



**HAL**  
open science

**Efficacy and mechanisms of action of tick defensins  
against the phytopathogenic and toxinogenic fungus  
*Fusarium graminearum***

Valentin Leannec-Rialland

► **To cite this version:**

Valentin Leannec-Rialland. Efficacy and mechanisms of action of tick defensins against the phytopathogenic and toxinogenic fungus *Fusarium graminearum*. Microbiology and Parasitology. Université de Bordeaux, 2022. English. NNT : 2022BORD0411 . tel-03982043

**HAL Id: tel-03982043**

**<https://theses.hal.science/tel-03982043>**

Submitted on 10 Feb 2023

**HAL** is a multi-disciplinary open access archive for the deposit and dissemination of scientific research documents, whether they are published or not. The documents may come from teaching and research institutions in France or abroad, or from public or private research centers.

L'archive ouverte pluridisciplinaire **HAL**, est destinée au dépôt et à la diffusion de documents scientifiques de niveau recherche, publiés ou non, émanant des établissements d'enseignement et de recherche français ou étrangers, des laboratoires publics ou privés.

THÈSE PRÉSENTÉE  
POUR OBTENIR LE GRADE DE

**DOCTEUR DE**

**L'UNIVERSITÉ DE BORDEAUX**

ÉCOLE DOCTORALE des Sciences de la Vie et de la Santé

SPÉCIALITÉ Microbiologie - Immunologie

Par Valentin LEANNEC-RIALLAND

**Efficacité et mécanismes d'action des défensines de tiques contre le champignon phytopathogène et toxigène *Fusarium graminearum***

Sous la direction de : Florence RICHARD-FORGET

Soutenue le 19/12/2022

Membres du jury :

M. Thierry CANDRESSE, Directeur de recherche, INRAe (Villenave d'Ornon), Président  
M. Massimo REVERBERI, Professeur des universités, Sapienza University of Rome (Roma, ITALIE), Rapporteur  
M. Vincent PHALIP, Professeur des universités, Université de Lille (Villeneuve-d'Ascq), Rapporteur  
Mme Florence RICHARD-FORGET, Directrice de recherche, INRAe (Villenave-d'Ornon), Directrice de thèse  
Mme Karine DEMENTHON, Associate Professor, Université de Bordeaux (Bordeaux), Examinatrice  
Mme Caroline STRUB, Associate Professor, Université de Montpellier (Montpellier), Examinatrice



## Greetings - Remerciements

Je tiens à adresser mes plus sincères remerciements aux membres du jury pour avoir accepté d'évaluer ces travaux de thèse.

Je tiens à remercier tous les membres du laboratoire MycSA pour leur accueil lors de ces quatre dernières années.

Tout d'abord, je tiens à remercier tout particulièrement ma cheffe Florence Richard-Forget, directrice d'unité du laboratoire MycSa, d'avoir accepté de me superviser depuis quatre ans. Je vous remercie de m'avoir fait confiance, de m'avoir poussé à donner le maximum de mes capacités et de ma réflexion pour pouvoir répondre à votre exigence, de m'avoir montré ce qu'est un véritable chercheur ainsi qu'un excellent superviseur. Je vous remercie d'avoir cru en moi et j'espère sincèrement ne pas vous avoir fait honte.

Je remercie aussi tout particulièrement les autres étudiants en thèse au sein du laboratoire MycSA. Vous êtes tous amenés à avoir de très belles carrières.

Aurélie, cela fait quatre ans que nous trimons dans ce laboratoire et que nous partageons nos victoires et nos peines de travail. Sans ta présence lors des moments difficiles et nos réunions de plaintes hebdomadaires, je n'aurais sans doute pas supporté l'entiereté de la thèse et n'aurait pas pu en venir finalement à bout. Je te remercie d'être l'amie que nous souhaiterions tous avoir pour collègue. Tu as été la meilleure des étudiants thésards de notre génération au sein de MycSA.

Jean-Marie, je te remercie pour être le meilleur voisin de bureau. Tu m'as permis de me motiver à travailler et de penser à autre chose que le travail lorsque cela était nécessaire. Nos pauses cigarette vont me manquer. Aurélie et Jean-Marie, je suis très heureux d'avoir pu partager ces trois années de thèse et cette éprouvante rédaction avec vous.

Antoine et Marie-Anne, je vous remercie de ne pas nous avoir trop durement jugé à votre arrivé. Je suis très content de pouvoir vous compter parmi mes amis. Nos repas, nos sorties et nos discussions sont des moments que je chérie.

Je remercie les autres membres du laboratoire. Je remercie Corine, Marie-France et Thierry pour les nombreux services qu'ils m'ont rendus. Je remercie les techniciennes de laboratoires Marie-Noelle, Christine, Magalie et Nathalie pour leur gentillesse et leur soutien. Je remercie Nadia pour avoir toujours pris le temps pour m'expliquer et m'aider, ainsi que pour sa patience malgré mes provocations. Je remercie Stéphane et Anne pour leur gentillesse à mon égard et j'aurais aimé avoir eu plus de temps pour faire votre connaissance. Je remercie Jean-Michel, Gérard et Marie pour leur amabilité et pour avoir toujours pris le temps de m'aider. Un grand merci à Laetitia pour avoir toujours été là pour moi et pour m'avoir montré comment montrer mes résultats sans que cela ne soit absolument moche. Encore merci pour ces moments passés avec toi à Parme et à Aussois. Un très grand merci à Sylvain, pour m'avoir tellement appris et participé à m'inculquer la rigueur. Ton sarcasme sur mes réflexions idiotes m'ont permis de continuer à me remettre en question !

Je remercie Oriane pour avoir été une excellente stagiaire et m'avoir ramené si souvent de délicieux cookies.

Je souhaite remercier Michel, qui m'a donné la passion pour la biologie et a cru en moi au début de mes études.

Je remercie mes amies Kim et Marie-Dominique. Je suis fier de ce que nous avons accompli tous les trois depuis notre rencontre.

Je tiens à remercier mes amis les plus fidèles Hugo, Florent, Rémi, Clément, Pierre, Alan, Adrian, Gandalf, Adou, Youj, Tristan, Chloé, Léo, Jane et Sofija. Vous avez été mes plus fidèles supports pendant cette thèse. Vous avez cru en moi et m'avez toujours soutenu. Je remercie également tous les autres membres de « Ah Pet Rot », ce groupe de potes plus bizarres et différents les uns que les autres, qui se rejoignent principalement pour faire la fête, mais qui forment aussi une petite famille dont les membres tiennent les uns aux autres.

Je tiens à remercier du fond du cœur mon amour et meilleure amie Maïlys qui partage ma vie depuis plus de quatre années. Tu as dû me supporter pendant toute cette thèse et a subi les pires moments. Sans toi, je n'aurais jamais pu tenir tout ce temps. Tu as été d'un grand soutien, tu m'as permis de rire aux éclats régulièrement et ton sourire au quotidien est ma plus belle récompense. Je t'aime amour !

Enfin je souhaite effectuer le plus grand des remerciements à ma famille.

Tout d'abord à mes parents qui ont tout fait pour me donner l'occasion de faire des études. Ces parents qui m'ont toujours poussé à donner le meilleur de moi-même et à être une meilleure personne au quotidien. J'espère vous rendre fiers.

Et enfin, un remerciement gigantesque à ma sœur, Julie, qui est mon plus grand soutien dans la vie. Tu as toujours cru en moi et m'as toujours protégé. Tu es la meilleure sœur que l'on puisse espérer. Je ne sais pas comment vous remercier pour tout ce que vous avez fait pour moi et vous témoigner la fierté de faire parti de cette famille.

Maman, Papa et Julie, je vous aime et vous dédie cette thèse.

## Scientific publications and communications

### Publication:

#### Review:

- Leannec-Rialland, V.; Atanasova, V.; Chereau, S.; Tonk-Rügen, M.; Cabezas-Cruz, A.; Richard-Forget, F. Use of Defensins to Develop Eco-Friendly Alternatives to Synthetic Fungicides to Control Phytopathogenic Fungi and Their Mycotoxins. *J. Fungi* 2022, 8, 229.  
<https://doi.org/10.3390/jof8030229>  
(article published in *Journal of Fungi*, doi.org/10.3390/jof8030229)

#### Scientific papers:

- Leannec-Rialland, V., Cabezas-Cruz, A., Atanasova, V. et al. Tick defensin  $\gamma$ -core reduces *Fusarium graminearum* growth and abrogates mycotoxins production with high efficiency. *Sci Rep* 11, 7962 (2021). <https://doi.org/10.1038/s41598-021-86904-w>  
(article published in scientific report, doi.org/10.1038/s41598-021-86904-w)
- Leannec-Rialland V., Atanasova V., Cabezas-Cruz A. et al. Susceptibility of different *Fusarium* species and strains involved in *Fusarium* Head Blight to the promising TickCore3-based biocontrol solution.  
(to be submitted in *Journal of Agricultural and Food Chemistry*.)
- Leannec-Rialland V., Ducos C., Cabezas-Cruz A. et al. Comparative transcriptome analysis of *Fusarium graminearum* revealed the multi-faceted mechanism of the peptide TickCore3, an efficient inhibitor of fungal growth and mycotoxin production.  
(Manuscript under preparation)

### Oral communications:

- “Tick defensin  $\gamma$ -core reduces *Fusarium graminearum* growth and abrogates mycotoxins production with high efficiency.”
  - 15th European *Fusarium* Seminar; June 1, 2021; Online
  - Journées Jean Chevaugéon - 13èmes Rencontres de Phytopathologie-Mycologie; May 24, 2022; Aussois
- “Unravelling the mechanism of action of an environmentally friendly defensin-based solution holding the promise to reduce mycotoxin contamination of wheat.”
  - 13th conference of the World Mycotoxin Forum; May 17, 2021; Parme
  - Journées des doctorants du département SPE de l'INRAe 2022; June 23, 2022; Bordeaux



# Table of contents – Table des matières

Foreword - Avant propos	1
<b>Introduction and bibliographic context</b>	<b>3</b>
1. Fusarium Head Blight	5
2. The fungal species responsible for FHB	7
3. Fusarium spp. genome and intra/interspecific diversity	10
4. The life cycle of Fusarium spp.	11
4.1. Sexual and asexual life cycle	11
4.2. Sexual and asexual transcriptional regulation	12
4.3. Infection cycle	12
5. Pathogenicity factors	14
6. Mycotoxins produced by Fusarium species	16
6.1. Trichothecenes (TCTs)	17
6.1.1. Type A trichothecenes (TCTA)	18
6.1.2. Type B trichothecenes (TCTB)	20
6.1.2.1. Chemotype distribution	20
6.1.2.2. DON, 3-ADON and 15-ADON	22
6.1.2.3. NIV and FX	22
6.1.3. Biosynthesis and regulations of the TCTs production	23
6.1.3.1. The Tri genes	23
6.1.3.2. TCT biosynthetic pathway	24
6.1.3.3. Regulation of the TCTBs biosynthesis	26
6.1.3.3.1. The production of DON is tightly controlled by environmental factors	26
6.1.3.3.2. Regulation of DON yield involves multiscale mechanisms	28
6.1.3.3.2.1. Specific transcription factors	28
6.1.3.3.2.2. Signal transduction pathways	28
6.1.3.3.2.3. Global regulators	28
6.1.3.3.2.4. Chromatin structure	30
6.2. Zearalenone	31
6.3. Emerging mycotoxins	32
6.4. Mycotoxin multi contamination	33
7. Pre-harvest strategies to control FHB	34
7.1. Agronomic methods	35
7.1.1. Crop Rotation	35
7.1.2. Tillage and Fertilization	35
7.1.3. Forecasting models	36
7.2. Use of genotype with a high level of tolerance to FHB	36
7.3. Use of antifungal phytochemicals	37
7.3.1. Active ingredients / their targets / effectiveness	38
7.3.2. Warning date application	39

7.3.3.	Unintended and adverse effect of fungicide use	39
7.3.3.1.	Inefficiency	39
7.3.3.2.	Emergence of resistance	39
7.3.3.3.	Environmental and regulatory issues	40
7.4.	Biocontrol solutions	41
7.4.1.	Biological control agents	41
7.4.2.	Marketed Biocontrol Agents	43
7.4.3.	Antimicrobial peptides as promising solutions to minimize FHB and DON accumulation	44
Use of Defensins to Develop Eco-Friendly Alternatives to Synthetic Fungicides to Control Phytopathogenic Fungi and Their Mycotoxins		45
1)	Introduction	46
2)	Origin and Characteristic of Defensins	47
3)	Activity of Defensins against Fungal phytopathogens	49
4)	Antifungal mechanisms of Action of Defensins	64
4.1)	Interactions with Host Membrane Components and Induction of Fungal Membranes Disorders	65
4.2)	Induction of Oxidative Stress and Apoptosis	68
4.3)	Internalization and Intracellular Targets	68
5)	Exploiting Defensins to Protect Crops from Phytopathogenic Fungi Mycotoxin Contamination	68
5.1)	Transgenic Plants Overexpressing Defensin for an Enhances Resistance to Phytopathogenic Fungi	69
5.2)	Developing Defensin-Based Plant Protection Products for the Control of Phytopathogenic Fungi	70
6)	Conclusion	72
	References	72
8.	Tickcore 3, a peptide from the tick <i>Ixodes ricinus</i> could be an excellent candidate for biofungicide development	82
	Thesis project	83
<b>Chapter 1: Assessment of TC3 antifungal and anti-mycotoxin properties and investigation of the structural determinants required for the bioactivity</b>		<b>85</b>
A)	<i>Tick defensin <math>\gamma</math>-core reduces <i>Fusarium graminearum</i> growth and abrogates Mycotoxins production with high efficiency</i>	89
	Abstract	89
I.	Introduction	89
II.	Material and methods	90
III.	Results	92
IV.	Discussion	96
V.	Conclusion	97
	References	98

B) Complementary data: comparative efficiency of DefMT3 and TC3	101
C) Complementary data: comparative efficiency of TC3 and synthetic fungicides commonly used to control FHB	102
D) Efficiency of TC3 when tested in in planta assays	104
a) TC3 efficiency in detached leaf assays	104
b) Greenhouse trials with TC3 application at wheat anthesis	107
Conclusion	109
<b>Chapter 2: Bioactivity of TC3 against the different FHB causal agents</b>	<b>111</b>
Abstract	113
I. Introduction	114
II. Material and methods	115
III. Results	120
IV. Discussion	127
V. Conclusion	129
References	130
<b>Chapter 3: Determination of the fungal metabolic pathways affected by TickCore3 in relation to DON and 15-ADON production.</b>	<b>133</b>
A) Comparative transcriptome analysis reveals antifungal molecular mechanisms triggered by the peptide TickCore3 against <i>Fusarium graminearum</i>	
Abstract	135
I. Introduction	136
II. Material and methods	137
III. Results	141
IV. Discussion	156
V. Conclusion	159
References	160
Supplementary documents	162
B) Complementary data: effect of TC3 on <i>F. graminearum</i> mutant strains affected for their response to oxidative stress and pH changes	185
C) Complementary data: Comparative metabolomic analysis of <i>F. graminearum</i> response to TC3 and synthetic fungicides	188
<b>Discussion / Conclusion</b>	<b>195</b>
References	205



## Table of figures - Table des illustrations

### Introduction

Figure 1. Worldmap of FHB epidemics and its consequences.—————	6
Figure 2. Phylogram of the <i>Fusarium</i> genus. —————	8
Figure 3. Gene and RNA distribution across the four <i>Fusarium graminearum</i> 's chromosomes (Chr 1–4). —————	10
Figure 4. Generalized life cycle of <i>Fusarium</i> depicting varying reproduction strategies.—	11
Figure 5. Regulation and Dynamics of Gene Expression During the Life Cycle of <i>Fusarium graminearum</i> . —————	12
Figure 6. The life cycle of <i>Fusarium graminearum</i> , the causal pathogen of <i>Fusarium</i> head blight disease of wheat. —————	13
Figure 7. <i>Fusarium</i> pathogenicity and host defense mechanisms. —————	14
Figure 8. Major <i>Fusarium</i> species and their fusariotoxins. —————	17
Figure 9. Chemical Structure of Type A, Type B, Type C, and Type D Trichothecenes.	18
Figure 10. Structure of TCTA mycotoxins. —————	19
Figure 11. Structure of TCTB mycotoxins. —————	20
Figure 12. Spatial distribution of chemotypes and <i>Fusarium</i> species in Europe. ————	21
Figure 13. Gene clusters involved in trichothecene biosynthetic pathway in <i>Fusarium</i> , including a Tri cluster containing 12 genes, a two-gene Tri1-Tri16 cluster and a single gene Tri101. —————	23
Figure 14. Comparison of the proposed trichothecene biosynthetic gene cluster of <i>Fusarium sporotrichioides</i> , <i>F. graminearum</i> , and <i>F. equiseti</i> . —————	24
Figure 15. Proposed trichothecene biosynthetic pathway. —————	26
Figure 16. Overview of metabolic pathways, indicating the relationship between the production of TCTB by <i>F. graminearum</i> and other primary and secondary metabolic pathways. —————	27
Figure 17. Environmental factors can influence tri genes expression and DON biosynthesis. This regulation involves various global regulators.—————	29
Figure 18. Regulation of DON production through chromatin structure modifications. —	30
Figure 19. Structure of Zearalenone. —————	31
Figure 20. Structure of Beauvericin. —————	32
Figure 21. Enniatin structure with the main analogs (ENNs A, A1, B, and B1) described. —————	33
Figure 22. Main mycotoxin mixtures and their geographic distribution. —————	34
Figure 23. Pre- and Post-harvest strategies to reduce FHB and mycotoxin presence in grains and processed food. —————	35
Figure 24. Mechanism of action of biocontrol agents to reduce FHB. —————	42
Review Figure 1. Tridimensional structure of the typical representative of the four groups of AMPs classified according to the presence of $\alpha$ -helix and/or $\beta$ -sheet secondary elements. —————	47
Review Figure 2. Disulfide bridges' connectivity pattern characteristic of defensin families: vertebrate $\alpha$ -defensin, vertebrate $\beta$ -defensin, invertebrate cis-oriented defensin and plant defensin. —————	49
Review Figure 3. Representation of the cysteine-stabilized alpha-beta (CS $\alpha\beta$ ) motif present in the structure of plant and of some invertebrate defensins. —————	50
Review Figure 4. Summary of known and suspected modes of action of defensins displaying antifungal. —————	66
Figure 25. Tertiary structures of <i>I. ricinus</i> defensins. —————	82

## Chapter 1

Figure 1. Antifungal and anti-mycotoxin activity of natural and oxidized TC3. _____	92
Figure 2. Membrane binding of TickCore3. _____	93
Figure 3. Recruitment of TC3 by POPA and POPG phospholipids. _____	94
Figure 4. Antifungal and anti-mycotoxin activity of linear, methylated and oxidized TC3. _____	95
Figure 5. Role of positively charged amino acids on the activity of TC3. _____	96
Figure 6. Antifungal and anti-mycotoxin activity of the defensin DefMT3 and its $\gamma$ -core motif TC3. _____	101
Figure 7. Three synthetic fungicides, Carbendazim, Tebuconazole and Azoxystrobin, and their mode of actions. _____	102
Figure 8. Antifungal and anti-mycotoxin activity of synthetic fungicides. _____	103
Figure 9. Antifungal and anti-mycotoxin activity of TC3, carbendazim, tebuconazole and azoxystrobin. _____	104
Figure 10. Necrotic zones observed on wheat leaves treated with TCA or sterile water at 3-day post inoculation with <i>F. graminearum</i> . _____	106
Figure 11. Necrosis surfaces (in mm <sup>2</sup> ) on wheat leaves inoculated with <i>F. graminearum</i> pre-treated with TC3 125 $\mu$ M (in blue) or with sterile water (in grey). _____	106
Figure 12. Quantification of fungal DNA (A) and Zearalenone (B) extracted from wheat leaves treated or not with TC3. _____	107
Figure 13. Fungal DNA (A) and DON (B) quantified in wheat heads at two maturity stages and treated according to four modalities, inoculated at anthesis by <i>F. graminearum</i> . _____	108

## Chapter 2

Figure 1. Effect of TC3 at 50 $\mu$ M on the fungal biomass weight (a) of <i>F. graminearum</i> (INRAE 349), <i>F. avenaceum</i> (INRAE 498), <i>F. tricinctum</i> (INRAE 104), <i>F. langsethiae</i> (INRAE 502), <i>F. poe</i> (INRAE 488) and <i>F. culmorum</i> (INRAE 134) and on the production of TCTB by <i>F. graminearum</i> and <i>F. culmorum</i> (b,f), ENN by <i>F. avenaceum</i> and <i>F. tricinctum</i> (c,e) and T2+HT2 by <i>F. langsethiae</i> (d) in 10-day-old broths. _____	120
Figure 2. Effect of TC3 at 50 $\mu$ M on the fungal biomass weight of <i>F. graminearum</i> strains (a) and on the production of TCTB by strains INRAE215 (b), INRAE349 (c), INRAE 605(d) and PH1 (e) in 10-day-old broths. _____	121
Figure 3. Effect of TC3 at 50 $\mu$ M on the fungal biomass weight of <i>F. avenaceum</i> strains (a) and on the production of ENN in strains INRA112 (b), INRA495 (c), INRA498 (d) and INRA873 (e) in 10-day-old broths. _____	122
Figure 4. Effect of TC3 at 50 $\mu$ M supplemented at different day post-inoculation on <i>F. graminearum</i> . Kinetics of <i>F. graminearum</i> INRAE 349 growth without treatment (a). Effect of TC3 at 50 $\mu$ M (supplemented at 0, 1, 3 and 5 dpi) on the fungal biomass weight of <i>F. graminearum</i> INRAE 349 (b) and on the production of DON + 15-ADON (c) in 14-day-old broths. _____	123
Figure 5. Effect of TC3 at 25 $\mu$ M and 50 $\mu$ M on the number of spores of <i>F. graminearum</i> INRAE 349 (a) and <i>F. avenaceum</i> INRAE 498 (b) in 3-day-old CMC medium. _____	124
Figure 6. Effect of TC3 at 25 $\mu$ M and 50 $\mu$ M on the percentage of germinated spores relative to the total spores of <i>F. graminearum</i> INRAE 349 (a) and <i>F. avenaceum</i> INRAE 498 (b) at 0, 4 and 8 HAI. _____	125
Figure 7. Analysis on fluorescence microscopy of <i>F. graminearum</i> strain and <i>F. avenaceum</i> spores in presence of TC3 peptide labeled with FITC (25 $\mu$ M) in green and the fluorescent dye FM4-64 in red. _____	126

## Chapter 3

Figure 1. Phenotypic response of <i>F. graminearum</i> to TC3. _____	142
Figure 2. Differential regulation of transcripts of <i>F. graminearum</i> treated or not with TC3 at two developmental stages (3 and 5 DPI). _____	143
Figure 3. Enrichment analysis of the negatively regulated transcripts in presence of TC3 at both 3DPI and 5DPI in <i>F. graminearum</i> . _____	144
Figure 4. Enrichment analysis of the positively regulated transcripts in presence of TC3 at both 3DPI and 5DPI in <i>F. graminearum</i> . _____	146
Figure 5. Heatmap reporting the comparative expression profile of all the differentially regulated genes with or without TC3 at 3 DPI and 5 DPI. _____	148
Figure 6. Differential expression of genes related to the GO terms “DNA replication” (a), “DNA repair” (b) and “Chromatin organization” (c) in the clusters 2 and 12.-	151
Figure 7. Differential expression of genes related to Intrinsic component of membrane, Fungal-type cell wall and Ergosterol biosynthetic process. _____	152
Figure 8. Differential expression of tri genes in <i>F. graminearum</i> treated or not with TC3 at two developmental stages. _____	154
Figure 9. Differential expression of genes related to the primary metabolism. _____	155
Figure 10. Validation of RNA-Seq results by quantitative PCR (qPCR). _____	156
Figure 11. Summary of the main biological processes and metabolic pathways in <i>F. graminearum</i> affected by the antifungal and anti-mycotoxin peptide TickCore 3. _____	159
Figure 12. Antifungal and anti-mycotoxin activity of TC3 on <i>F. graminearum</i> strain INRA349 and its mutants on gene <i>FgPac1</i> . _____	187
Figure 13. Antifungal and anti-mycotoxin activity of TC3 and synthetic fungicides on <i>F. graminearum</i> . _____	190
Figure 14. Scores from PCA decomposition of mycelium extracts (a) and culture supernatants extracts (b) at 3 DPI, 5 DPI, 7 DPI and 14 DPI of <i>F. graminearum</i> treated or not with TC3, Carbendazim, Tebuconazole and Azoxystrobin at the respective concentrations of 50µM, 5.25µM, 1.625µM and 5µM. _____	191
Figure 15. Scores from PCA decomposition of mycelium extracts (a) and culture supernatants extracts (b) at 14DPI of <i>F. graminearum</i> treated or not with TC3, Carbendazim, Tebuconazole and Azoxystrobin at the respective concentrations of 50µM, 5.25µM, 1.625µM and 5µM. _____	191
Figure 16. Volcano plot representing the differential concentration of detected molecules in mycelium extracts (a) and culture supernatant extracts (b) between TC3 and the control at 14DPI. _____	192

## Discussion

Figure 1. The antifungal and anti-mycotoxin activity of TC3 is related to a multi-faceted mechanism. _____	198
--	-----

## Table of tables

### Introduction

Table 1. Important food-borne <i>Fusarium</i> species, their habitat (cereal related), mycotoxins and physiological characteristics. _____	9
Table 2. List of CWDEs in <i>Fusarium graminearum</i> . _____	14
Table 3. List of pathogenicity and virulence factors of <i>Fusarium graminearum</i> (non-CWDEs and non-toxin). _____	15
Table 4. Major mycotoxins and associated US and EU limits in food. _____	16

Review Table 1. List of defensins and DLPs with antifungal effect on phytopathogenic and mycotoxigenic fungi. _____	50
<b>Chapter 1</b>	
Table 1. List of peptides synthesized and used in this study. _____	90
Table 2. Primers used for the fungal DNA quantification using qPCR. _____	106
<b>Chapter 2</b>	
Table 1. Fungal species and strains used in this study. _____	116
Table 2. Elution gradient used in the multi-mycotoxin method. _____	118
Table 3. LC-HRMS parameters for the quantification of mycotoxins, including the retention time, analyte formula, ion m/z (extracted with a 3 ppm tolerance) for quantification and for confirmation. _____	118
<b>Chapter 3</b>	
Table 1. Primers used for the RNA-Seq validation using RT-qPCR. _____	141
Table 2. Clusters of genes differentially expressed with their centroid expression profile and the Gene Ontology terms associated. _____	149
Table 3. Fungal wild and mutant strains used in this study. _____	186
<b>Supplementary Figure</b>	
Supplementary Figure 1. Hierarchical clustering of normalized concentration of detected molecules from culture supernatant extracts (a) and in mycelium extracts (b) between TC3 and the control at 14DPI. _____	193
<b>Supplementary Tables</b>	
Supplementary Table 1. GO terms related to “Molecular function” obtained from enrichment analysis on the transcripts down-regulated at both times, 3 and 5 DPI. _____	162
Supplementary table 2. GO terms related to “Cellular component” obtained from enrichment analysis on the transcripts down-regulated at both times, 3 and 5 DPI. _____	165
Supplementary table 3. GO terms related to “Biological process” obtained from enrichment analysis on the transcripts down-regulated at both times, 3 and 5 DPI. _____	165
Supplementary table 4. GO terms related to “Molecular function” obtained from enrichment analysis on the transcripts up-regulated at both times, 3 and 5 DPI. _____	167
Supplementary table 5. GO terms related to “Cellular component” obtained from enrichment analysis on the transcripts up-regulated at both times, 3 and 5 DPI. _____	170
Supplementary table 6. GO terms related to “Biological process” obtained from enrichment analysis on the transcripts up-regulated at both times. _____	171
Supplementary table 7. Top 50 genes most down-regulated and top 50 genes most up-regulated in presence of TC3 at 3DPI. _____	178
Supplementary table 8. Top 50 genes most down-regulated and top 50 genes most up-regulated in presence of TC3 at 5DPI. _____	180

## Table des abbreviations

<b>γ-core :</b>	functional region of defensin	<b>IC50 :</b>	half- maximal inhibitory concentration
<b>3-ADON :</b>	3-acetyl deoxynivalenol	<b>IPM :</b>	integrated pest management
<b>15-ADON :</b>	15-acetyl deoxynivalenol	<b>MD :</b>	molecular dynamic
<b>AF :</b>	aflatoxin	<b>MFP :</b>	microbial fermentation-based product
<b>AITD :</b>	antibacterial ancient invertebrate-type defensin	<b>MIC :</b>	minimum inhibitory concentration
<b>AMP :</b>	antimicrobial peptide	<b>MM :</b>	molecular mass
<b>BCA :</b>	biocontrol agent	<b>MMT :</b>	million metric tonne
<b>BEA :</b>	beauvericin	<b>MON :</b>	moniliformin
<b>cDNA :</b>	complementary DNA	<b>MS medium :</b>	mycotoxin synthetic medium
<b>CITD :</b>	antibacterial classical insect-type defensin	<b>MW :</b>	molecular weight
<b>CMC medium :</b>	carboxy methyl cellulose medium	<b>NIV :</b>	nivalenol
<b>CWDE :</b>	cell wall–degrading enzyme	<b>OTA :</b>	ochratoxin A
<b>Cys :</b>	cysteine	<b>PCR :</b>	polymerase chain reaction
<b>DAD :</b>	diode-array detection	<b>PDA medium :</b>	Potato dextrose agar medium
<b>DAS :</b>	diacetoxyscirpenol	<b>PGPM :</b>	plant growth promoting microorganism
<b>DefMT3 :</b>	defensin from the tick <i>Ixodes Ricinus</i>	<b>PITD :</b>	antifungal plant/insect-type defensin
<b>DLP :</b>	defensin-like peptide	<b>PKS :</b>	polyketide synthase
<b>DNA :</b>	deoxyribonucleic acid	<b>PMTDI :</b>	provisional maximum tolerable daily intake
<b>DON :</b>	deoxynivalenol	<b>POPA :</b>	phosphatidic acid
<b>DPI :</b>	day post-inoculation	<b>POPC :</b>	phosphatidylcholine
<b>EFSA :</b>	European Food Safety Authority	<b>POPE :</b>	phosphatidylethanolamine
<b>ENN :</b>	enniatin	<b>POPG :</b>	phosphatidylglycerol
<b>ESI-MS :</b>	electrospray mass-spectroscopy	<b>POPI :</b>	phosphatidylinositol
<b>FAO :</b>	Food and Agriculture Organization	<b>POPS :</b>	phosphatidylserine
<b>FE :</b>	Fold-enrichment	<b>RNA :</b>	ribonucleic acid
<b>FGSC :</b>	<i>Fusarium graminearum</i> species complex	<b>RNAseq :</b>	RNA sequencing
<b>FHB :</b>	<i>Fusarium</i> Head Blight	<b>ROS :</b>	reactive oxygen species
<b>FIESC :</b>	<i>Fusarium incarnatum-equiseti</i> species complex	<b>RT-qPCR :</b>	reverse transcriptase quantitative PCR
<b>FITC :</b>	fluorescein isothiocyanate	<b>TC3 :</b>	TickCore 3
<b>FPP :</b>	farnesyl pyrophosphate	<b>TC3-CH3 :</b>	TickCore 3 methylated on cysteine
<b>FSAMSC :</b>	<i>Fusarium sambucinum</i> species complexes	<b>TC3-K6T :</b>	TickCore with lysine 6 substituted by threonine
<b>FUM :</b>	fumonisin	<b>TC3Ox :</b>	oxydized TickCore 3
<b>FX :</b>	fusarenon X	<b>TCA cycle :</b>	tricarboxylic acid cycle
<b>GABA :</b>	γ-aminobutyric acid	<b>TCTA :</b>	type A trichothecenes
<b>GO :</b>	gene ontology	<b>TCTB :</b>	type B trichothecenes
<b>HAI :</b>	Hours after inoculation	<b>TDI :</b>	tolerable daily intake
<b>HPLC :</b>	high performance liquid chromatography	<b>ZEA :</b>	zearalenon



## Foreword - Avant propos

Agricultural production systems are currently facing unprecedented challenges worldwide including increased demand for food resulting from population growth, rising hunger and malnutrition, consumer's expectations that evolve, climate change, soil erosion, reduced list of licensed pesticides and food loss.

Food and agriculture systems are sustainable when they contribute to each of the four pillars of food security (availability, access, use and stability) as well as the three dimensions of sustainability (environmental, social and economic). Food production has to cope with the requirements of the current and future generations while being cost effective, preserving the health of the environment and ensuring social and economic equity.

Cereals have been an important part of human diet for thousands of years. Rice, wheat and maize are important food crops in the world contributing for more than half of all the calories consumed by humans. Sorghum and millets are important contributors to daily survival in certain parts of the world, particularly in some semi-arid regions of Africa and Asia.

Wheat is considered the main food for more than one third of world's populations and the second most important source of calories and proteins for humans, following closely rice (FAO, 2018)<sup>1</sup>. Thanks to its adaptability to a wide range of growth conditions compared to other major cereal crops, wheat is the most widely cultivated food plant worldwide with 760 million metric tonne (MMT) of grains produced on 219 million ha in 2019/2020 (FAOSTAT, 2020)<sup>2</sup>. China and India are the world's largest producers, with China and India producing approximately 30% of the wheat world's production in 2020 (FAOSTAT, 2020)<sup>2</sup>. On a *per capita* basis, however, Australia and Canada are among the largest wheat producers, with about 1 MMT *per capita* in 2020 (FAO, 2020)<sup>3</sup>. Major wheat exporters include Russia (36 million tons), the European Union (26 million tons), the United States of America (25 million tons), Canada (22.5 million tons), Australia (17.5 million tons), and Argentina (13.7 million tons) (USDA-FAS, 2018)<sup>4</sup>. Wheat is a good source of carbohydrates (78.10% of its composition), proteins (14.70%), minerals (2.10%), fat (2.10%), B-group vitamins and dietary fiber (Yadav RK, 2011)<sup>5</sup>. It can be consumed as an ingredient in foods such as bread, pasta, crackers, cakes, noodles and couscous.

Among the growing challenges, climate change and plant disease epidemics are the most worrying threats for wheat production (Friesen et al., 2008; Gurung et al., 2012)<sup>6,7</sup>. Among the numerous diseases threats cereals including abiotic (such as extreme temperatures, drought, salinity and soil nutrient limitations) and biotic ones (viruses, fungi, bacteria, weeds, insects, and other pests), the fungal disease *Fusarium* Head Blight (FHB) is a major cause of worldwide yield losses.

In addition, even when grains develop, FHB may induce a decreased grain quality and be responsible for the contamination of grains with mycotoxins which are harmful to humans and livestock health (Xia et al., 2020)<sup>8</sup>.

Current recommended control methods for FHB in wheat include agronomic practices (crop rotation, residues management, sowing date), genotype selection and phytosanitary

treatments. These methods reduce wheat contamination by *Fusarium* spp. and their mycotoxins to some extent, but remain insufficiently effective. Besides, the use of synthetic pesticides can be detrimental to health and the environment, and *Fusarium* spp. may develop resistances to these fungicides. In a context where the use of synthetic fungicides is one of the primary control methods for *Fusarium* Head Blight, it is important to find new sustainable and eco-friendly alternative approaches for diversifying the way to control it.

This work aims to contribute to the definition of new eco-friendly strategies to minimize FHB disease. It will consider a new biofungicide solution with antifungal and anti-mycotoxin properties.

# **Introduction and bibliographic context**



## Introduction and bibliographic context

### 1. *Fusarium* Head Blight

*Fusarium* Head Blight (FHB) is a devastating fungal disease affecting wheat and other cereals, including barley or oat. Fungal species causing FHB are mainly of the *Fusarium* genus. These species can also infect maize leading to the Gibberella Ear Rot disease (Parry et al., 1995, Sutton, 1982)<sup>9,10</sup>. First identified and described in 1884 by W. G. Smith in England (Parry et al., 1995)<sup>9</sup>, FHB (originally called wheat scab) was shown as responsible for significant damage in wheat heads. Arthur (Parry et al., 1995)<sup>9</sup> suggested in 1891 that the florets were the sites of infection and reported differences in symptom severity related to the general plant vigor and the flowering time. In 1920, Atanasoff (D. Atanasoff, 1920)<sup>11</sup> renamed the disease as *Fusarium* Head Blight. In 1926, Douin used the French term “fusariose” to nominate the disease (Leonard & Bushnell, 2003)<sup>12</sup>.

Infection by FHB related species is most likely to occur during flowering, when the wheat florets are open in warm and humid weather conditions; abundant dew and prolonged rainfall during the flowering stage are primary factors conducive to FHB (Walter et al., 2010; Lenc L., 2015)<sup>13,14</sup>. Typical symptoms of the disease are visible on heads starting from the milk stage when the kernel begins forming. Pink sporodochia with conidia spores, as well as a layer of mycelium, appear on infected chaff in spikes few days after infection. Kernels that develop in infected heads are usually smaller, gray, shriveled and often covered with sporodochia and *Fusarium* spp. mycelium. The disease also affects the nutritional qualities of the grain by changing the composition of storage proteins and damaging starch granules (Bechtel et al., 1985)<sup>15</sup>. The germinal quality of contaminated seeds is also affected, which can lead to seedling melting and symptoms on the stems of young seedlings (Pirgozliev et al., 2003)<sup>16</sup>.

FHB not only leads to significant losses in yield and quality, but is also of high concern for food and feed safety. Indeed, fungal pathogens causing FHB can produce various mycotoxins that pose a risk to human and animal health (Kang and Buchenauer, 1999)<sup>17</sup>.

Despite intensive efforts to develop strategies to combat FHB in the past decades, this fungal disease is still one of the most important plant diseases affecting cereals (Fig. 1).

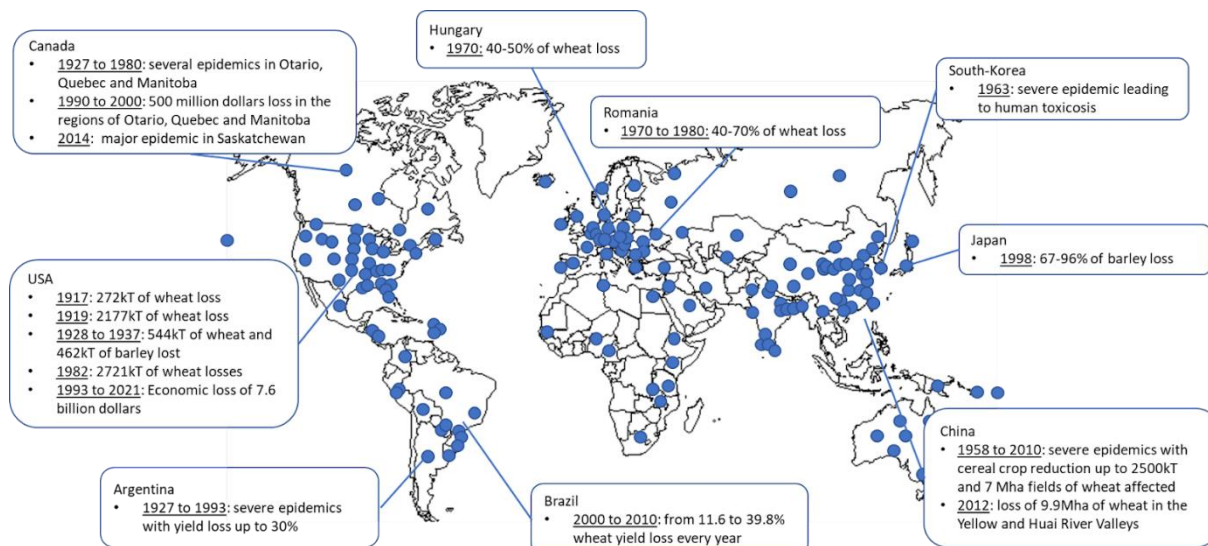


Figure 1. Worldmap of FHB epidemics and its consequences (based on J. Powell and V. Vujanovic, 2021<sup>18</sup>; Reis and Carmona, 2013<sup>19</sup>; Leonard and Bushnell, 2003<sup>12</sup>; Parry et al., 1995<sup>9</sup>; Zhu et al., 2016<sup>20</sup>; Windels, 2000<sup>21</sup>; McMullen et al., 2012<sup>22</sup>; McCartney et al., 2016<sup>23</sup>; Dill-Macky and Jones, 1997<sup>24</sup>; McMullen et al., 1997<sup>25</sup>; Choo Thin Meiw, 2009<sup>26</sup>; Zhang et al., 2011<sup>27</sup>; Tusa et al., 1981<sup>28</sup>)

An estimated loss of 272kT of wheat has been associated with the first FHB epidemic recorded in the USA in 1917 (Powell and Vujanovic, 2021)<sup>18</sup>. The economic loss resulting from FHB epidemics that have occurred between 1993 to 2001 in the US and have led to a reduced wheat production of approximately four percents was reported to reach 7.6 billion US dollars (Windels 2000; McMullen et al., 2012)<sup>21,22</sup>. During the two first decades of the 20<sup>th</sup> century, FHB wreaked havoc in the US and also extended to Canada where it was first reported in 1919. Losses incurred by the Canadian wheat sector during the 1990s major outbreak amounted to 200 million US dollars for the regions of Ontario and Quebec and 300 million US dollars for Manitoba. In 2014, an FHB epidemic caused drastic yield losses in Saskatchewan, the largest wheat producing province in Canada (McCartney et al., 2016)<sup>23</sup>. The main reasons explaining the severe FHB epidemics during the 20<sup>th</sup> century occurring in Canada and the USA were attributed to inefficient crop management strategies, the poor level of resistance of the used cultivars and detrimental environmental conditions (Dill-Macky and Jones, 2000; McMullen et al., 1997)<sup>24,25</sup>.

In China, FHB is considered to be the most harmful disease affecting barley and wheat crops. The first officially recorded epidemic has occurred in southern China in 1936. From 1951 to 1990, seven severe epidemics have been reported in various areas of China leading to more than 40% of yield losses for wheat and barley production (Leonard and Bushnell, 2003)<sup>12</sup>. The 2012 FHB epidemic was the most devastating, affecting more than 9.9 Mha in the major wheat producing area in China, the Yellow and Huai River Valleys (Zhu et al., 2020)<sup>20</sup>.

In Europe, several epidemics have been recorded, leading to yield losses reaching up to 40-50% in Hungary in 1970 and 40% in Romania in the 1980s (Parry et al., 1995)<sup>9</sup>.

In Japan, in 1998, barley yield losses due to FHB were estimated at 67-96% (Leonard and Bushnell, 2003)<sup>12</sup>. In Brazil, FHB has been reported to lead to yield losses ranging from 11.6 to 39.8% each year between 2000 and 2010 (Reis and Carmona, 2013)<sup>19</sup>. In developing countries, few data and estimations are available (Schmale and Munkvold, 2009)<sup>29</sup>.

FHB infection and development are principally modulated by the abundance and aggressiveness of inoculum at flowering, the environmental conditions and the susceptibility of the plant.

## 2. The fungal species responsible for FHB

FHB can be caused by more than 20 species of the *Fusarium* and *Microdochium* genus (Arseniuk et al., 1999; Liddell, 2003)<sup>30,31</sup>. In a survey released in 2012 listing the top ten fungal pathogens according to their worldwide economic relevance, the only genus appearing twice was the *Fusarium* genus, with *Fusarium graminearum* ranking at the fourth position and *Fusarium oxysporum* at the fifth.

*Fusarium* species concepts have undergone multiple revisions. The first description of the *Fusarium* genus was made by Link in 1809. *Fusarium* owes its name to the Latin *fuscus* (spindle) in relation to the shape of its fusiform and partitioned macroconidia. The *Fusarium* genus belongs to the division of the Ascomycetes and the Nectriaceae family. During the 20<sup>th</sup> century, taxonomic differentiation of *Fusarium* species mainly rested on morphological characters. The classification derived from Nelson et al. (1983)<sup>32</sup> which groups *Fusarium* species in 15 sections was the most commonly used.

From the 2000s to present, the species concept has evolved to be based on sexual compatibility and molecular phylogeny. The *Fusarium* genus has been divided into 23 informal multispecies lineages, termed species complexes. A genealogical concordance phylogenetic species recognition (GCPSR)-based analysis indicated that the genus comprises at least 300 phylogenetically distinct species, 20 species complexes, and 9 monotypic lineages (O'Donnell et al., 2015)<sup>33</sup> (Fig. 2).

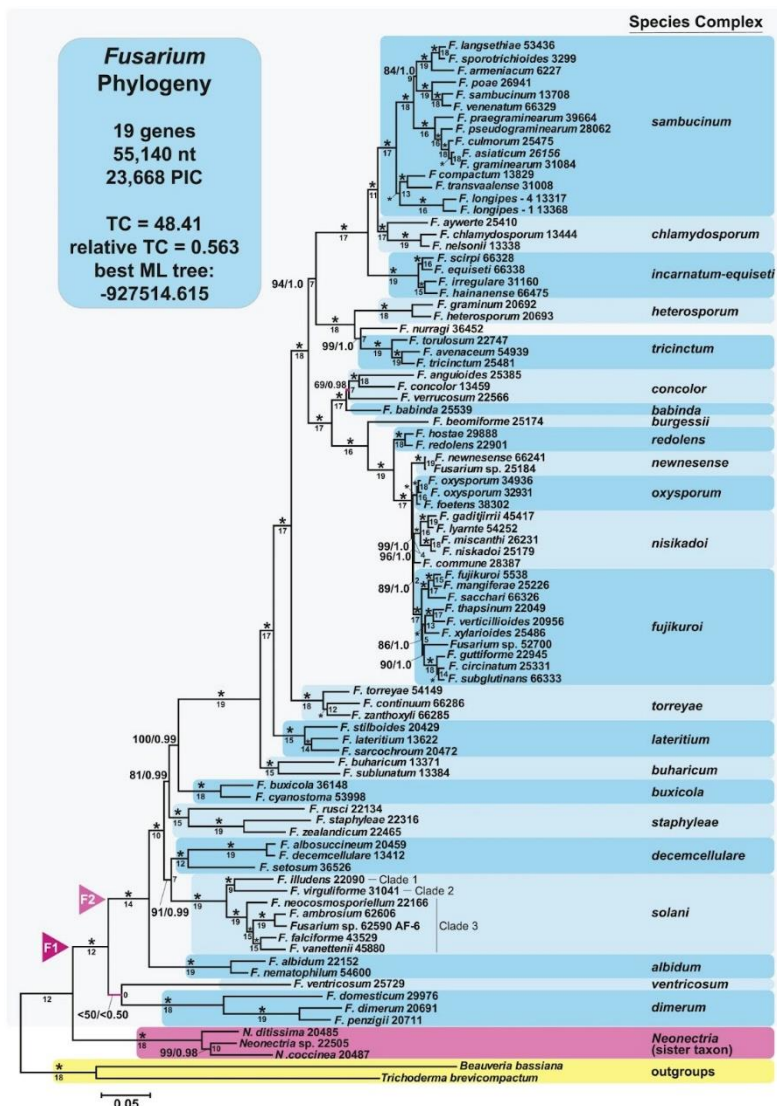


Figure 2. Phylogram of the *Fusarium* genus (D. Geiser et al., 2021)<sup>34</sup>.

Most *Fusarium* species involved in agriculturally important diseases are members of the *Fusarium sambucinum* (FSAMSC) and *Fusarium fujikuroi* species complexes. The major fungal pathogens associated with FHB include isolates from the *F. graminearum* species complex (FGSC), part of the FSAMSC, and related species such as *Fusarium avenaceum*, *Fusarium culmorum* and *Fusarium poae* (O'Donnell et al., 2004; Leslie and Summerell, 2006; van der Lee et al., 2015; Pasquali, 2016; Dweba et al., 2017)<sup>35–39</sup>. Other species, e.g. *Fusarium acuminatum*, *Fusarium chlamydosporum*, *Fusarium equiseti*, *Fusarium langsethiae*, *Fusarium sporotrichioides*, *Fusarium cerealis* and *Fusarium tricinctum*, are also acknowledged to contribute to FHB (Bottalico and Perrone, 2002; Van der Lee et al., 2015)<sup>37,40</sup>.

The distribution and predominance of the various species associated with FHB depends on the geographic region, the climatic conditions and cultivated cereal species (Leonard and Bushnell, 2003)<sup>12</sup>.

In general, *Fusarium* species prefer humid conditions, i.e. water activity higher than 0.86, and grow well at temperatures around 20–25°C. *Fusarium* species have however different climatic

preferences as regards temperature and water activity ( $a_w$ ) which explains partially their different habitats (table 1).

Table 1. Important food-borne *Fusarium* species, their habitat (cereal related), mycotoxins and physiological characteristics (based on Ulf Thrane, 1999)<sup>41</sup>.

Fusarium species	Habitat	Host	Growth conditions
<i>F. avenaceum</i>	Worldwide	Cereals, peaches, apples, pears, potatoes, peanuts, peas, asparagus, tomatoes	Temperature: -3–31°C ; Min $a_w$ 0.90 at 25°C
<i>F. culmorum</i>	Mainly temperate region	Cereals, potatoes, apples, sugar beet	Temperature: 0–35°C ; Min $a_w$ 0.87 at 25°C
<i>F. equiseti</i>	Worldwide	Cereals and fruits contaminated with soil, vegetables, nuts, spices, UHT-processed juices	Temperature: -3–35°C ; Min $a_w$ 0.92 at 25°C ; Growth at pH 3.3–10.4
<i>F. graminearum</i>	Worldwide	Cereals and grasses	Temperature: 0-35°C ; Min $a_w$ 0.90 at 25°C ; Min pH 2.4 at 30°C ; Max pH 10.2 at 37°C
<i>F. oxysporum</i>	Worldwide	Cereals, peas, beans, nuts, bananas, onions, potatoes, citrus fruits, apples, UHT-processed juices, spices, cheese	Temperature: 5–37°C ; pH range 2.2–9 ; Min $a_w$ 0.89 at 25°C
<i>F. poae</i>	Temperate regions	Cereals, soybeans, sugar cane, rice	Temperature: 2.5–33°C ; Min $a_w$ 0.90 at 25°C
<i>F. proliferatum</i>	Warmer to tropical regions	Corn, rice, figs, fruits	Temperature: 2.5–35°C ; Min $a_w$ 0.92 at 25°C
<i>F. sambucinum</i>	Worldwide	Cereals, potatoes	Temperature: 2–32.5°C
<i>F. solani</i>	Worldwide	Fruits and vegetables, spices	Temperature: up to 37°C ; Min $a_w$ 0.90 at 20°C
<i>F. sporotrichioides</i>	Worldwide	Cereals, pome fruits	Temperature: -2–35°C ; Min $a_w$ 0.88 at 20°C
<i>F. tricinctum</i>	Worldwide	Cereals	Temperature: 0–32.5°C
<i>F. verticillioides</i>	Subtropical and tropical region	Corn, rice, sugarcane, bananas, asparagus, spices, cheese, garlic	Temperature: 2.5–37.5°C ; Min $a_w$ 0.87 at 25°C

Most frequently, different species co-exist at the scale of the region, the plot, the spike and even the kernel (Xu and Nicholson, 2009)<sup>42</sup>. Indeed, FHB is in most cases caused by a mixture of pathogens of the FHB complex, its composition varying according to the year and geographic location (Xu, 2005; Audenaert, 2009; Oerke et al., 2010)<sup>43–45</sup>.

*F. graminearum* is recognized as the leading cause of cereal head blight and ear rot in many North and South American countries, as well as in Southern Europe and Asia. *F. graminearum*, considered as one of the most virulent *Fusarium* species infecting wheat, predominates in warm regions where temperature is at 25 to 28°C prior and during host plant anthesis and rainfall is superior to 195mm (Backhouse and Burgess, 2002)<sup>46</sup>. *F. culmorum* is more tolerant to changing thermal conditions therefore more common in colder regions, although more harmful to cereals at higher temperatures. Series of hot summers in Europe and increased maize production have seen the occurrence of the once predominant species, *F. culmorum*, to be replaced by *F. graminearum* (Parry et al., 1995; Brennan et al., 2003; Nielsen et al., 2012; Valverde-Bogantes et al., 2019)<sup>9,47–49</sup>.

*F. culmorum*, *F. avenaceum* and *F. poae* species usually infect cereals in colder regions. *F. avenaceum* usually occurs in areas with an average annual air temperature of 5–15°C (Bottalico and Perrone, 2002; Xu, 2007; Yli-Mattila, 2010)<sup>40,50,51</sup>.

### 3. *Fusarium* spp. genome and intra/interspecific diversity

The genome sizes within the FGSC range from 34.7 to 37.4 Mb (Kulik et al., 2022)<sup>52</sup>. Intraspecific variation was found ranging from 1,032,686 to 1,955,620 Single Nucleotide Polymorphisms (SNPs) for closely related morphospecies *F. culmorum*, *F. pseudograminearum*, *F. sambucinum* and *F. venenatum* (Kulik et al., 2022)<sup>52</sup>. *F. graminearum* genome (PH-1 reference strain) comprises 36,563,796 bp with a total gene call of 14,164 distributed genes among four chromosomes (King et al., 2015)<sup>53</sup> (Fig. 3). The mitochondrial draft is evaluated at 95,638 bp. Among all the genes, 12,691 are GO (Gene Ontology) annotated or have blast hits, whilst 5,442 genes have no GO annotation (38.4 %).

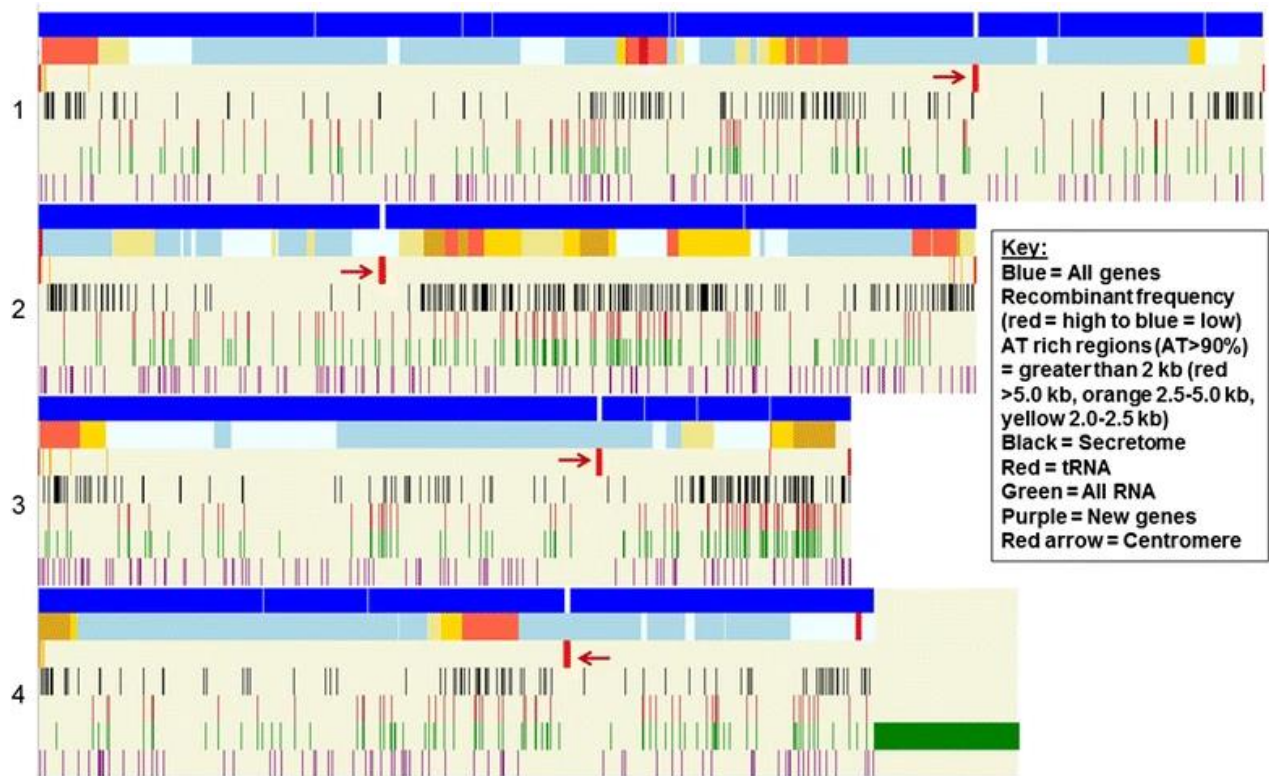


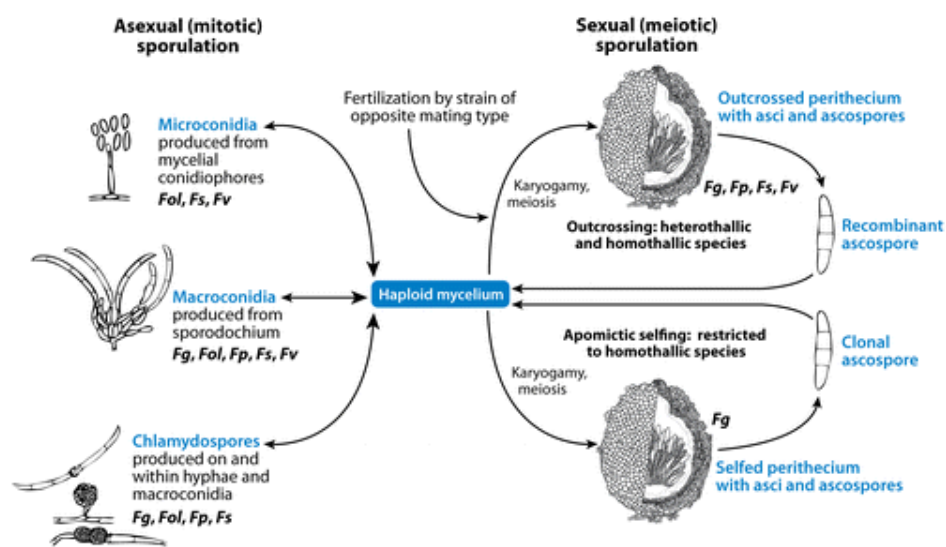
Figure 3. Gene and RNA distribution across the four *Fusarium graminearum*'s chromosomes (Chr 1–4) (R. King et al., 2015).

Fungal genomes are relatively small in comparison to plant and animal genomes, but vary from several to nearly 1,000 Mb (Stajich, 2017)<sup>54</sup>. Inter-strain comparative analysis of *F. graminearum* revealed nearly 21,000 non-redundant sequences and gathered a common base of 9250 conserved core-genes. Intraspecific variation calculated *via* comparison of *F. graminearum* strain genomes ranged from around 86,000 to nearly 158,000 SNPs (Kulik et al., 2022)<sup>52</sup>. Interspecific variation from cryptic species of the FGSC complex ranged from 304,164 to 706,454 SNPs (Kulik et al., 2022)<sup>52</sup>. About 900 secreted protein clusters (SPCs) have been described in *F. graminearum* (Alouane et al., 2021)<sup>55</sup>.

## 4. The life cycle of *Fusarium* spp.

### 4.1. Sexual and asexual life cycle

The life cycle of most *Fusarium* spp. infecting cereals contains sexual and asexual stages with haploid mycelial structures forming in both stages (Goswami and Kistler, 2004; Ma et al., 2013)<sup>56,57</sup>. Among the *Fusarium* species, the life cycle of *F. graminearum* is the most documented. Generally, *Fusarium* spp. is haploid during its life cycle, growing as a colony of hyphae. It spends its asexual cycle on infested crop debris and its sexual cycle on living wheat tissues (Gunupuru et al., 2017)<sup>58</sup>. *Fusarium* species can possess three forms of mitotic (asexual) spores with chlamydoconidia (protective structures) derived from hyphae and macroconidia produced in sporodochium, and microconidia from conidiophores and one form of sexual spores called ascospores, which are produced in ascus (one ascus contains eight ascospores). However, it is important to distinguish the species according to the specificities of their life cycle. *F. graminearum* can produce macroconidia, chlamydoconidia and ascospores but doesn't produce microconidia. *F. solani* can produce each type of spores, *F. oxysporum* cannot produce sexual spores and *F. verticillioides* cannot produce chlamydoconidia (Fig. 4).



Ma L-J, et al. 2013.  
Annu. Rev. Microbiol. 67:399–416

Figure 4. Generalized life cycle of *Fusarium* depicting varying reproduction strategies. Abbreviations Fg, *F. graminearum*; Fol, *F. oxysporum* f. sp. *lycopersici*; Fp, *F. pseudograminearum*; Fs, *F. solani* f. sp. *pisi*; Fv, *F. verticillioides* (Source Ma et al., 2013)<sup>57</sup>.

Ascospores formed within perithecia are wind and rain dispersed and believed to be the primary inoculum of the FHB disease (Trail, 2009; Dweba et al., 2017)<sup>39,59</sup>. Macroconidia develop on infected crop residues under humid conditions and are largely responsible for short-distance dispersion (Deacon 2005)<sup>60</sup>. The sexual lifecycle is triggered by warm, humid, and wet conditions. It is homothallic and dikaryotic, leading to the formation of perithecia containing ascospores (Khan et al., 2020)<sup>61</sup>. Sexual reproduction permits genetic diversity

through genetic exchanges in *F. graminearum* populations via recombination (Lee et al., 2009; Cuomo et al., 2007).

## 4.2. Sexual and asexual transcriptional regulation

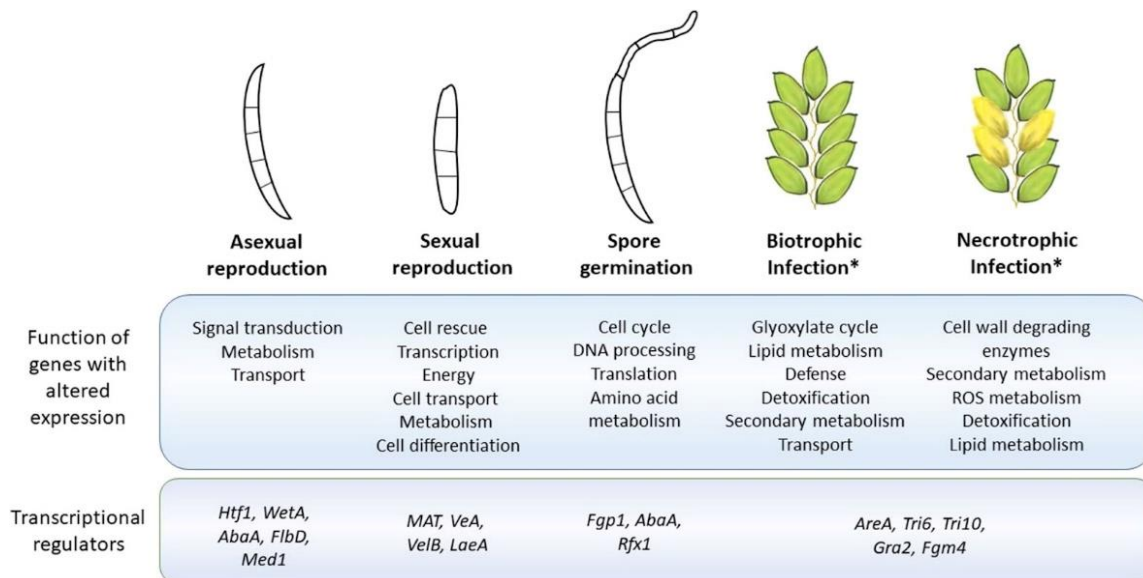


Figure 5. Regulation and Dynamics of Gene Expression During the Life Cycle of *Fusarium graminearum* (Brauer et al., 2020)<sup>62</sup>.

As reviewed by Brauer et al. (2020)<sup>62</sup>, transcriptional profiling revealed that genes specifically associated with sexual development are involved in cell rescue, transcription, metabolism, cell type differentiation, energy, and cell transport (Hallen et al., 2007; Sikhakolli et al., 2012)<sup>63,64</sup> (Fig. 5). The mating type transcription factor genes (MAT) are involved in initiating sexual spore formation (Lee et al., 2003)<sup>6</sup>, the Velvet transcriptional regulators (*VeA* and *VelB*) are important for sexual development (Lee et al., 2012)<sup>65</sup>, *Htf1* gene promotes conidial formation (Zheng et al., 2012)<sup>66</sup>, *WetA* and *AbaA* genes are involved in conidiogenesis (Son et al., 2013, 2014b)<sup>67,68</sup>, *FGP1* promotes rapid and polar germination of conidia (Jonkers et al., 2012)<sup>69</sup> and *RFX1* was also shown to be required for rapid conidial germination (Min et al., 2014)<sup>70</sup> (Fig. 5).

## 4.3. Infection cycle

*Fusarium* spp. live as saprophytes on plant debris or on plant surfaces without causing disease and can turn into pathogens with a rather narrow infection window and a relatively short parasitic period in the case of FHB (Shaner, 2003)<sup>71</sup> (Fig. 6). Most *Fusarium* species are classified as hemibiotrophs: the early infection resembles that of a pathogen that relies on a living host (biotrophic phase), but in the later stage of infections, they become necrotrophic, actively killing host cells and using the contents of dead cells to support their own growth (necrotrophic phase).

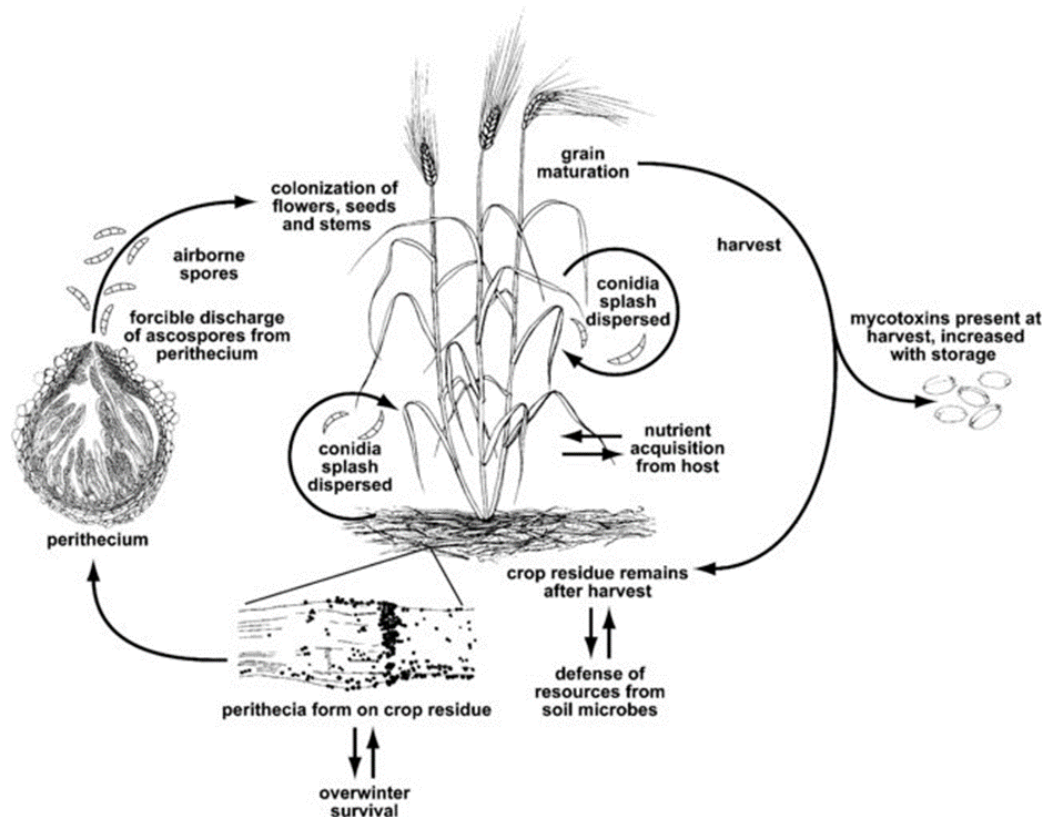
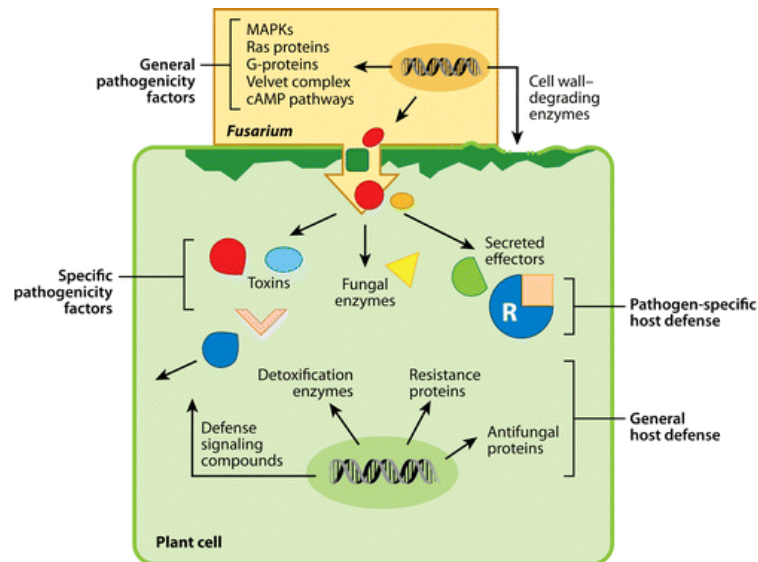


Figure 6. The life cycle of *Fusarium graminearum*, the causal pathogen of *Fusarium* head blight disease of wheat (Trail et al., 2009)<sup>59</sup>.

The infection cycle of *F. graminearum* in wheat starts with the settling of spores on wheat spikelets during anthesis, with germ tube penetrating the plants through wounds or natural openings (Inoue et al., 2002; Rodríguez-Molina, 2003; Hardham, 2001; Mary Wanjiru et al., 2002; Mandeel, 2007)<sup>72–76</sup>. The penetration process is enhanced by enzymes secreted by the pathogen (Walter et al., 2010)<sup>13</sup> (Fig. 7). The intercellular biotrophic infection of *Fusarium* continues with hyphae penetration. This first biotrophic phase is followed by a necrotrophic one during which, hyphae spread within the cell apoplast leading to the appearance of symptoms in the host tissues (Walter et al., 2010; Trail, 2009; Dweba et al., 2017)<sup>13,39,59</sup>. The cellular damages are occurring at the cell wall, mitochondria, chloroplasts, and the membranes (Miller and Ewen 1997)<sup>77</sup>. The mycelia spreading within the host produce conidia which are released. The new spores can either finish to the soil at plant death or be dispersed to new plants by wind or rain.



Ma L-J, et al. 2013.  
 Annu. Rev. Microbiol. 67:399–416

Figure 7. *Fusarium* pathogenicity and host defense mechanisms (Ma et al., 2013)<sup>57</sup>.

## 5. Pathogenicity factors

Most pathogenic *Fusarium* use both general and pathogen-specific mechanisms. General pathogenicity factors include components of cellular signaling pathways, which are often required for proper development, and fungal enzymes used for degradation of the plant cell wall.

Specialized pathogenicity genes are directly involved in host-pathogen interactions. *F. graminearum* genome analysis suggested the presence of small secreted proteins, including possible effector molecules such as small, cysteine-rich, internal amino acid repeat-containing proteins (Brown et al., 2012)<sup>78</sup>. The pathogenicity and virulence factors of *F. graminearum* can be conveniently summed under cell wall–degrading enzymes (CWDEs), toxins, and other pathogenicity and virulence determinants. The pathogenicity and virulence factors were summarized by Rauwane et al in 2020<sup>79</sup>.

Table 2. List of CWDEs in *Fusarium graminearum* (M. Rauwane, et al., 2020)<sup>79</sup>.

Cell Wall Degrading Enzymes	Function
Depolymerase enzyme	Catalyses depolymerization reactions
Pectinase	Breaks down pectin
Cellulase	Breaks down cellulose
Extracellular endoglucanase	Breaks down glucan
Endo-1,4-b-glucanase	Breaks down glucan
Proteolytic enzyme	Breaks down proteins
Xylanolytic enzyme	Breaks down xylan
Lipolytic enzyme	Breaks down lipids

*F. graminearum* produces CWDEs, such as pectinases, amylases, cellulases, xylanases, proteases, and lipases, and other hydrolytic enzymes presumed to be deployed during infection, promoting the penetration and proliferation of the fungal pathogen in the host (Jenczmionka and Schäfer, 2005; Lee et al., 2009)<sup>80,81</sup>. The secreted lipase FGL1 has been reported to contribute to *F. graminearum* virulence on wheat, barley, and maize (Voigt et al., 2005)<sup>82</sup> (table 2).

Specific virulence factors are employed by one or a few related *Fusarium* species and may include host-specific toxins and secreted effectors (Rauwane et al., 2020)<sup>79</sup> (table 3). The MAP kinase Gpmk1 regulates the induction of extracellular endoglucanase, xylanolytic as well as proteolytic activities (Jenczmionka and Schäfer, 2005)<sup>80</sup>.

Table 3. List of pathogenicity and virulence factors of *Fusarium graminearum* (non-CWDEs and non-toxin) (Rauwane, et al., 2020)<sup>79</sup>.

Pathogenicity and virulence determinants	Category/Type/Classification	Function
Gpmk1 MAP kinase	MAP kinase	Involved in mating, conidiation, and pathogenicity
OS-2	Stress activated kinase	Involved in conferring resistance to a soybean phytoalexin
FGL1	Lipase gene	Enhances the fungal pathogenicity against wheat and maize
<i>FgNoxR</i>	A regulatory subunit of NADPH oxidase	Involved in conidiation, sexual development and pathogenicity of <i>F. graminearum</i>
<i>fg2_54</i>	Putative secondary metabolite biosynthesis gene cluster	Responsible for cell-to-cell invasiveness
Protein kinase	Kinase cascade in trichothecene biosynthesis	Involved in trichothecene production
Histidine kinase	Kinase	Involved in trichothecene production
GzSNF1	Serine/threonine-protein kinase	Responsible sexual, asexual development, and virulence
GzXYL1	Endo-1,4-β-xylanase 1 precursor gene	Involved in plant cell wall degradation
GzXYL2	Endo-1,4-β-xylanase 2 precursor gene	Involved in plant cell wall degradation
GzXLP	Extracellular β-xylosidase gene	Involved in depolymerization and plant cell wall degradation
v-SNARE protein	Vesicle related proteins SNARE	Interacts with t-SNARE to catalyze the fusion of the apposing membranes of the transport intermediate and the target compartment
t-SNARE protein	Target membrane-related SNARE	Interacts with v-SNARE to catalyze the fusion of the apposing membranes of the transport intermediate and the target compartment
Syntaxin-like t-SNARE protein	Syntaxin-like membrane-integrated protein	Required for vegetative growth, sexual reproduction, and virulence. Proteins are also encoded by GzSYN1 and GzSYN2 in <i>F. graminearum</i> that enhanced virulence of the fungus on barley
GzSYN1	Syntaxin-like SNARE gene	Enhances perithecia and radial hyphal growth
GzSYN2	Syntaxin-like SNARE gene	Enhances perithecia and radial hyphal growth
Multiple ATP-binding cassette transporter	Major facilitator superfamily of membrane transporter	Involved in virulence
FgABCC9	ATP-binding cassette transporter gene	Involved in the fungal pathogenicity towards wheat
FGRAMPH1_01G16085	Gene-encoding polyketide synthase PKS2	Responsible for mycelial growth and fungal virulence
PKS2	Polyketide synthase gene	Responsible for secondary metabolism and virulence
presilphiperfolan-8-beta-ol synthase	Terpene synthase-encoding gene	Involved in the virulence of the fungus
transcription factor ZC116	Terpene synthase-encoding gene	Involved in the virulence of the fungus
trichodiene oxygenase	Putative cytochrome P450 gene	Responsible for the expression of disease in fungus-infected cereals
Cytochrome P450 4F12	Putative cytochrome P450 gene	Responsible for the expression of disease in fungus-infected cereals
ent-kaurene oxidase	Putative cytochrome P450 gene	Responsible for the expression of disease in fungus-infected cereals
ZIF1	Encodes bZIP transcription factor	Involved in virulence and reproduction ability of <i>F. graminearum</i>
bZIP transcription factor	Transcription factor	Enhances the virulence of <i>F. graminearum</i> in infected plants
TOP11	Enzyme	Involved in sporulation and pathogenicity
FGRAMPH1_01G07179	Conserved hypothetical protein	Involved in growth and virulence
Zn(II)2Cys6-type transcription factor	Transcription factor	Regulates fungal reproduction and pathogenicity

In *F. graminearum*, there is an association between the mycotoxin biosynthesis and the colonization of host tissues in wheat (Jansen et al., 2005; Ilgen et al., 2008)<sup>83,84</sup>. In the plant, genes for the mycotoxin deoxynivalenol (DON) biosynthesis are expressed at the beginning of infection by the fungus (Schwarz et al., 2002; Jansen et al., 2005; Maier et al., 2006; Proctor

et al., 1995)<sup>83,85–87</sup>. In wheat, DON is not essential for the initial infection of *F. graminearum* but plays a critical role in the spreading of infectious growth (Boddu et al., 2007)<sup>88</sup>.

## 6. Mycotoxins produced by *Fusarium* species

Mycotoxins are secondary metabolites produced by filamentous fungi that are capable of causing disease and death in humans and livestock. Three main fungal genera are responsible for the contamination of food and feed with mycotoxin: *Aspergillus*, *Penicillium*, and *Fusarium* (table 4). For the cereal sector, the risk associated with *Claviceps* species that can produce ergot alkaloids should also not be overlooked.

The consumption of food contaminated with mycotoxins can cause symptoms such as headache, food poisoning, abdominal pain, and diarrhea in humans as well as emaciation in animals (Wegulo 2012; Uzma et al., 2018)<sup>89,90</sup>. Furthermore, they can be mutagenic, teratogenic and oestrogenic.

Table 4. Major mycotoxins and associated US and EU limits in food (Alshannaq and Yu, 2017)<sup>91</sup>.

Mycotoxin	Fungal species	Food commodity	US FDA (µg/kg)	EU (EC 2006) (µg/kg)
Aflatoxins B1, B2, G1, G2	<i>Aspergillus flavus</i> , <i>Aspergillus parasiticus</i>	Maize, wheat, rice, peanut, sorghum, pistachio, almond, ground nuts, tree nuts, figs, cottonseed, spices	20 for total	2-12 for B1, 4-15 for total
Aflatoxin M1	Metabolite of aflatoxin B1	Milk, milk products	0.5	0.05 in milk, 0.025 in infant formulae and infant milk
Ochratoxin A	<i>Aspergillus ochraceus</i> <i>Penicillium verrucosum</i> <i>Aspergillus carbonarius</i>	Cereals, dried vine fruit, wine, grapes, coffee, cocoa, cheese	Not set	2-10
Fumonins B1, B2, B3	<i>Fusarium verticillioides</i> <i>Fusarium proliferatum</i>	Maize, maize products, sorghum, asparagus	2000-4000	200-1000
Zearalenone	<i>Fusarium graminearum</i> <i>Fusarium culmorum</i>	Cereals, cereal products, maize, wheat, barley	Not set	20-100
Deoxynivalenol	<i>Fusarium graminearum</i> <i>Fusarium culmorum</i>	Cereals, cereals products	1000	200-50
Patulin	<i>Penicillium expansum</i>	Apples, apple juice and concentrate	50	10-50

Numerous mycotoxins are regulated in many countries worldwide including the European Union (EU) and the United States. For each mycotoxin, the maximal authorized limits are different according to the country, the cereal grain and the derived product. Non-compliance with the thresholds leads to exclusion of agricultural crops, feed and food products from commercial trade (European Commission. Commission regulation (EU) 1881/2006 of 19 December 2006 setting maximum levels for certain contaminants in foodstuffs. Off. J. Eur. Union. 2006, 364, 5–24.)<sup>92</sup>. In contrast to human food, excepting for the aflatoxins (AF), there are no limits but only recommendations addressing the presence of mycotoxins in animal feed.

Fusariotoxins are mycotoxins produced by certain species of the *Fusarium* genus. Three fusariotoxin families are particularly important because of their well-documented and

acknowledged toxicity and their frequent occurrence in European agricultural products: (i) type A and type B trichothecenes (TCTA and TCTB) that are mainly T-2 and HT2 toxins, deoxynivalenol (DON) and its acetylated derivatives (15 and 3 ADON), nivalenol (NIV) and its acetylated derivative fusarenon X (FX), (ii) fumonisins (FUM), and (iii) zearalenone (ZEA) (Fig. 8). Moreover, several *Fusarium* species can produce the beauvericin (BEA), enniatins (ENNs), and moniliformin (MON) that belong to the family of emerging mycotoxins (Jestoi 2008). In the following, we will focus principally on the most economically important groups of fusariotoxins for the wheat cereal sector and/or on the most frequently occurring ones. These include the TCTA and TCTB, ZEA, BEA and ENNs.

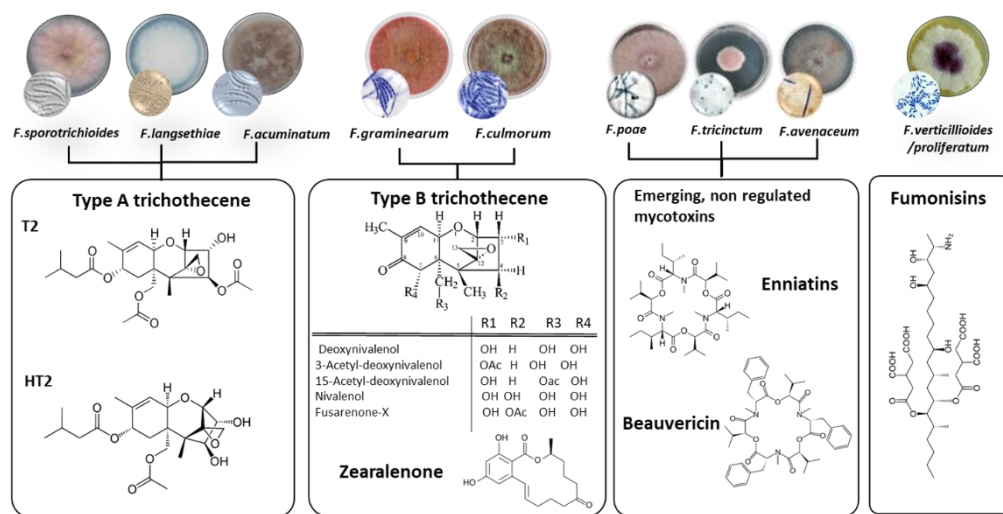


Figure 8. Major *Fusarium* species and their fusariotoxins (MycSA laboratory, 2022).

## 6.1. Trichothecenes (TCTs)

TCTs are produced by several genera of fungi, including *Trichoderma*, *Stachybotrys*, *Cephalosporium*, and *Fusarium* (McCormick et al., 2011)<sup>93</sup>. TCTs include more than 200 analogs and are the largest and most economically important group of fusariotoxins associated with human and livestock mycotoxicosis. All TCTs contain the same central skeleton. They are sesquiterpenoids with a tetracyclic ring system; the presence of an epoxide linked to carbon 12 confers their toxicity (Bennett and Klich, 2003)<sup>94</sup>. TCTs are divided into four groups - types A, B, C and D - based on substitution patterns of oxygen containing functional groups at various possible sites on carbons 3, 4, 7, 8, and 15, hydrogen (-H), hydroxyl (-OH), ester-linked acetyl (-OC(=O)CH<sub>3</sub>) or ester-linked isovalerate (-OC(=O)CH<sub>2</sub>CH(CH<sub>3</sub>)<sub>2</sub>) groups (McCormick et al., 2011)<sup>93</sup> (Fig. 9).

*Fusarium* spp. can produce Type A (TCTA) and Type B (TCTB) TCTs, which have respectively a hydroxyl or ester substitution or no oxygen atom at C-8, and have a keto (carbonyl) group at C-8.

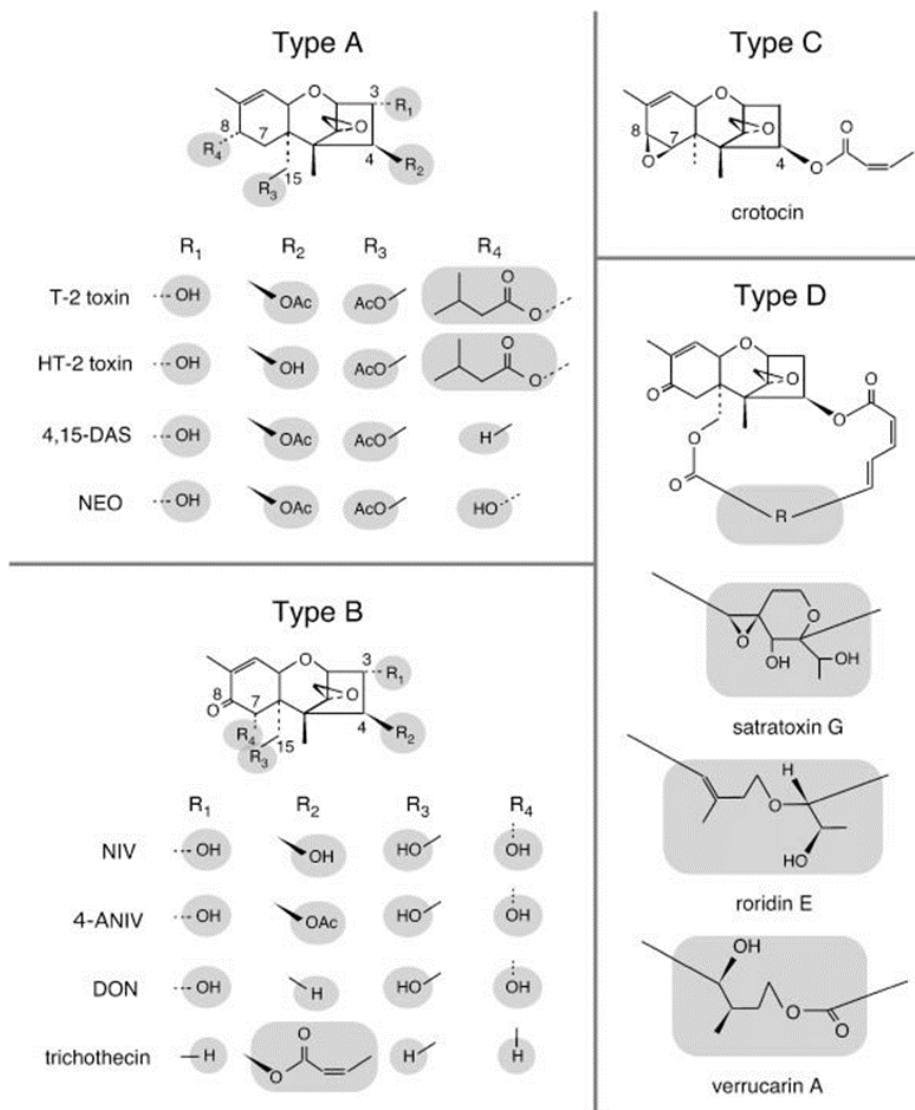
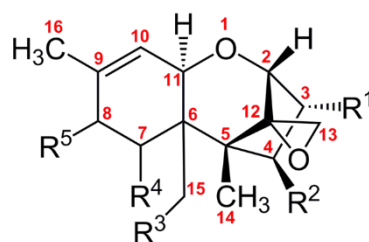


Figure 9. Chemical Structure of Type A, Type B, Type C, and Type D Trichothecenes (Kimura et al., 2007)<sup>95</sup>.

TCTA were reported as less phytotoxic than TCTB (Eudes et al., 2000, Steinmetz et al., 2009)<sup>96,97</sup>, more toxic in mammals than TCTB (Trusal and O'Brien, 1986; Minervini et al., 2004)<sup>98,99</sup>, but are produced at lower levels compared to TCTB. TCTs are small, amphipathic molecules that move across cell membranes, inhibit protein synthesis in eukaryotes, preventing peptide formation in the ribosome, reducing mitochondrial protein synthesis and inactivating thiol-enzymes (Carrasco et al., 1973; Cundliffe et al., 1974; Ueno and Matsumoto, 1975; Cundliffe and Davies, 1977; Pace et al., 1988)<sup>100-104</sup>.

### 6.1.1. Type A trichothecenes (TCTA)

TCTA include the following toxins: T-2, HT-2, trichodermol, trichodermin, diacetoxyscirpenol (DAS) as well as NX-2 and NX-3 (Fig. 10).



TCTA	R1	R2	R3	R4	R5
T-2 toxin (T-2)	OH	OAc	OAc	H	OCOCH <sub>2</sub> CH(CH <sub>3</sub> ) <sub>2</sub>
HT-2 toxin (HT-2)	OH	OH	OAc	H	OCOCH <sub>2</sub> CH(CH <sub>3</sub> ) <sub>2</sub>
Diacetoxyscirpenol (DAS)	OH	OAc	OAc	H	H
Trichodermol	H	OH	H	H	H
Trichodermin	H	OCH <sub>2</sub> =OCH <sub>3</sub>	H	H	H
NX-2	OAc	H	OH	OH	H
NX-3	OH	H	OH	OH	H

Figure 10. Structure of TCTA mycotoxins.

T-2 toxin and its deacetylated derivative HT-2 toxin are TCTA produced by some members of the FSAMSC, such as *F. langsethiae*, *F. sporotrichioides* and *F. poae*. Those species are more frequently isolated from oat and barley than from wheat and mainly occur in northern regions of Europe (SCOOP report, 2003; Edwards et al., 2009)<sup>105,106</sup>.

The T-2 toxin is an inhibitor of protein synthesis and mitochondrial function (JG Pace et al., 1988), shows immunosuppressive and cytotoxic effects and has a local irritant effect, can cause ulceration and necrosis in the digestive tract as well as alterations in the kidneys, heart, brain, and peripheral ganglia (SCOOP report, 2003; Edwards et al., 2009)<sup>105,106</sup>.

The estimates of chronic dietary exposure to the sum of T-2 and HT-2 ranged from 0.3 to 210 ng/kg bw per day. The Joint FAO/WHO Expert Committee on Food Additives (JECFA) Committee established a group tolerable daily intake (TDI) of 25 ng/kg bw for T-2, HT-2 and DAS, alone or in combination, and a group acute reference dose (ARfD) for T-2, HT-2 and DAS of 320 ng/kg bw (JECFA, 2022)<sup>107</sup>.

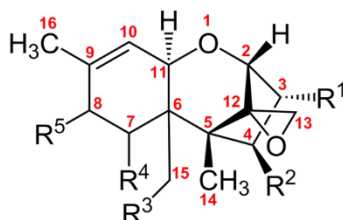
Diacetoxyscirpenol (DAS) and T-2 are produced by the same species, including *F. sporotrichioides* and *F. poae*, and are causing similar toxic effects. DAS is not of major economic importance although it can be toxic to food-producing animals (Hoerr et al., 1981)<sup>108</sup>.

Trichodermin is a trichothecene produced by species of the genera *Trichoderma*. It possesses inhibitory effects on some phytopathogenic fungi and phytotoxicity (Tijerino et al., 2011; Shentu et al., 2014)<sup>109,110</sup>. Trichodermol is the biosynthetic precursor of trichodermin.

NX toxins (1-6) are toxins produced by strain from the FGSC complex recently identified in the United States and Canada (Liang et al., 2014; Varga et al., 2015, Kelly et al., 2016)<sup>111-113</sup>. NX-2, and its deacetylated form NX-3, are very similar to 3-ADON and DON, but missed the keto-group at C-8 position. They are phytotoxic (Wipfler et al., 2019)<sup>114</sup>, induce oxidative stress (Woelflingseder et al., 2020)<sup>115</sup>, can inhibit eukaryotic protein synthesis (Varga et al., 2015, 2018)<sup>112,116</sup> and modulate inflammatory and immune response (Pierron et al., 2022)<sup>117</sup>.

### 6.1.2. Type B trichothecenes (TCTB)

TCTB include the following toxins: Deoxynivalenol (DON) and its acetylated forms 3-acetyl and 15-acetyl DON (3-ADON and 15-ADON), nivalenol (NIV) and its acetylated form fusarenol X (FX). In addition, two TCTBs less frequently observed in grains have been reported: 4-acetyl nivalenol (4-ANIV) and trichotecin (Fig. 11).



TCTB	R1	R2	R3	R4	R5
Deoxynivalenol (DON)	OH	H	OH	OH	=O
3-Acetyldeoxynivalenol (3-ADON)	OAc	H	OH	OH	=O
15-Acetyldeoxynivalenol (15-ADON)	OH	H	OAc	OH	=O
Nivalenol (NIV)	OH	OH	OH	OH	=O
4-Acetyl nivalenol (4-ANIV)	OH	OH	OH	OAc	=O
Fusarenol X (FX)	OH	OAc	OH	OH	=O
Trichotecin	H	OCOCH=HCHCH3	H	H	=O

Figure 31. Structure of TCTB mycotoxins.

TCTB are produced by species members of the FGSC complex including *F. graminearum*, *F. culmorum* and *F. asiaticum*, among others. Within TCTB producing species, strains can produce only one toxin and one associated acetylated form, which defines their chemotype. The following chemotypes were distinguished in *Fusarium* spp. based on the profile of produced mycotoxins: DON chemotype for strains producing DON and its acetyl derivatives and NIV chemotype for strains producing NIV and/or FX. Within DON chemotypes, the DON/3-ADON and DON/15-ADON are distinguished.

#### 6.1.2.1. Chemotype distribution

The species members of the FGSC complex and their chemotypes, DON/3-ADON, DON/15-ADON or NIV/FX producing populations are differentially distributed among the world. In western European countries, including England, France and Italy, the dominance of *F. graminearum* was observed, with predominant DON-15ADON populations but some NIV/FX types can also be observed (Jennings et al., 2004; Prodi et al., 2011; Somma et al., 2014; Boutigny et al., 2014)<sup>118–121</sup> (Fig. 12).

*F. culmorum* was the main cause of FHB in the Netherlands before the year 2000, but appears to be replaced by *F. graminearum* (Waalwijk et al., 2003)<sup>122</sup>. In Finland as well as in the

northern part of Russia exclusively the 3-ADON chemotype of *F. graminearum* was observed (Yli-Mattila et al., 2009)<sup>123</sup>. In contrast, in the southern part of Russia only 15-ADON isolates were encountered (Yli-Mattila et al., 2009)<sup>123</sup>.

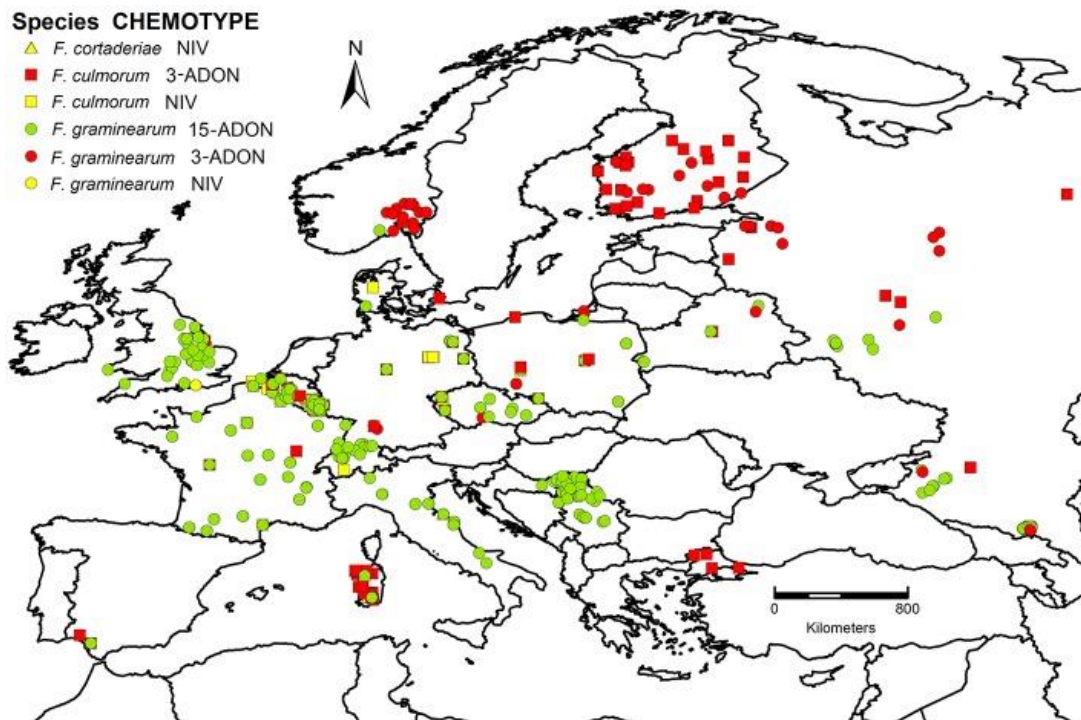


Figure 42. Spatial distribution of chemotypes and *Fusarium* species in Europe (Pasquali et al., 2016)<sup>38</sup>.

Concerning the chemotypes, DON/15-ADON is one of the most widespread and dominant *F. graminearum* chemotypes (Boutigny et al., 2012)<sup>124</sup>. The 15-ADON type dominates in North America, Central Europe, Southern Russia, and South America and the 3-ADON type dominates in Northern Europe, China, Australia, New Zealand and Korea (Van der Lee et al., 2015; Yli-Mattila et al., 2009)<sup>37,123</sup>. In Canada and the United States of America, a significant increase in the 3-ADON type over the 15-ADON has been observed in recent years (Gale et al., 2011; Guo et al., 2008, Puri and Zhong, 2010; Ward et al., 2008)<sup>125–128</sup>. This shift, from 1980 to 2008, has been related to the high aggressiveness of strains from the 3-ADON chemotype (Puri and Zhong, 2010)<sup>127</sup>. Strains of the NIV chemotype have been isolated in China, Japan and other Asian countries and less frequently in Europe, South Africa and the Americas (Gale et al., 2011; Suga et al., 2008; Van der Lee et al., 2015; Zhang et al., 2012)<sup>37,125,129,130</sup>.

In Japan, harvests from the north are mainly contaminated 15-ADON producing strains, while NIV and DON/3-ADON were the chemotypes isolated in the south (Yoshizawa and Jin, 1995; Suga et al., 2008)<sup>129,131</sup>. Diverse FGSC populations were observed in China, the gradient of NIV versus DON chemotypes along the Yangtze River was suggested to have been caused by a shift in the population (Yang et al., 2008)<sup>132</sup>. In Canada a migration event was reported, where 3ADON-producing *F. graminearum* was reported to replace 15-ADON-producing *F. graminearum* (Ward et al., 2008)<sup>128</sup>. In Argentina, the main causal pathogen appears to be *F. graminearum* of the 15-ADON chemotype (Reynoso et al., 2011; Castañares et al., 2014;

Malbrán et al., 2014)<sup>133–135</sup>. The same results were obtained in Southern Brazil (Scoz et al., 2009; Astolfi et al., 2011)<sup>136,137</sup>. Interestingly, NIV producers were also identified (Scoz et al., 2009; Sampietro et al., 2010, 2011; Umpiérrez-Failache et al., 2013)<sup>136,138,139</sup>. In south-Africa, more than 85% of the isolates from wheat or barley were *F. graminearum* with the 15-ADON chemotype (Boutigny et al., 2012)<sup>124</sup>.

In contrast to *F. graminearum*, *F. culmorum*'s worldwide dominant chemotype is DON/3-ADON (Quarta et al., 2006; Kammoun et al., 2010; Tok and Arslan, 2016)<sup>140–142</sup>.

#### 6.1.2.2. DON, 3-ADON and 15-ADON

DON, also known as vomitoxin, is one of the most commonly occurring trichothecenes produced by *F. graminearum* and *F. culmorum* in cereals such as wheat, barley, oat, and corn, and cereal-derived food products. It commonly prevails in all regions, with a 59% average incidence rate, ranging from 50% in Asia to 76% in Africa, but tends to occur at higher concentrations in Europe and Asia from 1990 to now (Chen et al., 2019)<sup>143</sup>. A report from the European Food Safety Authority (EFSA) published in 2013 indicated that DON was found in half of 18 884 tested samples of food, feed and unprocessed grains collected in 21 European countries between 2007 and 2012, with less than 2% exceeding the maximum limits (EFSA 2013)<sup>144</sup>.

DON is an inhibitor of ribosomal protein synthesis, which explains its high toxicity for humans and animals. Both acute and chronic toxicity due to ingestion of DON are reported. Acute symptoms include abdominal discomfort, diarrhea, vomiting, anorexia, a deregulation of the immune system and a teratogenic effect (Pestka, 2010; Reddy et al., 2010)<sup>145,146</sup>. Chronic consumption of DON causes weight loss, anorexia, and decreased nutritional efficiency.

DON and its acetylated form 15-ADON seems to possess an equivalent toxicity, but the acetylated variant 3-ADON was reported as more toxic (Alassane-Kpembé et al., 2013)<sup>147</sup>.

During wheat-based food processing, only a small amount of degradation of DON (less than 20%) is observed in most studies (Feizollahi & Roopesh, 2021; Wu, et al., 2017)<sup>148,149</sup>.

The JECFA established a group provisional maximum tolerable daily intake (PMTDI) 1 µg/kg bw/d for DON and its acetylated variants, alone or in combination, and a group ARfD of 8µg/kg bw (JECFA, 2011)<sup>150</sup>. The No observed effect level (NOEL) is set at 0.25 mg/kg bw in the diet.

#### 6.1.2.3. NIV and FX

NIV is produced by members of the *F. sambucinum* species complex, including *F. poae*, some strains of *F. culmorum* and *F. graminearum*, and some members of the *F. incarnatum-equiseti* species complex (FIESC). NIV can contaminate kernels from various types of cereals including wheat, maize, barley, oats, and rye. NIV inhibits ribosomal protein synthesis and can deregulate the immune system (Ueno et al., 1968)<sup>151</sup>. NIV is more toxic than DON and its acetylated form, FX, is even more so (Eriksen et al., 2004; Alassane-Kpembé et al., 2013)<sup>147,152</sup>.

### 6.1.3. Biosynthesis and regulations of the TCTs production

#### 6.1.3.1. The Tri genes

Nearly all the genes (called *Tri* genes) implicated in the biosynthetic pathway of the different TCTBs have been identified (Alexander et al., 2009)<sup>153</sup> (Fig. 13).

The trichothecenes are secondary metabolites encoded by genes arranged in a core Biosynthesis Gene Cluster (BGC) called the “Tri 5 cluster” comprising 12 genes, associated with two genes in the “Two genes cluster” and one isolated gene (Alexander et al., 2009)<sup>153</sup>. The “Tri 5 cluster” consists of the following genes: *Tri3* encoding a C-15 acetyltransferase, *Tri4* encoding a cytochrome P450 oxygenase for hydroxylation at C-2, *Tri5* encoding a trichodiene synthase, the *Tri6* regulatory gene, *Tri7* encoding a C-4 acetyltransferase, *Tri8* encoding a C-3 or C-15 esterase, *Tri9* gene with an unknown function, the *Tri10* regulatory gene, *Tri11* encoding a cytochrome P450 oxygenase responsible for hydroxylation at C-15, the *Tri12* trichothecene efflux pump, *Tri13* encoding a C-4 hydroxylase and the *Tri14* gene with an unknown function (Alexander et al., 2009)<sup>153</sup>. The *Tri1* gene encoding a cytochrome P450 oxygenase, the *Tri16* gene encoding a C-8 acyltransferase and the *Tri101* gene encoding a 3-O-acetyltransferase are outside of the “Tri 5 cluster”.

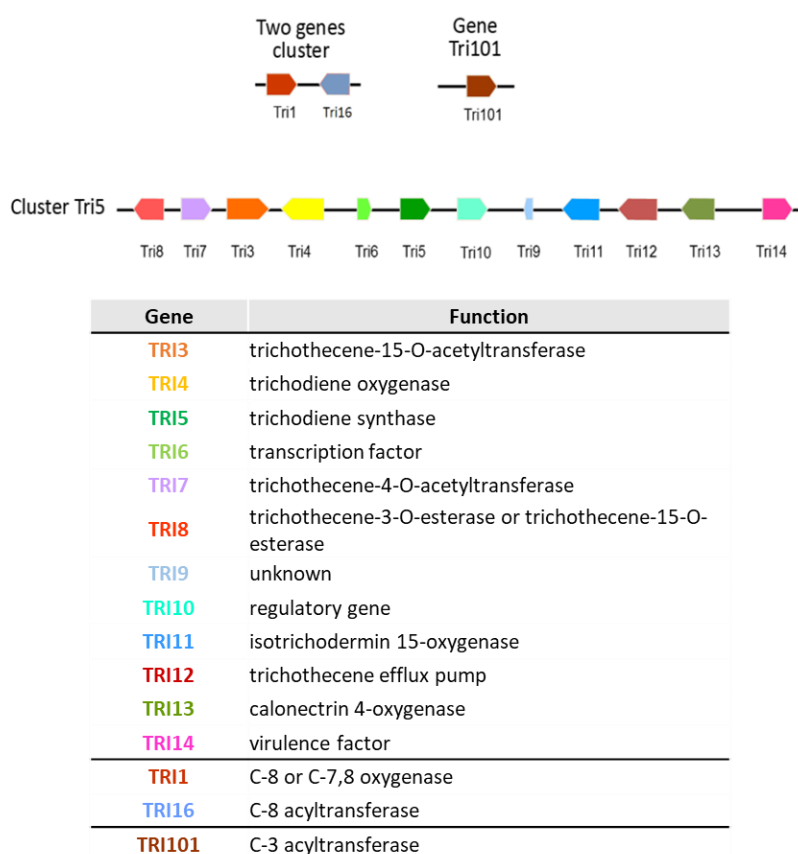


Figure 53. Gene clusters involved in trichothecene biosynthetic pathway in *Fusarium*, including a *Tri* cluster containing 12 genes, a two-gene *Tri1-Tri16* cluster and a single gene *Tri101* (adapted from Chen, 2019)<sup>154</sup>.

The chemotypes are determined genetically through the polymorphism of some *Tri* genes (Fig. 14). In particular, the esterase encoded by *Tri8* has been reported as the determinant factor of the DON/3-ADON or DON/15-ADON chemotype. TRI8 of strains of the DON/15-ADON chemotype was shown to catalyse the C-3 deacetylation of 3,15-diADON to yield 15-ADON whereas TRI8 from strains of the DON/3-ADON chemotype catalyzes the C-5 deacetylation of 3,15-diADON (Alexander et al., 2011)<sup>155</sup>. *Tri7* encoding a C-4 acetyltransferase and *Tri13* encoding a C-4 hydroxylase are only functional in the NIV/FX chemotype; in DON/ADON chemotypes, several insertions and deletions have been evidenced in their sequence (Lee et al., 2002; Villafana et al., 2019)<sup>156,157</sup>.

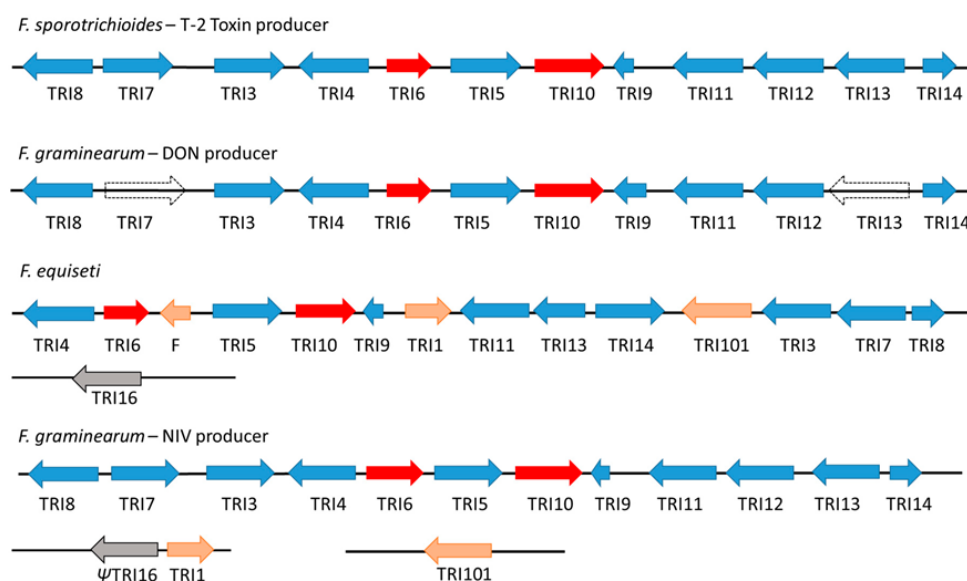


Figure 64. Comparison of the proposed trichothecene biosynthetic gene cluster of *Fusarium sporotrichioides*, *F. graminearum*, and *F. equiseti* (Villafana et al., 2019)<sup>157</sup>.

### 6.1.3.2. TCT biosynthetic pathway

The trichothecene biosynthetic pathway is well elucidated (Fig. 15). It begins with the cyclization of farnesyl pyrophosphate, derived from the metabolism of isoprenoids, into trichodiene; this first step being catalyzed by a trichodiene synthase called TRI5. This first step is followed by four reactions catalyzed by a trichodiene oxygenase called TRI4: (i) transformation of trichodiene into 2-hydroxytrichodiene by hydroxylation on carbon C2, (ii) C-12,13 epoxidation of 2-hydroxytrichodiene to lead 12-13-epoxy-9,10-trichoene-2-ol, (iii) addition of a hydroxyl group on C11 to form isotrichodiol and (iv) finally hydroxylation on C3 to yield isotrichotriol. The cyclization of isotrichotriol to isotrichodermol undergoes a transient intermediate form as trichotriol (Kimura et al., 2007). The TRI101 C3-acyltransferase catalyzes the substitution of the hydroxyl group on C3 by an acetyl group. 15-decalonectrin is formed by an oxygenation of the methyl group on C6 of the isotrichodermin catalyzed by the TRI11 isotrichodermin 15-oxygenase. Then 15-decalonectrin is modified into calonectrin through the transfer of an acetyl group to the lastly formed alcohol group; this reaction being catalyzed by

the enzyme TRI3 trichothecene-15-O-acetyltransferase (Alexander et al., 2009; Kimura et al., 2007; McCormick et al., 2011)<sup>93,95,153</sup>. The steps following the formation of calonectrin determine the differentiation between species producing TCTA and TCTB.

The TRI13 trichothecene-15-O-acetyltransferase, responsible for the formation of 3,15-diacetoxyscirpenol from calonectrin, is involved in production of NIV; disruption of *Tri13* gene was evidenced in DON-producing chemotypes (Lee et al., 2002)<sup>156</sup>. The C4 of 3-15-diacetoxyscirpenol can be oxygenated, with a reaction catalyzed by TRI7 trichothecene-4-O-acetyltransferase, forming 3,4-15-diacetoxyscirpenol.

The differentiation between TCTA and TCTB producing species is related to functional divergence of the monooxygenase enzymes encoded by the *Tri1* gene homologs. The C-8 oxygenase occurring in TCTA-producing, encoded by the *fsTri1* homolog, permits the addition of a hydroxyl group on C8 of 3,4,15-triacetoxyscirpenol to form 3-acetylneosolaniol. This step is followed by two reactions successively catalyzed by the fsTRI16 C-8 acyltransferase and TRI8 trichothecene-3-O-esterase to obtain T-2 toxin.

In the case of TCTB producing species, C-7,8 oxygenase coded by the *fgTri1* homolog catalyzes the formation of 3,15-acetyldeoxynivalenol from 7,8-dihydroxycalonectrin for DON and NIV producing species or 7,8-dihydroxy-TAS from 3,4,5-triacetoxyscirpenol only in NIV producing species. NIV precursor is either 3,15-acetyldeoxynivalenol or 7,8-dihydroxy-triacetoxyscirpenol modified until obtaining 3,4,15-triANIV.

In the case of DON producing species, the precursor is 3,15-acetyldeoxynivalenol. The differential activity of the esterase enzyme encoded by *Tri8*, trichothecene-3-O-esterase or trichothecene-15-O-esterase, determines respectively the 3-ADON and 15-ADON chemotypes in *F. graminearum* (Alexander et al., 2009; McCormick et al., 2011)<sup>93,153</sup>.

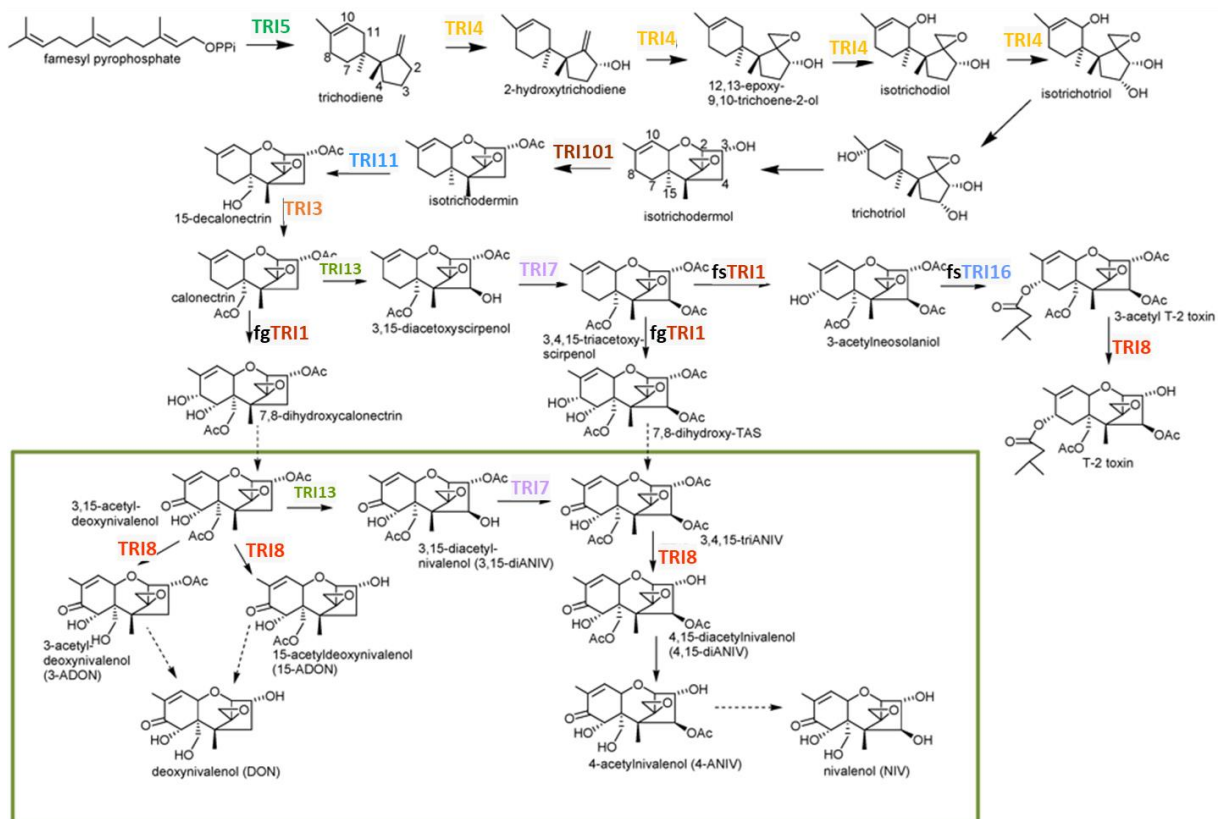


Figure 75. Proposed trichothecene biosynthetic pathway. Genes encoding an enzymatic step are identified near the arrow indicating the step. Dashed arrows indicate steps for which a gene has not been assigned. Green box identifies Type B trichothecenes (adapted from McCormick et al., 2011)<sup>93</sup>.

### 6.1.3.3. Regulation of the TCTBs biosynthesis

#### 6.1.3.3.1. The production of DON is tightly controlled by environmental factors

Various factors related to the environment have been shown to impact (positively or negatively) the production of DON by *F. graminearum* and/or *F. culmorum*. The most documented knowledge is gathered on Figure 17. Water activity ( $a_w$ ), temperature and their interactions are acknowledged to modulate the production of DON and its acetylated forms (Ramírez Albuquerque et al., 2021; 2022)<sup>158,159</sup>. The nature of the substrate is a primary determinant. Sources of carbon and/or nitrogen have been evidenced to influence the levels of TCTB produced by *F. graminearum* (Jiao et al., 2008; Chen et al., 2011; Giese et al., 2013)<sup>160–162</sup>. For instance, the production of toxins was reported to be enhanced when glucose is replaced by sucrose (Jiao et al., 2008)<sup>160</sup>. Regarding the nitrogen source, Gardiner et al. (2009, 2010)<sup>163</sup> have shown that amino acids associated with the polyamine biosynthetic pathway, such as agmatine or putrescine, were inducers of the production of DON. PH or more precisely pH changes is also a key factor influencing DON production. An acidification of the extracellular pH was shown to result in an increased *Tri* gene expression resulting in a higher TCTB production (Gardiner et al., 2009, Merhej et al., 2010; 2011)<sup>164–166</sup>. Variation in pH leading to non-acid environments surrounding *F. graminearum* hyphae induces a repression

of the *Tri* gene expression (Merhej et al., 2010)<sup>165</sup>. As for many fungal secondary metabolites, light can regulate the production of TCTB in *F. graminearum* (Merhej et al., 2012)<sup>167</sup>. The impact of an oxidative stress was widely investigated and it has been demonstrated that a peroxide stress enhanced the production of TCTB (Ponts et al., 2007; Montibus et al., 2013)<sup>168,169</sup>. This result is particularly important when dealing with plant-pathogen interactions since production of reactive oxygen species (ROS) including hydrogen peroxide (H<sub>2</sub>O<sub>2</sub>) is one of the first response of plant triggered by *F. graminearum* infection (Audenaert et al., 2010)<sup>170</sup>.

Besides, as reviewed by Richard-Forget et al. (2021)<sup>171</sup>, metabolomics analysis has allowed demonstrating the interdependence between the biosynthetic pathway of TCTB and several primary and specialized metabolic pathways. Actually, several metabolomics reports have shown the strong link between DON production and primary metabolism including amino acid and fatty acid pools, carbon flux and energy turnover, carbon and nitrogen metabolism and sugar metabolism (Lowe et al., 2010; Panagiotou et al., 2005; Chen et al., 2011; Smith et al., 2012; Atanasova-Penichon et al., 2018; Liu et al., 2019)<sup>161,172–176</sup>.

Farnesyl-pyrophosphate, which is the precursor of the TCTB production, results from the metabolization of acetyl coenzyme A (Acetyl-CoA), a compound which is an intermediate in various primary metabolic pathways, including glycolysis, fatty acid degradation through  $\beta$ -oxidation, protein degradation and tricarboxylic acid cycle (TCA cycle) (Fig. 15).

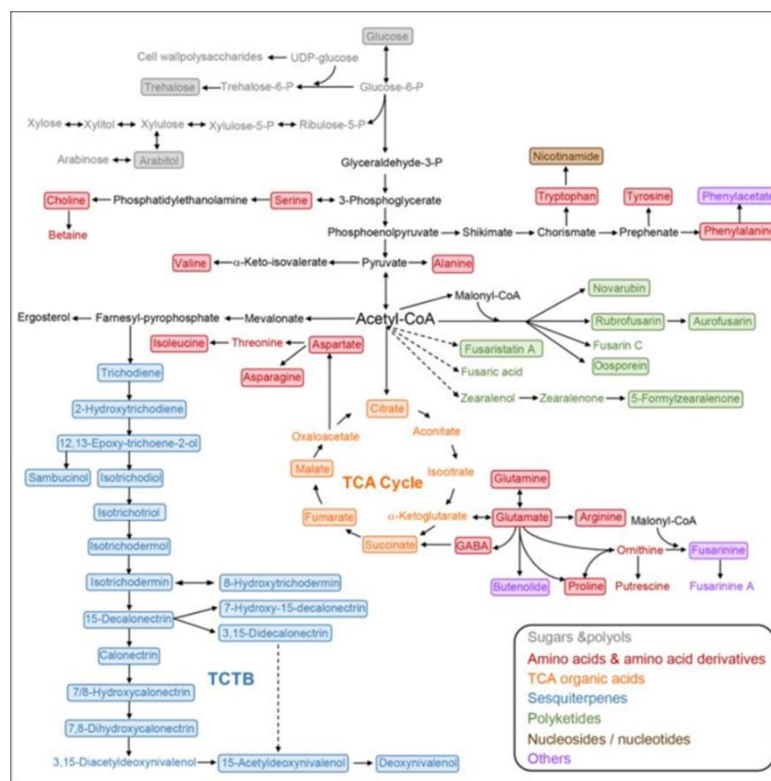


Figure 86. Overview of metabolic pathways, indicating the relationship between the production of TCTB by *F. graminearum* and other primary and secondary metabolic pathways (Atanasova-Penichon et al., 2018)<sup>175</sup>.

Thus, every external factor that will influence the development of *F. graminearum* could theoretically affect the production of DON by modifying the metabolic balance.

#### 6.1.3.3.2. Regulation of DON yield involves multiscale mechanisms

Regulation of DON biosynthesis operates at different levels including pathway specific and global regulators, signal transduction pathways and chromatin-mediated regulation.

##### 6.1.3.3.2.1. Specific transcription factors

In the TRI gene cluster, *Tri6* and *Tri10* have been identified as positive specific regulator genes of the trichothecene biosynthetic pathway in *F. graminearum*. *Tri6*, encoding a transcription factor, positively regulates the expression of *Tri* genes (Tag et al., 2001; Seong et al., 2009)<sup>177,178</sup>. *Tri6* autoregulates its own expression under nutrient-rich conditions (Seong et al., 2009; Nasmith et al., 2011)<sup>178,179</sup>. *Tri10* encodes a protein without any known functional domains but acts as an essential regulatory gene in trichothecene biosynthesis (Tag et al., 2001)<sup>177</sup>. In *F. sporotrichioides*, *Tri10* was suggested to act upstream of *Tri6*. In *F. graminearum*, *Tri6* negatively regulates *Tri10* expression (Seong et al., 2009)<sup>178</sup>. By implementing Chromatin immunoprecipitation followed by Illumina sequencing (ChIP-Seq), Nasmith et al. (2011)<sup>179</sup> have however demonstrated that *Tri6* was more than a specific transcription factor. Indeed, in addition to *tri* genes, more than 190 *F. graminearum* genes were shown as potential targets of *tri6*.

##### 6.1.3.3.2.2. Signal transduction pathways

The modulation of DON biosynthesis under specific conditions is related to the ability of *F. graminearum* to sense and transduce external signals to downstream targets, e.g. transcription factors, which in turn will affect the expression of *tri* genes. Several signal transduction pathways have been investigated in *F. graminearum*. They include targets of rapamycin (TOR) (Gu Q et al., 2015; Liu N et al., 2019; Yu et al., 2015; Boenisch MJ et al., 2017)<sup>176,180–182</sup>, mitogen-activated protein kinase (MAPK) cascades (Hou ZM et al., 2002; Yun et al., 2015)<sup>183,184</sup>, and cyclic adenosine monophosphate (cAMP)–protein kinase A (PKA) (Guo et al., 2016; Jiang et al., 2016; Yin et al., 2018)<sup>185–187</sup>.

##### 6.1.3.3.2.3. Global regulators

Secondary metabolites biosynthetic gene clusters may be positively or negatively controlled by global regulators. TCTB production is linked to various transcriptional regulators, including those involved in response to pH, light or oxidative stress (Merhej et al., 2011; Woloshuk & Shim, 2013)<sup>188,189</sup> (Fig. 17).

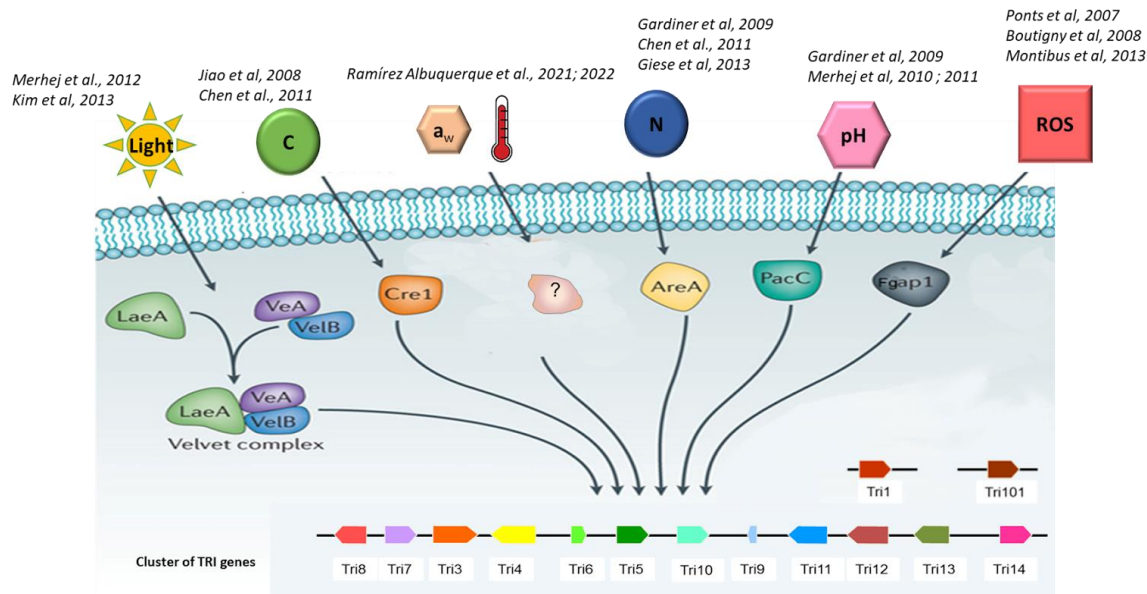


Figure 97. Environmental factors can influence *tri* genes expression and DON biosynthesis. This regulation involves various global regulators.

Light has been known to influence the expression of TCTB through the fungal-specific regulator velvet complex VeB/VeA/LaeA (Merhej et al., 2012; Niehaus et al., 2013)<sup>167,190</sup>. Overexpression of *FgLaeA* has been reported to led to an 11-fold increase in the amounts of 15-ADON (Kim et al., 2013)<sup>191</sup>. It has also been suggested that *LaeA* regulates gene transcription via epigenetic modification of the chromatin structure (Bok and Keller, 2004)<sup>192</sup>.

The key regulator of carbon metabolism is the transcription factor CreA/Cre1, which represses the transcription of target genes by binding to the promoters in response to glucose (Ronne, 1995)<sup>193</sup>. Sequence analysis indicated that some *Tri* genes, including *Tri6*, contain the typical CreA DNA binding sites (Rui and Chenfang, 2018)<sup>194</sup>.

The two main regulators of nitrogen metabolism, *AreA* and *AreB*, recognize and bind to a consensus DNA sequence (Tudzynski, 2014)<sup>195</sup>. In *F. graminearum*, *AreA* was shown to regulate DON production. *AreA* can interact with the regulator *Tri10* and therefore indirectly regulate the expression of the other *Tri* genes. Moreover, multiple *AreA* binding sites have been detected in several *Tri* genes, suggesting that *AreA* may directly regulate their expression (Hou et al., 2015)<sup>196</sup>. The second nitrogen-dependent transcriptional factor *AreB* physically interacts with *AreA*, which can act as both a positive and negative regulator.

The TCTBs biosynthesis in *F. graminearum* is not allowed under alkaline conditions (Gardiner et al., 2009; Merhej et al., 2010)<sup>164,165</sup>. *PacC* is the key transcription factor for pH regulation in filamentous fungi. In *F. graminearum*, the *PacC* homolog (*FgPac1*) represses the transcription of *tri* genes and negatively regulates DON production. Plural *PacC* binding motifs are found in the core *Tri* gene cluster, indicating *FgPac1* may regulate *Tri* gene expression by directly binding to their promoters (Merhej et al., 2011)<sup>166</sup>.

Oxidative stress induction in *F. graminearum* and the formation of reactive oxygen species (ROS) stimulate the expression of *Tri* genes, and therefore the accumulation of DON (Ponts et al., 2007; Boutigny et al., 2008)<sup>168,197</sup>. FgAP1 is one major regulator involved in the regulation of toxin accumulation through modulation of the expression of *Tri* genes in response to oxidative stress (Montibus et al., 2013)<sup>169</sup>.

#### 6.1.3.3.2.4. Chromatin structure

Another level of gene regulation of fungal secondary metabolism is linked to the chromatin structure, which is thought to enable a swift and reversible expression of a given secondary metabolite biosynthetic gene cluster. Regulatory circuits control chromatin alterations, leading to modifications in the structure of the chromatin, changing between lightly packed chromatin (euchromatin) with accessible genes, active for transcription, and the tightly packed chromatin structure with less accessibility for gene transcription. Chromatin modifications during the fungal development and/or induced by environmental conditions can lead to variations in targeted gene expression and silencing of genes (Etier et al., 2022)<sup>198</sup>. Several genes encoding chromatin-modifying enzymes and histone marks that could be involved in *Tri* gene expression modulation have been identified (Atanasoff-Kardjalieff and Studt, 2022; Mapook et al., 2022)<sup>199,200</sup> (Fig. 18).

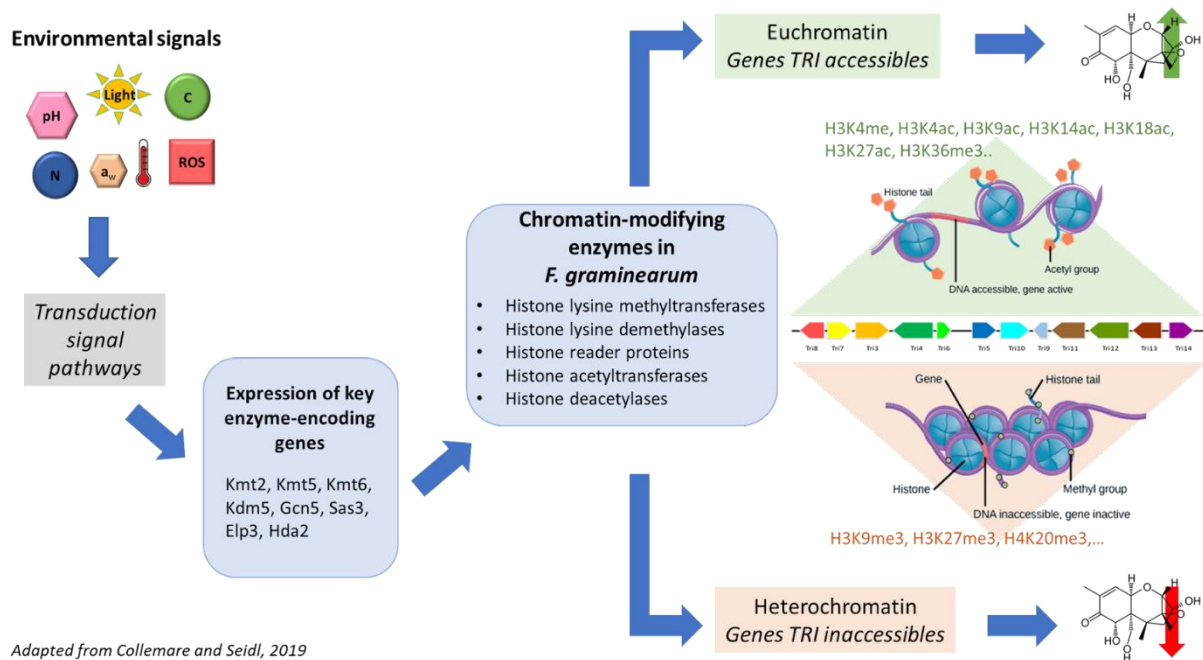


Figure 18. Regulation of DON production through chromatin structure modifications (adapted from Collemare and Seidl, 2019)<sup>201</sup>.

Genes coding for chromatin-modifying enzymes including histone lysine methyltransferases, histone lysine demethylases, histone reader proteins, histone acetyltransferases and histone deacetylases, catalyzing the deposit/removal of histone marks, are responsible for the compacted or opened conformation of chromatin and could modulate the accessibility/inaccessibility of *Tri* genes and in fine the production of DON. For instance, the H3K4me marks are largely located in euchromatic regions in *F. graminearum* (Connolly et al., 2013)<sup>202</sup> and deletion of CCL1, a component required for full H3K4me<sub>3</sub>, was shown to result in an altered secondary metabolite profile (Studt et al., 2016a, b)<sup>203,204</sup>. The deposit of H3K4me<sub>2/3</sub> and its removal by Set1 and Kdm5 has also been associated with a modulation of secondary metabolites production (Liu et al., 2015a, b; Janevska et al., 2018a, b)<sup>205–207</sup>. Two methylation marks, H3K9me<sub>3</sub> and H3K27me<sub>3</sub>, have been linked with a downregulation of secondary metabolite genes in *F. graminearum* (Reyes-Dominguez et al., 2012; Connolly et al., 2013)<sup>202,208</sup>. H4K20me<sub>3</sub> is known as contributing to gene silencing in higher eukaryotes (Kourmouli et al., 2004; Schotta et al., 2004)<sup>209,210</sup>, and deletion of Kmt5, a writer of methylation on H4K20, was reported to affect the biosynthesis of fungal secondary metabolites (Bachleitner et al., 2021)<sup>211</sup>. The acetylation of several histone 3 lysine residues, H3K4, H3K9, H3K18, and H3K27, was also described as a key event regulating the expression of fungal genes (Rösler et al., 2016)<sup>212</sup>. Deletion of Gcn5, the histone acetyltransferase responsible for the deposit of those marks, affected the transcription of putative secondary metabolite gene clusters (Atanasoff-Kardjalieff and Studt, 2022)<sup>199</sup>. Thus, the intervention of chromatin control through specific changes in histone marks appears today as a major mechanism that can control the biosynthesis of mycotoxins.

## 6.2. Zearalenone

Zearalenone (ZEA) is a non-steroidal estrogenic mycotoxin mainly produced by members of the FSAMSC and FIESC, including *F. graminearum* and *F. culmorum* and some strains of *F. poae* and *F. equiseti*. ZEA is a resorcylic acid lactone derived from the polyacetate pathway; its occurrence has been reported in cereal crops (maize, wheat, barley, oat, rye, sorghum, millet and rice) and processed food from many regions of the world including Europe, Asia and Africa (Almeida et al., 2012; Pleadin et al., 2012; Queiroz et al., 2012; Rai et al., 2018; Mousavi Khaneghah et al., 2018)<sup>213–217</sup>.

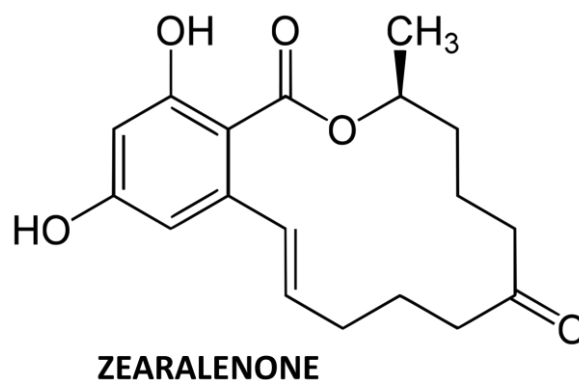


Figure 19. Structure of Zearalenone.

ZEA can cause alterations in the reproductive system, induce anestrus, hypoestrogenism, ovarian atrophy, and changes in the endometrium (Reddy et al., 2010)<sup>146</sup>. After ingestion, ZEA can be metabolized in the liver into  $\alpha$ -zearalenol, which is more estrogenic than zearalenone. NOEL was set at 40  $\mu\text{g}/\text{kg}$  bw/day. JECFA established a PMTDI for ZEA and its metabolites at 0.5  $\mu\text{g}/\text{kg}$  bw/d (JECFA 2000).

Knowledge regarding the genetic basis of zearalenone biosynthesis is less documented than that associated with DON. Four genes have been reported: *PKS4* encoding a reducing polyketide synthase, *PKS13* encoding a nonreducing polyketide synthase, one gene (*ZEB2*) encoding a transcription factor carrying a basic leucine zipper DNA-binding domain and a gene (*ZEB1*) encoding an isoamyl alcohol oxidase (Kim et al., 2018)<sup>218</sup>.

### 6.3. Emerging mycotoxins

The term emerging mycotoxins gathers “mycotoxins, which are neither routinely determined, nor legislatively regulated; however, the evidence of their incidence is rapidly increasing” (Gautier et al., 2020)<sup>219</sup>. *Fusarium* mycotoxins designed as emerging mycotoxins, include beauvericin (BEA), enniatins (ENNs), fusaproliferin (FUP), fusaric acid (FA), fusarins (FUSs), and moniliformin (MON). Among these, BEA and ENNs are the most frequently detected in harvests (Gauthier et al., 2020)<sup>219</sup>.

BEA is produced by diverse *Fusarium* species and could represent a health concern as it is frequently encountered at high concentrations in feed and food. BEA is a cyclic hexadepsipeptide. Most of the studies that have addressed the BEA toxicity are *in vitro* studies. The toxic effects of BEA are related to an increased ion permeability of biological membranes (ionophoric properties) and the production of an intracellular oxidative stress; BEA causes genotoxicity and induces apoptosis in many cellular lines (Mallebrera et al., 2017)<sup>220</sup>.

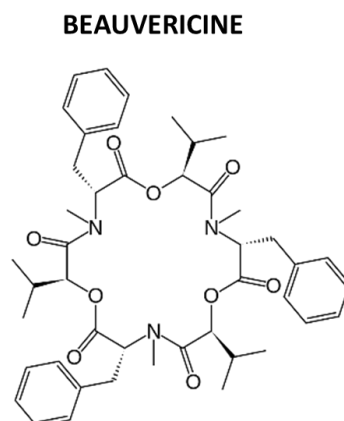
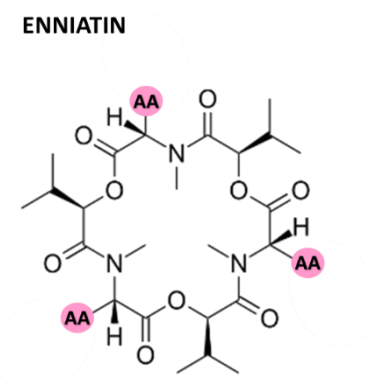


Figure 20. Structure of Beauvericin.

ENNs are produced by members of the FSAMSC and FIESC, including *F. avenaceum*, *F. equiseti* and *F. tricinctum*. ENNs are structurally similar to BEA. Differences between ENNs and BEA are related to the three amino acid residues: aromatic N-methyl-phenylalanines in beauvericin,

whereas in type A and B enniatins, the amino acid residues are N-methyl-valine, or N-methyl-isoleucine, or mixtures of these amino acids. A core enzyme, a nonribosomal peptide synthetase (NRPS) named enniatin synthetase (ESYN), is responsible for the biosynthesis of BEA and ENNs. Among ENNS, 29 analogs have been characterized with ENNs A, A1, B, and B1 as the most commonly detected in cereal grains.



Enniatin	Amino acids
A	3 Isoleucine
A1	2 Isoleucine + 1 L-Valine
B	3 L-Valine
B1	1 Isoleucine + 2 L-Valine

Figure 101. Enniatin structure with the main analogs (ENNs A, A1, B, and B1) described.

As BEA, ENNs are characterized by ionophoric properties. In-vitro studies demonstrated that ENNs can cause mitochondrial dysfunction, lysosomal alteration, genotoxicity, cell cycle disruption, cell membrane disruption and lipid peroxidation.

In 2014, The European Food Safety Authority (EFSA) has concluded that the acute exposure to ENNs was not a concern to human health but that chronic exposure required to be more studied (EFSA, 2014)<sup>221</sup>. Indeed, the frequent detection of ENNs in human urine supports the possible high incidence of human exposure to these mycotoxins (Rodriguez-Carrasco et al., 2018, 2020)<sup>222,223</sup>. Furthermore, the potential of ENNs to synergistically interact with other mycotoxins is of high concern.

#### 6.4. Mycotoxin multi contamination

Cereals are often contaminated by various species of toxigenic fungi, which can themselves produce more than one mycotoxin. This is particularly true for *Fusarium* spp. Several surveys have reported the natural co-occurrence of mycotoxins in various agricultural commodities cultivated all over the world. The fusariotoxins FUMs, TCTs, and ZEA occur persistently, according to Biomin's global mycotoxin occurrence reports, with prevalence superior to 50% in the tested samples (BIOMIN; 2021)<sup>224</sup>. AF with FUM, DON with ZEA, AF with ochratoxin A

(OTA), and FUM with ZEA were quoted as the mycotoxin combinations the most frequently observed, with occurrence depending on the geographical regions (Smith et al., 2016)<sup>225</sup> (Fig. 22).

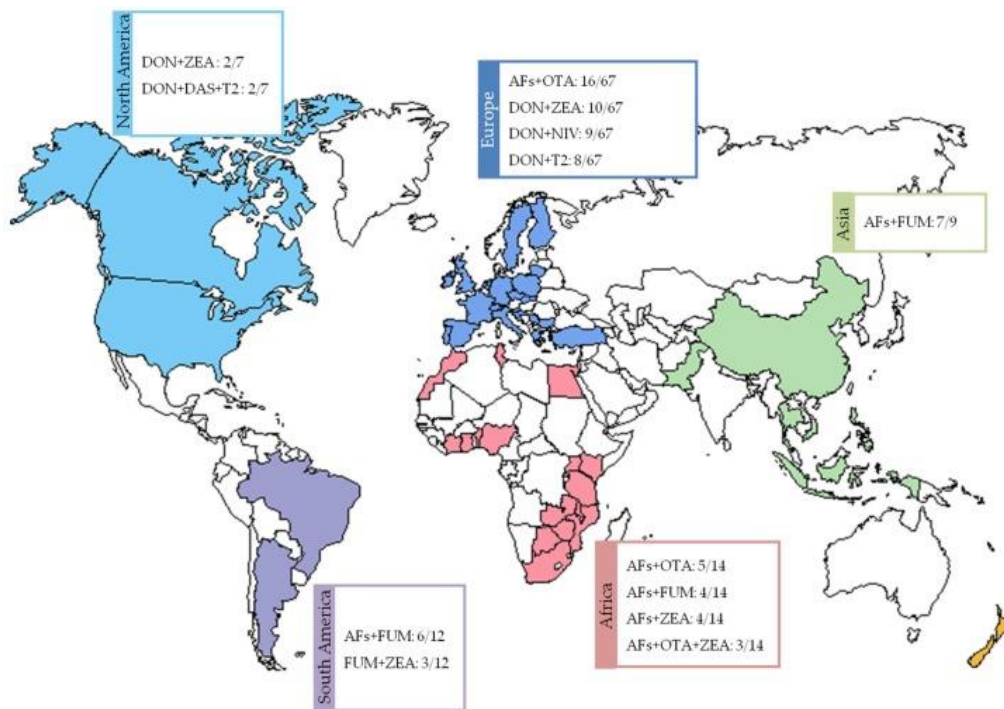


Figure 112. Main mycotoxin mixtures and their geographic distribution (Smith et al., 2016)<sup>225</sup>.

There is little information on the toxic effects of combinations of mycotoxins, synergistic or antagonist, in plant, animal or humans (Smith et al., 2016)<sup>225</sup>. Furthermore, mycotoxins are chemically and thermally stable and therefore highly difficult to eliminate from contaminated matrices; they can be retrieved all along the food/feed transformation chain and persist in end-products (Karlovsky et al., 2016; Peivasteh-Roudsari et al., 2021)<sup>226,227</sup>. Even if the risks of acute toxicity to humans due to high levels of these toxins in grains are now well controlled, the risks of chronic toxicity remain poorly controlled. Consequently, a preharvest control of mycotoxins is required, all the more that current decontamination strategies are not sufficiently efficient (Kabak et al., 2006)<sup>228</sup>.

## 7. Pre-harvest strategies to control FHB

In order to limit and manage FHB infection and associated mycotoxins, it is important to define effective, safe and sustainable strategies.

The strategies in place are based on limiting the environmental factors that favor *Fusarium* infection, increasing the resistance of plants to *Fusarium* invasion, and the direct control of the pathogenic fungus. These strategies include cultural, chemical, and biological strategies, as well as the development of resistant host plant species. These strategies are required to be combined, as a single strategy is frequently insufficiently efficient.

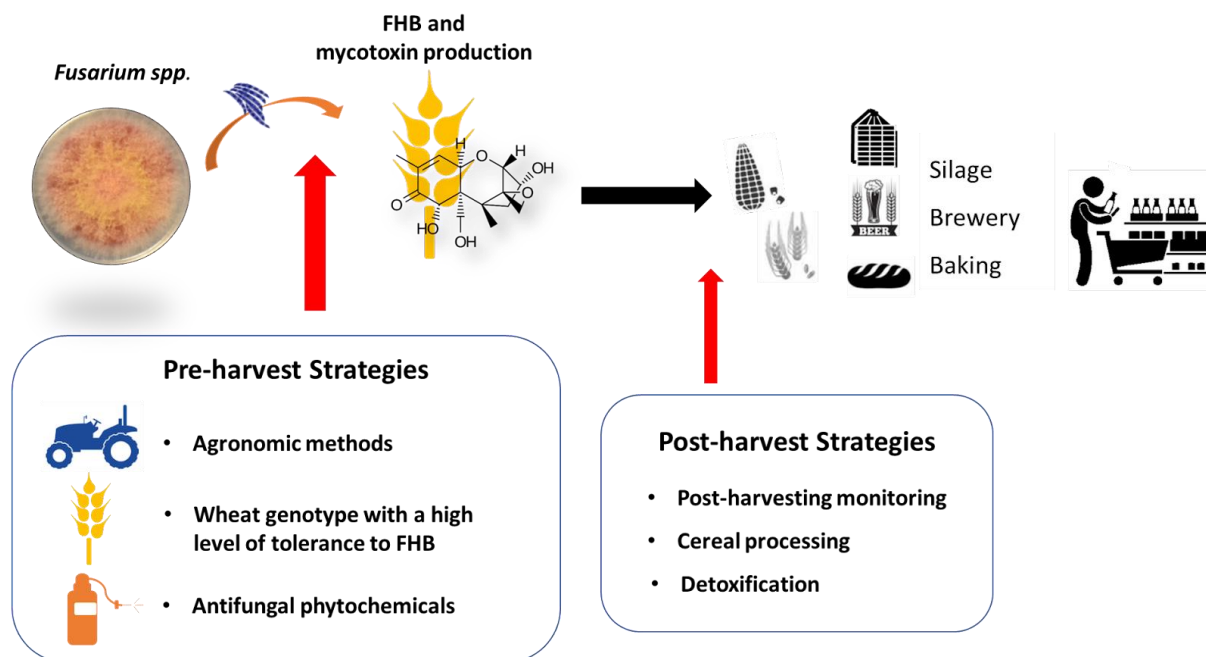


Figure 123. Pre- and Post-harvest strategies to reduce FHB and mycotoxin presence in grains and processed food.

## 7.1. Agronomic methods

### 7.1.1. Crop Rotation

Suitable crop rotation involving non-host crops is one of the main efficient measures against *F. graminearum* (Wegulo et al., 2015)<sup>229</sup>. Survival of *Fusarium* spp. on residues in soil have been largely documented and considered as one of the main sources of inoculum. Thus, introducing *Fusarium*-free plant varieties/species in a crop rotation schema is reported as an efficient practice to reduce the risk of infection and grain contamination with mycotoxins (Parry et al., 1995; McMullen et al., 1997; Marburger et al., 2015, Tillmann et al., 2017)<sup>9,25,230,231</sup>. For instance, a wheat previous crop is known as more at risk than a non-cereal previous crop (Parry et al., 1995; Obst et al.; 1997; Fernandez et al., 2005)<sup>9,232,233</sup>. Root crops and legume plants are interesting previous crops, limiting the occurrence of *Fusarium* spp. It was for long recommended to introduce soybean in crop rotation to reduce FHB and DON content in wheat or maize (Pioli et al., 2004; Broders et al., 2007)<sup>234,235</sup>, but further studies have demonstrated that soybean can also be a host plant for *F. graminearum*.

### 7.1.2. Tillage and Fertilization

Tillage, which is a running method to bury infected crop remnants, is recommended to avoid contamination related to crop residues (Wegulo et al., 2015)<sup>229</sup>. The absence of tillage was shown to significantly promote FHB and high DON contents in harvested wheat grains (Obst et al., 1997)<sup>232</sup>. Efficacy of tillage is increased with the use of a plow with moldboard and with deeper plowing. Furthermore, tilling associated with a resistant cultivar and fungicide

application has been shown to reduce DON contamination in wheat by 94% (Blandino et al., 2012)<sup>236</sup>.

Mineral fertilization used in cereal farming systems can influence FHB by affecting the rate of residue decomposition, by creating a physiological stress on the host plant, by altering the crop canopy structure or by changing the soil structure. In the case of *F. graminearum*, an excess of nitrogen applied to cereals or in the soil was shown to increase the frequency of grain infection (Teich et al 1989; Martin et al., 1991)<sup>237,238</sup>. The form of nitrogen fertilization (urea, ammonium nitrate, calcium nitrate or calcium cyanamide) was also reported to affect the level of FHB symptoms but not the mycotoxin production (Martin et al., 1997; Teich et al 1991, Yi et al., 2001)<sup>237–239</sup>.

### 7.1.3. Forecasting models

Because the weather conditions are acknowledged as the most determinant factors in FHB infection and cannot be controlled, forecasting systems are important for farmers to improve and/or adapt the FHB management. Multiple forecasting models have been developed for both FHB and DON accumulation; they are mainly based on climatic data including relative humidity, rain and temperature and can also consider some agronomic parameters. One key climatic variable frequently introduced in forecasting models is rainfall at the wheat flowering stage, i.e. the most sensitive stage for *F. graminearum* infection. Predictions are nowadays mainly realized based on mathematical predictive models; some mechanistic models have also been developed. The empiric modeling approach describes the relation between the key variables (i.e. rainfall during flowering) and the event to be predicted (i.e. FHB symptoms and/or DON contamination in grain at harvest) using statistical analysis. The mechanistic approach is based on the cause and effect relationships between variables; these relationships being described by mathematical functions. The DONcast<sup>®</sup> model, which was one of the first empirical developed models, aims to predict DON contamination at harvest based on rainfall and temperature around flowering, on the susceptibility of the planted cultivar and on the previous crop in the field (Schaafsma and Hooker, 2007)<sup>240</sup>. In France, the Myco-LIS<sup>®</sup> model developed by Arvalis Institut du Végétal includes residues management in addition to climatic factors and crop rotation. Use of such forecasting models allows farmers to react and implement the most suitable preventive strategy according to the level of risk (De Wolf et al., 2003; Shah et al., 2014)<sup>241,242</sup>. For instance, use of chemical spray or choice of sowing date can be decided and adjusted according to the predictions (Prandini et al., 2009)<sup>243</sup>. Actually, use of forecasting models was demonstrated to permit a significant reduction of yield loss and mycotoxin contamination (Prandini et al., 2009)<sup>243</sup>.

## 7.2. Use of genotype with a high level of tolerance to FHB

Use of varieties showing resistance to FHB or the use of plants genetically modified through breeding or transgenesis (in countries where it is allowed) is an efficient control method to

prevent and/or reduce FHB damage. However, breeding programs are hindered by the complexity of FHB resistance mechanisms and the current lack of available European FHB fully resistant germplasms.

Resistance mechanisms of wheat to FHB have been shown to include five components. Schroeder and Christensen (1963)<sup>244</sup> first discriminated two types of resistance: type I—resistance to initial infection and type II—resistance to the spread of the infection within the plant tissues. Three other types were further identified: type III refers to kernel resistance to infection, type IV to host tolerance to yield losses and type V to resistance to the accumulation of deoxynivalenol in grain through metabolization of the toxin into non-toxic derivatives or inhibition of its biosynthesis.

In the early 20th century the development of knowledge in heritability and genetics allowed researchers to identify sources of heritable resistance, called resistance genes (R genes). Qualitative (monogenic) disease resistance is related to R genes, which identification facilitates the improvement of breeding programs. However and unfortunately, wheat resistance to FHB is reported as a quantitative resistance related to a wide set of genes with additive effects. More than 100 quantitative traits loci (QTLs) related to FHB resistance have been identified in wheat; these QTLs are located on all chromosomes with exception of chromosome 7D (Dhokane et al., 2016)<sup>245</sup>. Some QTLs located on chromosomes 5AL and 4BS were reported to have a significant contribution to resistance of type I and some located on chromosomes 3BS, 6BS, and 2DL to type II resistance. The QTLs reported as having major effects on FHB resistance include Fhb1, Fhb2, Fhb4 and Fhb5 (Buerstmayr et al., 2002; Cuthbert et al., 2007; McCartney et al., 2007; Dokāne et al., 2016)<sup>246–249</sup>. To date, a number of differentially FHB-tolerant wheat landraces around the world have been selected by local farmers (Talas et al., 2011; Zhu et al., 2019; Li et al., 2011, 2016; Jia et al., 2018)<sup>250–254</sup>. FHB resistance in several cultivars such as ‘Wangshuibai’, ‘Sumai 3’, ‘Gamenya’, ‘Alondra’, ‘Nyubai’, ‘Romanus’, ‘Frontana’, ‘Spark’, ‘Wangshuibai’, ‘Arina’ and ‘F201R’ has been determined using specific locus markers (Buerstmayr et al., 2009)<sup>255</sup>.

### 7.3. Use of antifungal phytochemicals

Since the introduction of the first fungicides in the 1800s, synthetic pesticides remain the primary strategy to control fungal diseases. Over 110 new fungicides have been developed during the last century; their use is thought to be responsible for an increase in food production corresponding to a value of USD 12.8 billions in the US annually (Ons et al., 2020<sup>256</sup>). Chemical control methods have been preferred in commercial crop production due to their effectiveness and their easy application. The use of synthetic pesticides has therefore become an integral part of agriculture. In the case of FHB, the application of fungicides during flowering has been considered a few decades ago as one of the first approaches to manage the disease (Wegulo et al., 2015)<sup>229</sup>. The use of insecticides (Bagga et al., 2008; Olotuah, 2016;

Drakulic et al., 2016)<sup>257–259</sup> and herbicides (Johal and Huber, 2009; Fernandez et al., 2009; Drakopoulos et al., 2020)<sup>260–262</sup> can also have a slight impact on FHB disease management (weeds being potential reservoirs of *Fusarium* inoculum and insects can act as vectors of inoculum or create damages promoting fungal infection) but in the following we will focus on fungicide treatments.

### 7.3.1. Active ingredients / their targets / effectiveness

Many fungicides have been commonly used to reduce FHB, including triazoles, carbendazim, mancozeb, benomyl, prochloraz, propiconazole and triadimenol. Among them, the most widely used are triazoles such as metconazole, propiconazole, prothioconazole, and tebuconazole.

Triazoles-based fungicides belong to the demethylase inhibitors (DMI) group: they inhibit the cytochrome P450 sterol 14 $\alpha$ -demethylase (CYP51/ERG11) leading to disruption of fungal ergosterol biosynthesis. Ergosterol is a component of fungal cell membranes and its reduction negatively affects the membrane integrity and lowers fungal viability (Becher et al., 2011)<sup>263</sup>. Triazoles fungicides, such as tebuconazole, metconazole and prothioconazole (Paul et al., 2008; Pirgozliev et al., 2002)<sup>264,265</sup> currently provide the most effective control of FHB. Triazole fungicide application can reduce FHB incidence, disease severity and DON accumulation but is not a guarantee of a lack of disease.

Another commonly used active substance for controlling FHB is prochloraz, a compound belonging to the imidazole group characterized by a mode of action similar to triazoles.

Benzimidazole fungicides block the GTP-cap during tubulin polymerization, inhibiting nuclear and cell division. This group of fungicide, mainly represented by carbendazim, has a longer history of use in FHB control compared to triazoles. They are still widely used in China as a result of their relatively lower cost compared with triazoles (Chen et al., 2015; Mesterházy, 2003)<sup>266,267</sup>.

Strobilurins, including azoxystrobin, inhibit the fungal growth by interfering with mitochondrial electron transport. Strobilurins interact with the Qo site of cytochrome bc1 complex, which leads to a decreased aerobic respiration and energy production (Audenaert, 2010)<sup>170</sup>. Efficacy of strobilurins as part of FHB control strategies has been tested since the end of the 1990s: results range from efficacy to decrease FHB disease, to no effect on yield or DON accumulation (Milus & Weight, 1998; Haidukowski et al., 2005)<sup>268,269</sup>, to an increase in DON accumulation compared to the non-treated condition (Hollingsworth & Motteberg, 2006)<sup>270</sup>.

None of the aforementioned chemicals, however, suffice by themselves to completely control FHB (Dweba et al., 2017; Spolti et al., 2013; Yuan and Zhou, 2005)<sup>39,271,272</sup>. Some reports recommend combining triazoles with strobilurins for a more efficient control (Gilbert and Haber, 2013; McMullen et al., 2008; Ramirez et al., 2004)<sup>273–275</sup>. Besides, the efficiency of fungicide application to reduce FHB severity and DON is reported as higher when moderately resistant cultivars are used (Mesterhazy et al., 2011; Willyerd et al., 2012)<sup>276,277</sup>. Actually, the application of tebuconazole + prothioconazole in combination with cultivar resistance may be

a much better solution in limiting FHB and DON in grain than using breeding-resistance and chemical methods separately (Paul et al., 2019)<sup>278</sup>. Fungicide effectiveness depends also on other agronomic practices, e.g. crop rotation, tillage, nitrogen fertilization and seed treatment (Ács et al., 2018; Beyer et al., 2006; Edwards, 2004)<sup>279–281</sup>.

### 7.3.2. Warning date application

The most suitable fungicide's date of application depends on the plant stage of growth and the presence of fungal inoculum. The time window for an optimal application is of about two days during early anthesis (Blandino and Reyneri, 2009; Barber et al., 2020)<sup>282,283</sup>. Farmers may not be able to spray during this short time window due to various reasons including bad weather and the efficacy of the treatments can be significantly reduced. The timing of application of fungicides is a critical point since it may affect DON accumulation. For instance, an increase in DON accumulation has been observed in some situations when strobilurin fungicides were applied after pathogen infection (Simpson et al., 2001; Hollingsworth et al., 2006; Blandino and Reyneri, 2009)<sup>270,282,284</sup>.

### 7.3.3. Unintended and adverse effect of fungicide use

Although synthetic fungicides have benefited crop production for decades, the use of such chemicals is currently restricted or discouraged for several reasons.

#### 7.3.3.1. Inefficiency

Improper use of fungicides may cause reduced efficacy or increased mycotoxin concentrations in the grains. Certain compounds, such as strobilurins or tebuconazole, resulted in no direct effect on mycotoxin content in cereals or a significant increase in DON contamination (Jennings et al., 2000, Simpson et al., 2001; Pirgozliev et al., 2002; Ramirez et al., 2004; Blandino et al., 2006; Paul et al., 2008)<sup>264,265,275,284–286</sup>. Among the various rationales that can explain such an unintended effect, one can mention: (i) the removal of competitive species more sensitive to the fungicide than *F. graminearum* itself, (ii) the increase in DON production as a result of stressful conditions perceived by the fungus.

In a context of global warming, many pesticides are predicted to have their activity limited by dry conditions and to be degraded faster with higher temperatures; which will probably necessitate higher dose levels or more frequent applications to protect crops (Bailey, 2004)<sup>287</sup>. Besides, under epidemic conditions, even the most efficient fungicides may not be good enough to keep the toxin level below the critical threshold (D'Angelo et al., 2014; Mesterhazy et al., 2011)<sup>276,288</sup>.

#### 7.3.3.2. Emergence of resistance

Repeated applications of the same fungicide can lead to appearance of fungicide resistance in targeted pathogens.

Farmers have been struggled with emergence of resistance against some commonly known fungicides since the 1970s. Fungicides such as benzimidazoles, are very successful in the treatment of many crop diseases worldwide; however, they are predisposed to the emergence of resistance by crop pathogens. Carbendazim has been applied regularly to control FHB for over 40 years during wheat heading and flowering in areas with warm and moist weather. Unfortunately, the emergence of resistant isolates worldwide, particularly in China, has been reported; this emergence threatens the efficacy of carbendazim against *F. graminearum* (Chen and Zhou, 2009; Liu et al., 2019)<sup>289,290</sup>. Carbendazim is no longer available on the market in several countries including countries from the European Union as a result of this resistance concern. Resistance to Carbendazim has been shown to be associated with mutations in  $\beta$ 1-tubulin and  $\beta$ 2-tubulin (Y. Zhou et al., 2016; Duan et al., 2014)<sup>291,292</sup>. Similarly, mutations on CYP51A and CYP51C have been identified and reported to be responsible for *F. graminearum* resistance to triazoles (X. Liu et al 2011; Y. Duan et al., 2018)<sup>293,294</sup>.

#### 7.3.3.3. Environmental and regulatory issues

The most widespread model of agriculture involves intensive use of agricultural inputs, including fertilizers and pesticides. The overapplication or misuse of synthetic fungicides (associated with the toxicity of the active component) has raised serious concerns such as their impact on the environment, the contamination of drinking water and their negative effects on human health and livestock.

Fungicide poisoning to farmers is reported as a critical issue in many countries, especially in developing countries. For example, certain fungicides have recently been linked to cancer, respiratory and hormone imbalance diseases (Mamane et al., 2015; Piel et al., 2019; Hoppin et al., 2017; Juntarawijit and Juntarawijit, 2018)<sup>295–298</sup>. Several authors have however argued that mycotoxin contamination could be more problematic for humans and domesticated animals than fungicide overapplication (Torres et al., 2019)<sup>299</sup>. This assumption is based on the fact that MTDI in humans for DON and its acetylated variants is 1  $\mu$ g/kg body weight/day while the MTDIs for the fungicides range from 18 to 40  $\mu$ g/kg body weight/day. According to some studies, fungicides can be degraded under field conditions within two weeks of application, while mycotoxins may persist for years and are stable to heat (Mesterházy et al., 2018)<sup>300</sup>. The two aforementioned comments are however the subject of high controversy.

Concerning the environmental impact, pesticides are known to potentially affect non-targeted species such as soil microorganisms causing imbalance in ecosystems. Agricultural intensification is not compatible with sustainable agriculture and is a threat to future production. Additionally, consumers from industrial countries are willing to pay more for food produced organically, which is not compatible with the application of most synthetic fungicides.

Regulators have approved laws that result in either banning or restricting the use of synthetic fungicide by imposing lower maximum residue limits (MRLs). In the European Union, the MRL review program was implemented under Regulation 396/2005 to restrict the use of synthetic pesticides.

In the light of the high concern associated with the use of synthetic chemical fungicides, we can observe an increased effort of research to identify eco-friendly alternatives (Lee et al., 2010)<sup>301</sup>.

#### 7.4. Biocontrol solutions

The International Biocontrol Manufacturers Association (IBMA) defines biocontrol (or biological control) as: “pest and disease control for plant protection based on living organisms and naturally-sourced compounds.” In France, the definition in the article L.253-6 of the Rural and maritime fishing code (CPMR) is more detailed: biocontrol is based on “agents and products using natural mechanisms in the context of integrated pest management of crops, which include in particular macroorganisms and plant protection products comprising micro-organisms, chemical mediators such as pheromones and kairomones and natural substances of plant, animal or mineral origin.”

When considering FHB, numerous potential biological control agents or natural products have been tested in laboratories and have shown interesting efficiency to inhibit the fungal growth and DON production. However, very few of them have shown efficiency in field trials. This is particularly true for natural compounds which use as plant care products is frequently hampered by the poor solubility of the identified active compounds. Among these natural compounds, phenylpropanoids have raised a wide attention. The recent review of Ahmed et al. (2022)<sup>302</sup> illustrates the promising potential of phenolic compounds from botanical extracts as anti-mycotoxin agents but underlines also the necessity to improve formulation solutions to overcome their solubility and stability.

##### 7.4.1. Biological control agents

Biocontrol agents (BCA) are organisms used to control a pest species. As summarized on Figure 24, BCA can interact with the pathogen either directly (parasitism, antibiosis, secretion of lytic enzymes) or indirectly (competition for space and nutrients); they can also affect the susceptibility of the host plant through induction of resistance or plant growth promotion (Pal and McSpadden Gardener, 2006; Vujanovic and Goh, 2011; Kim and Vujanovic, 2016; Legrand et al., 2017)<sup>303–306</sup>.

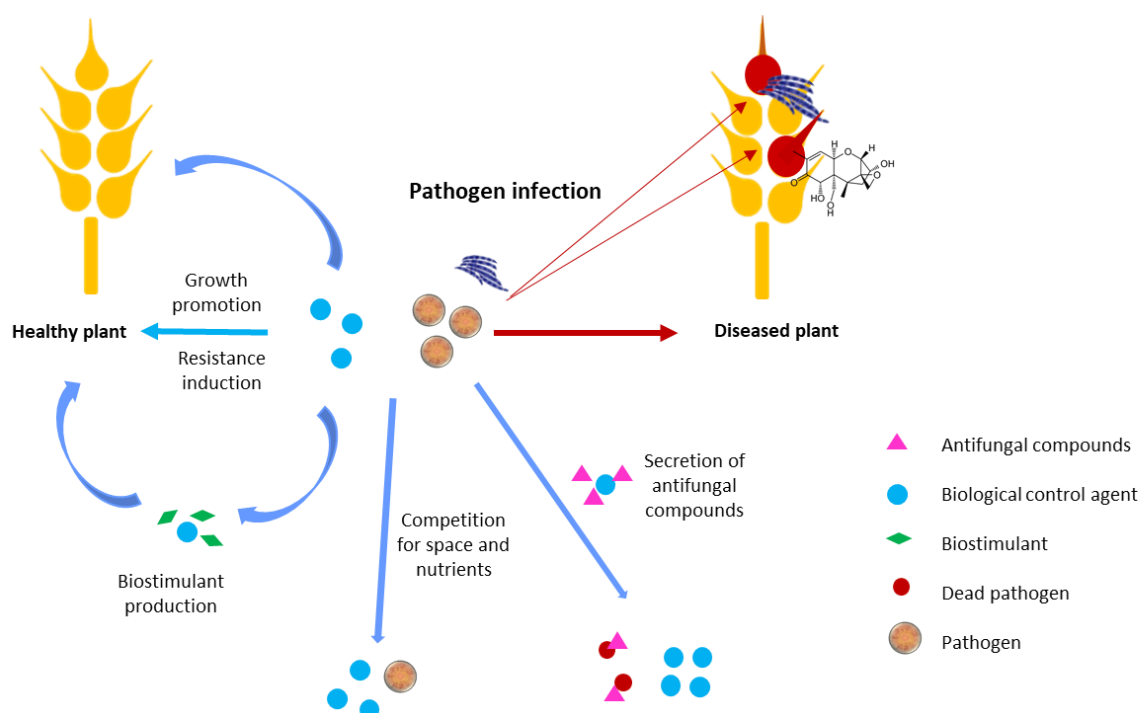


Figure 134. Mechanism of action of biocontrol agents to reduce FHB.

Several reports have illustrated the interest biocontrol agents could have to minimize FHB disease (Legrand et al., 2017; Byrne et al., 2021)<sup>306,307</sup>. Bacteria including *Bacillus*, *Pseudomonas* and *Streptomyces* have been reported as able to reduce the FHB incidence and DON contamination. This was also the case for some fungi including *Clonostachys*, *Pythium* and *Trichoderma* (Khan et al., 2004; Jochum et al., 2006; Błaszczyk et al., 2014; Woo et al., 2014)<sup>308–311</sup>.

Some BCAs are antagonists of *Fusarium* sp. through competition for space and nutrients; they share the same ecological niche and have the same nutritional needs. *T. harzianum*, *Microsphaeropsis* sp., *Streptomyces* sp. RC 87B and *C. rosea* are saprophytic fungi limiting the growth of *F. graminearum* on residues. In addition, they can inhibit the formation of *F. graminearum* perithecial and ascospores (Fernandez, 1992; Bujold et al., 2001; Xue et al., 2009; Palazzini et al., 2013, 2017)<sup>312–316</sup>. *C. rosea* is also a mycoparasitic fungus that can directly kill its targets including *F. graminearum* (Nygren et al., 2018)<sup>317</sup>. Two strains of *Paenibacillus polymyxa* were also characterized for their antagonistic potential against *F. graminearum* colonization and DON accumulation (He et al., 2009)<sup>318</sup>.

*Bacillus* spp., *Lactobacillus* spp., *Lysobacter enzymogenes*, *Pseudomonas fluorescens*, *Trichoderma* spp. and *Streptomyces* sp. were shown to produce a wide variety of antibiotics, bacteriocins, enzymes and volatile compounds that are active against several plant pathogens (Ghisalberti and Sivasithamparam, 1991; Lavermicocca et al., 2000; Jochum et al., 2006; Nourozian et al., 2006; Palazzini et al., 2007; Crane and Bergstrom, 2014; Gong et al., 2015; Grosu et al., 2015; Wang et al., 2016)<sup>309,319–326</sup>. Fengycin and iturin are two inhibitory lipopeptides produced by some *Bacillus* spp. with strong antagonistic effects against *F. graminearum* (Dunlap et al., 2013; Wang et al., 2007; Zhao et al., 2014)<sup>327–329</sup>. *C. rosea*

produces fungal cell wall degrading enzymes and antibiotics to kill the host cells (Chatterton and Punja 2009; Rodríguez et al., 2011)<sup>330,331</sup>.

Plant growth promoting microorganism (PGPM) can enhance seed germination, improve wheat growth and protection (Larran et al., 2016; Toumatia et al., 2016)<sup>332,333</sup>. Some microorganisms can also induce plant defense response. Actually, it is widely documented that plants respond to a variety of chemical stimuli produced by soil- and plant-associated microbes and that such stimuli can either induce or condition plant host defenses against infection by a variety of pathogens including toxigenic fusaria. Thus, inoculation of *Clonostachys* spp. to the soil was reported to induce systemic resistance in wheat and protection against *F. culmorum* (Roberti et al., 2008)<sup>334</sup>. Similarly, wheat seed treatment with *P. fluorescens* CHAO or *L. enzymogenes* C3 was shown to allow a significant reduction of FHB symptoms and mycotoxin content in wheat (Jochum et al., 2006; Henkes et al., 2011)<sup>309,335</sup>. Maize seed treatment with *T. harzianum* T22 has been described as an efficient treatment to control kernel colonization by *F. verticillioides* and fumonisin accumulation (Ferrigo et al., 2014)<sup>336</sup>. In addition, several microbial products have been identified as elicitors of host defenses. These inducers include lipopolysaccharides and flagellin from Gram-negative bacteria, cold shock proteins of diverse bacteria, transglutaminase, elicitors, and  $\beta$ -glucans from Oomycetes, invertase from yeast, chitin and ergosterol from fungi and xylanase from *Trichoderma* (Nürnberg et al., 2004)<sup>337</sup>. As an example, one can mention PSP1 that exploits the protease activity of *Acremonium strictum* and has demonstrated significant effect to increase resistance against FHB (Chalfoun et al., 2018)<sup>338</sup>. Similarly, a microbial fermentation-based product (MFP), a blend of bacteria and yeasts from fermentation brewing media, has been shown to allow a significant reduction of FHB symptoms in wheat (Twamley et al., 2022)<sup>339</sup>.

Many reports have concluded that the use of BCAs was more efficient when they were included in an integrated pest management (IPM) strategy to reduce and not replace synthetic fungicides (Palazzini et al., 2007; Xue et al., 2009)<sup>314,322</sup>. For instance, a combination of *Lysobacter enzymogenes* strain C3 with tebuconazole, applied during wheat cultivation, was shown to reduce FHB incidence or severity, up to 16% and 24% respectively (Jochum et al., 2006)<sup>309</sup>.

#### 7.4.2. Marketed Biocontrol Agents

Despite promising results, most solutions based on biological control agents are still stuck at the in vitro lab-scale. Only one *Bacillus* strain TrigoCor 148 and one *C. rosea* strain ACM941 have been developed as biofungicide. These two strains were patented in 2003 and 2002 respectively but are hitherto not available on the market (Xue et al., 2008, 2014; Bergstrom & Da Luz, 2005)<sup>314,340,341</sup>. Only one biocontrol product for FHB management is available on the French market (Polyversum® authorized in France since August 2015). Regarding all plant pathogens, fifty-two active chemical ingredients were registered in the EU between 1996 and 2000, whereas only 10 biocontrol agents were approved during the same span of time. From

2005 to 2010, 22 biocontrol agents were authorized in the EU and only 20 synthetic chemical pesticides. The worldwide annual increase in market is predicted reach 12.3% for biopesticides versus 5% for chemical pesticides in 2025 (Market and Markets, 2022)<sup>340</sup>.

Commercialization of a BCA as a biopesticide remains a long and complex process, mainly because the efficacy demonstrated in the laboratory and/or greenhouse experiments does not always result in field success, with a lack of reproducibility and consistency across experiments and because the registration process of biopesticides is highly challenging with different regulation policies across countries (Kiewnick, 2007; Lahlali et al., 2022)<sup>341,342</sup>. Furthermore, cost and convenience are important factors to be taken into account. According to Pal and McSpadden Gardener (2006)<sup>303</sup>, biocontrol solutions should be applied only when cultural practices and host resistance are insufficient for an effective disease control.

#### 7.4.3. Antimicrobial peptides as promising solutions to minimize FHB and DON accumulation

**Use of Defensins to Develop Eco-Friendly Alternatives to Synthetic Fungicides to Control Phytopathogenic Fungi and Their Mycotoxins**  
(review published in Journal of Fungi, doi.org/10.3390/jof8030229)

Review

# Use of Defensins to Develop Eco-Friendly Alternatives to Synthetic Fungicides to Control Phytopathogenic Fungi and Their Mycotoxins

Valentin Leannec-Rialland <sup>1</sup>, Vessela Atanasova <sup>2</sup> , Sylvain Chereau <sup>2</sup> , Miray Tonk-Rügen <sup>3,4</sup> , Alejandro Cabezas-Cruz <sup>5,\*</sup>  and Florence Richard-Forget <sup>2,\*</sup>

<sup>1</sup> Université de Bordeaux, UR1264 Mycology and Food Safety (MycSA), INRAE, 33882 Villenave d'Ornon, France; valentin.leanec-rialland@inrae.fr

<sup>2</sup> UR1264 Mycology and Food Safety (MycSA), INRAE, 33882 Villenave d'Ornon, France; vessela.atanasova@inrae.fr (V.A.); sylvain.chereau@inrae.fr (S.C.)

<sup>3</sup> Institute for Insect Biotechnology, Justus Liebig University, Heinrich-Buff-Ring 26-32, 35392 Giessen, Germany; miray.tonk@agr.uni-giessen.de

<sup>4</sup> Institute of Nutritional Sciences, Justus Liebig University, Wilhelmstrasse 20, 35392 Giessen, Germany

<sup>5</sup> Anses, Ecole Nationale Vétérinaire d'Alfort, UMR Parasitic Molecular Biology and Immunology (BIPAR), Laboratoire de Santé Animale, INRAE, 94700 Maison-Alfort, France

\* Correspondence: alejandro.cabezas@vet-alfort.fr (A.C.-C.); florence.forget@inrae.fr (F.R.-F.)



**Citation:** Leannec-Rialland, V.; Atanasova, V.; Chereau, S.; Tonk-Rügen, M.; Cabezas-Cruz, A.; Richard-Forget, F. Use of Defensins to Develop Eco-Friendly Alternatives to Synthetic Fungicides to Control Phytopathogenic Fungi and Their Mycotoxins. *J. Fungi* **2022**, *8*, 229. <https://doi.org/10.3390/jof8030229>

Academic Editor: Luis V. Lopez-Llorca

Received: 24 January 2022

Accepted: 18 February 2022

Published: 25 February 2022

**Publisher's Note:** MDPI stays neutral with regard to jurisdictional claims in published maps and institutional affiliations.



**Copyright:** © 2022 by the authors. Licensee MDPI, Basel, Switzerland. This article is an open access article distributed under the terms and conditions of the Creative Commons Attribution (CC BY) license (<https://creativecommons.org/licenses/by/4.0/>).

**Abstract:** Crops are threatened by numerous fungal diseases that can adversely affect the availability and quality of agricultural commodities. In addition, some of these fungal phytopathogens have the capacity to produce mycotoxins that pose a serious health threat to humans and livestock. To facilitate the transition towards sustainable environmentally friendly agriculture, there is an urgent need to develop innovative methods allowing a reduced use of synthetic fungicides while guaranteeing optimal yields and the safety of the harvests. Several defensins have been reported to display antifungal and even—despite being under-studied—antimycotoxin activities and could be promising natural molecules for the development of control strategies. This review analyses pioneering and recent work addressing the bioactivity of defensins towards fungal phytopathogens; the details of approximately 100 active defensins and defensin-like peptides occurring in plants, mammals, fungi and invertebrates are listed. Moreover, the multi-faceted mechanism of action employed by defensins, the opportunity to optimize large-scale production procedures such as their solubility, stability and toxicity to plants and mammals are discussed. Overall, the knowledge gathered within the present review strongly supports the bright future held by defensin-based plant protection solutions while pointing out the obstacles that still need to be overcome to translate defensin-based in vitro research findings into commercial products.

**Keywords:** plant disease; fungal pathogens; mycotoxins; biocontrol strategies; defensins

## 1. Introduction

Fungal plant diseases jeopardize global food security. Actually, staple crops with high economical and agronomical value, including rice, wheat, maize, potato and soybean, are threatened by various fungal diseases that can lead to substantial yield losses [1–3]. Using the harvest statistics provided by the Food and Agriculture Organization (FAO) for the period 2009–2010, Fisher et al. [4] estimated that the losses caused by fungal diseases with regard to wheat, rice, maize potato and soybean were equivalent to the food necessary to feed 600 million humans over one year. Of greater concern is that the currently available knowledge does not allow ruling out the possibility that climate change would increase the impact of major fungal plant diseases as well as create environmental conditions promoting the emergence of new devastating fungal diseases [5,6]. Among the phytopathogenic fungal species recognized as the most economically important, one can mention *Magnaporthe*

*oryzae*, which is responsible for rice blast that can lead to up to 35% harvest losses; *Botrytis cinerea*, which causes severe damages to a broad range of plant species; *Puccinia* species and the two *Fusarium* species, *Fusarium graminearum* and *Fusarium oxysporum*, which cause significant damages to diverse crops [7]. In addition to jeopardizing crop yields, some phytopathogenic fungi can also significantly affect crop safety as a result of their capacity to produce mycotoxins. This is notably the case of several *Fusarium* species infecting cereal crops [8] but also of various species within the *Aspergillus*, *Penicillium*, *Alternaria*, and *Claviceps* genera that can contaminate a wide variety of agricultural products [9]. Mycotoxins are fungal secondary metabolites causing serious adverse health effects to both humans and livestock [10]. The most important mycotoxins that affect health and agro-economy are aflatoxins, patulin, trichothecenes, zearalenone, fumonisins, ochratoxin A and ergot alkaloids [11]. According to FAO estimates, 25% of the world's crops are contaminated by mycotoxins above the limits set by national and agricultural regulations, which leads to annual losses close to 1 billion metric tons [10]. These estimates were recently refined in the report of Eskola et al. [12] which indicates that 60–80% of agricultural products contain detectable levels of mycotoxins. Despite increasing efforts to develop agronomic and cultural practices to manage and control plant infecting fungi including crop rotation, and to improve appropriate management of crop residues and the appropriate use of resistant cultivar when available [13,14], the application of synthetic fungicides has been the primary strategy adopted by farmers and is still widely used. However, concerns over environmental contamination and human health risks [15], restrictions or cancellations of authorization by some countries, have driven research to develop safe and efficient alternatives to synthetic fungicides. To prevent the emergence of resistant fungal strains, as has been observed with the intensive use of single-target site fungicides, priority should be given to multi-target solutions [16–18]. Based on their nature, control methods' alternatives to conventional fungicides can be classified as chemical or biological. Biological solutions include the use of plant growth-promoting bacteria, mycorrhizal fungi to promote plant fortification and/or enhance plant defense, and the use of antagonists microorganisms that are able to counteract the spread of the fungal pathogen [19–21]. Chemical solutions leverage the capacity of molecules from natural origin to prevent or reduce fungal growth. Among natural molecules, antimicrobial peptides (AMPs), that can be produced either by animals, plants or fungi, have been the subject of increasing research in recent decades. AMPs are low molecular mass biomolecules, generally between 12 and 50 amino acids, that play an important role in innate host defense against microbial colonization [22] and possess a wide range of antimicrobial activities against bacteria, fungi, viruses and protozoa [23]. According to the presence of  $\alpha$ -helix and/or  $\beta$ -sheet secondary structural elements, AMPs are commonly divided into four categories represented in Figure 1;  $\alpha$ ,  $\beta$ ,  $\alpha\beta$  and non- $\alpha\beta$  [24]. For instance, the human cathelicidin LL37, which has been widely studied due to its large repertoire of functional activities including direct antimicrobial activities against various types of microorganisms, belongs to the  $\alpha$ -helical peptide category of AMPs [25]. As an example of  $\beta$ -sheet peptides, one can mention gomesin, which has been isolated from the spider *Acanthoscurria gomesiana* and contains two  $\beta$ -sheets linked through two disulfide bridges forming a  $\beta$ -hairpin motif [26]. Indolicidin, a 13-amino-acid-long peptide with a linear structure isolated from bovine neutrophils is a typical example of the class of non- $\alpha\beta$  AMPs [27]. Regarding the mixed  $\alpha\beta$  category, this class includes, but is not limited to, several microcins such as the microcin B17 that is produced by strains of *Escherichia coli* and displays efficient bactericidal activity [28]. Of all the AMPs reported thus far, the defensin family which comprises peptides with  $\alpha$ -helix and/or  $\beta$ -sheet has been the most extensively studied. Their antimicrobial activity has been evidenced against a broad range of human and plant pathogens, including bacteria, oomycetes, virus, fungi or even apicomplexan parasites [29–34]. One specific defensin, such as MtDef4 or MtDef5 from *Medicago truncatula*, can exhibit a wide antimicrobial spectrum and can be active against both human and plant pathogens while others (such as the D2 defensin from *Spinacia oleracea*) exhibit a more narrow spectrum of activity [35]; additionally, one pathogen can be

affected by different defensins [32,34,36]. Interestingly, some defensins have been shown to display antifungal activity against pathogens, leading to devastating disease in crops. For instance, the defensins RsAFP2 from *Raphanus sativus* and Sa-AFP2 from *Sinapis alba* have been demonstrated as potent inhibitors of the fungal growth of major pathogens including *Fusarium culmorum* and *B. cinerea* [29]. This has led several authors to propose defensins as promising candidates for medical and agricultural applications, including the treatment of life-threatening microbial diseases or treatments against phytopathogens [37–39].

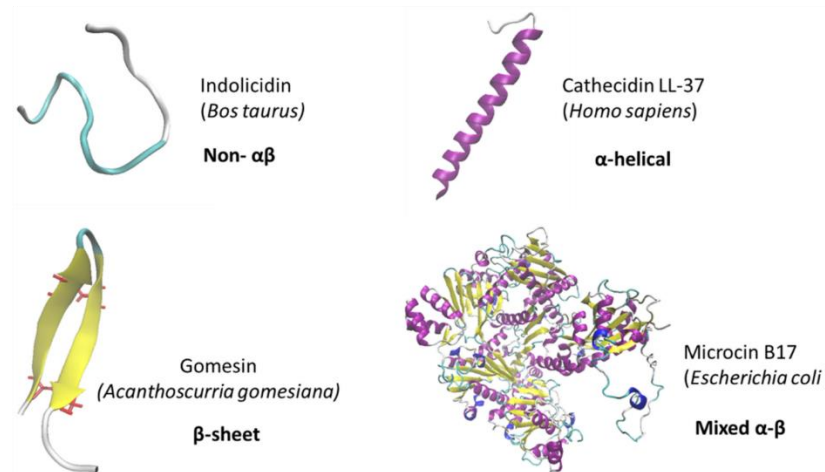


**Figure 1.** Tridimensional structure of the typical representative of the four groups of AMPs classified according to the presence of  $\alpha$ -helix and/or  $\beta$ -sheet secondary elements: non- $\alpha\beta$ ,  $\alpha$ -helical,  $\beta$ -sheet and mixed  $\alpha$ - $\beta$  AMPs.

In this review, we will specifically focus on the potential use of defensins as novel leads for the development of sustainable solutions to control plant fungal diseases, reduce yield losses and mycotoxin contamination and therefore improve food security and safety. Firstly, the most recent information on the major characteristics of defensins, their antifungal activity and mechanisms of action will be discussed. Secondly, the biological applications of plant defensins as eco-friendly alternatives to synthetic fungicides will be debated.

## 2. Origin and Characteristics of Defensins

The term defensin was introduced in 1985 to refer to peptides with antimicrobial activities isolated from humans [40]. Since then, the term defensin has been expanded to include peptides from non-human organisms possessing functional (antimicrobial properties) and structural (a compact cysteine-stabilized  $\beta$ -sheet structure) similarities. Defensins constitute the largest, and most studied, group of AMPs [41]. These small proteins of approximately 20–60 amino acids are ubiquitous and multipotent components of the innate immune system of a wide range of organisms within the animal, plant and fungi kingdoms [42,43]. The defensins are cationic cysteine-rich peptides with a high diversity of amino acid sequence. However, despite this low level of amino acid sequence identity, most defensins bear some similarities in their tertiary structure stabilized into compact shapes [44].

Defensins are separated into two principal super-families, the cis- and trans- defensins, with an independent evolutionary origin and a convergent evolution of their structural folds [44,45]. The cis- and trans-classification is based on the spacing and pairing of the cysteine residues and the orientation of the peptide's secondary structure. Defensins of the cis-family contain two parallel cis-oriented disulfide bridges pointing in the same direction and stabilizing the same  $\beta$ -strand to an  $\alpha$ -helix. Cis-defensins have been reported in a wide array of invertebrate animals, fungi and spermatophyte plants [44]. The cis-defensins

have generally more diverse and longer amino acid sequences than trans-defensins. The trans-family of defensins is characterized by two trans-oriented disulfide bridges pointing in opposite directions from the final  $\beta$ -strand and thus stabilizing different structural elements. Trans-defensins have either been observed in invertebrates or vertebrates [45] and include  $\alpha$ -defensins,  $\beta$ -defensins and big defensins, this last family being supposed to be the ancestors of  $\beta$ -defensins [46]. In addition to these families, it is worth mentioning the occurrence of  $\theta$ -defensins, which are the only cyclic peptides of animal origin reported to date [47].

The tertiary structure of defensins is characterized by the connectivity pattern of their disulfide bridges, which is unique to their phylum and conserved within the defensin family as represented in Figure 2 [44]. Thus, all vertebrate  $\alpha$ -defensins have three disulfide bridges between cysteine (Cys) residues, Cys1–Cys6, Cys2–Cys4, and Cys3–Cys5. In vertebrate  $\beta$ -defensins, the three-disulfide bridges are between Cys1–Cys5, Cys2–Cys4, and finally Cys3–Cys6. For cis-oriented defensins in invertebrates, the common linkage pattern is Cys1–Cys4, Cys2–Cys5, Cys3–Cys6. In plant defensins, the disulfide bonds between cysteine residues commonly share the same following pattern, Cys1–Cys8, Cys2–Cys5, Cys3–Cys6, and Cys4–Cys7 [42]. In plant and some invertebrate (notably arthropods and mussels) defensins, disulfide bridges connect one  $\alpha$ -helix and three or two-strand antiparallel  $\beta$  sheets leading to a stabilized motif called cysteine-stabilized alpha-beta ( $CS\alpha\beta$ ) schematized in Figure 3 [48]. Defensins containing a  $CS\alpha\beta$  motif, also designed as  $CS\alpha\beta$ -defensins, have been categorized in three major types, namely antibacterial ancient invertebrate-type defensins (AITDs), antibacterial classical insect-type defensins (CITDs) and antifungal plant/insect-type defensins (PITDs) [49]. In contrast to plant and invertebrate defensins, mammal defensins usually do not contain  $\alpha$ -helices and consequently no  $CS\alpha\beta$  motif [50]. The presence of disulfide bridges in the defensin structure confers a high stability against chemical and thermal extreme conditions to this class of peptides [51,52], such as protection from cleavage by proteolysis [53]. Defensins often adopt an amphipathic structure with a hydrophobic side facing a hydrophilic one, which, in addition to their typically cationic state (net charge inter-quartile range from +1 to +5), facilitates the interaction and insertion of the peptides into the anionic cell walls and the double layer of phospholipid membranes of microorganisms [54]. Defensins possess a structural residue characterized as functionally important located in the C-terminal  $\beta$ -sheet domain. This motif, conserved across all classes of  $CS\alpha\beta$ -defensins, is called  $\gamma$ -core. The  $\gamma$ -core is assumed to be responsible for the antimicrobial activity of defensins as it has been demonstrated for several plant defensins including RsAFP2, Psd1, MsDef1, and MtDef4 [55–57], but also of metazoan defensins such as tick defensins [36].

Defensins are synthesized as precursor proteins that possess an N-terminal endoplasmic reticulum targeting signal peptide followed by the mature defensin domain and an optional C-terminal prodomain [58,59]. According to the presence or absence of the C-terminal prodomain, plant defensins are divided into two classes: class I (absence of the C-terminal prodomain) and class II (presence of the C-terminal prodomain). The role of the C-terminal prodomain in the *N. alata* NaD1 defensin was investigated by Lay et al. [60]. The previous authors have shown that this pro-peptide which is rich in hydrophobic and acidic amino acids is involved in targeting the vacuoles and eliminating the potential detrimental effects caused by the basic nature of the defensin in the plant host cells [60].



**Table 1.** List of defensins and DLPs with antifungal effect on phytopathogenic and mycotoxigenic fungi.

Defensin	Amino Acid (AA) Sequence (Accession n°)	AA n°ber	MM (Da)/pI	Organism (Family)	Targeted Species (IC50 and MIC)	Ref.
Plant defensin						
AX1	AICKKPSKFFKGACGR-DADCEKACDQENWPG-GVCVPFLRCECQRSC (P81493)	44	4895.72/7.14	<i>Beta vulgaris</i> L ( <i>Amaranthaceae</i> )	<i>Cercospora beticola</i> (IC <sub>50</sub> = 0.79 μM *)	[62]
AX2	ATCRKPSMYFSGACFSD-TNCQKACNREDWPNG-KCLVGFKCECQRPC (P82010)	46	5185.01/7.31		<i>C. beticola</i> (IC <sub>50</sub> = 0.39 μM *)	
Dm-AMP1	ELCEKASKTWSGNCNGN-TGHCDNQCKSWEGA-AHGACHVRNGKHMCFYFNC (P0C8Y4)	46	4997.63/6.87	<i>Dahlia merckii</i> ( <i>Asteraceae</i> )	<i>B. cinerea</i> K1147 (IC <sub>50</sub> = 2.17 μM *); <i>Cladosporium sphaerospermum</i> K0791 (IC <sub>50</sub> = 0.54 μM *); <i>F. culmorum</i> K0311 (IC <sub>50</sub> = (0.18–0.9) μM *); <i>Leptosphaeria maculans</i> LM36uea (IC <sub>50</sub> = 0.27 μM *); <i>Penicillium digitatum</i> K0879 (IC <sub>50</sub> = 0.36 μM *); <i>Trichoderma viride</i> K1127 (IC <sub>50</sub> = 18.1 μM *); <i>Septoria tritici</i> K1097 (IC <sub>50</sub> = 0.18 μM *); <i>Verticillium albo-atrum</i> K0937 (IC <sub>50</sub> = 0.72 μM *)	[63]
Dm-AMP2	EVCEKASKTWSGNCNGN-TGHC	20	2111.33/6.36		<i>B. cinerea</i> K1147 (IC <sub>50</sub> = 1.81 μM *); <i>C. sphaerospermum</i> K0791 (IC <sub>50</sub> = 0.54 μM *); <i>F. culmorum</i> K0311 (IC <sub>50</sub> = 0.54 μM *); <i>L. maculans</i> LM36uea (IC <sub>50</sub> = 0.18 μM *); <i>P. digitatum</i> K0879 (IC <sub>50</sub> = 0.36 μM *); <i>T. viride</i> K1127 (IC <sub>50</sub> = 18.1 μM *); <i>S. tritici</i> K1097 (IC <sub>50</sub> = 0.18 μM *); <i>V. albo-atrum</i> K0937 (IC <sub>50</sub> = 0.36 μM *)	
AhPDF1.1	QRLCEKPSGTWSGVCG-NNGACRNQCIRLEKAR-HGS	51	5707.65/7.74		<i>Arabidopsis helleri</i> ( <i>Brassicaceae</i> )	
At-AFP1	KLCERPSGTWSGVCG-NSNACKNQCNLEKARHGSCNYVFPAAHKCICYFPC (P30224)	50	5539.44/7.53	<i>Arabidopsis thaliana</i> ( <i>Brassicaceae</i> )	<i>Alternaria brassicicola</i> MUCL 20,297 (IC <sub>50</sub> = 1.8 μM *); <i>B. cinerea</i> MUCL 30,158 (IC <sub>50</sub> = 0.7 μM *); <i>F. culmorum</i> IMI 180,420 (IC <sub>50</sub> = 0.54 μM *); <i>F. oxysporum</i> f. sp. lycopersici MUCL 909 (IC <sub>50</sub> = 0.54 μM *); <i>Pyricularia oryzae</i> MUCL 30,166 (IC <sub>50</sub> = 0.05 μM *); <i>Verticillium dahliae</i> MUCL 6963 (IC <sub>50</sub> = 0.27 μM *)	[29]
AtPDF2.3	RTCESKSHRFKGPCVST-HNCANVCHNEFGGG-KCRGFRRCYCTRHC (Q9ZUL7)	49	5348.15/8.49		<i>B. cinerea</i> B05-10 (IC <sub>50</sub> = 5.8 μM); <i>B. cinerea</i> R16 (IC <sub>50</sub> = 5.8 μM); <i>F. oxysporum</i> 5176 (IC <sub>50</sub> = 4.4 μM); <i>F. culmorum</i> MUCL 30,162 (IC <sub>50</sub> = 1.0 μM); <i>V. dahliae</i> MUCL 19,210 (IC <sub>50</sub> = 4.4 μM); <i>F. graminearum</i> PH-1 (IC <sub>50</sub> = 1.4 μM)	

Table 1. Cont.

Defensin	Amino Acid (AA) Sequence (Accession n°)	AA n°ber	MM (Da)/pI	Organism (Family)	Targeted Species (IC50 and MIC)	Ref.
Hc-AFP1	RYCERSSGTWSGVCGN-SGKCSNQQRLEGAA-HGSCSNYVFAHKCICYPC (G8GZ62)	50	5483.21/7.33	<i>Heliophila coronopifolia</i> (Brassicaceae)	<i>B. cinerea</i> (IC <sub>50</sub> = 4.56 μM *); <i>Fusarium solani</i> (IC <sub>50</sub> = 4.56 μM *)	[66]
Hc-AFP2	QKLCERPSGTWSGVCGN-NNNACRNQCINLEKARHGSCSNYVFAHKCICYPC (G8GZ63)	51	5722.61/7.54		<i>B. cinerea</i> (IC <sub>50</sub> = (1.75–2.62) μM *); <i>F. solani</i> (IC <sub>50</sub> = (1.75–2.62) μM *)	
Hc-AFP3	RYCERSSGTWSGVCGN-NTDKCSSQQRLEGA-AHGSCSNYVFAHKCICYPC (G8GZ64)	50	5528.24/7.09		<i>B. cinerea</i> (IC <sub>50</sub> = (3.62–4.52) μM *); <i>F. solani</i> (IC <sub>50</sub> = 4.52 μM *)	
Hc-AFP4	QKLCERPSGTWSGVCGNNGACRNQCIRLE-RARHGSCSNYVFAHKCICYPC (G8GZ65)	51	5735.66/7.75		<i>B. cinerea</i> (IC <sub>50</sub> = (2.61–3.49) μM *); <i>F. solani</i> (IC <sub>50</sub> = (0.87–1.74) μM *)	
Rs-AFP1	QKLCERPSGTWSGVCGN-NNNACKNQCNLEKARHGSCSNYVFAHKCICYPC (P69241)	51	5694.60/7.53	<i>R. sativus</i> (Brassicaceae)	<i>A. brassicicola</i> MUCL 20,297 (IC <sub>50</sub> = 2.64 μM *); <i>B. cinerea</i> MUCL 30,158 (IC <sub>50</sub> = 1.41 μM *); <i>F. culmorum</i> IMI 180,420 (IC <sub>50</sub> = 0.88 μM *); <i>F. oxysporum</i> f. sp. lycopersici MUCL 909 (IC <sub>50</sub> = 5.28 μM *); <i>P. oryzae</i> MUCL 30,166 (IC <sub>50</sub> = 0.05 μM *); <i>V. dahliae</i> MUCL 6963 (IC <sub>50</sub> = 0.88 μM *)	[29]
					<i>Ascochyta pisi</i> (IC <sub>50</sub> = 0.88 μM *); <i>C. beticola</i> (IC <sub>50</sub> = 0.35 μM *); <i>Colletotrichum lindemuthianum</i> (IC <sub>50</sub> = 17.61 μM *); <i>F. oxysporum</i> f. sp. pisi (IC <sub>50</sub> = 2.64 μM *); <i>Mycosphaerella fijiensis</i> var. <i>fijiensis</i> (IC <sub>50</sub> = 0.7 μM *); <i>Nectria haematococca</i> (IC <sub>50</sub> = 1.06 μM *); <i>Phoma betae</i> (IC <sub>50</sub> = 0.35 μM *); <i>Pyrenophora tritici-repentis</i> (IC <sub>50</sub> = 0.53 μM *); <i>P. oryzae</i> (IC <sub>50</sub> = 0.05 μM *); <i>Rhizoctonia solani</i> (IC <sub>50</sub> = 17.61 μM *); <i>Sclerotinia sclerotiorum</i> (IC <sub>50</sub> = 3.52 μM *); <i>Septoria nodorum</i> (IC <sub>50</sub> = 3.52 μM *); <i>Trichoderma hamatum</i> (IC <sub>50</sub> = 1.06 μM *); <i>V. dahliae</i> (IC <sub>50</sub> = 0.88 μM *)	[67]

Table 1. Cont.

Defensin	Amino Acid (AA) Sequence (Accession n°)	AA n°ber	MM (Da)/pI	Organism (Family)	Targeted Species (IC50 and MIC)	Ref.
Rs-AFP2	QKLCQRPSGTWSGVC- NNNACKNQCI- RLEKAR- HGSCNYVFP- PAHK- CICYFPC (P30230)	51	5735.70/7.94		<i>B. cinerea</i> K1147 (IC <sub>50</sub> = 1.75 μM *); <i>C. sphaerospermum</i> K0791 (IC <sub>50</sub> = 0.52 μM *); <i>F. culmorum</i> K0311 (IC <sub>50</sub> = 0.26 μM *); <i>F. culmorum</i> K0311 (IC <sub>50</sub> = 0.87 μM *); <i>L. maculans</i> LM36uea (IC <sub>50</sub> = 2.1 μM *); <i>P. digitatum</i> K0879 (IC <sub>50</sub> = 0.26 μM *); <i>T. viride</i> K1127 (IC <sub>50</sub> = 5.25 μM *); <i>S. tritici</i> K1097 (IC <sub>50</sub> = 0.26 μM *); <i>V. albo-atrum</i> K0937 (IC <sub>50</sub> = 2.1 μM *)	[63]
					<i>A. brassicicola</i> MUCL 20,297 (IC <sub>50</sub> = 0.35 μM *); <i>B. cinerea</i> MUCL 30,158 (IC <sub>50</sub> = 0.35 μM *); <i>F. culmorum</i> IMI 180,420 (IC <sub>50</sub> = 0.35 μM *); <i>F. oxysporum</i> f. sp. <i>lycopersici</i> MUCL 909 (IC <sub>50</sub> = 0.35 μM *); <i>P. oryzae</i> MUCL 30,166 (IC <sub>50</sub> = 0.7 μM *); <i>V. dahliae</i> MUCL 6963	[29]
					<i>A. pisi</i> (IC <sub>50</sub> = 0.7 μM *); <i>C. beticola</i> (IC <sub>50</sub> = 0.35 μM *); <i>C. lindemuthianum</i> (IC <sub>50</sub> = 0.52 μM *); <i>F. oxysporum</i> f. sp. <i>Pisi</i> (IC <sub>50</sub> = 0.35 μM *); <i>M. fijiensis</i> var. <i>fijiensis</i> (IC <sub>50</sub> = 0.26 μM *); <i>N. haematococca</i> (IC <sub>50</sub> = 0.35 μM *); <i>P. betae</i> (IC <sub>50</sub> = 0.17 μM *); <i>P. tritici-repentis</i> (IC <sub>50</sub> = 0.26 μM *); <i>R. solani</i> (IC <sub>50</sub> = 17.49 μM *); <i>S. sclerotiorum</i> (IC <sub>50</sub> = 17.49 μM *); <i>S. nodorum</i> (IC <sub>50</sub> = 2.62 μM *); <i>T. hamatum</i> (IC <sub>50</sub> = 0.35 μM *); <i>V. dahliae</i> (IC <sub>50</sub> = 0.26 μM *); <i>Venturia inaequalis</i> (IC <sub>50</sub> = 4.37 μM *)	[67]
Defensin-like protein 4	QKLCERSSTWSG- VCGNNNACKNQCI- NLEGARHGSCNYI- FPYHRCICYFPC (O24331)	51	5747.58/7.33		<i>A. brassicicola</i> (IC <sub>50</sub> = 0.87 μM *); <i>B. cinerea</i> (IC <sub>50</sub> = 1.57 μM *); <i>F. culmorum</i> (IC <sub>50</sub> = 1.92 μM *)	[68]
Defensin-like protein 3	KLCERSSTWSG- VCGNNNACKN- QCIRLEGAQH- GSCNYVFP- PAHKCI-CYFPC (O24332)	50	5499.34/7.33		<i>A. brassicicola</i> (IC <sub>50</sub> = 0.36 μM *); <i>B. cinerea</i> (IC <sub>50</sub> = 0.36 μM *); <i>F. culmorum</i> (IC <sub>50</sub> = 0.36 μM *)	

Table 1. Cont.

Defensin	Amino Acid (AA) Sequence (Accession n°)	AA n°ber	MM (Da)/pI	Organism (Family)	Targeted Species (IC50 and MIC)	Ref.
Sa-AFP2	QKLCQRPSGTWSG-VCGNNNACRNQC-INLEKARHGSCNY-VFPAHKCICYFPC (P30232)	51	5721.63/7.74	<i>S. alba</i> (Brassicaceae)	<i>A. brassicicola</i> MUCL 20,297 (IC <sub>50</sub> = 0.79 µM *); <i>B. cinerea</i> MUCL 30,158 (IC <sub>50</sub> = 0.61 µM *); <i>F. culmorum</i> IMI 180,420 (IC <sub>50</sub> = 0.4 µM *); <i>F. oxysporum</i> f. sp. lycopersici MUCL 909 (IC <sub>50</sub> = 0.4 µM *); <i>P. oryzae</i> MUCL 30,166 (IC <sub>50</sub> = 0.05 µM *); <i>V. dahliae</i> MUCL 6963 (IC <sub>50</sub> = 0.21 µM *)	[29]
WT1	QKLCEKSSGTWSG-VCGNNNACKNQC-INLEGARHGSC-NYIFPYHRCICY-FPC (Q9FS38)	51	5719.56/7.33	<i>Eutrema japonicum</i> (Brassicaceae)	<i>Magnaporthe grisea</i> (IC <sub>50</sub> = 0.87 µM *); <i>B. cinerea</i> (IC <sub>50</sub> = 3.5 µM *)	[69]
Sm-AMP-D1	KICERASGTWK-GICHSNDCNNQC-VKWENAGSGSCHY-QFPNYMFCFY-FDC (COHL82)	50	5763.55/6.28	<i>Stellaria media</i> L. (Caryophyllaceae)	<i>Bipolaris sorokiniana</i> 6/10 (IC <sub>50</sub> = 0.5 µM); <i>F. oxysporum</i> 16/10 (IC <sub>50</sub> = 0.35 µM); <i>F. graminearum</i> VKM F-1668 (IC <sub>50</sub> = 0.52 µM); <i>Fusarium avenaceum</i> VKM F-2303 (IC <sub>50</sub> = 0.52 µM); <i>B. cinerea</i> SGR-1 (IC <sub>50</sub> = 1.0 µM); <i>P. betae</i> VKM F-2532 (IC <sub>50</sub> = 0.52 µM); <i>Pythium debaryanum</i> VKM F-1505 (IC <sub>50</sub> = 1.0 µM)	[70]
Sm-AMP-D2	KICERASGTWKGI-CIHSNDCNNQC-VKWENAGSGSCHYQFPNYMFCFY-FNC (COHL83)	50	5762.57/6.77		<i>B. sorokiniana</i> 6/10 (IC <sub>50</sub> = 0.5 µM); <i>F. oxysporum</i> 16/10 (IC <sub>50</sub> = 0.35 µM); <i>F. graminearum</i> VKM F-1668 (IC <sub>50</sub> = 0.52 µM); <i>F. avenaceum</i> VKM F-2303 (IC <sub>50</sub> = 0.52 µM); <i>B. cinerea</i> SGR-1 (IC <sub>50</sub> = 1.0 µM); <i>P. betae</i> VKM F-2532 (IC <sub>50</sub> = 0.52 µM); <i>P. debaryanum</i> VKM F-1505 (IC <sub>50</sub> = 1.0 µM)	
So-D2	GIFSSRKCKTPSK-TFKGICTRDSNCDTSC-RYEGYPAGDC-KGIRRRRCMCKPC	52	5803.79/8.34	<i>S. oleracea</i> (Chenopodiaceae)	<i>F. culmorum</i> (IC <sub>50</sub> = 0.2 µM); <i>F. solani</i> (IC <sub>50</sub> = 11 µM); <i>Colletotrichum lagenarium</i> (IC <sub>50</sub> = 11 µM); <i>Bipolaris maydis</i> (IC <sub>50</sub> = 6 µM)	[71]
AB2	RTCENLANTYRG-PCITTGSCDDHC-KNKEHLRSGRCRD-DFRCW	47	5469.18/7.33	<i>Adzuckia angularia</i> (Fabaceae)	<i>B. cinerea</i> (IC <sub>50</sub> = 3.5 µM)	[72]
Beta-astratide bM1	CEKPSKFFSGP-CIGSSGKTQCAYL-CRRGEGLQDGNCK-GLKCVAC	45	4734.58/7.52	<i>Astragalus membranaceus</i> (Fabaceae)	<i>F. oxysporum</i> CICC 2532 (IC <sub>50</sub> = 4.92 µM *); <i>Alternaria alternata</i> CICC 2465 (IC <sub>50</sub> = 4.75 µM *); <i>R. solani</i> CICC 40,259 (IC <sub>50</sub> = 27.52 µM *); <i>Curvularia lunata</i> CICC 40,301 (IC <sub>50</sub> = 0.57 µM *)	[73]
Coccinin	KQTENLADTY (P84785)	10	1182.25/4.19	<i>Phaseolus coccineus</i> cv. 'Major' (Fabaceae)	<i>F. oxysporum</i> (MIC = 81 µM); <i>B. cinerea</i> (MIC = 109 µM); <i>R. solani</i> (MIC = 134 µM); <i>Mycosphaerella arachidicola</i> (MIC = 75 µM)	[74]

Table 1. Cont.

Defensin	Amino Acid (AA) Sequence (Accession n°)	AA n°ber	MM (Da)/pI	Organism (Family)	Targeted Species (IC50 and MIC)	Ref.
Phaseococcin	KTCENLADTYKGPPP-FFTTG	20	2187.46/6.03	<i>P. coccineus</i> cv. 'Minor' (Fabaceae)	<i>F. oxysporum</i> (MIC = 89 µM); <i>B. cinerea</i> (MIC = 102 µM); <i>R. solani</i> (MIC = 140 µM); <i>M. arachidicola</i> (MIC = 70 µM)	[75]
Ct-AMP1	NLCERASLTWTGN-CGNTGHCDTQCRNW-ESAKHGACHKRGKRWK-CFCYFNC (Q7M1F2)	49	5613.32/7.33	<i>Clitoria ternatea</i> (Fabaceae)	<i>B. cinerea</i> K1147 (IC <sub>50</sub> = 3.56 µM *); <i>C. sphaerospermum</i> K0791 (IC <sub>50</sub> = 1.07 µM *); <i>F. culmorum</i> K0311 (PDB medium) (IC <sub>50</sub> = 1.78 µM *); <i>F. culmorum</i> K0311 (SMF medium) (IC <sub>50</sub> = 0.11 µM *); <i>L. maculans</i> LM36uea (IC <sub>50</sub> = 1.07 µM *); <i>P. digitatum</i> K0879 (IC <sub>50</sub> = 3.56 µM *); <i>T. viride</i> K1127 (IC <sub>50</sub> = 17.81 µM *); <i>S. tritici</i> K1097 (IC <sub>50</sub> = 0.36 µM *); <i>V. albo-atrum</i> K0937 (IC <sub>50</sub> = 0.36 µM *)	[63]
Gymnin	KTCENLADDDY (P84200)	10	1171.25/3.8	<i>Gymnocladus chinensis</i> (Fabaceae)	<i>F. oxysporum</i> (IC <sub>50</sub> = 2 µM); <i>Cercospora arachidicola</i> (IC <sub>50</sub> = 10 µM)	[76]
Lc-def	KTCENLSDSFKG-PCIPDGNCKNH-CKEKEHLLSGR-CRDDDFRCWCTRNC (B3F051)	47	5449.23/7.08	<i>Lens culinaris</i> (Fabaceae)	<i>Aspergillus niger</i> VKM F-2259 (IC <sub>50</sub> = 18.5 µM); <i>Aspergillus versicolor</i> VKM F-1114 (IC <sub>50</sub> = 18.5 µM); <i>B. cinerea</i> VKM F-3700 (IC <sub>50</sub> = 9.25 µM); <i>F. culmorum</i> VKM F-844 (IC <sub>50</sub> = (18.5–37.0) µM)	[77]
Limenin	KTCENLADTY-KGPCFTTGGCDD-HCKNKEHLLSGR-RCRDDDFRCWCTRNC	47	5403.12/6.77	<i>Phaseolus limensis</i> (Fabaceae)	<i>B. cinerea</i> (MIC = 2.9 µM); <i>F. oxysporum</i> (MIC = 2.1 µM); <i>M. arachidicola</i> (MIC = 0.34 µM)	[78]
Limyin	KTCENLATYYRGPCF	15	1766.03/7.51		<i>F. solani</i> (IC <sub>50</sub> = 8.6 µM)	[79]
Ms-Def1 (alfAFP)	RTCENLADKYRGPCF-SGCDTHCTTKENAVSG-RCRDDDFRCWCTKR-C (Q4G3V1)	45	5194.90/7.32	<i>Medicago sativa</i> (Fabaceae)	<i>F. graminearum</i> (IC <sub>50</sub> = (1.2–2.3) µM *)	[80]
					<i>F. graminearum</i> PH-1 (IC <sub>50</sub> = (2–4) µM *); <i>F. graminearum</i> PH-1 (MIC > 6 µM)	[56]
					<i>V. dahliae</i> (MIC = 1 µM *)	[81]
Mt-Def2	KTCENLADKYRG-PCFSGCDTHCTTKE-NAVSGRCRDDDFRCWC-TKRC (Q5YLG8)	45	5166.89/7.32	<i>M. truncatula</i> (Fabaceae)	<i>F. graminearum</i> PH-1 (IC <sub>50</sub> = (0.75–1) µM)	[56]
					<i>F. oxysporum</i> f. sp. <i>medicaginis</i> 7F-3 (IC <sub>50</sub> = 0.7 µM); <i>F. oxysporum</i> f. sp. <i>medicaginis</i> 31F-3 (IC <sub>50</sub> = 1.9 µM); <i>Phoma medicaginis</i> STC (IC <sub>50</sub> = 0.3 µM); <i>P. medicaginis</i> WS-2 (IC <sub>50</sub> = 2.6 µM); <i>Clavibacter insidiosus</i> (IC <sub>50</sub> = 0.1 µM)	[35]
Mt-Def4	RTCESQSHKFK-GPCASDHNCASV-CQTERFSGGR-CRGRFRRCFCCTHC (G7L736)	47	5343.08/7.97		<i>F. graminearum</i> PH-1 (IC <sub>50</sub> = (0.75–1) µM)	[56]
					<i>F. oxysporum</i> f. sp. <i>medicaginis</i> 7F-3 (IC <sub>50</sub> = 0.7 µM); <i>F. oxysporum</i> f. sp. <i>medicaginis</i> 31F-3 (IC <sub>50</sub> = 1.9 µM); <i>P. medicaginis</i> STC (IC <sub>50</sub> = 0.3 µM); <i>P. medicaginis</i> WS-2 (IC <sub>50</sub> = 2.6 µM)	[35]

Table 1. Cont.

Defensin	Amino Acid (AA) Sequence (Accession n°)	AA n°ber	MM (Da)/pI	Organism (Family)	Targeted Species (IC50 and MIC)	Ref.
PsD1	KTCEHLADTYRG-VCFTNASCDDHC-KNKAHLISGTCHN-WKCFCTQNC (P81929)	46	5208.93/6.81	<i>Pisum sativum</i> (Fabaceae)	<i>A. niger</i> EK0197 (IC <sub>50</sub> = 2.3 μM *); <i>A. versicolor</i> 40028LMR/INCQS (IC <sub>50</sub> = 1 μM *); <i>Fusarium moniliforme</i> 2414UFPe (IC <sub>50</sub> = 4.2 μM *); <i>F. oxysporum</i> 2665UFPe (IC <sub>50</sub> = 19.2 μM *); <i>F. solani</i> 2389UFPe (IC <sub>50</sub> = 2.3 μM *)	[82]
PsD2	KTCENLSGTFKGPC-IPDGNCKNHCRNN-EHLLSGRCRDDFR-CWCTNRC (P81930)	47	5404.15/7.33		<i>A. niger</i> EK0197 (IC <sub>50</sub> = 1.9 μM *); <i>A. versicolor</i> 40028LMR/INCQS (IC <sub>50</sub> = 0.06 μM *); <i>F. moniliforme</i> 2414UFPe (IC <sub>50</sub> = 1.85 μM *); <i>F. oxysporum</i> 2665UFPe (IC <sub>50</sub> = 18.5 μM *); <i>F. solani</i> 2389UFPe (IC <sub>50</sub> = 1.57 μM *)	
PvD1_PTA2c	KTCENLADTYKGPCF-TTGCDDHCKNKEHLR-SGRRCRDDFRWCCTK-NC (F8QXP9)	47	5448.16/7.08	<i>Phaseolus vulgaris</i> (Fabaceae)	<i>F. solani</i> (IC <sub>50</sub> = 18.35 μM *); <i>Fusarium laterithium</i> (IC <sub>50</sub> = 18.35 μM *); <i>R. solani</i> (IC <sub>50</sub> = 18.35 μM *); <i>F. oxysporum</i> (IC <sub>50</sub> = 18.35 μM *)	[83]
P. vulgaris white cloud defensin	KTCENLADTFRGP-CFATSNCDHCKN-KEHLLSGRCRD-DFRCWCTRNC	47	5472.18/6.77	<i>P. vulgaris</i> cv. "white cloud bean" (Fabaceae)	<i>B. cinerea</i> (MIC = 2.8 μM); <i>F. oxysporum</i> (MIC = 2.3 μM); <i>M. arachidicola</i> (MIC = 0.72 μM)	[84]
Sesquin	KTCENLADTY (P84868)	10	1157.27/4.19	<i>Vigna unguiculate</i> (Fabaceae)	<i>B. cinerea</i> (IC <sub>50</sub> = 2.5 μM); <i>F. oxysporum</i> (IC <sub>50</sub> = 1.4 μM); <i>M. arachidicola</i> (IC <sub>50</sub> = 0.15 μM)	[85]
SPE10	KTCENLADTFRG-PCFTDGSCD-DHCKNKEHLI-KGRCRDDFRWCCT-RNC (Q6B519)	47	5500.24/6.77	<i>Pachyrhizus erosus</i> (Fabaceae)	<i>Aspergillus flavus</i> (IC <sub>50</sub> = 5.45 μM *); <i>A. niger</i> (IC <sub>50</sub> = 8.18 μM *); <i>B. maydis</i> (IC <sub>50</sub> = 2.73 μM *); <i>B. cinerea</i> (IC <sub>50</sub> = 18.18 μM *); <i>Colletotrichum gloeosporides</i> (IC <sub>50</sub> = 18.18 μM *); <i>F. oxysporum</i> f.sp. lycopersic (IC <sub>50</sub> = 18.18 μM *); <i>F. oxysporum</i> f.sp. vasinfectum (IC <sub>50</sub> = 18.18 μM *); <i>Penicillium</i> spp. (IC <sub>50</sub> = 18.18 μM *); <i>Rhizopus stolonifer</i> (IC <sub>50</sub> = 18.18 μM *); <i>V. dahliae</i> (IC <sub>50</sub> = 18.18 μM *)	[86]
TvD1	KTCENLADTYRGP-CFTTGSCDDHCKN-KEHLLSGRCRD-DFRCWCTK-RC (Q2KM12)	47	5475.23/7.09	<i>Tephrosia villosa</i> (Fabaceae)	<i>Nothopassalora personata</i> (MIC = 2.05 μM *); <i>F. oxysporum</i> (MIC = 5.12 μM *); <i>Fusarium verticillioides</i> (MIC = 5.12 μM *); <i>B. cinerea</i> (MIC = 5.12 μM *); <i>Curvularia</i> sp (MIC = 5.12 μM *); <i>R. solani</i> (MIC = 7.78 μM *)	[87]
VaD1	KTCMTKKEGWG-RCLIDTTCAHSCRK-QGYKGGNCKGMR-RTCYCLLDC (A0A053QXX7)	46	5209.23/8.12	<i>Vigna angularis</i> (Fabaceae)	<i>F. oxysporum</i> (IC <sub>50</sub> = 5.76 μM *); <i>F. oxysporum</i> f. sp. pisi (IC <sub>50</sub> = 10.21 μM *)	[88]

Table 1. Cont.

Defensin	Amino Acid (AA) Sequence (Accession n°)	AA n°ber	MM (Da)/pI	Organism (Family)	Targeted Species (IC50 and MIC)	Ref.
VrD1	RTCMIKKEGWGK-CLIDTTCAHSKN-RGYIGGNCKGM-TRTCYCLVNC (Q6T418)	46	5122.15/7.92	<i>Vigna radiata</i> (Fabaceae)	<i>F. oxysporum</i> (IC <sub>50</sub> = 1.1 μM *); <i>F. oxysporum</i> CCRC 35,270 (IC <sub>50</sub> = 3.4 μM *); <i>F. oxysporum</i> f. sp. Pisi (IC <sub>50</sub> = 2.4 μM *); <i>P. oryzae</i> (IC <sub>50</sub> = 4 μM *); <i>R. solani</i> (IRTENLADKYRGPFCFGCDT-HCTTKENAVSGRCRDDFRWCWTKRCC <sub>50</sub> = 17.7 μM *)	[89]
PgD1	RTCKTPSGKFKGVC-ASSNNCKNVCQTEGF-PSGSCDFHVANRKCYSKPCP (Q6RSS6)	50	5377.21/7.91	<i>Picea glauca</i> (Pinaceae)	<i>Nectria galligena</i> (MIC = 2.6 μM *); <i>F. oxysporum</i> (MIC = 2.6 μM *)	[51]
PgD5	RMCESQSHKFKGYC-ASSNCKVVCQTE-KFLTGSCRDTHTFGNRR-CFCEKPC	50	5729.62/7.72		<i>F. oxysporum</i> (MIC = 1.92 μM *); <i>V. dahliae</i> (MIC = 0.35 μM *); <i>B. cinerea</i> (MIC = 0.7 μM *)	
PsDef1	RMCKTPSGKFKGY-CVNNNTNCKNVCRTG- GFPTGSCDFHVAGR-KCYCYKPCP (A4L7R7)	50	5601.58/8.12	<i>Pinus sylvestris</i> (Pinaceae)	<i>F. solani</i> UKM F-50639 (IC <sub>50</sub> = 0.16 μM *); <i>F. oxysporum</i> UKM F-52897 (IC <sub>50</sub> = 0.52 μM *); <i>B. cinerea</i> UKM F-16753 (IC <sub>50</sub> = 0.07 μM *)	[90]
Ec-AMP-D1	RECQSQSHRYK-GACVHDTNCASV-CQTEGFSGGKC-VGFRGRFCFTKAC (P86518)	47	5107.82/7.54	<i>Echinochloa crusgalli</i> (Poaceae)	<i>F. graminearum</i> (IC <sub>50</sub> = 2.94 μM *); <i>F. verticillioides</i> (IC <sub>50</sub> = 1.66 μM *); <i>Diplodia maydis</i> (IC <sub>50</sub> = 2.45 μM *); <i>F. oxysporum</i> (IC <sub>50</sub> = 19.97 μM *)	[91]
Ec-AMP-D2	RECQSQSHRYK-GACVHDTNCASV-CQ-TEGFSGGKCVGF-RGRFCFTKHC (P86519)	47	5173.89/7.54		<i>F. oxysporum</i> (IC <sub>50</sub> = 19.71 μM *)	
Pp-AMP1	KSCCRSTQARNI-YNAPRFAGGSRP-LCALGSGCKIVD-DKKTTPND	44	4697.39/8.61	<i>Phyllostachys pubescens</i> (Poaceae)	<i>F. oxysporum</i> IFO 6384 (IC <sub>50</sub> = 0.43 μM *)	[92]
Pp-AMP2	KSCCRSTTART-ARVPCAKKSNIYN-GCRVPPGGCKIQE-AKKCEPPYD	45	4919.76/8.52		<i>F. oxysporum</i> IFO 6384 (IC <sub>50</sub> = 0.41 μM *)	
Sd1	RYCLSQSHRF-KGLCMSSNCA-NVCQTFENFPGGEC-KADGATRKCFCCKIC (B2CNV2)	49	5412.32/7.72	<i>Saccharum officinarum</i> (Poaceae)	<i>A. niger</i> (IC <sub>50</sub> = 2.0 μM); <i>F. solani</i> (IC <sub>50</sub> = 1.0 μM)	[93]
Sd3	RHRHCFQSQSHKFGA-CLRESNCENVCKTEGF-PSGECKWHGIVSK-CHCKRIC	51	5864.82/7.73		<i>A. niger</i> (IC <sub>50</sub> = 1.0 μM); <i>F. solani</i> (IC <sub>50</sub> > 20 μM)	
Sd5	HTPTPTPICKSRSE-YKGRCIQDMDCNAAC-VKESESYTGGFCNGR-PPFKQCFCTKPKCKRE-RAAATLRWPGL (A0A1B3B2K6)	71	7967.21/7.91		<i>A. niger</i> (IC <sub>50</sub> > 20 μM); <i>F. solani</i> (IC <sub>50</sub> = 10 μM)	

Table 1. Cont.

Defensin	Amino Acid (AA) Sequence (Accession n°)	AA n°ber	MM (Da)/pI	Organism (Family)	Targeted Species (IC50 and MIC)	Ref.
SI alpha-1	RVCMGKSQHHSFPCI-SDRLCSNECVKEEGGW-TAGYCHLRYCRCQKAC (P21923)	47	5382.26/7.33	<i>Sorghum bicolor</i> (Poaceae)	<i>B. cinerea</i> K1147 (IC <sub>50</sub> = 18.58 μM *); <i>C. sphaerospermum</i> K0791 (IC <sub>50</sub> = 14.86 μM *); <i>F. culmorum</i> K0311 (IC <sub>50</sub> = 37.16 μM *); <i>P. digitatum</i> K0879 (IC <sub>50</sub> = 37.16 μM *); <i>T. viride</i> K1127 (IC <sub>50</sub> = 9.29 μM *)	[63]
Tk-AMP-D1	RTCQSQSHKFKGAC-FSDTNCDSVCRTEFN-PRGQCNQHHVERK-CYCERDC (P84963)	49	5744.40/7.1	<i>Triticum kiharae</i> (Poaceae)	<i>F. graminearum</i> (IC <sub>50</sub> = 5.22 μM *); <i>F. verticillioides</i> (IC <sub>50</sub> = 5.22 μM *)	[91]
ZmD32	RTCQSQSHRFRGPCL-RRSNCANVCRTGEGF-PGGRRCRGFRRRCFC-TTHC (A0A317Y7J2)	47	5466.33/10.85	<i>Zea mays</i> (Poaceae)	<i>F. graminearum</i> PH-1 (IC <sub>50</sub> = 1 μM)	[94]
ZmESR6	KLCSTTMDLLICGGA-IPGAVNQACDDTCRN-KGYTGGGFNCNMK-IQRCVCRKPC (D1MAH4)	52	5516.57/7.52		<i>F. oxysporum</i> f.sp. Conglutinans (IC <sub>50</sub> = 3 μM); <i>F. oxysporum</i> f.sp.lycopersici (IC <sub>50</sub> = 3 μM); <i>Plectosphaerella cucumerina</i> (IC <sub>50</sub> = 2 μM)	[95]
Fa-AMP1	AQCGAQGGGATCP-GGLCCSQWGWCGSTPKYCGAGCQSN-CK (P0DKH7)	40	3887.42/7.07	<i>Fagopyrum esculentum</i> (Polygonaceae)	<i>F. oxysporum</i> IFO 6384 (IC <sub>50</sub> = 4.89 μM *)	[96]
Fa-AMP2	AQCGAQGGGATCPGG-LCCSQWGWCGSTPKYCGAGCQSNCR (P0DKH8)	40	3915.44/7.07		<i>F. oxysporum</i> IFO 6384 (IC <sub>50</sub> = 7.41 μM *)	
Ns-D1	KFCEKPSGTWSGV-CGNSGACKDQCIR-LEGAKHGSCNY-KPPAHRICICYEC (P86972)	50	5487.32/7.32	<i>Nigella sativa</i> (Ranunculaceae)	<i>A. niger</i> VKM F-33 (IC <sub>50</sub> = 0.64 μM *); <i>B. sorokiniana</i> VKM F-1446 (IC <sub>50</sub> = 0.55 μM *); <i>F. oxysporum</i> (IC <sub>50</sub> = 1.73 μM *); <i>F. graminearum</i> VKM F-1668 (IC <sub>50</sub> = 1.26 μM *); <i>F. culmorum</i> VKM F-2303 (IC <sub>50</sub> = 1.26 μM *); <i>B. cinerea</i> (IC <sub>50</sub> = 4.99 μM *)	[97]
Ns-D2	KFCEKPSGTWSGV-CGNSGACKDQCIRLE-GAKHGSNYKLP-AHRICICYEC (P86973)	50	5503.36/7.32		<i>A. niger</i> VKM F-33 (IC <sub>50</sub> = 0.64 μM *); <i>B. sorokiniana</i> VKM F-1446 (IC <sub>50</sub> = 0.33 μM *); <i>F. oxysporum</i> (IC <sub>50</sub> = 0.96 μM *); <i>F. graminearum</i> VKM F-1668 (IC <sub>50</sub> = 1.25 μM *); <i>F. culmorum</i> VKM F-2303 (IC <sub>50</sub> = 1.25 μM *); <i>B. cinerea</i> (IC <sub>50</sub> = 2.49 μM *)	

Table 1. Cont.

Defensin	Amino Acid (AA) Sequence (Accession n°)	AA n°ber	MM (Da)/pI	Organism (Family)	Targeted Species (IC50 and MIC)	Ref.
Ah-AMP1	LCNERPSQTWSGNC-GNTAHCDKQCQD-WEKASHGACH-KRENHWKFCYFNC (Q7M1F3)	50	5863.53/6.82	<i>Aesculus hippocastanum</i> (Sapindaceae)	<i>B. cinerea</i> K1147 (IC <sub>50</sub> = 4.26 μM *); <i>C. sphaerospermum</i> K0791 (IC <sub>50</sub> = 0.85 μM *); <i>F. culmorum</i> K0311 (IC <sub>50</sub> = 2.05 μM *); <i>F. culmorum</i> K0311 (IC <sub>50</sub> = 0.12 μM *); <i>L. maculans</i> LM36uea (IC <sub>50</sub> = 0.09 μM *); <i>P. digitatum</i> K0879 (IC <sub>50</sub> = 1.02 μM *); <i>T. viride</i> K1127 (IC <sub>50</sub> = 17.05 μM *); <i>S. tritici</i> K1097 (IC <sub>50</sub> = 0.85 μM *); <i>V. albo-atrum</i> K0937 (IC <sub>50</sub> = 1.02 μM *)	[63]
Hs-AFP1	DGVKLCDVPSGTWS-GHCGSSSKCSQQCKD-REHFAYGGACHYQ-FPSVKCFCKRQC (P0C8Y5)	54	5948.76/7.32	<i>Heuchera sanguinea</i> (Saxifragaceae)	<i>B. cinerea</i> K1147 (IC <sub>50</sub> = 1 μM *); <i>C. sphaerospermum</i> K0791 (IC <sub>50</sub> = 0.2 μM *); <i>F. culmorum</i> K0311 (IC <sub>50</sub> = 0.2 μM *); <i>L. maculans</i> LM36uea (IC <sub>50</sub> = 4.2 μM *); <i>P. digitatum</i> K0879 (IC <sub>50</sub> = 0.2 μM *); <i>T. viride</i> K1127 (IC <sub>50</sub> = 2.5 μM *); <i>S. tritici</i> K1097 (IC <sub>50</sub> = 0.1 μM *); <i>V. albo-atrum</i> K0937 (IC <sub>50</sub> = 1 μM *)	
NaD1	RECKTESNTFPGICITK-PPCRKACISEKFTDGH-CSKILRRRCLCTKPC (Q8GTM0)	47	5304.37/7.91	<i>Nicotiana alata</i> (Solanaceae)	<i>A. niger</i> 5181 (IC <sub>50</sub> = 2.1 ± 0.76 μM); <i>A. flavus</i> 5310 (IC <sub>50</sub> > 10 μM); <i>F. oxysporum</i> f.sp. Vasinfectum (IC <sub>50</sub> = 1.5 ± 0.25 μM); <i>F. graminearum</i> (IC <sub>50</sub> = 0.4 ± 0.3 μM); <i>Colletotrichum graminicola</i> (IC <sub>50</sub> = 4.4 ± 0.1 μM); <i>Aspergillus parasiticus</i> 4467 (IC <sub>50</sub> = 4.5 ± 0.27 μM)	[98]
NaD2	RTCESQSHRFKGPCA-RDSNCATVCLTEGFSG-GDCRGFRRRCFCTRPC (A0A1B2YL15)	47	5264.02/7.76		<i>V. dahliae</i> (IC <sub>50</sub> = 0.75 μM); <i>Thielaviopsis basicola</i> (IC <sub>50</sub> = 1 μM); <i>Aspergillus nidulans</i> (IC <sub>50</sub> = 0.8 μM); <i>Puccinia coronata</i> f.sp. Avenae (IC <sub>50</sub> = 2.5 μM); <i>Puccinia sorghi</i> (IC <sub>50</sub> = 2 μM)	[99]
					<i>F. oxysporum</i> f.sp. Vasinfectum (IC <sub>50</sub> = 8.3 μM); <i>F. graminearum</i> (IC <sub>50</sub> = 2 μM); <i>V. dahliae</i> (IC <sub>50</sub> > 10 μM); <i>T. basicola</i> (IC <sub>50</sub> = 7 μM); <i>A. nidulans</i> (IC <sub>50</sub> = 5 μM); <i>P. coronata</i> f.sp. Avenae (IC <sub>50</sub> = 4 μM); <i>P. sorghi</i> (IC <sub>50</sub> = 5 μM)	

Table 1. Cont.

Defensin	Amino Acid (AA) Sequence (Accession n°)	AA n°ber	MM (Da)/pI	Organism (Family)	Targeted Species (IC50 and MIC)	Ref.
PhD1	ATCKAECPTWDSVC-INKKPCVACCKKAKFS-DGHCSKILRRCLCTKEC (Q8H6Q1)	47	5211.33/7.67	<i>Petunia hybrida</i> (Solanaceae)	<i>F. oxysporum</i> (MIC = (0–0.38) μM *); <i>B. cinerea</i> (MIC = (0.38–1.92) μM *)	[100]
PhD2	GTCKAECPTWEGIC-INKAPCVKCKKAQPE-KFTDGHCSKILRRCL-CTKPC (Q8H6Q0)	49	5403.55/7.52		<i>F. oxysporum</i> (MIC = (0.38–1.92) μM *); <i>B. cinerea</i> (MIC = (0.38–1.92) μM *)	
Vv-AMP1	RTCESQSHRFKGTG-VRQSNCAAVCQTEGFH-GGNCRGFRRRRCFCTKHC (D7TAI4)	47	5355.13/8.24	<i>Vitis vinifera</i> (Vitaceae)	<i>F. oxysporum</i> ATCC 10,913 (IC <sub>50</sub> = 1.12 μM *); <i>V. dahliae</i> ATCC 96,522 (IC <sub>50</sub> = 0.34 μM *); <i>F. solani</i> (IC <sub>50</sub> = 1.79 μM *); <i>B. cinerea</i> (IC <sub>50</sub> = 2.43 μM *)	[101]
Invertebrate defensin						
AgDef1	ATCDLASGFGVGSLL-CAAHCIARRYRGGYCN-NSKAVCVCRN (B2FZB7)	40	4141.80/7.82	<i>Anopheles gambiae</i> (Insecta)	<i>F. culmorum</i> (MIC = (3–6) μM); <i>F. oxysporum</i> (MIC = (1.5–3) μM)	[30]
Defensin ARD1	DKLIGSCVWGA VNYTS-NCNAECKRRRGYKGGH-CGSFANVNCWCET (P84156)	44	4803.43/7.24	<i>Archaeoprepone demophon</i> (Insecta)	<i>Aspergillus fumigatus</i> GASP 4707 (MIC = 2.6 μM *)	[102]
DEFC	ATCDLLSGFGVGD SA-CAAHCIARRNRGGYCN-AKKVCVCRN (P81603)	40	4161.84/7.81	<i>Aedes aegypti</i> (Insecta)	<i>F. culmorum</i> (MIC = (50–100) μM)	[30]
Drosomycin	DCLSGRYKGPCAVWD-NETCRRVCKEEGRSS-GHCSPSLKCWCEGC (P41964)	44	4897.59/6.75	<i>Drosophila melanogaster</i> (Insecta)	<i>B. cinerea</i> MUCL 30,158 (IC <sub>50</sub> = 1.2 μM); <i>F. culmorum</i> IMI 180,420 (IC <sub>50</sub> = 1.0 μM); <i>A. brassicicola</i> MUCL 20,297 (IC <sub>50</sub> = 0.9 μM); <i>Alternaria longipes</i> CBS 62,083 (IC <sub>50</sub> = 1.4 μM); <i>N. haematococca</i> Collection VanEtten160-2-2 (IC <sub>50</sub> = 1.8 μM); <i>F. oxysporum</i> MUCL 909 (IC <sub>50</sub> = 4.2 μM); <i>A. pisi</i> MUCL 30,164 (IC <sub>50</sub> = 3.2 μM)	[103]
Gm defensin-like peptide	DKLIGSCVWGATNYTS-DCNAECKRRRGYKGGH-CGSFWNVNCWCEE (P85215)	44	4949.53/6.21	<i>Galleria mellonella</i> (Insecta)	<i>A. niger</i> (MIC = (1.4–2.9) μM); <i>Trichoderma harzianum</i> (MIC = (1.4–2.9) μM)	[104]
Galleria defensin	DTLIGSCVWGATNY-TSDCNAECKRRRGYKGGH-CGSFNLVNCWCE (P85213)	43	4720.29/6.2		<i>F. oxysporum</i> (MIC = (8.5–16.9) μM); <i>A. niger</i> (MIC = (1.1–2.1) μM); <i>T. harzianum</i> (MIC = (2.1–4.2) μM)	
Heliomicin	DKLIGSCVWGA VNYTS-DCNGECKRRRGYKGGH-CGSFANVNCWCET (D3G9G5)	44	4790.39/6.87	<i>Heliothis virescens</i> (Insecta)	<i>F. culmorum</i> IMI 180,420 (MIC = (0.2–0.4) μM); <i>F. oxysporum</i> MUCL 909 (MIC = (1.5–3.0) μM); <i>N. haematococca</i> 160.2.2 (MIC = (0.4–0.8) μM); <i>A. fumigatus</i> (MIC = (6–12) μM); <i>T. viride</i> MUCL 19,724 (MIC = (1.5–3) μM)	[105]

Table 1. Cont.

Defensin	Amino Acid (AA) Sequence (Accession n°)	AA n°ber	MM (Da)/pI	Organism (Family)	Targeted Species (IC50 and MIC)	Ref.
PduDef	ATCDLLSAFGVGH-ACA AHCIHG YRGG- YCNSKAVCTCRR (P83404)	40	4101.74/7.55	<i>Phlebotomus duboscqi</i> (Insecta)	<i>A. fumigatus</i> (MIC = 12.5–25 µM); <i>F. culmorum</i> (MIC = 1.56–3.12 µM); <i>F. oxysporum</i> (MIC = 3.12–6.25 µM); <i>T. viride</i> (MIC = 3.12–6.25 µM)	[30]
Phormicin	ATCDLLSGTGINHSA-CAAHCLLRGNRGGY-CNGKGVCCVRN (P10891)	40	4066.69/7.55	<i>Protophormia terraenovae</i> (Insecta)	<i>F. culmorum</i> IMI 180,420 (MIC = 3 µM); <i>F. oxysporum</i> MUCL 909 (MIC = 6 µM)	[105]
					<i>F. culmorum</i> (MIC = (1.5–3.0) µM); <i>F. oxysporum</i> (MIC = (3–6) µM); <i>N. haematococca</i> (MIC = (0.8–1.5) µM); <i>T. viride</i> (MIC = (6–12) µM)	[106]
PxDef	RIPCQYEDATEDTICQ-QHCLPKGYSYGICVSYRCSVCV	37	4233.84/5.27	<i>Plutella xylostella</i> (Insecta)	<i>B. cinerea</i> (MIC = 15.0 µM); <i>Penicillium crustosum</i> (MIC = 13.0 µM); <i>Colletotrichum gloeosporioides</i> Penz. (MIC = 17.3 µM); <i>Colletotrichum orbiculare</i> (MIC = 12.5 µM); <i>F. oxysporum</i> (MIC = 8.0 µM)	[107]
Royalisin	VTCDLLSFKGQVND-ACAANCLSLGKAGG-HCEKGVCI CRKTSFK-DLWDKRF (P17722)	51	5525.45/7.5	<i>Apis mellifera</i> (Insecta)	<i>B. cinerea</i> (MIC = 4.9 µM *)	[108]
Termicin	ACNFQSCWATCQA-QHSIYFRR AFCDRSQ-CKCVFVRG (P82321)	36	4221.89/7.82	<i>Pseudacanthothermes springer</i> (Insecta)	<i>F. culmorum</i> (MIC = (0.2–0.4) µM); <i>F. oxysporum</i> (MIC = (0.8–1.5) µM); <i>N. haematococca</i> (MIC = (0.05–0.1) µM); <i>Trichoderma viridae</i> (MIC = (6–12) µM)	[106]
Cg-Def	GFGCPGNQLKCNH-CKSISCRAGYCDAA TLW-LRCTCTDCNGKK (Q4GWV4)	43	4642.40/7.53	<i>Crassostrea gigas</i> (Bivalvia)	<i>B. cinerea</i> (MIC > 20 µM); <i>P. crustosum</i> (MIC > 20 µM); <i>F. oxysporum</i> (MIC = 9 µM)	[109]
MGD-1	GFGCPNNYQCHRHC-KSIPGRCCGYCGW-HRLRCTCYRC (P80571)	38	4351.07/7.99	<i>Mytilus galloprovincialis</i> (Bivalvia)	<i>F. oxysporum</i> (MIC = 5 µM)	[110]
DefMT3	GYC PFRQDKCHRHC-RSFGRKAGYCGNF-LKRTCICVKK (A0A089VRA3)	38	4531.39/9.09	<i>Ixodes ricinus</i> (Arachnida)	<i>F. culmorum</i> (IC <sub>50</sub> = 4 µM); <i>F. graminearum</i> 8/1 (IC <sub>50</sub> = 4 µM)	[36]
DefMT5	GFFCPYNGYCDRHCR-KKLRRRGGYCGG-RWKLTCICIMN	38	4533.43/9.11		<i>F. culmorum</i> (IC <sub>50</sub> = 4 µM); <i>F. graminearum</i> 8/1 (IC <sub>50</sub> = 4 µM)	
DefMT6	GFGCPLNQGACHNH-CRSIKRRGGYCSGII-KQTCTCYRK	38	4217.95/8.76		<i>F. culmorum</i> (IC <sub>50</sub> = 12 µM); <i>F. graminearum</i> 8/1 (IC <sub>50</sub> = 2 µM)	

Table 1. Cont.

Defensin	Amino Acid (AA) Sequence (Accession n°)	AA n°ber	MM (Da)/pI	Organism (Family)	Targeted Species (IC50 and MIC)	Ref.
Holosin 2	GFGCPLNQRACHR-HCRSIGRRGGFCA-GLIKQTCTCYRK (A0A5C1Z8V5)	38	4256.05/9.39	<i>Ixodes holocyclus</i> (Arachnida)	<i>F. graminearum</i> PH-1 (MIC = 5 µM)	[111]
Holosin 3	GFGCPNEWRCNAH-CKRNRFRGGYCDSWF-RRRCHCYG (A0A5C1ZAY3)	36	4400.01/8.59		<i>F. graminearum</i> PH-1 (MIC = 5 µM)	
Juruin	FTCAISCDIKVNGKPC-KGSGEKKCSGGW-SCKFNVCVKV (B3EWQ0)	38	4012.80/7.99	<i>Avicularia juruensis</i> (Arachnida)	<i>A. niger</i> (MIC = (5–10) µM)	[112]
Scapularisin-3	AFGCPFDQGTCHSHC-RSIRRRGERCSGFAKRT-CTCYQK (B7Q4Z2)	38	4355.00/8.49	<i>Ixodes scapularis</i> (Arachnida)	<i>F. culmorum</i> (IC <sub>50</sub> = 0.5 µM); <i>F. graminearum</i> 8/1 (IC <sub>50</sub> = 1 µM)	[113]
Scapularisin-6	GFGCPFDQGACHR-HCQSIGRRGGYAG-FIKQTCTCYHN (Q5Q979)	38	4180.76/7.55		<i>F. culmorum</i> (IC <sub>50</sub> = 1 µM); <i>F. graminearum</i> 8/1 (IC <sub>50</sub> = 2 µM)	
Vertebrate defensin						
Hepcidin-1 (Hepcidin-6)	CRFCCRCPPMRGC-GLCCRF	20	2374.04/7.77	<i>Acanthopagrus schlegelii</i> (Sparidae)	<i>A. niger</i> CGMCC 3.316 (MIC = 20–40 µM); <i>F. graminearum</i> CGMCC 3.3490 (MIC = 20–40 µM); <i>F. solani</i> CGMCC 3.5840 (MIC = 20–40 µM)	[114]
Hepcidin-2	SPAGCRFCGCGCPN-MRGCGVCCRF (Q68M56)	24	2531.12/7.33		<i>A. niger</i> CGMCC 3.316 (MIC = 40–60 µM); <i>F. graminearum</i> CGMCC 3.3490 (MIC > 60 µM); <i>F. solani</i> CGMCC 3.5840 (MIC > 60 µM)	
Hepcidin	GCRFCCNCCPNMSGC-GVCCRF (P82951)	21	2263.79/7.08		<i>A. niger</i> (MIC = 44 µM)	[115]
Crotamine	YKQCHKKGGHG-FPKEKICLPPSSDFGKM-DCRWRWKCKKGGSG (Q9PWF3)	42	4889.85/8.58	<i>Crotalus durissus terrificus</i> (Viperidae)	<i>A. fumigatus</i> IOC 4526 (MIC >25.5 µM *)	[116]
Spheniscin-2	SFGLCRLRRGFCARGRC-RFPSIPIGRCSRFBVQCCRR-VW (P83430)	38	4507.47/11.47	<i>Aptenodytes patagonicus</i> (Spheniscidae)	<i>A. fumigatus</i> (MIC = (3–6) µM)	[117]
Human drosomycin-like defensin	CLAGRLDKQCTCR-RSQPSRRSGHEVGRP-SPHCGPSRQCGCHMD	43	4751.43/8.15	<i>Homo sapiens</i> (Hominidae)	<i>A. fumigatus</i> ATCC MYA1163 (MIC = 6.25 µM); <i>A. nidulans</i> AZN 2867 (MIC = 6.25 µM); <i>Aspergillus ustus</i> (MIC = 12.5 µM); <i>F. solani</i> AZN 6836 (MIC = 25 µM); <i>F. oxysporum</i> (MIC = 6.25 µM)	[118]

Table 1. Cont.

Defensin	Amino Acid (AA) Sequence (Accession n°)	AA n°ber	MM (Da)/pI	Organism (Family)	Targeted Species (IC50 and MIC)	Ref.
Fungus defensin						
AFP	ATYNGKCYKKD-NICKYKAQSGKTAICK-CYVKKCPRDGAKCEFD-SYKGGKCYC (P17737)	51	5805.86/8.34	<i>Aspergillus giganteus</i> (Trichocomaceae)	<i>Fusarium sporotrichioides</i> IfGB 39/1601 (MIC = 0.02 µM *); <i>F. moniliforme</i> IfGB 39/1402 (MIC = 0.02 µM *); <i>A. niger</i> ATCC 9029 (MIC = 0.17 µM *); <i>A. niger</i> NRRL 372 (MIC = 0.17 µM *); <i>A. niger</i> IfGB 15/1803 (MIC = 0.17 µM *); <i>Fusarium equiseti</i> IfGB 39/0701 (MIC = 0.17 µM *); <i>Fusarium lactis</i> IfGB 39/0701 (MIC = 0.17 µM *); <i>F. oxysporum</i> IfGB 39/1201 (MIC = 0.17 µM *); <i>Fusarium proliferatum</i> IfGB 39/1501 (MIC = 0.17 µM *); <i>Fusarium sp.</i> IfGB 39/1101 (MIC = 0.17 µM *); <i>Aspergillus awamori</i> ATCC 22,342 (MIC = 0.34 µM *); <i>F. oxysporum</i> f.sp. lini IfGB 39/0801 (MIC = 1.38 µM *); <i>Fusarium bulbigenum</i> IfGB 39/0301 (MIC = 1.72 µM *); <i>F. oxysporum</i> f.sp. vasinfectum IfGB 39/1301 (MIC = 1.72 µM *); <i>F. solani</i> IfGB 39/1001 (MIC = 20.67 µM *); <i>Fusarium poae</i> IfGB 39/0901 (MIC = 31 µM *); <i>A. nidulans</i> DSM 969 (MIC = 34.45 µM *); <i>A. nidulans</i> G191 (MIC = 34.45 µM *); <i>A. giganteus</i> IfGB 15/0903 (MIC = 68.90 µM *); <i>A. giganteus</i> MDH 18,894 (MIC = 68.90 µM *); <i>Fusarium aquaeductuum</i> IfGB 39/0101 (MIC = 68.90 µM *); <i>F. culmorum</i> IfGB 39/0403 (MIC = 68.90 µM *)	[119]
PAFB	LSKFGGECSLKHNTCT-YLKGGKNHVVNCGS-AANKKCKSDRHHCE-YDEHHKRVDCQTPV (D0EXD3)	58	6500.36/7.74	<i>Penicillium chrysogenum</i> (Trichocomaceae)	<i>A. fumigatus</i> (MIC = 0.25 µM); <i>A. niger</i> (MIC = 0.50 µM); <i>Aspergillus terreus</i> (MIC = 1 µM)	[120]
PAF	AKYTGKCTKSKNEC-KYKNDAGKDTFIKC-PKFDNKKCTKDNNK-CTVDTYNNAVDCCD (Q01701)	55	6250.08/7.89		<i>A. fumigatus</i> (MIC = 1 µM); <i>A. niger</i> (MIC = 0.25 µM); <i>A. terreus</i> (MIC = 32 µM)	
AnAFP	LSKYGGECSEVHNCT-TYLKGGKDHI VSCPSA-ANLRCRTERHHCEY-DEHHKTVDCCQTPV (A2QM98)	58	6517.29/6.24	<i>A. niger</i> (Trichocomaceae)	<i>A. flavus</i> KCTC 1375 (MIC = 8 µM); <i>A. fumigatus</i> KCTC 6145 (MIC = (4–8) µM); <i>F. oxysporum</i> KCTC 6076 (MIC = (8–15) µM); <i>F. solani</i> KCTC 6326 (MIC = 8 µM)	[121]

Table 1. Cont.

Defensin	Amino Acid (AA) Sequence (Accession n°)	AA n°ber	MM (Da)/pI	Organism (Family)	Targeted Species (IC50 and MIC)	Ref.
AcAFP	ATYDGCKCYKK-DNICKYKAQSGKT (D3Y2M3)	24	2717.14/8.43	<i>Aspergillus clavatus</i> (Trichocomaceae)	<i>F. oxysporum</i> (MIC = 8.57 $\mu$ M *); <i>F. oxysporum</i> (IC50 = 1.25 $\mu$ M *)	[122]
NFAP	LEYKGECFTKDNTC-KYKIDGKTYLAKCP-SAANTKCEKDGKCT-YDSYNRKVKCDFRH (A1D8H8)	57	6625.56/7.92	<i>Neosartorya fischeri</i> (Trichocomaceae)	<i>A. niger</i> (MIC = (3.77–15.09) $\mu$ M *); <i>A. nidulans</i> (MIC = 30.19 $\mu$ M *)	[123]

The literature, from which the data presented were compiled, was selected from papers published from 1990 to 2021, using the search engines PubMed and ResearchGate, with different associations of the keywords “defensin”, “antifungal” and “plant”. Defensins were classified into four groups based on their organism of origin: the vertebrates, the invertebrates, the plants and the fungi. The minimum inhibitory concentration (MICs) and half-maximal inhibitory concentrations (IC50) noted “\*” were calculated from the mass concentrations and molecular mass. The molecular mass (MM) was calculated as the average mass with peptide 2.0. The iso-electric was calculated with IPC 2.0. The accession number is the reference from Uniprot.

As shown in Table 1, most defensins that have been characterized to date for their capacity to restrain the growth of plant-infecting fungi belong to the plant defensin group. Among the 67 plant defensins and DLPs identified through our literature search, the majority of them were isolated from plants of the *Fabaceae* (mainly related to various *Medicago*, *Vigna* and *Pisum* species) and *Brassicaceae* (e.g., *Raphanus*, *Sinapis*, *Arabidopsis* and *Brassica* species) families. RsAFP1 and RsAFP2 from *Raphanus* and *Brassica* species [29,63,67], MtDef2 and MtDef4 from *M. truncatula* [35,56] and Nad1 and Nad2 from *N. alata* [98,99] were those for which the antifungal activity against plant pathogens were the most extensively documented. Regarding invertebrate defensins, 22 peptides have been shown as efficient to restrain the growth of plant infecting fungi. With the exception of Cg-Def isolated from *C. gigas* [109] and MGD-1 from *M. galloprovincialis* [110], these antifungal invertebrate defensins have been found in insect and arachnid species. The literature review highlighted six defensins from filamentous fungi and six defensins from vertebrates with a reported activity against phytopathogenic fungi: three occurring in fish species, one from a snake species, one in a penguin species and one homologue of the *Drosophila*-derived drosomycin observed in humans [114–118]. The small proportion of fungi and animal defensins listed in Table 1 supports previously published conclusions indicating that plant defensins primarily exhibited activity against fungi while fungal and animal defensins have efficient antibacterial properties [48]. The previous statement should, however, be put in balance with the history of research dedicated to defensins. Actually, as illustrated in the review of Silva et al. [41], the research addressing the antifungal bioactivity of defensins has only increased in a really more recent past that dedicated to antibacterial effects. It is therefore reasonable to assume that the antifungal activity of animal defensins, which were the first identified defensins, has been understudied. To evidence the antifungal properties of defensins, a broad set of targeted fungi has been used. The list reported in Table 1 includes fungi responsible for major plant diseases, such as the phytopathogenic fungi of cereal crops (*F. culmorum* and *F. graminearum*, *S. tritici* and *Pycularia oryzae*) or of cruciferous crops (*Leptosphaeria maculans*), fungi affecting grape quality (*B. cinerea*) and fungi infecting fruit and vegetable crops (*F. oxysporum*, *F. solani*, *N. haematococca*). Among this list of targeted fungi, several species are acknowledged as responsible for crop contamination by mycotoxins. This is the case, for example, of *F. graminearum* and *F. culmorum* that are the main causal agents of cereal contamination with deoxynivalenol mycotoxin [8] of *F. verticillioides* that produces fumonisins on maize grains [124] and of the ochratoxin-producing *A. niger* species and the sterigmatocystin-producing *A. versicolor* and *nidulans* species [125].

To assess the antifungal efficacy of defensins, MIC and/or IC<sub>50</sub> were used (Table 1). It should be borne in mind that the heterogeneity of experimental procedures targeting

the fungal strain and fungal growth assessment method—especially with regard to culture conditions—makes it difficult to compare results from different studies. Nevertheless, for the tests realized within a same study and using similar protocols, differences in MIC and IC<sub>50</sub> values may reveal the occurrence of variations in the specificity of defensins towards pathogens and/or in their mode of action. Thus, the data reported in Table 1 indicate a significantly higher efficacy of the AFP defensin from *A. giganteus* against *F. sporotrichioides* (MIC value of 0.1 µg/mL which corresponds to a 0.02 µM concentration) than against *F. culmorum* (MIC value higher than 70 µM) [119]. Such differences in antifungal efficacy were also reported for the RsAFP1 defensin from *R. sativus* that has been characterized by a 0.05 µM MIC value when tested against the rice blast fungus *P. oryzae* and a 17.6 µM MIC value against the Basidiomycota *R. solani* [67]. The RsAFP1 defensin was also shown to be twice as efficient against *F. oxysporum* f. sp. *Pisi* (IC<sub>50</sub> = 2.65 µM) than against *F. oxysporum* f. sp. *Lycopersici* (IC<sub>50</sub> = 5.3 µM) [29,67]. Additionally, as illustrated with PAF and PAFB from *P. chrysogenum* tested against various *Aspergillus* species [120], different defensins from the same origin can display important disparity in their antifungal effectiveness and their target specificity. Finally, data gathered in Table 1 also support the point that one fungal species can be more or less affected by defensins of different origin. Thus, *B. cinerea* was shown to be approximately twice as sensitive to the DM-AMP1 defensin from *D. merckii* than to the Ah-AMP1 defensin from horse chestnut *A. hippocastanum* [63].

In addition to assessing the antifungal efficacy of defensins, some authors have considered the specific activity of their  $\gamma$ -core. For instance, Tonk et al. [36] have reported that the  $\gamma$ -core of the defensin DefMT3 was two to four times more efficient in inhibiting the spore germination of *F. graminearum* and *F. culmorum* than the mature defensin. In contrast, the  $\gamma$ -core of the defensins MtDef4 and MtDef5 exhibited a lower inhibitory potential against Ascomycota *F. oxysporum* and *P. medicaginis* than the parental defensins [35]. These opposite results may be related to the absence/presence of disulfide bridges and/or creation of oligomers. To identify the determinants of the  $\gamma$ -core activity, structure/function investigations have been implemented; and  $\gamma$ -core sequences and degree of inhibitory efficiency have been compared. Such approaches have allowed Lacerda et al. [126] and Leannec-Rialland et al. [127] to demonstrate that the positively charged amino acids located in the  $\gamma$ -core were essential for the antifungal activity; other structural motifs responsible for antimicrobial activity being the  $\alpha$ -patch, the  $\gamma$ -patch, and m-loop [128,129].

Although several reports have documented the antifungal activity of defensins against plant pathogens, very few have investigated their potential to inhibit the yield of mycotoxins. To our knowledge, this potential was first demonstrated by Leannec-Rialland et al. [127], who showed the remarkable efficacy of the  $\gamma$ -core of the tick defensin DefMT3 to inhibit the production of type B trichothecenes by *F. graminearum*. The previous authors also evidenced that the tertiary structure of the peptide, the occurrence of dimer forms and its cationic properties were primary factors involved in the mycotoxin inhibition activity of DefMT3  $\gamma$ -core.

#### 4. Antifungal Mechanism of Action of Defensins

Defensins with an acknowledged antifungal activity are classified into two groups according to their antimicrobial action: (i) the morphogenic defensins, causing a reduced hyphal elongation with an increase in hyphal branching; and (ii) the non-morphogenic defensins that lead to a reduction in the hyphal elongation without provoking observable changes in hyphae morphology [80,130,131]. For instance, MsDef1 from *M. sativa* that induces the important hyperbranching of fungal hyphae belongs to morphogenic group while MtDef4, from *M. truncatula*, is non-morphogenic [132]. A variety of key features have been proposed to explain the antifungal activity of defensins. These features, schematized in Figure 4 and detailed in the following, are related to fungal membrane binding and the induction of membrane disorders, as well as to the production of reactive oxygen species (ROS) and their interaction with fungal specific targets once the defensin has entered the cytoplasm. According to this multifaceted mechanism of action, defensins have been shown

to affect various fungal pathways. In the recent publication of Aumer et al. [133], the use of a proteomic approach has allowed evidencing the alteration of spliceosome, ribosome protein processing in endoplasmic reticulum, endocytosis, MAPK signaling pathway and oxidative phosphorylation in *B. cinerea* exposed to an analogue of the insect defensin heliomicin. In addition to being comprehensively reviewed by Parisi et al. [134] and Struyfs et al. [135], the antifungal activity of different defensins can result from different mechanisms. While some defensins require crossing the fungal cell wall and plasma membrane to induce cell death, others can exert their toxic effects from the extracellular side of the fungal cells. Moreover, a single defensin can have different mechanisms of action depending on the targeted fungal species [136].

#### 4.1. Interactions with Host Membrane Components and Induction of Fungal Membranes Disorders

For some defensins, the interaction with specific sphingolipids and phospholipids of the plasma membrane is a prerequisite for their antifungal activity [137]. For example, the binding of the DmAPM1 defensin from *D. merckii* to the sphingolipid mannosyl di(inositolphosphoryl)-ceramide has been shown to be critical for triggering its antifungal activity [138]. The specific target of several defensins including MsDef1 from the barre clover *M. sativa*, Sd5 from the sugarcane *S. officinarum*, RsAFP2 from the radish *R. sativus* and Psd1 from the pea *P. sativum* has been identified as glucosylceramide [139–142]. MtDef4 from *M. truncatula* has been shown to specifically interact with phosphatidic acid, a precursor of membrane phospholipids and a signaling lipid, and this interaction has been indicated as necessary for MtDef4 entry into fungal cells [143]. Regarding the defensin NaD1 from *N. alata* and the tomato defensin TPP3, their interaction with phosphatidylinositol (4,5)-bisphosphate, located in the inner leaflet of the membrane, has been reported as essential for the initiation of their cytotoxic effects [144,145]. More recently, the membrane modeling approach used by Leannec-Rialland et al. [127] indicated that the  $\gamma$ -core of the tick defensin DefMT3 was recruited by the phospholipids POPS, POPA and POPG that are present in the *F. graminearum* membrane. Using the in silico modeling or mutational analysis of amino acids, some specific residues located in the loop region of the  $\gamma$ -core motif, such as Phenyl-alanine 28 and Isoleucine 29 in the DefMet3 protein [32] or the RGFRRR motif in MtDef4 [143], have been predicted as critical for the interaction with the lipid bilayer membrane. The binding site of NaD1 was also characterized: this binding site is formed by the Lysine 4 residue and a KILRR motif located between the  $\beta$ -strands of its  $\gamma$ -core motif [144]. In addition to structural features of the  $\gamma$ -core motif, the specific residues located in loop 1 of some defensins have been demonstrated to be involved in the binding with fungal membranes. For example, the Phenylalanine 15 and the Threonine 16 residues present in Loop 1 of the Psd1 defensin have been shown to be involved in the interaction with glucosylceramide [146].

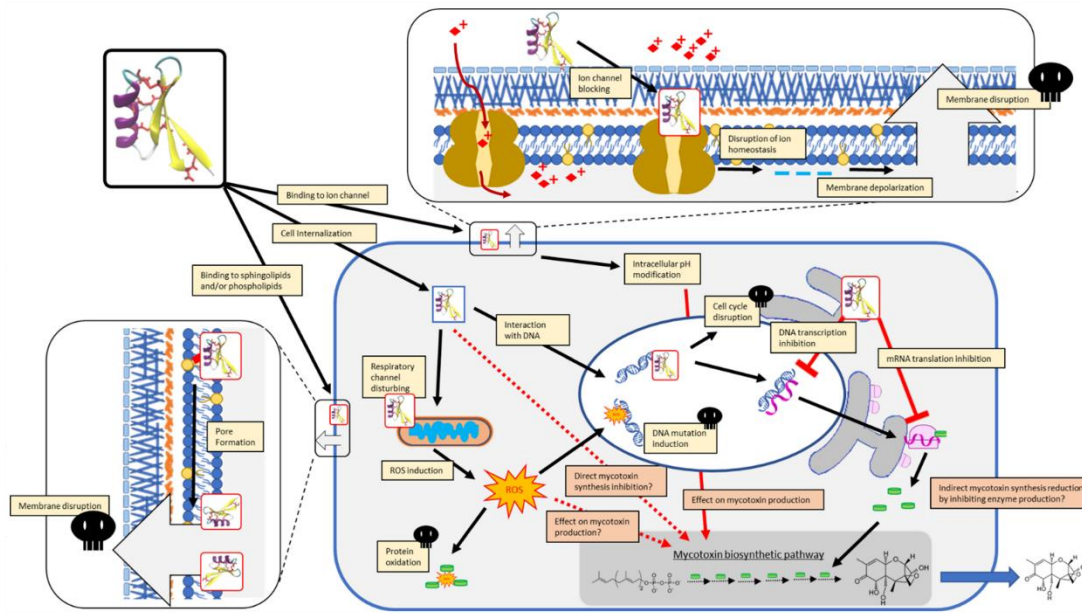


Figure 4. Summary of known and suspected modes of action of defensins displaying antifungal (yellow inserts) and/or antimycotoxin (orange inserts) activity.

As a result of the binding with membrane components, defensins can create pores and permeabilize the membranes, which is, however, acknowledged as only one among several mechanisms involved in the antimicrobial action of defensins [147]. This capacity of pore formation is not shared by all defensins; certain defensins such as plectasin—a fungal defensin from *Pseudoplectania nigrella*—does not affect fungal membrane integrity [148]. Actually, neither pore formation, nor changes in membrane potential, nor carboxy-fluorescein efflux from liposomes were detected by the previous authors when *Bacillus subtilis* were exposed to plectasin. The mechanism involved in plectasin bactericidal activity was reported to be associated with an inhibition of membrane-associated steps of cell-wall biosynthesis [148]. The membrane permeabilization of *Neurospora crassa* caused by various plant defensins was reported by Thevissen et al. [149]—the extent of which is dependent on the defensin dose. Such a membrane-permeabilizing activity was also evidenced for NaD1, which was reported to form a relatively stable aperture with an internal diameter ranging between 14 and 23 Å in *F. oxysporum* membrane [150] and for MtDef5 in *F. graminearum* and *N. crassa* [151]. The capacity of defensins to cause membrane permeabilization is dependent on the fungal target as illustrated for MtDef4. Indeed, while MtDef4 has been shown to induce permeabilization in *F. graminearum*, this mechanism did not appear to contribute to the antifungal effect of MtDef4 against *N. crassa* [136]. Some defensins form oligomers and those oligomers were reported as being the active structures associated with membrane permeabilization and antimicrobial activity [152]. This is the case of defensin SPE10, from the plant *P. erosus*, for which the dimeric form was shown to possess high antifungal properties, possibly favored by its increased hydrophobicity [86]. Similarly, the TPP3 tomato defensin can form a dimeric cationic grip through antiparallel alignment of the  $\beta$  strands, stabilized by hydrogen bonds and salt bridge interactions, which was shown as critical for its interaction with PIP2 (phosphatidylinositol 4,5-bisphosphate) and cytolytic activity [145]. NAD1 from *N. alata* was observed to create an arrangement with seven dimers binding to the anionic headgroups of 14 PIP2, leading to a complex oligomer seemingly important for cell permeabilization [144].

There are currently at least three different commonly accepted models describing the possible membrane-permeabilizing activity of defensins: the barrel-stave pore model, the toroidal pore model and the carpet model. To address these specific pore models in greater depth, we strongly encourage the readers to consult the relevant review of Brogden published in 2005 [153]. Briefly, in the barrel-stave model, antifungal peptides self-aggregate in the membrane in a way that their hydrophobic sites face the phospholipid layers of the membrane while their hydrophilic segments face the lumen of transmembrane pores. In the toroidal model, antifungal peptides and membrane lipids interact to form pores that are lined by both peptide and lipid headgroups. In the carpet model, antifungal peptides bind, in a monomeric or oligomeric form, onto the surface of the negatively charged target membrane and surround it in a carpet-like manner, leading to the disruption of the bilayer curvature and the disintegration of the membrane. The immediate consequence of pore-formation induced by some defensins in fungal membranes is the dissipation of ionic gradients and membrane potential across the cytoplasmic membrane of target cells, triggering cell death. The such dysfunction of calcium influx and potassium efflux can also directly result from the binding of defensins with fungal membrane components. In this way, a membrane potential disruption effect has been proposed to explain the activity of a synthetic tick defensin against *Micrococcus luteus* [154]. Similarly, the plectasin fungal defensin [155] and the *Arabidopsis* defensin AtPDF2.3 [65] were proven to interfere with potassium channels. The pea defensin Psd1 was also characterized for its capacity to disturb potassium channels in mammalian cells; however, this activity was not observed in fungal cells [156]. The maize defensin called  $\gamma$ -zethionin was also reported to affect sodium currents by hindering voltage-operated channels [157]. In the same way, MsDef1 was evidenced to perturb calcium exchanges in mammalian cells; a blocking of calcium channels was also supposed to be involved in its antimicrobial action against *F. graminearum* [80]. According to the reports of Zhu et al. [158] and Meng et al. [159], the structural  $C\alpha\beta$ -

motif could be a key determinant involved in the capacity of defensins or DLPs to block ion channels.

#### 4.2. Induction of Oxidative Stress and Apoptosis

There is compelling evidence that defensins can induce ROS accumulation within the targeted fungal cells. This has been notably demonstrated for RsAFP2 in *C. albicans* [160,161], for NaD1 in *C. albicans* [162,163] or in *F. oxysporum* [150] and for HsAFP1 in *C. albicans* [164]. It should be noted that internalization is not required for inducing ROS production as RsAFP2, which is not internalized, induces the production of ROS [161]. ROS can instantaneously and nonspecifically react with essential biological molecules and lead to an alteration of cellular functions by inducing damages such as mutations in DNA, oxidations of proteins, or the peroxidation of lipids. These damages are generally deleterious, and could lead to apoptosis and cell death. The induction of apoptosis in *C. albicans* cells exposed to the OsAFP1, RsAFP2 and HsAFP1 defensins, has been clearly demonstrated thanks to the use of epifluorescence methods [161,164,165]. Regarding the effect of RsAFP2 in *C. albicans*, apoptosis induction was shown to concomitantly occur with an activation of caspases or caspase-like proteases [161]. Since it is strongly suspected that the biosynthesis of mycotoxins could help the fungal cell maintain safe levels of intracellular ROS [166], it makes sense to suggest that ROS accumulation triggered by defensins could affect the production of mycotoxins by toxigenic fungi. However, to date, this potential link between ROS induction by defensins and modulation of mycotoxin yield has not been addressed.

#### 4.3. Internalization and Intracellular Targets

The use of fluorescently labeled peptides coupled to confocal microscopy has boosted the demonstration of cell internalization of various defensins. The translocation of defensins across fungal cell membrane can occur in a non-disruptive manner, frequently for peptide concentrations and/or exposure times that do not lead to significant growth alteration. For instance, while MtDef4 was shown to permeabilize the plasma membrane of *F. graminearum* before its entry into fungal cells, the internalization of MtDef4 into *N. crassa* cells was reported to occur without membrane permeabilization [136]. According to previous works, MtDef4 internalization in *N. crassa* could be related to endocytosis. Similarly, NaD1 has been reported to bind to a putative cell wall receptor of *C. albicans* and to be taken up to the cytoplasm through endocytosis, causing cytoplasm granulation [150,163]. In fact, the mechanism of non-lytic defensin internalization remains poorly understood [135]. When internalized, defensins can bind intracellular specific targets, inducing signaling cascades. Due to their cationic nature, most defensins are likely to bind nucleic acids which might result in a broad inhibition of DNA synthesis, transcription and/or mRNA translation inside the target cells [167,168]. Such an effect on gene expression could explain the non-morphogenic activity of some defensins and their capacity to interfere with the fungal secondary metabolism, including mycotoxin biosynthesis [127]. One of the most documented defensins for its interaction with intracellular targets is certainly the pea defensin, Psd1. Psd1 has been shown to be translocated to *N. crassa* fungal nucleus and to interact with distinct nuclear proteins including cyclin F and consequently to lead to the disruption of the cell cycle control function in the nuclei [169].

### 5. Exploiting Defensins to Protect Crops from Phytopathogenic Fungi and Mycotoxin Contamination

As illustrated above, several defensins possess efficient and interesting capacities to prevent and/or restrain the growth of phytopathogenic fungi including toxigenic ones and their mechanisms of action have been the subject of numerous investigations. This bioactivity makes defensins promising candidates for consideration in control methods as alternatives to the use of synthetic fungicides. Two application strategies might be explored: the creation of transgenic plants overexpressing antifungal defensins and the formulation of defensin-based plant-care products.

### 5.1. Transgenic Plants Overexpressing Defensin for an Enhanced Resistance to Phytopathogenic Fungi

Gene constructions based on sequences coding for defensins have been expressed in various plant models and/or crops of economic interest. As first reviewed by Montesinos in 2007 [170] and thereafter by Sher Khan et al. [171], these biotechnological developments can provide higher degrees of protection against distinct plant fungal pathogens, either biotrophic, hemi biotrophic or necrotrophic ones. Thus, Gao et al. [81] and Abdallah et al. [172] have reported the increased protection against *F. oxysporum* and *Verticillium dahlia* of potato and tomato plants overexpressing the MsDef1 defensin from *M. sativa*. Similarly, tobacco transformation with MsDef1 led to an improved resistance to *Ralstonia solanacearum* and *A. niger* [173]. DmAMP1 from *D. merckii*, when expressed in papaya, was shown to upscale the resistance to *Phytophthora palmivora* [174] and to reduce symptoms caused by *M. oryzae* and *R. solani* when expressed in rice [175]. The use of RsAFP2 from radish as transgene was demonstrated to enhance tobacco resistance to the pathogen *A. longipes* [68], tomato resistance to *F. oxysporum* [176] and wheat resistance to *R. solani* [177]. Tobacco and potato genetically engineered with NmDef02 from *Nicotiana megalosiphon* were reported to be more tolerant against the oomycete *Phytophthora infestans* [178]. The introduction of the previous NmDef03 transgene was also shown to protect soybean from *Phakopsora pachyrhizi* and *Colletotrichum truncatum* [179]. Lastly, the overexpression of WT1 from *Wasabia japonica* in rice, tomato, potato, egusi melon or tobacco was reported as an efficient strategy to decrease their susceptibility to several phytopathogenic fungi [180–183]. In several studies, a combination of two defensin genes was used. Thus, the genetic engineering of *A. thaliana* with DmAMP1 and RsAFP1 [184], of rice with DmAMP1 and RsAFP2 [185] and of peanut with NPR1 and Tfgd was successfully experimented. Defensins from non-plant origin were also considered in these biotechnological applications. For example, rice transformation with a transgene related to the fungal defensin AFP from *A. giganteus* was shown to improve plant resistance to the pathogen *M. grisea* [186]. Genetically modified tobacco with genes coding for the arthropod defensins, heliomycin or drosomycin, was reported to exhibit a slight but statistically significant enhanced resistance to the fungal pathogen *Cercospora nicotianae* [187]. Lastly, in a few studies, the inserted DNA fragment contains a defensin gene associated with a non-defensin one. Thus, the co-expression of the RsAFP1 gene and the chitinase Chit42 gene from *Trichoderma atroviride* was demonstrated to enhance canola resistance to sclerotinia stem rot disease [188].

Genetic engineering exploiting the bioactivity of plant defensins could also offer a promising approach for manipulating susceptibility to disease induced by toxigenic fungi and for minimizing mycotoxins in harvests. A small number of defensin transgenes have been explored in order to generate crops that display enhanced resistance or tolerance to Fusarium head blight which is mainly caused by *F. graminearum* or to *Aspergillus* spp. disease. The study of Li et al. [177] described reduced symptoms in wheat lines transformed with RsAFP2 compared to the transgenic control cultivar, cultivated in greenhouse and field trials and artificially inoculated with *F. graminearum*. Similarly, an increased resistance to Fusarium head blight was reported in transgenic wheat lines overexpressing the TAD1 defensin gene [189]. Moreover, the potential of defensin-based engineering strategies to alleviate contamination with mycotoxins was clearly demonstrated in the report of Kaur et al. [190] that indicated significantly reduced amounts of deoxynivalenol in the siliques of *Arabidopsis* transgenic lines expressing MtDef4.2 that were inoculated with a toxigenic *F. graminearum* strain. MtDef4 and MtDef5 from *M. truncatula* have also been used to boost the resistance of peanut against *A. flavus* and to minimize the contamination of seeds with aflatoxin [151,191].

However, despite the promising results described above, no defensin transgenic plants that confer improved resistance to pathogenic fungi are yet in the market. Indeed, most of the developed countries have set up full and detailed genetically modified organism regulations that require the achievement of a comprehensive risk assessment procedure prior release on the market and this risk assessment is far from being completed with regard

to defensin transgenic plants. Moreover, the implementation of field trials also remains highly insufficient to allow concluding on critical issues including reproducibility, stability and environmental effects such as the potential occurrence of side effects affecting the crop productivity. Actually, while the expression of Dm-AMP1 in *Solanum melongena* [192] or MtDef4.2 in wheat [193] was reported as harmless to mycorrhizal fungi, some detrimental effects were also observed in a few defensin transgenic plants. The overexpression of DEF2 was reported to alter the architecture of the tomato plant, to reduce pollen viability as well as seed production [194]. Transgenic *A. thaliana* expressing the plant defensins MsDef1, MtDef2, and RsAFP2, were also negatively affected in their growth, root and root hair development [195]. Lastly, political and ethical concerns related to genetically modified organisms should also not be neglected, representing an additional obstacle that the development of defensin transgenic crops has to overcome before reaching the market.

### 5.2. Developing Defensin-Based Plant Protection Products for the Control of Phytopathogenic Fungi

Given their antifungal efficiency even at low doses, defensins are attractive candidates to replace synthetic fungicides or to reduce their amount by a combinatorial use in plant disease management strategy. The capacity demonstrated by some defensins to inhibit the production of mycotoxins, more precisely of deoxynivalenol [127], is an additional argument in favor of their exploitation in agro-products. Indeed, deoxynivalenol is acknowledged to act as a virulence factor for *F. graminearum* infecting wheat; the fungus used deoxynivalenol production to circumvent the plant's defense system and invade spikelets [196]. In addition, since deoxynivalenol production is reported as part of the adaptive response of *F. graminearum* to stressful conditions as those induced by exposure to fungicides [197], it is highly recommended that a fungicide solution that also target the production of deoxynivalenol is applied, which will allow avoiding an increased yield of toxins as has been observed with some synthetic fungicide treatments [198]. Moreover, the multifaceted mechanism employed by defensins against fungi is likely to reduce the risk of the emergence of resistant fungal strains through selective pressures [23]. Actually, as exhaustively reviewed by Fisher et al. [199], the emergence of new virulent and fungicide-resistant strains, mainly due to the intensive use of single-target fungicides, has become a critical threat for agriculture of today and tomorrow. Available published data support the fact that AMPs seem to not induce neither antibacterial nor antifungal resistance [200,201]. Furthermore, some fungal defensins were reported to be able to kill antibiotic-resistant bacteria isolates, supporting the promising use of this class of AMPs [202]. Nevertheless, even though unlikely, it cannot be entirely ruled out that phytopathogenic fungi, that are known as remarkable in their ability to adapt in response to selection pressures, could evolve and develop mechanisms to counter the fungicidal action of pesticide, including cell membrane rearrangement, membrane potential and ionic currents change, or peptide degrading enzyme production [41]. Despite increasing evidence supporting the promising use of defensins, the development of defensin-based protection products requires solutions to several hurdles which will be briefly addressed in the following. The first one is the insufficient amount of data supporting the *in vivo* lack of toxicity of defensins, which hampers a comprehensive assessment of risk and health hazards related to their use as plant protection products and their registration by competent authorities. Indeed, while *in vitro* cytotoxicity studies converged on the null or reduced the toxic side effects of defensins [203], the body of knowledge that has been developed using animal models remains limited and mainly restricted to defensins of bacterial origin [204].

The second major limitation to the application of defensins for controlling phytopathogenic fungi is the lack of optimized process for their production on a large scale. The yields of defensins from natural sources are generally low and the extraction and purification steps are time-consuming and expensive. Chemical synthesis has for a long time been considered as an economically viable solution but only for short peptides and high-value applications [205]. However, recent advances in peptide synthesis method-

ologies have paved the way for the successful synthesis of defensins conserving their biological activity and for reducing associated costs. One of the latest successes of defensin chemical synthesis is the production of the PvD1 defensin from the *P. vulgaris* [206]. In recent years, genetic engineering, which is the privileged technology for the production of large amounts of proteins, has been subject of intense investigation for the large-scale production of defensins. Different heterologous expression systems were studied, including *E. coli* [207], yeasts (*Saccharomyces cerevisiae* or *Pichia pastoris*) and insects. Indeed, the use of advanced insect cell-based expression systems was proposed to overcome limitations due to the antimicrobial activity of defensins that could hamper their heterologous production in bacteria and yeasts and to allow the proper synthesis of folded functional peptides which is more challenging using bacteria [208]. In addition, to minimize the lethal effects of the peptide in the host cell, to protect them from proteolytic degradation and improve their solubility, various strategies were elaborated. The most common strategy is based on the use of fusion proteins, associating a defensin and a carrier protein [209,210]. Thus, thioredoxin [211] and small ubiquitin-related modifier [212–215] have frequently been used as AMPs fusion partner for improving the folding and solubility of the peptide. The promising use of heterologous expression technology to produce defensins and preserve their bioactivity against toxigenic fungal species has been reported by Kant et al. [216] who described the capacity of a recombinant PDC1 corn defensin, expressed in *E. coli* or *P. pastoris*, to inhibit the growth of *F. graminearum*. Interest in the *E. coli* expression system was also recently supported by the study of Al Kashgry et al. [217] which reported the successful production of the MzDef maize defensin and its antifungal activity against *F. verticillioides* and *A. niger*.

Another factor that must be considered for the development of defensin-based plant care products is their stability. As generally small peptides, defensins can be subject to proteolytic degradation by various proteases, resulting in their poor bioavailability and decreased efficacy. However, the intramolecular structure stabilized by disulfide bonds that characterizes defensin makes this class of peptides less proteolytically degradable compared to linear peptides. The occurrence of disulfide bonds has also been reported to confer a high structural stability to defensin at extreme temperatures and pH values [218]. To protect defensins from degradation, improve their solubility and consequently their bioavailability, the use of engineered nano-carriers may be a promising route. Nanoencapsulation systems including micro/nano-suspensions, -emulsions, -particles, -capsules and -hybrids are currently under practice for chemical pesticide application [219], and intensively investigated for medicinal applications of defensins [220].

Last but certainly not least, economic and social acceptance of the use of defensin-based plant fungicides should not be neglected. While integrated pest management practices with less environmental impact including the adoption of biofungicide solutions are convincing an increasing number of farmers [221], the balance between the efficiency and cost of environmentally friendly pesticides can be a barrier for the adoption of these new plant protection solutions. As previously mentioned, efforts should be dedicated to improving the large-scale and low-cost production of defensins and demonstrate their efficiency in field trials. Once these issues are solved, defensin-plant-based solutions will have to be integrated in the framework of policies implemented to change farmer behavior and incentivize the adoption of new practices, which includes advisory services and training, the demonstration of the economic benefits of new and sustainable protection products but also financial support to accompany the transition towards agricultural systems with less use of chemical pesticides [222]. Actually, the adoption and acceptability of defensin-based biopesticides will be impossible without the relevant and wide dissemination of the benefits of their use to stakeholders, which represents a critical step to combat the sometimes negative perception related to new sustainable solutions and avoid their dismissal as a feasible and efficient option for pest management [223]. Defensin-plant-based solutions will also have to meet the requirements for their registration as biofungicides. The term biofungicide mostly refers to fungicides that contain a microorganism as active ingredient, but also in-

volve formulations exploiting the bioactivity of naturally occurring substances. Antifungal peptides with native chemical structure fall within the former definition. The biopesticide registration data portfolio is close to that required for conventional chemical pesticides and includes, among others, information about the mode of action and proof of efficacy, host range testing, toxicological and eco-toxicological evaluations [223]. The guidance of the Organisation for Economic Co-operation and Development (OECD) is that biopesticides should only be authorized if they pose minimal or zero risk. This registration procedure is cumbersome and expensive and can jeopardize the commercialization of a biopesticide such as a defensin-based one if the market seems too small to justify the expenses inherent to its registration. To try solving this issue and boost the development of biopesticides, some countries have modified their legislation so that biological products automatically enter a fast-track review process. This is for instance the case of Canada and the United States, which have implemented a joint review process for biological products whereby a registration dossier receives speedier analysis and once the biopesticide is approved and granted, its commercialization is allowed in both countries simultaneously [224].

## 6. Conclusions

The present review highlights the promising potential of defensins in plant disease treatments to protect crops from phytopathogenic fungi including toxigenic ones. In addition to their efficient antifungal activity and capacity to inhibit the production of mycotoxins, several rationales support the bright future held by this class of natural peptides: defensins exhibit low toxicity to plants and mammals, high stability and solubility, fall within the biopesticide definition and have a possibly low cost of production through microorganism engineering. The development of defensin-based plant protection products could be a new lever to facilitate the transition between current crop production systems based on an intensive use of chemical pesticides towards more sustainable ones. However, despite this outstanding potential, the development of defensin-based biocontrol solutions still faces numerous obstacles. Efforts should be pursued to translate defensin-based in vitro research findings into plant protection products. In addition, the potential offered by defensins in plant disease management is today certainly largely underestimated. Indeed, available knowledge on defensin bioactivity against phytopathogenic fungi is mainly restricted to their antifungal effect and to defensins from plant origin. As previously published [111,113,127], defensins could also exhibit highly promising antimycotoxin efficiency and defensins of invertebrate origin could be an additional source of bioactive peptides. The expansion of peptide libraries and defensin databases, together with the development of bioinformatics and proteomics tools, will certainly contribute to broaden the field of defensin investigation [225].

**Author Contributions:** Conceptualization: V.L.-R., A.C.-C. and F.R.-F.; writing—original draft: V.L.-R. and F.R.-F.; writing—editing and reviewing: M.T.-R., V.A. and S.C. All authors have read and agreed to the published version of the manuscript.

**Funding:** The research was financially supported by INRAE, MICA department (TickTox project, MICA20202021).

**Conflicts of Interest:** Authors declare that there is no conflict of interest.

## References

1. Pennisi, E. Armed and Dangerous. *Science* **2010**, *327*, 804–805. [[CrossRef](#)] [[PubMed](#)]
2. Godfray, H.C.J.; Mason-D’Croz, D.; Robinson, S. Food System Consequences of a Fungal Disease Epidemic in a Major Crop. *Philos. Trans. R. Soc. B Biol. Sci.* **2016**, *371*, 20150467. [[CrossRef](#)] [[PubMed](#)]
3. Savary, S.; Willocquet, L.; Pethybridge, S.J.; Esker, P.; McRoberts, N.; Nelson, A. The Global Burden of Pathogens and Pests on Major Food Crops. *Nat. Ecol. Evol.* **2019**, *3*, 430–439. [[CrossRef](#)] [[PubMed](#)]
4. Fisher, M.C.; Henk, D.A.; Briggs, C.J.; Brownstein, J.S.; Madoff, L.C.; McCraw, S.L.; Gurr, S.J. Emerging Fungal Threats to Animal, Plant and Ecosystem Health. *Nature* **2012**, *484*, 186–194. [[CrossRef](#)] [[PubMed](#)]
5. Velásquez, A.C.; Castroverde, C.D.M.; He, S.Y. Plant–Pathogen Warfare under Changing Climate Conditions. *Curr. Biol.* **2018**, *28*, R619–R634. [[CrossRef](#)] [[PubMed](#)]

6. Fones, H.N.; Beber, D.P.; Chaloner, T.M.; Kay, W.T.; Steinberg, G.; Gurr, S.J. Threats to Global Food Security from Emerging Fungal and Oomycete Crop Pathogens. *Nat. Food* **2020**, *1*, 332–342. [[CrossRef](#)]
7. Dean, R.; Van Kan, J.A.L.; Pretorius, Z.A.; Hammond-Kosack, K.E.; Di Pietro, A.; Spanu, P.D.; Rudd, J.J.; Dickman, M.; Kahmann, R.; Ellis, J.; et al. The Top 10 Fungal Pathogens in Molecular Plant Pathology: Top 10 Fungal Pathogens. *Mol. Plant Pathol.* **2012**, *13*, 414–430. [[CrossRef](#)]
8. Perincherry, L.; Lalak-Kańczugowska, J.; Stępień, Ł. Fusarium-Produced Mycotoxins in Plant-Pathogen Interactions. *Toxins* **2019**, *11*, 664. [[CrossRef](#)]
9. Marin, S.; Ramos, A.J.; Cano-Sancho, G.; Sanchis, V. Mycotoxins: Occurrence, Toxicology, and Exposure Assessment. *Food Chem. Toxicol.* **2013**, *60*, 218–237. [[CrossRef](#)]
10. Bhat, R.; Rai, R.V.; Karim, A.A. Mycotoxins in Food and Feed: Present Status and Future Concerns. *Compr. Rev. Food Sci. Food Saf.* **2010**, *9*, 57–81. [[CrossRef](#)]
11. Awuchi, C.G.; Ondari, E.N.; Ogbonna, C.U.; Upadhyay, A.K.; Baran, K.; Okpala, C.O.R.; Korzeniowska, M.; Guiné, R.P.F. Mycotoxins Affecting Animals, Foods, Humans, and Plants: Types, Occurrence, Toxicities, Action Mechanisms, Prevention, and Detoxification Strategies—A Revisit. *Foods* **2021**, *10*, 1279. [[CrossRef](#)] [[PubMed](#)]
12. Eskola, M.; Kos, G.; Elliott, C.T.; Hajšlová, J.; Mayar, S.; Krska, R. Worldwide Contamination of Food-Crops with Mycotoxins: Validity of the Widely Cited “FAO Estimate” of 25. *Crit. Rev. Food Sci. Nutr.* **2020**, *60*, 2773–2789. [[CrossRef](#)] [[PubMed](#)]
13. Arya, A.; Perelló, A.E. (Eds.) *Management of Fungal Plant Pathogens*; CABI: Wallingford, UK, 2010; ISBN 978-1-84593-603-7.
14. Ghanney, N. Management of Fungal Plants Diseases. *Eur. J. Biol. Res.* **2017**, *7*, 309–4314. [[CrossRef](#)]
15. Agrios, G.N. *Plant Pathology*; Elsevier: Amsterdam, The Netherlands, 1988; ISBN 978-0-12-044563-9.
16. Oliver, R.P.; Hewitt, H.G. *Fungicides in Crop Protection*, 2nd ed.; CABI: Boston, MA, USA, 2014; ISBN 978-1-78064-166-9.
17. Fisher, M.C.; Hawkins, N.J.; Sanglard, D.; Gurr, S.J. Worldwide Emergence of Resistance to Antifungal Drugs Challenges Human Health and Food Security. *Science* **2018**, *360*, 739–742. [[CrossRef](#)] [[PubMed](#)]
18. Steinberg, G.; Gurr, S.J. Fungi, Fungicide Discovery and Global Food Security. *Fungal Genet. Biol.* **2020**, *144*, 103476. [[CrossRef](#)]
19. Pellegrino, E.; Bedini, S. Enhancing Ecosystem Services in Sustainable Agriculture: Biofertilization and Biofortification of Chickpea (*Cicer Arietinum* L.) by Arbuscular Mycorrhizal Fungi. *Soil Biol. Biochem.* **2014**, *68*, 429–439. [[CrossRef](#)]
20. Mahanty, T.; Bhattacharjee, S.; Goswami, M.; Bhattacharyya, P.; Das, B.; Ghosh, A.; Tribedi, P. Biofertilizers: A Potential Approach for Sustainable Agriculture Development. *Environ. Sci. Pollut. Res.* **2017**, *24*, 3315–3335. [[CrossRef](#)]
21. Balasubramanian, P.; Karthickumar, P. Biofertilizers and Biopesticides: A Holistic Approach for Sustainable Agriculture. In *Sustainable Utilization of Natural Resources*; Mondal, P., Dalai, A.K., Eds.; CRC Press: Boca Raton, FL, USA, 2017; pp. 255–284, ISBN 978-1-315-15329-2.
22. Wang, G. Human Antimicrobial Peptides and Proteins. *Pharmaceuticals* **2014**, *7*, 545–594. [[CrossRef](#)]
23. Zasloff, M. Antimicrobial Peptides of Multicellular Organisms. *Nature* **2002**, *415*, 389–395. [[CrossRef](#)]
24. Lei, J.; Sun, L.; Huang, S.; Zhu, C.; Li, P.; He, J.; Mackey, V.; Coy, D.H.; He, Q. The Antimicrobial Peptides and Their Potential Clinical Applications. *Am. J. Transl. Res.* **2019**, *11*, 3919–3931.
25. Xhindoli, D.; Pacor, S.; Benincasa, M.; Scocchi, M.; Gennaro, R.; Tossi, A. The Human Cathelicidin LL-37—A Pore-Forming Antibacterial Peptide and Host-Cell Modulator. *Biochim. Biophys. Acta—Biomembr.* **2016**, *1858*, 546–566. [[CrossRef](#)] [[PubMed](#)]
26. Tanner, J.; Deplazes, E.; Mancera, R. The Biological and Biophysical Properties of the Spider Peptide Gomesin. *Molecules* **2018**, *23*, 1733. [[CrossRef](#)] [[PubMed](#)]
27. Vergis, J.; Malik, S.S.; Pathak, R.; Kumar, M.; Ramanjaneya, S.; Kurkure, N.V.; Barbuddhe, S.B.; Rawool, D.B. Antimicrobial Efficacy of Indolicidin Against Multi-Drug Resistant Enterococcal *Escherichia Coli* in a *Galleria Mellonella* Model. *Front. Microbiol.* **2019**, *10*, 2723. [[CrossRef](#)] [[PubMed](#)]
28. Rebuffat, S. Microcins. In *Handbook of Biologically Active Peptides*; Elsevier: Amsterdam, The Netherlands, 2013; pp. 129–137, ISBN 978-0-12-385095-9.
29. Terras, F.R.G.; Torrekens, S.; Van Leuven, F.; Osborn, R.W.; Vanderleyden, J.; Cammue, B.P.A.; Broekaert, W.F. A New Family of Basic Cysteine-Rich Plant Antifungal Proteins from Brassicaceae Species. *FEBS Lett.* **1993**, *316*, 233–240. [[CrossRef](#)]
30. Boulanger, N.; Lowenberger, C.; Volf, P.; Ursic, R.; Sigutova, L.; Sabatier, L.; Svobodova, M.; Beverley, S.M.; Späth, G.; Brun, R.; et al. Characterization of a Defensin from the Sand Fly *Phlebotomus Duboscqi* Induced by Challenge with Bacteria or the Protozoan Parasite *Leishmania Major*. *Infect. Immun.* **2004**, *72*, 7140–7146. [[CrossRef](#)] [[PubMed](#)]
31. Wilson, S.S.; Wiens, M.E.; Smith, J.G. Antiviral Mechanisms of Human Defensins. *J. Mol. Biol.* **2013**, *425*, 4965–4980. [[CrossRef](#)]
32. Cabezas-Cruz, A.; Tonk, M.; Bouchut, A.; Pierrot, C.; Pierce, R.J.; Kotsyfakis, M.; Rahnamaeian, M.; Vilcinskas, A.; Khalife, J.; Valdés, J.J. Antiplasmodial Activity Is an Ancient and Conserved Feature of Tick Defensins. *Front. Microbiol.* **2016**, *7*, 1682. [[CrossRef](#)]
33. Kudryashova, E.; Seveau, S.M.; Kudryashov, D.S. Targeting and Inactivation of Bacterial Toxins by Human Defensins. *Biol. Chem.* **2017**, *398*, 1069–1085. [[CrossRef](#)]
34. Couto, J.; Tonk, M.; Ferrolho, J.; Antunes, S.; Vilcinskas, A.; de la Fuente, J.; Domingos, A.; Cabezas-Cruz, A. Antiplasmodial Activity of Tick Defensins in a Mouse Model of Malaria. *Ticks Tick-Borne Dis.* **2018**, *9*, 844–849. [[CrossRef](#)]
35. Sathoff, A.E.; Velivelli, S.; Shah, D.M.; Samac, D.A. Plant Defensin Peptides Have Antifungal and Antibacterial Activity Against Human and Plant Pathogens. *Phytopathology* **2019**, *109*, 402–408. [[CrossRef](#)]

36. Tonk, M.; Cabezas-Cruz, A.; Valdés, J.J.; Rego, R.O.M.; Grubhoffer, L.; Estrada-Peña, A.; Vilcinskas, A.; Kotsyfakis, M.; Rahnamaeian, M. Ixodes Ricinus Defensins Attack Distantly-Related Pathogens. *Dev. Comp. Immunol.* **2015**, *53*, 358–365. [[CrossRef](#)]
37. De Souza Cândido, E.; e Silva Cardoso, M.H.; Sousa, D.A.; Viana, J.C.; de Oliveira-Júnior, N.G.; Miranda, V.; Franco, O.L. The Use of Versatile Plant Antimicrobial Peptides in Agribusiness and Human Health. *Peptides* **2014**, *55*, 65–78. [[CrossRef](#)] [[PubMed](#)]
38. Falanga, A.; Nigro, E.; De Biasi, M.; Daniele, A.; Morelli, G.; Galdiero, S.; Scudiero, O. Cyclic Peptides as Novel Therapeutic Microbicides: Engineering of Human Defensin Mimetics. *Molecules* **2017**, *22*, 1217. [[CrossRef](#)] [[PubMed](#)]
39. Wei, H.; Movahedi, A.; Xu, C.; Sun, W.; Li, L.; Li, D.; Zhuge, Q. Characterization, Expression Profiling, and Functional Analysis of a Populus Trichocarpa Defensin Gene and Its Potential as an Anti-Agrobacterium Rooting Medium Additive. *Sci. Rep.* **2019**, *9*, 15359. [[CrossRef](#)] [[PubMed](#)]
40. Ganz, T.; Selsted, M.E.; Szklarek, D.; Harwig, S.S.; Daher, K.; Bainton, D.F.; Lehrer, R.I. Defensins. Natural Peptide Antibiotics of Human Neutrophils. *J. Clin. Invest.* **1985**, *76*, 1427–1435. [[CrossRef](#)] [[PubMed](#)]
41. Silva, P.M.; Gonçalves, S.; Santos, N.C. Defensins: Antifungal Lessons from Eukaryotes. *Front. Microbiol.* **2014**, *5*, 97. [[CrossRef](#)]
42. Lay, F.; Anderson, M. Defensins—Components of the Innate Immune System in Plants. *Curr. Protein Pept. Sci.* **2005**, *6*, 85–101. [[CrossRef](#)] [[PubMed](#)]
43. Xu, D.; Lu, W. Defensins: A Double-Edged Sword in Host Immunity. *Front. Immunol.* **2020**, *11*, 764. [[CrossRef](#)]
44. Shafee, T.M.A.; Lay, F.T.; Hulett, M.D.; Anderson, M.A. The Defensins Consist of Two Independent, Convergent Protein Superfamilies. *Mol. Biol. Evol.* **2016**, *33*, 2345–2356. [[CrossRef](#)]
45. Shafee, T.M.A.; Lay, F.T.; Phan, T.K.; Anderson, M.A.; Hulett, M.D. Convergent Evolution of Defensin Sequence, Structure and Function. *Cell. Mol. Life Sci.* **2017**, *74*, 663–682. [[CrossRef](#)]
46. Gerdol, M.; Schmitt, P.; Venier, P.; Rocha, G.; Rosa, R.D.; Destoumieux-Garzón, D. Functional Insights From the Evolutionary Diversification of Big Defensins. *Front. Immunol.* **2020**, *11*, 758. [[CrossRef](#)] [[PubMed](#)]
47. Lehrer, R.I.; Cole, A.M.; Selsted, M.E.  $\theta$ -Defensins: Cyclic Peptides with Endless Potential. *J. Biol. Chem.* **2012**, *287*, 27014–27019. [[CrossRef](#)] [[PubMed](#)]
48. De Dias, R.O.; Franco, O.L. Cysteine-Stabilized A $\beta$  Defensins: From a Common Fold to Antibacterial Activity. *Peptides* **2015**, *72*, 64–72. [[CrossRef](#)] [[PubMed](#)]
49. Dimarcq, J.L.; Bulet, P.; Hetru, C.; Hoffmann, J. Cysteine-Rich Antimicrobial Peptides in Invertebrates. *Biopolymers* **1998**, *47*, 465–477. [[CrossRef](#)]
50. Dorin, J.R.; McHugh, B.J.; Cox, S.L.; Davidson, D.J. Mammalian Antimicrobial Peptides; Defensins and Cathelicidins. In *Molecular Medical Microbiology*; Elsevier: Amsterdam, The Netherlands, 2015; pp. 539–565, ISBN 978-0-12-397169-2.
51. Picart, P.; Pirttilä, A.; Raventos, D.; Kristensen, H.-H.; Sahl, H.-G. Identification of Defensin-Encoding Genes of Picea Glauca: Characterization of PgD5, a Conserved Spruce Defensin with Strong Antifungal Activity. *BMC Plant Biol.* **2012**, *12*, 180. [[CrossRef](#)] [[PubMed](#)]
52. Chan, Y.S.; Ng, T.B. Northeast Red Beans Produce a Thermostable and PH-Stable Defensin-Like Peptide with Potent Antifungal Activity. *Cell Biochem. Biophys.* **2013**, *66*, 637–648. [[CrossRef](#)]
53. Maemoto, A.; Qu, X.; Rosengren, K.J.; Tanabe, H.; Henschen-Edman, A.; Craik, D.J.; Ouellette, A.J. Functional Analysis of the  $\alpha$ -Defensin Disulfide Array in Mouse Cryptdin-4. *J. Biol. Chem.* **2004**, *279*, 44188–44196. [[CrossRef](#)]
54. White, S.H.; Wimley, W.C.; Selsted, M.E. Structure, Function, and Membrane Integration of Defensins. *Curr. Opin. Struct. Biol.* **1995**, *5*, 521–527. [[CrossRef](#)]
55. De Samblanx, G.W.; Goderis, I.J.; Thevissen, K.; Raemaekers, R.; Fant, F.; Borremans, F.; Acland, D.P.; Osborn, R.W.; Patel, S.; Broekaert, W.F. Mutational Analysis of a Plant Defensin from Radish (*Raphanus sativus* L.) Reveals Two Adjacent Sites Important for Antifungal Activity. *J. Biol. Chem.* **1997**, *272*, 1171–1179. [[CrossRef](#)]
56. Sagaram, U.S.; Pandurangi, R.; Kaur, J.; Smith, T.J.; Shah, D.M. Structure-Activity Determinants in Antifungal Plant Defensins MsDef1 and MtDef4 with Different Modes of Action against *Fusarium graminearum*. *PLoS ONE* **2011**, *6*, e18550. [[CrossRef](#)]
57. De Coninck, B.; Cammue, B.P.A.; Thevissen, K. Modes of Antifungal Action and in Planta Functions of Plant Defensins and Defensin-like Peptides. *Fungal Biol. Rev.* **2013**, *26*, 109–120. [[CrossRef](#)]
58. Contreras, G.; Shirdel, I.; Braun, M.S.; Wink, M. Defensins: Transcriptional Regulation and Function beyond Antimicrobial Activity. *Dev. Comp. Immunol.* **2020**, *104*, 103556. [[CrossRef](#)]
59. Wilson, C.L.; Schmidt, A.P.; Piriilä, E.; Valore, E.V.; Ferri, N.; Sorsa, T.; Ganz, T.; Parks, W.C. Differential Processing of  $\alpha$ - and  $\beta$ -Defensin Precursors by Matrix Metalloproteinase-7 (MMP-7). *J. Biol. Chem.* **2009**, *284*, 8301–8311. [[CrossRef](#)] [[PubMed](#)]
60. Lay, F.T.; Poon, S.; McKenna, J.A.; Connelly, A.A.; Barbeta, B.L.; McGinness, B.S.; Fox, J.L.; Daly, N.L.; Craik, D.J.; Heath, R.L.; et al. The C-Terminal Propeptide of a Plant Defensin Confers Cytoprotective and Subcellular Targeting Functions. *BMC Plant Biol.* **2014**, *14*, 41. [[CrossRef](#)] [[PubMed](#)]
61. Hegedüs, N.; Marx, F. Antifungal Proteins: More than Antimicrobials? *Fungal Biol. Rev.* **2013**, *26*, 132–145. [[CrossRef](#)]
62. Kragh, K.M. Characterization and Localization of New Antifungal Cysteine-Rich Proteins from Beta vulgaris. *Mol. Plant Microb. Interact.* **1995**, *8*, 424. [[CrossRef](#)] [[PubMed](#)]
63. Osborn, R.W.; De Samblanx, G.W.; Thevissen, K.; Goderis, I.; Torreken, S.; Van Leuven, F.; Attenborough, S.; Rees, S.B.; Broekaert, W.F. Isolation and Characterisation of Plant Defensins from Seeds of Asteraceae, Fabaceae, Hippocastanaceae and Saxifragaceae. *FEBS Lett.* **1995**, *368*, 257–262. [[CrossRef](#)]

64. Marquès, L.; Oomen, R.J.F.J.; Aumelas, A.; Le Jean, M.; Berthomieu, P. Production of an *Arabidopsis Halleri* Foliar Defensin in *Escherichia Coli*. *J. Appl. Microbiol.* **2009**, *106*, 1640–1648. [[CrossRef](#)]
65. Vriens, K.; Peigneur, S.; De Coninck, B.; Tytgat, J.; Cammue, B.P.A.; Thevissen, K. The Antifungal Plant Defensin AtPDF2.3 from *Arabidopsis Thaliana* Blocks Potassium Channels. *Sci. Rep.* **2016**, *6*, 32121. [[CrossRef](#)]
66. De Beer, A.; Vivier, M.A. Four Plant Defensins from an Indigenous South African Brassicaceae Species Display Divergent Activities against Two Test Pathogens despite High Sequence Similarity in the Encoding Genes. *BMC Res. Notes* **2011**, *4*, 459. [[CrossRef](#)]
67. Terras, F.R.; Schoofs, H.M.; De Bolle, M.F.; Van Leuven, F.; Rees, S.B.; Vanderleyden, J.; Cammue, B.P.; Broekaert, W.F. Analysis of Two Novel Classes of Plant Antifungal Proteins from Radish (*Raphanus sativus* L.) Seeds. *J. Biol. Chem.* **1992**, *267*, 15301–15309. [[CrossRef](#)]
68. Terras, F.R.; Eggermont, K.; Kovaleva, V.; Raikhel, N.V.; Osborn, R.W.; Kester, A.; Rees, S.B.; Torrekens, S.; Van Leuven, F.; Vanderleyden, J. Small Cysteine-Rich Antifungal Proteins from Radish: Their Role in Host Defense. *Plant Cell* **1995**, *7*, 573–588. [[CrossRef](#)] [[PubMed](#)]
69. Saitoh, H.; Kiba, A.; Nishihara, M.; Yamamura, S.; Suzuki, K.; Terauchi, R. Production of Antimicrobial Defensin in *Nicotiana Benthamiana* with a Potato Virus X Vector. *Mol. Plant-Microbe Interact.* **2001**, *14*, 111–115. [[CrossRef](#)] [[PubMed](#)]
70. Slavokhotova, A.A.; Odintsova, T.I.; Rogozhin, E.A.; Musolyamov, A.K.; Andreev, Y.A.; Grishin, E.V.; Egorov, T.A. Isolation, Molecular Cloning and Antimicrobial Activity of Novel Defensins from Common Chickweed (*Stellaria media* L.) Seeds. *Biochimie* **2011**, *93*, 450–456. [[CrossRef](#)]
71. Segura, A.; Moreno, M.; Molina, A.; García-Olmedo, F. Novel Defensin Subfamily from Spinach (*Spinacia oleracea*). *FEBS Lett.* **1998**, *435*, 159–162. [[CrossRef](#)]
72. Ye, X.Y.; Ng, T.B. Peptides from Pinto Bean and Red Bean with Sequence Homology to Cowpea 10-KDa Protein Precursor Exhibit Antifungal, Mitogenic, and HIV-1 Reverse Transcriptase-Inhibitory Activities. *Biochem. Biophys. Res. Commun.* **2001**, *285*, 424–429. [[CrossRef](#)]
73. Huang, J.; Wong, K.H.; Tay, S.V.; Serra, A.; Sze, S.K.; Tam, J.P. Astratides: Insulin-Modulating, Insecticidal, and Antifungal Cysteine-Rich Peptides from *Astragalus membranaceus*. *J. Nat. Prod.* **2019**, *82*, 194–204. [[CrossRef](#)]
74. Ngai, P.H.K.; Ng, T.B. Coccinin, an Antifungal Peptide with Antiproliferative and HIV-1 Reverse Transcriptase Inhibitory Activities from Large Scarlet Runner Beans. *Peptides* **2004**, *25*, 2063–2068. [[CrossRef](#)]
75. Ngai, P.H.K.; Ng, T.B. Phaseococcin, an Antifungal Protein with Antiproliferative and Anti-HIV-1 Reverse Transcriptase Activities from Small Scarlet Runner Beans. *Biochem. Cell Biol.* **2005**, *83*, 212–220. [[CrossRef](#)]
76. Wong, J.H.; Ng, T.B. Gymnin, a Potent Defensin-like Antifungal Peptide from the Yunnan Bean (*Gymnocladus Chinensis* Baill.). *Peptides* **2003**, *24*, 963–968. [[CrossRef](#)]
77. Shenkarev, Z.O.; Gizatullina, A.K.; Finkina, E.I.; Alekseeva, E.A.; Balandin, S.V.; Mineev, K.S.; Arseniev, A.S.; Ovchinnikova, T.V. Heterologous Expression and Solution Structure of Defensin from Lentil Lens Culinaris. *Biochem. Biophys. Res. Commun.* **2014**, *451*, 252–257. [[CrossRef](#)] [[PubMed](#)]
78. Wong, J.H.; Ng, T.B. Limenin, a Defensin-like Peptide with Multiple Exploitable Activities from Shelf Beans. *J. Pept. Sci. Off. Publ. Eur. Pept. Soc.* **2006**, *12*, 341–346. [[CrossRef](#)] [[PubMed](#)]
79. Wang, S.; Rao, P.; Ye, X. Isolation and Biochemical Characterization of a Novel Leguminous Defense Peptide with Antifungal and Antiproliferative Potency. *Appl. Microbiol. Biotechnol.* **2009**, *82*, 79–86. [[CrossRef](#)]
80. Spelbrink, R.G.; Dilmac, N.; Allen, A.; Smith, T.J.; Shah, D.M.; Hockerman, G.H. Differential Antifungal and Calcium Channel-Blocking Activity among Structurally Related Plant Defensins. *Plant Physiol.* **2004**, *135*, 2055–2067. [[CrossRef](#)] [[PubMed](#)]
81. Gao, A.G.; Hakimi, S.M.; Mittanck, C.A.; Wu, Y.; Woerner, B.M.; Stark, D.M.; Shah, D.M.; Liang, J.; Rommens, C.M. Fungal Pathogen Protection in Potato by Expression of a Plant Defensin Peptide. *Nat. Biotechnol.* **2000**, *18*, 1307–1310. [[CrossRef](#)] [[PubMed](#)]
82. Almeida, M.S.; Cabral, K.M.S.; Zingali, R.B.; Kurtenbach, E. Characterization of Two Novel Defense Peptides from Pea (*Pisum Sativum*) Seeds. *Arch. Biochem. Biophys.* **2000**, *378*, 278–286. [[CrossRef](#)] [[PubMed](#)]
83. Games, P.D.; dos Santos, I.S.; Mello, É.O.; Diz, M.S.S.; Carvalho, A.O.; de Souza-Filho, G.A.; Da Cunha, M.; Vasconcelos, I.M.; dos Ferreira, B.S.; Gomes, V.M. Isolation, Characterization and Cloning of a cDNA Encoding a New Antifungal Defensin from *Phaseolus Vulgaris* L. Seeds. *Peptides* **2008**, *29*, 2090–2100. [[CrossRef](#)] [[PubMed](#)]
84. Wong, J.H.; Zhang, X.Q.; Wang, H.X.; Ng, T.B. A Mitogenic Defensin from White Cloud Beans (*Phaseolus Vulgaris*). *Peptides* **2006**, *27*, 2075–2081. [[CrossRef](#)]
85. Wong, J.H.; Ng, T.B. Sesquin, a Potent Defensin-like Antimicrobial Peptide from Ground Beans with Inhibitory Activities toward Tumor Cells and HIV-1 Reverse Transcriptase. *Peptides* **2005**, *26*, 1120–1126. [[CrossRef](#)]
86. Song, X.; Wang, J.; Wu, F.; Li, X.; Teng, M.; Gong, W. cDNA Cloning, Functional Expression and Antifungal Activities of a Dimeric Plant Defensin SPE10 from *Pachyrrhizus Erosus* Seeds. *Plant Mol. Biol.* **2005**, *57*, 13–20. [[CrossRef](#)]
87. Vijayan, S.; Guruprasad, L.; Kirti, P.B. Prokaryotic Expression of a Constitutively Expressed Tephrosia Villosa Defensin and Its Potent Antifungal Activity. *Appl. Microbiol. Biotechnol.* **2008**, *80*, 1023–1032. [[CrossRef](#)] [[PubMed](#)]
88. Chen, G.-H.; Hsu, M.-P.; Tan, C.-H.; Sung, H.-Y.; Kuo, C.G.; Fan, M.-J.; Chen, H.-M.; Chen, S.; Chen, C.-S. Cloning and Characterization of a Plant Defensin VaD1 from Azuki Bean. *J. Agric. Food Chem.* **2005**, *53*, 982–988. [[CrossRef](#)] [[PubMed](#)]
89. Chen, J.-J.; Chen, G.-H.; Hsu, H.-C.; Li, S.-S.; Chen, C.-S. Cloning and Functional Expression of a Mungbean Defensin VrD1 in *Pichia Pastoris*. *J. Agric. Food Chem.* **2004**, *52*, 2256–2261. [[CrossRef](#)] [[PubMed](#)]

90. Kovaleva, V.; Krynytskyi, H.; Gout, I.; Gout, R. Recombinant Expression, Affinity Purification and Functional Characterization of Scots Pine Defensin 1. *Appl. Microbiol. Biotechnol.* **2011**, *89*, 1093–1101. [[CrossRef](#)] [[PubMed](#)]
91. Odintsova, T.I.; Rogozhin, E.A.; Baranov, Y.; Musolyamov, A.K.; Yalpani, N.; Egorov, T.A.; Grishin, E.V. Seed Defensins of Barnyard Grass *Echinochloa Crusgalli* (L.) Beauv. *Biochimie* **2008**, *90*, 1667–1673. [[CrossRef](#)]
92. Fujimura, M.; Ideguchi, M.; Minami, Y.; Watanabe, K.; Tadera, K. Amino Acid Sequence and Antimicrobial Activity of Chitin-Binding Peptides, *Pp*-AMP 1 and *Pp*-AMP 2, from Japanese Bamboo Shoots (*Phyllostachys pubescens*). *Biosci. Biotechnol. Biochem.* **2005**, *69*, 642–645. [[CrossRef](#)]
93. De-Paula, V.S.; Razzera, G.; Medeiros, L.; Miyamoto, C.A.; Almeida, M.S.; Kurtenbach, E.; Almeida, F.C.L.; Valente, A.P. Evolutionary Relationship between Defensins in the Poaceae Family Strengthened by the Characterization of New Sugarcane Defensins. *Plant Mol. Biol.* **2008**, *68*, 321–335. [[CrossRef](#)]
94. Kerenga, B.K.; McKenna, J.A.; Harvey, P.J.; Quimbar, P.; Garcia-Ceron, D.; Lay, F.T.; Phan, T.K.; Veneer, P.K.; Vasa, S.; Parisi, K.; et al. Salt-Tolerant Antifungal and Antibacterial Activities of the Corn Defensin ZmD32. *Front. Microbiol.* **2019**, *10*, 795. [[CrossRef](#)]
95. Balandín, M.; Royo, J.; Gómez, E.; Muniz, L.M.; Molina, A.; Hueros, G. A Protective Role for the Embryo Surrounding Region of the Maize Endosperm, as Evidenced by the Characterisation of ZmESR-6, a Defensin Gene Specifically Expressed in This Region. *Plant Mol. Biol.* **2005**, *58*, 269–282. [[CrossRef](#)]
96. Fujimura, M.; Minami, Y.; Watanabe, K.; Tadera, K. Purification, Characterization, and Sequencing of a Novel Type of Antimicrobial Peptides, *Fa*-AMP1 and *Fa*-AMP2, from Seeds of Buckwheat (*Fagopyrum esculentum* Moench.). *Biosci. Biotechnol. Biochem.* **2003**, *67*, 1636–1642. [[CrossRef](#)]
97. Rogozhin, E.A.; Oshchepkova, Y.I.; Odintsova, T.I.; Khadeeva, N.V.; Veshkurova, O.N.; Egorov, T.A.; Grishin, E.V.; Salikhov, S.I. Novel Antifungal Defensins from *Nigella sativa* L. Seeds. *Plant Physiol. Biochem.* **2011**, *49*, 131–137. [[CrossRef](#)]
98. Bleackley, M.R.; Payne, J.A.E.; Hayes, B.M.E.; Durek, T.; Craik, D.J.; Shafee, T.M.A.; Poon, I.K.H.; Hulett, M.D.; van der Weerden, N.L.; Anderson, M.A. *Nicotiana glauca* Defensin Chimeras Reveal Differences in the Mechanism of Fungal and Tumor Cell Killing and an Enhanced Antifungal Variant. *Antimicrob. Agents Chemother.* **2016**, *60*, 6302–6312. [[CrossRef](#)] [[PubMed](#)]
99. Dracatos, P.M.; Weerden, N.L.; Carroll, K.T.; Johnson, E.D.; Plummer, K.M.; Anderson, M.A. Inhibition of Cereal Rust Fungi by Both Class I and II Defensins Derived from the Flowers of *Nicotiana glauca*. *Mol. Plant Pathol.* **2014**, *15*, 67–79. [[CrossRef](#)] [[PubMed](#)]
100. Lay, F.T.; Brugliera, F.; Anderson, M.A. Isolation and Properties of Floral Defensins from Ornamental Tobacco and Petunia. *Plant Physiol.* **2003**, *131*, 1283–1293. [[CrossRef](#)] [[PubMed](#)]
101. De Beer, A.; Vivier, M.A. Vv-AMP1, a Ripening Induced Peptide from *Vitis vinifera* Shows Strong Antifungal Activity. *BMC Plant Biol.* **2008**, *8*, 75. [[CrossRef](#)] [[PubMed](#)]
102. Landon, C. Lead Optimization of Antifungal Peptides with 3D NMR Structures Analysis. *Protein Sci.* **2004**, *13*, 703–713. [[CrossRef](#)] [[PubMed](#)]
103. Fehlbauer, P.; Bulet, P.; Michaut, L.; Lagueux, M.; Broekaert, W.F.; Hetru, C.; Hoffmann, J.A. Insect Immunity. Septic Injury of *Drosophila* Induces the Synthesis of a Potent Antifungal Peptide with Sequence Homology to Plant Antifungal Peptides. *J. Biol. Chem.* **1994**, *269*, 33159–33163. [[CrossRef](#)]
104. Cytryńska, M.; Mak, P.; Zdybicka-Barabas, A.; Suder, P.; Jakubowicz, T. Purification and Characterization of Eight Peptides from *Galleria mellonella* Immune Hemolymph. *Peptides* **2007**, *28*, 533–546. [[CrossRef](#)]
105. Lamberty, M.; Ades, S.; Uttenweiler-Joseph, S.; Brookhart, G.; Bushey, D.; Hoffmann, J.A.; Bulet, P. Insect Immunity. Isolation from the Lepidopteran *Heliothis virescens* of a Novel Insect Defensin with Potent Antifungal Activity. *J. Biol. Chem.* **1999**, *274*, 9320–9326. [[CrossRef](#)]
106. Lamberty, M.; Zachary, D.; Lanot, R.; Bordereau, C.; Robert, A.; Hoffmann, J.A.; Bulet, P. Insect Immunity. Constitutive Expression of a Cysteine-Rich Antifungal and a Linear Antibacterial Peptide in a Termite Insect. *J. Biol. Chem.* **2001**, *276*, 4085–4092. [[CrossRef](#)]
107. Xu, X.-X.; Zhang, Y.-Q.; Freed, S.; Yu, J.; Gao, Y.-F.; Wang, S.; Ouyang, L.-N.; Ju, W.-Y.; Jin, F.-L. An Anionic Defensin from *Plutella xylostella* with Potential Activity against *Bacillus thuringiensis*. *Bull. Entomol. Res.* **2016**, *106*, 790–800. [[CrossRef](#)] [[PubMed](#)]
108. Bíliková, K.; Wu, G.; Simúth, J. Isolation of a Peptide Fraction from Honeybee Royal Jelly as a Potential Antifouling Factor. *Apidologie* **2001**, *32*, 275–283. [[CrossRef](#)]
109. Gueguen, Y.; Herpin, A.; Aumelas, A.; Garnier, J.; Fievet, J.; Escoubas, J.-M.; Bulet, P.; Gonzalez, M.; Lelong, C.; Favrel, P.; et al. Characterization of a Defensin from the Oyster *Crassostrea gigas*: Recombinant Production, Folding, Solution Structure, Antimicrobial Activities, and Gene Expression. *J. Biol. Chem.* **2006**, *281*, 313–323. [[CrossRef](#)]
110. Romestand, B.; Molina, F.; Richard, V.; Roch, P.; Granier, C. Key Role of the Loop Connecting the Two Beta Strands of Mussel Defensin in Its Antimicrobial Activity. *Eur. J. Biochem.* **2003**, *270*, 2805–2813. [[CrossRef](#)] [[PubMed](#)]
111. Cabezas-Cruz, A.; Tonk, M.; Bleackley, M.R.; Valdés, J.J.; Barrero, R.A.; Hernández-Jarguín, A.; Moutailler, S.; Vilcinskis, A.; Richard-Forget, F.; Anderson, M.A.; et al. Antibacterial and Antifungal Activity of Defensins from the Australian Paralysis Tick, *Ixodes holocyclus*. *Ticks Tick-Borne Dis.* **2019**, *10*, 101269. [[CrossRef](#)]
112. Ayroza, G.; Ferreira, I.L.C.; Sayegh, R.S.R.; Tashima, A.K.; da Silva Junior, P.I. Juruin: An Antifungal Peptide from the Venom of the Amazonian Pink Toe Spider, *Avicularia juruensis*, Which Contains the Inhibitory Cystine Knot Motif. *Front. Microbiol.* **2012**, *3*, 324. [[CrossRef](#)]
113. Tonk, M.; Cabezas-Cruz, A.; Valdés, J.J.; Rego, R.O.; Chrudimská, T.; Strnad, M.; Šima, R.; Bell-Sakyi, L.; Franta, Z.; Vilcinskis, A.; et al. Defensins from the Tick *Ixodes scapularis* Are Effective against Phytopathogenic Fungi and the Human Bacterial Pathogen *Listeria grayi*. *Parasit. Vectors* **2014**, *7*, 554. [[CrossRef](#)]

114. Yang, M.; Chen, B.; Cai, J.-J.; Peng, H.; Ling-Cai; Yuan, J.-J.; Wang, K.-J. Molecular Characterization of Hepcidin AS-Hepc2 and AS-Hepc6 in Black Porgy (*Acanthopagrus schlegelii*): Expression Pattern Responded to Bacterial Challenge and in Vitro Antimicrobial Activity. *Comp. Biochem. Physiol. B Biochem. Mol. Biol.* **2011**, *158*, 155–163. [[CrossRef](#)]
115. Lauth, X.; Babon, J.J.; Stannard, J.A.; Singh, S.; Nizet, V.; Carlberg, J.M.; Ostland, V.E.; Pennington, M.W.; Norton, R.S.; Westerman, M.E. Bass Hepcidin Synthesis, Solution Structure, Antimicrobial Activities and Synergism, and in Vivo Hepatic Response to Bacterial Infections. *J. Biol. Chem.* **2005**, *280*, 9272–9282. [[CrossRef](#)]
116. Yamane, E.S.; Bizerra, F.C.; Oliveira, E.B.; Moreira, J.T.; Rajabi, M.; Nunes, G.L.C.; de Souza, A.O.; da Silva, I.D.C.G.; Yamane, T.; Karpel, R.L.; et al. Unraveling the Antifungal Activity of a South American Rattlesnake Toxin Crotamine. *Biochimie* **2013**, *95*, 231–240. [[CrossRef](#)]
117. Thouzeau, C.; Le Maho, Y.; Froget, G.; Sabatier, L.; Le Bohec, C.; Hoffmann, J.A.; Bulet, P. Spheniscins, Avian  $\beta$ -Defensins in Preserved Stomach Contents of the King Penguin, *Aptenodytes patagonicus*. *J. Biol. Chem.* **2003**, *278*, 51053–51058. [[CrossRef](#)]
118. Simon, A.; Kullberg, B.J.; Tripet, B.; Boerman, O.C.; Zeeuwen, P.; van der Ven-Jongekrijg, J.; Verweij, P.; Schalkwijk, J.; Hodges, R.; van der Meer, J.W.M.; et al. Drosomycin-Like Defensin, a Human Homologue of *Drosophila melanogaster* Drosomycin with Antifungal Activity. *Antimicrob. Agents Chemother.* **2008**, *52*, 1407–1412. [[CrossRef](#)]
119. Theis, T.; Wedde, M.; Meyer, V.; Stahl, U. The Antifungal Protein from *Aspergillus Giganteus* Causes Membrane Permeabilization. *Antimicrob. Agents Chemother.* **2003**, *47*, 588–593. [[CrossRef](#)] [[PubMed](#)]
120. Huber, A.; Hajdu, D.; Bratschun-Khan, D.; Gáspári, Z.; Varbanov, M.; Philippot, S.; Fizil, Á.; Czajlik, A.; Kele, Z.; Sonderegger, C.; et al. New Antimicrobial Potential and Structural Properties of PAFB: A Cationic, Cysteine-Rich Protein from *Penicillium Chrysogenum* Q176. *Sci. Rep.* **2018**, *8*, 1751. [[CrossRef](#)] [[PubMed](#)]
121. Gun Lee, D.; Shin, S.Y.; Maeng, C.Y.; Jin, Z.Z.; Kim, K.L.; Hahm, K.S. Isolation and Characterization of a Novel Antifungal Peptide from *Aspergillus niger*. *Biochem. Biophys. Res. Commun.* **1999**, *263*, 646–651. [[CrossRef](#)]
122. Skouri-Gargouri, H.; Gargouri, A. First Isolation of a Novel Thermostable Antifungal Peptide Secreted by *Aspergillus Clavatus*. *Peptides* **2008**, *29*, 1871–1877. [[CrossRef](#)]
123. Kovács, L.; Virágh, M.; Takó, M.; Papp, T.; Vágvölgyi, C.; Galgóczy, L. Isolation and Characterization of *Neosartorya fischeri* Antifungal Protein (NFAP). *Peptides* **2011**, *32*, 1724–1731. [[CrossRef](#)]
124. Mielniczuk, E.; Skwaryło-Bednarz, B. Fusarium Head Blight, Mycotoxins and Strategies for Their Reduction. *Agronomy* **2020**, *10*, 509. [[CrossRef](#)]
125. Varga, J.; Baranyi, N.; Muthusamy, C.; Vágvölgyi, C.; Kocsubé, S. Mycotoxin Producers in the *Aspergillus* Genus: An Update. *Acta Biol. Szeged.* **2015**, *59*, 151–167.
126. Lacerda, A.F.; Vasconcelos, Á.A.R.; Pelegrini, P.B.; Grossi de Sa, M.F. Antifungal Defensins and Their Role in Plant Defense. *Front. Microbiol.* **2014**, *5*, 116. [[CrossRef](#)]
127. Leanne-Rialland, V.; Cabezas-Cruz, A.; Atanasova, V.; Chereau, S.; Ponts, N.; Tonk, M.; Vilcinskas, A.; Ferrer, N.; Valdés, J.J.; Richard-Forget, F. Tick Defensin  $\gamma$ -Core Reduces *Fusarium Graminearum* Growth and Abrogates Mycotoxins Production with High Efficiency. *Sci. Rep.* **2021**, *11*, 7962. [[CrossRef](#)]
128. Zhang, Z.-T.; Zhu, S.-Y. Drosomycin, an Essential Component of Antifungal Defence in *Drosophila*. *Insect Mol. Biol.* **2009**, *18*, 549–556. [[CrossRef](#)] [[PubMed](#)]
129. Tian, C.; Gao, B.; del Rodriguez, M.C.; Lanz-Mendoza, H.; Ma, B.; Zhu, S. Gene Expression, Antiparasitic Activity, and Functional Evolution of the Drosomycin Family. *Mol. Immunol.* **2008**, *45*, 3909–3916. [[CrossRef](#)]
130. Broekaert, W.F.; Terras, F.; Cammue, B.; Osborn, R.W. Plant Defensins: Novel Antimicrobial Peptides as Components of the Host Defense System. *Plant Physiol.* **1995**, *108*, 1353–1358. [[CrossRef](#)] [[PubMed](#)]
131. Thomma, B.P.H.J.; Cammue, B.P.A.; Thevissen, K. Mode of Action of Plant Defensins Suggests Therapeutic Potential. *Curr. Drug Targets Infect. Disord.* **2003**, *3*, 1–8. [[CrossRef](#)] [[PubMed](#)]
132. Vriens, K.; Cammue, B.; Thevissen, K. Antifungal Plant Defensins: Mechanisms of Action and Production. *Molecules* **2014**, *19*, 12280–12303. [[CrossRef](#)]
133. Aumer, T.; Voisin, S.N.; Knobloch, T.; Landon, C.; Bulet, P. Impact of an Antifungal Insect Defensin on the Proteome of the Phytopathogenic Fungus *Botrytis Cinerea*. *J. Proteome Res.* **2020**, *19*, 1131–1146. [[CrossRef](#)] [[PubMed](#)]
134. Parisi, K.; Shafee, T.M.A.; Quimbar, P.; van der Weerden, N.L.; Bleackley, M.R.; Anderson, M.A. The Evolution, Function and Mechanisms of Action for Plant Defensins. *Semin. Cell Dev. Biol.* **2019**, *88*, 107–118. [[CrossRef](#)]
135. Struyfs, C.; Cammue, B.P.A.; Thevissen, K. Membrane-Interacting Antifungal Peptides. *Front. Cell Dev. Biol.* **2021**, *9*, 706. [[CrossRef](#)]
136. El-Mounadi, K.; Islam, K.T.; Hernández-Ortiz, P.; Read, N.D.; Shah, D.M. Antifungal Mechanisms of a Plant Defensin MtDef4 Are Not Conserved between the Ascomycete Fungi *Neurospora crassa* and *Fusarium graminearum*. *Mol. Microbiol.* **2016**, *100*, 542–559. [[CrossRef](#)]
137. Thevissen, K.; Francois, I.E.; Aerts, A.; Cammue, B. Fungal Sphingolipids as Targets for the Development of Selective Antifungal Therapeutics. *Curr. Drug Targets* **2005**, *6*, 923–928. [[CrossRef](#)] [[PubMed](#)]
138. Aerts, A.M.; François, I.E.J.A.; Bammens, L.; Cammue, B.P.A.; Smets, B.; Winderickx, J.; Accardo, S.; De Vos, D.E.; Thevissen, K. Level of M(IP)2C Sphingolipid Affects Plant Defensin Sensitivity, Oxidative Stress Resistance and Chronological Life-Span in Yeast. *FEBS Lett.* **2006**, *580*, 1903–1907. [[CrossRef](#)] [[PubMed](#)]

139. Ramamoorthy, V.; Cahoon, E.B.; Li, J.; Thokala, M.; Minto, R.E.; Shah, D.M. Glucosylceramide Synthase Is Essential for Alfalfa Defensin-Mediated Growth Inhibition but Not for Pathogenicity of *Fusarium graminearum*. *Mol. Microbiol.* **2007**, *66*, 771–786. [[CrossRef](#)] [[PubMed](#)]
140. De Paula, V.S.; Razzera, G.; Barreto-Bergter, E.; Almeida, F.C.L.; Valente, A.P. Portrayal of Complex Dynamic Properties of Sugarcane Defensin 5 by NMR: Multiple Motions Associated with Membrane Interaction. *Structure* **2011**, *19*, 26–36. [[CrossRef](#)] [[PubMed](#)]
141. Thevissen, K.; de Mello Tavares, P.; Xu, D.; Blankenship, J.; Vandenbosch, D.; Idkowiak-Baldys, J.; Govaert, G.; Bink, A.; Rozental, S.; de Groot, P.W.J.; et al. The Plant Defensin RsAFP2 Induces Cell Wall Stress, Septin Mislocalization and Accumulation of Ceramides in *Candida albicans*: RsAFP2 Affects C. Albicans Cell Wall and Septin. *Mol. Microbiol.* **2012**, *84*, 166–180. [[CrossRef](#)] [[PubMed](#)]
142. Fernandes, C.M.; de Castro, P.A.; Singh, A.; Fonseca, F.L.; Pereira, M.D.; Vila, T.V.M.; Atella, G.C.; Rozental, S.; Savoldi, M.; Del Poeta, M.; et al. Functional Characterization of the *A. Spergillus nidulans* Glucosylceramide Pathway Reveals That LCB  $\Delta 8$ -Desaturation and C9-Methylation Are Relevant to Filamentous Growth, Lipid Raft Localization and *Ps* D1 Defensin Activity: *Aspergillus nidulans* Glucosylceramide Pathway. *Mol. Microbiol.* **2016**, *102*, 488–505. [[CrossRef](#)]
143. Sagaram, U.S.; El-Mounadi, K.; Buchko, G.W.; Berg, H.R.; Kaur, J.; Pandurangi, R.S.; Smith, T.J.; Shah, D.M. Structural and Functional Studies of a Phosphatidic Acid-Binding Antifungal Plant Defensin MtDef4: Identification of an RGFRRR Motif Governing Fungal Cell Entry. *PLoS ONE* **2013**, *8*, e82485. [[CrossRef](#)]
144. Poon, I.K.; Baxter, A.A.; Lay, F.T.; Mills, G.D.; Adda, C.G.; Payne, J.A.; Phan, T.K.; Ryan, G.F.; White, J.A.; Veneer, P.K.; et al. Phosphoinositide-Mediated Oligomerization of a Defensin Induces Cell Lysis. *eLife* **2014**, *3*, e01808. [[CrossRef](#)]
145. Baxter, A.A.; Richter, V.; Lay, F.T.; Poon, I.K.H.; Adda, C.G.; Veneer, P.K.; Phan, T.K.; Bleackley, M.R.; Anderson, M.A.; Kvensakul, M.; et al. The Tomato Defensin TPP3 Binds Phosphatidylinositol (4,5)-Bisphosphate via a Conserved Dimeric Cationic Grip Conformation To Mediate Cell Lysis. *Mol. Cell. Biol.* **2015**, *35*, 1964–1978. [[CrossRef](#)]
146. De Medeiros, L.N.; Angeli, R.; Sarzedas, C.G.; Barreto-Bergter, E.; Valente, A.P.; Kurtenbach, E.; Almeida, F.C.L. Backbone Dynamics of the Antifungal Psd1 Pea Defensin and Its Correlation with Membrane Interaction by NMR Spectroscopy. *Biochim. Biophys. Acta—Biomembr.* **2010**, *1798*, 105–113. [[CrossRef](#)]
147. Aerts, A.M.; François, I.E.J.A.; Cammue, B.P.A.; Thevissen, K. The Mode of Antifungal Action of Plant, Insect and Human Defensins. *Cell. Mol. Life Sci.* **2008**, *65*, 2069–2079. [[CrossRef](#)]
148. Schneider, T.; Kruse, T.; Wimmer, R.; Wiedemann, I.; Sass, V.; Pag, U.; Jansen, A.; Nielsen, A.K.; Mygind, P.H.; Raventos, D.S.; et al. Plectasin, a Fungal Defensin, Targets the Bacterial Cell Wall Precursor Lipid II. *Science* **2010**, *328*, 1168–1172. [[CrossRef](#)]
149. Thevissen, K.; Terras, F.R.; Broekaert, W.F. Permeabilization of Fungal Membranes by Plant Defensins Inhibits Fungal Growth. *Appl. Environ. Microbiol.* **1999**, *65*, 5451–5458. [[CrossRef](#)] [[PubMed](#)]
150. Van der Weerden, N.L.; Lay, F.T.; Anderson, M.A. The Plant Defensin, NaD1, Enters the Cytoplasm of *Fusarium Oxysporum* Hyphae. *J. Biol. Chem.* **2008**, *283*, 14445–14452. [[CrossRef](#)] [[PubMed](#)]
151. Islam, K.T.; Velivelli, S.L.S.; Berg, R.H.; Oakley, B.; Shah, D.M. A Novel Bi-Domain Plant Defensin MtDef5 with Potent Broad-Spectrum Antifungal Activity Binds to Multiple Phospholipids and Forms Oligomers. *Sci. Rep.* **2017**, *7*, 16157. [[CrossRef](#)]
152. Lay, F.T.; Mills, G.D.; Poon, I.K.H.; Cowieson, N.P.; Kirby, N.; Baxter, A.A.; van der Weerden, N.L.; Dogovski, C.; Perugini, M.A.; Anderson, M.A.; et al. Dimerization of Plant Defensin NaD1 Enhances Its Antifungal Activity. *J. Biol. Chem.* **2012**, *287*, 19961–19972. [[CrossRef](#)] [[PubMed](#)]
153. Brogden, K.A. Antimicrobial Peptides: Pore Formers or Metabolic Inhibitors in Bacteria? *Nat. Rev. Microbiol.* **2005**, *3*, 238–250. [[CrossRef](#)] [[PubMed](#)]
154. Nakajima, Y.; Ishibashi, J.; Yukuhiro, F.; Asaoka, A.; Taylor, D.; Yamakawa, M. Antibacterial Activity and Mechanism of Action of Tick Defensin against Gram-Positive Bacteria. *Biochim. Biophys. Acta—Gen. Subj.* **2003**, *1624*, 125–130. [[CrossRef](#)]
155. Xiang, F.; Xie, Z.; Feng, J.; Yang, W.; Cao, Z.; Li, W.; Chen, Z.; Wu, Y. Plectasin, First Animal Toxin-Like Fungal Defensin Blocking Potassium Channels through Recognizing Channel Pore Region. *Toxins* **2015**, *7*, 34–42. [[CrossRef](#)]
156. Almeida, M.S.; Cabral, K.M.S.; Kurtenbach, E.; Almeida, F.C.L.; Valente, A.P. Solution Structure of *Pisum sativum* Defensin 1 by High Resolution NMR: Plant Defensins, Identical Backbone with Different Mechanisms of Action. *J. Mol. Biol.* **2002**, *315*, 749–757. [[CrossRef](#)]
157. Kushmerick, C.; de Souza Castro, M.; Santos Cruz, J.; Bloch, C.; Beirão, P.S.L. Functional and Structural Features of  $\gamma$ -Zeathonins, a New Class of Sodium Channel Blockers. *FEBS Lett.* **1998**, *440*, 302–306. [[CrossRef](#)]
158. Zhu, S.; Peigneur, S.; Gao, B.; Umetsu, Y.; Ohki, S.; Tytgat, J. Experimental Conversion of a Defensin into a Neurotoxin: Implications for Origin of Toxic Function. *Mol. Biol. Evol.* **2014**, *31*, 546–559. [[CrossRef](#)] [[PubMed](#)]
159. Meng, L.; Xie, Z.; Zhang, Q.; Li, Y.; Yang, F.; Chen, Z.; Li, W.; Cao, Z.; Wu, Y. Scorpion Potassium Channel-Blocking Defensin Highlights a Functional Link with Neurotoxin. *J. Biol. Chem.* **2016**, *291*, 7097–7106. [[CrossRef](#)] [[PubMed](#)]
160. Aerts, A.M.; François, I.E.J.A.; Meert, E.M.K.; Li, Q.-T.; Cammue, B.P.A.; Thevissen, K. The Antifungal Activity of RsAFP2, a Plant Defensin from *Raphanus Sativus*, Involves the Induction of Reactive Oxygen Species in *Candida albicans*. *J. Mol. Microbiol. Biotechnol.* **2007**, *13*, 243–247. [[CrossRef](#)]
161. Aerts, A.M.; Carmona-Gutierrez, D.; Lefevre, S.; Govaert, G.; François, I.E.J.A.; Madeo, F.; Santos, R.; Cammue, B.P.A.; Thevissen, K. The Antifungal Plant Defensin RsAFP2 from Radish Induces Apoptosis in a Metacaspase Independent Way in *Candida albicans*. *FEBS Lett.* **2009**, *583*, 2513–2516. [[CrossRef](#)]

162. Hayes, B.M.E.; Bleackley, M.R.; Wiltshire, J.L.; Anderson, M.A.; Traven, A.; van der Weerden, N.L. Identification and Mechanism of Action of the Plant Defensin NaD1 as a New Member of the Antifungal Drug Arsenal against *Candida Albicans*. *Antimicrob. Agents Chemother.* **2013**, *57*, 3667–3675. [[CrossRef](#)] [[PubMed](#)]
163. Hayes, B.M.E.; Bleackley, M.R.; Anderson, M.A.; van der Weerden, N.L. The Plant Defensin NaD1 Enters the Cytoplasm of *Candida Albicans* via Endocytosis. *J. Fungi* **2018**, *4*, 20. [[CrossRef](#)] [[PubMed](#)]
164. Aerts, A.M.; Bammens, L.; Govaert, G.; Carmona-Gutierrez, D.; Madeo, F.; Cammue, B.P.A.; Thevissen, K. The Antifungal Plant Defensin HsAFP1 from *Heuchera Sanguinea* Induces Apoptosis in *Candida Albicans*. *Front. Microbiol.* **2011**, *2*, 47. [[CrossRef](#)]
165. Ochiai, A.; Ogawa, K.; Fukuda, M.; Otori, M.; Kanaoka, T.; Tanaka, T.; Taniguchi, M.; Sagehashi, Y. Rice Defensin OsAFP1 Is a New Drug Candidate against Human Pathogenic Fungi. *Sci. Rep.* **2018**, *8*, 11434. [[CrossRef](#)]
166. Montibus, M.; Ducos, C.; Bonnin-Verdal, M.-N.; Bormann, J.; Ponts, N.; Richard-Forget, F.; Barreau, C. The BZIP Transcription Factor Fgap1 Mediates Oxidative Stress Response and Trichothecene Biosynthesis But Not Virulence in *Fusarium Graminearum*. *PLoS ONE* **2013**, *8*, e83377. [[CrossRef](#)]
167. Hale, J.D.; Hancock, R.E. Alternative Mechanisms of Action of Cationic Antimicrobial Peptides on Bacteria. *Expert Rev. Anti Infect. Ther.* **2007**, *5*, 951–959. [[CrossRef](#)]
168. Do Nascimento, V.V.; de Mello, É.O.; Carvalho, L.P.; de Melo, E.J.T.; de O. Carvalho, A.; Fernandes, K.V.S.; Gomes, V.M. PvD1 Defensin, a Plant Antimicrobial Peptide with Inhibitory Activity against *Leishmania amazonensis*. *Biosci. Rep.* **2015**, *35*, e00248. [[CrossRef](#)] [[PubMed](#)]
169. Lobo, D.S.; Pereira, I.B.; Fragel-Madeira, L.; Medeiros, L.N.; Cabral, L.M.; Faria, J.; Bellio, M.; Campos, R.C.; Linden, R.; Kurtenbach, E. Antifungal *Pisum Sativum* Defensin 1 Interacts with *Neurospora Crassa* Cyclin F Related to the Cell Cycle †. *Biochemistry* **2007**, *46*, 987–996. [[CrossRef](#)] [[PubMed](#)]
170. Montesinos, E. Antimicrobial Peptides and Plant Disease Control. *FEMS Microbiol. Lett.* **2007**, *270*, 1–11. [[CrossRef](#)] [[PubMed](#)]
171. Sher Khan, R.; Iqbal, A.; Malak, R.; Shehryar, K.; Attia, S.; Ahmed, T.; Ali Khan, M.; Arif, M.; Mii, M. Plant Defensins: Types, Mechanism of Action and Prospects of Genetic Engineering for Enhanced Disease Resistance in Plants. *Biotech.* **2019**, *9*, 192. [[CrossRef](#)]
172. Abdallah, N.A.; Shah, D.; Abbas, D.; Madkour, M. Stable Integration and Expression of a Plant Defensin in Tomato Confers Resistance to *Fusarium Wilt*. *GM Crops* **2010**, *1*, 344–350. [[CrossRef](#)]
173. Deb, D.; Shrestha, A.; Sethi, L.; Das, N.C.; Rai, V.; Das, A.B.; Maiti, I.B.; Dey, N. Transgenic Tobacco Expressing Medicago Sativa Defensin (Msdef1) Confers Resistance to Various Phyto-Pathogens. *Nucleus* **2020**, *63*, 179–190. [[CrossRef](#)]
174. Zhu, Y.J.; Agbayani, R.; Moore, P.H. Ectopic Expression of Dahlia Merckii Defensin DmAMP1 Improves Papaya Resistance to *Phytophthora palmicoora* by Reducing Pathogen Vigor. *Planta* **2007**, *226*, 87–97. [[CrossRef](#)]
175. Jha, S.; Tank, H.G.; Prasad, B.D.; Chattoo, B.B. Expression of Dm-AMP1 in Rice Confers Resistance to Magnaporthe Oryzae and Rhizoctonia Solani. *Transgenic Res.* **2009**, *18*, 59–69. [[CrossRef](#)]
176. Kostov, K.; Christova, P.; Slavov, S.; Batchvarova, R. Constitutive Expression of a Radish Defensin Gene *Rs-AFP2* in Tomato Increases the Resistance to Fungal Pathogens. *Biotechnol. Biotechnol. Equip.* **2009**, *23*, 1121–1125. [[CrossRef](#)]
177. Li, Z.; Zhou, M.; Zhang, Z.; Ren, L.; Du, L.; Zhang, B.; Xu, H.; Xin, Z. Expression of a Radish Defensin in Transgenic Wheat Confers Increased Resistance to *Fusarium graminearum* and *Rhizoctonia cerealis*. *Funct. Integr. Genom.* **2011**, *11*, 63–70. [[CrossRef](#)]
178. Portieles, R.; Ayra, C.; Gonzalez, E.; Gallo, A.; Rodriguez, R.; Chacón, O.; López, Y.; Rodriguez, M.; Castillo, J.; Pujol, M.; et al. NmDef02, a Novel Antimicrobial Gene Isolated from *Nicotiana megalosiphon* Confers High-Level Pathogen Resistance under Greenhouse and Field Conditions: NmDef02, a Novel Antimicrobial Protein. *Plant Biotechnol. J.* **2010**, *8*, 678–690. [[CrossRef](#)]
179. Soto, N.; Hernández, Y.; Delgado, C.; Rosabal, Y.; Ortiz, R.; Valencia, L.; Borrás-Hidalgo, O.; Pujol, M.; Enríquez, G.A. Field Resistance to Phakopsora Pachyrhizi and Colletotrichum Truncatum of Transgenic Soybean Expressing the NmDef02 Plant Defensin Gene. *Front. Plant Sci.* **2020**, *11*, 562. [[CrossRef](#)] [[PubMed](#)]
180. Kanzaki, H.; Nirasawa, S.; Saitoh, H.; Ito, M.; Nishihara, M.; Terauchi, R.; Nakamura, I. Overexpression of the Wasabi Defensin Gene Confers Enhanced Resistance to Blast Fungus (*Magnaporthe grisea*) in Transgenic Rice. *Theor. Appl. Genet.* **2002**, *105*, 809–814. [[CrossRef](#)]
181. Khan, R.S.; Nishihara, M.; Yamamura, S.; Nakamura, I.; Mii, M. Transgenic Potatoes Expressing Wasabi Defensin Peptide Confer Partial Resistance to Gray Mold (*Botrytis cinerea*). *Plant Biotechnol.* **2006**, *23*, 179–183. [[CrossRef](#)]
182. Ntui, V.O.; Thirukkumaran, G.; Azadi, P.; Khan, R.S.; Nakamura, I.; Mii, M. Stable Integration and Expression of Wasabi Defensin Gene in “Egusi” Melon (*Colocynthis citrullus* L.) Confers Resistance to *Fusarium Wilt* and *Alternaria Leaf Spot*. *Plant Cell Rep.* **2010**, *29*, 943–954. [[CrossRef](#)] [[PubMed](#)]
183. Kong, K.; Ntui, V.O.; Makabe, S.; Khan, R.S.; Mii, M.; Nakamura, I. Transgenic Tobacco and Tomato Plants Expressing Wasabi Defensin Genes Driven by Root-Specific LjNRT2 and AtNRT2.1 Promoters Confer Resistance against *Fusarium Oxysporum*. *Plant Biotechnol.* **2014**, *31*, 89–96. [[CrossRef](#)]
184. François, I.E.J.A.; Dwyer, G.I.; De Bolle, M.F.C.; Goderis, I.J.W.M.; Van Hemelrijck, W.; Proost, P.; Wouters, P.; Broekaert, W.F.; Cammue, B.P.A. Processing in Transgenic Arabidopsis Thaliana Plants of Polyproteins with Linker Peptide Variants Derived from the Impatiens Balsamina Antimicrobial Polyprotein Precursor. *Plant Physiol. Biochem.* **2002**, *40*, 871–879. [[CrossRef](#)]
185. Jha, S.; Chattoo, B.B. Transgene Stacking and Coordinated Expression of Plant Defensins Confer Fungal Resistance in Rice. *Rice* **2009**, *2*, 143–154. [[CrossRef](#)]

186. Coca, M.; Bortolotti, C.; Rufat, M.; Peñas, G.; Eritja, R.; Tharreau, D.; del Pozo, A.M.; Messeguer, J.; San Segundo, B. Transgenic Rice Plants Expressing the Antifungal AFP Protein from *Aspergillus Giganteus* Show Enhanced Resistance to the Rice Blast Fungus *Magnaporthe grisea*. *Plant Mol. Biol.* **2004**, *54*, 245–259. [[CrossRef](#)]
187. Banzet, N.; Latorse, M.-P.; Bulet, P.; François, E.; Derpierre, C.; Dubald, M. Expression of Insect Cystein-Rich Antifungal Peptides in Transgenic Tobacco Enhances Resistance to a Fungal Disease. *Plant Sci.* **2002**, *162*, 995–1006. [[CrossRef](#)]
188. Zarinpanjeh, N.; Motallebi, M.; Zamani, M.R.; Ziaei, M. Enhanced Resistance to *Sclerotinia sclerotiorum* in *Brassica napus* by Co-Expression of Defensin and Chimeric Chitinase Genes. *J. Appl. Genet.* **2016**, *57*, 417–425. [[CrossRef](#)] [[PubMed](#)]
189. Sasaki, K.; Kuwabara, C.; Umeki, N.; Fujioka, M.; Saburi, W.; Matsui, H.; Abe, F.; Imai, R. The Cold-Induced Defensin TAD1 Confers Resistance against Snow Mold and Fusarium Head Blight in Transgenic Wheat. *J. Biotechnol.* **2016**, *228*, 3–7. [[CrossRef](#)]
190. Kaur, J.; Thokala, M.; Robert-Seilaniantz, A.; Zhao, P.; Peyret, H.; Berg, H.; Pandey, S.; Jones, J.; Shah, D. Subcellular Targeting of an Evolutionarily Conserved Plant Defensin MtDef4.2 Determines the Outcome of Plant–Pathogen Interaction in Transgenic Arabidopsis. *Mol. Plant Pathol.* **2012**, *13*, 1032–1046. [[CrossRef](#)] [[PubMed](#)]
191. Sharma, K.K.; Pothana, A.; Prasad, K.; Shah, D.; Kaur, J.; Bhatnagar, D.; Chen, Z.-Y.; Raruang, Y.; Cary, J.W.; Rajasekaran, K.; et al. Peanuts That Keep Aflatoxin at Bay: A Threshold That Matters. *Plant Biotechnol. J.* **2018**, *16*, 1024–1033. [[CrossRef](#)]
192. Turrini, A.; Sbrana, C.; Pitto, L.; Ruffini Castiglione, M.; Giorgetti, L.; Briganti, R.; Bracci, T.; Evangelista, M.; Nuti, M.P.; Giovannetti, M. The Antifungal Dm-AMP1 Protein from *Dahlia Merckii* Expressed in *Solanum melongena* Is Released in Root Exudates and Differentially Affects Pathogenic Fungi and Mycorrhizal Symbiosis. *New Phytol.* **2004**, *163*, 393–403. [[CrossRef](#)]
193. Kaur, J.; Fellers, J.; Adholeya, A.; Velivelli, S.L.S.; El-Mounadi, K.; Nersesian, N.; Clemente, T.; Shah, D. Expression of Apoplast-Targeted Plant Defensin MtDef4.2 Confers Resistance to Leaf Rust Pathogen *Puccinia triticina* but Does Not Affect Mycorrhizal Symbiosis in Transgenic Wheat. *Transgenic Res.* **2017**, *26*, 37–49. [[CrossRef](#)]
194. Stotz, H.U.; Spence, B.; Wang, Y. A Defensin from Tomato with Dual Function in Defense and Development. *Plant Mol. Biol.* **2009**, *71*, 131–143. [[CrossRef](#)]
195. Allen, A.; Snyder, A.K.; Preuss, M.; Nielsen, E.E.; Shah, D.M.; Smith, T.J. Plant Defensins and Virally Encoded Fungal Toxin KP4 Inhibit Plant Root Growth. *Planta* **2007**, *227*, 331–339. [[CrossRef](#)]
196. Audenaert, K.; Vanheule, A.; Höfte, M.; Haesaert, G. Deoxynivalenol: A Major Player in the Multifaceted Response of Fusarium to Its Environment. *Toxins* **2014**, *6*, 1–19. [[CrossRef](#)]
197. Ponts, N. Mycotoxins Are a Component of *Fusarium graminearum* Stress-Response System. *Front. Microbiol.* **2015**, *6*, 1234. [[CrossRef](#)]
198. Paul, P.A.; Bradley, C.A.; Madden, L.V.; Lana, F.D.; Bergstrom, G.C.; Dill-Macky, R.; Esker, P.D.; Wise, K.A.; McMullen, M.; Grybauskas, A.; et al. Meta-Analysis of the Effects of QoI and DMI Fungicide Combinations on Fusarium Head Blight and Deoxynivalenol in Wheat. *Plant Dis.* **2018**, *102*, 2602–2615. [[CrossRef](#)]
199. Fisher, M.C.; Gurr, S.J.; Cuomo, C.A.; Bleher, D.S.; Jin, H.; Stukenbrock, E.H.; Stajich, J.E.; Kahmann, R.; Boone, C.; Denning, D.W.; et al. Threats Posed by the Fungal Kingdom to Humans, Wildlife, and Agriculture. *mBio* **2020**, *11*, e00449-20. [[CrossRef](#)]
200. Mahlapuu, M.; Håkansson, J.; Ringstad, L.; Björn, C. Antimicrobial Peptides: An Emerging Category of Therapeutic Agents. *Front. Cell. Infect. Microbiol.* **2016**, *6*, 194. [[CrossRef](#)] [[PubMed](#)]
201. Assoni, L.; Milani, B.; Carvalho, M.R.; Nepomuceno, L.N.; Waz, N.T.; Guerra, M.E.S.; Converso, T.R.; Darrieux, M. Resistance Mechanisms to Antimicrobial Peptides in Gram-Positive Bacteria. *Front. Microbiol.* **2020**, *11*, 593215. [[CrossRef](#)] [[PubMed](#)]
202. Wu, J.; Liu, S.; Wang, H. Invasive Fungi-Derived Defensins Kill Drug-Resistant Bacterial Pathogens. *Peptides* **2018**, *99*, 82–91. [[CrossRef](#)] [[PubMed](#)]
203. Kaewklom, S.; Wongchai, M.; Petvises, S.; Hanpithakphong, W.; Aunpad, R. Structural and Biological Features of a Novel Plant Defensin from *Brugmansia × candida*. *PLoS ONE* **2018**, *13*, e0201668. [[CrossRef](#)] [[PubMed](#)]
204. Benítez-Chao, D.F.; León-Buitimea, A.; Lerma-Escalera, J.A.; Morones-Ramírez, J.R. Bacteriocins: An Overview of Antimicrobial, Toxicity, and Biosafety Assessment by in Vivo Models. *Front. Microbiol.* **2021**, *12*, 677. [[CrossRef](#)]
205. Andersson, L.; Blomberg, L.; Flegel, M.; Lepsa, L.; Nilsson, B.; Verlander, M. Large-Scale Synthesis of Peptides. *Biopolymers* **2000**, *55*, 227–250. [[CrossRef](#)]
206. Skalska, J.; Andrade, V.M.; Cena, G.L.; Harvey, P.J.; Gaspar, D.; Mello, É.O.; Henriques, S.T.; Valle, J.; Gomes, V.M.; Conceição, K.; et al. Synthesis, Structure, and Activity of the Antifungal Plant Defensin PvD1. *J. Med. Chem.* **2020**, *63*, 9391–9402. [[CrossRef](#)] [[PubMed](#)]
207. Li, Y. Recombinant Production of Antimicrobial Peptides in *Escherichia coli*: A Review. *Protein Expr. Purif.* **2011**, *80*, 260–267. [[CrossRef](#)]
208. Druzinec, D.; Salzig, D.; Brix, A.; Kraume, M.; Vilcinskis, A.; Kollewe, C.; Czermak, P. Optimization of Insect Cell Based Protein Production Processes—Online Monitoring, Expression Systems, Scale Up. In *Yellow Biotechnology II*; Vilcinskis, A., Ed.; Advances in Biochemical Engineering/Biotechnology; Springer: Berlin/Heidelberg, Germany, 2013; Volume 136, pp. 65–100, ISBN 978-3-642-39901-5.
209. Kozlov, S.; Vassilevski, A.; Grishin, E. Antimicrobial Peptide Precursor Structures Suggest Effective Production Strategies. *Recent Pat. Inflamm. Allergy Drug Discov.* **2008**, *2*, 58–63. [[CrossRef](#)] [[PubMed](#)]
210. Deng, T.; Ge, H.; He, H.; Liu, Y.; Zhai, C.; Feng, L.; Yi, L. The Heterologous Expression Strategies of Antimicrobial Peptides in Microbial Systems. *Protein Expr. Purif.* **2017**, *140*, 52–59. [[CrossRef](#)]

211. Li, Y. Carrier Proteins for Fusion Expression of Antimicrobial Peptides in *Escherichia coli*. *Biotechnol. Appl. Biochem.* **2009**, *54*, 1–9. [[CrossRef](#)] [[PubMed](#)]
212. Butt, T.R.; Edavettal, S.C.; Hall, J.P.; Mattern, M.R. SUMO Fusion Technology for Difficult-to-Express Proteins. *Protein Expr. Purif.* **2005**, *43*, 1–9. [[CrossRef](#)] [[PubMed](#)]
213. Bommarius, B.; Jenssen, H.; Elliott, M.; Kindrachuk, J.; Pasupuleti, M.; Gieren, H.; Jaeger, K.-E.; Hancock, R.E.W.; Kalman, D. Cost-Effective Expression and Purification of Antimicrobial and Host Defense Peptides in *Escherichia Coli*. *Peptides* **2010**, *31*, 1957–1965. [[CrossRef](#)]
214. Sadr, V.; Saffar, B.; Emamzadeh, R. Functional Expression and Purification of Recombinant Hepcidin25 Production in *Escherichia Coli* Using SUMO Fusion Technology. *Gene* **2017**, *610*, 112–117. [[CrossRef](#)]
215. Mo, Q.; Fu, A.; Lin, Z.; Wang, W.; Gong, L.; Li, W. Expression and Purification of Antimicrobial Peptide AP2 Using SUMO Fusion Partner Technology in *Escherichia Coli*. *Lett. Appl. Microbiol.* **2018**, *67*, 606–613. [[CrossRef](#)]
216. Kant, P.; Liu, W.-Z.; Pauls, K.P. PDC1, a Corn Defensin Peptide Expressed in *Escherichia Coli* and *Pichia Pastoris* Inhibits Growth of *Fusarium graminearum*. *Peptides* **2009**, *30*, 1593–1599. [[CrossRef](#)]
217. Al Kashgry, N.A.T.; Abulreesh, H.H.; El-Sheikh, I.A.; Almaroai, Y.A.; Salem, R.; Mohamed, I.; Waly, F.R.; Osman, G.; Mohamed, M.S.M. Utilization of a Recombinant Defensin from Maize (*Zea Mays L.*) as a Potential Antimicrobial Peptide. *AMB Express* **2020**, *10*, 208. [[CrossRef](#)]
218. Kovaleva, V.; Bukhteeva, I.; Kit, O.Y.; Nesmelova, I.V. Plant Defensins from a Structural Perspective. *Int. J. Mol. Sci.* **2020**, *21*, 5307. [[CrossRef](#)] [[PubMed](#)]
219. Tleuova, A.B.; Wielogorska, E.; Talluri, V.S.S.L.P.; Štěpánek, F.; Elliott, C.T.; Grigoriev, D.O. Recent Advances and Remaining Barriers to Producing Novel Formulations of Fungicides for Safe and Sustainable Agriculture. *J. Control. Release Off. J. Control. Release Soc.* **2020**, *326*, 468–481. [[CrossRef](#)]
220. Gao, X.; Ding, J.; Liao, C.; Xu, J.; Liu, X.; Lu, W. Defensins: The Natural Peptide Antibiotic. *Adv. Drug Deliv. Rev.* **2021**, *179*, 114008. [[CrossRef](#)] [[PubMed](#)]
221. Markets and Markets. *Biofungicides Market by Type (Microbial Species, Botanical), Mode of Application (Soil Treatment, Foliar Application, Seed Treatment), Species (Bacillus, Trichoderma, Streptomyces, Pseudomonas), Crop Type, Formulation, and Region—Global Forecast to 2025*; Markets and Markets: Pune, India, 2020.
222. Mateo-Sagasta, J.; Zadeh, S.M.; Turrall, H.; Burke, J. *Water Pollution from Agriculture: A Global Review*; Executive, Summary; FAO: Rome, Italy; International Water Management Institute (IWMI); CGIAR Research Program on Water, Land and Ecosystems (WLE): Colombo, Sri Lanka, 2017.
223. Barratt, B.I.P.; Moran, V.C.; Bigler, F.; van Lenteren, J.C. The Status of Biological Control and Recommendations for Improving Uptake for the Future. *BioControl* **2018**, *63*, 155–167. [[CrossRef](#)]
224. NAFTA Technical Working Group on Pesticides North American Free Trade Agreement Technical Working Group on Pesticides—Updated Procedures for the Joint Review of Biopesticides (i.e., Microbials and Biochemicals). 2010. Available online: <https://www.canada.ca/en/health-canada/services/consumer-product-safety/pesticides-pest-management/public/protecting-your-health-environment/public-registry/north-american-free-trade-agreement-technical-working-group-pesticides-updated-procedures-joint-review-biopesticides-microbials-biochemicals.html> (accessed on 23 January 2022).
225. Neelabh; Singh, K.; Rani, J. Sequential and Structural Aspects of Antifungal Peptides from Animals, Bacteria and Fungi Based on Bioinformatics Tools. *Probiotics Antimicrob. Proteins* **2016**, *8*, 85–101. [[CrossRef](#)]

## 8. Tickcore 3, a peptide from the tick *Ixodes ricinus* could be an excellent candidate for biofungicide development

Ticks are ectoparasitic arthropods that obligatorily suck blood from vertebrate hosts (Boulanger et al., 2019)<sup>343</sup>. The castor bean tick *Ixodes ricinus* is the most common tick species in Europe. *I. ricinus* is a vector of causative agents of diseases that affect humans and animals such as bacteria, fungi, viruses, protozoa, and nematodes. It is responsible for Lyme disease, tick-borne encephalitis, human granulocytic anaplasmosis, rickettsioses and babesiosis. Ticks possess an efficient innate immune system that allow them to maintain the pathogens and commensal microbes at the level, which does not impair their fitness and further development. Antimicrobial peptides (AMPs) including defensins constitute an important feature of the tick immune system.

Many defensins isolated from ticks have been characterized (Nakajima et al., 2001; Fogaça et al., 2004, Hynes et al., 2005, Johns et al., 2001, Lai et al., 2004, Nakajima et al., 2001, Nakajima et al., 2002b, Saito et al., 2009, Todd et al., 2007, Tsuji et al., 2007, Wang and Zhu, 2011, Cabezas-Cruz et al., 2019)<sup>344,344–354</sup>. Before 2014, only two defensins were described for *I. ricinus* (Rudenko et al., 2005, Rudenko et al., 2007)<sup>355,356</sup>. In 2014, Tonk et al.<sup>357</sup> identified a diverse family of CS- $\alpha\beta$  defensins (DefMT2–7) (Fig. 25).

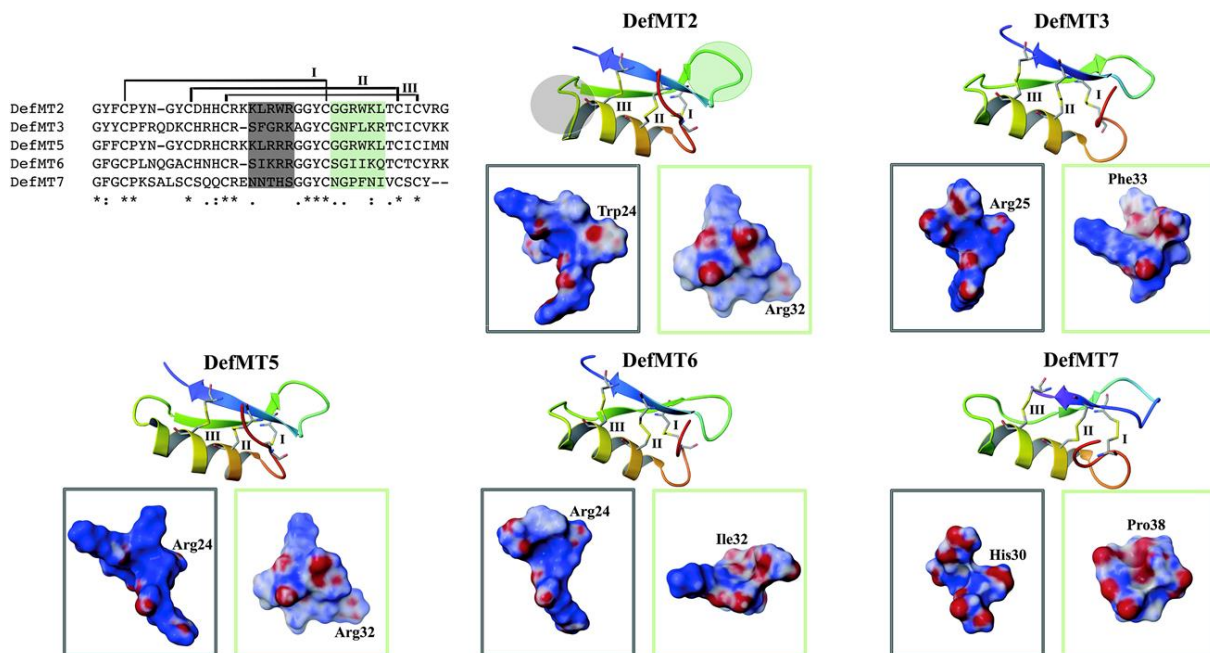


Figure 145. Tertiary structures of *I. ricinus* defensins (Tonk et al., 2015).

Among the five unique defensins reported in the above Figure, only DefMT3, DefMT5 and DefMT6 showed *in vitro* antimicrobial efficiency against different species of fungi (*F. culmorum* and *F. graminearum*), Gram-negative (*Escherichia coli* and *Pseudomonas aeruginosa*) and Gram-positive (different *Listeria* and *Staphylococcus* species) bacteria that are not transmitted by tick confirming the broad-spectrum activity of defensins (Tonk et al., 2015)<sup>358</sup>. Whereas *I. ricinus* defensins were active against distantly related pathogens, the defensin Scapularisin-6

from the tick is *Ixodes scapularis* was shown as only active against the Gram-positive bacterium *Listeria grayi*, but not against Gram-negative bacteria or any other *Listeria* species (Tonk et al., 2014)<sup>359</sup>.

DefMT3 (GenBank accession number: JAA71488) is an isoform of the defensins Def 1 and Def 2 from *I. ricinus* (Rudenko et al., 2005, Rudenko et al., 2007)<sup>355,356</sup>. DefMT3 possesses an amphipathic structure with  $\alpha$ -helix/ $\beta$ -sheet mixed structures. Its CS- $\alpha\beta$  tertiary fold structure is believed to be essential for antimicrobial action (Bulet et al., 2004)<sup>360</sup>. Furthermore, defensins possess specific functional motifs known as the  $\alpha$ -patch, the m-loop and the  $\gamma$ -patch responsible for bactericidal/fungicidal activity (Zhang and Zhu, 2009)<sup>361</sup>. The ' $\gamma$ -core motif' functional region of defensins is located in the C-terminal  $\beta$ -sheet domain (Wang and Zhu, 2011)<sup>353</sup>.

The  $\gamma$ -core motifs of DefMT3 and DefMT6, respectively TickCore 3 (TC3) and 6, showed higher antifungal activity on spore germination compared to whole peptides, with TickCore 3 displaying stronger activity (Tonk et al., 2015)<sup>358</sup>. However, the bactericidal effect of the  $\gamma$ -core of DefMT3 and DefMT6 was reduced compared to the full peptides, suggesting the  $\gamma$ -core isn't the only responsible for the antimicrobial effect of those peptides.

## Thesis project

As mentioned previously, there is an increasing request for new alternatives utilizing natural antifungal compounds to control *Fusarium* pathogens and replace the use of synthetic fungicides. The defensin DefMT3 and its  $\gamma$ -core TC3 showed promising results as antifungal compounds against *F. graminearum*. Moreover, the DefMT3 defensin, as a naturally occurring substance that has been identified in its natural state, could be used as a biocontrol product. However, its efficacy against the various FHB agents and mechanisms of action were largely unknown. The purpose of this thesis project was to decipher the mechanisms underlying the bioactivity of TC3 against FHB causal agents (with a strong focus on *F. graminearum*) and its capacity to reduce TCTB accumulation.

To reach this objective, three research axes (corresponding to the three result chapters of this manuscript) have been implemented:

The first one aims to precise the efficacy of DefMT3 and TC3 against *F. graminearum* and DON yield and to determine the structural elements of the TC3 peptide responsible for its bioactivity.

The second axis aims to deepen the knowledge regarding the bioactivity of TC3 by considering the different developmental stages of *F. graminearum* and introducing various strains from *F. graminearum* and other FHB causal agents

The third axis aims to reach a comprehensive view of the mechanisms that explain the activity of TC3 by the use of an experimental strategy combining metabolomics and transcriptomics approaches.



**Chapter 1:**  
**Assessment of TC3 antifungal and anti-  
mycotoxin properties and investigation  
of the structural determinants required  
for the bioactivity**



## **Chapter 1: Assessment of TC3 antifungal and anti-mycotoxin properties and investigation of the structural determinants required for the bioactivity**

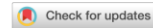
As highlighted in the introduction part of this thesis manuscript, the focus of our work will be the tick defensin DefMT3 and mostly its  $\gamma$ -core TickCore3 or TC3. These two peptides have been previously reported to inhibit spore germination in *F. graminearum* (Tonk et al., 2015)<sup>358</sup>. However, nothing was known regarding their capacity to decrease the fungal growth after incubation in a rich medium and even less regarding their potential to inhibit TCTB yield.

Therefore, the aim of this first chapter was to deepen the knowledge on the bioactivity of TC3 against *F. graminearum* by quantifying both the amount of mycelium and the TCTB levels in liquid broths supplemented with TC3 at different concentrations. To go further, the use of TC3 variants was considered to identify the structural elements of TC3 that are involved in its bioactivity. Finally, in planta assays were implemented to validate the potential of TC3 to be used as part of a plant protection strategy.

### **A) Tick defensin $\gamma$ -core reduces *Fusarium graminearum* growth and abrogates mycotoxins production with high efficiency**

(article published in scientific report, [doi.org/10.1038/s41598-021-86904-w](https://doi.org/10.1038/s41598-021-86904-w))





OPEN

# Tick defensin $\gamma$ -core reduces *Fusarium graminearum* growth and abrogates mycotoxins production with high efficiency

Valentin Leannec-Rialland<sup>1,10</sup>, Alejandro Cabezas-Cruz<sup>2,10</sup>✉, Vessela Atanasova<sup>3</sup>, Sylvain Chereau<sup>3</sup>, Nadia Ponts<sup>3</sup>, Miray Tonk<sup>4,5</sup>, Andreas Vilcinskas<sup>4,5,6</sup>, Nathalie Ferrer<sup>3</sup>, James J. Valdés<sup>7,8,9</sup> & Florence Richard-Forget<sup>3</sup>✉

*Fusarium graminearum* is a major fungal pathogen affecting crops of worldwide importance. *F. graminearum* produces type B trichothecene mycotoxins (TCTB), which are not fully eliminated during food and feed processing. Therefore, the best way to minimize TCTB contamination is to develop prevention strategies. Herein we show that treatment with the reduced form of the  $\gamma$ -core of the tick defensin DefMT3, referred to as TickCore3 (TC3), decreases *F. graminearum* growth and abrogates TCTB production. The oxidized form of TC3 loses antifungal activity, but retains anti-mycotoxin activity. Molecular dynamics show that TC3 is recruited by specific membrane phospholipids in *F. graminearum* and that membrane binding of the oxidized form of TC3 is unstable. Capping each of the three cysteine residues of TC3 with methyl groups reduces its inhibitory efficacy. Substitutions of the positively-charged residues lysine (Lys) 6 or arginine 7 by threonine had the highest and the lesser impact, respectively, on the anti-mycotoxin activity of TC3. We conclude that the binding of linear TC3 to *F. graminearum* membrane phospholipids is required for the antifungal activity of the reduced peptide. Besides, Lys6 appears essential for the anti-mycotoxin activity of the reduced peptide. Our results provide foundation for developing novel and environment-friendly strategies for controlling *F. graminearum*.

*Fusarium graminearum* is the major causal agent of two devastating diseases affecting cereal-growing areas around the world. Fusarium head blight (FHB) affects small grain cereals including wheat, oat, barley, rice and rye, a Gibberella ear rot (GER) has a major impact on maize production. In addition to cause grain yield losses<sup>1,2</sup>, *F. graminearum* can produce mycotoxins of the family type B trichothecenes (TCTB), including deoxynivalenol (DON) and its 15- or 3-acetylated forms (15- and 3-ADON), that constitute important food contaminants. DON toxicity has been well-documented and represents a public health concern<sup>3</sup>. To protect consumers, maximum admissible DON content for cereals and maize-based food were set by the European Commission in June 2005 (EC No856/2005) and revised in July 2007 (EC No1126/2007). DON is resistant to biodegradation and food processing and currently, there is no suitable detoxification procedure available. As a consequence, the occurrence of TCTB in cereal-derived products cannot be reduced by post-harvest treatments. Although good agricultural practices have been proposed to reduce the impact of *Fusarium* and DON contamination on cereal grains,

<sup>1</sup>Université de Bordeaux, INRAE, Mycology and Food Safety (MycSA), 33882 Villenave d'Ornon, France. <sup>2</sup>Anses, INRAE, Ecole Nationale Vétérinaire D'Alfort, UMR BIPAR, Laboratoire de Santé Animale, 94700 Maisons-Alfort, France. <sup>3</sup>INRAE, Mycology and Food Safety (MycSA), 33882 Villenave d'Ornon, France. <sup>4</sup>Institute for Insect Biotechnology, Justus Liebig University of Giessen, Heinrich-Buff-Ring 26-32, 35392 Giessen, Germany. <sup>5</sup>LOEWE Centre for Translational Biodiversity Genomics (LOEWE-TBG), Senckenberganlage 25, 60325 Frankfurt, Germany. <sup>6</sup>Department of Bioresources, Fraunhofer Institute for Molecular Biology and Applied Ecology, Ohlebergsweg 12, 35392 Giessen, Germany. <sup>7</sup>Faculty of Science, University of South Bohemia, Branišovská 1160/31, 37005 České Budějovice, Czech Republic. <sup>8</sup>Institute of Parasitology, Biology Centre, Czech Academy of Sciences, Branišovská 1160/31, 37005 České Budějovice, Czech Republic. <sup>9</sup>Department of Virology, Veterinary Research Institute, Hudcova 70, 62100 Brno, Czech Republic. <sup>10</sup>These authors contributed equally: Valentin Leannec-Rialland and Alejandro Cabezas-Cruz. ✉email: alejandro.cabezas@vet-alfort.fr; florence.forget@inrae.fr

Peptide names	Sequence <sup>a</sup>	Synthesis modification
TC3	CGNFLKRTCICVKK	Reduced
TC3Ox	CGNFLKRTCICVKK	Oxidation
TC3-CH3-123	C(CH <sub>3</sub> )GNFLKRTC(CH <sub>3</sub> )IC(CH <sub>3</sub> )VKK	Methylation
TC3-CH3-1	C(CH <sub>3</sub> )GNFLKRTCICVKK	Methylation
TC3-CH3-2	CGNFLKRTC(CH <sub>3</sub> )ICVKK	Methylation
TC3-CH3-3	CGNFLKRTCIC(CH <sub>3</sub> )VKK	Methylation
TC3-CH3-1Ox	C(CH <sub>3</sub> )GNFLKRTCICVKK	Methylation followed by oxidation
TC3-CH3-2Ox	CGNFLKRTC(CH <sub>3</sub> )ICVKK	Methylation followed by oxidation
TC3-CH3-3Ox	CGNFLKRTCIC(CH <sub>3</sub> )VKK	Methylation followed by oxidation
TC3-K6T	CGNFL <u>TR</u> TCICVKK	Amino acid substitution
TC3-R7T	CGNFLK <u>T</u> TCICVKK	Amino acid substitution
TC3-K13T	CGNFLKRTCICV <u>T</u> K	Amino acid substitution
TC3-K14T	CGNFLKRTCICV <u>K</u> T	Amino acid substitution

**Table 1.** List of peptides synthesized and used in this study. <sup>a</sup>Amino acids substitutions are underlined and in bold letters.

they are not always efficient to guarantee the compliance with the safety regulations. Thus, the development of innovative sustainable and environment-friendly solutions to reduce contaminations of cereals with mycotoxins produced by *F. graminearum* is particularly encouraged.

Ticks are important vectors of pathogens affecting human and animal health worldwide<sup>4</sup>. Ticks carry a high diversity of pathogenic and non-pathogenic microorganisms including bacteria, viruses, protozoa, helminths and fungi<sup>4–6</sup>. Ticks develop a vast array of humoral and cellular immune reactions in response to microbial challenge<sup>7</sup>. Defensins, a family of antimicrobial peptides (AMP), are major effector molecules of tick humoral immunity<sup>7</sup>. Tick defensins have a wide spectrum of antimicrobial activity against gram-negative and gram-positive bacteria, but also against eukaryotes such as fungi and apicomplexan parasites<sup>8–11</sup>. Similar to plant defensins, tick defensins inhibit the growth of *F. graminearum*<sup>8,12,13</sup>. Previous studies showed that the  $\gamma$ -cores of *Ixodes ricinus* defensins, DefMT3 and DefMT6, are potent antifungal agents that inhibit *F. graminearum* germination in a dose-dependent manner<sup>9</sup>. In this study, we asked whether tick defensin  $\gamma$ -cores would inhibit TCTB production by *F. graminearum* and aimed to identify the structural determinants of such activity. Our study, focusing on the  $\gamma$ -core of DefMT3, showed that Cys cyclization is not necessary for the antifungal and anti-mycotoxin activity of tick  $\gamma$ -cores. Furthermore, we demonstrated the key role of positively charged amino acids for both types of activity.

## Material and methods

**Synthesis of tick  $\gamma$ -core TickCore3.** TickCore3 (TC3) is the  $\gamma$ -core of the *Ixodes ricinus* defensin DefMT3 (GenBank accession number: JAA71488)<sup>9</sup>. Peptide synthesis was commissioned to Pepmic (Suzhou, China) that uses solid-phase peptide synthesis (SPPS) to obtain highly-pure peptides as previously described<sup>10</sup>. Briefly, peptide synthesis was performed using 2-chlorotrityl chloride resin as the solid support, using the base labile 9-fluorenyl-methyloxy-carbonyl (Fmoc) as protecting group. Amino acids were protected as follows: Fmoc-Cys(Trt)-OH, Fmoc-Gly-OH, Fmoc-Asn(Trt)-OH, Fmoc-Phe-OH, Fmoc-Leu-OH, Fmoc-Lys(Boc)-OH, Fmoc-Arg(Pbf)-OH, Fmoc-Thr(tBu)-OH, Fmoc-Ile-OH and Fmoc-Val-OH. All the peptide sequences were synthesized according to the principles of SPPS. High Performance Liquid Chromatography (HPLC)-grade Fmoc chloride (Fmoc-Cl)-protected amino acid-based peptide chemistry was used with standard peptide chemistry coupling protocols. Peptides were purified by reverse phase HPLC and peptide sequence was confirmed by electrospray mass spectrometry (ESI-MS) using a mass spectrometer LCMS-2020 (Shimadzu, Kyoto, Japan). Oxidation was achieved using a folding buffer containing 1 M urea, 100 mM Tris (pH 8.0), 1.5 mM oxidized glutathione, 0.75 mM reduced glutathione and 10 mM methionine. Oxidation of Cys residues was confirmed by Ellman reagent reaction and sulfide bond formation was characterized by ESI-MS on a mass spectrometer LCMS-2020 (Shimadzu, Kyoto, Japan). The peptide TC3Ox was synthesized as TC3, but synthesis was followed by oxidation using folding buffer. The peptides TC3-CH3-123, TC3-CH3-1, TC3-CH3-2 and TC3-CH3-3, TC3-CH3-1Ox, TC3-CH3-2Ox and TC3-CH3-3Ox were synthesized as above but Fmoc-Cys(Me)-OH was added instead of Fmoc-Cys(Trt)-OH and the synthesis of TC3-CH3-1Ox, TC3-CH3-2Ox and TC3-CH3-3Ox was followed by oxidation using folding buffer. Capping the sulfur (S) of the thiol group of all Cys prevents Cys cyclization (*i.e.*, no disulfide bridge can be formed). Conversely, capping the S of the thiol group of individual Cys followed by oxidation directs the cyclization of the reduced Cys (*i.e.*, those that were not capped). Four peptides were synthesized as TC3 with amino acid substitutions, referred as TC3-K6T (Lys6 substituted by Thr), TC3-R7T (Arg7 substituted by Thr), TC3-K13T (Lys13 substituted by Thr) and TC3-K14T (Lys 14 substituted by Thr). The sequences of TC3 and all TC3 variants are available in Table 1.

**Classical molecular dynamics.** *TC3 and membrane structures.* The tertiary structure of the linearized TC3 peptide was constructed in silico by truncating the predicted DefMT3 *Ixodes ricinus* salivary defensin from our previous study<sup>9</sup>. Both termini of the TC3 were capped with an acetyl group (amine terminus) and a N-methyl amide group (carboxyl terminus). The electrostatic potential of TC3 was generated using tools from the

Schrodinger's Maestro molecular software package, release 2020–4<sup>14</sup>. The CHARMM-GUI automated server<sup>15</sup> was used to construct the heterogenous bilayer membrane. The upper leaflet of the membrane bilayer consisted of 62 phospholipids [32 phosphatidylcholine (POPC), 14 phosphatidylethanolamine (POPE), 6 phosphatidylinositol (POPI), 4 phosphatidylserine (POPS), 2 phosphatidic acid (POPA), 2 phosphatidylglycerol (POPG), and tetraoleoyl cardiolipin 2 (TOCL)]. The lower leaflet consisted of 64 phospholipids (36 POPC and 28 POPE). The heterogenous bilayer membrane therefore consisted of 126 phospholipids. The TC3 and membrane systems were then prepared separately and the hydrogen-bond network was optimized using the Schrodinger's Maestro Protein Preparation Wizard<sup>16</sup>. After preparation and optimization, a global minimization was performed using Maestro default settings to remove any steric clashes.

**All-atom molecular simulation protocol.** The optimized TC3 peptide and bilayer membrane were oriented separately in an orthorhombic box (40 Å × 40 Å × 40 Å and 64 Å × 64 Å × 130 Å, respectively) with a TIP3P explicit model, neutralized and salted with 0.15 M NaCl. The force fields used to parameterize the two systems were, TIP3P CHARMM<sup>17</sup> for the solvent, AMBER99SB-ILDN<sup>18–20</sup> for the TC3 peptide, and CHARMM36<sup>21</sup> for the membrane and ions. The program CGenFF<sup>22,23</sup>, based on CHARMM36<sup>21</sup>, was used to retrieve force field parameters for phospholipids POPI and TOCL. Classical molecular dynamics (MD) calculations were performed using Desmond<sup>24</sup>. Semi-isotropic conditions for MD were used under an NPT ensemble coupled with a Nose–Hoover thermostat<sup>25</sup> and Martyna–Tobias–Klein barostat<sup>26</sup>. The temperature was set at 37 °C with a RESPA<sup>27</sup> integrator at an inner time step of 2.5 fs. All MD calculations were conducted using a GPU-accelerated (*i.e.*, graphics card) workstation.

The phospholipid bilayer membrane was first equilibrated using the Desmond<sup>24</sup> protocol provided by the CHARMM-GUI automated server<sup>15</sup>. The final CHARMM-GUI membrane production frame generated and the TC3 were separately equilibrated for 4 μs and 1 μs, respectively, using the MD protocol above. The final frame from the TC3 and membrane equilibration was used as the starting conformations for the combined peptide-membrane system. The TC3 was positioned 30 Å from its residue α-carbons to the phospholipid phosphorus atoms of the upper membrane surface and was equilibrated, as before, for 100 ns in an orthorhombic box 64 Å × 64 Å × 130 Å. Production MD calculations for analyses were then conducted for 1 μs using the last equilibrated frame under the same above protocol except using an NVT ensemble (where the volume is kept constant, not the pressure). The MD calculations for the cysteine oxidized form of TC3 (TC3Ox) was conducted using the same aforementioned protocol. The MD calculations were analysed using the Schrodinger's Maestro software package<sup>14</sup>.

**Mycotoxin production inhibition assay.** *Fusarium strain and culture conditions.* The *F. graminearum* CBS185.32 strain (Westerdijk Institute, The Netherlands) was selected for its capacity to produce high concentrations of DON and 15-ADON and was used throughout the study. Fungal culture was maintained at 4 °C on Potato Dextrose Agar (PDA) (Difco, Le Ponts de Claix, France) slants under mineral oil. Conidia were prepared by inoculating agar plugs in CMC medium (15 g/L carboxymethyl cellulose, 1 g/L yeast extract, 0.5 g/L MgSO<sub>4</sub>·7H<sub>2</sub>O, 1 g/L NH<sub>4</sub>NO<sub>3</sub>, 1 g/L KH<sub>2</sub>PO<sub>4</sub>), incubating at 150 rpm and 25 °C for three to five days, and harvesting by filtration through Seifar Nitex 03–100 (SEFAR AG, Heiden, Switzerland). Liquid-culture experiments were performed in 24-well static plates. Each well containing 2 mL of a mycotoxin synthetic (MS) medium (20 g/L glucose, 0.5 g/L KH<sub>2</sub>PO<sub>4</sub>, 0.6 g/L K<sub>2</sub>HPO<sub>4</sub>, 17 mg/L MgSO<sub>4</sub>, 1 g/L (NH<sub>4</sub>)<sub>2</sub>SO<sub>4</sub>, 0.1 mL/L Vogel mineral salts solution<sup>28</sup>) prepared as previously described<sup>29</sup>, supplemented or not with TC3 or its variants at three concentrations (12.5, 25 and 50 μM), was inoculated with 2 × 10<sup>4</sup> spores/mL. Fungal liquid cultures were incubated at 25 °C in the dark for 10 days. Following incubation, mycelia were recovered by centrifugation and fungal biomass was measured by weighing the mycelia after 48 h of freeze-drying (Flexi-Dry, Oerlikon Leybold, Germany). Culture media were stored at –20 °C until TCTB analysis. All peptides were tested at three concentrations 12.5, 25 and 50 μM. Five repetitions were made for each condition. Controls using TC3-free control media and non-inoculated control media were included.

**Extraction and analysis of TCTB.** The procedure was adapted from a previously published procedure<sup>29</sup>. Briefly, 1.5 mL sample of culture medium was extracted with 3 mL of ethyl acetate. A volume of 2.5 mL of the organic phase was evaporated to dryness at 45 °C under nitrogen flux. Dried samples were dissolved in 200 μL of methanol/water (1/1, v/v) and filtered through a 0.2 μm filter before analysis. TCTB were quantified by HPLC–DAD using an Agilent Technologies 1100 series liquid chromatograph equipped with an auto sampler system, an Agilent photodiode array detector (DAD) and the ChemStation chromatography manager software (Agilent, France). Separation was achieved on a Kinetex XB-C18 100 Å column (4.6 × 150 mm, 2.6 μm) (Phenomenex, France) maintained at 45 °C. The mobile phase consisted of water acidified with ortho-phosphoric acid to pH 2.6 (solvent A) and acetonitrile (solvent B). The flow was kept at 1 mL min<sup>–1</sup>. The injection volume was set to 5 μL. TCTB were separated using a gradient elution as follows: 7–30% B in 10 min, 30–90% B in 5 min, 90% B for 5 min, 90–7% B for 2 min, 7% B for 5 min. The UV–Vis spectra were recorded from 190 to 400 nm and peak areas were measured at 230 nm. Quantification was performed by external calibration with standard solutions (Romer Labs, Austria). Toxin yields were expressed in μg g<sup>–1</sup> of fungal dry biomass.

**Statistical analyses.** All presented values are mean ± standard deviation including five biological replications. Since the data were non-normally distributed (Shapiro–Wilk normality test), the Kruskal–Wallis one-way analysis was used, with mean comparisons performed using the Mann–Whitney U test. Statistical analysis was conducted with R<sup>30</sup> and figures were produced using the package ggplot2<sup>31</sup>. The statistical thresholds  $p = 0.05$  (\*),  $p = 0.01$  (\*\*) and  $p = 0.005$  (\*\*\*) were used throughout the study.

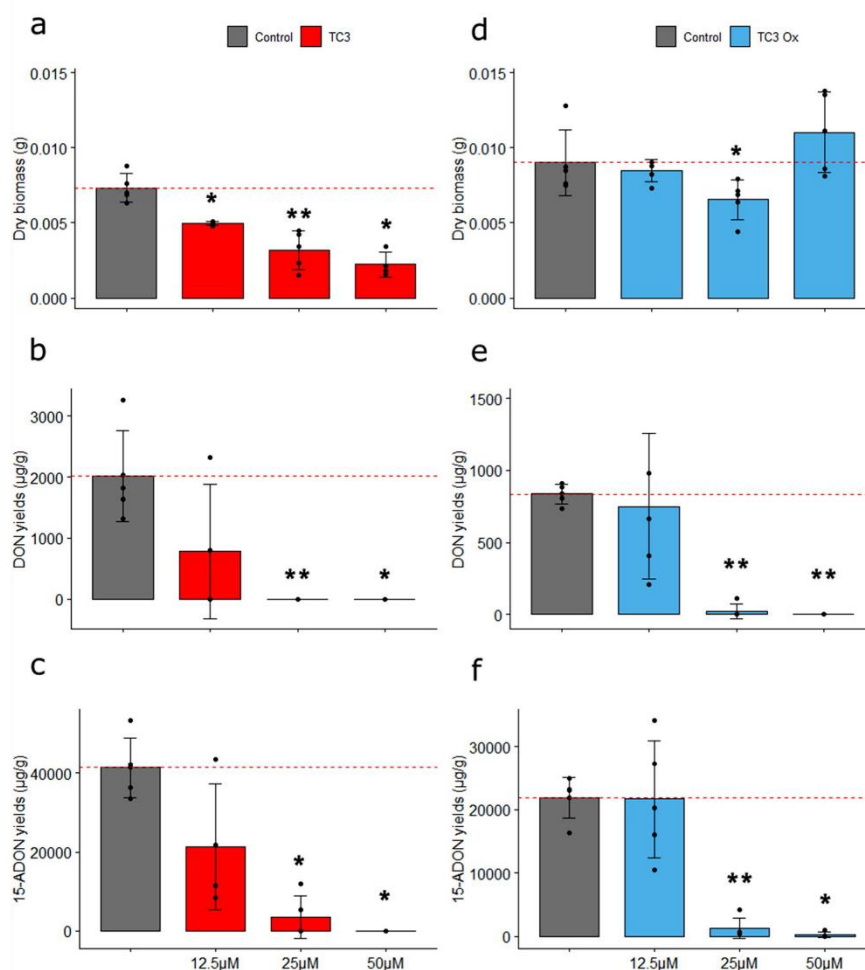


**Figure 1.** Antifungal and anti-mycotoxin activity of natural and oxidized TC3. Effect of reduced TC3 (a–c) and oxidized TC3 (d–f) at 12.5, 25 and 50 µM on the fungal biomass weight of *F. graminearum* (a, d) and on the production of DON (b, e) and 15-ADON (c, f) in 10-day-old broths. Significant differences are labelled (\* $p < 0.05$ , \*\* $p < 0.01$  and \*\*\* $p < 0.005$ ).

## Results

**Linear TC3 is a strong inhibitor of TCTB production by *F. graminearum*.** *F. graminearum* cultures were supplemented or not with the peptide TC3. A significant dose-dependent inhibition of fungal growth was registered under all tested TC3 concentrations compared with control samples (Fig. 1a). Concerning mycotoxin production, 15-ADON was the more abundant TCTB detected in the liquid media (Fig. 1b,c). In control samples, production of 15-ADON ( $41,347 \pm 7622$  µg/g) was 20 times higher than that of DON ( $2014 \pm 742$  µg/g). Supplementation with 25 and 50 µM TC3 reduced both DON (Fig. 1b) and 15-ADON (Fig. 1c) synthesis to trace amounts. However, only a non-significant reduction of DON (Fig. 1b) and 15-ADON (Fig. 1c) was observed with 12.5 µM TC3. Compared to TC3, the TC3Ox had a reduced effect on the dry fungal biomass (Fig. 1d). However, similar to TC3, the detected amounts of DON (Fig. 1e) and 15-ADON (Fig. 1f) were significantly decreased in the 25 µM and 50 µM TC3Ox-treated samples.

The purity, amino acid sequence and reduction status of the TC3 and TC3Ox cysteine (Cys) residues were evaluated by HPLC and ESI-MS (Supplementary Figure S1). A major peak, representing 95% of the composition

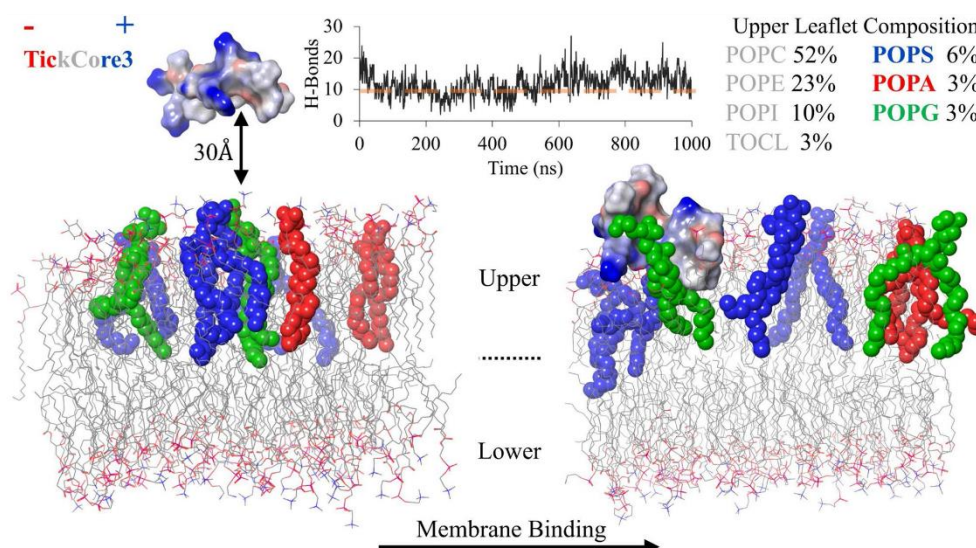


**Figure 2.** Membrane binding of TickCore3. The TC3 electrostatic potential of its residues are color-labeled as red (negative), grey (neutral) and blue (positive). The TC3 was placed 30 Å—from residue  $\alpha$ -carbons to the phospholipid phosphorus atoms of the upper membrane surface. The upper and lower membrane leaflets, before and after 1  $\mu$ s of MD, are shown with the majority of phospholipids depicted as sticks (grey = carbon, red = oxygen, and blue = nitrogen) (hydrogen atoms not shown). The main phospholipids (POPS, POPA and POPG) forming hydrogen bonds with TC3 are depicted as colored spheres (see legend for color scheme and percent composition). The line graph depicts the number hydrogen bond contacts (H-Bonds; y-axis) throughout the 1  $\mu$ s of MD (x-axis; in ns). The dashed orange line in the graph is the average H-Bond contacts ( $\bar{x} = 9.7$ ) between the membrane and the TC3Ox.

of the purified peptide, was observed in the HPLC chromatogram of TC3. The observed molecular weight (MW) of the purified TC3 (*i.e.*, 1613 Da) matched the theoretical MW of TC3 (Supplementary Figure S1) and included the three hydrogen ( $H^+$ , considering that the MW of  $H^+$  is approximately 1) of the thiol groups of the three Cys. TC3Ox was purified and refolded in folding buffer to obtain the oxidized form of TC3. HPLC analysis of the final purified and oxidized TC3Ox revealed a complex mix of peptides eluted with different retention times (Supplementary Figure S1). The identity of the most abundant peptide, representing 44% of the area, was characterized by ESI-MS and revealed the presence of a peptide with a MW that matches the MW of a homodimer TC3, referred here to as TC3-TC3. The MW of TC3-TC3 having three  $-S-S-$  bonds should be approximately 6 Da less than the double of the MW of a monomer of TC3 before the oxidation (*i.e.*,  $(1613 \times 2) - 6 = 3220$ ), resulting from the loss of 6  $H^+$  from the six reduced sulfhydryl groups ( $-SH$ ). This was confirmed using ESI-MS; the observed MW of TC3-TC3 was indeed 3220 Da (Supplementary Figure S1). In addition to the dimer TC3-TC3, three possible disulphide bridge combinations (Cys1-Cys9, Cys1-Cys11 and Cys9-Cys11) could result in three different oxidized monomers of TC3. However, no oxidized TC3 monomer was detected by ESI-MS probably due to the lower representation within the oxidized mix and concentrations below detection thresholds (Supplementary Figure S1).

**Linear TC3 is recruited by specific membrane phospholipids.** The *in silico* TC3 peptide for the MD calculations is a truncated form of the previous predicted tertiary structure of the *I. ricinus* DefMT3<sup>9</sup>. The TC3 electrostatic potential is mainly neutral with four highly positive residues (Lys/Arg) (Fig. 2). To approximate a natural heterogenous membrane, the upper leaflet was based on the actual phospholipid composition of *E. graminearum*<sup>32</sup> (Fig. 2). The TC3 was positioned with most of its residues facing away from or parallel to the upper membrane leaflet (Fig. 2). After equilibration (100 ns; see Material and Methods), the TC3 was immediately recruited by the upper leaflet. During the 1  $\mu$ s MD production stage, the hydrogen bond contacts formed between the TC3 and the upper leaflet reduced for the first 500 ns, but later increased after 600 ns (line graph in Fig. 2). The specific upper leaflet phospholipid types that recruit TC3 are POPS, POPA and POPG (color-coded in Fig. 2). Although multiple copies of these phospholipid types were present in the upper leaflet (Fig. 2), TC3 only formed contacts with a single POPS, POPA and/or POPG during the last 400 ns of the 1  $\mu$ s MD.

The TC3 was membrane-bound after equilibration, but, as indicated by the increased distances from POPA and POPG (Fig. 3A), disassociates from the upper leaflet during the first 500 ns. The membrane recruitment of TC3 then stabilizes with POPA and POPG approximately at 600 ns (Fig. 3A). After 600 ns, TC3-POPA average

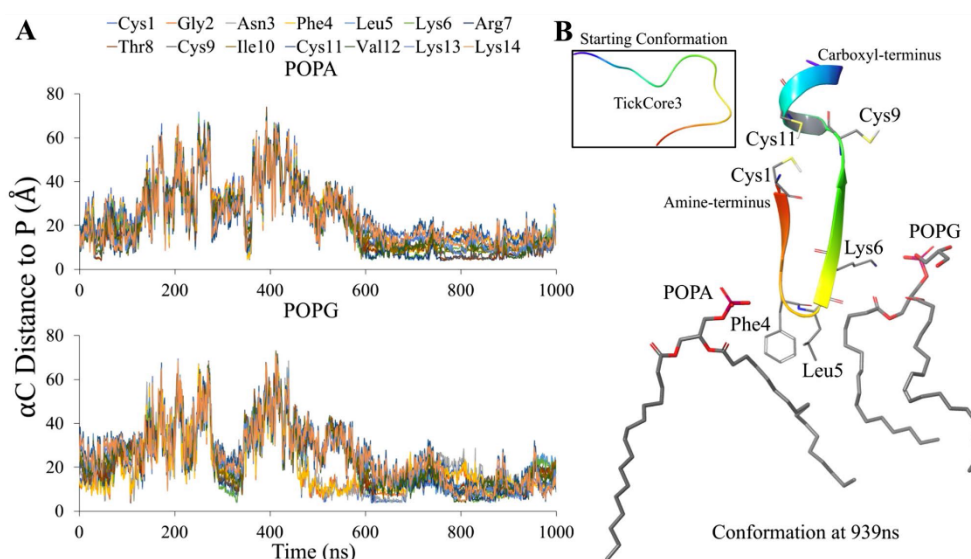


**Figure 3.** Recruitment of TC3 by POPA and POPG phospholipids. The line graphs (A) are the distances measured (y-axis) between the  $\alpha$ -carbon ( $\alpha$ C) of TC3 residues and the phosphorus (P) atom of POPA (upper) and POPG (lower) throughout the 1  $\mu$ s of MD (x-axis; in ns). The structural conformation at 0.939  $\mu$ s of MD (B) shows the specific TC3 residues 4–6 that interact with POPA and POPG (hydrogen atoms not shown). The tertiary structure of TC3 also depicts the Cys residues (with hydrogen caps) and is color-coded from the amine-terminus (red) to the carboxyl-terminus (purple).

contact distances were between 7–14 Å and 11–15 Å with POPG (Fig. 3A). Association with POPS demonstrated greater distances with TC3 after 600 ns of MD (averaging 18–25 Å; Supplementary Figure S2). Between the two phospholipids, on average, POPA forms closer contacts (< 11 Å) with half of TC3 than POPG, namely with residues Leu5—Ile10 and Val12 (Fig. 3A). The closest average distance, however, for both POPA (6.8 Å) and POPG (11.2 Å), is with TC3 residue Arg7 (Fig. 3A).

The TC3Ox formed an average of 9.7 hydrogen bond contacts with the membrane throughout the 1  $\mu$ s MD, similarly as the first 500 ns of the TC3 MD calculations (line graph A in Fig. 3). The TC3Ox MD calculations show unstable contacts formed with POPA, POPG and POPS (Supplementary Figure S3A). The TC3Ox secondary structure conformations during the 1  $\mu$ s MD are dominated by simple turns and coils with helical folding occurring at both peptide termini after ~400 ns of MD (Supplementary Figure S3B). The helical folding coincides when TC3Ox momentarily associates with the membrane (Supplementary Figure S3).

Depending on membrane disassociation and association (Fig. 3A and Supplementary Figure S2), TC3 undergoes considerable secondary structure conformations throughout the 1  $\mu$ s MD (Supplementary Figure S4). The TC3 during the first half of the 1  $\mu$ s MD is marked by coils and turns with sporadic helices forming throughout residues Cys4—Ile10 (Supplementary Figure S4). These dynamics are quite similar to the folds occurring during the 1  $\mu$ s MD of TC3Ox frequent disassociation with the membrane (Supplementary Figure S3). Only after 580 ns, while approximating membrane association (Fig. 3A and Supplementary Figure S2), does TC3 fold into more ordered secondary structures (Supplementary Figure S4). The MD timeline demonstrates (Supplementary Figure S4) that TC3 transitions between a simple coil-turn structure (membrane disassociation) to a  $\beta$ -hairpin/ $\alpha$ -helix structure (membrane association)—as shown in complex with POPA and POPG (Fig. 3B).

**Methylation of Cys reduces the antifungal and anti-mycotoxin activities of TC3.** The purity and sequence of all methylated variants of TC3, TC3-CH3-1Ox, TC3-CH3-2Ox and TC3-CH3-3Ox, were confirmed by HPLC and ESI-MS, respectively (Supplementary Figure S5). As shown in the HPLC chromatogram, high purity (*i.e.*, ~95%) was achieved for the oxidized peptides TC3-CH3-1Ox, TC3-CH3-2Ox and TC3-CH3-3Ox (Supplementary Figure S5). The observed MW (*i.e.*, 1627 Da) of the purified  $\gamma$ -cores TC3-CH3-1, TC3-CH3-2 and TC3-CH3-3 before oxidation corresponded with the theoretical MW for each of them (*i.e.*, 1627 Da). The ESI-MS analysis performed after the oxidation protocol confirmed the loss of two H<sup>+</sup> in each peptide. Quantitative analysis of -SH revealed that no Cys residue was available for reaction with the Ellman's reagent, indicating, in combination with the ESI-MS results, that all the non-capped Cys residues were involved in intramolecular disulphide linkages.

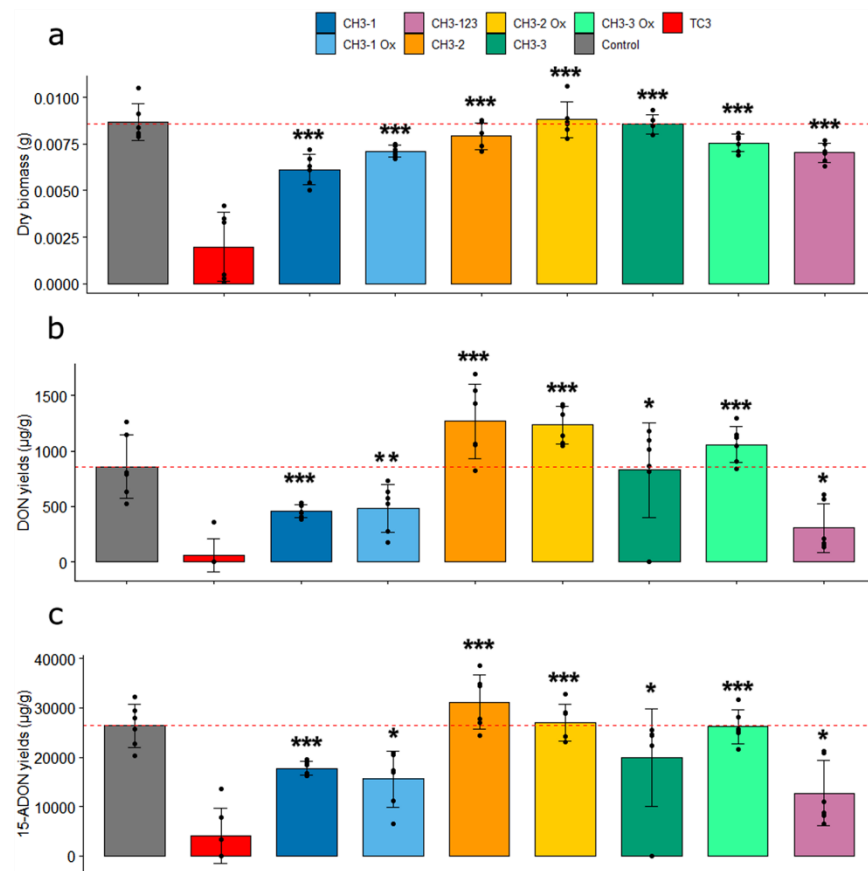


**Figure 4.** Antifungal and anti-mycotoxin activity of linear, methylated and oxidized TC3. Effect of reduced TC3, TC3-CH<sub>3</sub>-1, TC3-CH<sub>3</sub>-2, TC3-CH<sub>3</sub>-3, TC3-CH<sub>3</sub>-1 Ox, TC3-CH<sub>3</sub>-2 Ox, TC3-CH<sub>3</sub>-3 Ox and TC3-CH<sub>3</sub>-123 at 50 µM on the fungal biomass weight of *F. graminearum* (a) and on the production of DON (b) and 15-ADON (c) in 10-day-old broths. Significant differences are labelled (\* $p < 0.05$ , \*\* $p < 0.01$  and \*\*\* $p < 0.005$ ).

All the methylated variants TC3-CH<sub>3</sub>-1, TC3-CH<sub>3</sub>-2, TC3-CH<sub>3</sub>-3 and the cyclized variants TC3-CH<sub>3</sub>-1Ox, TC3-CH<sub>3</sub>-2Ox, TC3-CH<sub>3</sub>-3Ox had significantly less effect on fungal mycelium growth when compared with TC3 (Fig. 4a). Mycotoxin production of *F. graminearum* was then measured after adding the different methylated-reduced and methylated-oxidized-cyclized variants at 50 µM. All variants had a significantly lower inhibitory effect on DON and 15-ADON production compared with TC3. However, the treatments with TC3-CH<sub>3</sub>-1 and TC3-CH<sub>3</sub>-1Ox led to a reduction in DON (Fig. 4b) and 15-ADON (Fig. 4c) levels compared to the control.

Thus, the production of 15-ADON was reduced by about 33% in presence of TC3-CH<sub>3</sub>-1 ( $p$  value = 0.002) and by about 42% in presence of TC3-CH<sub>3</sub>-1Ox ( $p$  value = 0.017). An additional peptide, TC3-CH<sub>3</sub>-123, with all Cys capped with CH<sub>3</sub> groups was synthesized. *F. graminearum* exposed to TC3-CH<sub>3</sub>-123 produced significantly more DON and 15-ADON than TC3. The reduction in the ability to inhibit TCTB production was similar in all methylated-reduced and methylated-oxidized-cyclized variants, suggesting that Cys capping reduces the activity of TC3, regardless of oxidation and cyclization status. However, methyl caps on Cys9 (TC3-CH<sub>3</sub>-2Ox) and Cys11 (TC3-CH<sub>3</sub>-3Ox) had the most negative impact in the activity of TC3.

**The positively charged residues are essential for the antifungal and anti-mycotoxin activities of TC3.** The role of cationic charges on the biological activity of TC3 was tested using TC3 variants in which positive residues Lys6 (TC3-K61), Arg7 (TC3-R71), Lys13 (TC3-K13T) and Lys14 (TC3-K14T) were individu-

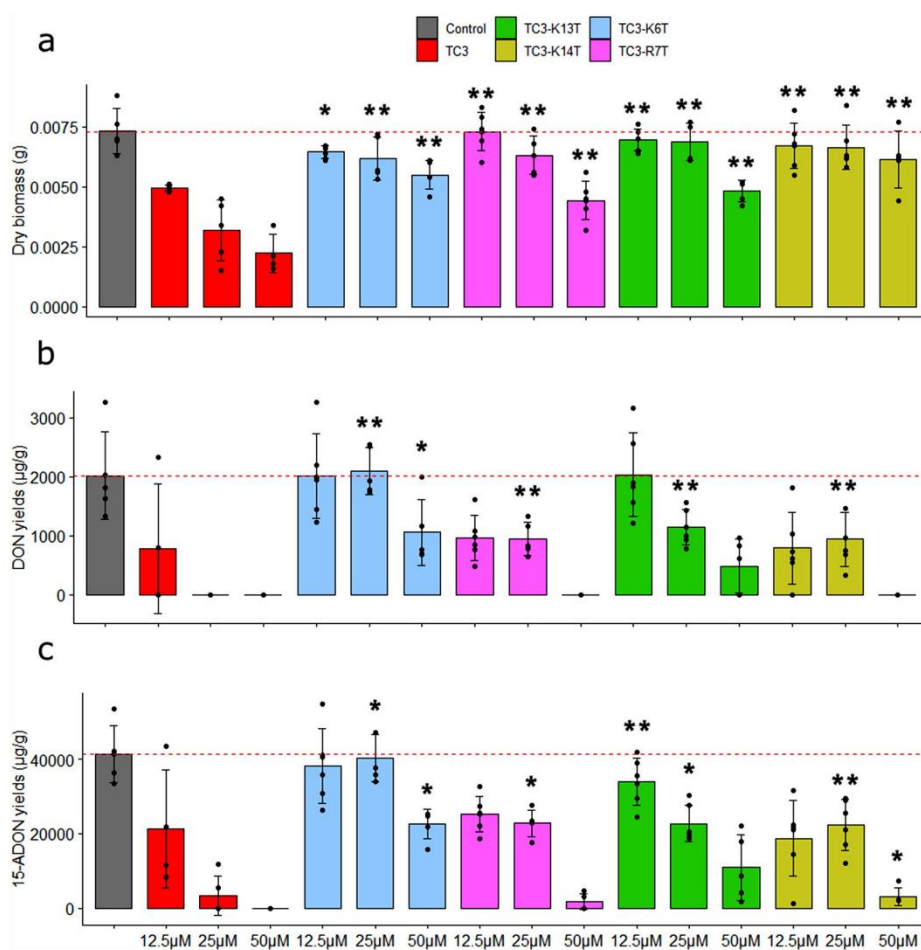


**Figure 5.** Role of positively charged amino acids on the activity of TC3. Effect of reduced TC3, TC3-K6T, TC3-R7T, TC3-K13T or TC3-K14T at 12.5, 25 and 50 μM on the fungal biomass weight of *F. graminearum* (a) and on the production of DON (b) and 15-ADON (c) in 10-day-old broths. Significant differences are labelled (\* $p < 0.05$ , \*\* $p < 0.01$  and \*\*\* $p < 0.005$ ).

ally substituted by the neutral amino acid Thr. Purity (*i.e.*, ~95%) and sequence of the TC3 variants were confirmed by HPLC and ESI-MS, respectively. The variants TC3-K6T, TC3-R7T and TC3-K13T had significant effect on fungal growth at 50 μM, when compared to the control (with respective  $p$ -values of 0.012, 0.004 and 0.012), while TC3-K14T had no effect at the tested concentrations. However, the antifungal activity of all variants was significantly reduced in comparison with that of native peptide TC3 (Fig. 5a).

Mycotoxin production by *F. graminearum* was measured in media supplemented with TC3-K6T, TC3-R7T, TC3-K13T and TC3-K14T at three different concentrations 12.5, 25 and 50 μM. All variants showed a lower DON (Fig. 5b) and 15-ADON (Fig. 5c) production inhibition activity compared with the native peptide TC3. Peptide TC3-K6T had the lowest inhibitory activity on TCTB production, suggesting that Lys6 plays important roles in the anti-mycotoxin activity of TC3.

## Discussion

The current study demonstrates that the  $\gamma$ -core motif TC3 reduces the growth of *F. graminearum* strain CBS 185.32 in a dose-dependent manner. In agreement with our findings, TC3 was previously reported to decrease germination in *F. graminearum* strain 8/1 with little or no effect on bacterial growth<sup>9</sup>. It is noteworthy that while

DefMT3 has both antibacterial and antifungal effects<sup>9</sup>, TC3 has only antifungal effect suggesting that this  $\gamma$ -core is responsible for the antifungal activity of DefMT3. This also suggests that the structural bases of the antifungal and antibacterial activity of DefMT3 are independent. Previous studies showed that the  $\gamma$ -core of the plant defensin MtDef4 alone was capable of inhibiting *F. graminearum* growth, but not that of MsDef1<sup>33</sup>. Remarkably, 50  $\mu$ M of TC3 reduced fungal growth 1.8 times and abrogated the production of mycotoxins DON and 15-ADON by *F. graminearum*. The moderate antifungal effect and high anti-mycotoxin effect suggest that the mechanism of inhibition of toxin biosynthesis is independent from the fungicide effect.

Arthropod defensins have six cysteine residues that form a conserved pattern of disulfide bridges in the combinations Cys1–Cys4, Cys2–Cys5 and Cys3–Cys6<sup>34,35</sup>. The formation of disulfide bridges by Cys cyclization confers stability to insect and chelicerate defensins<sup>34,35</sup>. Consequently, cyclization is expected to enhance the activity of defensins. For example, while both fully-oxidized and linear persulcatusin, a defensin from *Ixodes persulcatus* ticks, showed activity against *Staphylococcus aureus*, the activity of fully-oxidized peptides was significantly higher than that of linear peptides<sup>36</sup>. In addition, loss of a single disulphide bridge was enough to disrupt the antibacterial activity of Coprisin, a defensin of the beetle *Copris tripartitus*<sup>34</sup>. TC3 contains the last three Cys of DefMT3 (Cys4, Cys5 and Cys6-named in this study Cys1, Cys9 and Cys11 considering their position in TC3) and oxidation of TC3 forms three possible disulfide bridge combinations (i.e. Cys1–Cys9 or Cys1–Cys11 or Cys9–Cys11). None of these monomeric disulfide combinations was observed when oxidation was induced in the non-methylated TC3. Instead of oxidized monomers, a TC3 dimer (TC3–TC3) was detected by mass spectrometry suggesting that inter-molecular, and not intra-molecular, disulfide bridges prevail in spontaneous oxidative folding of TC3. The dimerization decreased the antifungal activity of TC3, contrasting with results obtained on plant defensin NaD1 where dimerization enhances its antifungal activity<sup>37</sup>. Antifungal activity assays showed that cyclic TC3 peptides have a severely reduced capacity to inhibit the fungal growth and the production of TCTB, compared with the linear TC3. This is in contrast with previous reports on human defensins in which cyclization enhanced the antimicrobial activity of  $\gamma$ -cores<sup>38,39</sup>.

Antifungal peptides were originally considered as lytic molecules acting primarily by permeabilizing the plasma membrane after interactions with cell wall components. Recently published data have indicated the preference of some defensins to interact with sphingolipids and phospholipids contained in lipid rafts, that house critical proteins for the regulation of membrane potential, intracellular pH, and nutrient transport<sup>40,41</sup>. Protein-lipid overlay assays showed that the plant defensin Psd2 targets the phospholipid POPC in the membrane of *Fusarium solani*<sup>41</sup>. In contrast to Psd2, our membrane modelling showed that TC3 is recruited by POPS, POPA and POPG, but not by POPC. Further studies using *F. graminearum* mutants lacking membrane phospholipids POPS, POPA, POPG or POPC could be used to test in vitro or in silico results. Besides, our results suggest that the four cationic acids contained in TC3 are partly responsible for its antifungal activity. Particularly, results show that Lys6 plays a key role in the anti-mycotoxin activity of TC3. The importance of Lys6 may be due to its positive charge combined with its position close to the Phe28 and Leu29 in the native protein DefMT3, which were predicted to interact with a lipid bilayer membrane in silico<sup>10,42</sup>. The role of cationic charges in the activity of antimicrobial peptides has been reported<sup>43</sup>. These cationic charges have been shown to be involved in the interaction of defensins with the negatively charged phospholipids of the fungal membrane leading to pore formation, dysregulation of ion homeostasis and cell death<sup>44</sup>.

Moreover, there are currently several evidences that antifungal peptides, including plant defensins, can reach intracellular targets and exert their activity by mechanisms in addition to permeabilization of the membrane<sup>45,46</sup>. In particular, these mechanisms involve the production of reactive oxygen species (ROS) in fungal cells and the inhibition of substrate acidification<sup>47</sup>, which are two environmental factors with a recognized modulating effect on the production of TCTB<sup>48</sup>. Defensins also interact with components of the tricarboxylic acid (TCA) cycle and GABA shunt<sup>49</sup> that are tightly related with the mycotoxin biosynthesis pathway<sup>50</sup>. Despite being derived from a tick defensin, the mechanistic action of TC3 may be similar to that of insect antimicrobial peptides (AMP). For example, the AMP metchnikowin from *Drosophila melanogaster* has potent activity against *F. graminearum*<sup>49</sup>. Metchnikowin affects *F. graminearum* by inhibiting the activity of the fungal enzyme iron-sulfur subunit of succinate-coenzyme Q reductase, a key enzyme in the TCA cycle and the electron transport chain<sup>49</sup>. Alternatively, TC3 may specifically inhibit the activity of some enzymatic components of the TCTB biosynthetic pathway, in the same way that some phenolic compounds inhibit the activity of trichodiene synthase, the first and key enzyme of the cascade leading to the accumulation of TCTB<sup>51</sup>.

## Conclusion

TC3 is a potent antifungal peptide that inhibits germination<sup>9</sup> and does not require Cys cyclization to inhibit the growth and TCTB production of *F. graminearum*. TC3 cyclization reduces the antifungal activity, especially when disulphide bridges are formed between Cys1–Cys11 or Cys1–Cys9. This suggests structural rigidity of the N-terminus having Cys1 reduced the activity of TC3. The cationic amino acids are partly responsible for the antifungal and anti-mycotoxin activities of TC3, notably Lys6. The results reported here advance our current understanding of the mechanism of action of tick molecules with antifungal and anti-mycotoxin activities and pave the way for developing novel and environment-friendly strategies for the control of *F. graminearum* using arthropod-derived peptides.

Received: 9 December 2020; Accepted: 19 March 2021

Published online: 12 April 2021

## References

- Ferrigo, D., Raiola, A. & Causin, R. Fusarium toxins in cereals: occurrence, legislation, factors promoting the appearance and their management. *Molecules* **21**, 627 (2016).
- Wilson, W., Dahl, B. & Nganje, W. Economic costs of *Fusarium* head blight, scab and deoxynivalenol. *World Mycotoxin J.* **11**, 291–302 (2018).
- Sobrova, P. *et al.* Deoxynivalenol and its toxicity. *Interdiscip. Toxicol.* **3**, 94–99 (2010).
- de la Fuente, J. *et al.* Tick-pathogen interactions and vector competence: identification of molecular drivers for tick-borne diseases. *Front. Cell. Infect. Microbiol.* **7**, 144 (2017).
- Angelo, I. C. *et al.* Physiological changes in *Rhipicephalus microplus* (Acari: Ixodidae) experimentally infected with entomopathogenic fungi. *Parasitol. Res.* **114**, 219–225 (2015).
- Cabezas-Cruz, A. *et al.* Antibacterial and antifungal activity of defensins from the Australian paralysis tick, *Ixodes holocyclus*. *Ticks Tick Borne Dis.* **10**, 101269 (2019).
- Hajdušek, O. *et al.* Interaction of the tick immune system with transmitted pathogens. *Front. Cell. Infect. Microbiol.* **3**, 26 (2013).
- Tonk, M. *et al.* Defensins from the tick *Ixodes scapularis* are effective against phytopathogenic fungi and the human bacterial pathogen *Listeria grayi*. *Parasites Vectors* **7**, 554 (2014).
- Tonk, M. *et al.* Ixodes ricinus defensins attack distantly-related pathogens. *Dev. Comp. Immunol.* **53**, 358–365 (2015).
- Cabezas-Cruz, A. *et al.* Antiplasmodial activity is an ancient and conserved feature of tick defensins. *Front. Microbiol.* **7**, 1682 (2016).
- Couto, J. *et al.* Antiplasmodial activity of tick defensins in a mouse model of malaria. *Ticks Tick Borne Dis.* **9**, 844–849 (2018).
- Spelbrink, R. G. *et al.* Differential antifungal and calcium channel-blocking activity among structurally related plant defensins. *Plant Physiol.* **135**, 2055–2067 (2004).
- Ramamoorthy, V., Zhao, X., Snyder, A. K., Xu, J.-R. & Shah, D. M. Two mitogen-activated protein kinase signalling cascades mediate basal resistance to antifungal plant defensins in *Fusarium graminearum*. *Cell. Microbiol.* **9**, 1491–1506 (2007).
- Schrödinger Release 2020–3: Maestro, Schrödinger, LLC, New York, NY (2020).
- Jo, S., Kim, T., Iyer, V. G. & Im, W. CHARMM-GUI: a web-based graphical user interface for CHARMM. *J. Comput. Chem.* **29**, 1859–1865 (2008).
- Madhavi Sastry, G., Adzhigirey, M., Day, T., Annabhimoju, R. & Sherman, W. Protein and ligand preparation: parameters, protocols, and influence on virtual screening enrichments. *J. Comput. Aided Mol. Des.* **27**, 221–234 (2013).
- Jorgensen, W. L., Chandrasekhar, J., Madura, J. D., Impey, R. W. & Klein, M. L. Comparison of simple potential functions for simulating liquid water. *J. Chem. Phys.* **79**, 926–935 (1983).
- Wang, J., Cieplak, P. & Kollman, P. A. How well does a restrained electrostatic potential (RESP) model perform in calculating conformational energies of organic and biological molecules? *J. Comput. Chem.* **21**, 1049–1074 (2000).
- Hornak, V. *et al.* Comparison of multiple Amber force fields and development of improved protein backbone parameters. *Proteins* **65**, 712–725 (2006).
- Lindorff-Larsen, K. *et al.* Improved side-chain torsion potentials for the Amber ff99SB protein force field. *Proteins* **78**, 1950–1958 (2010).
- Kluda, J. B. *et al.* Update of the CHARMM all-atom additive force field for lipids: validation on six lipid types. *J. Phys. Chem. B* **114**, 7830–7843 (2010).
- Vanommeslaeghe, K. & MacKerell, A. D. Automation of the CHARMM General Force Field (CGenFF) I: bond perception and atom typing. *J. Chem. Inf. Model.* **52**, 3144–3154 (2012).
- Vanommeslaeghe, K., Raman, E. P. & MacKerell, A. D. Automation of the CHARMM General Force Field (CGenFF) II: assignment of bonded parameters and partial atomic charges. *J. Chem. Inf. Model.* **52**, 3155–3168 (2012).
- Bowers, K. J. *et al.* Scalable algorithms for molecular dynamics simulations on commodity clusters. In *SC '06: Proceedings of the 2006 ACM/IEEE Conference on Supercomputing* 43–43 (2006). <https://doi.org/10.1109/SC.2006.54>.
- Hoover, W. G. Canonical dynamics: equilibrium phase-space distributions. *Phys. Rev. A* **31**, 1695–1697 (1985).
- Martyna, G. J., Tobias, D. J. & Klein, M. L. Constant pressure molecular dynamics algorithms. *J. Chem. Phys.* **101**, 4177–4189 (1994).
- Tuckerman, M., Berne, B. J. & Martyna, G. J. Reversible multiple time scale molecular dynamics. *J. Chem. Phys.* **97**, 1990–2001 (1992).
- Vogel, H. J. A convenient growth medium for *Neurospora crassa*. *Microb. Genet. Bull.* **13**, 42–47 (1956).
- Boutigny, A.-L. *et al.* Ferulic acid, an efficient inhibitor of type B trichothecene biosynthesis and Tri gene expression in *Fusarium* liquid cultures. *Mycol. Res.* **113**, 746–753 (2009).
- R Core Team. *R: A language and environment for statistical computing*. R Foundation for Statistical Computing, Vienna, Austria. <https://www.r-project.org/index.html>.
- Wickham, H. *ggplot2: Elegant Graphics for Data Analysis*. (Springer International Publishing: Imprint: Springer, 2016). doi:<https://doi.org/10.1007/978-3-319-24277-4>.
- Wiebe, M. G., Robson, G. D. & Trinci, A. P. J. Effect of choline on the morphology, growth and phospholipid composition of *Fusarium graminearum*. *Microbiology* **135**, 2155–2162 (1989).
- Sagaram, U. S., Pandurangi, R., Kaur, J., Smith, T. J. & Shah, D. M. Structural and functional studies of a phosphatidic acid-binding antifungal plant defensin MtDef4: identification of an RGFRRR motif governing fungal cell entry. *PLoS ONE* **8**(12), e82485 (2013).
- Lee, J. *et al.* Structure-activity relationships of the intramolecular disulfide bonds in coprisin, a defensin from the dung beetle. *BMB Rep.* **47**, 625–630 (2014).
- Miyoshi, N. *et al.* Functional structure and antimicrobial activity of persulcatusin, an antimicrobial peptide from the hard tick *Ixodes persulcatus*. *Parasites Vectors* **9**, 85 (2016).
- Isogai, E. *et al.* Tertiary structure-related activity of tick defensin (persulcatusin) in the taiga tick, *Ixodes persulcatus*. *Exp. Appl. Acarol.* **53**, 71–77 (2011).
- Lay, F. T. *et al.* Dimerization of plant defensin NaD1 enhances its antifungal activity. *J. Biol. Chem.* **287**, 19961–19972 (2012).
- Scudiero, O. *et al.* Design and activity of a cyclic mini- $\beta$ -defensin analog: a novel antimicrobial tool. *Int. J. Nanomed.* **10**, 6523–6539 (2015).
- Nigro, E. *et al.* An ancestral host defence peptide within human  $\beta$ -defensin 3 recapitulates the antibacterial and antiviral activity of the full-length molecule. *Sci. Rep.* **5**, 18450 (2015).
- Thevissen, K., Ferket, K. K. A., François, I. E. J. A. & Cammue, B. P. A. Interactions of antifungal plant defensins with fungal membrane components. *Peptides* **24**, 1705–1712 (2003).
- Amaral, V. S. G. *et al.* Psd2 pea defensin shows a preference for mimetic membrane rafts enriched with glucosylceramide and ergosterol. *Biochim. Biophys. Acta Biomembr.* **1861**, 713–728 (2019).
- Victor, K. G. & Cafiso, D. S. Location and dynamics of basic peptides at the membrane interface: electron paramagnetic resonance spectroscopy of tetramethyl-piperidine-N-oxyl-4-amino-4-carboxylic acid-labeled peptides. *Biophys. J.* **81**, 2241–2250 (2001).
- López Cascales, J. J. *et al.* Small cationic peptides: influence of charge on their antimicrobial activity. *ACS Omega* **3**, 5390–5398 (2018).

44. De Coninck, B., Cammue, B. P. A. & Thevissen, K. Modes of antifungal action and in planta functions of plant defensins and defensin-like peptides. *Fungal Biol. Rev.* **26**, 109–120 (2013).
45. van der Weerden, N. L., Lay, F. T. & Anderson, M. A. The plant defensin, NaD1, enters the cytoplasm of *Fusarium Oxysporum* hyphae. *J. Biol. Chem.* **283**, 14445–14452 (2008).
46. van der Weerden, N. L., Hancock, R. E. W. & Anderson, M. A. Permeabilization of fungal hyphae by the plant defensin NaD1 occurs through a cell wall-dependent process. *J. Biol. Chem.* **285**, 37513–37520 (2010).
47. Mello, E. O. *et al.* Antifungal activity of PvD1 defensin involves plasma membrane permeabilization, inhibition of medium acidification, and induction of ROS in fungi cells. *Curr. Microbiol.* **62**, 1209–1217 (2011).
48. Merhej, J., Richard-Forget, F. & Barreau, C. Regulation of trichothecene biosynthesis in *Fusarium*: recent advances and new insights. *Appl. Microbiol. Biotechnol.* **91**, 519–528 (2011).
49. Moghaddam, M.-R.B., Gross, T., Becker, A., Vilcinskis, A. & Rahnamaeian, M. The selective antifungal activity of *Drosophila melanogaster* metchnikowin reflects the species-dependent inhibition of succinate-coenzyme Q reductase. *Sci. Rep.* **7**, 8192 (2017).
50. Atanasova-Penichon, V. *et al.* Mycotoxin biosynthesis and central metabolism are two interlinked pathways in *Fusarium graminearum*, as demonstrated by the extensive metabolic changes induced by caffeic acid exposure. *Appl. Environ. Microbiol.* **84**, e01705–e01717 (2018).
51. Pani, G. *et al.* Natural phenolic inhibitors of trichothecene biosynthesis by the wheat fungal pathogen *Fusarium culmorum*: a computational insight into the structure-activity relationship. *PLoS ONE* **11**, e0157316 (2016).

### Acknowledgements

JJV is supported by Project FIT (Pharmacology, Immunotherapy, nanoToxicology), which was funded by the European Regional Development Fund and acknowledge a grant for the development of a research organization RVO: RO0516. This research has benefited from an INRAE MICA department funding (“TickTox” Project, 2020–2021).

### Author contributions

A.C.-C. and F.R.-F. conceived the study and designed the experiments. V.L.-R., V.A., N.P., M.T., and N.F. performed the experiments. A.C.-C., V.L.-R. and V.A. performed data analysis. J.J.V. performed structural and bioinformatics analyses. A.C.-C., F.R.-F., J.J.V. and N.P. wrote the manuscript. All authors approved and contributed to the final version of the manuscript.

### Competing interests

The authors declare no competing interests.

### Additional information

**Supplementary Information** The online version contains supplementary material available at <https://doi.org/10.1038/s41598-021-86904-w>.

**Correspondence** and requests for materials should be addressed to A.C.-C. or F.R.-F.

**Reprints and permissions information** is available at [www.nature.com/reprints](http://www.nature.com/reprints).

**Publisher's note** Springer Nature remains neutral with regard to jurisdictional claims in published maps and institutional affiliations.



**Open Access** This article is licensed under a Creative Commons Attribution 4.0 International License, which permits use, sharing, adaptation, distribution and reproduction in any medium or format, as long as you give appropriate credit to the original author(s) and the source, provide a link to the Creative Commons licence, and indicate if changes were made. The images or other third party material in this article are included in the article's Creative Commons licence, unless indicated otherwise in a credit line to the material. If material is not included in the article's Creative Commons licence and your intended use is not permitted by statutory regulation or exceeds the permitted use, you will need to obtain permission directly from the copyright holder. To view a copy of this licence, visit <http://creativecommons.org/licenses/by/4.0/>.

© The Author(s) 2021



## B) Complementary data: comparative efficiency of DefMT3 and TC3

Using the same protocols as those described in the previously reported publication (Leanne-Rialland et al., 2021)<sup>362</sup>, the efficiency of TC3 and DefMT3 were compared in *in vitro* MS liquid cultures inoculated with the DON/15-ADON producing *F. graminearum* CBS185.32 strain. As for TC3, DefMT3 synthesis was commissioned to Pepmic (Suzhou, China) following a similar procedure (production and quality check) as that employed for TC3 and its variants. Results regarding the biomass and 15-ADON yield are gathered in Figure 6.

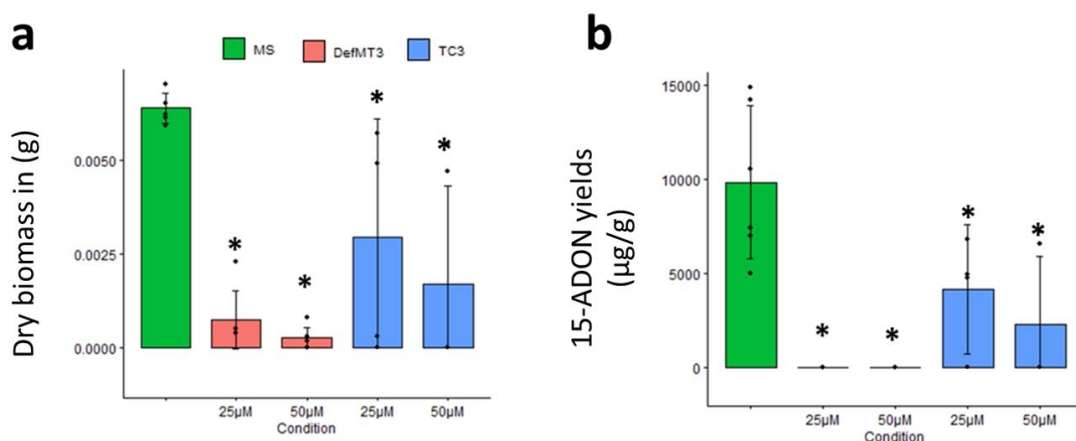


Figure 6. Antifungal and anti-mycotoxin activity of the defensin DefMT3 and its  $\gamma$ -core motif TC3. Effect of DefMT3 and TC3 at 25 and 50  $\mu\text{M}$  on the fungal biomass weight of *F. graminearum* (a) and on the production of 15-ADON (b) in 12-day-old broths. Significant differences are labeled by \* ( $p < 0.05$ ).

A significant dose-dependent inhibition of fungal growth was registered under all tested DefMT3 and TC3 concentrations compared with control samples. DefMT3 at 25 and 50  $\mu\text{M}$  inhibited *F. graminearum* growth by 88% (p-value=0.0046) and 95% (p-value=0.0049) respectively, when TC3 reduced fungal growth by 54% (p-value=0.045) at 25  $\mu\text{M}$  and 73% (p-value=0.0043) at 50  $\mu\text{M}$ . However, differences in antifungal activity between DefMT3 and TC3 for a same concentration, 25 or 50  $\mu\text{M}$ , were not statistically significant.

Concerning mycotoxin production, supplementation with 25 and 50  $\mu\text{M}$  TC3 reduced 15-ADON significantly, with a reduction by about 58% (p-value=0.03) and 76% (p-value=0.018) respectively at 25 and 50  $\mu\text{M}$ . The whole peptide DefMT3 showed higher anti-mycotoxin activity than its  $\gamma$ -core TC3, with no-detectable 15-ADON in the samples treated with DefMT3 at both 25 and 50  $\mu\text{M}$ .

Thus, according to our data, the whole defensin DefMT3 appears as more efficient than its  $\gamma$ -core TC3. Such data were slightly different to those obtained by Tonk et al. (2015)<sup>358</sup> who have evidenced a higher capacity of TC3 compared to DefMT3 to reduce *F. graminearum* spore germination. Such discrepancies could be ascribed to differences in experimental protocols, quantified variables (germination rate vs fungal biomass) and also targeted *F. graminearum* strain.

### C) Complementary data: comparative efficiency of TC3 and synthetic fungicides commonly used to control FHB

To go further, we have compared the efficiency of our eco-friendly alternative candidate TC3 to reduce *F. graminearum* growth and its mycotoxin production with those of three synthetic fungicides characterized by three different modes of action: carbendazim, tebuconazole and azoxystrobin (Fig. 7). Carbendazim exerts fungicidal effects by inhibiting cell division through the inhibition of tubulin polymerization by blocking GTP-cap formation (Vela-Corcía et al., 2018)<sup>363</sup>. Tebuconazole is a demethylase inhibitor (DMI) fungicide, interfering with the biosynthesis of ergosterol, an essential membrane sterol of fungi, by binding to the active site of the 14- $\alpha$ -demethylase that catalyses the transformation of lanosterol into ergosterol (Roberts et al., 2007)<sup>364</sup>. Azoxystrobin is a quinone outside inhibitors (QoI) that inhibits mitochondrial respiration by binding to a specific site in the mitochondria, the quinol oxidation (Qo) site of cytochrome b (Cyt b), and thereby hampering electron transfer between Cyt b and cytochrome c (Cyt c).

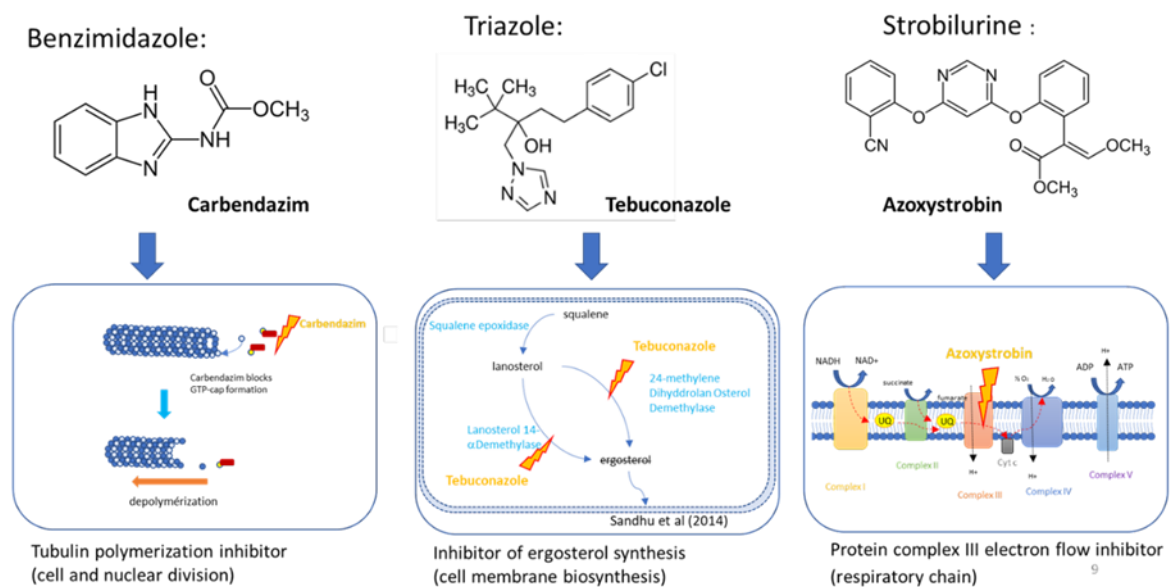


Figure 7. Three synthetic fungicides, Carbendazim, Tebuconazole and Azoxystrobin, and their mode of actions.

The first step was to define the concentrations for each fungicide which induce a measurable growth inhibition in our experimental conditions. The second step was to compare the effect of TC3 on *F. graminearum* with that of chosen fungicides. For this study, the DON/15-ADON *F. graminearum* CBS185.32 strain was used and the protocols were adapted to those described in Leannec-Rialland *et al.* (2021)<sup>362</sup> with one major difference; liquid MS cultures were performed in 55 mm diameter static Petri dishes instead of 24-well plates. 8mL of MS medium supplemented or not with TC3 (25  $\mu$ M or 50 $\mu$ M) or the synthetic fungicides carbendazim (5.25, 10.5, 15.7 and 26  $\mu$ M), tebuconazole (0.325, 0.65, 0.975 and 1.625  $\mu$ M) or

azoxystrobin (2.5, 5, 7.5 and 12.5  $\mu\text{M}$ ) was inoculated with  $2 \times 10^4$  spores/mL. Maximum concentrations of fungicides were defined according to their solubility in water. It was verified that neither TC3, carbendazim, tebuconazole or azoxystrobin supplementation modified the pH values of the treated broths compared to control conditions. Cultures were stopped at day 12. Collected mycelia were washed with 5 ml of sterile water and freeze-dried for fungal biomass quantification. 4 mL sample of supernatants were extracted with 8 mL of ethyl acetate. A volume of 7 mL of the organic phase was evaporated to dryness at 45  $^{\circ}\text{C}$  under a nitrogen flux. Dried samples were dissolved in 200  $\mu\text{L}$  of methanol/water (1/1, v/v) and filtered through a 0.2  $\mu\text{m}$  filter before analysis. TCTB quantification was done as previously described (Leanne-Rialland *et al.*, 2021)<sup>362</sup>. Results (Fungal biomass and TCTB) are gathered in Figure 8.

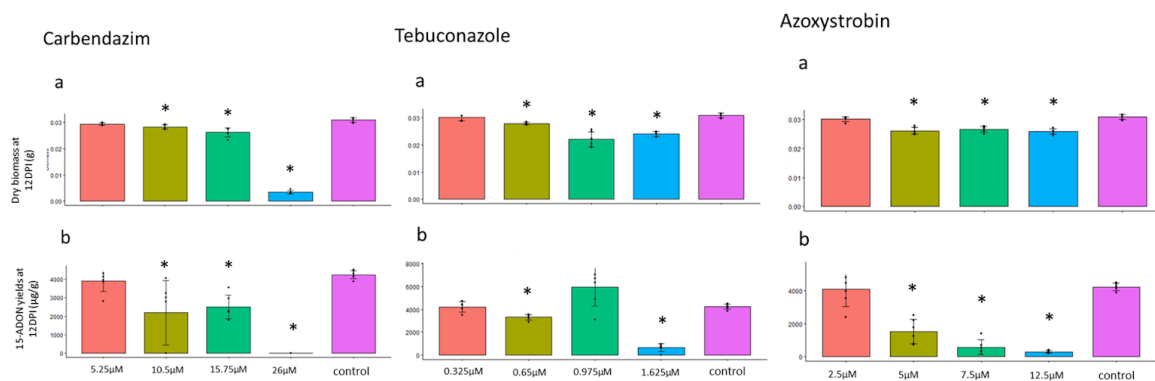


Figure 8. Antifungal and anti-mycotoxin activity of synthetic fungicides. Effect of Carbendazim at 5.25, 10.5, 15.7 and 26  $\mu\text{M}$ , Tebuconazole at 0.325, 0.65, 0.975 and 1.625  $\mu\text{M}$  and of Azoxystrobin at 2.5, 5, 7.5 and 12.5  $\mu\text{M}$  on the fungal biomass weight of *F. graminearum* and on the production of 15-ADON in 12-day-old broths. Significant differences are labeled (\* $p < 0.05$ ).

If we first focus on carbendazim, a significant inhibition of fungal growth was registered for the carbendazim concentration of 26  $\mu\text{M}$  (78% reduction) while 5.25  $\mu\text{M}$  did not induce any modification of fungal biomass and concentrations of 10.5 and 15.75  $\mu\text{M}$  were responsible for a slight reduction (lower than 10%). Concerning mycotoxin production, supplementation with carbendazim from 10.5  $\mu\text{M}$  to 26  $\mu\text{M}$  significantly reduced the 15-ADON yield. Because carbendazim is difficult to solubilize in water, the antifungal and anti-toxicogenic effect of this fungicide may have been underestimated in this experiment. When tebuconazole was supplied to the cultures, a statistically significant but low growth inhibition was observed for concentrations of 0.65  $\mu\text{M}$ , 0.975  $\mu\text{M}$  and 1.625  $\mu\text{M}$ . 0.65  $\mu\text{M}$  and 1.625  $\mu\text{M}$  were shown to induce an inhibition of the mycotoxin production. The surprising lack of significant effect obtained with 0.975  $\mu\text{M}$  could be ascribed to the large standard deviation. Treatment with 2.5  $\mu\text{M}$  azoxystrobin had no effect compared to control condition. However, from 5  $\mu\text{M}$  to 12.5  $\mu\text{M}$ , all concentrations induced a significant antifungal and anti-mycotoxin effect.

For the following comparative study including TC3, the concentrations of 5.25  $\mu\text{M}$  for carbendazim, 1.625  $\mu\text{M}$  for tebuconazole and 5  $\mu\text{M}$  for azoxystrobin were selected. Results are reported on Figure 9.

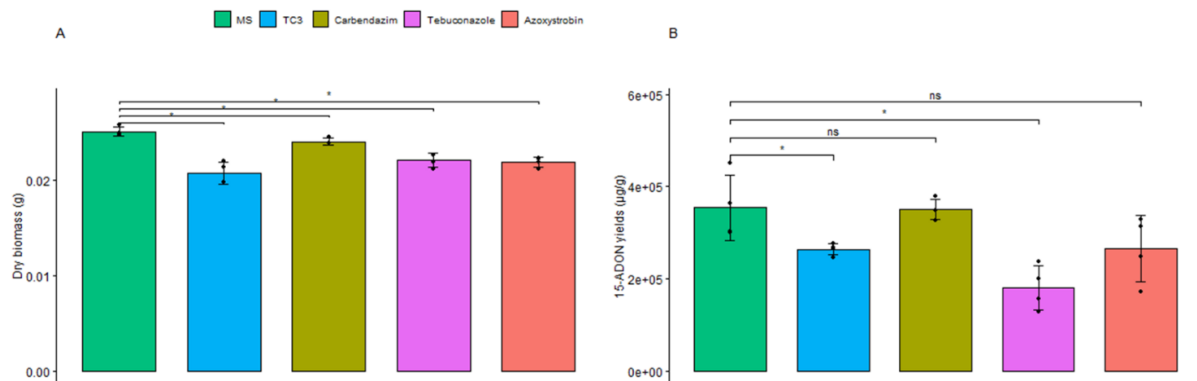


Figure 9. Antifungal and anti-mycotoxin activity of TC3, carbendazim, tebuconazole and azoxystrobin. Effect of TC3 at 50 $\mu\text{M}$ , carbendazim at 5.25  $\mu\text{M}$ , tebuconazole at 1.625  $\mu\text{M}$  and azoxystrobin at 5  $\mu\text{M}$  on fungal biomass weight of *F. graminearum* (A) and 15-ADON yield (B) in 14-day-old broths.

According to fungal biomass data, 50  $\mu\text{M}$  of TCT3 exhibited a similar antifungal potential than 5.25  $\mu\text{M}$  carbendazim, 1.625  $\mu\text{M}$  tebuconazole and 5  $\mu\text{M}$  azoxystrobin, which suggests a lower efficacy of the peptide compared to the three tested fungicides. However, it has to be noticed that the reduction induced by TC3 in this experiment was significantly lower than that previously observed (Fig. 6). Such variation in TC3 efficacy has been observed several times throughout this PhD work. This could be associated with the batch of the purchased peptide and/or the dimerization of the peptides that could occur and was clearly evidenced in the microscopy study described in chapter 2. When considering the 15-ADON yield, 50  $\mu\text{M}$  TC3 led to a decrease in 15-ADON close to that observed with 1.625  $\mu\text{M}$  tebuconazole.

Altogether, while corroborating TC3 bioactivity, the previous data clearly demonstrate the lower potential of the peptide compared to that of some synthetic fungicides. This lower bioactivity can however be outweighed by a higher solubility of the peptide, a low or lack of toxicity (Leannec-Rialland et al., 2022) such as a natural origin.

#### D) Efficiency of TC3 when tested in *in planta* assays

Two types of *in planta* assays were considered: detached leaf assays and greenhouse trials. As for previously described experiments, TC3 was chemically synthesized by Pepmic (Suzhou, China).

##### a) TC3 efficiency in detached leaf assays

###### *Experimental design:*

The detached leaf assay is a nondestructive method, that partially mimics interaction between a plant host and a disease-causing agent, frequently used to test the efficacy of a pesticide treatment. In this study, the effect of TC3 at 125  $\mu\text{M}$  was investigated on wheat detached

leaves. The DON/15-ADON *F. graminearum* CBS185.32 strain was used and conidia solutions were prepared as described in Leannec-Rialland *et al.* (2021)<sup>362</sup>. Leaf segments of 6 cm were cut from the tip of the first leaves of 10-day-old seedlings. The leaves were wounded using a 10- $\mu$ L sterile pipette tip in the center prior to placing them on water agar plates amended with 40 mg/L benzimidazole. To assess the effects of TCA on the infection and mycotoxin production by *F. graminearum*, 10  $\mu$ L of TCA 125  $\mu$ M were transferred to the center of detached leaves followed by 1  $\mu$ L of spore suspension ( $10^6$  spores/mL). Sterile water (10 $\mu$ L) was used as a control. Images were taken at 3, 4, and 5 days after infection (dai). The infection severity was assessed via necrosis areas using FIJI software. At 5 dai, for each treatment, three leaves were pooled into one sample and dried overnight by lyophilization. Each sample was divided into two subsamples (5mg per each) in which one was used for quantification of total fungal DNA levels and the other one for mycotoxin analysis. Three biological replicates were done per each treatment.

#### *Mycotoxin analysis:*

The procedure was adapted from a previously published procedure (Nicaise *et al.*, 2022)<sup>365</sup>. Briefly, 5 mg of ground wheat leaf was extracted with 1.5 mL of ethyl acetate supplemented with 1% formic acid and agitated for 1 hour. A volume of 1.3 mL of the organic phase was collected after 5 min of centrifugation at 4800 rpm and evaporated to dryness at 45 °C under nitrogen flux. Dried samples were dissolved in 125  $\mu$ L of methanol/water (1/1, v/v) and filtered through a 0.2  $\mu$ m filter before analysis. TCTB and zearalenone were quantified by HPLC–DAD (same protocol as described previously in Leannec-Rialland *et al.*, 2021)<sup>362</sup>. Toxin yields were expressed in  $\mu$ g/g of dried leaf.

#### *Fungal DNA quantification:*

The protocol was adapted from Nicaise *et al.* (2022)<sup>365</sup>. DNA extraction was realized using 5mg of freeze-dried wheat leaf and ground with a TissueLyser II (Qiagen, Venlo, The Netherlands), using the NucleoMag Plant kit (Macherey-Nagel, Hoerdt, France) according to the manufacturer's instructions. The quality and quantification of the prepared DNA were evaluated by spectrometry (DeNovix, DeNovix Inc, Wilmington DE, USA) and the concentration was adjusted to 20 ng/ $\mu$ L with nuclease-free water. Fusarium and wheat DNA contents in each sample were measured by quantitative polymerase chain reaction (qPCR) with SYBR green detection using a QuantStudio5™ (ThermoFisher Scientific, Vantaa, Finland). Fusarium DNA abundance was assayed by quantification of the beta-tubulin gene and wheat DNA abundance using the Rubisco gene (primers reported in Table 2). Each qPCR consisted of 5 mM MgCl<sub>2</sub>, 0.5  $\mu$ M primers, 20 ng of purified DNA, and 2  $\mu$ L of 1X QuantiFast SYBR Green PCR Master Mix (Qiagen) in a final volume of 10  $\mu$ L. The amplification conditions consisted of a first denaturation step for 5 min at 95 °C, followed by 40 cycles of 15 s at 95 °C and 40 s at 60 °C. The melting curve was generated using the following profile: 0 s at 95 °C, 15 s at 65 °C, 0 s at 95 °C (linear temperature transition from 65 °C to 95 °C at 0.1 °C s<sup>-1</sup>), and 30 s at 40 °C. All the reactions were performed in triplicate. Quantification was performed using external calibration curves with standard solutions of *F. graminearum* DNA extracted from pure cultures and wheat DNA extracted from an uncontaminated wheat sample. Relative

quantification of the presence of fungal DNA in the tested sample was calculated as the quantity of fungal DNA/quantity of wheat DNA.

Table 2. Primers used for the fungal DNA quantification using qPCR.

Gene	Forward primer sequence (5' to 3')	Reverse primer sequence (5' to 3')
Beta-tubuline	GGTAACCAAATCGGTGCTGCTTTC	GATTGACCGAAAACGAAGTTG
Rubisco	CCCAAAGATTTTCGGTCAGAG	AAGATCGTGCTCCCGGTAT
TRI5	GGTCAAGAACTTTGTCACTG	CAATCGTGCCATCACCTGAG

Results:

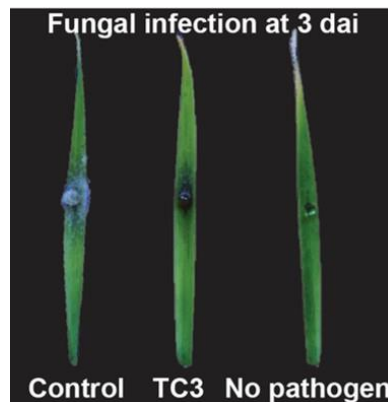


Figure 10. Necrotic zones observed on wheat leaves treated with TCA or sterile water at 3-day post inoculation with *F. graminearum*. Wounded leaves not inoculated with *F. graminearum* serves as negative control.

First *F. graminearum* symptoms on inoculated detached leaves were observed 48 h after inoculation. At 3, 4 and 5 dai, symptoms on treated leaves with TC3 consisted of restricted areas of necrotic zones, which was not the case for control leaves which showed extensive areas of necrosis. This clearly appears on the photography taken at 3 dai reported on Figure 10.

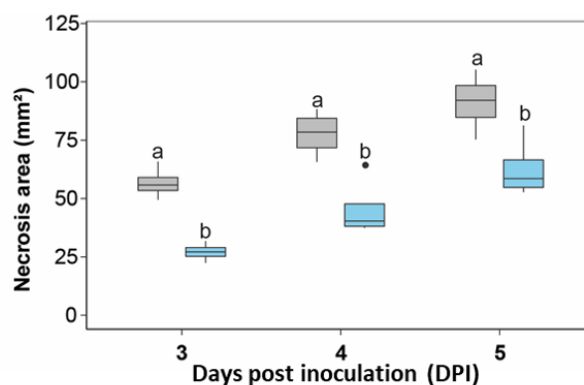


Figure 11. Necrosis surfaces (in mm<sup>2</sup>) on wheat leaves inoculated with *F. graminearum* pre-treated with TC3 125 µM (in blue) or with sterile water (in grey). Significant differences are labeled with different letters ( $p < 0.05$ ).

The capacity of TC3 125  $\mu\text{M}$  to reduce the disease symptoms induced by *F. graminearum* was clearly evidenced when comparing the necrosis surfaces between the different treatments, as shown in Figure 11. Moreover, the fungal DNA quantification allowed to demonstrate the efficiency of the TC3 treatment to inhibit the spread of *F. graminearum* on wheat leaves (Fig. 12A). When considering mycotoxin data, the quantification limit of the LC-DAD procedure used in this study did not allow quantifying TCTB. Nevertheless, a significant amount of zearalenone was detected and the TC3 treatment was shown to considerably decrease the level of contamination (Fig. 12B).

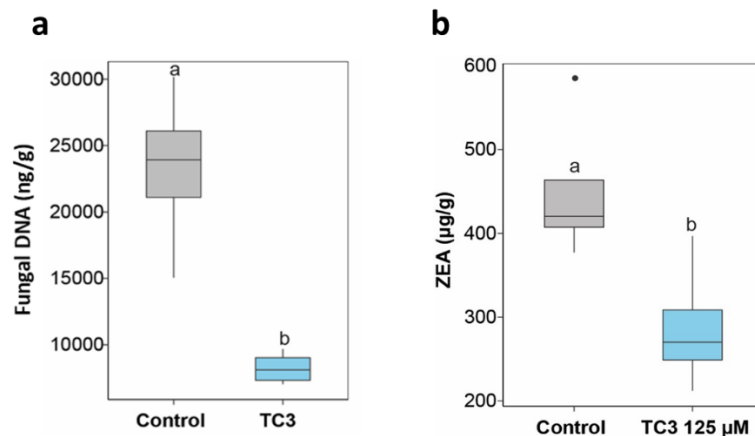


Figure 12. Quantification of fungal DNA (A) and Zearalenone (B) extracted from wheat leaves treated or not with TC3. Significant differences are labeled with different letters ( $p < 0.05$ ).

Thus, results of the previously described detached leaf assay strongly provide new arguments supporting the promising bioactivity of TC3.

## b) Greenhouse trials with TC3 application at wheat anthesis

### Experimental design

This assay was subcontracted to Staphyt (a french company focusing on AgroSciences) in partnership with the Elephant Vert company (a French company that develops biocontrol solutions). A FHB susceptible wheat variety was treated or not (C1) with TC3 at two dosages (100  $\mu\text{M}$  / C2 and 12.5  $\mu\text{M}$  / C3) or with a synthetic fungicide Prosaro (5 ml/l - C4). 24 plants per condition were considered. 1 ml of a suspension of  $10^4$  conidia/ml of the *F. graminearum* INRAE 164 strain (a DON/15-ADON strain with a long history of use for wheat inoculation at the MycSA laboratory) was inoculated by spraying into each central spikelet at anthesis. The fungal strain was inoculated 24 hours after the treatments (TC3 or fungicide). Wheat heads were harvested at two times for each modality: (i) when the extent of symptoms on the ears of the control condition C1 reached 20/30% of the ear and (ii) when they reached 50% of the ear. Four biological replicates composed of 6 ears were harvested per condition and per time. At reception, the samples were freeze-dried and ground into flour using a TissueLyser II (Qiagen, Venlo, The Netherlands) with a 2.5 cm diameter metal bead for 45 seconds.

### Mycotoxin analysis and DNA fungal quantification:

The procedures were similar to those implemented for the detached leaf assay with very slight differences. For mycotoxin analysis, the amount of extracted plant material was 30 mg of wheat flour. For fungal DNA quantification, the extraction was realized with 50 mg of wheat flour and the gene targeted for quantifying *F. graminearum* DNA was the *tri5* gene (primers are reported in table 2).

### Results:

DON and fungal DNA quantified in the different modalities are reported in Figures 13a and 13b.

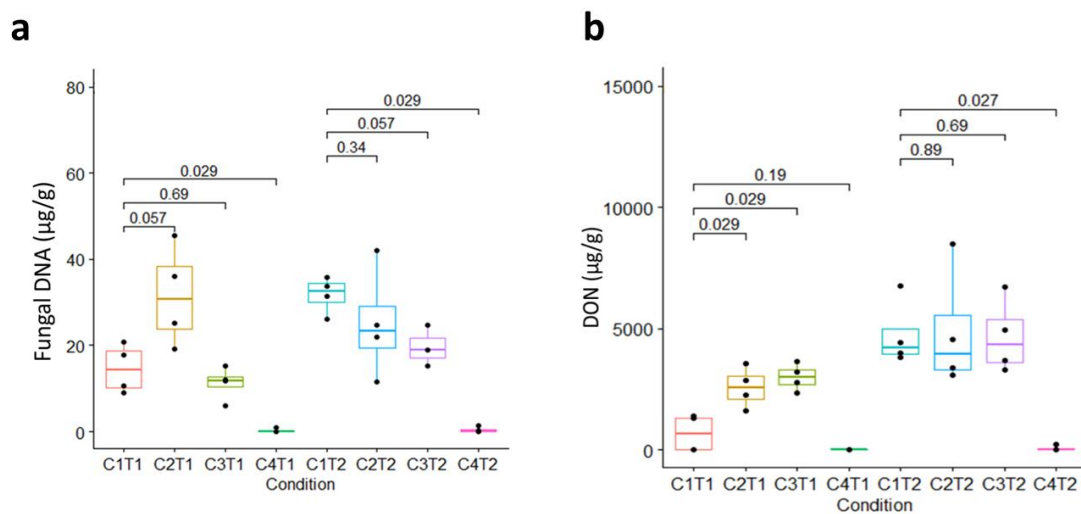


Figure 13. Fungal DNA (A) and DON (B) quantified in wheat heads at two maturity stages and treated according to four modalities, inoculated at anthesis by *F. graminearum*. C1: control condition, C2: TC3 12.5 µM treatment, C3: TC3 100 µM treatment, C4: synthetic fungicide treatment - T1: ears collected when the FHB symptoms in C1 reached 20-30 % of the ear, T2: ears collected when the FHB symptoms in C1 reached 50 % of the ear.

FHB symptoms (data not shown), fungal DNA and DON were detected in all modalities, supporting the proper functioning of the inoculation procedure. However, for each modality/maturity stage (with the exception of the C4/Prosaro treatment), a high variability between the four biological replicates was observed, for both fungal DNA and DON amounts. In the untreated modality (C1), a consequent level of fungal DNA was quantified with higher concentrations at T2 (50% infection) compared to T1 (20-30% infection). For modalities with TC3 (C2 and C3), the DNA levels quantified at T1 and T2 were not significantly different from those of the untreated control condition (C1). However, for the T2 sampling time, the fungal DNA levels quantified in the pretreated wheat ears with 100 µM TC3 were lower than those of the untreated condition (the differences were not statistically different with the selected threshold of 0.05). In comparison, the synthetic antifungal product (C4) was highly efficient to prevent the fungal spread.

Regarding DON amounts, very high levels of mycotoxins were quantified. Indeed, in the untreated modality (C1), the amount of DON at T2 reached values comprised between 3800 and 7000 µg DON/kg wheat. Such high levels could have masked slight differences between

the modalities. For the two maturity stages and TC3 treatments, DON was detected in an equivalent or a higher amount compared to the untreated conditions (C1). Very low levels of DON (between 0 and 240 µg of DON/kg of wheat) were quantified in modality (C4), evidencing the efficiency of the Prosaro synthetic fungicide.

Altogether, the previous data suggest that TC3 100 µM could lead to a reduction of *F. graminearum* spread when applied at wheat anthesis before fungal inoculation. This observation was however not statistically significant and not associated with a reduction in DON amount. It should however be kept in mind that this experiment was a preliminary one with no optimization regarding the dose of TC3 neither the formulation of the product (to improve its stability and persistence). Besides, the *F. graminearum* strain used in this experiment such as the spore concentration (and also the susceptibility of the wheat genotype) has led to a very high severity of symptoms and amount of toxins, far from what could happen in field conditions. Lastly, four biological replicates were really not enough.

## Conclusion

Key results of Chapter 1 that aimed to describe the bioactivity of TC3 against *F. graminearum* and the production of TCTB are:

- TC3 (at concentrations ranging between 12.5 and 50 µM) showed a great potential to reduce the growth of *F. graminearum* and mycotoxin production in liquid cultures. This efficiency was confirmed for higher concentrations (125 µM) on detached wheat leaves inoculated with *F. graminearum*. The in-planta bioactivity of TC3 was also suggested by greenhouse experiments: a pretreatment by TC3 before *F. graminearum* inoculation at wheat anthesis seemed to hamper the fungal spread within the ears (this observation required however to be confirmed).
- Some structural features involved in TC3 bioactivity have been evidenced: (i) the linear form of the TC3 peptide is the most active, (ii) the cationic charge is a key factor driving the TC3 bioactivity, (iii) the Lys 6 residue significantly contributes to the inhibition efficiency.
- A first modeling approach has suggested that TC3 is recruited by the *F. graminearum* membrane's upper leaflet, more specifically by the phospholipids POPS, POPA and POPG. This modeling was however based on old data (Wiebe et al., 1989) regarding the lipidic composition of *F. graminearum* membrane (but they were the only ones published hitherto) and requires to be repeated with updated information. Furthermore, this modelling has corroborated the importance of Lys6 which is located close to Phe4 and Leu5, two residues that were predicted to interact with the lipid membrane in silico.

One observation related to these first studies is also that the efficacy of TC3 could be lower than expected in some experiments. With the aim to reduce this variation in efficacy, a same

batch of peptide was used for the following experiments. TC3 preparations were received as 1mg aliquots that were immediately stored at -20°C and no opened aliquot was reused.

**Chapter 2:**  
**Bioactivity of TC3 against the different**  
**FHB causal agents**



## Chapter 2: Bioactivity of TC3 against the different FHB causal agents

In the first chapter, we have evidenced the efficacy of TC3 in inhibiting the growth of *F. graminearum* CBS185.32 strain and its production of mycotoxins. However, considering the genomic and phenotypic diversity of *F. graminearum* (Aamot et al., 2015; Laurent et al., 2017)<sup>366,367</sup>, focusing on only one strain is really insufficient to develop a biocontrol solution. Besides, even if *F. graminearum* is acknowledged as the main causal agent of FHB, *F. graminearum* is only one member of the *Fusarium* community associated with this fungal disease. To ascertain that a biocontrol solution will not strongly unbalance this community leading to an over occurrence of *F. graminearum* (suppression of one or several species competitive of *F. graminearum*) and/or to the increased occurrence of another toxigenic species, it is important to assess the different susceptibilities of the FHB species towards the active molecule. Considering the intraspecific and interspecific diversity of FHB *Fusarium* species will be the core subject of this Chapter 2.

*Article to be submitted in Journal of Agricultural and Food Chemistry.*

Susceptibility of different *Fusarium* species and strains involved in *Fusarium* Head Blight to the promising TickCore3-based biocontrol solution.

Leannec-Rialland V., Atanasova V., Cabezas-Cruz Alejandro, Chereau S., Minh Tran T., Pinson-Gadais L., Richard-Forget F.

### Abstract

Cereal crops are frequently affected by *Fusarium* species that are responsible for the devastating fungal disease *Fusarium Head Blight* (FHB). *Fusarium* species also produce grain contamination with mycotoxins. Reducing the use of synthetic fungicides in agriculture while guaranteeing low levels of mycotoxin contamination in crops requires the development of innovative and environment-friendly solutions. TickCore3 (TC3) is an antimicrobial peptide derived from a defensin DefMT3 of the tick *Ixodes ricinus*. This peptide was previously reported as a potent antifungal and anti-mycotoxin agent when tested against *Fusarium graminearum*, one of the most prevalent species causing FHB. In this study, we demonstrated that TC3 is active against major *Fusarium* species infecting wheat and has the capacity to inhibit the production of various mycotoxins. However, fungal susceptibility to this peptide showed great variability across the *Fusarium* species and strain tested. We also found that TC3 is highly efficient when applied at the spore stage and has a strong anti-germination activity. FITC-labeled TC3 was tracked using confocal microscopy to study the possible mechanism of the anti-germination activity. Results showed that TC3 has strong affinity for the conidia surface and surrounds this fungal structure. While this study supports the potential of TC3 as a novel and highly effective anti-fungal agent, it also highlights the need of further studies to

ensure that the application of TC3 in wheat fields will not induce a shift in *Fusarium* population such as in mycotoxin profile contaminating grains.

**Keywords:** *Fusarium*, Fusarium head blight, mycotoxins, tick defensins, biocontrol

## I. Introduction

*Fusarium graminearum* is a major fungal pathogen responsible of the disease Fusarium Head Blight (FHB) that affects wheat and other small grain cereals leading to significant losses in yield and harvest quality. *Fusarium graminearum* is however not the sole causal agent of FHB and is never observed solitary on developing kernels. The disease is caused by a complex of species of the genera *Fusarium* and *Microdochium*, with more than 20 species identified hitherto. Among them, *F. graminearum*, *Fusarium culmorum*, *Fusarium avenaceum* and *Fusarium poae* have been identified as the most prevalent in Europe (Birr et al., 2020)<sup>1</sup>. Additional species, including *Fusarium sporotrichioides*, *Fusarium langsethiae* and *Fusarium tricinctum*, are also reported to contribute to FHB (Bottalico and Perrone, 2002; Van der Lee et al., 2015, Dweba et al., 2017)<sup>2-4</sup>, but to play a subordinate role in the development of the disease (Birr et al., 2020)<sup>1</sup>. All the aforementioned *Fusarium* species can produce various mycotoxins that pose a risk to human and animal health (Kang and Buchenauer, 1999)<sup>5</sup>. *Fusarium graminearum*, *F. culmorum* and *F. poae* can produce type B trichothecenes that include deoxynivalenol (DON) and its acetylated forms (3-acetyl and 15-acetyl DON / 3-ADON and 15-ADON), nivalenol (NIV) and its acetylated form fusarenon X (FX). Besides, *F. graminearum* and *F. culmorum* are the main producers of zearalenone. *Fusarium poae* is also reported as a producer of trichothecenes of type A (mainly diacetoxyscirpenol / DAS and monoacetoxyscirpenol / MAS) such as *F. langsethiae* and *F. sporotrichioides* that are the main responsible for contamination of grains with T-2 and HT-2 toxins. Last but not least, the production of the so-called emerging mycotoxins, enniatins (ENNs) and beauvericin (BEA), by *F. avenaceum* and *F. tricinctum* is widely documented (Gautier et al., 2020)<sup>6</sup>. ENNs and BEA are among the most frequently mycotoxins found in small grain cereals and with the highest levels; their physiological role for the fungus, their toxic effects such as the factors governing their occurrence are however misunderstood (Gautier et al., 2020)<sup>6</sup>. The FHB disease is even more complex that it is not only associated with a diversity of species but also a diversity of isolates that, even if they belong to a same species, can exhibit various phenotypes. This has been particularly evidenced for the *F. graminearum* species, which isolates are characterized by large differences in aggressiveness (Fabre et al., 2019)<sup>7</sup>, in toxigenic potential (Laurent et al., 2017)<sup>8</sup> or in resistance to antifungal treatments (Zhang et al., 2009, Hou et al., 2017)<sup>9,10</sup>. Unfortunately, this complexity is frequently overlooked in researches aiming at identifying alternative solutions to the use of synthetic fungicides to reduce FHB, which could be one reason why demonstrated efficiency in controlled conditions is not retrieved in field trials. Actually, various scenarios can be imagined: (i) all FHB species have a similar susceptibility to

the antifungal treatment; the disease symptoms and the whole mycotoxin content could be reduced, (ii) *F. graminearum* or *F. culmorum* are significantly less susceptible than the other FHB species; the treatment could preferentially eliminate competitive species of the two former ones and induce an increase in contamination with DON, (iii) *F. graminearum* and *F. culmorum* are significantly more susceptible than the other FHB species; the treatment could lead to an over representation of FHB species considered as minors, resulting in an increased content of some mycotoxins such as ENNs.

A package of preharvest practices are recommended to reduce *Fusarium* mycotoxins in cereals; they include the adaptation of the crop sequence, a rational crop residue management, the choice of tolerant cultivar, a proper use of fungicides and an appropriate sowing date and rate (Leslie et al., 2021)<sup>11</sup>. However, there are so far no management strategies that are efficient enough to guarantee the compliance of harvested grains with the mycotoxin thresholds set by the European commission for cereals intended to human consumption (EC N°856/2005 that has been revised in July 2007 / EC N°1126/2007)<sup>12,13</sup>. In recent years, the environmental and health concerns associated with chemical pesticides, and the increased spreading of *Fusarium* strains resistant to commonly-applied synthetic fungicides, have stimulated research into alternative methods of FHB disease management. Defensins are a well-characterized family of naturally occurring antimicrobial peptides in many species, including ticks (Tonk et al., 2014; 2015; Cabezas-Cruz et al., 2016)<sup>14-16</sup>. Tick defensins have antibacterial and antifungal (Tonk et al., 2014; 2015)<sup>14,15</sup> activity, and have been recently described as an alternative for the control of *Fusarium* spp. (Leannec-Rialland et al., 2022)<sup>17</sup>. In previous studies, we showed that the  $\gamma$ -core of the *Ixodes ricinus* defensin DefMT3 (TickCore3, hereafter referred to as TC3) inhibits the spore germination and growth (Tonk et al., 2015)<sup>15</sup> and mycotoxin (Leannec-Rialland et al., 2021)<sup>18</sup> production of *F. graminearum*. As reviewed by Leannec-Rialland et al. (2022)<sup>17</sup>, such defensin peptides possess interesting characteristics, in addition to their bioactivity, that support the development of plant care products: low toxicity to plants and mammals, high solubility and a possible low cost of production through recombinant expression in microorganisms.

In the present study, the capacity of TC3 to inhibit the growth and mycotoxin production of several *Fusarium* species and strains causing FHB was assessed. In addition, we aimed at identifying some features that could explain differences in strain susceptibility. Even though the main FHB species have been considered, a specific focus was done on the couple of species, *F. graminearum* and *F. avenaceum*, the two most prevalent species infecting European cereals (Birr et al., 2020)<sup>1</sup>. For these two species, anti-sporulating, anti-germinating and effect on the developed mycelium were investigated such as the occurrence of internalization of the peptide within the fungal cells.

## II. Material and methods

- a) Synthesis of tick  $\gamma$ -core (TC3) and fluorescent labeled peptide FITC-TC3

TC3 is the  $\gamma$ -core of the *Ixodes ricinus* defensin DefMT3 (GenBank accession number: JAA71488). Peptide synthesis was commissioned to Pepmic (Suzhou, China) that uses solid-phase peptide synthesis (SPPS) to obtain highly-pure peptides as previously described (Leannec-Riolland et al., 2021)<sup>18</sup>. Briefly, peptide synthesis was performed using 2-chlorotrityl chloride resin as the solid support, using the base labile 9-fluorenyl-methyloxy-carbonyl (Fmoc) as protecting group. Amino acids were protected as follows: Fmoc-Cys(Trt)-OH, Fmoc-Gly-OH, Fmoc-Asn(Trt)-OH, Fmoc-Phe-OH, Fmoc-Leu-OH, Fmoc-Lys(Boc)-OH, Fmoc-Arg(Pbf)-OH, Fmoc-Tr(tBu)-OH, Fmoc-Ile-OH and Fmoc-Val-OH. All the peptide sequences were synthesized according to the principles of SPPS. High Performance Liquid Chromatography (HPLC)-grade Fmoc chloride (Fmoc-Cl)-protected amino acid-based peptide chemistry was used with standard peptide chemistry coupling protocols. Peptides were purified by reverse phase HPLC and peptide sequence was confirmed by electrospray mass spectroscopy (ESI-MS) using a mass spectrometer LCMS-2020 (Shimadzu, Kyoto, Japan). The peptide 'TC3-FITC' was synthesized as TC3 but the fluorescent label fluorescein isothiocyanate (FITC) was incorporated at the N-terminal end with the spacer 1,6-aminohexanoic acid (Ahx).

b) *Fusarium* strains

Several *Fusarium* strains (n = 26) of six different FHB causing species were used in this study. These strains together with information relative to their origin and capacity to produce mycotoxins are summarized in table 1.

Table 1. Fungal species and strains used in this study.

<i>Fusarium</i> species	Strains	Mycotoxins	Origin
<i>Fusarium graminearum</i>			
	CBS185.32/INRAE 349	DON/15-ADON and ZEA	Westerdijk Institute, The Netherlands
	INRAE 156	DON/15-ADON and ZEA	INRAE MycSA collection, France
	INRAE 164	DON/ 15-ADON and ZEA	INRAE MycSA collection, France
	INRAE 215	DON/15-ADON and ZEA	AgResearch, Hamilton
	INRAE 605	DON/15-ADON and ZEA	Technical University of Denmark
	PH-1	DON/15-ADON and ZEA	Fungal Genetic, USA
<i>Fusarium avenaceum</i>			
	INRAE 498	ENNs, BEA	Bayer, France
	INRAE 112	ENNs, BEA	INRAE MycSA collection, France
	INRAE 113	ENNs, BEA	INRAE MycSA collection, France
	INRAE 495	ENNs, BEA	Bayer, France
	INRAE 873	ENNs, BEA	Canadian Collection of fungal cultures, Canada
<i>Fusarium culmorum</i>			
	INRAE 134	NIV/FX and ZEA	INRAE MycSA collection, France
<i>Fusarium poae</i>			
	INRAE 488	NIV, MAS and DAS	Bayer, France
<i>Fusarium tricinctum</i>			
	INRAE 104	ENNs, BEA	INRAE MycSA collection, France
<i>Fusarium langsethiae</i>			
	INRAE 502	T2, HT2	Bayer, France

DON: deoxynivalenol, A-DON: acetyldeoxynivalenol, NIV: nivalenol, FX: fusarenone X, ZEA: zearalenone, ENNs: enniatins, BEA: beauvericin, T2: toxin T2, HT2: toxin HT2, DAS: diacetoxyscirpenol and MAS: monoacetoxyscirpenol.

Stock cultures were maintained at 4°C on Potato Dextrose Agar (PDA) (Difco, France) slants under mineral oil. When inoculum was required, spore suspensions were prepared by inoculating six agar plugs in 75 mL of Carboxymethyl Cellulose (CMC) medium (15 g/L carboxymethyl cellulose, 1 g/L yeast extract, 0.5 g/L MgSO<sub>4</sub>·7H<sub>2</sub>O, 1 g/L NH<sub>4</sub>NO<sub>3</sub>, 1 g/L KH<sub>2</sub>PO<sub>4</sub>) in culture flasks and incubating at 180 rpm and 25°C in darkness for five days. After filtration through Sefar Nitex 03-100 (100 µm, SEFAR AG - Switzerland) and concentration by centrifugation, spores were counted on a Malassez cell before immediate use.

#### c) Liquid fungal cultures

Liquid-cultures were performed in 24-well static plates. Each well containing 2 mL of a mycotoxin synthetic (MS) medium (20 g/L glucose, 0.5 g/L KH<sub>2</sub>PO<sub>4</sub>, 0.6 g/L K<sub>2</sub>HPO<sub>4</sub>, 17 mg/L MgSO<sub>4</sub>, 1 g/L (NH<sub>4</sub>)<sub>2</sub>SO<sub>4</sub>, 0.1 mL/L Vogel mineral salts solution) supplemented or not with TC3 was inoculated with 2e+04 spores/mL. For experiments aiming at comparing the susceptibilities of strains, TC3 (50 µM in the medium) was supplied before strain inoculation. For kinetic experiments with TC3 added at different times pre- and post-inoculation, TC3 (50 µM in the medium) was supplied at 0, 1, 3 and 5-days post inoculation. Fungal liquid cultures were incubated at 25 °C in the dark for 10 days. Following incubation, mycelia were recovered by centrifugation and fungal biomass was measured by weighing the mycelia after 48 h of freeze-drying (Flexi-Dry, Oerlikon Leybold, Germany). Culture media were stored at -20 °C until mycotoxin analysis. Six repetitions were made for each condition. Controls using non-supplemented control media and non-inoculated control media were included.

#### d) Extraction and analysis of mycotoxins

For each assay, mycotoxins were extracted according to a protocol adapted from Leannec-Rialland et al. (2021)<sup>18</sup>. Briefly, 1 mL sample of culture medium was extracted with 2 mL of ethyl acetate. A volume of 1.5 mL of the organic phase was evaporated to dryness at 45 °C under nitrogen flux. Dried samples were dissolved in 200 µL of methanol/water (1/1, v/v) and filtered through a 0.2 µm filter before analysis.

TCTB produced by *F. graminearum* strains were analyzed by HPLC/DAD using the method described in Leannec-Rialland et al. (2021). For all other toxigenic isolates (*F. culmorum*, *F. avenaceum*, *F. tricinctum*, *F. poae* and *F. langsethiae*), mycotoxins were analyzed using a multimycotoxin LC-HRMS method. Analyses were performed with a Q-Exactive Focus mass spectrometer (Thermo Fisher Scientific, Bremen, Germany) equipped with a heated electrospray ionization (HESI) source and a Vanquish UHPLC System (Thermo Fisher Scientific, Bremen, Germany). Separation was achieved on a Thermo Scientific™ Accucore™ aQ C18 Polar

Endcapped HPLC column (2.1 × 100 mm, 2.6 μm) (Thermo Fisher Scientific, USA) maintained at 40 °C. The mobile phase consisted of water/methanol (98/2) with 10 mM AcNH<sub>4</sub> and 0.1% acetic acid (solvent A) and methanol/water (98/2) with 10 mM AcNH<sub>4</sub> and 0.1% acetic acid (solvent B). The flow was kept at 0.4 mL min<sup>-1</sup>. The injection volume was set to 2 μL. Thirteen mycotoxins can be separated using the gradient elution described in Table 2.

Table 2. Elution gradient used in the multi-mycotoxin method.

Time (min)	Solvent A (%)	Solvent B (%)
0	98	2
0.5	98	2
5.0	2	98
9.7	2	98
9.8	98	2
12.0	98	2

TheTraceFinder software (version 5.0.889.0) was used to control the LC-MS system and to acquire and process data. The mass spectrometer was operated in the positive ESI mode with 70k resolving power full scan acquisition in the 150-1000 m/z range. Nitrogen was used as the sheath and auxiliary gas. The main MS parameters were optimized and finally set as follows: sheath gas flow rate, 50 a.u.; auxiliary gas flow rate, 13 a.u.; sweep gas flow rate, 0 a.u.; spray voltage, 3.5 kV; capillary temperature, 320 °C; S-lens RF level 50%; auxiliary gas heater temperature, 350°C. LC-HRMS parameters associated with the multi-mycotoxin method are gathered in table 3. Quantification was performed by external calibration with standard solutions of ENNs (A, A1, B, B1), BEA, DON, ADON, NIV, FX, ZEA, T2, HT2, and DAS. (Romer Labs, Getzersdorf, Austria). Toxin yields were expressed in μg/g of fungal dry biomass.

Table 3. LC-HRMS parameters for the quantification of mycotoxins, including the retention time, analyte formula, ion m/z (extracted with a 3 ppm tolerance) for quantification and for confirmation.

Mycotoxin	Retention time (min)	Formula	Ion for quantification (m/z)	Ion for confirmation (m/z)
Acetyl-deoxynivalenol	3.85	C <sub>17</sub> H <sub>22</sub> O <sub>7</sub>	361.1258	339.1438
Beauvericin	6.22	C <sub>45</sub> H <sub>57</sub> N <sub>3</sub> O <sub>9</sub>	801.4433	806.3987
Diacetoxyscirpenol	4.50	C <sub>19</sub> H <sub>26</sub> O <sub>7</sub>	389.1571	384.2017
Deoxynivalenol	2.90	C <sub>15</sub> H <sub>20</sub> O <sub>6</sub>	319.1152	297.1333
Enniatin A	6.35	C <sub>36</sub> H <sub>63</sub> N <sub>3</sub> O <sub>9</sub>	699.4903	704.4456
Enniatin A1	6.30	C <sub>35</sub> H <sub>61</sub> N <sub>3</sub> O <sub>9</sub>	685.4746	690.4300
Enniatin B	6.10	C <sub>34</sub> H <sub>59</sub> N <sub>3</sub> O <sub>9</sub>	657.4433	662.3987
Enniatin B1	6.30	C <sub>34</sub> H <sub>59</sub> N <sub>3</sub> O <sub>9</sub>	671.4590	676.4143
Fusarenone X	3.90	C <sub>17</sub> H <sub>22</sub> O <sub>8</sub>	377.1207	355.1387
Nivalenol	2.30	C <sub>15</sub> H <sub>20</sub> O <sub>7</sub>	335.1101	313.1282
Toxin T-2	5.10	C <sub>24</sub> H <sub>34</sub> O <sub>9</sub>	489.2095	484.2541
Toxin HT-2	4.95	C <sub>22</sub> H <sub>32</sub> O <sub>8</sub>	447.1989	442.2435
Zearalenone	5.40	C <sub>18</sub> H <sub>22</sub> O <sub>5</sub>	341.1359	319.1540

e) Sporulation and germination assays

The *F. graminearum* strain CBS185.32/INRAE 349 and the *F. avenaceum* strain INRAE 498 were selected for these assays.

For conidiation assays, one mycelial plug (5 mm in diameter) of each strain, taken from the periphery of a 7-day old colony grown on PDA plates was inserted in a 50 mL-filter screw cap conical tube containing 10 mL of CMC medium supplemented or not with TC3 at 25 and 50  $\mu$ M, and incubated for up to three days at 25°C and 180 rpm in darkness in an Infors Multitron (INFORS-HT). After three days, the spore solutions were filtered through Sefar Nitex 03–100 (SEFAR AG, Heiden, Switzerland), then spores were counted in a Mallassez cell counting chamber under microscope (three independent counts per sample). Three biological replicates for each condition were done. Three counts for each biological repetition were made and the value for one biological repetition is represented as the mean of the three counts.

For germination assays, conidia of *Fusarium* spp. were prepared by transferring 4 fungal agar plugs (5 mm in diameter) into 20 mL CMC medium and incubation at 200 rpm and 25 °C for three days. The conidia were harvested by filtration through a 100  $\mu$ m Sefar Nitex 03–100 (SEFAR AG, Heiden, Switzerland) followed by centrifugation at 4000 rpm for 20 min. The conidial pellet was redissolved with sterile water and diluted to reach 1e+06 spores/mL. To assess the effect of TC3 on the germination of *Fusarium* species, 20  $\mu$ L of spore suspension was added to 0.5 mL tubes containing 200  $\mu$ L of MS medium supplemented with TC3 at 25 and 50  $\mu$ M or with water for control. The tubes were incubated at 25 °C in the dark. The effect of TC3 on conidial germination was assessed at 0, 4 and 8 hours after inoculation (HAI). Then spores were counted in a Mallassez cell counting chamber under microscope (two independent counts per biological repetition) and the number of germinated spores was determined by observation. The density of spores was determined for each sample to confirm the comparability of the results. Four biological repetitions were done for each condition.

f) Fluorescence microscopy

The *F. graminearum* strain CBS185.32/INRAE 349 and the *F. avenaceum* strain INRAE 498 were considered in this assay.  $1.10^4$  Conidia / ml of *F. graminearum* and *F. avenaceum*, prepared in CMC medium as previously described, were incubated for 45 minutes in MS medium supplemented with TC3 labeled with the fluorophore fluorescein isothiocyanate (FITC) at 25  $\mu$ M and with 5  $\mu$ g/mL FM 4-64 prepared according to the supplier's recommendations. The imaging was performed using a confocal microscope (Zeiss LSM 880) equipped with a Plan-Apochromat 40X/1.3 oil and 63X/1.4 oil objectives. Laser excitation lines for the different fluorophores were 488 nm for TC3-FITC or FM4-64. Fluorescence emissions were detected at 490–561 nm for FITC and 642–695 nm for FM4-64. In multi-labeling acquisitions, detection was in sequential line-scanning mode with a line average of 4. Confocal microscope images were processed using the Zen Black Software (V2.3 Zeiss) for intensity optimization.

### g) Statistical analyses

All presented values are mean  $\pm$  standard deviation including six biological replications, except for the sporulation assay which included three biological replications. Since the data were non-normally distributed (Shapiro–Wilk normality test), the Kruskal–Wallis one-way analysis was used, with mean comparisons performed using the Mann–Whitney U test. Statistical analysis was conducted with R (R Core Team) and figures were produced using the package ggplot (Wickham, H., 2016)<sup>19</sup>. Statistical significance was considered when  $p < 0.05$ .

## III. Results

### 1) Species- and strain-dependent antifungal activity of TC3

The peptide TC3 was tested at 50 $\mu$ M against different *Fusarium* species involved in FHB including *F. graminearum*, *F. avenaceum*, *F. tricinctum*, *F. langsethiae*, *F. poae* and *F. culmorum*. Results are reported in Figure 1.

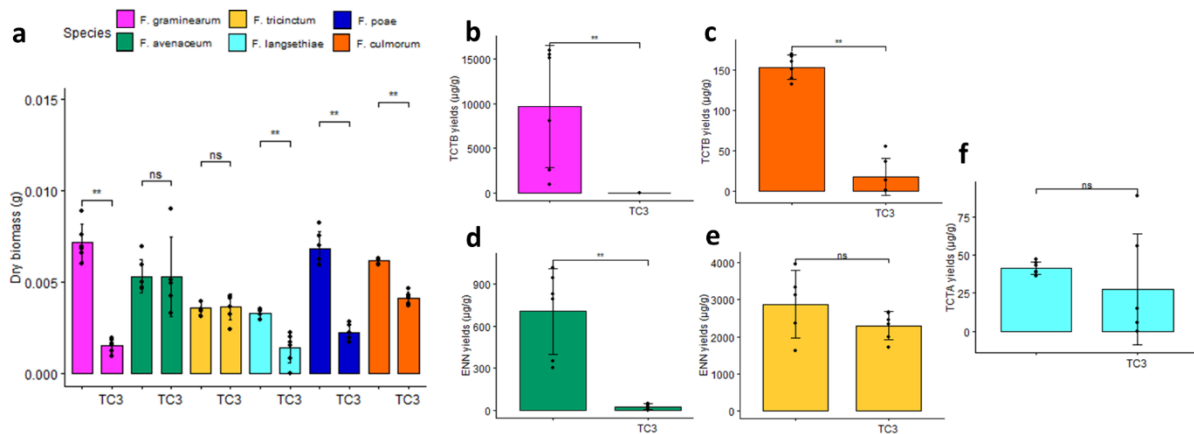


Figure 1. Effect of TC3 at 50  $\mu$ M on the fungal biomass weight (a) of *F. graminearum* (INRAE 349), *F. avenaceum* (INRAE 498), *F. tricinctum* (INRAE 104), *F. langsethiae* (INRAE 502), *F. poae* (INRAE 488) and *F. culmorum* (INRAE 134) and on the production of TCTB by *F. graminearum* and *F. culmorum* (b,f), ENN by *F. avenaceum* and *F. tricinctum* (c,e) and T2+HT2 by *F. langsethiae* (d) in 10-day-old broths. Results shown are means and standard deviation values. Results in control and TC3-treated groups within each species were compared by Mann–Whitney U test (\*\*  $p < 0.01$ ; ns: not significant).

A significant reduction in fungal growth was registered for *F. graminearum*, *F. langsethiae*, *F. poae* and *F. culmorum* when cultures were supplemented with the peptide TC3 compared to non-supplemented cultures (Fig. 1a). In contrast, the growth of the species *F. avenaceum* and *F. tricinctum* was not affected by the peptide at the tested concentration.

No detectable levels of mycotoxins (i.e., NIV, DAS or MAS) was observed after 10 days in TC3-treated and control cultures for *F. poae*. The TCTB production by *F. graminearum* (DON + 15-ADON) and *F. culmorum* (NIV + FX) was reduced significantly by the TC3 treatment (Fig. 1b, 1c). In *F. graminearum* control cultures, the mean value of DON + 15-ADON reached 9600

µg/g, while no quantifiable TCTB was observed in TC3-supplemented cultures ( $p < 0.01$ ). Similarly, the production of NIV + FX by *F. culmorum* in control conditions was close to 150 µg/g while in TC3-treated cultures this production was reduced to 20 µg/g, which indicates a reduction of 86% (Fig. 1c,  $p < 0.01$ ). The production of ENNs by *F. avenaceum* was also significantly reduced by TC3 (reduction factor close to 95 %) ( $p < 0.01$ ) (Fig. 1d). This was however not the case for the production of ENNs by *F. tricinctum* that was not affected by TC3 supplementation neither for the production of the sum of T2+HT2 by *F. langsethiae* (Fig. 1e, 1f). These results suggest that *F. graminearum* and *F. avenaceum*, which are the two most prevalent species associated with FHB in Europe, showed significant differences in their susceptibility to TC3. However, and surprisingly, whereas TC3 did not impact *F. avenaceum* growth, it significantly modulated the production of ENNs. To go further, the effect of TC3 was investigated considering a panel of isolates of the two former species.

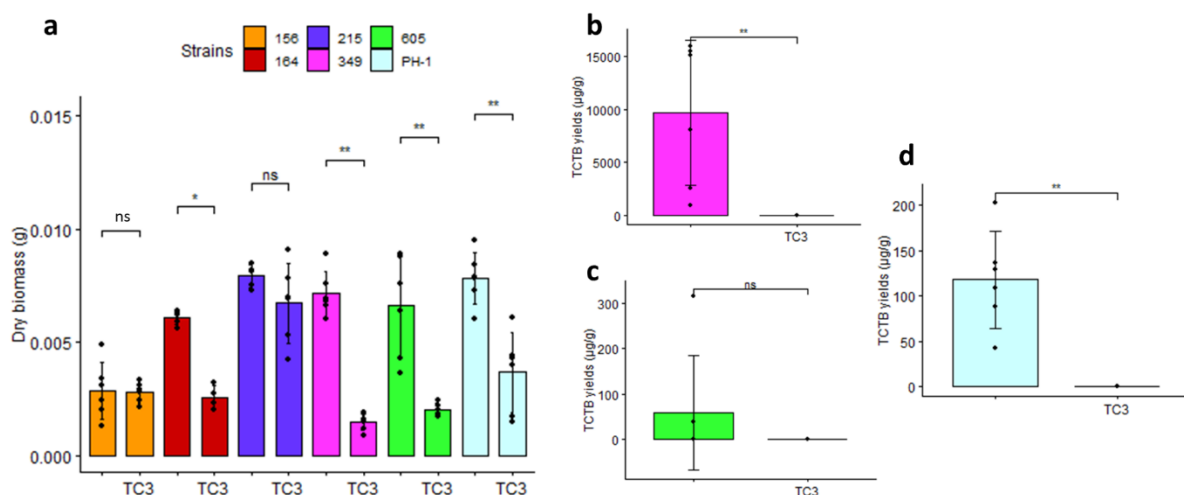
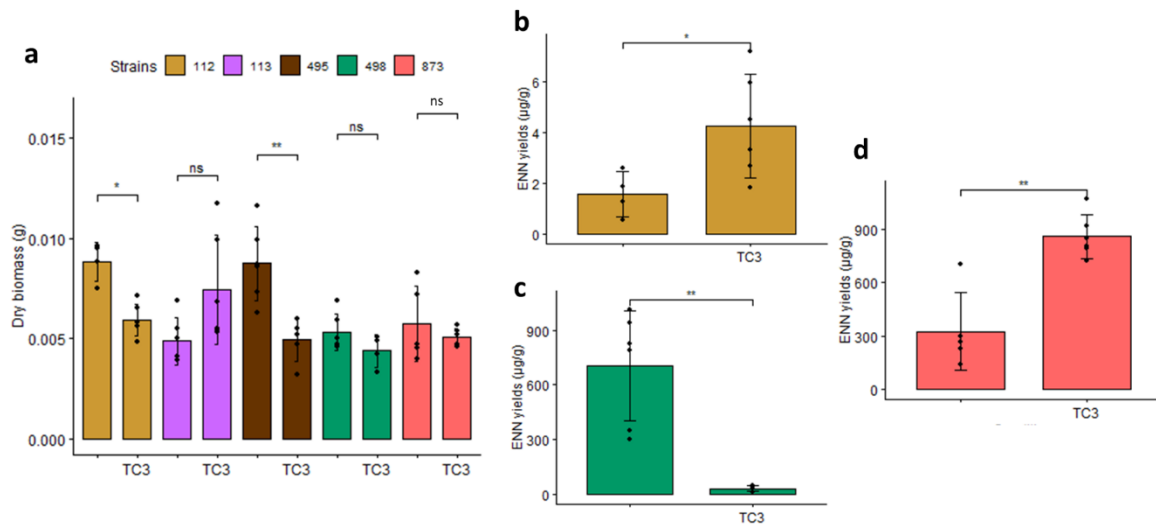


Figure 2. Effect of TC3 at 50 µM on the fungal biomass weight of *F. graminearum* strains (a) and on the production of TCTB by strains INRAE215 (b), INRAE349 (c), INRAE 605(d) and PH1 (e) in 10-day-old broths. Results shown are means and standard deviation values. Results in control and TC3-treated groups within each *F. graminearum* strains were compared by Mann–Whitney U test (\*\*  $p < 0.01$ , \*  $p < 0.05$ ; NS: not significant)

Results displayed in Figure 2a indicated a significant reduction in fungal biomass induced by the TC3 treatment for four of the six considered *F. graminearum* strains (INRAE 164, INRAE 349, INRAE 605 and PH-1). Inhibition percentages were ranging between 50 (PH-1) and 80 % (INRAE 349). For the INRAE 215 isolate, a reduction trend in biomass was also suggested by our data; this decrease was however not statistically different when comparing with the control. The growth of INRAE 156, that showed a lower biomass after 10 days of incubation compared to the five other strains, was not affected when exposed to TC3. Concerning the production of DON + 15-ADON, the levels of produced mycotoxins by the strains INRAE 156, INRAE 164 and INRAE 215 in control conditions were below the limit of quantification of the HPLC-DAD method. For the three strains for which a quantifiable amount of toxins was

observed in untreated conditions, the supplementation with TC3 led to a reduction of DON + 15-ADON yields. This reduction was statistically significant and drastic for INRAE 349 and PH-1, and not significant for INRAE 605.



Results regarding the effect of 50 µM TC3 on a panel of *F. avenaceum* isolates are gathered in Figure 3. A significant reduction in fungal biomass was observed for the strains INRAE 112 and INRAE 495. The reduction in fungal growth was close to 33% ( $p$ -value $<0.05$ ) for INRAE 112 and 44% ( $p$ -value $<0.01$ ) for INRAE 495 compared to their respective control groups. The fungal biomass of strains INRAE 113, INRAE 498 and INRAE 873 was not affected by the defensin  $\gamma$ -core. Regarding the production of ENNs, three strains were capable of producing quantifiable amounts of ENNs in our experimental conditions. For these three strains, a significant inhibition of ENNs yield induced by TC3 was only observed for INRAE 498 (Fig. 3c). At the opposite, an increase in ENNs accumulated in TC3-supplemented broths was evidenced for INRAE 112 and INRAE 873 (Fig. 3b, 3d). It should however be noticed that the production of ENNs by INRAE 112 was very weak, lower than 10 µg/g. Altogether, the above described data support that TC3 has a wider antifungal activity (i.e., can affect more fungal strains) against *F. graminearum* compared with that against *F. avenaceum*.

2) The fungal life cycle stage impacts TC3 fungicidal and anti-mycotoxin actions

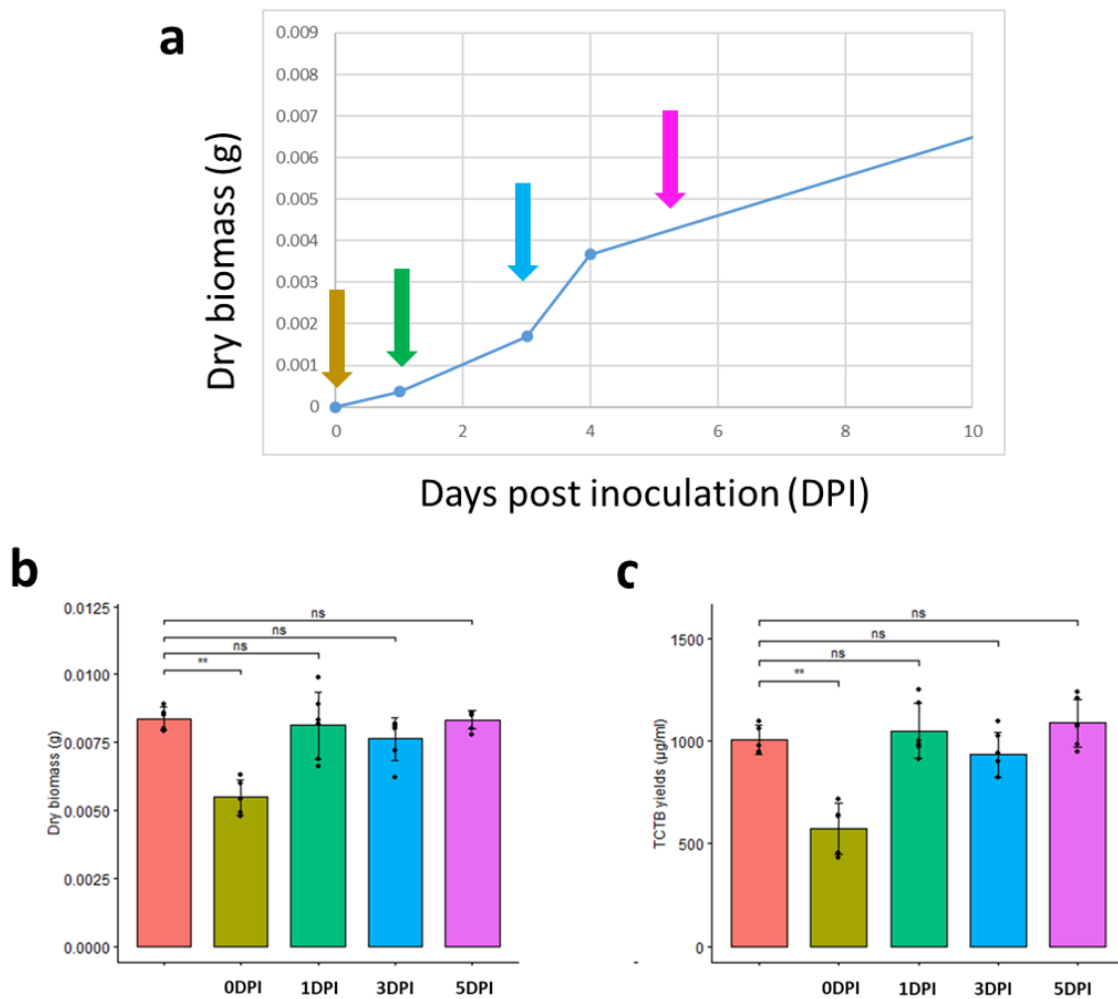


Figure 4. Effect of TC3 at 50  $\mu$ M supplemented at different day post-inoculation on *F. graminearum* INRAE 349 growth without treatment (a). The arrows represent the supplementation day for test of TC3 on different life cycle stages. Effect of TC3 at 50  $\mu$ M (supplemented at 0, 1, 3 and 5 dpi) on the fungal biomass weight of *F. graminearum* INRAE 349 (b) and on the production of DON + 15-ADON (c) in 14-day-old broths. Results in control and TC3-treated groups were compared to the control by Mann–Whitney U test (\*\*  $p < 0.01$ ; NS: not significant).

To determine the effect of the peptide TC3 according to the life cycle stage of *F. graminearum* INRAE 349, TC3 was supplemented before fungal inoculation (0 dpi), at 1 and 3 dpi (during the exponential phase of growth) and at 5 dpi (inflection of the growth kinetics). Results are reported in Figure 4. It clearly appears that TC3 induced a significant inhibition of fungal growth and mycotoxin yield only when it is applied at 0 dpi (at the spore stage). For all other conditions, i.e. when the peptide was applied when the mycelium starts to develop (1 dpi), during the exponential phase of growth (3 dpi) or at the beginning of growth kinetics inflexion (5 dpi), no effect was evidenced concerning both fungal growth and mycotoxin production. These results suggested that the spore germination stage is the most susceptible stage to the TC3 peptide.

### 3) TC3 affects *F. graminearum* and *F. avenaceum* sporulation and germination

To study the effect of TC3 on the early stages of fungal development, the effect of TC3 on sporulation and germination of *F. graminearum* INRAE 349 and *F. avenaceum* INRAE 498 was investigated and compared. The two strains were demonstrated as highly toxigenic in previous experiments (Figures 2 and 3).

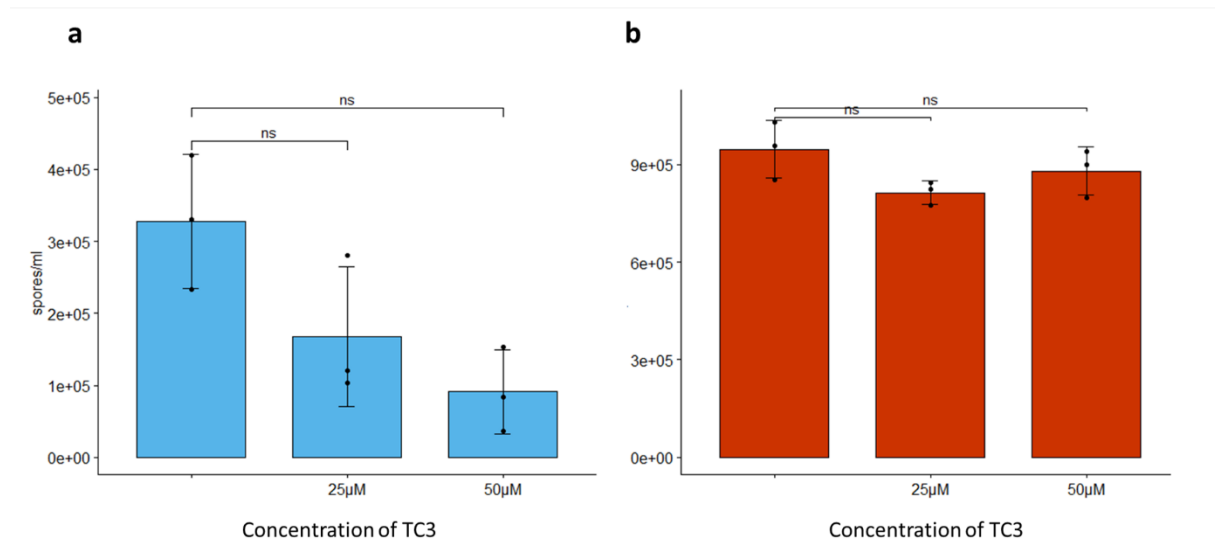


Figure 5. Effect of TC3 at 25  $\mu\text{M}$  and 50  $\mu\text{M}$  on the number of spores of *F. graminearum* INRAE 349 (a) and *F. avenaceum* INRAE 498 (b) in 3-day-old CMC medium. Results shown are means and standard deviation values. Results in control and TC3-treated groups within each species were compared by Mann–Whitney U test (ns: not significant).

One mycelial plug of each studied strain was incubated in CMC conidiation medium supplemented with TC3 at 0, 25 and 50  $\mu\text{M}$  for 3 days. The numbers of counted spores in each condition and for each strain are reported in Figures 5a and 5a. The peptide TC3 induced a dose-dependent anti-sporulation effect on *F. graminearum* (Fig. 5a). The mean number of spores was 32e+04/ml in the CMC control conditions while this number was reduced to 16e+04 spores/ml with 25  $\mu\text{M}$  TC3 and 9e+04 spores/ml with 50  $\mu\text{M}$  TC3. This inhibition effect was however not statistically significant, certainly as a result of the large standard deviation and insufficient number of biological repetitions. When considering *F. avenaceum* INRAE 498, it clearly appeared that the TC3 peptide had no effect on its sporulation (Fig. 5b).

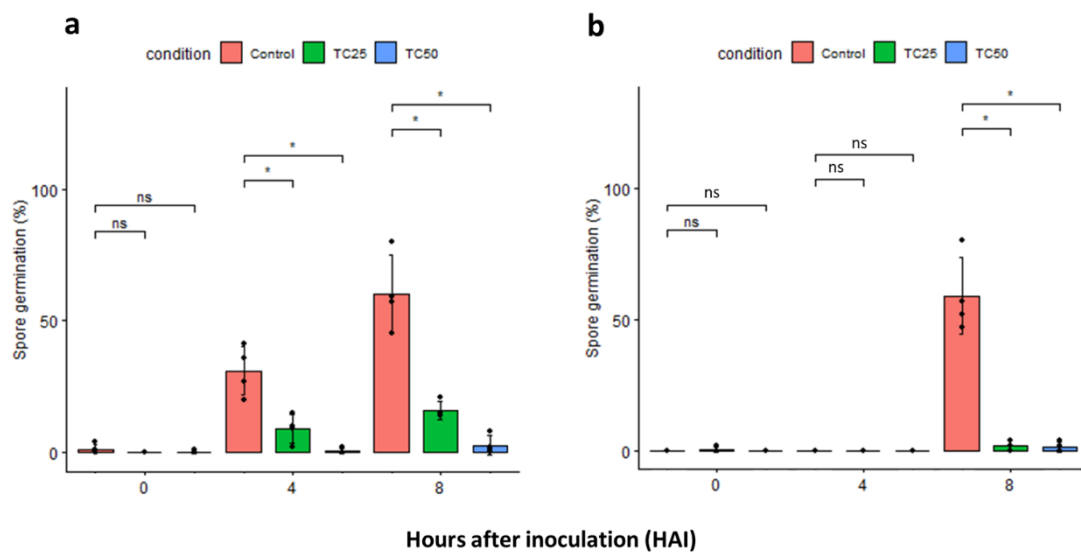


Figure 6. Effect of TC3 at 25  $\mu\text{M}$  and 50  $\mu\text{M}$  on the percentage of germinated spores relative to the total spores of *F. graminearum* INRAE 349 (a) and *F. avenaceum* INRAE 498 (b) at 0, 4 and 8 HAI. Results shown are means and standard deviation values. Results in control and TC3-treated groups within each species were compared by Mann–Whitney U test (\*  $p < 0.05$ ; NS: not significant).

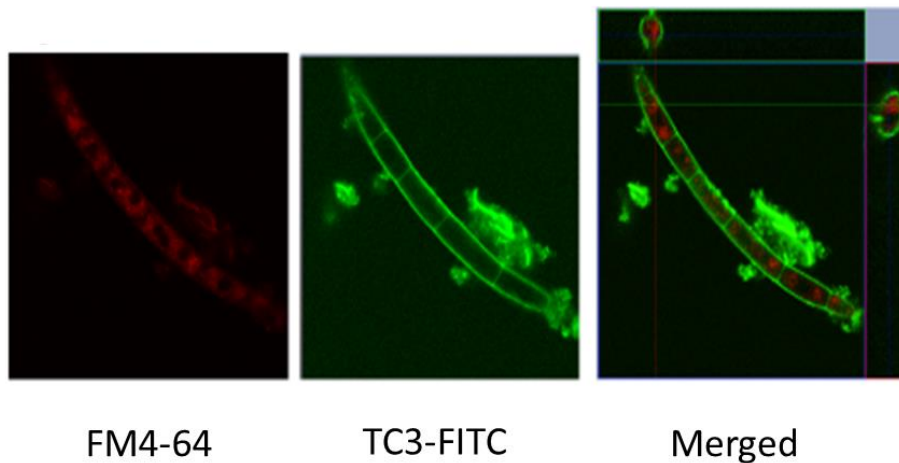
To determine the effect of the antifungal peptide TC3 on *Fusarium* spore germination, a similar concentration of spores ( $4 \times 10^4/\text{ml}$ ) of *F. graminearum* INRAE 349 and *F. avenaceum* INRAE 498 were incubated in presence of TC3 25 and 50  $\mu\text{M}$  and the number of germinated spores was counted over 8 hours. Results are reported in Figures 6a and 6b. When first looking at the spore germination kinetics of *F. graminearum* in MS control medium, data reported on Figure 6a indicate that 30 % and 60% of the spores were germinated after 4h and 8h incubation, respectively. Treatment with TC3 led to a sharp and dose-dependent inhibition of spore germination. At 4 HAI, the percentage of germinated spores was 9% ( $p\text{-value} < 0.05$ ) and 1% ( $p\text{-value} < 0.05$ ) with 25 $\mu\text{M}$ , and 50 $\mu\text{M}$  TC3, respectively, compared to not-supplemented MS. This effect was even more pronounced at 8 HAI: while 60 % of germinated spores were recorded in the control MS condition, this percentage was reduced to 16% ( $p\text{-value} < 0.05$ ) and 3% ( $p\text{-value} < 0.05$ ) with TC3 at 25 $\mu\text{M}$  and 50 $\mu\text{M}$ , respectively. When focusing on *F. avenaceum* INRAE 498, data reported in Figure 6b clearly indicate that, in our experimental conditions, the kinetic of spore germination was significantly delayed compared to that of *F. graminearum* INRAE 349. No germinated spore or a few germinated spores were detected in control MS at 4 HAI. Germination appeared to start between 4 and 8 h of incubation to reach a 60 % percentage at 8 HAI. However, as it has been observed for *F. graminearum*, TC3 at both 25 and 50  $\mu\text{M}$  was able to drastically inhibit the germination of *F. avenaceum* spores.

To summarize, TC3 possesses an anti-sporulation activity against *F. graminearum* but not against *F. avenaceum* and a significant capacity to inhibit spore germination for both species. This inhibition of spore germination is associated with a reduction of fungal biomass in 10-day-old broths of *F. graminearum* but not for *F. avenaceum* (Fig. 1a).

4) TC3 is recruited by the cell envelope of *F. graminearum* and *F. avenaceum* spores

To investigate the interactions of the TC3 peptide with *F. graminearum* and *F. avenaceum* spores and visualize the potential internalization of TC3 within the fungal cell, a fluorescence microscopy assay was implemented with the use of a TC3 peptide labeled with a fluorescent reagent. The fluorescein isothiocyanate (FITC) was privileged due to its high luminous yield, a rather low molecular weight (389 Da) and the fact that FITC possesses the same excitation wavelength with the fluorescent stain FM4-64 (488 nm) but different emission wavelength. Indeed, spores were simultaneously treated with TC3-FITC and FM4-64. FM4-64 is known to insert into the outer leaflet of the fungal plasma membrane.

*F. graminearum*



*F. avenaceum*

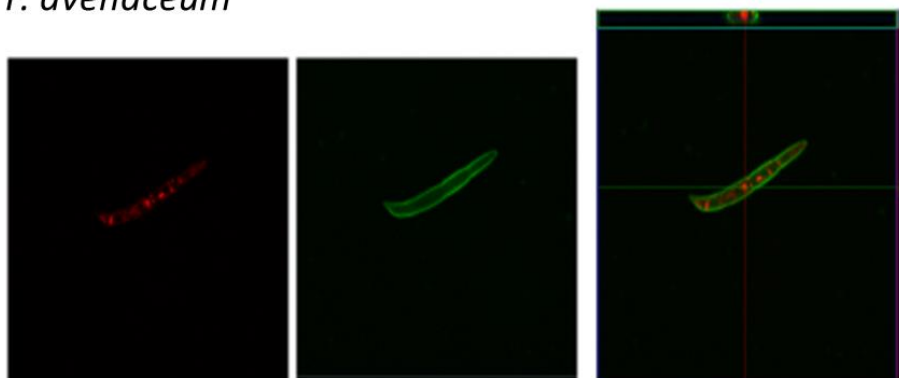


Figure 7. Analysis on fluorescence microscopy of *F. graminearum* strain and *F. avenaceum* spores in presence of TC3 peptide labeled with FITC (25  $\mu$ M) in green and the fluorescent dye FM4-64 in red. The merged pictures present a cross-section observation of the spores. *F. graminearum* was observed with a Plan-Apochromat at resolution 63X/1.4 oil and *F. avenaceum* with a Plan-Apochromat at resolution 40X/1.3 oil.

Within 45 min of treatment, TC3-FITC was clearly found to bind on the conidial surface for the two studied species. The interaction was characterized by a homogeneous distribution of the green fluorescent signal along the hyphae and septa. In order to reach a more accurate location of the FITC-TC3 peptide at the cellular envelope, spores were treated by a mixture of FITC-TC3 and FM4-64. Membranes stained by FM4-64 were clearly visualized, including membranes around organelles (red fluorescence in Figure 7). But no green fluorescence within the fungal cells was observed whatever the considered *Fusarium* species suggesting that TC3-FITC was not internalized. Besides, the green patches observed in Figure 7 indicate the occurrence of aggregates of peptides.

#### IV. Discussion

The present study demonstrates that the  $\gamma$ -core motif TC3 reduces the growth of numerous of the *Fusarium* species causing FHB, including *F. graminearum*, *F. culmorum*, *F. poae* and *F. langsethiae*. However, while confirming previously published data on the efficiency of TC3 towards *F. graminearum* (Tonk et al., 2015, Leannec-Rialland et al., 2021)<sup>15,18</sup>, the present study also evidenced that the sensitivity of mycotoxin-producing fungi varies according to the species and even of the strain. Such differences in fungal species susceptibilities to defensins have already been described and are discussed in the review of Leannec-Rialland et al. (2022)<sup>17</sup>. For instance, in the study of Theis et al. (2003)<sup>20</sup> focusing on the activity of a defensin from *Aspergillus giganteus*, the *F. sporotrichioides* species was significantly more susceptible than *F. culmorum*. According to our data, the growth of *F. avenaceum* appears to be much less affected by a TC3 treatment than the other tested *Fusarium* species, and particularly compared to *F. graminearum*. Surprisingly, this lower susceptibility was not related to differences in the capacity of TC3 to inhibit the germination of spores from both species, *F. avenaceum* and *F. graminearum*. We could imagine that TC3 induces a delayed germination rather than a stop or/and that the residual number of *F. avenaceum* germinated spores in TC3 treated conditions is sufficient to initiate a mycelium growth that will rapidly offset the germination inhibitory effect of TC3. This hypothesis requires however to be demonstrated. Besides, our data illustrated that TC3 was not only capable of affecting the fungal growth but also the production of various mycotoxins by most of the species involved in FHB. In addition to an inhibition of DON and 15-ADON yield, TC3 supplementation was shown to induce decreased amounts of NIV and FX, T2 and HT2 and ENNs. The observed reduction of ENNs production was not associated with an inhibition of fungal biomass. Such a result supporting the assumption that inhibition of fungal growth and of production of mycotoxins by TC3 suggests that the two effects could be independent. They corroborated first data published on the activity of TC3 (at lower concentrations than used in the present study) towards *F. graminearum* and DON+15-ADON production (Leannec-Rialland et al., 2021)<sup>18</sup> or previously published work focusing on other natural products including phenylpropanoids (Boutigny et al., 2009; Gautier et al., 2020)<sup>21,22</sup>. This specific effect on

mycotoxin yields was partially ascribed to the capacity of biomolecules to affect the transcription of key genes involved in the biosynthesis of mycotoxins (Atanasova-Penichon et al., 2016)<sup>23</sup>. Altogether, our results that have documented the species and strain-dependent efficacy of TC3 raise a potential concern of shifts in FHB community induced by a TC3-based plant care treatment applied during cereal cultivation. An overrepresentation of *F. avenaceum* and consequently an increased in ENNs contamination levels cannot be excluded (Audenaert et al., 2011)<sup>24</sup>. Such unexpected effect mediated by fungicide treatment has already been documented. In their report, Audenaert *et al.* (2011)<sup>24</sup> indicated that application of azole fungicides in wheat fields caused a shift in *Fusarium* population with *F. poae* (more resistant to azole fungicides) being dominant and supplanting *F. graminearum*. Besides, not only different susceptibilities to a biosolution but also the occurrence of interactions between the *Fusarium* species that share a common niche when infecting cereals require to be considered. Yet, the recent publication of Tan et al. (2021)<sup>25</sup> has clearly demonstrated that the biocontrol capacity of actinobacteria against *F. graminearum* was critically hampered by the presence of *F. poae* and has highlighted the limits of single-strain and/or single-species approach. In next experiments, the antifungal and anti-mycotoxin efficiency of TC3 will be assessed considering *F. graminearum* in interaction with the other *Fusarium* species that infect European wheat harvests.

According to our data, the conidiation and germination stage of *F. graminearum* and only the germination stage for *F. avenaceum* were sensitive to the  $\gamma$ -core motif TC3. The peptide appeared as not efficient to restrain the mycelial growth. These data corroborate previous results published by Tonk et al. (2014, 2015)<sup>14,15</sup> who have highlighted the anti-germination activity of *Ixodes scapularis* and *Ixodes ricinus* defensins. They also support the frequently reported observation that the fungal germination stage is the most sensitive developmental stage to antifungal compounds including phenolic compounds (Ahmed et al., 2021)<sup>26</sup>. Similarly, strobilurin fungicides, which block electron transport at the site of quinol oxidation in the cytochrome bc1 complex of the mitochondrial electron transport chain, are highly efficient inhibitors of spore germination but much less active to restrain mycelial growth (Bartlett et al., 2022)<sup>27</sup>. On the opposite, some fungicides are reported as more active on mycelial growth than on spore germination. This is for instance the case of azole fungicides that are inhibitors of ergosterol biosynthesis (Wang et al., 2022).

According to our previously published study (Leannec-Rialland et al., 2021)<sup>18</sup>, the  $\gamma$ -core motif TC3 was predicted to interact with specific membrane phospholipids of *F. graminearum*. However, the membrane composition used for this *in silico* prediction was based on old data, published in 1989 (Wiebe et al., 1989)<sup>28</sup>, and no further information on *F. graminearum* membrane composition has been delivered since. Using a fluorescent labelled TC3 peptide, the microscopy observations made in the present study seem to corroborate the TC3 interactions with *F. graminearum* membranes. But, unfortunately, our experimental conditions did not allow to unambiguously conclude whether the TC3 fixation was carried out at the fungal cell wall or the plasma membrane. TC3 appeared to accumulate on the surface of the spores and to surround them. This evokes a carpet-like interaction, which is one of the

described mode of interactions of defensins with fungal membrane (Leannec-Rialland et al., 2022)<sup>17</sup>. By this way, TC3 could induce dysfunctions of calcium influx and potassium efflux. Besides, with the concentration of labeled peptide and the time of application used in this study, no internalization of the peptide was evidenced. Since defensin internalization has been shown as time and concentration dependent (Tetorya et al., 2022)<sup>29</sup>, we can however not exclude that TC3 internalization could occur with other experimental parameters.

## V. Conclusion

The  $\gamma$ -core motif of the defensin DefMT3 from *Ixodes ricinus* is a potent antifungal peptide that inhibits the fungal growth and mycotoxin production by various *Fusarium* species when applied at the spore stage. The peptide has the capacity to surround the spores and is likely to interfere with fungal cell ionic exchanges, which is certainly one of the first rationale that can explain its bioactivity. By increasing the knowledge on the efficacy and mechanisms of action of the TC3 peptide, the present study supports the promising use of defensin-based products as environment-friendly treatments for controlling FHB. However, the demonstrated species-dependent efficiency of the peptide raises the concern of potential shift in *Fusarium* population such as in mycotoxin profile contaminating grains mediated by its application in wheat fields. Further studies are required to support or negate the occurrence of such unintended effects.

## References

1. Birr, T., Hasler, M., Verreet, J.-A. & Klink, H. Composition and Predominance of Fusarium Species Causing Fusarium Head Blight in Winter Wheat Grain Depending on Cultivar Susceptibility and Meteorological Factors. *Microorganisms* **8**, 617 (2020).
2. Bottalico, A. & Perrone, G. Toxigenic Fusarium species and Mycotoxins Associated with Head Blight in Small-Grain Cereals in Europe. *European Journal of Plant Pathology* **108**, 611–624 (2002).
3. van der Lee, T., Zhang, H., van Diepeningen, A. & Waalwijk, C. Biogeography of Fusarium graminearum species complex and chemotypes: a review. *Food Addit Contam Part A Chem Anal Control Expo Risk Assess* **32**, 453–460 (2015).
4. Dweba, C. C. *et al.* Fusarium head blight of wheat: Pathogenesis and control strategies. *Crop Protection* **91**, 114–122 (2017).
5. Kang, Z. & Buchenauer, H. Immunocytochemical localization of fusarium toxins in infected wheat spikes by Fusarium culmorum. *Physiological and Molecular Plant Pathology* **55**, 275–288 (1999).
6. Gautier, C., Pinson-Gadais, L. & Richard-Forget, F. Fusarium Mycotoxins Enniatins: An Updated Review of Their Occurrence, the Producing Fusarium Species, and the Abiotic Determinants of Their Accumulation in Crop Harvests. *J. Agric. Food Chem.* **68**, 4788–4798 (2020).
7. Fabre, F. *et al.* Unbalanced Roles of Fungal Aggressiveness and Host Cultivars in the Establishment of the Fusarium Head Blight in Bread Wheat. *Frontiers in Microbiology* **10**, (2019).
8. Laurent, B. *et al.* Landscape of genomic diversity and host adaptation in Fusarium graminearum. *BMC Genomics* **18**, 203 (2017).
9. Zhang, Y.-J. *et al.* Effect of Carbendazim Resistance on Trichothecene Production and Aggressiveness of Fusarium graminearum. *MPMI* **22**, 1143–1150 (2009).
10. Hou, Y.-P., Mao, X.-W., Wang, J.-X., Zhan, S.-W. & Zhou, M.-G. Sensitivity of Fusarium asiaticum to a novel succinate dehydrogenase inhibitor fungicide pydiflumetofen. *Crop Protection* **96**, 237–244 (2017).
11. Leslie, J. F. *et al.* Key Global Actions for Mycotoxin Management in Wheat and Other Small Grains. *Toxins* **13**, 725 (2021).
12. Règlement (CE) N° 396/2005 du Parlement européen et du Conseil du 23 février 2005 concernant les limites maximales applicables aux résidus de pesticides présents dans ou sur les denrées alimentaires et les aliments pour animaux d'origine végétale et animale et modifiant la directive 91/414/CEE du Conseil Texte présentant de l'intérêt pour l'EEE. *OJ L* vol. 070 (2005).
13. Règlement (CE) n° 1126/2007 de la Commission du 28 septembre 2007 modifiant le règlement (CE) n° 1881/2006 portant fixation de teneurs maximales pour certains contaminants dans les denrées alimentaires en ce qui concerne les toxines du Fusarium dans le maïs et les produits à base de maïs (Texte présentant de l'intérêt pour l'EEE). *OJ L* vol. 255 (2007).
14. Tonk, M. *et al.* Defensins from the tick Ixodes scapularis are effective against phytopathogenic fungi and the human bacterial pathogen *Listeria grayi*. *Parasites Vectors* **7**, 554 (2014).
15. Tonk, M. *et al.* Ixodes ricinus defensins attack distantly-related pathogens. *Developmental & Comparative Immunology* **53**, 358–365 (2015).
16. Cabezas-Cruz, A. *et al.* Antiplasmodial Activity Is an Ancient and Conserved Feature of Tick Defensins. *Front. Microbiol.* **7**, (2016).
17. Leannec-Rialland, V. *et al.* Use of Defensins to Develop Eco-Friendly Alternatives to Synthetic Fungicides to Control Phytopathogenic Fungi and Their Mycotoxins. *J Fungi (Basel)* **8**, 229 (2022).

18. Leannec-Rialland, V. *et al.* Tick defensin  $\gamma$ -core reduces *Fusarium graminearum* growth and abrogates mycotoxins production with high efficiency. *Sci Rep* **11**, 7962 (2021).
19. Wickham, H. *ggplot2: Elegant Graphics for Data Analysis*. (Springer International Publishing : Imprint: Springer, 2016). doi:10.1007/978-3-319-24277-4.
20. Theis, T., Wedde, M., Meyer, V. & Stahl, U. The antifungal protein from *Aspergillus giganteus* causes membrane permeabilization. *Antimicrob Agents Chemother* **47**, 588–593 (2003).
21. Boutigny, A.-L. *et al.* Ferulic acid, an efficient inhibitor of type B trichothecene biosynthesis and Tri gene expression in *Fusarium* liquid cultures. *Mycological Research* **113**, 746–753 (2009).
22. Gautier, C. *et al.* Investigating the Efficiency of Hydroxycinnamic Acids to Inhibit the Production of Enniatins by *Fusarium avenaceum* and Modulate the Expression of Enniatins Biosynthetic Genes. *Toxins* **12**, 735 (2020).
23. Atanasova-Penichon, V., Barreau, C. & Richard-Forget, F. Antioxidant Secondary Metabolites in Cereals: Potential Involvement in Resistance to *Fusarium* and Mycotoxin Accumulation. *Frontiers in Microbiology* **7**, (2016).
24. Audenaert, K. *et al.* *Impact of Fungicide Timing on the Composition of the Fusarium Head Blight Disease Complex and the Presence of Deoxynivalenol (DON) in Wheat. Fungicides - Beneficial and Harmful Aspects* (IntechOpen, 2011). doi:10.5772/26322.
25. Tan, J. *et al.* Presence of the Weakly Pathogenic *Fusarium poae* in the *Fusarium* Head Blight Disease Complex Hampers Biocontrol and Chemical Control of the Virulent *Fusarium graminearum* Pathogen. *Front Plant Sci* **12**, 641890 (2021).
26. Ahmed, O. S. *et al.* Naturally occurring phenolic compounds as promising antimycotoxin agents: Where are we now? *Comprehensive Reviews in Food Science and Food Safety* **21**, 1161–1197 (2022).
27. Bartlett, D. W. *et al.* The strobilurin fungicides. *Pest. Manag. Sci.* **58**, 649–662 (2002).
28. Wiebe, M. G., Robson, G. D. & Trinci, A. P. J. Effect of Choline on the Morphology, Growth and Phospholipid Composition of *Fusarium graminearum*. *Microbiology* **135**, 2155–2162 (1989).
29. Tetorya, M. *et al.* *Plant defensin MtDef4-derived antifungal peptide with multiple modes of action and potential as a bioinspired fungicide*. <http://biorxiv.org/lookup/doi/10.1101/2022.10.02.510465> (2022) doi:10.1101/2022.10.02.510465.



**Chapter 3:  
Determination of the fungal metabolic  
pathways affected by TickCore3 in  
relation to DON and 15-ADON  
production.**



## Chapter 3: Determination of the fungal metabolic pathways affected by TickCore3 in relation to DON and 15-ADON production.

Results presented in Chapter 1 and 2 have highlighted the promising efficiency of the  $\gamma$ -core of the DefMet3 defensin from *Ixodes ricinus*, TickCore3 (TC3), against toxigenic *Fusarium* species infecting cereals. They have also provided first indications as regards the mechanisms underlying its bioactivity, supporting the involvement of a multifaceted mode of action: interactions with the spore fungal surface, a toxic effect that seems to be exerted from the extracellular side of the fungal cells, a specific modulation of the mycotoxin biosynthetic pathway. To go further and reach a comprehensive view of the fungal metabolic pathways that could be affected by exposure to TickCore3, a comparative transcriptomic approach coupled with a metabolomic one has been implemented. Deciphering how TickCore3 works is actually mandatory to help defining the most appropriate formulation and, in fine, developing an efficient plant care solution. Besides, this knowledge is also required to help anticipating the emergence of resistant fungal strain.

- A) Comparative transcriptome analysis reveals antifungal molecular mechanisms triggered by the peptide TickCore3 against *Fusarium graminearum* (article under preparation)

Leannec-Rialland V., Ducos C., Cabezas-Cruz Alejandro, Ponts N., Richard-Forget F.

### Abstract:

*Fusarium graminearum* is a fungal pathogen causing Fusarium Head Blight (FHB) in wheat. Contamination of grains with the deoxynivalenol (DON) mycotoxin produced by *F. graminearum* is a major concern in the path to food safety and security. The several drawbacks of synthetic fungicides have prompted the search of innovative and eco-friendly biosolutions. Recently, TickCore3 (TC3), a peptide derived from the defensin DefMT3 of the tick *Ixodes ricinus*, was shown to reduced *F. graminearum* fungal growth and, importantly, DON production. However, the mechanism of action of TC3 remained unknown. In this study, the transcriptomic profiles of *F. graminearum* challenged or not with TC3 were investigated to uncover potential antifungal and anti-mycotoxin mechanisms. Results showed that the tick peptide TC3 induced the differential regulation of 6,667 transcripts out of the 14,145 contained in *F. graminearum* transcriptome. Among the differentially expressed genes, 3545 were upregulated and 3783 downregulated in at least one modality. Multiple biological processes and cellular components were shown to be affected by the peptide TC3. The peptide induced a transcriptional repression of genes related to the cell wall and membrane organization as well as DNA organization and DNA transcription. Moreover, the expression of genes related to the TCA cycle, a pathway that shares a common precursor with DON biosynthesis, was enhanced. The results suggest that TC3 has the capacity to reduce mycotoxin biosynthesis, to permeabilize the membrane and affect the intracellular

environment. These data provide key insights into the multifaceted mode of action employed by TC3 and new knowledge in favor of the development of a TC3-based plant care solution to control FHB epidemics.

## I. Introduction

Currently, there is evidence that antimicrobial peptides, including defensins, possess a wide range of antimicrobial activities against bacteria, fungi, viruses and protozoa (Fernández de Ullivarri et al., 2020)<sup>1</sup>. The antimicrobial activity of defensins has been extensively documented (Sathoff and Samac, 2019)<sup>2</sup>. Besides, the promising potential of defensin-based solutions as alternatives to synthetic fungicides to control plant pathogenic fungi including fungal species capable of producing mycotoxins has also been highlighted (Martínez-Culebras et al., 2021; Leannec-Rialland et al., 2022)<sup>3,4</sup>. Mycotoxin-producing fungi are responsible for major fungal diseases affecting cereal crops, including *Fusarium* Head Blight (FHB) in small grain cereals, *Aspergillus* and *Fusarium* ear rot and *Giberella* rot in maize (Leslie et al., 2021)<sup>5</sup>. Fungal contamination by these fungi that mainly belong to the *Aspergillus*, *Penicillium* and *Fusarium* genera, is a threat for both the food and feed security and safety. They are not only responsible for dramatic losses in crop yields but also for the contamination of harvests with various mycotoxins, that pose a significant health concern to human and livestock. In Europe, *Fusarium graminearum* that produces the type B trichothecene mycotoxins with deoxynivalenol (DON) as major representant is acknowledged as the most worrying toxigenic species infecting cereals (Li et al., 2019). At present, synthetic fungicides are still a common component of agronomic strategies that aim to control *F. graminearum* in fields (Shah et al., 2017; Leslie et al., 2022)<sup>5,6</sup>. Their extensive and repeated use is however associated with environmental pollution, acute and delayed toxic effects on human and selection of fungal resistant strains. Such side effects have prompted intensive research for the identification of natural antifungal products. In a recent publication, we demonstrated that the  $\gamma$ -core of the defensin DefMt3 named TickCore3 (TC3) had a remarkable antifungal and anti-mycotoxin efficacy against *F. graminearum* (Leannec-Rialland et al., 2021)<sup>7</sup> and could be the basis for a new eco-friendly alternative to synthetic fungicides. Reaching this last objective requires however to hold a precise and comprehensive knowledge on the mechanisms underlying the capacity of TC3 to inhibit the fungal growth and the production of DON. A variety of key features have been proposed to explain the antifungal activity of antimicrobial peptides including defensins (Parisi et al., 2019; Struyfs et al., 2021; Leannec-Rialland et al., 2022)<sup>4,8,9</sup>. The biological activity of defensins is reported to involve membrane binding, binding to the cell wall, membrane permeabilization and interaction with intracellular targets. Regarding TC3, our first experiments have evidenced the key role of its positively charged amino acid residues and strongly suggested its interaction with negatively charged phospholipid head groups of *F. graminearum* membranes (Leannec-Rialland et al., 2021)<sup>7</sup>. However, the dysfunctions of the fungal metabolism and biological processes induced by the binding of TC3 to the fungal membrane remained unknown. Valuable insights into the mode of action of antifungal defensins can be gained from omics investigations, as it has been recently

illustrated by the study of Aumer et al. (2020)<sup>10</sup>. Using a proteomic strategy, the previous authors have evidenced alterations in various biological processes (including endocytosis, MAPK signaling pathway, oxidative phosphorylation and ribosome processing in endoplasmic reticulum) in *Botrytis cinerea* challenged with an analogue of the heliomycin defensin. Transcriptomics could also be a powerful tool to reveal the complex mechanism of action of an antifungal peptide. This was recently demonstrated by the work of Feng et al. (2020)<sup>11</sup> who have explored the inhibitory activity of the thanatin peptide against *Penicillium digitatum*. Thanatin was shown to alter the expression of genes encoding RNA polymerases and genes involved in ribosome biogenesis and amino acid metabolisms and was suggested to perturb the information transmission pathway in *P. digitatum*.

In this study, we used a high-throughput RNA-seq strategy to investigate dysfunctions in the biological processes and metabolic pathways of *F. graminearum* induced by the antifungal and anti-mycotoxin peptide TC3.

## II. Material and methods

### a) Synthesis of TickCore3

TickCore3 (TC3) is the  $\gamma$ -core of the *Ixodes ricinus* defensin DefMT3 (GenBank accession number: JAA71488). Peptide synthesis was commissioned to Pepmic (Suzhou, China) that uses solid-phase peptide synthesis (SPPS) to obtain highly-pure peptides as previously described (Leannec-Rialland et al., 2021)<sup>7</sup>. Briefly, peptide synthesis was performed using 2-chlorotrityl chloride resin as the solid support, using the base labile 9-fluorenyl-methyloxy-carbonyl (Fmoc) as protecting group. Amino acids were protected as follows: Fmoc-Cys(Trt)-OH, Fmoc-Gly-OH, Fmoc-Asn(Trt)-OH, Fmoc-Phe-OH, Fmoc-Leu-OH, Fmoc-Lys(Boc)-OH, Fmoc-Arg(Pbf)-OH, Fmoc-Tr(tBu)-OH, Fmoc-Ile-OH and Fmoc-Val-OH. The peptide sequence was synthesized according to the principles of SPPS. High Performance Liquid Chromatography (HPLC)-grade Fmoc chloride (Fmoc-Cl)-protected amino acid-based peptide chemistry was used with standard peptide chemistry coupling protocols. The peptide was purified by reverse phase HPLC and peptide sequence was confirmed by electrospray mass spectroscopy (ESI-MS) using a mass spectrometer LCMS-2020 (Shimadzu, Kyoto, Japan).

### b) *Fusarium graminearum* culture conditions

The *F. graminearum* CBS185.32 strain (Westerdijk Institute, The Netherlands)/INRAE 349 was selected for its capacity to produce high concentrations of DON and 15-acetyldeoxynivalenol (15-ADON) and was used throughout the study. Fungal culture was maintained at 4 °C on Potato Dextrose Agar (PDA) (Difco, Le Ponts de Claix, France) slants under mineral oil. Conidia were prepared by inoculating agar plugs in CMC medium (15 g/L carboxymethyl cellulose, 1 g/L yeast extract, 0.5 g/L MgSO<sub>4</sub>·7H<sub>2</sub>O, 1 g/L NH<sub>4</sub>NO<sub>3</sub>, 1 g/L KH<sub>2</sub>PO<sub>4</sub>) that was incubated at 150 rpm and 25 °C for three to five days. Conidia were harvested by filtration through Sefar Nitex 03–100 (SEFAR AG, Heiden, Switzerland). Liquid-culture experiments were performed in

55 mm in diameter static Petri dishes. Each Petri dish containing 8 mL of a mycotoxin synthetic (MS) medium (20 g/L glucose, 0.5 g/L KH<sub>2</sub>PO<sub>4</sub>, 0.6 g/L K<sub>2</sub>HPO<sub>4</sub>, 17 mg/L MgSO<sub>4</sub>, 1 g/L (NH<sub>4</sub>)<sub>2</sub>SO<sub>4</sub>, 0.1 mL/L Vogel mineral salts solution), supplemented or not with TC3 at 50 µM. *F. graminearum* spores were inoculated at a  $2 \times 10^4$  spores/mL concentration. Fungal liquid cultures were incubated at 25 °C in the dark for 5 days. At the third and fifth day of incubation, the culture media were removed with Supelco visiprep vacuum and stored at -20°C until analysis, while the mycelia were washed with 5 ml of sterile water and freeze-dried for fungal biomass quantification, RNA extraction and sequencing. Fungal biomass was measured by weighing the mycelia after 48 h of freeze-drying (Flexi-Dry, Oerlikon Leybold, Germany). Thirty-eight repetitions were made for each condition. At day 3 post inoculation (DPI), eighteen cultures per conditions were stopped, with ten repetitions for fungal biomass quantification and eight repetitions for RNA-seq. At day 5, eight cultures per condition were stopped with four repetitions for fungal biomass quantification and four for RNA-seq. Non-inoculated media was also collected at days 3 and 5. Controls using non-supplemented control media and non-inoculated control media were included. It was verified that TickCore3 does not modify the pH values of the treated broths compared to those of the control.

#### c) Extraction and analysis of mycotoxins

The procedure was adapted from a previously published procedure (Montibus et al., 2021)<sup>12</sup>. Briefly, 4 mL sample of culture medium was extracted with 8 mL of ethyl acetate. A volume of 7 mL of the organic phase was evaporated to dryness at 45 °C under nitrogen flux. Dried samples were dissolved in 200 µL of methanol/water (1/1, v/v) and filtered through a 0.2 µm filter before analysis. TCTB were quantified by HPLC–DAD using an Agilent Technologies 1100 series liquid chromatograph equipped with an autosampler system, an Agilent photodiode array detector (DAD) and the ChemStation chromatography manager software (Agilent, France). Separation was achieved on a Kinetex XB-C18 100 Å column (4.6 × 150 mm, 2.6 µm) (Phenomenex, France) maintained at 45 °C. The mobile phase consisted of water (solvent A) and acetonitrile (solvent B). The flow was kept at 1 mL /min. The injection volume was set to 5 µL. TCTB were separated using a gradient elution as follows: 7–30% B in 6 min, 30–90% B in 2 min, 90% B for 2 min, 90–7% B for 1 min, 7% B for 6 min. The UV–Vis spectra were recorded from 190 to 400 nm and peak areas were measured at 230 nm. Quantification was performed by external calibration with standard solutions (Romer Labs, Austria). Toxin yields were expressed in µg/g of fungal dry biomass.

#### d) RNA extraction

Total RNA was extracted from 3 and 5-day-old flash-frozen mycelia of *F. graminearum* I349 cultivated in MS-glucose media supplemented or not with 50 µM of TC3. 5 mg of flash-frozen mycelium were grinded with 5 mm stainless steel balls (IKA™, Staufen, Germany) in 2 mL Eppendorf tubes in the presence of 0.7 mL TRIzol (Invitrogen™, USA) at 20Hz using a TissueLyser II (Qiagen, Venlo, The Netherlands) with 2x20 second cycle and 10s break to avoid

samples to heat. 140  $\mu$ L of chloroform were added to the homogenate and the mixture was incubated 3 min at room temperature. After 15 min centrifugation at 4°C and 12000 g, the supernatant ( $\approx$ 300 $\mu$ L) was recovered, 300  $\mu$ L ethanol 70% was added and the mixture was vortexed. After transfer on a RNeasy Mini column, the RNA was cleaned using the RNeasy Mini Kit (Qiagen, Venlo, The Netherlands) following the instructions of the manufacturer and including a DNase treatment with ezDNase™ (Invitrogen™, USA).

The absence of DNA contamination in the RNA extracts was investigated through DNA quantification by spectrophotometry (DeNovix, DeNovix Inc, Wilmington DE, USA) and quantitative PCR (qPCR) analyses targeting the *F. graminearum*  $\beta$ -*tub* gene (table 1) performed with a QuantStudio5™ (ThermoFisher Scientific, Vantaa, Finland) using 1  $\mu$ L of RNA extract mixed with 9  $\mu$ L of Power Track SYBR® Green Master Mix (Applied Biosystems, Vilnius, Lithuania). The primers final concentration in the reaction mix was 0.5  $\mu$ M. The PCR cycling conditions were set at 95 °C for 2 min, 40  $\times$  [95 °C for 3 s, 60 °C for 20 s]. The quality and quantification of the prepared RNA were evaluated using E-gel® EX 2% agarose (Invitrogen™, USA) and fluorescent quantification with Quantifluor® RNA System kit (Promega, USA) following the instructions of manufacturers.

#### e) Construction of CDNA library and sequencing

Reverse transcription was performed on 20ng/ $\mu$ L RNA samples with the NEBNext® Single Cell/Low Input RNA Library Prep Kit for Illumina® according to the manufacturer's instructions (New England Biolabs, USA). Fragmentation of cDNA and amplification were done using NEBNext® Ultra™ II FS DNA Library Prep Kit for Illumina and following the manufacturer's instructions (New England Biolabs, USA). The size of cDNA fragments was measured on a High Sensitivity D1000 ScreenTape® (Agilent Technologies, USA) with an Agilent 2200 TapeStation system (Agilent Technologies, USA). Libraries were prepared with Swift RNA Library Kit (Cambridge Bioscience) and samples were indexed with Swift Single Indexing Primers Set A (12-plex, 24 rxns) according to the manufacturer's instructions (Swift Biosciences Inc., Integrated DNA Technologies, Inc., USA). Libraries sequencing for RNA-sequencing as paired-end 100 base reads realized on Illumina HiSeq 4000 sequencer was commissioned by the GenomEast platform, a member of the 'France Genomique' consortium (ANR-10-INBS-0009).

#### f) Bioinformatics analysis

Sequencing results were analyzed with EdgeR (Robinson et al., 2010; McCarthy et al.; 2012)<sup>13,14</sup> mediated by the wrapper SARTools (Varet et al., 2016)<sup>15</sup> using the reference genome and annotation of *F. graminearum* PH-1 v5 (King et al., 2015)<sup>16</sup>. The transcripts from the online FungiDB database release 57 (April 21th, 2022) were used as references for transcript abundance quantification to compare the response of *F. graminearum* after 3 and 5 days of exposition to TC3. The p-value threshold was 0.05.

A hierarchical clustering using the Ward D2 method was performed to group genes with comparable expression variations. This clustering was realized on genes whose expression was significantly altered ( $p$ -value = 0.05) between all conditions. The optimal number of clusters for further analysis was determined using decision support methods (Silhouette, Bouldin, Calinski-Harabasz and Gap-statistic methods). These tools allowed us to determine that the optimal number of clusters was between 11 and 15. The silhouette and profile methods were used to represent the distribution and appearance of the different clusters helping us to choose 12 as the appropriate cluster number for analysis. K-means clustering was performed on the means of the biological replicates (data mean centered and reduced to unit variance, euclidean correlation distance, and average linkage).

Enrichment analysis of gene ontology (GO) terms related to biological process, cellular component and molecular function were realized on the online FungiDB database release 57 based on the *F. graminearum* PH-1 reference. GO terms were selected based on the  $p$ -value (inferior to 0,05). The fold – enrichment (FE) was obtained on FungiDB by dividing the percent of genes with the GO term in the results by the percent of genes with the same GO term in the background.

Volcano plots were obtained using DESeq2 software (Love et al., 2014)<sup>17</sup>. Venn diagrams were obtained using Venny 2.1 (Oliveros J.C., 2007-2015)<sup>18</sup>. Heatmaps were prepared on R using the package pheatmap (Kolde R., 2012)<sup>19</sup> with the normalized values of transcripts by centering and scaling on the average number of reads per gene using three biological replicates per condition.

#### g) Differential gene expression validation by RT-qPCR

RNA-Seq gene expression validation was achieved by qPCR. Primers (table 1) were designed with Primer3 using gene sequences of *F. graminearum* PH-1 reference strain from the FungiDB database targeting 100- to 200-bp fragments. Complementary DNA (cDNA) was synthesized from total RNA stored at  $-80^{\circ}\text{C}$  (remaining from samples shipped for sequencing) using the NEBNext® Single Cell/Low Input RNA Library Prep Kit for Illumina® according to the manufacturer's instructions (New England Biolabs, USA). The relative transcript abundance of the selected genes was assessed by QuantStudio™ 5 Real-Time PCR (Applied Biosystems™), using the PowerTrack™ SYBR Green Master Mix (Thermo Fisher) along with approximately 1 ng of cDNA template and 500 nM of each of the primers in a 10- $\mu\text{l}$  reaction volume. The following program was used for reverse transcription-qPCR:  $95^{\circ}\text{C}$  for 20 s followed by 40 cycles of 1 s at  $95^{\circ}\text{C}$  and 20 s at  $60^{\circ}\text{C}$ . Normalized relative expression values ( $\Delta\Delta\text{CT}$ ) of the selected candidates were calculated using the SATQPCR tool, with the three genes phosphoglycerate kinase,  $\beta$ -tubuline and citrate synthase designated as reference genes and the control samples at 3DPI chosen to rescale. Serial dilutions of cDNA samples were used to develop standard curves for primer sets to confirm their efficiency according to the Livak relative-gene expression quantification method.

Table 1. Primers used for the RNA-Seq validation using RT-qPCR.

Gene name	FungiDB ID	Forward primer sequence (5' to 3')	Reverse primer sequence (5' to 3')
ubiquitin	FGRAMPH1_01G10777	CGCTGCTGGCATTACTATCA	CCAGAATGGGAGGCAAAGTA
murein transglycosylase	FGRAMPH1_01G11857	TCCAAGACGGATTCCAAGAC	CTTGGCGGTAGAAGAAGCAC
S-formylglutathione hydrolase	FGRAMPH1_01G22905	AACCTCGAGAAGGCTGTCAA	CCTCGCCAAAGGTAGAGATG
phospho-2-dehydro-3-deoxyheptonate aldolase	FGRAMPH1_01G01229	ATCACAAGAACCAGCCCAAG	GATGGTGTCTCCAGCTAA
phosphoglycerate kinase	FGRAMPH1_01G14205	ACTCTTCATGGTCGGTGTC	TGTCGATGAGCTGGATCTTG
C-5 sterol desaturase	FGRAMPH1_01G06005	ACGGCGAGTATCTACCAAC	CAACGACCTTCGGACATTTT
NAD-specific glutamate dehydrogenase	FGRAMPH1_01G14529	TGGCTGCATTCTGTACAAGG	ATCTTGAGCTGCACCTGCTT
Enolase	FGRAMPH1_01G03321	GAGGCTCTCGAGCTCATCAC	TGGAGACGATGGGGTACTTC
trichodiene oxygenase	FGRAMPH1_01G13107	TCCCTTACCTGAACGGTGTC	CGGTGTGCATGAAATAGGTG
$\beta$ -tubuline	FGRAMPH1_01G26865	GGTAACCAAATCGGTGCTGCTTTC	GATTGACCGAAAACGAAG TTG
citrate synthase	FGRAMPH1_01G03497	AGTCGTTCCGCTATGATTC	CTCCAAGTTGCCTGACG
H3	FGRAMPH1_01G14931	AAGAAGCCTCACCGCTACAA	TCGAAGAGGGAGACGAGGTA

#### h) Statistical analyses applied to fungal biomass and biochemical data

Data for TCTB production and fungal growth were reported as mean values  $\pm$  standard deviations from four biological replications. Since the data were non-normally distributed (Shapiro–Wilk normality test), the Kruskal–Wallis one-way analysis was used, with mean comparisons performed using the Mann–Whitney U test. Statistical analysis was conducted with R and figures were produced using the package ggplot2. The statistical thresholds p-value = 0.05 was used throughout the study.

### III. Results

#### 1) Effect of TC3 on *F. graminearum* transcripts

As previously demonstrated (Leannec-Rialland et al., 2021), 50 $\mu$  M TC3 induced a significant reduction of both fungal growth and TCTB production (Fig. 1).

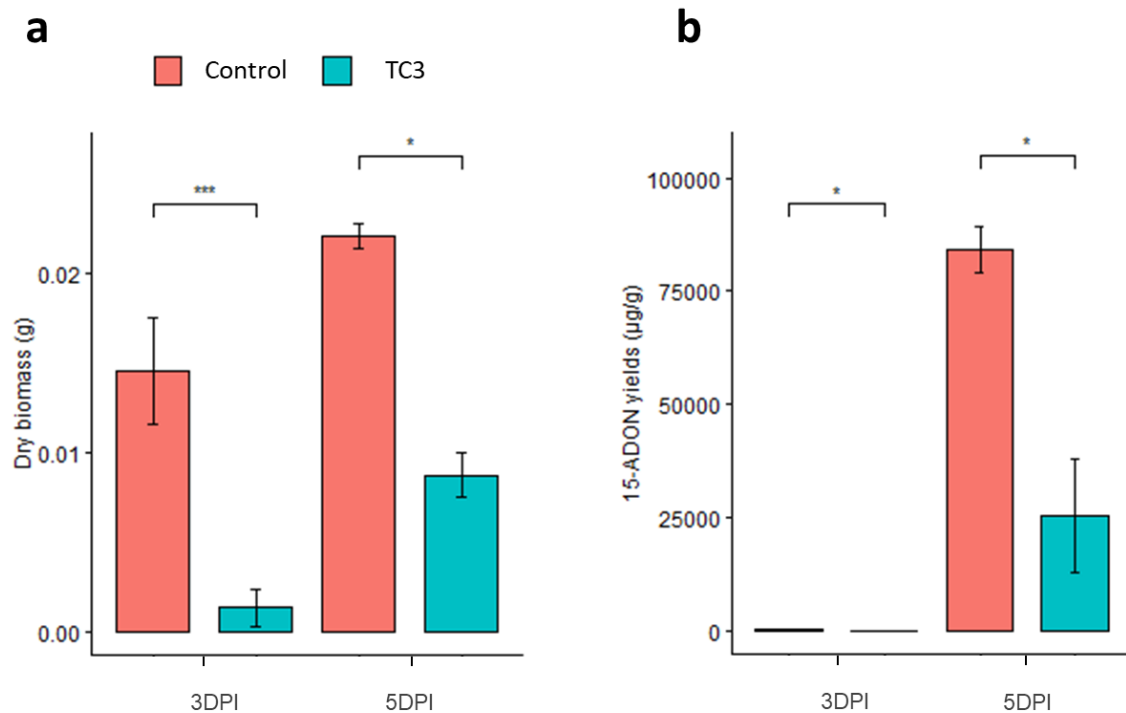


Figure 1. Phenotypic response of *F. graminearum* to TC3. Effect of TC3 at 50 µM on the fungal biomass weight of *F. graminearum* (a) and on the production of 15-ADON (b) in 3 and 5-day-old broths. Significant differences are labeled (\*p-value < 0.05, \*\*\*p-value < 0.005).

We observed an important number of differentially regulated transcripts in *F. graminearum* treated or not with TC3, at 3 DPI (Fig. 2a) and 5 DPI (Fig. 2b). Of the 14,145 transcripts, 6,667 transcripts were differentially regulated in *F. graminearum* treated with TC3, with 4,914 transcripts differentially regulated at 3DPI and 3703 transcripts at 5DPI. At 3 DPI, exposure to TC3 led to a decrease in the expression of 2502 genes and an increase of the expression of 2,422 genes. At 5 DPI, 1,873 genes were shown to be down-regulated and 1830 to be up-regulated. Notably, among the differentially regulated genes, 592 (Fig. 2c) and 707 (Fig. 2d) were found to be down-regulated and up-regulated, respectively, at both 3 and 5 DPI, suggesting the occurrence of common pathways of regulation at these two time points. On the total of transcripts differentially regulated, 1910 were down-regulated only at 3DPI while 1281 were down-regulated uniquely at 5DPI. Similarly, the expression of 1715 genes was increased only at 3DP and 1123 exclusively at 5DPI. This indicates a differential regulation induced by TC3 on *F. graminearum* gene expression over time.

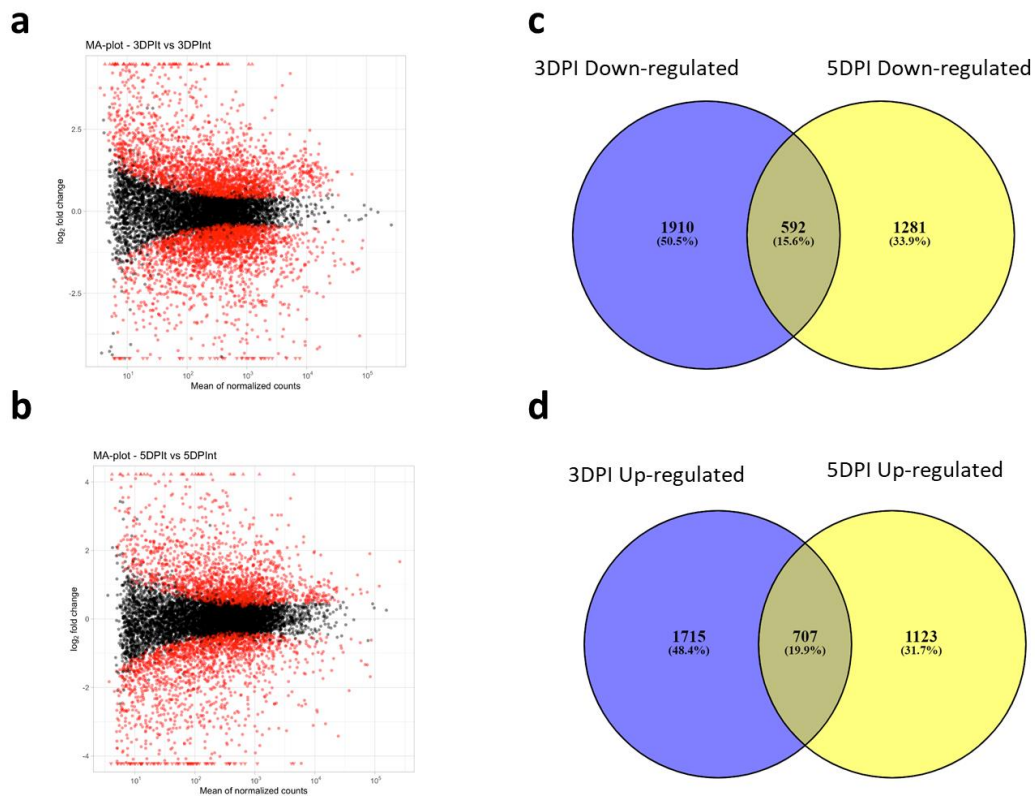


Figure 2. Differential regulation of transcripts of *F. graminearum* treated or not with TC3 at two developmental stages (3 and 5 DPI). Volcano plots of differential gene expression treated and non-treated with TC3 at 3DPI (2a) and at 5DPI (2b). Volcano plots were obtained using DESeq2 software. Venn diagrams representing the genes downregulated (2c) and upregulated in presence of TC3 at 3DPI and 5DPI (2d). Venn diagrams were obtained using Venny 2.1.

## 2) Results of enrichment analysis

In order to better characterized the different pathways affected by TC3 treatment, we performed an enrichment analysis of the gene ontology term (GO) by their annotation using the FungiDB database.

The genes with their expression downregulated at both times were enriched by 65 GO terms for molecular function (supplementary table 1), 10 GO terms for cellular components (supplementary table 2) and 114 GO terms for biological processes (supplementary table 3) (Fig. 3).

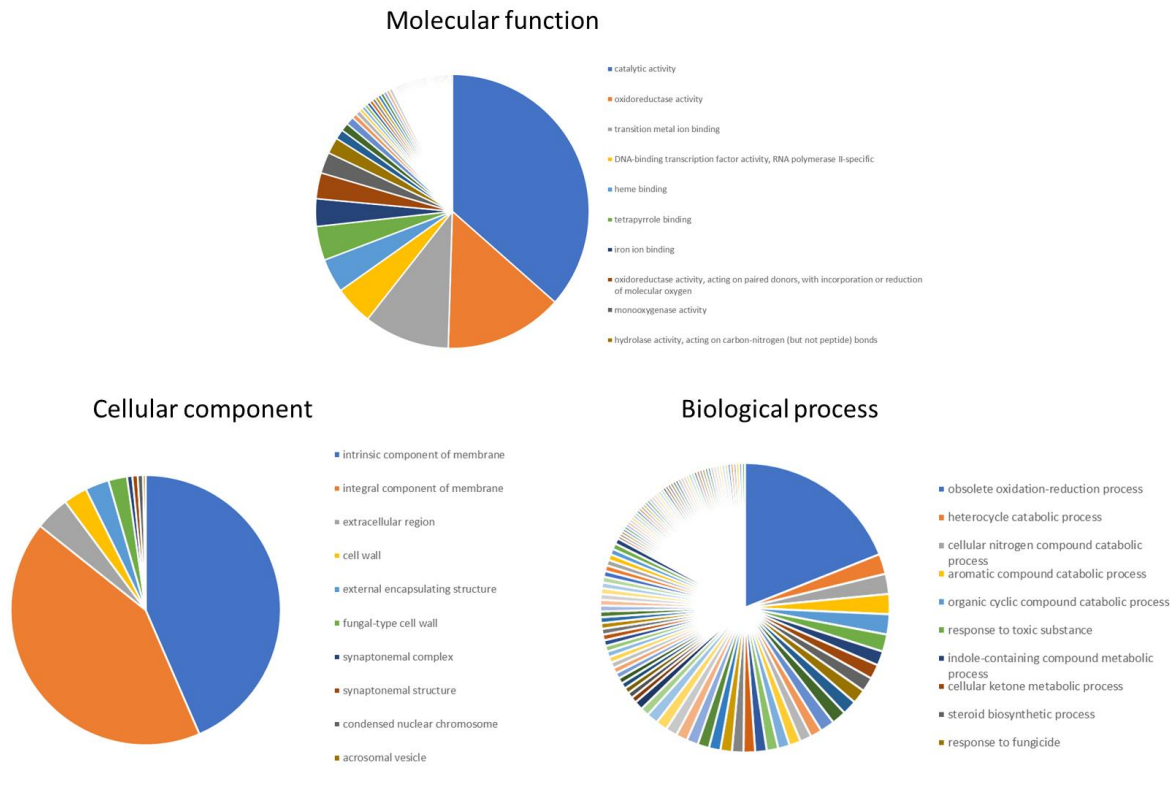


Figure 3. Enrichment analysis of the negatively regulated transcripts in presence of TC3 at both 3DPI and 5DPI in *F. graminearum*. Pie Chart of the GO terms obtained through an enrichment analysis on FungiDB for ontology to “Molecular function”, “Cellular component” and “Biological process” with a p-value inferior to 0.05. The size of each slice represents the number of genes enriched with the GO term. The genes enriched with multiple GO terms are represented for each term. Only the ten terms with the higher number of genes are represented in the legend. Additional terms with a lower number of genes are reported in supplementary tables 1-3.

The GO terms related to the molecular function enriched in the higher number of genes with downregulation in presence of TC3 include “catalytic activity”, “oxidoreductase activity”, “transition metal ion binding”, “DNA-binding transcription factor activity, RNA polymerase II-specific” and “heme binding” (Fig. 3 and supplementary table 1). The enrichment analysis focusing on the molecular function of transcripts that decreased at both 3 and 5 DPI allowed identifying oxidoreductase and hydrolase activities as significantly enriched with 1.56 and 2.34-fold increases, respectively. Indeed, among the 1048 genes annotated with “oxidoreductase activity” GO term on FungiDB, the expression of 73 (7%) genes were found downregulated in TC3-treated group. Similarly, the expression of 10 genes were downregulated among the 96 annotated for “hydrolase activity, acting on carbon-nitrogen (but not peptide) bonds” GO term.

The GO terms related to the cellular component enriched in the higher number of genes with downregulation in presence of TC3 include “intrinsic component of membrane”, “integral component of membrane”, “extracellular region”, “cell-wall” and “external encapsulating structure” (Fig. 3 and supplementary table 2). Notably, the cellular components of the enrichment analysis highlighted two major cellular targets, for which the expression of associated genes was repressed in presence of TC3. Firstly, a decrease in the expression of

genes related to synaptonemal complex (FE = 22.49), synaptonemal structure (FE = 14.99) and condensed nuclear chromosome (FE = 5.62) was observed. Secondly, the expression of various genes related to the fungal envelope (Fig. 3) were shown to be negatively affected by TC3. Indeed, the expression of a high number of genes associated with the plasmic membrane was decreased in the presence of TC3; 137 within the 2665 total genes annotated with the GO term “intrinsic component of membrane” (FE = 1.16) and 133 among the 2644 genes with the GO term “integral component of membrane” (FE = 1.13) were pointed out by the analysis. Besides, our data indicated that the TC3 treatment negatively impacted the expression of genes related to the fungal cell wall: 7 of the 57 genes annotated with the GO term “fungal-type cell wall” (FE = 2.76), 9 of the 99 genes annotated with the GO term “cell wall” (FE = 2.04) and 9 of the 103 genes for GO term “external encapsulating structure” (FE = 1.97) were affected by TC3. Furthermore, the GO term “extracellular region” (FE = 1.66) was shown to emerge from the analysis with 13 genes annotated and 9 of them in common with the genes annotated to the cell wall. Lastly, four genes related to ergosterol had their expression downregulated when *F. graminearum* was treated with TC3.

The GO terms related to the biological process enriched in the higher number of genes with downregulation in presence of TC3 include “obsolete oxidation-reduction process”, “heterocycle catabolic process”, “cellular nitrogen compound catabolic process”, “aromatic compound catabolic process” and “organic cyclic compound catabolic process” (Fig. 3 and supplementary table 3). The set of genes related to “response to toxic substance” with a downregulated expression (FE = 3.00) comprised 6 genes of the 45 annotated. A decreased expression of genes related to the response to toxic substances could enhance the fungal cell susceptibility to the toxic peptide TC3. An important number of GO terms related to “tryptophan catabolic process to kynurenine” (FE = 8.18), “DNA catabolic process” (FE = 22.49), “amine metabolic process” (FE = 3.21) and “triterpenoid biosynthetic process” (FE = 22.49) have also been highlighted. These results indicate that TC3 could be responsible for a decreased catabolism of cyclic and aromatic compounds. It is important to recall that tryptophan is a pivotal metabolite for living organism: its catabolism is critical for maintaining the metabolism of organic cyclic compounds, such as the nitrogenous base purine component of DNA, or steroids such as triterpenoids. Thus, a decreased tryptophan catabolism is likely to indirectly impact processes related to DNA repair and secondary metabolites production. In the presence of TC3, expression of genes related to the “regulation of protein secretion” was shown to be affected (FE = 22.49). Finally, the TC3 treatment led to the decrease of transcripts of 4 genes from the 12 annotated with “carbohydrate derivative transport” GO term (FE = 7.5). These genes are related to the transmembrane transport of carbohydrates such as the N-acetylglucosamine which is important for the polymerization of peptidoglycans in the cell wall of numerous species. Those results are consistent with the “fungal-type cell wall” discussed above.

The genes with their expression up-regulated at both times were enriched by 93 GO terms for molecular function (supplementary table 4), 28 GO terms for cellular components

(supplementary table 5) and 277 GO terms for biological processes (supplementary table 6) (Fig. 4).

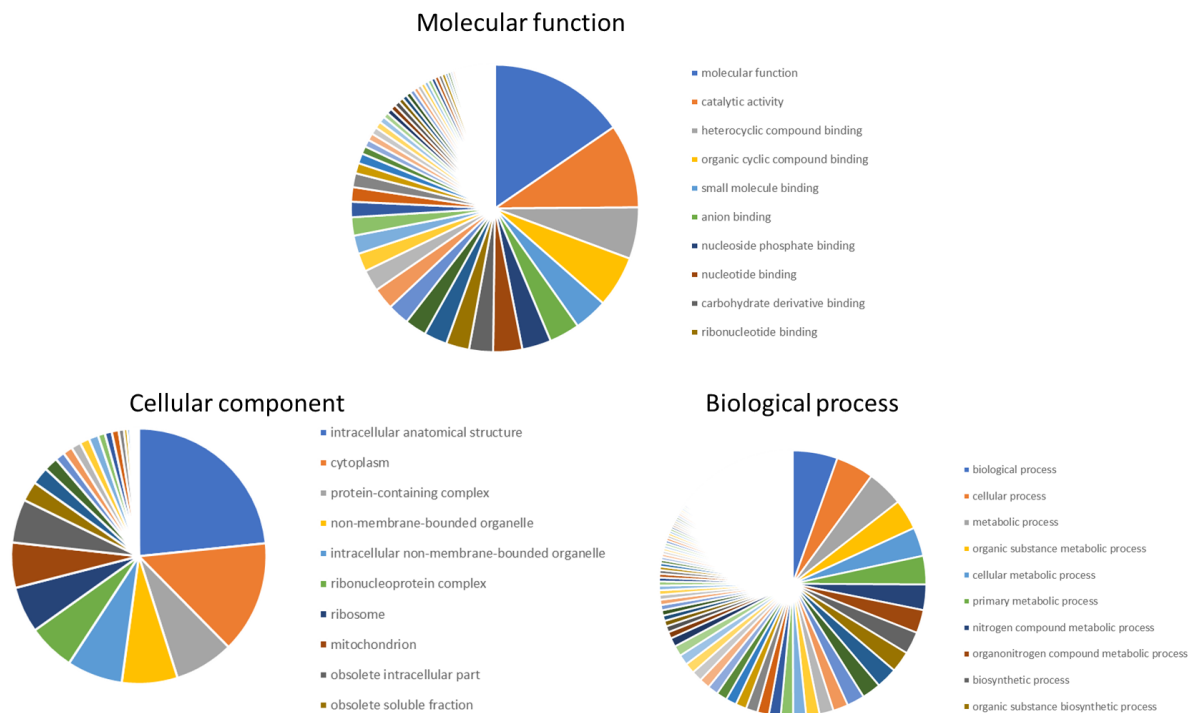


Figure 4. Enrichment analysis of the positively regulated transcripts in presence of TC3 at both 3DPI and 5DPI in *F. graminearum*. Pie Chart of the GO terms obtained through an enrichment analysis on FungiDB for ontology to “Molecular function”, “Cellular component” and “Biological process” with a *p*-value inferior to 0.05. The size of each slice represents the number of genes enriched with the GO term. The genes enriched with multiple GO terms are represented for each term. Only the ten terms with the higher number of genes are represented in the legend. Additional terms with a lower number of genes are reported in supplementary tables 4-6.

Concerning the expression of genes positively regulated by TC3, the GO terms related to the molecular function enriched in the higher number of genes with downregulation in presence of TC3 include “molecular function”, “catalytic activity”, “heterocyclic compound binding”, “organic cyclic compound binding” and “small molecule binding” (Fig. 4 and supplementary table 4). The enrichment analysis permitted to highlight the effect of TC3 on the expression of genes related to “structural constituent of ribosome” (FE = 5.66), “structural molecule activity” (FE = 4.23), “translation factor activity, RNA binding” (FE = 5.92), “RNA binding” (FE = 2.62) and “rRNA binding” (FE = 4.44), as well as “ligase activity” (FE = 3.3), “GTPase activity” (FE = 1.92) and “lyase activity” (FE = 2.57) (supplementary table 4). Most of these terms are related to the translation activity within the cell.

The GO terms related to the cellular component enriched in the higher number of genes with downregulation in presence of TC3 include “intracellular anatomical structure”, “cytoplasm”, “protein-containing complex”, “non-membrane-bounded organelle” and “intracellular non-membrane-bounded organelle” (Fig. 4 and supplementary table 5). The enrichment analysis

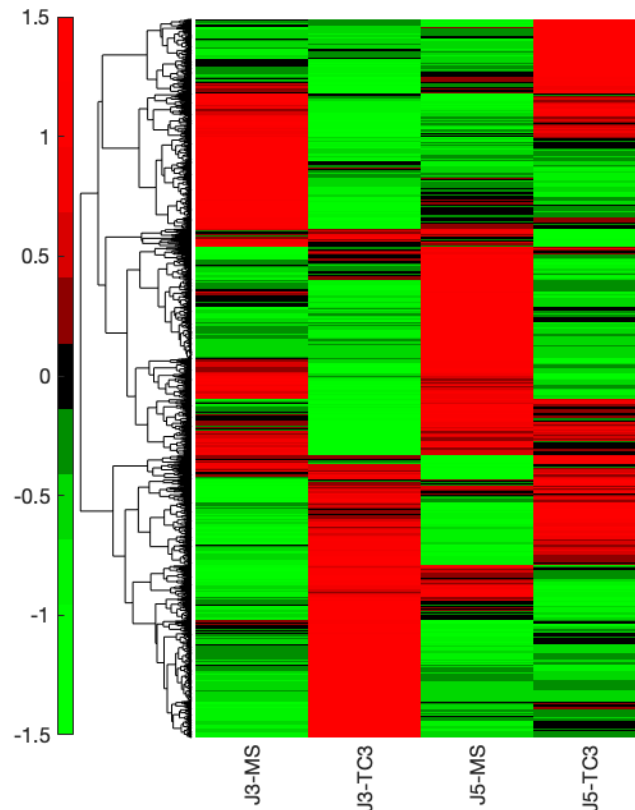
highlighted the “ribosome” as one of the central cellular components positively impacted. Indeed, 53 transcripts on the 151 annotated with the GO term “ribosome” (35%) were modulated by TC3. Among them, 47 are related to translation and peptide biosynthetic process. The “cytoplasm” and the “mitochondrion” GO terms were also well represented with respective fold-enrichment of 1.34 and 1.46. The “mitochondrion” genes identified are mostly related to the cellular amino acid metabolic process and the generation of precursor metabolites and energy.

The GO terms related to the biological process enriched in the higher number of genes with downregulation in presence of TC3 include “biological process”, “cellular process”, “metabolic process”, “organic substance metabolic process” and “cellular metabolic process” (Fig. 4 and supplementary table 6). The previous indications on a TC3 effect towards the mitochondrion were confirmed by the enrichment analysis towards biological process that has revealed that the GO terms related to “cellular amino acid metabolic process” (FE = 4.72), “cytoplasmic translation” (FE = 11.4) and “tRNA metabolic process” (FE = 3.42) were the main biological processes affected by the TC3 treatment. Besides, an enrichment of the GO term “ribosome biogenesis” (FE = 2.15) was observed, supporting the TC3-induced modulation of the translation activity within the fungal cell. Lastly, the “generation of precursor metabolites and energy” GO term was highlighted (FE = 3.42) with 20 on the 91 annotated genes which expression was enhanced by the TC3 treatment.

When comparing the genes with an expression that was differentially regulated according to the incubation time (3 and 5 DPI) the enrichment analysis demonstrated similar results at early and late stage for gene up-regulation. However, 348 transcripts were up-regulated at 3DPI and down-regulated at 5DPI. Similarly, there were 707 transcripts down-regulated at 3DPI which were up-regulated at 5DPI (data not shown). The occurrence of a different effect of TC3 according to the duration of the exposure was supported by the distribution of gene ontology (GO) terms associated with transcripts upregulated and down regulated at the 3DPI and 5DPI stages. For example, 95 (39%) and 122 (50%) transcripts with GO terms related to “cellular amino acid metabolic process” were up-regulated at 3DPI and 5DPI, respectively. A further analysis focusing on the top 50 differentially expressed genes from each timepoint (3DPI and 5DPI) was implemented (supplementary table 7). Among these genes, 6 were positively affected for their expression at both 3 and 5 DPI while none of the genes with a decreased expression at 3DPI was down regulated at 5 DPI and *vice-versa*. These findings that underscored substantial changes in the type of transcripts being up- and down-regulated between the two incubation times, demonstrate that the TC3 effect on *F. graminearum* transcriptome is dependent on the fungal developmental stage. Besides, the higher number of genes differentially expressed at 3 DPI compared to 5 DPI suggests that the perturbations induced by TC3 are more severe in the early stages of fungal development.

### 3) Clustering analysis

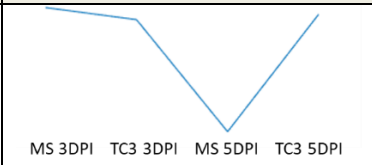
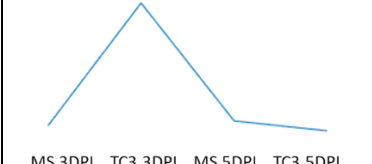
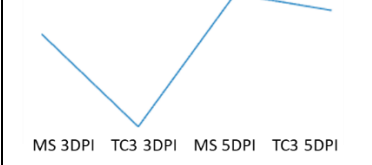
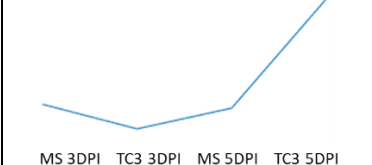
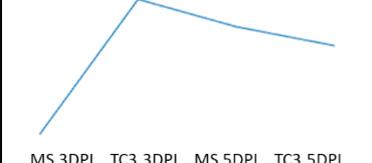
To deepen our analysis, a number of gene groups (clusters) characterized by a same pattern of expression modulation in the presence or absence of TC3 at different stages of development was defined. A hierarchical clustering using the Ward D2 method was performed to group genes with comparable expression variations (Fig. 5).

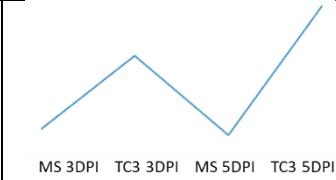
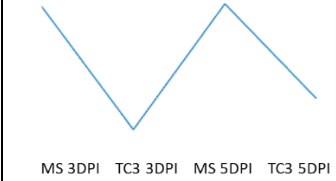
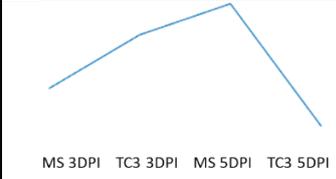


*Figure 5. Heatmap reporting the comparative expression profile of all the differentially regulated genes with or without TC3 at 3 DPI and 5 DPI. This heatmap shows the normalized values by centering and scaling by gene the average number of reads on three biological replicates per condition. In green are represented the slightly or non-expressed genes and in red the strongly expressed genes.*

This clustering was realized on genes whose expression was significantly altered (p-value 0.05) between all conditions. A k-means clustering with K=12 was realized in accordance with decision support methods. Study of the expression of the genes in the 12 different clusters has allowed providing additional support to the results issued from the enrichment analysis discussed above (Table 2).

Table 2. Clusters of genes differentially expressed with their centroid expression profile and the Gene Ontology terms associated. MS: control medium, TC3: TC3 treatment.

Cluster	Number of genes	K-means centroid profiles	GO terms related to biological process (genes in the cluster/ genes in the background with this term)	GO terms related to molecular function (genes in the cluster/ genes in the background with this term)	GO terms related to cellular component (genes in the cluster/ genes in the background with this term)
Cluster 1	227		GO:0042254: ribosome biogenesis (24/130) GO:0006399: tRNA metabolic process (10/109) GO:0006520: cellular amino acid metabolic process (15/244)	GO:0003723: RNA binding (21/309) GO:0016874: ligase activity (11/160)	GO:0005730: nucleolus (22/100) GO:0005739: mitochondrion (27/552) GO:0005622: intracellular anatomical structure (88/2998) GO:0043226: organelle (80/2708)
Cluster 2	526		GO:0016192: vesicle-mediated transport (28/153) GO:0006325: chromatin organization (14/58) GO:0006486: protein glycosylation (11/59) GO:0036211: protein modification process (35/391) GO:0006260: DNA replication (11/68) GO:0006281: DNA repair (16/130) GO:0006886: intracellular protein transport (14/106)	GO:0008092: cytoskeletal protein binding (12/72)	GO:0043226: organelle (183/2708) GO:0005622: intracellular anatomical structure (195/2998) GO:0032991: protein-containing complex (72/814) GO:0005783: endoplasmic reticulum (29/208) GO:0005794: Golgi apparatus (20/119) GO:0031410: cytoplasmic vesicle (20/145) GO:0005737: cytoplasm (103/1492) GO:0005634: nucleus (94/1410) GO:0005575: cellular component (301/5611)
Cluster 3	927		GO:0006355: regulation of transcription, DNA-templated (70/582) GO:0006914: autophagy (10/32) GO:0055085: transmembrane transport (76/703)	GO:0003700: DNA-binding transcription factor activity (61/445) GO:0016491: oxidoreductase activity (112/1048) GO:0022857: transmembrane transporter activity (78/717) GO:0043167: ion binding (203/2365)	
Cluster 4	1013		GO:0042254: ribosome biogenesis (22/130) GO:0055086: nucleobase-containing small molecule metabolic process (24/189)	GO:0003735: structural constituent of ribosome (66/129) GO:0005198: structural molecule activity (68/180) GO:0003723: RNA binding (47/309) GO:0019843: rRNA binding (6/14)	GO:0005840: ribosome (73/151) GO:0032991: protein-containing complex (109/814) GO:0005829: cytosol (17/49) GO:0005739: mitochondrion (71/552)
Cluster 5	422		GO:0006629: lipid metabolic process (23/302)		
Cluster 6	562		GO:0006790: sulfur compound metabolic process (13/98) GO:0006091: generation of precursor metabolites and energy (12/91) GO:0005975: carbohydrate metabolic process (29/348)	GO:0016491: oxidoreductase activity (77/1048)	
Cluster 7	322		GO:0036211: protein modification process (23/391) GO:0008150: biological process (154/5316) GO:0023052: signaling (13/189) GO:0048856: anatomical structure development (11/153) GO:0016192: vesicle-mediated transport (13/224)	GO:0043167: ion binding (83/2365) GO:0016301: kinase activity (15/254)	

<b>Cluster 8</b>	486		GO:0006520: cellular amino acid metabolic process (62/244) GO:0006091: generation of precursor metabolites and energy (15/91) GO:0006399: tRNA metabolic process (16/109)	GO:0016874: ligase activity (25/160) GO:0016829: lyase activity (25/212) GO:0043167: ion binding (134/2365)	
<b>Cluster 9</b>	446				
<b>Cluster 10</b>	336		GO:0006914: autophagy (5/32)		
<b>Cluster 11</b>	609		GO:0002181: cytoplasmic translation (11/15) GO:0055086: nucleobase-containing small molecule metabolic process (27/189) GO:0065003: protein-containing complex assembly (19/115) GO:0006520: cellular amino acid metabolic process (27/244) GO:0006091: generation of precursor metabolites and energy (14/91) GO:0008150: biological process (320/5316)	GO:0008135: translation factor activity, RNA binding (26/63) GO:0003723: RNA binding (45/309) GO:0003735: structural constituent of ribosome (23/129) GO:0005198: structural molecule activity (24/180)	GO:0005840: ribosome (27/151) GO:0005737: cytoplasm (114/1492) GO:0005739: mitochondrion (48/552)
<b>Cluster 12</b>	791		GO:0006281: DNA repair (37/130) GO:0006260: DNA replication (24/68) GO:0016071: mRNA metabolic process (27/133) GO:0140014: mitotic nuclear division (9/21) GO:0006325: chromatin organization (15/58) GO:0007059: chromosome segregation (14/53) GO:0000278: mitotic cell cycle (16/70) GO:0006310: DNA recombination (9/35) GO:0006486: protein glycosylation (12/59)	GO:0003677: DNA binding (65/517) GO:0016779: nucleotidyltransferase activity (16/81) GO:0004386: helicase activity (16/90) GO:0140657: ATP-dependent activity (30/232)	GO:0043226: organelle (313/2708) GO:0005622: intracellular anatomical structure (33/2998) GO:0005634: nucleus (187/1410) GO:0032991: protein-containing complex (128/814) GO:0005694: chromosome (50/170) GO:0005654: nucleoplasm (22/72) GO:0005794: Golgi apparatus (27/119) GO:0005575: cellular component (456/5611) GO:0005783: endoplasmic reticulum (35/208) GO:0000228: nuclear chromosome (13/45) GO:0005737: cytoplasm (11/40) GO:0005635: nuclear envelope (11/40)

### 3.1 The peptide TickCore3 negatively impacts the expression of genes related to *F. graminearum* DNA at an early stage.

Gene ontology analysis of genes gathered in cluster 2 and 12 has allowed to corroborate the strong repression of the expression of genes related to DNA replication (FE = 3.35 and respectively 4.95), DNA repair (FE = 2.55 and 3.99 respectively) and chromatin organization (FE = 5.01 and 3.63 respectively) at 3DPI (Fig. 8). Furthermore, the GO terms “mitotic nuclear division” (FE = 3.21), “chromosome segregation” (FE = 3.71), “mitotic cell cycle” (FE = 3.21) and “DNA recombination” (FE = 3.61) were shown to be enriched in cluster 12. These data support the potential strong activity of TC3 towards the nucleus and DNA at an early stage.

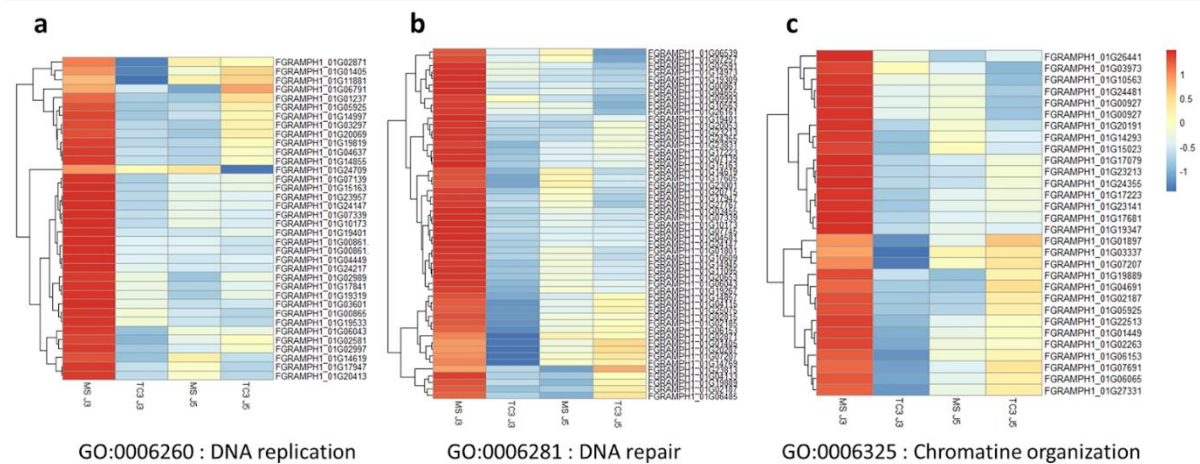


Figure 6. Differential expression of genes related to the GO terms “DNA replication” (a), “DNA repair” (b) and “Chromatine organization” (c) in the clusters 2 and 12. These heatmaps show the normalized values by centering and scaling the average number of reads per gene on three biological replicates per condition. In blue are represented the slightly or non-expressed genes and in red the strongly expressed genes.

### 3.2 TC3 negatively impacts the *F. graminearum* biosynthetic process by interfering with its DNA-templated transcription.

Gene ontology analysis of genes gathered in cluster 3 (gene expression slightly downregulated at 3DPI and strongly at 5DPI) has led to evidence terms related to DNA-templated” (FE = 1.69) and “DNA-binding transcription factor activity” (FE = 1.93). In cluster 12 (genes strongly repressed at 3DPI and slightly at 5DPI), the term “mRNA metabolic process” was shown to be enriched. These results support a downregulation exerted by TC3 on the transcription process at the two stages of *F. graminearum* development.

### 3.3 The peptide TC3 impacts the *F. graminearum* membrane organization and the intracellular vesicle mediated transport.

The GO terms “intracellular protein transport” (FE = 2.74) and “vesicle-mediated transport” (FE = 3.8) were emerged from cluster 2 analysis (cluster 2 is composed of genes with expression strongly down-regulated at 3DPI and up-regulated at 5DPI). The term “vesicle-mediated transport” (FE = 2.95) was also found associated with cluster 7 (genes with a higher expression at 3DPI in presence of TC3 than in the control). The term “lipid metabolic process” (FE = 2.08) was pointed out by the GO analysis of cluster 5, that contains genes with an expression strongly down-regulated at 3 DPI and slightly down-regulated at 5 DPI. Despite a non-significant adjusted p-value according to Bonferroni, the terms “lysosome organization” (2 genes on 5 annotated and FE = 10.91), “membrane organization” (5 genes on 44 annotated and FE = 3.1) and “cell wall organization or biogenesis” (7genes on 87 annotated and FE = 2.19) were emerged from the analysis of the cluster 5 with a p-value according to Fisher below 0.05. The differential expression of genes related to intrinsic component of membrane, fungal-type

cell wall and ergosterol biosynthetic process are represented in Figure 7. Altogether, the previous data support the perturbations induced by TC3 to the fungal membrane.

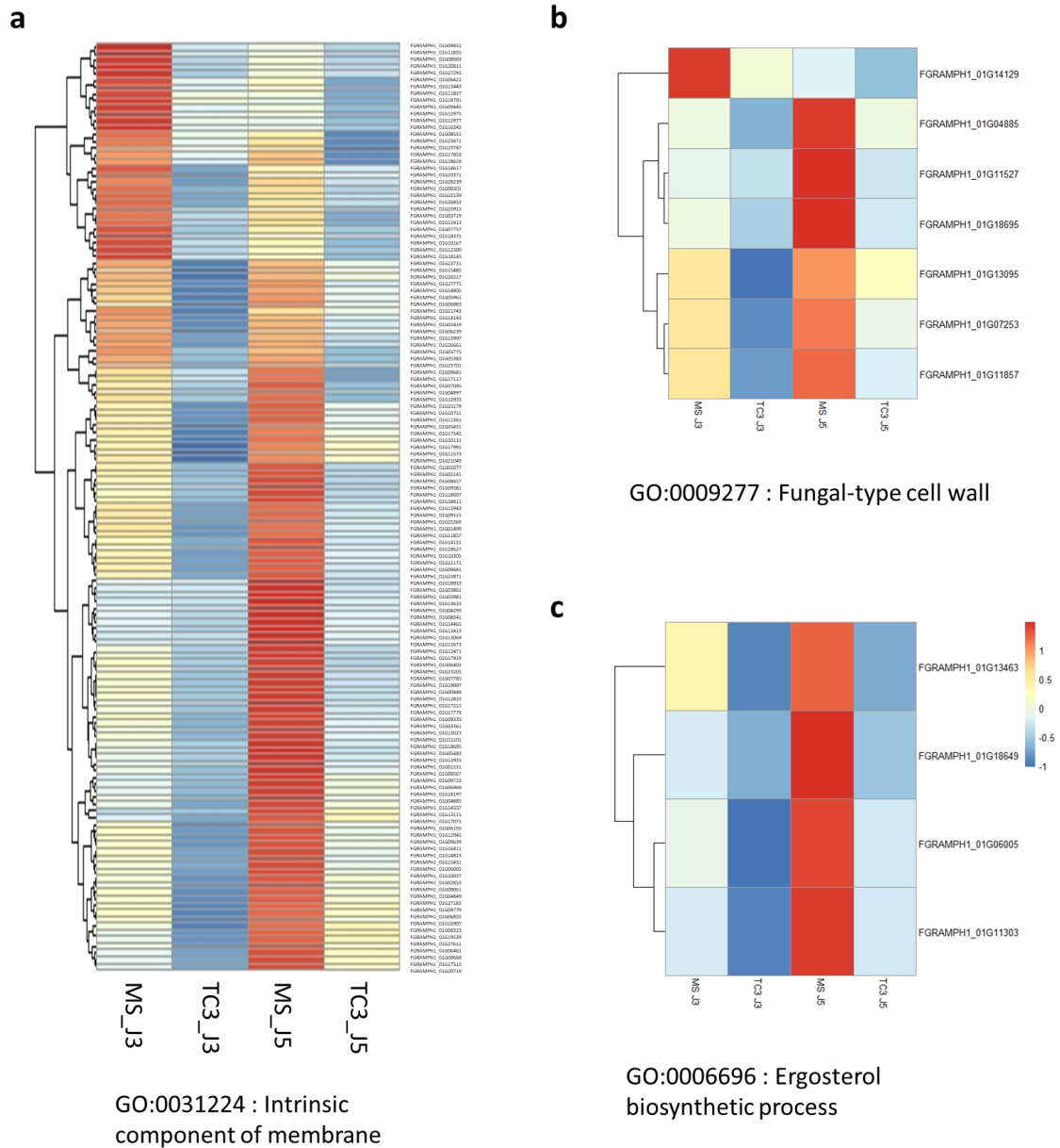


Figure 7. Differential expression of genes related to Intrinsic component of membrane, Fungal-type cell wall and Ergosterol biosynthetic process. Heatmap representing the differential expression of genes related to the GO terms “Intrinsic component of membrane” (a), “Fungal-type cell wall” (b) and “Ergosterol biosynthetic process” (c) downregulated in presence of TC3.

### 3.4 TC3 induces a down-regulation of genes related to autophagy at 5 DPI in *F. graminearum*.

This hypothesis was consolidated by the GO analysis of clusters 3 and 10, which contain genes strongly downregulated at 5 DPI. The GO term autophagy appears in both clusters

(respectively FE = 4.39 and FE = 6.42). These results suggest the potential occurrence of a decrease in lipid biosynthesis induced by TC3 and therefore a failure in vesicles and lysosomes.

### 3.5 TC3 increases the expression of genes related to the ribosome biogenesis, the translation and the generation of precursor metabolites and energy.

Genes grouped in both the cluster 8 and 11 show an upregulation of their expression induced by TC3 at 3 and 5 DPI, but with a higher amplitude at 3DPI compared to 5DPI. The analysis of these two clusters has indicated shared related GO terms such as “cellular amino acid metabolic process” (FE = 5.99 and 2.04 respectively), “generation of precursor metabolites and energy” (FE = 3.89 and respectively 2.84). The term “tRNA metabolic process” (FE = 3.46) was evidenced in cluster 8 while the terms “cytoplasmic translation” (FE = 13.54), “nucleobase-containing small molecule metabolic process” (FE = 2.64), “protein-containing complex assembly” (3.05), “structural constituent of ribosome” (3.29) and “translation factor activity, RNA binding” (7.62) were underscored in cluster 11. In clusters 1 and 6 (gathering genes with a high expression in presence of TC3 at 5 DPI), the terms “ribosome biogenesis” (FE = 8.5), “tRNA metabolic process” (FE = 4.23) and “cellular amino acid metabolic process” (FE = 2.83) for cluster 1, and the terms “sulfur compound metabolic process” (FE = 2.97), “generation of precursor metabolites and energy” (FE = 2.95) and “carbohydrate metabolic process” (FE = 1.87) for cluster 6 were represented in the enrichment analysis. Furthermore, the GO terms “ribosome biogenesis” (FE = 2.21) and “nucleobase-containing small molecule metabolic process” (FE = 1.66) have been identified when analyzing the cluster 4 (genes with a higher level of transcripts in presence of TC3 compared to the control). Emergence of the previous GO terms strongly argues in favor of an impact of TC3 on the ribosome biogenesis, the translation and the generation of precursor metabolites and energy.

#### 4) Genes related to the production of mycotoxins.

In a last part of this RNA-seq analysis, a targeted approach focusing on genes and pathways of interest related to the TCTB production has been implemented. Genes involved in TCTB and other secondary metabolite biosynthetic pathways, genes involved in stress response - the link between stress response and TCTB yield is widely documented (Pons et al., 2015)<sup>20</sup> - and genes involved in some primary metabolism pathways that have been previously reported as intimately linked to TCTB production (Atanasova-Penichon et al., 2018)<sup>21</sup> were followed.

67 predicted secondary metabolism gene clusters (C01 to C67) in *F. graminearum* genome have been identified by Sieber et al. (2014)<sup>22</sup>. RNA-Seq expression data of *F. graminearum* treated or not with TC3 showed that several of these gene clusters were affected in their expression by the peptide. When first looking at the expression of *tri* genes that are responsible for the trichothecene biosynthesis (C23), data reported on Figure 8 clearly indicate a downregulation of the expression of all *tri* genes (with the exception of *tri7A*) induced by TC3 at 3DPI. Those results are consistent with the significant decrease of 15-ADON

yield observed in TC3-treated media (Fig. 1). Furthermore, when scrutinizing the list of genes which were the most affected in their expression at 3 DPI, the genes *Tri3*, *Tri5*, *Tri9*, *Tri4* and *Tri1* were among the 50 genes characterized by a strong expression divergence between culture conditions (supplementary Table 7). As mentioned above, the expression of genes related to triterpenoid and sterol metabolic processes has also been shown as reduced. We can therefore hypothesize that the decrease in TCTB production can also be partly due to lower amounts of farnesyl pyrophosphate (FPP), which is the precursor of the trichothecene biosynthetic pathway. Among the other downregulated clusters in presence of TC3, we can mention the cluster C42 responsible for Fusarin C production, the cluster C2 associated with the gramilin metabolite, the cluster C64 containing genes coding for NRPS5 and NRPS9, the cluster C47 involved in fusaristatin A yield and cluster C11 related to the fusarubin. In contrast, the expression of genes included in several biosynthetic clusters was shown to be increased in presence of TC3. This was the case of genes of cluster C33 (ferricrocin) at both 3 and 5 DPI, of cluster C28 (carotenoids) and cluster C49 (butanolide) at 5DPI. Concerning genes of the cluster C15, related to zearalenone, another mycotoxin of concern produced by *F. graminearum*, no transcripts were found.

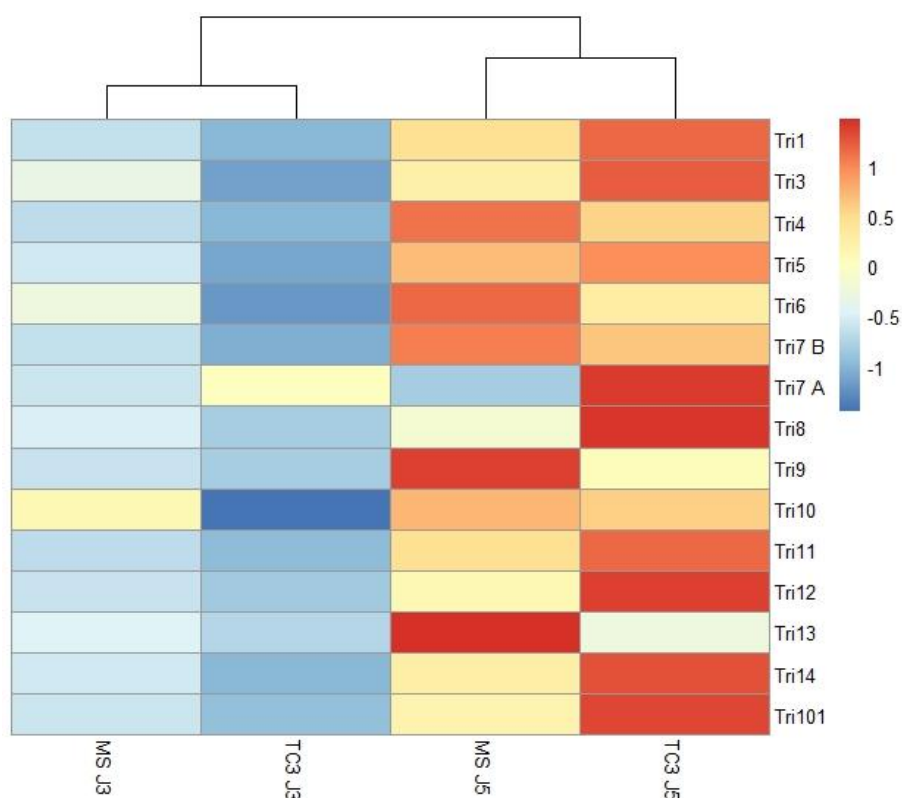


Figure 8. Differential expression of tri genes in *F. graminearum* treated or not with TC3 at two developmental stages.

Several genes involved in *F. graminearum* stress response were shown to be affected in their expression when *F. graminearum* was exposed to TC3. Thus, the expression of the gene

*FgFUM1* coding for the fumarate hydratase, which is associated with the response to water stress, stress temperature and starvation in *F. graminearum* was slightly enhanced by TC3. The transcripts of the gene *FgYCF1*, coding for an ABC transporter related to metal toxicity alleviation by sequestration of metal-glutathione conjugates to vacuoles and the gene coding for the heat shock protein Ssb1 were more importantly expressed in presence of TC3 at both stages. At 3DPI, an important increase in the expression of the pH-response transcription factor *FgPAC*, a key actor of pH homeostasis was also evidenced. Lastly, when focusing on some primary metabolism pathways, multiple genes involved in the tricarboxylic acid cycle (TCA), glycolysis and trehalose were shown to be affected in their expression by the TC3 treatment (Fig. 9). While the expression of most of the genes involved in TCA cycle (Fig. 9c) at 3 and 5 DPI, in glycolysis (Fig. 9b) and trehalose metabolism (Fig. 9d) at 5 DPI was increased in presence of TC3, genes related to the gamma-aminobutyric acid (GABA) shunt were downregulated at 3 and 5 DPI (Fig. 9a).

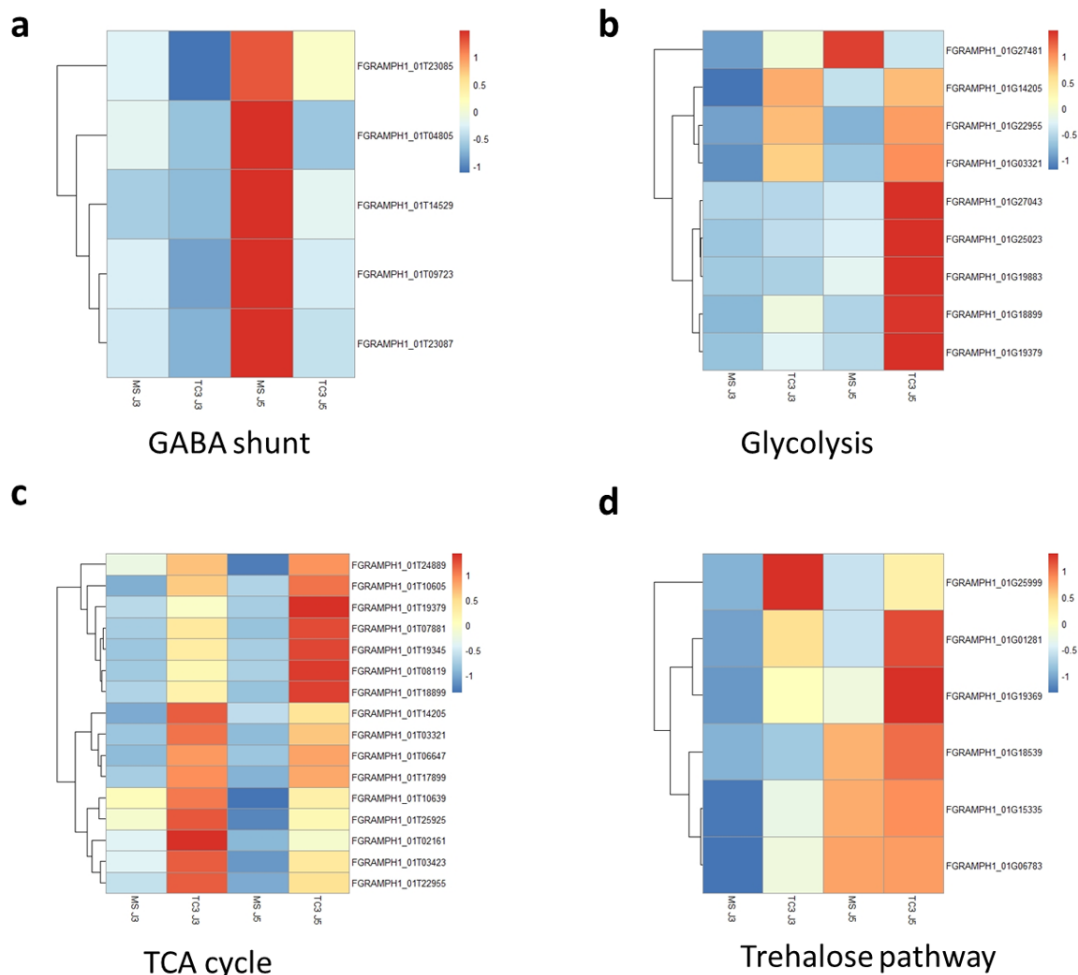


Figure 9. Differential expression of genes related to the primary metabolism. Heatmap of genes differentially expressed related to the GABA shunt (a), glycolysis (b), TCA cycle (c) and trehalose metabolism (d).

## 5) RNA-seq validation by RT-qPCR

To confirm the veracity of the RNA-Seq expression data, quantitative PCR (qPCR) primers were designed against candidate *F. graminearum* transcripts whose expression was either not affected, up-regulated or downregulated for one or both exposition times (Fig. 10). With the exception of H3, whose transcript have shown different profiles between qPCR and RNA-Seq analysis, data from targeted qPCR experiments (Fig. 10a) corroborated the RNA-Seq expression profiles (Fig. 10b). Therefore, the RNA-Seq analysis results were deemed sufficiently reliable to represent the biological events occurring when *F. graminearum* was exposed or not to the antifungal peptide TC3.

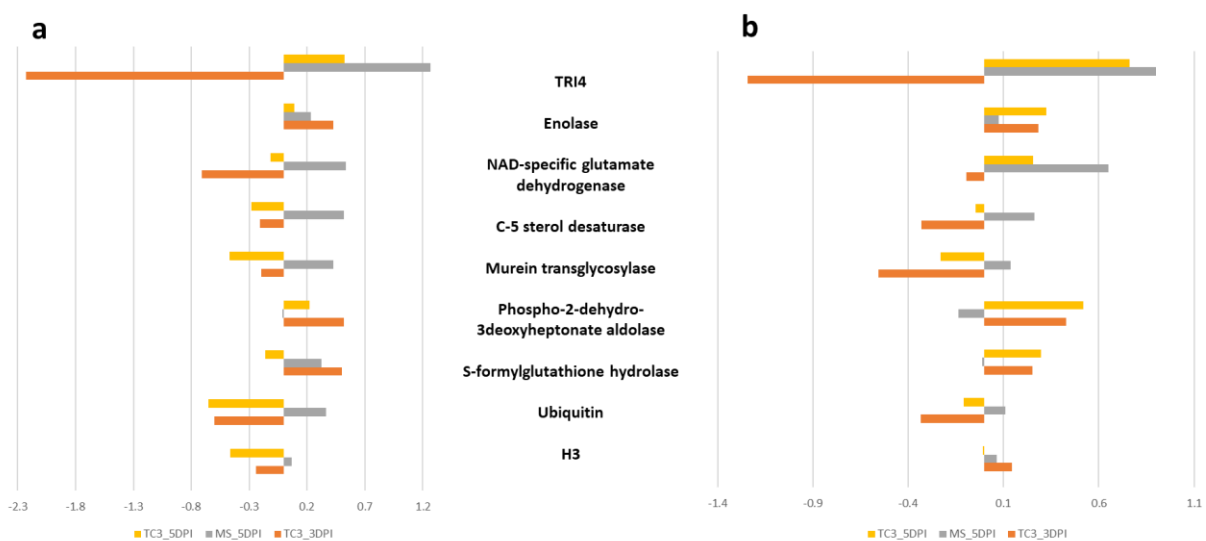


Figure 10. Validation of RNA-Seq results by quantitative PCR (qPCR). Results arising from a set of selected unaffected, upregulated, and downregulated transcripts at 3DPI and 5DPI in RT-qPCR (a) and RNA-Seq (b). The relative expression values of genes from RT-qPCR are represented as Log10 of normalized values obtained with SATQPCR tool using the reference genes and the control samples at 3DPI chosen to rescale. The relative expression values of genes from RNA-Seq are represented as Log10 values obtained with EdgeR using the control samples at 3DPI for normalization.

## IV. Discussion

In a previous study (Leannec-Rialland et al., 2021)<sup>7</sup>, the  $\gamma$ -core TickCore3 (TC3) was demonstrated to significantly reduce the fungal growth and mycotoxin yield by *F. graminearum* CBS185.32 strain/INRAE 349 in 10-day-old broths. These first data have evidenced the promising potential of TC3 to be part of an environment-friendly strategy to control the FHB fungal disease and the contamination of cereals with the DON mycotoxin. In the present study, the TC3 bioactivity was confirmed for earlier stages of fungal development: antifungal and anti-mycotoxin efficacies were demonstrated for 3 and 5-day old broths. Besides and more importantly, first evidences on the molecular and cellular disturbances induced by TC3 exposure were provided by comparing whole transcriptome data of *F.*

*graminearum* challenged or not with TC3. Almost 47% of *F. graminearum* transcripts were shown to be differentially regulated in the presence of TC3 and more severe transcriptome disorders were observed after three days of exposure compared to 5 days (33 % and 26 % of genes differentially expressed in 3 and 5-day treatments, respectively). The GO enrichment analysis has allowed evidencing various biological processes and metabolic pathways that were affected by TC3, the most important being schematically summarized in Figure 11.

Notably, the expression of numerous genes related to the regulation of membrane and fungal cell wall composition and organization was shown to be disturbed by TC3 peptide exposure. For instance, we can mention the observed downregulation of genes involved in ergosterol and lipid biosynthetic pathway, which suggests that TC3 is likely to induce potential modification in the fungal membrane stability resulting in its embrittlement and permeabilization. These data are in accordance with the widely documented assumption that the antifungal activity of most defensins first results from interactions with fungal envelope components and induction of membrane disorders (Van der Weerden et al., 2010; Leannec-Rialland et al., 2022)<sup>4,23</sup>. As a result of the binding with membrane components, defensins can create pores and permeabilize the membranes (Thevissen et al., 2005; Aerts et al., 2008)<sup>24</sup>. Using an *in-silico* strategy, we previously demonstrated the probable recruitment of TC3 by specific membrane phospholipids present in the *F. graminearum* membrane (Leannec-Rialland et al., 2021)<sup>7</sup>. Some antimicrobial peptides have also been proved to target cell wall components (Yount and Yeaman., 2013)<sup>25</sup>. For instance, the plant defensin NaD1 was reported to permeabilize fungal hyphae of *Fusarium oxysporum* through specific cell wall interaction and the plant defensin RsAFP2 induced cell wall integrity disorder in *Candida albicans* (Van der Weerden et al., 2010; Thevissen et al., 2012)<sup>23,26</sup>.

Besides, the dysfunction of several intra-cellular and intra-nuclear biological processes induced by TC3 was evidenced, which is in accordance with a probable internalization of the peptide. Indeed, internalization of defensins allowed by plasma membrane permeabilization or endocytosis has been shown to frequently occur and to lead to direct action towards intra-cellular targets inducing signaling cascades (Van der Weerden et al., 2008; Hayes et al., 2018)<sup>27,28</sup>. Previous data that have demonstrated the importance of the cationic charges in the antifungal activity of TC3 (Leannec-Rialland et al., 2021)<sup>7</sup> support the hypothesis of a binding of TC3 to nucleic acids. Binding of defensins to nucleic acids has been proved to induce a broad inhibition of DNA synthesis, transcription and/or mRNA translation inside the target cells (do Nascimento, 2015)<sup>29</sup>. Our transcriptomic analysis has evidenced that *F. graminearum* exposure to TC3 resulted in a dysregulation of the expression of genes related to DNA replication, DNA repair, chromatin organization and DNA-templated transcription. Such effects are close to those observed for the defensin Psd1 which has been reported to translocate to the nucleus of fungal cells of *Neurospora crassa* and to interact with intra-nuclear proteins leading to a disruption of the cell cycle (Lobo et al., 2007)<sup>30</sup>. The reported effect of TC3 on DNA organization and transcription could explain the antifungal activity of TC3 and its capacity to interfere with the fungal secondary metabolism, including mycotoxin biosynthesis. Interestingly, the decrease in gene expression related to transcription was

shown to be accompanied by an upregulation of gene expression related to ribosomal biogenesis, translation, generation of energy and precursor metabolites. According to the previous observation, we could hypothesize that cellular processes are triggered to compensate for the decrease in mRNA synthesis and damage caused by the peptide.

Our transcriptomic analysis has also highlighted that TC3 could negatively affect oxidoreductase activities within the cell and therefore disturb redox homeostasis within the fungal cell. Intracellular accumulation of Reactive Oxygen Species (ROS) induced by antifungal defensins has already been described (Van der Weerden et al., 2008)<sup>27</sup>; this accumulation is not mandatory associated with the defensin internalization as it has been demonstrated for the plant defensin RsAFP2 and its target *Candida albicans* (Aerts et al., 2009)<sup>31</sup>. According to the key roles played by intracellular ROS and their interplay with pH changes, calcium transport, protein phosphorylation and oxidation levels of pyridine nucleotides (Montibus et al., 2013)<sup>32</sup>, deregulation of redox homeostasis induced by TC3 is another rationale that could explain fungal growth inhibition. Besides, redox status and pH changes are also two well-known factors governing the production of DON by *F. graminearum* (Ponts, 2015)<sup>20</sup>. The TC3-induced decreased expression of genes coding for cytochrome P450, known as involved in detoxification of drugs and therefore as key actors for protecting cells from exposure to toxic compounds, could also contribute to the high antifungal efficiency of the peptide.

Lastly, expression of genes involved in various primary and secondary metabolism pathways of *F. graminearum* were shown to be affected by the peptide TC3. The *tri* genes that are responsible for the DON production were downregulated when *F. graminearum* was challenged to TC3, in accordance with the observed decrease in the mycotoxin yield. Other mycotoxin biosynthetic pathways such as those related to Fusarin C and Fusaristatin A were also negatively affected by the TC3 treatment; this lack of side-effect on *F. graminearum* toxinogenesis is an important result in the perspective of developing a biosolution to reduce DON contamination. Key primary metabolic pathways known to be tightly linked to the DON biosynthesis (Atanasova-Penichon et al., 2018)<sup>21</sup> were also shown to be transcriptionally controlled by TC3. Notably, the expression of several genes involved in the TCA cycle was increased in presence of TC3. Since both the TCA cycle and the DON biosynthetic pathway share the same precursor (acetyl-coA), an increase in acetyl-coA consumption to produce energy in the form of ATP will result in less available acetyl-coA to the synthesis of secondary metabolites. Our data also indicated that TC3 treatment caused a decrease in the expression of genes involved in the GABA metabolism. Since the GABA metabolism is known as an inducer of DON biosynthesis (Wang et al., 2018)<sup>33</sup>, its slowdown is consistent with the TC3-induced reduction of the DON yield.

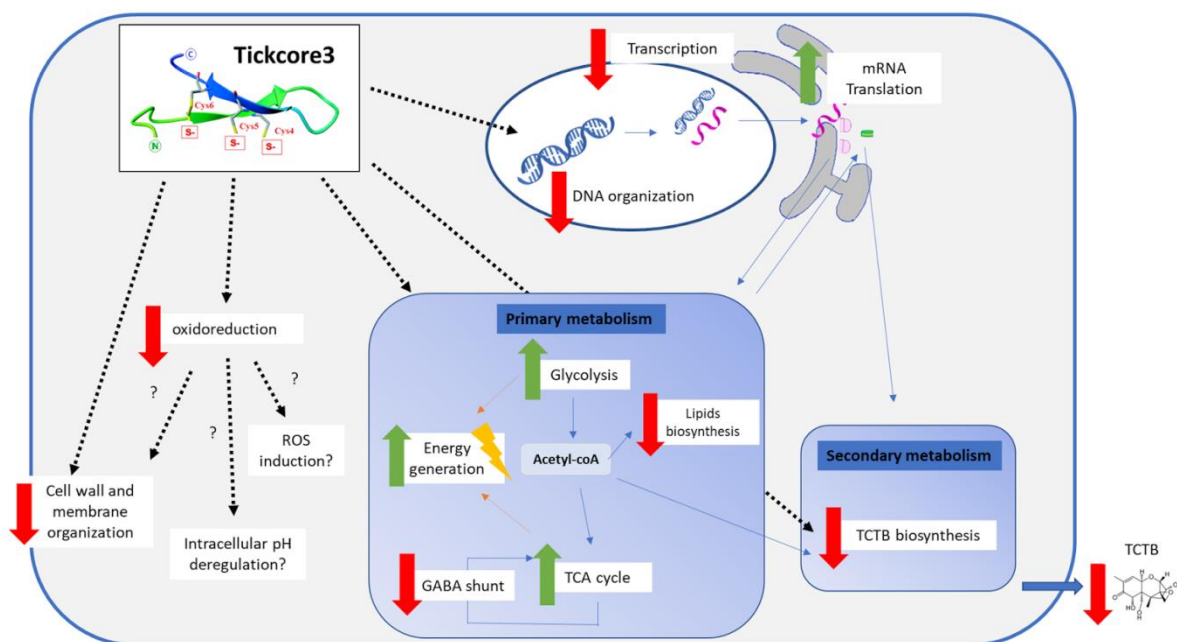


Figure 11. Summary of the main biological processes and metabolic pathways in *F. graminearum* affected by the antifungal and anti-mycotoxin peptide TickCore 3.

## V. Conclusion

The  $\gamma$ -core of the tick defensin DefMT3 demonstrated an efficient antifungal activity and capacity to inhibit the production of mycotoxins (Leannec-Rialland et al., 2021)<sup>7</sup>. Our analyses highlighted the expression of 6667 genes significantly modulated in *F. graminearum* challenged to TC3. Investigation of changes in *F. graminearum* transcriptome revealed multiple biological processes and cellular components affected by the peptide TC3, including the cell wall and membrane organization, DNA organization, DNA transcription, mRNA translation as well as several primary and secondary metabolism pathways. This study providing the first mechanistic clues explaining the bioactivity of TC3 illustrates the multifaceted mode of action employed by this promising antifungal peptide. Such a multifaceted mechanism is likely to reduce the emergence of resistant strains and is another argument corroborating that TC3 could be a candidate to protect crops from the phytopathogenic and toxigenic fungi *F. graminearum* and a solution to reduce the use of synthetic fungicides.

## References

1. Fernández de Ullivarri, M., Arbulu, S., Garcia-Gutierrez, E. & Cotter, P. D. Antifungal Peptides as Therapeutic Agents. *Front. Cell. Infect. Microbiol.* **10**, 105 (2020).
2. Sathoff, A. E. & Samac, D. A. Antibacterial Activity of Plant Defensins. *MPMI* **32**, 507–514 (2019).
3. Martínez-Culebras, P. V., Gandía, M., Garrigues, S., Marcos, J. F. & Manzanares, P. Antifungal Peptides and Proteins to Control Toxigenic Fungi and Mycotoxin Biosynthesis. *IJMS* **22**, 13261 (2021).
4. Leanne-Rialland, V. *et al.* Use of Defensins to Develop Eco-Friendly Alternatives to Synthetic Fungicides to Control Phytopathogenic Fungi and Their Mycotoxins. *J Fungi (Basel)* **8**, 229 (2022).
5. Leslie, J. F. *et al.* Key Global Actions for Mycotoxin Management in Wheat and Other Small Grains. *Toxins* **13**, 725 (2021).
6. Shah, L. *et al.* Integrated control of fusarium head blight and deoxynivalenol mycotoxin in wheat. *Plant Pathol* **67**, 532–548 (2018).
7. Leanne-Rialland, V. *et al.* Tick defensin  $\gamma$ -core reduces *Fusarium graminearum* growth and abrogates mycotoxins production with high efficiency. *Sci Rep* **11**, 7962 (2021).
8. Parisi, K. *et al.* The evolution, function and mechanisms of action for plant defensins. *Seminars in Cell & Developmental Biology* **88**, 107–118 (2019).
9. Struyfs, C., Cammue, B. P. A. & Thevissen, K. Membrane-Interacting Antifungal Peptides. *Frontiers in Cell and Developmental Biology* **9**, 706 (2021).
10. Aumer, T., Voisin, S. N., Knobloch, T., Landon, C. & Bulet, P. Impact of an Antifungal Insect Defensin on the Proteome of the Phytopathogenic Fungus *Botrytis cinerea*. *J. Proteome Res.* **19**, 1131–1146 (2020).
11. Feng, G., Li, X., Wang, W., Deng, L. & Zeng, K. Effects of Peptide Thanatin on the Growth and Transcriptome of *Penicillium digitatum*. *Frontiers in Microbiology* **11**, (2020).
12. Montibus, M. *et al.* Screening of Wood/Forest and Vine By-Products as Sources of New Drugs for Sustainable Strategies to Control *Fusarium graminearum* and the Production of Mycotoxins. *Molecules* **26**, 405 (2021).
13. Robinson, M. D., McCarthy, D. J. & Smyth, G. K. edgeR: a Bioconductor package for differential expression analysis of digital gene expression data. *Bioinformatics* **26**, 139–140 (2009).
14. McCarthy, D. J., Chen, Y. & Smyth, G. K. Differential expression analysis of multifactor RNA-Seq experiments with respect to biological variation. *Nucleic Acids Research* **40**, 4288–4297 (2012).
15. Varet, H., Brillet-Guéguen, L., Coppée, J.-Y. & Dillies, M.-A. SARTools: A DESeq2- and EdgeR-Based R Pipeline for Comprehensive Differential Analysis of RNA-Seq Data. *PLOS ONE* **11**, e0157022 (2016).
16. King, R., Urban, M., Hammond-Kosack, M. C. U., Hassani-Pak, K. & Hammond-Kosack, K. E. The completed genome sequence of the pathogenic ascomycete fungus *Fusarium graminearum*. *BMC Genomics* **16**, 544–544 (2015).
17. Love, M. I., Huber, W. & Anders, S. Moderated estimation of fold change and dispersion for RNA-seq data with DESeq2. *Genome Biology* **15**, 550 (2014).
18. Venny 2.1.0. <https://bioinfogp.cnb.csic.es/tools/venny/>.
19. Kolde, R. Pheatmap: pretty heatmaps. *R package version 1*, 726 (2012).
20. Ponts, N. Mycotoxins are a component of *Fusarium graminearum* stress-response system. *Front Microbiol* **6**, 1234–1234 (2015).

21. Atanasova-Penichon, V. *et al.* Mycotoxin Biosynthesis and Central Metabolism Are Two Interlinked Pathways in *Fusarium graminearum*, as Demonstrated by the Extensive Metabolic Changes Induced by Caffeic Acid Exposure. *Appl Environ Microbiol* **84**, (2018).
22. Sieber, C. M. K. *et al.* The *Fusarium graminearum* Genome Reveals More Secondary Metabolite Gene Clusters and Hints of Horizontal Gene Transfer. *PLOS ONE* **9**, e110311 (2014).
23. van der Weerden, N. L., Hancock, R. E. W. & Anderson, M. A. Permeabilization of fungal hyphae by the plant defensin NaD1 occurs through a cell wall-dependent process. *J Biol Chem* **285**, 37513–37520 (2010).
24. Thevissen, K. *et al.* SKN1, a novel plant defensin-sensitivity gene in *Saccharomyces cerevisiae*, is implicated in sphingolipid biosynthesis. *FEBS Letters* **579**, 1973–1977 (2005).
25. Yount, N. Y. & Yeaman, M. R. Peptide antimicrobials: cell wall as a bacterial target. *Annals of the New York Academy of Sciences* **1277**, 127–138 (2013).
26. Thevissen, K. *et al.* The plant defensin RsAFP2 induces cell wall stress, septin mislocalization and accumulation of ceramides in *Candida albicans*. *Mol Microbiol* **84**, 166–180 (2012).
27. van der Weerden, N. L., Lay, F. T. & Anderson, M. A. The Plant Defensin, NaD1, Enters the Cytoplasm of *Fusarium Oxysporum* Hyphae. *J. Biol. Chem.* **283**, 14445–14452 (2008).
28. Hayes, B. M. E., Bleackley, M. R., Anderson, M. A. & van der Weerden, N. L. The Plant Defensin NaD1 Enters the Cytoplasm of *Candida albicans* via Endocytosis. *JoF* **4**, 20 (2018).
29. do Nascimento, V. V. *et al.* PvD1 defensin, a plant antimicrobial peptide with inhibitory activity against *Leishmania amazonensis*. *Bioscience Reports* **35**, e00248 (2015).
30. Lobo, D. S. *et al.* Antifungal *Pisum sativum* Defensin 1 Interacts with *Neurospora crassa* Cyclin F Related to the Cell Cycle. *Biochemistry* **46**, 987–996 (2007).
31. Aerts, A. M. *et al.* The antifungal plant defensin RsAFP2 from radish induces apoptosis in a metacaspase independent way in *Candida albicans*. *FEBS Letters* **583**, 2513–2516 (2009).
32. Montibus, M., Pinson-Gadais, L., Richard-Forget, F., Barreau, C. & Ponts, N. Coupling of transcriptional response to oxidative stress and secondary metabolism regulation in filamentous fungi. *Critical Reviews in Microbiology* **41**, 295–308 (2015).
33. Wang, C. *et al.* The cotton MAPK kinase GhMPK20 negatively regulates resistance to *Fusarium oxysporum* by mediating the MKK4–MPK20–WRKY40 cascade. *Molecular Plant Pathology* **19**, 1624–1638 (2018).

## Supplementary documents

*Supplementary Table 1. GO terms related to “Molecular function” obtained from enrichment analysis on the transcripts down-regulated at both times, 3 and 5 DPI. “Bgd count” refers to the number of genes in the background with this term. “Result count” refers to the number of genes in the results with this term. “Pct of bgd” refers to the percentage of genes of the background in the results. The fold enrichment is the percent of genes with this term in the results divided by the percent of genes with this term in the background. Odds ratio and p-value are calculated with the Fisher’s exact test.*

<b>ID</b>	<b>Name</b>	<b>Bgd count</b>	<b>Result count</b>	<b>Pct of bgd</b>	<b>Fold enrichment</b>	<b>Odds ratio</b>	<b>P-value</b>
GO:0019441	tryptophan catabolic process to kynurenine	11	4	36.4	8.18	12.4	0.00099002
GO:0055114	obsolete oxidation-reduction process	895	59	6.6	1.48	1.61	0.00117252
GO:0070189	kynurenine metabolic process	12	4	33.3	7.5	10.85	0.00143325
GO:1901264	carbohydrate derivative transport	12	4	33.3	7.5	10.85	0.00143325
GO:0006308	DNA catabolic process	2	2	100	22.49	inf	0.00197227
GO:0002791	regulation of peptide secretion	2	2	100	22.49	inf	0.00197227
GO:0050708	regulation of protein secretion	2	2	100	22.49	inf	0.00197227
GO:0042436	indole-containing compound catabolic process	14	4	28.6	6.43	8.67	0.00270024
GO:0046218	indolalkylamine catabolic process	14	4	28.6	6.43	8.67	0.00270024
GO:0006569	tryptophan catabolic process	14	4	28.6	6.43	8.67	0.00270024
GO:0042430	indole-containing compound metabolic process	23	5	21.7	4.89	6.03	0.00293428
GO:0042180	cellular ketone metabolic process	25	5	20	4.5	5.43	0.0043066
GO:0042402	cellular biogenic amine catabolic process	16	4	25	5.62	7.23	0.00457498
GO:0015780	nucleotide-sugar transmembrane transport	3	2	66.7	14.99	43.2	0.00574227
GO:0035825	homologous recombination	3	2	66.7	14.99	43.2	0.00574227
GO:0140527	reciprocal homologous recombination	3	2	66.7	14.99	43.2	0.00574227
GO:0007131	reciprocal meiotic recombination	3	2	66.7	14.99	43.2	0.00574227
GO:0009310	amine catabolic process	17	4	23.5	5.29	6.67	0.00577572
GO:0042537	benzene-containing compound metabolic process	18	4	22.2	5	6.19	0.00716948
GO:0006568	tryptophan metabolic process	18	4	22.2	5	6.19	0.00716948
GO:0006586	indolalkylamine metabolic process	18	4	22.2	5	6.19	0.00716948
GO:0006694	steroid biosynthetic process	29	5	17.2	3.88	4.52	0.00832162
GO:0070201	regulation of establishment of protein localization	4	2	50	11.24	21.6	0.01114702
GO:0030534	adult behavior	4	2	50	11.24	21.6	0.01114702
GO:0032880	regulation of protein localization	4	2	50	11.24	21.6	0.01114702
GO:1903530	regulation of secretion by cell	4	2	50	11.24	21.6	0.01114702
GO:0051046	regulation of secretion	4	2	50	11.24	21.6	0.01114702
GO:0051223	regulation of protein transport	4	2	50	11.24	21.6	0.01114702
GO:0009636	response to toxic substance	45	6	13.3	3	3.34	0.01395245
GO:0009074	aromatic amino acid family catabolic process	22	4	18.2	4.09	4.81	0.01489985

GO:0060992	response to fungicide	34	5	14.7	3.31	3.74	0.01627045
GO:0015764	N-acetylglucosamine transport	5	2	40	9	14.4	0.01803443
GO:0062012	regulation of small molecule metabolic process	5	2	40	9	14.4	0.01803443
GO:0009308	amine metabolic process	35	5	14.3	3.21	3.62	0.01830996
GO:0046700	heterocycle catabolic process	62	7	11.3	2.54	2.77	0.01949859
GO:0051235	maintenance of location	14	3	21.4	4.82	5.9	0.02202753
GO:0044270	cellular nitrogen compound catabolic process	64	7	10.9	2.46	2.67	0.02284994
GO:0008202	steroid metabolic process	37	5	13.5	3.04	3.39	0.02287835
GO:0016126	sterol biosynthetic process	25	4	16	3.6	4.13	0.02321304
GO:0046677	response to antibiotic	38	5	13.2	2.96	3.29	0.02541549
GO:0034627	'de novo' NAD biosynthetic process	6	2	33.3	7.5	10.8	0.02626263
GO:0009448	gamma-aminobutyric acid metabolic process	6	2	33.3	7.5	10.8	0.02626263
GO:0007127	meiosis I	6	2	33.3	7.5	10.8	0.02626263
GO:0045185	maintenance of protein location	6	2	33.3	7.5	10.8	0.02626263
GO:0051651	maintenance of location in cell	6	2	33.3	7.5	10.8	0.02626263
GO:0010817	regulation of hormone levels	6	2	33.3	7.5	10.8	0.02626263
GO:0061982	meiosis I cell cycle process	6	2	33.3	7.5	10.8	0.02626263
GO:0034354	'de novo' NAD biosynthetic process from tryptophan	6	2	33.3	7.5	10.8	0.02626263
GO:0032507	maintenance of protein location in cell	6	2	33.3	7.5	10.8	0.02626263
GO:0044106	cellular amine metabolic process	26	4	15.4	3.46	3.94	0.02649886
GO:0006576	cellular biogenic amine metabolic process	26	4	15.4	3.46	3.94	0.02649886
GO:0006144	purine nucleobase metabolic process	16	3	18.8	4.22	4.99	0.03173909
GO:0019439	aromatic compound catabolic process	70	7	10	2.25	2.41	0.03523757
GO:0043248	proteasome assembly	7	2	28.6	6.43	8.64	0.03569938
GO:0032024	positive regulation of insulin secretion	1	1	100	22.49	inf	0.04446471
GO:0010228	vegetative to reproductive phase transition of meristem	1	1	100	22.49	inf	0.04446471
GO:0045444	fat cell differentiation	1	1	100	22.49	inf	0.04446471
GO:0000737	DNA catabolic process, endonucleolytic	1	1	100	22.49	inf	0.04446471
GO:0007628	adult walking behavior	1	1	100	22.49	inf	0.04446471
GO:0046883	regulation of hormone secretion	1	1	100	22.49	inf	0.04446471
GO:0046887	positive regulation of hormone secretion	1	1	100	22.49	inf	0.04446471
GO:0048822	enucleate erythrocyte development	1	1	100	22.49	inf	0.04446471
GO:0051224	negative regulation of protein transport	1	1	100	22.49	inf	0.04446471
GO:0002793	positive regulation of peptide secretion	1	1	100	22.49	inf	0.04446471
GO:0050714	positive regulation of protein secretion	1	1	100	22.49	inf	0.04446471
GO:0002792	negative regulation of peptide secretion	1	1	100	22.49	inf	0.04446471
GO:0007631	feeding behavior	1	1	100	22.49	inf	0.04446471

GO:0006285	base-excision repair, AP site formation	1	1	100	22.49	inf	0.04446471
GO:1903829	positive regulation of protein localization	1	1	100	22.49	inf	0.04446471
GO:1904950	negative regulation of establishment of protein localization	1	1	100	22.49	inf	0.04446471
GO:0090276	regulation of peptide hormone secretion	1	1	100	22.49	inf	0.04446471
GO:0090277	positive regulation of peptide hormone secretion	1	1	100	22.49	inf	0.04446471
GO:0090659	walking behavior	1	1	100	22.49	inf	0.04446471
GO:1903531	negative regulation of secretion by cell	1	1	100	22.49	inf	0.04446471
GO:1903828	negative regulation of protein localization	1	1	100	22.49	inf	0.04446471
GO:1904951	positive regulation of establishment of protein localization	1	1	100	22.49	inf	0.04446471
GO:0000751	mitotic cell cycle G1 arrest in response to pheromone	1	1	100	22.49	inf	0.04446471
GO:0010514	induction of conjugation with cellular fusion	1	1	100	22.49	inf	0.04446471
GO:0006722	triterpenoid metabolic process	1	1	100	22.49	inf	0.04446471
GO:0090278	negative regulation of peptide hormone secretion	1	1	100	22.49	inf	0.04446471
GO:0015783	GDP-fucose transmembrane transport	1	1	100	22.49	inf	0.04446471
GO:0033298	contractile vacuole organization	1	1	100	22.49	inf	0.04446471
GO:0051048	negative regulation of secretion	1	1	100	22.49	inf	0.04446471
GO:0031919	vitamin B6 transport	1	1	100	22.49	inf	0.04446471
GO:0042755	eating behavior	1	1	100	22.49	inf	0.04446471
GO:0046676	negative regulation of insulin secretion	1	1	100	22.49	inf	0.04446471
GO:0046888	negative regulation of hormone secretion	1	1	100	22.49	inf	0.04446471
GO:0098742	cell-cell adhesion via plasma-membrane adhesion molecules	1	1	100	22.49	inf	0.04446471
GO:0030705	cytoskeleton-dependent intracellular transport	1	1	100	22.49	inf	0.04446471
GO:0090480	purine nucleotide-sugar transmembrane transport	1	1	100	22.49	inf	0.04446471
GO:0030242	autophagy of peroxisome	1	1	100	22.49	inf	0.04446471
GO:0042438	melanin biosynthetic process	1	1	100	22.49	inf	0.04446471
GO:0042554	superoxide anion generation	1	1	100	22.49	inf	0.04446471
GO:0043353	enucleate erythrocyte differentiation	1	1	100	22.49	inf	0.04446471
GO:0016339	calcium-dependent cell-cell adhesion via plasma membrane cell adhesion molecules	1	1	100	22.49	inf	0.04446471
GO:0009737	response to abscisic acid	1	1	100	22.49	inf	0.04446471
GO:0019628	urate catabolic process	1	1	100	22.49	inf	0.04446471
GO:0046415	urate metabolic process	1	1	100	22.49	inf	0.04446471
GO:0031142	induction of conjugation upon nitrogen starvation	1	1	100	22.49	inf	0.04446471
GO:0050709	negative regulation of protein secretion	1	1	100	22.49	inf	0.04446471
GO:0031140	induction of conjugation upon nutrient starvation	1	1	100	22.49	inf	0.04446471
GO:0050796	regulation of insulin secretion	1	1	100	22.49	inf	0.04446471
GO:0050872	white fat cell differentiation	1	1	100	22.49	inf	0.04446471

GO:0051222	positive regulation of protein transport	1	1	100	22.49	inf	0.04446471
GO:0036085	GDP-fucose import into Golgi lumen	1	1	100	22.49	inf	0.04446471
GO:0019442	tryptophan catabolic process to acetyl-CoA	1	1	100	22.49	inf	0.04446471
GO:0016104	triterpenoid biosynthetic process	1	1	100	22.49	inf	0.04446471
GO:1901361	organic cyclic compound catabolic process	74	7	9.5	2.13	2.27	0.04558552
GO:0043545	molybdopterin cofactor metabolic process	8	2	25	5.62	7.2	0.04622152
GO:0051189	prosthetic group metabolic process	8	2	25	5.62	7.2	0.04622152
GO:0019720	Mo-molybdopterin cofactor metabolic process	8	2	25	5.62	7.2	0.04622152
GO:0006777	Mo-molybdopterin cofactor biosynthetic process	8	2	25	5.62	7.2	0.04622152
GO:0033212	iron import into cell	8	2	25	5.62	7.2	0.04622152
GO:0016125	sterol metabolic process	31	4	12.9	2.9	3.21	0.04694015

Supplementary table 2. GO terms related to “Cellular component” obtained from enrichment analysis on the transcripts down-regulated at both times, 3 and 5 DPI. “Bgd count” refers to the number of genes in the background with this term. “Result count” refers to the number of genes in the results with this term. “Pct of bgd” refers to the percentage of genes of the background in the results. The fold enrichment is the percent of genes with this term in the results divided by the percent of genes with this term in the background. Odds ratio and p-value are calculated with the Fisher’s exact test.

ID	Name	Bgd count	Result count	Pct of bgd	Fold enrichment	Odds ratio	P-value
GO:0000795	synaptonemal complex	2	2	100	22.49	inf	0.00197227
GO:0099086	synaptonemal structure	3	2	66.7	14.99	43.2	0.00574227
GO:0009277	fungal-type cell wall	57	7	12.3	2.76	3.05	0.01265158
GO:0031224	intrinsic component of membrane	2665	137	5.1	1.16	1.25	0.02228597
GO:0005618	cell wall	99	9	9.1	2.04	2.18	0.03161262
GO:0030312	external encapsulating structure	103	9	8.7	1.97	2.08	0.03933754
GO:0001669	acrosomal vesicle	1	1	100	22.49	inf	0.04446471
GO:0000794	condensed nuclear chromosome	8	2	25	5.62	7.2	0.04622152
GO:0016021	integral component of membrane	2644	133	5	1.13	1.21	0.0470181
GO:0005576	extracellular region	176	13	7.4	1.66	1.74	0.04984606

Supplementary table 3. GO terms related to “Biological process” obtained from enrichment analysis on the transcripts down-regulated at both times, 3 and 5 DPI. “Bgd count” refers to the number of genes in the background with this term. “Result count” refers to the number of genes in the results with this term. “Pct of bgd” refers to the percentage of genes of the background in the results. The fold enrichment is the percent of genes with this term in the results divided by the percent of genes with this term in the background. Odds ratio and p-value are calculated with the Fisher’s exact test.

ID	Name	Bgd count	Result count	Pct of bgd	Fold enrichment	Odds ratio	P-value
GO:0020037	heme binding	154	21	13.6	3.07	3.53	4.13E-06
GO:0046906	tetrapyrrole binding	156	21	13.5	3.03	3.48	5.08E-06
GO:0016491	oxidoreductase activity	1048	73	7	1.57	1.75	4.86E-05
GO:0003838	sterol 24-C-methyltransferase activity	2	2	100	22.49	inf	0.00197227

GO:0004190	aspartic-type endopeptidase activity	22	5	22.7	5.11	6.39	0.00238201
GO:0070001	aspartic-type peptidase activity	22	5	22.7	5.11	6.39	0.00238201
GO:0016705	oxidoreductase activity, acting on paired donors, with incorporation or reduction of molecular oxygen	168	16	9.5	2.14	2.32	0.00324152
GO:0005338	nucleotide-sugar transmembrane transporter activity	3	2	66.7	14.99	43.2	0.00574227
GO:0004060	arylamine N-acetyltransferase activity	3	2	66.7	14.99	43.2	0.00574227
GO:0004316	3-oxoacyl-[acyl-carrier-protein] reductase (NADPH) activity	3	2	66.7	14.99	43.2	0.00574227
GO:0070403	NAD+ binding	9	3	33.3	7.5	10.82	0.00599654
GO:0016810	hydrolase activity, acting on carbon-nitrogen (but not peptide) bonds	96	10	10.4	2.34	2.54	0.01003751
GO:0005506	iron ion binding	208	17	8.2	1.84	1.95	0.01121482
GO:0015572	N-acetylglucosamine transmembrane transporter activity	5	2	40	9	14.4	0.01803443
GO:0008169	C-methyltransferase activity	5	2	40	9	14.4	0.01803443
GO:0004312	fatty acid synthase activity	5	2	40	9	14.4	0.01803443
GO:0003839	gamma-glutamylcyclotransferase activity	5	2	40	9	14.4	0.01803443
GO:0003824	catalytic activity	3842	191	5	1.12	1.24	0.02026186
GO:0051287	NAD binding	50	6	12	2.7	2.96	0.02263283
GO:0004061	arylformamidase activity	6	2	33.3	7.5	10.8	0.02626263
GO:0016151	nickel cation binding	6	2	33.3	7.5	10.8	0.02626263
GO:0003857	3-hydroxyacyl-CoA dehydrogenase activity	6	2	33.3	7.5	10.8	0.02626263
GO:0009987	cellular process	15	3	20	4.5	5.41	0.02664582
GO:0004497	monooxygenase activity	163	13	8	1.79	1.89	0.02951126
GO:0046914	transition metal ion binding	933	53	5.7	1.28	1.34	0.03531508
GO:0005457	GDP-fucose transmembrane transporter activity	1	1	100	22.49	inf	0.04446471
GO:0031559	oxidosqualene cyclase activity	1	1	100	22.49	inf	0.04446471
GO:0061799	cyclic pyranopterin monophosphate synthase activity	1	1	100	22.49	inf	0.04446471
GO:0033903	obsolete endo-1,3(4)-beta-glucanase activity	1	1	100	22.49	inf	0.04446471
GO:0043425	bHLH transcription factor binding	1	1	100	22.49	inf	0.04446471
GO:0047419	N-acetylgalactosamine-6-phosphate deacetylase activity	1	1	100	22.49	inf	0.04446471
GO:0036054	protein-malonyllysine demalonylase activity	1	1	100	22.49	inf	0.04446471
GO:0052862	glucan endo-1,4-beta-glucanase activity, C-3 substituted reducing group	1	1	100	22.49	inf	0.04446471
GO:0048306	calcium-dependent protein binding	1	1	100	22.49	inf	0.04446471
GO:0050664	oxidoreductase activity, acting on NAD(P)H, oxygen as acceptor	1	1	100	22.49	inf	0.04446471
GO:0052736	beta-glucanase activity	1	1	100	22.49	inf	0.04446471
GO:0061798	GTP 3',8'-cyclase activity	1	1	100	22.49	inf	0.04446471
GO:0031924	vitamin B6 transmembrane transporter activity	1	1	100	22.49	inf	0.04446471
GO:0005046	KDEL sequence binding	1	1	100	22.49	inf	0.04446471
GO:0000977	RNA polymerase II transcription regulatory region sequence-specific DNA binding	1	1	100	22.49	inf	0.04446471
GO:0003830	beta-1,4-mannosylglycoprotein 4-beta-N-	1	1	100	22.49	inf	0.04446471

	acetylglucosaminyltransferase activity						
GO:0001055	RNA polymerase II activity	1	1	100	22.49	inf	0.04446471
GO:0004846	urate oxidase activity	1	1	100	22.49	inf	0.04446471
GO:0016716	oxidoreductase activity, acting on paired donors, with incorporation or reduction of molecular oxygen, another compound as one donor, and incorporation of one atom of oxygen	1	1	100	22.49	inf	0.04446471
GO:0000250	lanosterol synthase activity	1	1	100	22.49	inf	0.04446471
GO:0000703	oxidized pyrimidine nucleobase lesion DNA N-glycosylase activity	1	1	100	22.49	inf	0.04446471
GO:0008691	3-hydroxybutyryl-CoA dehydrogenase activity	1	1	100	22.49	inf	0.04446471
GO:0010427	abscisic acid binding	1	1	100	22.49	inf	0.04446471
GO:0016176	superoxide-generating NADPH oxidase activator activity	1	1	100	22.49	inf	0.04446471
GO:0016504	peptidase activator activity	1	1	100	22.49	inf	0.04446471
GO:0004503	tyrosinase activity	1	1	100	22.49	inf	0.04446471
GO:0016663	oxidoreductase activity, acting on other nitrogenous compounds as donors, oxygen as acceptor	1	1	100	22.49	inf	0.04446471
GO:0016175	superoxide-generating NAD(P)H oxidase activity	1	1	100	22.49	inf	0.04446471
GO:0042123	glucanosyltransferase activity	1	1	100	22.49	inf	0.04446471
GO:0042300	beta-amyrin synthase activity	1	1	100	22.49	inf	0.04446471
GO:0019840	isoprenoid binding	1	1	100	22.49	inf	0.04446471
GO:0036055	protein-succinyllysine desuccinylase activity	1	1	100	22.49	inf	0.04446471
GO:0036080	purine nucleotide-sugar transmembrane transporter activity	1	1	100	22.49	inf	0.04446471
GO:0140033	acetylation-dependent protein binding	1	1	100	22.49	inf	0.04446471
GO:0052861	glucan endo-1,3-beta-glucanase activity, C-3 substituted reducing group	1	1	100	22.49	inf	0.04446471
GO:0070577	lysine-acetylated histone binding	1	1	100	22.49	inf	0.04446471
GO:0008448	N-acetylglucosamine-6-phosphate deacetylase activity	1	1	100	22.49	inf	0.04446471
GO:0140103	catalytic activity, acting on a glycoprotein	1	1	100	22.49	inf	0.04446471
GO:0016842	amidine-lyase activity	8	2	25	5.62	7.2	0.04622152
GO:0000981	DNA-binding transcription factor activity, RNA polymerase II-specific	378	24	6.3	1.43	1.49	0.04931358

Supplementary table 4. GO terms related to "Molecular function" obtained from enrichment analysis on the transcripts up-regulated at both times, 3 and 5 DPI. "Bgd count" refers to the number of genes in the background with this term. "Result count" refers to the number of genes in the results with this term. "Pct of bgd" refers to the percentage of genes of the background in the results. The fold enrichment is the percent of genes with this term in the results divided by the percent of genes with this term in the background. Odds ratio and p-value are calculated with the Fisher's exact test.

ID	Name	Bgd count	Result count	Pct of bgd	Fold enrichment	Odds ratio	P-value
GO:0003735	structural constituent of ribosome	129	47	36.4	5.67	9.01	4.52E-24
GO:0005198	structural molecule activity	180	49	27.2	4.23	5.87	8.11E-19
GO:0090079	translation regulator activity, nucleic acid binding	63	24	38.1	5.92	9.31	2.27E-13

GO:0008135	translation factor activity, RNA binding	63	24	38.1	5.92	9.31	2.27E-13
GO:0045182	translation regulator activity	67	24	35.8	5.57	8.44	1.10E-12
GO:0016875	ligase activity, forming carbon-oxygen bonds	40	18	45	7	12.27	8.12E-12
GO:0004812	aminoacyl-tRNA ligase activity	40	18	45	7	12.27	8.12E-12
GO:0003723	RNA binding	309	52	16.8	2.62	3.14	8.63E-11
GO:0003743	translation initiation factor activity	45	18	40	6.22	9.99	9.07E-11
GO:0016874	ligase activity	160	34	21.3	3.3	4.11	3.63E-10
GO:0140101	catalytic activity, acting on a tRNA	72	21	29.2	4.54	6.18	2.27E-09
GO:0016829	lyase activity	212	35	16.5	2.57	3	1.91E-07
GO:0016879	ligase activity, forming carbon-nitrogen bonds	39	13	33.3	5.18	7.42	4.81E-07
GO:0016769	transferase activity, transferring nitrogenous groups	44	13	29.5	4.59	6.22	2.28E-06
GO:0008483	transaminase activity	41	12	29.3	4.55	6.13	6.26E-06
GO:0016835	carbon-oxygen lyase activity	70	16	22.9	3.55	4.41	6.61E-06
GO:0036094	small molecule binding	1207	113	9.4	1.46	1.63	1.31E-05
GO:0016836	hydro-lyase activity	51	13	25.5	3.96	5.07	1.38E-05
GO:0016884	carbon-nitrogen ligase activity, with glutamine as amido-N-donor	11	6	54.5	8.48	17.64	2.41E-05
GO:0043168	anion binding	1097	103	9.4	1.46	1.62	3.08E-05
GO:0016646	oxidoreductase activity, acting on the CH-NH group of donors, NAD or NADP as acceptor	12	6	50	7.78	14.7	4.55E-05
GO:1901363	heterocyclic compound binding	2092	174	8.3	1.29	1.46	5.19E-05
GO:0097159	organic cyclic compound binding	2093	174	8.3	1.29	1.46	5.34E-05
GO:0051540	metal cluster binding	61	13	21.3	3.31	4.01	0.00010484
GO:0051536	iron-sulfur cluster binding	61	13	21.3	3.31	4.01	0.00010484
GO:0070279	vitamin B6 binding	73	14	19.2	2.98	3.52	0.00019015
GO:0030170	pyridoxal phosphate binding	73	14	19.2	2.98	3.52	0.00019015
GO:0140098	catalytic activity, acting on RNA	159	23	14.5	2.25	2.52	0.00019834
GO:1901265	nucleoside phosphate binding	1083	98	9	1.41	1.54	0.00020624
GO:0000166	nucleotide binding	1083	98	9	1.41	1.54	0.00020624
GO:0046912	acyltransferase, acyl groups converted into alkyl on transfer	10	5	50	7.78	14.67	0.00020755
GO:0097367	carbohydrate derivative binding	860	81	9.4	1.46	1.6	0.00022475
GO:0002161	aminoacyl-tRNA editing activity	6	4	66.7	10.37	29.3	0.00022865
GO:0004086	obsolete carbamoyl-phosphate synthase activity	3	3	100	15.55	inf	0.00026456
GO:0032553	ribonucleotide binding	829	78	9.4	1.46	1.59	0.00030722
GO:0003674	molecular function	6693	463	6.9	1.08	1.45	0.00036679
GO:0035639	purine ribonucleoside triphosphate binding	779	73	9.4	1.46	1.58	0.00054802
GO:0016645	oxidoreductase activity, acting on the CH-NH group of donors	18	6	33.3	5.18	7.34	0.00065565
GO:0003824	catalytic activity	3842	284	7.4	1.15	1.33	0.00071817
GO:0032555	purine ribonucleotide binding	791	73	9.2	1.44	1.55	0.00084836
GO:0017076	purine nucleotide binding	793	73	9.2	1.43	1.55	0.00091076
GO:0005524	ATP binding	653	62	9.5	1.48	1.59	0.00105518
GO:0051539	4 iron, 4 sulfur cluster binding	34	8	23.5	3.66	4.53	0.0011352
GO:0003746	translation elongation factor activity	14	5	35.7	5.55	8.15	0.00132836
GO:0032559	adenyl ribonucleotide binding	665	62	9.3	1.45	1.56	0.00165476

GO:0030554	adenyl nucleotide binding	667	62	9.3	1.45	1.55	0.00177969
GO:0003878	ATP citrate synthase activity	2	2	100	15.55	inf	0.00412799
GO:0004824	lysine-tRNA ligase activity	2	2	100	15.55	inf	0.00412799
GO:0004823	leucine-tRNA ligase activity	2	2	100	15.55	inf	0.00412799
GO:0003842	1-pyrroline-5-carboxylate dehydrogenase activity	2	2	100	15.55	inf	0.00412799
GO:0004088	carbamoyl-phosphate synthase (glutamine-hydrolyzing) activity	2	2	100	15.55	inf	0.00412799
GO:0016743	carboxyl- or carbamoyltransferase activity	2	2	100	15.55	inf	0.00412799
GO:0015603	iron chelate transmembrane transporter activity	6	3	50	7.78	14.62	0.00456772
GO:0015343	siderophore transmembrane transporter activity	6	3	50	7.78	14.62	0.00456772
GO:0016838	carbon-oxygen lyase activity, acting on phosphates	6	3	50	7.78	14.62	0.00456772
GO:0016668	oxidoreductase activity, acting on a sulfur group of donors, NAD(P) as acceptor	6	3	50	7.78	14.62	0.00456772
GO:0019238	cyclohydrolase activity	6	3	50	7.78	14.62	0.00456772
GO:0042929	ferrichrome transmembrane transporter activity	6	3	50	7.78	14.62	0.00456772
GO:0019842	vitamin binding	116	15	12.9	2.01	2.19	0.00721563
GO:0019843	rRNA binding	14	4	28.6	4.44	5.86	0.0100823
GO:0019200	carbohydrate kinase activity	14	4	28.6	4.44	5.86	0.0100823
GO:0000049	tRNA binding	14	4	28.6	4.44	5.86	0.0100823
GO:0004160	dihydroxy-acid dehydratase activity	3	2	66.7	10.37	29.2	0.01185485
GO:0003994	aconitate hydratase activity	3	2	66.7	10.37	29.2	0.01185485
GO:0016639	oxidoreductase activity, acting on the CH-NH2 group of donors, NAD or NADP as acceptor	3	2	66.7	10.37	29.2	0.01185485
GO:0016597	amino acid binding	3	2	66.7	10.37	29.2	0.01185485
GO:0003849	3-deoxy-7-phosphoheptulonate synthase activity	3	2	66.7	10.37	29.2	0.01185485
GO:0005544	calcium-dependent phospholipid binding	3	2	66.7	10.37	29.2	0.01185485
GO:0004055	argininosuccinate synthase activity	3	2	66.7	10.37	29.2	0.01185485
GO:0004826	phenylalanine-tRNA ligase activity	3	2	66.7	10.37	29.2	0.01185485
GO:0016741	transferase activity, transferring one-carbon groups	134	16	11.9	1.86	2	0.01189664
GO:0030145	manganese ion binding	15	4	26.7	4.15	5.32	0.01306199
GO:0009055	electron transfer activity	42	7	16.7	2.59	2.93	0.01652689
GO:0016810	hydrolase activity, acting on carbon-nitrogen (but not peptide) bonds	96	12	12.5	1.94	2.1	0.01967501
GO:0016740	transferase activity	971	78	8	1.25	1.31	0.02055196
GO:0043023	ribosomal large subunit binding	4	2	50	7.78	14.6	0.02270225
GO:0004084	branched-chain-amino-acid transaminase activity	4	2	50	7.78	14.6	0.02270225
GO:0031369	translation initiation factor binding	4	2	50	7.78	14.6	0.02270225
GO:0031420	alkali metal ion binding	4	2	50	7.78	14.6	0.02270225
GO:0140640	catalytic activity, acting on a nucleic acid	270	26	9.6	1.5	1.58	0.02491762
GO:0016763	pentosyltransferase activity	18	4	22.2	3.46	4.18	0.02513003
GO:0016462	pyrophosphatase activity	171	18	10.5	1.64	1.74	0.02625555
GO:0000287	magnesium ion binding	58	8	13.8	2.15	2.35	0.03107231
GO:0008312	7S RNA binding	5	2	40	6.22	9.73	0.03623829

GO:0003676	nucleic acid binding	927	73	7.9	1.22	1.28	0.03661834
GO:0016776	phosphotransferase activity, phosphate group as acceptor	12	3	25	3.89	4.87	0.03761663
GO:1904680	peptide transmembrane transporter activity	12	3	25	3.89	4.87	0.03761663
GO:0016861	intramolecular oxidoreductase activity, interconverting aldoses and ketoses	12	3	25	3.89	4.87	0.03761663
GO:0016667	oxidoreductase activity, acting on a sulfur group of donors	30	5	16.7	2.59	2.93	0.04045678
GO:0003924	GTPase activity	73	9	12.3	1.92	2.06	0.04344448
GO:0052689	carboxylic ester hydrolase activity	73	9	12.3	1.92	2.06	0.04344448
GO:0030248	cellulose binding	13	3	23.1	3.59	4.38	0.04662726
GO:0017111	nucleoside-triphosphatase activity	158	16	10.1	1.57	1.66	0.04701543

*Supplementary table 5. GO terms related to “Cellular component” obtained from enrichment analysis on the transcripts up-regulated at both times, 3 and 5 DPI. “Bgd count” refers to the number of genes in the background with this term. “Result count” refers to the number of genes in the results with this term. “Pct of bgd” refers to the percentage of genes of the background in the results. The fold enrichment is the percent of genes with this term in the results divided by the percent of genes with this term in the background. Odds ratio and p-value are calculated with the Fisher’s exact test.*

<b>ID</b>	<b>Name</b>	<b>Bgd count</b>	<b>Result count</b>	<b>Pct of bgd</b>	<b>Fold enrichment</b>	<b>Odds ratio</b>	<b>P-value</b>
GO:0005840	ribosome	151	53	35.1	5.46	8.58	4.04E-26
GO:1990904	ribonucleoprotein complex	226	54	23.9	3.72	4.95	7.66E-18
GO:0070993	translation preinitiation complex	13	11	84.6	13.16	81.6	4.91E-12
GO:0005852	eukaryotic translation initiation factor 3 complex	13	11	84.6	13.16	81.6	4.91E-12
GO:0016282	eukaryotic 43S preinitiation complex	13	11	84.6	13.16	81.6	4.91E-12
GO:0033290	eukaryotic 48S preinitiation complex	13	11	84.6	13.16	81.6	4.91E-12
GO:0044424	obsolete intracellular part	321	50	15.6	2.42	2.85	3.21E-09
GO:0044391	ribosomal subunit	43	16	37.2	5.79	8.85	3.61E-09
GO:0005625	obsolete soluble fraction	104	23	22.1	3.44	4.27	1.24E-07
GO:0015935	small ribosomal subunit	15	8	53.3	8.29	16.86	1.20E-06
GO:0043228	non-membrane-bounded organelle	570	64	11.2	1.75	1.95	6.11E-06
GO:0043232	intracellular non-membrane-bounded organelle	570	64	11.2	1.75	1.95	6.11E-06
GO:0005737	cytoplasm	1492	129	8.6	1.34	1.49	0.00013332
GO:0005829	cytosol	49	11	22.4	3.49	4.28	0.00021793
GO:0015934	large ribosomal subunit	28	8	28.6	4.44	5.89	0.00027368
GO:0022626	cytosolic ribosome	19	6	31.6	4.91	6.78	0.00090671
GO:0005739	mitochondrion	552	52	9.4	1.46	1.57	0.00314824
GO:0097361	CIA complex	2	2	100	15.55	inf	0.00412799
GO:0005746	mitochondrial respirasome	6	3	50	7.78	14.62	0.00456772
GO:0022625	cytosolic large ribosomal subunit	13	4	30.8	4.79	6.51	0.00758118
GO:0005576	extracellular region	176	20	11.4	1.77	1.9	0.0090914
GO:0032991	protein-containing complex	814	68	8.4	1.3	1.37	0.01358736
GO:0070069	cytochrome complex	4	2	50	7.78	14.6	0.02270225
GO:0022627	cytosolic small ribosomal subunit	4	2	50	7.78	14.6	0.02270225
GO:0098803	respiratory chain complex	4	2	50	7.78	14.6	0.02270225

GO:0005786	signal recognition particle, endoplasmic reticulum targeting	5	2	40	6.22	9.73	0.03623829
GO:0005622	intracellular anatomical structure	2998	212	7.1	1.1	1.17	0.04359298
GO:0009986	cell surface	63	8	12.7	1.97	2.13	0.04760553

*Supplementary table 6. GO terms related to “Biological process” obtained from enrichment analysis on the transcripts up-regulated at both times. “Bgd count” refers to the number of genes in the background with this term. “Result count” refers to the number of genes in the results with this term. “Pct of bgd” refers to the percentage of genes of the background in the results. The fold enrichment is the percent of genes with this term in the results divided by the percent of genes with this term in the background. Odds ratio and p-value are calculated with the Fisher’s exact test.*

ID	Name	Bgd count	Result count	Pct of bgd	Fold enrichment	Odds ratio	P-value
GO:1901566	organonitrogen compound biosynthetic process	595	157	26.4	4.1	6.84	2.25E-59
GO:0006412	translation	227	87	38.3	5.96	10.51	2.50E-46
GO:0043043	peptide biosynthetic process	231	87	37.7	5.86	10.21	1.34E-45
GO:0006518	peptide metabolic process	245	87	35.5	5.52	9.29	3.49E-43
GO:0043604	amide biosynthetic process	254	88	34.6	5.39	8.96	1.10E-42
GO:0043603	cellular amide metabolic process	293	88	30	4.67	7.22	4.55E-37
GO:0006520	cellular amino acid metabolic process	244	74	30.3	4.72	7.14	1.88E-31
GO:1901564	organonitrogen compound metabolic process	1346	194	14.4	2.24	3.21	1.98E-31
GO:0043436	oxoacid metabolic process	367	89	24.3	3.77	5.34	1.26E-29
GO:0019752	carboxylic acid metabolic process	362	88	24.3	3.78	5.35	2.25E-29
GO:0006082	organic acid metabolic process	375	89	23.7	3.69	5.19	7.12E-29
GO:0044281	small molecule metabolic process	634	118	18.6	2.89	3.94	6.29E-28
GO:0009058	biosynthetic process	1362	187	13.7	2.14	2.97	2.73E-27
GO:1901576	organic substance biosynthetic process	1259	176	14	2.17	2.98	2.17E-26
GO:0044249	cellular biosynthetic process	1268	176	13.9	2.16	2.96	5.22E-26
GO:0044271	cellular nitrogen compound biosynthetic process	787	126	16	2.49	3.28	1.55E-23
GO:0008652	cellular amino acid biosynthetic process	102	41	40.2	6.25	10.47	4.83E-23
GO:0016053	organic acid biosynthetic process	151	47	31.1	4.84	7.08	9.61E-21
GO:0046394	carboxylic acid biosynthetic process	146	45	30.8	4.79	6.96	1.03E-19
GO:0044283	small molecule biosynthetic process	220	55	25	3.89	5.27	3.98E-19
GO:1901607	alpha-amino acid biosynthetic process	87	34	39.1	6.08	9.87	7.75E-19
GO:1901605	alpha-amino acid metabolic process	160	44	27.5	4.28	5.9	3.48E-17
GO:0044267	cellular protein metabolic process	689	98	14.2	2.21	2.71	1.19E-14
GO:0044237	cellular metabolic process	2482	241	9.7	1.51	1.99	2.35E-14
GO:0006807	nitrogen compound metabolic process	2167	213	9.8	1.53	1.94	7.48E-13
GO:0044238	primary metabolic process	2551	239	9.4	1.46	1.88	2.38E-12
GO:0034641	cellular nitrogen compound metabolic process	1334	147	11	1.71	2.08	3.34E-12
GO:0006418	tRNA aminoacylation for protein translation	39	18	46.2	7.18	12.85	4.75E-12
GO:0001732	formation of cytoplasmic translation initiation complex	13	11	84.6	13.16	81.6	4.91E-12
GO:0071704	organic substance metabolic process	2781	253	9.1	1.41	1.83	9.42E-12
GO:0043038	amino acid activation	41	18	43.9	6.83	11.73	1.36E-11
GO:0043039	tRNA aminoacylation	41	18	43.9	6.83	11.73	1.36E-11

GO:0034645	cellular macromolecule biosynthetic process	766	97	12.7	1.97	2.34	2.15E-11
GO:0002183	cytoplasmic translational initiation	14	11	78.6	12.22	54.4	2.16E-11
GO:0071826	ribonucleoprotein complex subunit organization	38	17	44.7	6.96	12.11	3.51E-11
GO:0022618	ribonucleoprotein complex assembly	38	17	44.7	6.96	12.11	3.51E-11
GO:0006413	translational initiation	29	15	51.7	8.04	15.99	3.70E-11
GO:0010467	gene expression	905	108	11.9	1.86	2.2	5.20E-11
GO:0002181	cytoplasmic translation	15	11	73.3	11.4	40.79	7.63E-11
GO:0009059	macromolecule biosynthetic process	783	97	12.4	1.93	2.28	7.67E-11
GO:0019538	protein metabolic process	862	103	11.9	1.86	2.19	1.51E-10
GO:0008152	metabolic process	3697	305	8.2	1.28	1.67	2.53E-09
GO:0009064	glutamine family amino acid metabolic process	54	18	33.3	5.18	7.48	2.97E-09
GO:0009259	ribonucleotide metabolic process	91	23	25.3	3.93	5.09	8.41E-09
GO:0019693	ribose phosphate metabolic process	91	23	25.3	3.93	5.09	8.41E-09
GO:0009127	purine nucleoside monophosphate biosynthetic process	18	10	55.6	8.64	18.5	3.06E-08
GO:0006163	purine nucleotide metabolic process	83	21	25.3	3.93	5.08	3.69E-08
GO:0009156	ribonucleoside monophosphate biosynthetic process	28	12	42.9	6.66	11.13	5.23E-08
GO:0009987	cellular process	3976	317	8	1.24	1.6	5.61E-08
GO:0006399	tRNA metabolic process	109	24	22	3.42	4.25	7.21E-08
GO:0009117	nucleotide metabolic process	127	26	20.5	3.18	3.88	9.89E-08
GO:0009126	purine nucleoside monophosphate metabolic process	20	10	50	7.78	14.8	1.15E-07
GO:0006753	nucleoside phosphate metabolic process	128	26	20.3	3.16	3.84	1.17E-07
GO:0009124	nucleoside monophosphate biosynthetic process	30	12	40	6.22	9.89	1.32E-07
GO:0009161	ribonucleoside monophosphate metabolic process	30	12	40	6.22	9.89	1.32E-07
GO:0072521	purine-containing compound metabolic process	97	22	22.7	3.53	4.4	1.45E-07
GO:0046390	ribose phosphate biosynthetic process	54	16	29.6	4.61	6.28	1.48E-07
GO:0009260	ribonucleotide biosynthetic process	54	16	29.6	4.61	6.28	1.48E-07
GO:0022613	ribonucleoprotein complex biogenesis	157	29	18.5	2.87	3.42	1.91E-07
GO:0009168	purine ribonucleoside monophosphate biosynthetic process	21	10	47.6	7.41	13.45	2.06E-07
GO:0009150	purine ribonucleotide metabolic process	84	20	23.8	3.7	4.68	2.31E-07
GO:0009082	branched-chain amino acid biosynthetic process	13	8	61.5	9.57	23.6	2.69E-07
GO:0009123	nucleoside monophosphate metabolic process	32	12	37.5	5.83	8.9	3.06E-07
GO:0006189	'de novo' IMP biosynthetic process	10	7	70	10.89	34.37	4.44E-07
GO:0006526	arginine biosynthetic process	10	7	70	10.89	34.37	4.44E-07
GO:0009084	glutamine family amino acid biosynthetic process	23	10	43.5	6.76	11.38	5.95E-07
GO:0034660	ncRNA metabolic process	195	32	16.4	2.55	2.97	7.40E-07
GO:0009066	aspartate family amino acid metabolic process	47	14	29.8	4.63	6.31	8.31E-07
GO:0006091	generation of precursor metabolites and energy	91	20	22	3.42	4.21	9.19E-07
GO:0046040	IMP metabolic process	11	7	63.6	9.9	25.77	1.15E-06
GO:0006188	IMP biosynthetic process	11	7	63.6	9.9	25.77	1.15E-06

GO:0019637	organophosphate metabolic process	259	38	14.7	2.28	2.61	1.25E-06
GO:0009165	nucleotide biosynthetic process	78	18	23.1	3.59	4.48	1.52E-06
GO:1901293	nucleoside phosphate biosynthetic process	80	18	22.5	3.5	4.33	2.25E-06
GO:0009167	purine ribonucleoside monophosphate metabolic process	26	10	38.5	5.98	9.24	2.32E-06
GO:0072522	purine-containing compound biosynthetic process	51	14	27.5	4.27	5.62	2.47E-06
GO:0009081	branched-chain amino acid metabolic process	21	9	42.9	6.66	11.07	2.58E-06
GO:0009073	aromatic amino acid family biosynthetic process	12	7	58.3	9.07	20.62	2.61E-06
GO:0006164	purine nucleotide biosynthetic process	45	13	28.9	4.49	6.03	3.02E-06
GO:0009152	purine ribonucleotide biosynthetic process	45	13	28.9	4.49	6.03	3.02E-06
GO:0009067	aspartate family amino acid biosynthetic process	35	11	31.4	4.89	6.78	7.12E-06
GO:0022607	cellular component assembly	158	26	16.5	2.56	2.96	7.73E-06
GO:0055086	nucleobase-containing small molecule metabolic process	189	29	15.3	2.39	2.73	9.62E-06
GO:0009069	serine family amino acid metabolic process	36	11	30.6	4.75	6.51	9.66E-06
GO:0006525	arginine metabolic process	14	7	50	7.78	14.72	1.01E-05
GO:0006165	nucleoside diphosphate phosphorylation	19	8	42.1	6.55	10.72	1.12E-05
GO:0046939	nucleotide phosphorylation	19	8	42.1	6.55	10.72	1.12E-05
GO:0065003	protein-containing complex assembly	115	21	18.3	2.84	3.34	1.13E-05
GO:0042274	ribosomal small subunit biogenesis	15	7	46.7	7.26	12.88	1.79E-05
GO:0042255	ribosome assembly	15	7	46.7	7.26	12.88	1.79E-05
GO:0006414	translational elongation	15	7	46.7	7.26	12.88	1.79E-05
GO:0043933	protein-containing complex subunit organization	128	22	17.2	2.67	3.1	1.91E-05
GO:0044085	cellular component biogenesis	295	38	12.9	2	2.23	2.80E-05
GO:0034622	cellular protein-containing complex assembly	104	19	18.3	2.84	3.33	2.93E-05
GO:0009132	nucleoside diphosphate metabolic process	23	8	34.8	5.41	7.86	5.75E-05
GO:0006096	glycolytic process	18	7	38.9	6.05	9.36	7.47E-05
GO:0006757	ATP generation from ADP	18	7	38.9	6.05	9.36	7.47E-05
GO:0046112	nucleobase biosynthetic process	14	6	42.9	6.66	11.02	0.00013241
GO:0034248	regulation of cellular amide metabolic process	47	11	23.4	3.64	4.51	0.00014651
GO:0006417	regulation of translation	47	11	23.4	3.64	4.51	0.00014651
GO:0009185	ribonucleoside diphosphate metabolic process	21	7	33.3	5.18	7.35	0.00023018
GO:0046031	ADP metabolic process	21	7	33.3	5.18	7.35	0.00023018
GO:0009179	purine ribonucleoside diphosphate metabolic process	21	7	33.3	5.18	7.35	0.00023018
GO:0009135	purine nucleoside diphosphate metabolic process	21	7	33.3	5.18	7.35	0.00023018
GO:0009099	valine biosynthetic process	3	3	100	15.55	inf	0.00026456
GO:0006090	pyruvate metabolic process	22	7	31.8	4.95	6.86	0.00031906
GO:0000096	sulfur amino acid metabolic process	29	8	27.6	4.29	5.61	0.00035693
GO:0010608	posttranscriptional regulation of gene expression	52	11	21.2	3.29	3.96	0.00037892
GO:0090407	organophosphate biosynthetic process	168	23	13.7	2.13	2.36	0.00044805
GO:0006534	cysteine metabolic process	17	6	35.3	5.49	8.01	0.00046198

GO:0009070	serine family amino acid biosynthetic process	17	6	35.3	5.49	8.01	0.00046198
GO:0006541	glutamine metabolic process	17	6	35.3	5.49	8.01	0.00046198
GO:0006536	glutamate metabolic process	12	5	41.7	6.48	10.48	0.00058537
GO:0044260	cellular macromolecule metabolic process	1298	111	8.6	1.33	1.45	0.00067416
GO:0032268	regulation of cellular protein metabolic process	73	13	17.8	2.77	3.2	0.00067662
GO:0140694	non-membrane-bounded organelle assembly	25	7	28	4.35	5.72	0.00075942
GO:0006740	NADPH regeneration	8	4	50	7.78	14.65	0.00096132
GO:0019346	transsulfuration	8	4	50	7.78	14.65	0.00096132
GO:0050667	homocysteine metabolic process	8	4	50	7.78	14.65	0.00096132
GO:0009220	pyrimidine ribonucleotide biosynthetic process	8	4	50	7.78	14.65	0.00096132
GO:0051156	glucose 6-phosphate metabolic process	8	4	50	7.78	14.65	0.00096132
GO:0009092	homoserine metabolic process	8	4	50	7.78	14.65	0.00096132
GO:0006098	pentose-phosphate shunt	8	4	50	7.78	14.65	0.00096132
GO:0051246	regulation of protein metabolic process	76	13	17.1	2.66	3.05	0.00100333
GO:0000028	ribosomal small subunit assembly	4	3	75	11.66	43.88	0.00100746
GO:0000022	mitotic spindle elongation	4	3	75	11.66	43.88	0.00100746
GO:0042254	ribosome biogenesis	130	18	13.8	2.15	2.38	0.00159353
GO:0000097	sulfur amino acid biosynthetic process	21	6	28.6	4.44	5.87	0.00162392
GO:0042401	cellular biogenic amine biosynthetic process	9	4	44.4	6.91	11.72	0.00164273
GO:0030490	maturation of SSU-rRNA	9	4	44.4	6.91	11.72	0.00164273
GO:0009309	amine biosynthetic process	9	4	44.4	6.91	11.72	0.00164273
GO:0000462	maturation of SSU-rRNA from tricistronic rRNA transcript (SSU-rRNA, 5.8S rRNA, LSU-rRNA)	9	4	44.4	6.91	11.72	0.00164273
GO:0019878	lysine biosynthetic process via aminoadipic acid	9	4	44.4	6.91	11.72	0.00164273
GO:0009218	pyrimidine ribonucleotide metabolic process	9	4	44.4	6.91	11.72	0.00164273
GO:0009085	lysine biosynthetic process	15	5	33.3	5.18	7.33	0.00188817
GO:0070925	organelle assembly	29	7	24.1	3.75	4.68	0.00196975
GO:0006793	phosphorus metabolic process	451	45	10	1.55	1.67	0.00197864
GO:0009112	nucleobase metabolic process	22	6	27.3	4.24	5.5	0.00211324
GO:0008150	biological process	5316	374	7	1.09	1.3	0.00223194
GO:0043648	dicarboxylic acid metabolic process	46	9	19.6	3.04	3.58	0.00227523
GO:0015687	ferric-hydroxamate import into cell	5	3	60	9.33	21.94	0.00239818
GO:0051231	spindle elongation	5	3	60	9.33	21.94	0.00239818
GO:0006573	valine metabolic process	5	3	60	9.33	21.94	0.00239818
GO:0005991	trehalose metabolic process	5	3	60	9.33	21.94	0.00239818
GO:1901678	iron coordination entity transport	5	3	60	9.33	21.94	0.00239818
GO:0006549	isoleucine metabolic process	5	3	60	9.33	21.94	0.00239818
GO:0033214	siderophore-dependent iron import into cell	5	3	60	9.33	21.94	0.00239818
GO:0042928	ferrichrome import into cell	5	3	60	9.33	21.94	0.00239818
GO:0009097	isoleucine biosynthetic process	5	3	60	9.33	21.94	0.00239818
GO:0006796	phosphate-containing compound metabolic process	443	44	9.9	1.54	1.66	0.00241752
GO:0046653	tetrahydrofolate metabolic process	10	4	40	6.22	9.76	0.00259952

GO:1901135	carbohydrate derivative metabolic process	300	32	10.7	1.66	1.78	0.00314354
GO:0006555	methionine metabolic process	17	5	29.4	4.57	6.11	0.00349481
GO:0006553	lysine metabolic process	17	5	29.4	4.57	6.11	0.00349481
GO:0046034	ATP metabolic process	49	9	18.4	2.86	3.31	0.00357321
GO:0006790	sulfur compound metabolic process	98	14	14.3	2.22	2.46	0.00381476
GO:0006544	glycine metabolic process	11	4	36.4	5.66	8.37	0.003879
GO:0044208	'de novo' AMP biosynthetic process	2	2	100	15.55	inf	0.00412799
GO:0052031	modulation by symbiont of host defense response	2	2	100	15.55	inf	0.00412799
GO:0044416	induction by symbiont of host defense response	2	2	100	15.55	inf	0.00412799
GO:0006241	CTP biosynthetic process	2	2	100	15.55	inf	0.00412799
GO:0046036	CTP metabolic process	2	2	100	15.55	inf	0.00412799
GO:0046037	GMP metabolic process	2	2	100	15.55	inf	0.00412799
GO:0010133	proline catabolic process to glutamate	2	2	100	15.55	inf	0.00412799
GO:0006177	GMP biosynthetic process	2	2	100	15.55	inf	0.00412799
GO:0009209	pyrimidine ribonucleoside triphosphate biosynthetic process	2	2	100	15.55	inf	0.00412799
GO:0006430	lysyl-tRNA aminoacylation	2	2	100	15.55	inf	0.00412799
GO:0009208	pyrimidine ribonucleoside triphosphate metabolic process	2	2	100	15.55	inf	0.00412799
GO:0006429	leucyl-tRNA aminoacylation	2	2	100	15.55	inf	0.00412799
GO:0031349	positive regulation of defense response	2	2	100	15.55	inf	0.00412799
GO:0035999	tetrahydrofolate interconversion	6	3	50	7.78	14.62	0.00456772
GO:0019856	pyrimidine nucleobase biosynthetic process	6	3	50	7.78	14.62	0.00456772
GO:0006206	pyrimidine nucleobase metabolic process	6	3	50	7.78	14.62	0.00456772
GO:0000027	ribosomal large subunit assembly	6	3	50	7.78	14.62	0.00456772
GO:0006221	pyrimidine nucleotide biosynthetic process	12	4	33.3	5.18	7.32	0.00552581
GO:0006739	NADP metabolic process	12	4	33.3	5.18	7.32	0.00552581
GO:0006826	iron ion transport	19	5	26.3	4.09	5.23	0.00590111
GO:0009072	aromatic amino acid family metabolic process	35	7	20	3.11	3.67	0.00607078
GO:0072528	pyrimidine-containing compound biosynthetic process	20	5	25	3.89	4.88	0.00745958
GO:0043650	dicarboxylic acid biosynthetic process	13	4	30.8	4.79	6.51	0.00758118
GO:0006560	proline metabolic process	13	4	30.8	4.79	6.51	0.00758118
GO:0042273	ribosomal large subunit biogenesis	13	4	30.8	4.79	6.51	0.00758118
GO:0098754	detoxification	7	3	42.9	6.66	10.97	0.00761373
GO:0042435	indole-containing compound biosynthetic process	7	3	42.9	6.66	10.97	0.00761373
GO:0006220	pyrimidine nucleotide metabolic process	14	4	28.6	4.44	5.86	0.0100823
GO:0006760	folic acid-containing compound metabolic process	14	4	28.6	4.44	5.86	0.0100823
GO:0019344	cysteine biosynthetic process	8	3	37.5	5.83	8.77	0.01160517
GO:0009113	purine nucleobase biosynthetic process	8	3	37.5	5.83	8.77	0.01160517
GO:0033212	iron import into cell	8	3	37.5	5.83	8.77	0.01160517
GO:0006595	polyamine metabolic process	3	2	66.7	10.37	29.2	0.01185485
GO:0005992	trehalose biosynthetic process	3	2	66.7	10.37	29.2	0.01185485

GO:0052200	response to host defenses	3	2	66.7	10.37	29.2	0.01185485
GO:0052173	response to defenses of other organism	3	2	66.7	10.37	29.2	0.01185485
GO:0006596	polyamine biosynthetic process	3	2	66.7	10.37	29.2	0.01185485
GO:0008615	pyridoxine biosynthetic process	3	2	66.7	10.37	29.2	0.01185485
GO:0006432	phenylalanyl-tRNA aminoacylation	3	2	66.7	10.37	29.2	0.01185485
GO:0046351	disaccharide biosynthetic process	3	2	66.7	10.37	29.2	0.01185485
GO:0009148	pyrimidine nucleoside triphosphate biosynthetic process	3	2	66.7	10.37	29.2	0.01185485
GO:0075136	response to host	3	2	66.7	10.37	29.2	0.01185485
GO:0018216	peptidyl-arginine methylation	3	2	66.7	10.37	29.2	0.01185485
GO:1990748	cellular detoxification	3	2	66.7	10.37	29.2	0.01185485
GO:0044003	modulation by symbiont of host process	3	2	66.7	10.37	29.2	0.01185485
GO:0097237	cellular response to toxic substance	3	2	66.7	10.37	29.2	0.01185485
GO:0009423	chorismate biosynthetic process	3	2	66.7	10.37	29.2	0.01185485
GO:0044272	sulfur compound biosynthetic process	49	8	16.3	2.54	2.87	0.01207989
GO:0009086	methionine biosynthetic process	15	4	26.7	4.15	5.32	0.01306199
GO:0006730	one-carbon metabolic process	15	4	26.7	4.15	5.32	0.01306199
GO:0055072	iron ion homeostasis	15	4	26.7	4.15	5.32	0.01306199
GO:0042558	pteridine-containing compound metabolic process	15	4	26.7	4.15	5.32	0.01306199
GO:0042886	amide transport	15	4	26.7	4.15	5.32	0.01306199
GO:0072527	pyrimidine-containing compound metabolic process	23	5	21.7	3.38	4.07	0.01380481
GO:0048878	chemical homeostasis	51	8	15.7	2.44	2.73	0.01524844
GO:0098657	import into cell	9	3	33.3	5.18	7.31	0.01658639
GO:0046173	polyol biosynthetic process	9	3	33.3	5.18	7.31	0.01658639
GO:0007052	mitotic spindle organization	9	3	33.3	5.18	7.31	0.01658639
GO:0016052	carbohydrate catabolic process	151	17	11.3	1.75	1.87	0.01679646
GO:0000041	transition metal ion transport	33	6	18.2	2.83	3.26	0.01720555
GO:0055082	cellular chemical homeostasis	43	7	16.3	2.53	2.85	0.01868194
GO:0055076	transition metal ion homeostasis	25	5	20	3.11	3.66	0.01961011
GO:0046148	pigment biosynthetic process	25	5	20	3.11	3.66	0.01961011
GO:0006081	cellular aldehyde metabolic process	10	3	30	4.67	6.26	0.02258076
GO:0016226	iron-sulfur cluster assembly	10	3	30	4.67	6.26	0.02258076
GO:0031163	metallo-sulfur cluster assembly	10	3	30	4.67	6.26	0.02258076
GO:0000162	tryptophan biosynthetic process	4	2	50	7.78	14.6	0.02270225
GO:0070813	hydrogen sulfide metabolic process	4	2	50	7.78	14.6	0.02270225
GO:0006551	leucine metabolic process	4	2	50	7.78	14.6	0.02270225
GO:0008614	pyridoxine metabolic process	4	2	50	7.78	14.6	0.02270225
GO:0070814	hydrogen sulfide biosynthetic process	4	2	50	7.78	14.6	0.02270225
GO:0018195	peptidyl-arginine modification	4	2	50	7.78	14.6	0.02270225
GO:0006167	AMP biosynthetic process	4	2	50	7.78	14.6	0.02270225
GO:0019722	calcium-mediated signaling	4	2	50	7.78	14.6	0.02270225
GO:0046219	indolalkylamine biosynthetic process	4	2	50	7.78	14.6	0.02270225
GO:0009098	leucine biosynthetic process	4	2	50	7.78	14.6	0.02270225

GO:0009312	oligosaccharide biosynthetic process	4	2	50	7.78	14.6	0.02270225
GO:0032787	monocarboxylic acid metabolic process	98	12	12.2	1.9	2.05	0.02279662
GO:0044262	cellular carbohydrate metabolic process	87	11	12.6	1.97	2.13	0.02308602
GO:0006725	cellular aromatic compound metabolic process	1163	91	7.8	1.22	1.28	0.0238931
GO:0005996	monosaccharide metabolic process	36	6	16.7	2.59	2.93	0.02573158
GO:0006448	regulation of translational elongation	11	3	27.3	4.24	5.48	0.02959392
GO:0005984	disaccharide metabolic process	11	3	27.3	4.24	5.48	0.02959392
GO:0006563	L-serine metabolic process	11	3	27.3	4.24	5.48	0.02959392
GO:0045727	positive regulation of translation	11	3	27.3	4.24	5.48	0.02959392
GO:0034250	positive regulation of cellular amide metabolic process	11	3	27.3	4.24	5.48	0.02959392
GO:0051247	positive regulation of protein metabolic process	19	4	21.1	3.27	3.9	0.03025774
GO:0032270	positive regulation of cellular protein metabolic process	19	4	21.1	3.27	3.9	0.03025774
GO:0042819	vitamin B6 biosynthetic process	5	2	40	6.22	9.73	0.03623829
GO:0009147	pyrimidine nucleoside triphosphate metabolic process	5	2	40	6.22	9.73	0.03623829
GO:0042816	vitamin B6 metabolic process	5	2	40	6.22	9.73	0.03623829
GO:0046417	chorismate metabolic process	5	2	40	6.22	9.73	0.03623829
GO:1901701	cellular response to oxygen-containing compound	5	2	40	6.22	9.73	0.03623829
GO:0006207	'de novo' pyrimidine nucleobase biosynthetic process	5	2	40	6.22	9.73	0.03623829
GO:0006546	glycine catabolic process	5	2	40	6.22	9.73	0.03623829
GO:0044205	'de novo' UMP biosynthetic process	5	2	40	6.22	9.73	0.03623829
GO:0006566	threonine metabolic process	5	2	40	6.22	9.73	0.03623829
GO:0051701	biological process involved in interaction with host	5	2	40	6.22	9.73	0.03623829
GO:0006531	aspartate metabolic process	5	2	40	6.22	9.73	0.03623829
GO:0006562	proline catabolic process	5	2	40	6.22	9.73	0.03623829
GO:0031347	regulation of defense response	5	2	40	6.22	9.73	0.03623829
GO:0006575	cellular modified amino acid metabolic process	39	6	15.4	2.39	2.66	0.03668299
GO:0010557	positive regulation of macromolecule biosynthetic process	12	3	25	3.89	4.87	0.03761663
GO:0031328	positive regulation of cellular biosynthetic process	12	3	25	3.89	4.87	0.03761663
GO:0009891	positive regulation of biosynthetic process	12	3	25	3.89	4.87	0.03761663
GO:1902850	microtubule cytoskeleton organization involved in mitosis	12	3	25	3.89	4.87	0.03761663
GO:0005975	carbohydrate metabolic process	348	31	8.9	1.39	1.45	0.03969052
GO:0098771	inorganic ion homeostasis	40	6	15	2.33	2.58	0.04090563
GO:0050801	ion homeostasis	40	6	15	2.33	2.58	0.04090563
GO:0055080	cation homeostasis	40	6	15	2.33	2.58	0.04090563
GO:0072525	pyridine-containing compound biosynthetic process	21	4	19	2.96	3.44	0.04223353
GO:0071840	cellular component organization or biogenesis	624	51	8.2	1.27	1.32	0.04287697
GO:0019725	cellular homeostasis	62	8	12.9	2.01	2.17	0.04391927
GO:0009060	aerobic respiration	41	6	14.6	2.28	2.51	0.04542309
GO:0042440	pigment metabolic process	31	5	16.1	2.51	2.81	0.04578537
GO:0006879	cellular iron ion homeostasis	13	3	23.1	3.59	4.38	0.04662726

GO:0007051	spindle organization	13	3	23.1	3.59	4.38	0.04662726
GO:0046686	response to cadmium ion	13	3	23.1	3.59	4.38	0.04662726
GO:0046916	cellular transition metal ion homeostasis	22	4	18.2	2.83	3.25	0.04908719
GO:0072524	pyridine-containing compound metabolic process	22	4	18.2	2.83	3.25	0.04908719

Supplementary table 7. Top 50 genes most down-regulated and top 50 genes most up-regulated in presence of TC3 at 3DPI.

Gene	Description and informations from FungiDB	Gene ID	log 2 fold change
<b>Down-regulated genes</b>			
hypothetical protein FPSE_05362	secondary metabolite cluster, C19, predicted secreted, predicted Non-effector	FGRAMPH1_01G14021	-9.017
integral membrane		FGRAMPH1_01G16517	-8.659
hypothetical protein	predicted secreted, predicted Effector	FGRAMPH1_01G13355	-7.577
unnamed protein product		FGRAMPH1_01G04187	-6.931
alpha-ketoglutarate-dependent sulfonate dioxygenase	This gene is exclusively expressed in wheat, as identified from comparative transcriptomic analyses	FGRAMPH1_01G15839	-6.914
hypothetical protein		FGRAMPH1_01G16325	-6.632
hypothetical protein		FGRAMPH1_01G12133	-6.474
phthalate transporter		FGRAMPH1_01G25487	-6.403
fatty acid synthase beta subunit	secondary metabolite cluster, C2 gramillin (Expanded)	FGRAMPH1_01G00131	-6.174
hypothetical protein	secondary metabolite cluster, C2 gramillin (Expanded)	FGRAMPH1_01G00153	-5.999
branched-chain-amino-acid aminotransferase	secondary metabolite cluster, C2 gramillin (Expanded)	FGRAMPH1_01G00157	-5.93
Oxoglutarate iron-dependent oxygenase	secondary metabolite cluster, C2 gramillin (Expanded)	FGRAMPH1_01G00155	-5.754
hypothetical protein		FGRAMPH1_01G03971	-5.601
hypothetical protein	Tymovirus 45/70Kd protein	FGRAMPH1_01G04951	-5.461
taurine dioxygenase	secondary metabolite cluster, C40; This gene is exclusively expressed in wheat, as identified from comparative transcriptomic analyses	FGRAMPH1_01G25163	-5.359
short-chain dehydrogenase reductase	secondary metabolite cluster, C64(Expanded)	FGRAMPH1_01G20957	-5.355
thermophilic desulfurizing enzyme	This gene is exclusively expressed in wheat, as identified from comparative transcriptomic analyses	FGRAMPH1_01G13347	-5.348
Aspartyl-tRNA synthetase		FGRAMPH1_01G16673	-5.244
TRI 3	secondary metabolite cluster, C23 TRI	FGRAMPH1_01G13105	-5.175
fatty acid synthase alpha partial	secondary metabolite cluster, C2 gramillin (Expanded)	FGRAMPH1_01G00127	-5
cytochrome p450 family	secondary metabolite cluster, C64 FUMONISIN(Expanded)	FGRAMPH1_01G20961	-4.991
NRPS9	secondary metabolite cluster, C64 FUMONISIN (Expanded)	FGRAMPH1_01G20959	-4.988
nonribosomal peptide synthetase	secondary metabolite cluster, C22(Expanded); This gene is exclusively expressed in wheat, as identified from comparative transcriptomic analyses	FGRAMPH1_01G13581	-4.957
hypothetical protein	predicted secreted, predicted Non-effector	FGRAMPH1_01G25485	-4.918
hydrolase or acyltransferase of alpha beta superfamily	secondary metabolite cluster, C2 gramillin (Expanded)	FGRAMPH1_01G00147	-4.91
Tri 5	secondary metabolite cluster, C23 TRI; Tri 5	FGRAMPH1_01G13111	-4.9
thioredoxin reductase	secondary metabolite cluster, C2 gramillin (Expanded)	FGRAMPH1_01G00145	-4.88
acid phosphatase	predicted secreted, predicted Non-effector	FGRAMPH1_01G15463	-4.823
GRA1	NRPS; gramillin; secondary metabolite cluster, C2(Expanded); GRA1 gene encodes	FGRAMPH1_01G00143	-4.821

	nonribosomal peptide synthetase 8 which is required for the biosynthesis of two bicyclic lipopeptides, gramillin A and gramillin B		
O-methylsterigmatocystin oxidoreductase	secondary metabolite cluster, C1; CLM2 encodes a regio- and stereoselective cytochrome P450 monooxygenase for C-11 of longiborneol in culmorin biosynthesis.	FGRAMPH1_01G00053	-4.795
2-isopropylmalate synthase	secondary metabolite cluster, C64 FUMONISIN	FGRAMPH1_01G20965	-4.765
siderophore iron transporter mirb	secondary metabolite cluster, C22(Expanded)	FGRAMPH1_01G13583	-4.746
nad dependent epimerase		FGRAMPH1_01G10207	-4.665
trichothecene biosynthesis gene	secondary metabolite cluster, C23 TRI; Subcellular localization of Tri14 protein	FGRAMPH1_01G13123	-4.639
TRI9	secondary metabolite cluster, C23 TRI	FGRAMPH1_01G13115	-4.625
NRPS5	secondary metabolite cluster, C64 FUMONISIN (Expanded)	FGRAMPH1_01G20955	-4.573
glucose 1-dehydrogenase	secondary metabolite cluster, C64 FUMONISIN(Expanded)	FGRAMPH1_01G20963	-4.538
sterigmatocystin biosynthesis monooxygenase stcW		FGRAMPH1_01G15971	-4.509
Ferric reductase transmembrane component 4		FGRAMPH1_01G16299	-4.504
fusarin C cluster-cytochrome P450	secondary metabolite cluster, C42 FUSARIN C(Expanded)	FGRAMPH1_01G25705	-4.496
Cytochrome E- group I	secondary metabolite cluster, C2(Expanded)	FGRAMPH1_01G00129	-4.49
hypothetical protein		FGRAMPH1_01G16787	-4.469
hypothetical protein		FGRAMPH1_01G21999	-4.458
hypothetical protein	predicted secreted, predicted Effector	FGRAMPH1_01G13225	-4.458
Tri4	secondary metabolite cluster, C23 TRI	FGRAMPH1_01G13107	-4.367
chry1	nonribosomal peptide synthetase; secondary metabolite cluster, C66	FGRAMPH1_01G21959	-4.356
TRII	Calonectrin oxygenase	FGRAMPH1_01G00223	-4.34
hypothetical protein	secondary metabolite cluster, C22(Expanded)	FGRAMPH1_01G13579	-4.328
unnamed protein product	secondary metabolite cluster, C2, gramillin(Expanded)	FGRAMPH1_01G00133	-4.259
fusarin C cluster-transporter	secondary metabolite cluster, C42 FUSARIN C (Expanded)	FGRAMPH1_01G25701	-4.249
<b>Up-regulated genes</b>			
bifunctional lycopene cyclase phytoene synthase	secondary metabolite cluster, C28 CAROTENOID	FGRAMPH1_01G11973	4.568
endo- -beta-xylanase		FGRAMPH1_01G08045	4.591
ATPase		FGRAMPH1_01G13949	4.62
bHLH009	allergen fus c 3; Transcription factor	FGRAMPH1_01G14303	4.66
ZC242	cercosporin resistance; Transcription factor	FGRAMPH1_01G22663	4.662
thioredoxin reductase	secondary metabolite cluster, C27(Expanded)	FGRAMPH1_01G12441	4.681
hypothetical protein		FGRAMPH1_01G01495	4.687
GMC oxidoreductase	predicted secreted, predicted Non-effector	FGRAMPH1_01G21537	4.726
hypothetical protein		FGRAMPH1_01G25969	4.726
phytoene dehydrogenase	secondary metabolite cluster, C28 CAROTENOID	FGRAMPH1_01G11971	4.744
hypothetical protein		FGRAMPH1_01G08431	4.771
hypothetical protein		FGRAMPH1_01G08473	4.825
cryptochrome DASH		FGRAMPH1_01G10993	4.901
hypothetical protein FPSE_05362	secondary metabolite cluster, C19, predicted secreted, predicted Non-effector	FGRAMPH1_01G23453	4.913
hypothetical protein		FGRAMPH1_01G11591	4.927
n amino acid transport system	secondary metabolite cluster, C52	FGRAMPH1_01G27977	4.976

unnamed protein product	This gene is exclusively expressed in wheat, as identified from comparative transcriptomic analyses; predicted secreted, predicted Non-effector	FGRAMPH1_01G21223	5.013
amino acid transporter		FGRAMPH1_01G11689	5.062
unnamed protein product		FGRAMPH1_01G00093	5.064
neutral amino acid permease		FGRAMPH1_01G15375	5.081
probable lactonohydrolase	predicted secreted, predicted Non-effector	FGRAMPH1_01G13775	5.129
unnamed protein product		FGRAMPH1_01G22203	5.177
unnamed protein product		FGRAMPH1_01G11605	5.206
hypothetical protein	predicted secreted, predicted Non-effector	FGRAMPH1_01G04075	5.258
hypothetical protein		FGRAMPH1_01G20819	5.3
unnamed protein product	predicted secreted GPI anchored, predicted Non-effector	FGRAMPH1_01G11597	5.371
murein transglycosylase	predicted secreted, predicted Non-effector	FGRAMPH1_01G19765	5.557
conserved serine-rich		FGRAMPH1_01G16281	5.589
monophenol monooxygenase (tyrosinase)	predicted secreted, predicted Non-effector	FGRAMPH1_01G22097	5.636
hypothetical protein	secondary metabolite cluster, C66	FGRAMPH1_01G21951	5.693
3-dehydroquinate synthase	AroB, 3-dehydroquinate synthetase	FGRAMPH1_01G25135	5.696
dicarboxylic amino acid permease	secondary metabolite cluster, C6	FGRAMPH1_01G04077	5.703
mannose-specific lectin		FGRAMPH1_01G13805	5.762
g- coupled receptor		FGRAMPH1_01G11671	5.878
hypothetical protein		FGRAMPH1_01G22895	5.97
hypothetical protein		FGRAMPH1_01G18953	6.063
related to DUF124 domain		FGRAMPH1_01G04361	6.217
hypothetical protein	secondary metabolite cluster, C60 FUSARIELIN (Expanded)	FGRAMPH1_01G08181	6.221
sphingoid long-chain base transporter rsb1		FGRAMPH1_01G15495	6.41
Bifunctional xylanase deacetylase		FGRAMPH1_01G18451	6.665
mfs fhs l-fucose permease		FGRAMPH1_01G13917	7.027
unnamed protein product		FGRAMPH1_01G05799	7.05
neutral amino acid permease		FGRAMPH1_01G00331	7.2
integral membrane PTH11		FGRAMPH1_01G12565	7.257
hypothetical protein		FGRAMPH1_01G13777	7.301
murein transglycosylase	predicted secreted, predicted Non-effector	FGRAMPH1_01G13337	7.314
family inorganic phosphate transporter		FGRAMPH1_01G12227	7.689
related to monophenol monooxygenase (tyrosinase)	predicted secreted, predicted Non-effector	FGRAMPH1_01G04801	7.718
hypothetical protein	predicted secreted, predicted Effector	FGRAMPH1_01G04265	8.086
Ferric reductase transmembrane component 4	secondary metabolite cluster, C8	FGRAMPH1_01G04343	8.125

Supplementary table 8. Top 50 genes most down-regulated and top 50 genes most up-regulated in presence of TC3 at 5DPI.

Gene	Description and informations from FungiDB	Gene ID	log 2 fold change
<b>Down-regulated genes</b>			
choline monooxygenase		FGRAMPH1_01G12833	-10.983
alkaline ceramidase	predicted secreted, predicted Non-effector	FGRAMPH1_01G16201	-9.823
cytochrome oxidoreductase p450		FGRAMPH1_01G11593	-9.76

salicylate hydroxylase	secondary metabolite cluster, C52	FGRAMPH1_01G28011	-9.566
hypothetical protein		FGRAMPH1_01G03585	-8.81
endochitinase precursor	42 kDa endochitinase precursor	FGRAMPH1_01G13235	-8.616
dimethylglycine oxidase	secondary metabolite cluster, C25	FGRAMPH1_01G12827	-8.334
hypothetical protein		FGRAMPH1_01G15827	-8.141
related to ethionine resistance		FGRAMPH1_01G05323	-8.034
hypothetical protein		FGRAMPH1_01G18499	-7.54
related to GABA permease		FGRAMPH1_01G22565	-7.531
hypothetical protein		FGRAMPH1_01G10907	-7.48
multidrug resistance fnx1		FGRAMPH1_01G03861	-7.465
hypothetical protein		FGRAMPH1_01G09355	-7.324
hypothetical protein		FGRAMPH1_01G13491	-7.11
hypothetical protein		FGRAMPH1_01G06535	-6.951
cholin permease		FGRAMPH1_01G05325	-6.867
hypothetical protein	secondary metabolite cluster, C16(Expanded)	FGRAMPH1_01G15667	-6.823
urea active transporter 1		FGRAMPH1_01G12089	-6.795
aliphatic nitrilase		FGRAMPH1_01G22385	-6.793
agmatinase 1	predicted secreted, predicted Non-effector	FGRAMPH1_01G05321	-6.516
aldoxime dehydratase		FGRAMPH1_01G22389	-6.501
hypothetical protein		FGRAMPH1_01G28183	-6.469
aspergillopepsin-2 precursor	predicted secreted, predicted Non-effector	FGRAMPH1_01G09337	-6.381
membrane transporter	secondary metabolite cluster, C52	FGRAMPH1_01G28017	-6.38
integral membrane		FGRAMPH1_01G03981	-6.319
electron transport		FGRAMPH1_01G05711	-6.292
fad linked oxidase		FGRAMPH1_01G13987	-6.283
flavin-containing amine oxidase dehydrogenase		FGRAMPH1_01G28019	-6.152
hypothetical protein		FGRAMPH1_01G14193	-5.911
maleylacetoacetate isomerase		FGRAMPH1_01G11461	-5.854
Triacylglycerol lipase	predicted secreted, predicted Non-effector	FGRAMPH1_01G04165	-5.84
Lysine biosynthesis regulatory LYS14	Transcription factor	FGRAMPH1_01G05319	-5.722
hypothetical protein FPSE_03282		FGRAMPH1_01G22065	-5.672
extracellular lipase	predicted secreted, predicted Non-effector ; FGL1,extracellular lipase,	FGRAMPH1_01G19051	-5.639
hypothetical protein		FGRAMPH1_01G15825	-5.545
DAL5-Allantoate and ureidosuccinate permease		FGRAMPH1_01G00587	-5.355
ethanolamine utilization		FGRAMPH1_01G18503	-5.289
homoserine o-acetyltransferase		FGRAMPH1_01G28061	-5.201
L-amino-acid oxidase precursor		FGRAMPH1_01G08611	-5.18
glucosamine 6-phosphate N-acetyltransferase		FGRAMPH1_01G15549	-5.1
related to C6 transcription factor	secondary metabolite cluster, C25 ; Transcription factor	FGRAMPH1_01G12829	-5.086
hypothetical protein		FGRAMPH1_01G04325	-5.016
hypothetical protein		FGRAMPH1_01G00439	-5.012
serine threonine kinase		FGRAMPH1_01G18949	-5.011
hypothetical protein		FGRAMPH1_01G15155	-4.966

hypothetical protein		FGRAMPH1_01G22895	-4.926
hypothetical protein		FGRAMPH1_01G05205	-4.82
catalase		FGRAMPH1_01G11527	-4.76
hypothetical protein	predicted secreted, predicted Effector	FGRAMPH1_01G25985	-4.735
<b>Up-regulated genes</b>			
FAD-dependent monooxygenase	secondary metabolite cluster, C16(Expanded)	FGRAMPH1_01G15661	3.266
averantin oxidoreductase	secondary metabolite cluster, C16(Expanded)	FGRAMPH1_01G15651	3.276
asparagine synthase	secondary metabolite cluster, C66	FGRAMPH1_01G21961	3.288
amino acid transporter		FGRAMPH1_01G11689	3.29
vegetative incompatibility hte-1		FGRAMPH1_01G08559	3.298
unnamed protein product		FGRAMPH1_01G00181	3.318
Myb007	Transcriptional activator Myb	FGRAMPH1_01G06093	3.358
unnamed protein product		FGRAMPH1_01G04123	3.369
hypothetical protein		FGRAMPH1_01G05861	3.41
hypothetical protein		FGRAMPH1_01G13777	3.47
Transforming growth factor-beta-induced ig-h3	predicted secreted GPI anchored, predicted Non-effector	FGRAMPH1_01G22661	3.488
Ferric reductase transmembrane component 4	secondary metabolite cluster, C8	FGRAMPH1_01G04343	3.499
XYLC	endo-1,4-beta-xylanase precursor ; predicted secreted, predicted Effector	FGRAMPH1_01G22187	3.506
hypothetical protein		FGRAMPH1_01G04919	3.515
endo- -beta-xylanase		FGRAMPH1_01G08045	3.516
hypothetical protein		FGRAMPH1_01G10975	3.516
chry3	GA4 desaturase	FGRAMPH1_01G21963	3.6
unnamed protein product	secondary metabolite cluster, C1, predicted secreted, predicted Non-effector	FGRAMPH1_01G00071	3.609
hypothetical protein		FGRAMPH1_01G16219	3.631
o-methyltransferase domain	secondary metabolite cluster, C16(Expanded) ; O-methyltransferase in thePKS15cluster	FGRAMPH1_01G15649	3.647
heterokaryon incompatibility		FGRAMPH1_01G14101	3.648
serine threonine kinase		FGRAMPH1_01G15363	3.652
GMC oxidoreductase	predicted secreted, predicted Non-effector	FGRAMPH1_01G21537	3.683
C2H032	Transcription factor ; hypothetical protein	FGRAMPH1_01G16667	3.751
hypothetical protein	predicted secreted GPI anchored, predicted Non-effector	FGRAMPH1_01G04305	3.86
polyketide synthase	secondary metabolite cluster, C16(Expanded)	FGRAMPH1_01G15647	3.861
MIR1	siderophore iron transporter mirB	FGRAMPH1_01G01375	3.973
hypothetical protein		FGRAMPH1_01G06135	4.013
integral membrane	secondary metabolite cluster, C16(Expanded)	FGRAMPH1_01G15659	4.06
geranylgeranyl pyrophosphate synthetase	secondary metabolite cluster, C16(Expanded)	FGRAMPH1_01G15653	4.076
hypothetical protein		FGRAMPH1_01G19871	4.175
high-affinity fructose transporter ght6		FGRAMPH1_01G16951	4.222
WSC2 Glucoamylase III (alpha-1,4-glucan-glucosid	This gene is exclusively expressed in wheat, as identified from comparative transcriptomic analyses	FGRAMPH1_01G04303	4.258
Zinc finger ZZ-type and EF-hand domain-containin		FGRAMPH1_01G21459	4.436
related to phospholipid-translocating ATPase	secondary metabolite cluster, C54	FGRAMPH1_01G27657	4.463
chry1	nonribosomal peptide synthetase ; secondary metabolite cluster, C66	FGRAMPH1_01G21959	4.476

neutral amino acid permease		FGRAMPH1_01G00331	4.483
hypothetical protein	secondary metabolite cluster, C51	FGRAMPH1_01G08915	4.735
NACHT domain-containing		FGRAMPH1_01G21553	4.859
alpha-L-arabinofuranosidase precursor	predicted secreted, predicted Non-effector	FGRAMPH1_01G25243	4.91
peptidase m12		FGRAMPH1_01G09057	4.952
gnat family n-	secondary metabolite cluster, C49 BUTENOLIDE	FGRAMPH1_01G09073	5.217
plasma membrane yro2		FGRAMPH1_01G03539	5.407
six-bladed beta-propeller	predicted secreted, predicted Non-effector	FGRAMPH1_01G08675	5.447
small secreted	predicted secreted, predicted Effector	FGRAMPH1_01G08483	5.728
benzoate 4-monooxygenase	secondary metabolite cluster, C49 BUTENOLIDE	FGRAMPH1_01G09067	5.993
major facilitator superfamily transporter	secondary metabolite cluster, C49 BUTENOLIDE	FGRAMPH1_01G09077	6.031
glutamate decarboxylase	secondary metabolite cluster, C49 BUTENOLIDE	FGRAMPH1_01G09075	6.168
2og-fe oxygenase family	secondary metabolite cluster, C49 BUTENOLIDE	FGRAMPH1_01G09071	6.496
neutral amino acid permease		FGRAMPH1_01G15375	6.788



## B) Complementary data: effect of TC3 on *F. graminearum* mutant strains affected for their response to oxidative stress and pH changes

### I. Introduction

pH changes and oxidative stress are two key determinants governing the accumulation of mycotoxins by *F. graminearum* (Ponts, 2015)<sup>368</sup>. The fungal cell response to these abiotic factors is mediated by global transcription factors (FgPacC1 for pH and FgAP1 for oxidative stress) which were also previously reported as capable of affecting the expression of the *tri* genes (Merhej et al., 2011; Montibus et al., 2013)<sup>166,169</sup>. Results of the transcriptomic analysis described above have highlighted a modulation of the expression of various *F. graminearum* genes involved in redox and pH homeostasis. To go further and investigate the potential relation between TC3-induced perturbations in the fungal intracellular pH and redox status, the effect of TC3 was compared using wild strains and mutant strains (deleted strains for FgPacC1 and FgAP1 and strains containing truncated forms of the two previous transcription factors). This study was allowed by the availability of such mutant strains, built for previous research programs performed at the MycSA lab.

### II. Material and methods

#### a. Synthesis of tick $\gamma$ -core TickCore3

TickCore3 (TC3) is the  $\gamma$ -core of the *Ixodes ricinus* defensin DefMT3 (GenBank accession number: JAA71488). Peptide synthesis was commissioned to Pepmic (Suzhou, China) that uses solid-phase peptide synthesis (SPPS) to obtain highly-pure peptides as previously described.

#### b. *Fusarium graminearum* mutant strains, culture conditions, assessment of fungal biomass and mycotoxin yield

Characteristics of the wild and mutant strains used throughout this study are reported in Table 3.

Table 3. Fungal wild and mutant strains used in this study.

Wild strain	Mutant strain	Characteristics
Fg INRA 349 (CBS185.32)		
	Fg INRAE349- $\Delta$ FgPac1	deleted mutant strain
	Fg INRAE349 - $\Delta$ FgPac1 : FgPac1	complemented mutant strain
	Fg INRAE349 - FgPac1 <sup>C<sub>trunc</sub></sup>	mutant strain with a truncated constitutive form of FgPac1 (constitutively active)
Fg INRAE 605		
	Fg INRAE605 - $\Delta$ FgAp1	deleted mutant strain
	Fg INRAE605 - $\Delta$ FgAp1: FgAp1	complemented mutant strain
	Fg INRAE605-FgAp1 <sup>C<sub>trunc</sub></sup>	mutant strain with a truncated constitutive form of FgAP1 (constitutively expressed and located in the nucleus)

Cultures were performed in MS liquid medium supplemented or not with TC3 50  $\mu$ M, in 24-wells plates, as described in Leannec-Rialland et al. (2021)<sup>362</sup>. Mycelium biomass and mycotoxin production were quantified according to the protocols described in Leannec-Rialland et al. (2021)<sup>362</sup>.

### III. Results

Regarding strains affected in their response to oxidative stress, no difference in susceptibility towards the active TC3 peptide was observed between the wild INRAE Fg605 strain and the mutant Fg INRAE605 -  $\Delta$ FgAp1: and Fg INRAE605-FgAp1<sup>C<sub>trunc</sub></sup> strains. Their biomass and TCTB production were equally affected by TC3 (data not shown). This could suggest that a strain more or less sensitive to the presence of ROS is not more sensitive to TC3 and that a potential oxidative stress induced by TC3 exposure would not be the primary rationale for its bioactivity.

Results were different when considering *F. graminearum* FgPac1 mutant strains (Fig. 12). Corroborating the data of Merhej *et al.* (2011)<sup>166</sup>, the Fg INRAE349 - FgPac1<sup>C<sub>trunc</sub></sup> cultivated in MS medium did not produce detectable levels of TCTB. Our data also shown a reduced production of TCTB by the deleted strain, which was not previously reported in the study of Merhej *et al.* (2011)<sup>166</sup>. Nevertheless, results gathered in Figure 12 clearly evidenced that the deleted mutant strain was significantly more affected by the TC3 treatment than the wild and

complemented strain, both for its fungal biomass and its production of DON+15-ADON. Notably, a drastic reduction of the fungal biomass of the Fg INRAE349- $\Delta$ FgPac1 was induced by exposure to TC3. These observations could suggest a link between potential modifications of intracellular pH caused by TC3 and its bioactivity against *F. graminearum*. This hypothesis is also supported by the observed modulation of the expression of the FgPac1 transcription factor revealed by the transcriptomics analysis described above.

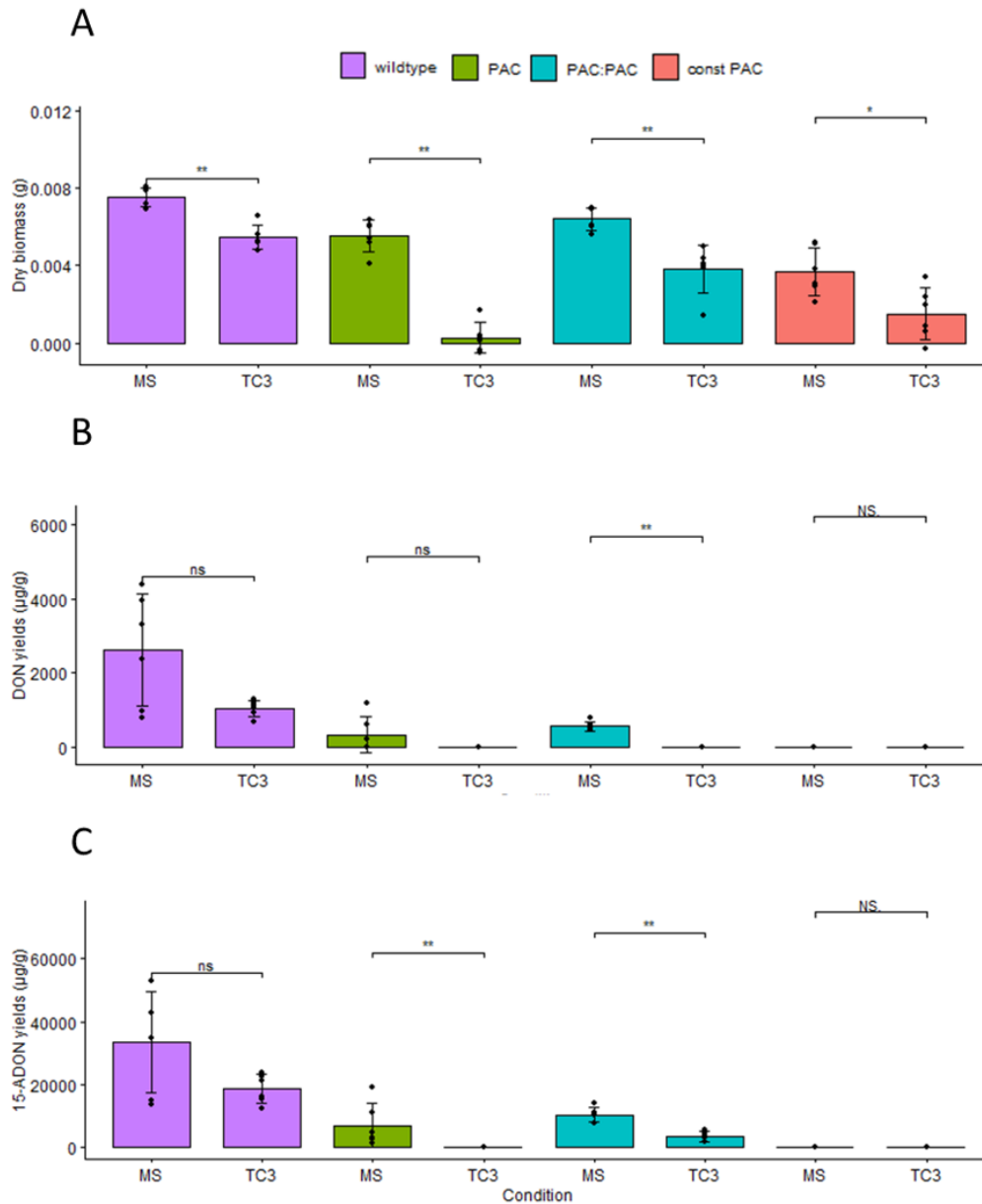


Figure 12. Antifungal and anti-mycotoxin activity of TC3 on *F. graminearum* strain INRA349 and its mutants on gene FgPac1. Effect of TC3 at 50  $\mu$ M on the fungal biomass weight of *F. graminearum* wild type, deleted mutant PAC, complemented mutant PAC:PAC and const PAC (a) and on the production of DON(b) and 15-ADON (c) in 10-day-old broths. Significant differences are labeled (\* $p$ <0.05, \*\* $p$ <0.01; ns = Not signif).

## C) Complementary data: Comparative metabolomic analysis of *F. graminearum* response to TC3 and synthetic fungicides

### I. Material and methods

#### a. Synthesis of tick $\gamma$ -core TickCore3

TickCore3 (TC3) is the  $\gamma$ -core of the *Ixodes ricinus* defensin DefMT3 (GenBank accession number: JAA71488). Peptide synthesis was commissioned to Pepmic (Suzhou, China) that uses solid-phase peptide synthesis (SPPS) to obtain highly-pure peptides as previously described.

#### b. *Fusarium graminearum* culture conditions

The *F. graminearum* CBS185.32 strain (Westerdijk Institute, The Netherlands) was selected for its capacity to produce high concentrations of DON and 15-ADON and was used throughout this study. The cultures conditions, fungal biomass weighing and mycotoxin analysis protocols were similar as those previously reported for the transcriptomic study. The control culture and 50  $\mu$ M TC3-supplemented cultures were the same as those used for RNA extraction and transcriptomic analysis. Additional cultures were performed with supplementation with synthetic fungicides including Carbendazim (Sigma-Aldrich, France), Tebuconazole (Sigma-Aldrich, France) or Azoxystrobin (Sigma-Aldrich, France) at respective concentrations of 5.25 $\mu$ M, 1.625 $\mu$ M and 5 $\mu$ M. It was verified that Carbendazim, Tebuconazole or Azoxystrobin supplementation did not modify the pH values of the treated broths compared to those of the control.

#### d. LC-MS/MS analysis of polar metabolites

LC-MS/MS analyses were performed on culture supernatants and methanolic extracts of freeze-dried and ground mycelia. For each sample, the flash-frozen mycelium was crushed using 2 stainless steel bulk beads 2.8 mm at 20Hz with 2x20 sec cycle and 10 sec break to avoid samples to heat, using a TissueLyser II (Qiagen, Venlo, The Netherlands). The powder was suspended with 1 ml of methanol-water (70:30, vol/vol) acidified with formic acid (0.1%) and containing 1.37 mM methyl vanillate (Sigma-Aldrich, France) as an internal standard. The suspension was sonicated for 15 min in an ice bath, centrifuged, and filtered on a 0.22- $\mu$ m polyvinylidene difluoride (PVDF) filter (Millex Millipore, Billerica, MA, USA) in HPLC vials. For each culture supernatant, 500 $\mu$ L were filtered on a 0.22- $\mu$ m PVDF filter (Millex Millipore, Billerica, MA, USA) and mixed with 500  $\mu$ l of methanol-water (1:1, vol/vol) and containing 2.74 mM methyl vanillate (Sigma-Aldrich, France) for a final concentration in HPLC vial of 1.37 mM methyl vanillate as an internal standard.

A vanquish UHPLC system was used to separate metabolites on a reversed-phase C18 column Hypersil GOLD aQ (100 x 2.1), 1.9  $\mu$ m. Using 0.1% acetic acid in water as solvent A, 0.1% acetic acid in acetonitrile as solvent B, and the following gradient: 0 to 1.4min, 5%B; 1.4 to 4.5min, 5%B; 4.5 to 11min, 25%; 11 to 14min, 70%; 14 to 17.5min, 95%; 17.5 to 18min, 95%; 18 to

23min, 5%. The flow rate was set at 0.4 ml/min. The column temperature was set at 35°C. The injection volume was 5 µl. Metabolites were detected using a quadrupole mass filter associated with Q Exactive Focus mass spectrometer. Electrospray ionization in positive mode with Full scan and data dependent MS2 was used. The mass spectrometer was operated in the positive ESI mode with 70k resolving power full scan acquisition in the 80-1100 m/z range. For the Data dependent MS2 (ddMS2), the resolving power is 17 500 m/z 200 with isolation window of 3.0 m/z and dynamic exclusion at 2.0s. Ion fragmentation was performed in the HCD cell and normalized collision energy was set at 30 %. The Orbitrap analyzer was calibrated with the ESI+ tune mix. Nitrogen was used as the sheath and auxiliary gas. The main MS parameters were optimized and finally set as follows: sheath gas flow rate, 50 a.u; auxiliary gas flow rate, 13 a.u.; sweep gas flow rate, 0 a.u.; spray voltage, 3.5 kV; capillary temperature, 320 °C; S lens RF level 50%; auxiliary gas heater temperature, 350°C. Each extracted sample was injected twice as technological replicates. One vial containing 10µl of each sample was used as a quality control (QC) sample and injected each 10 injections. A blank extraction was also injected to identify potential contaminants. Raw data were processed in a targeted manner using the Coumpound Discoverer 3.3 software (Thermo Scientific™).

## II.Results

The concentrations of fungicides used in this metabolomics approach have been selected after preliminary experiments, with the aim to obtain comparable reduction of biomass and mycotoxin yield between the four treatments. As observed in Figure 13, in our experimental conditions, the inhibition of fungal growth and of TCTB production induced by 50 µM TC3, 5.25 µM carbendazim, 1.625 µM tebuconazole and 5 µM azoxystrobin were in the same order of magnitude.

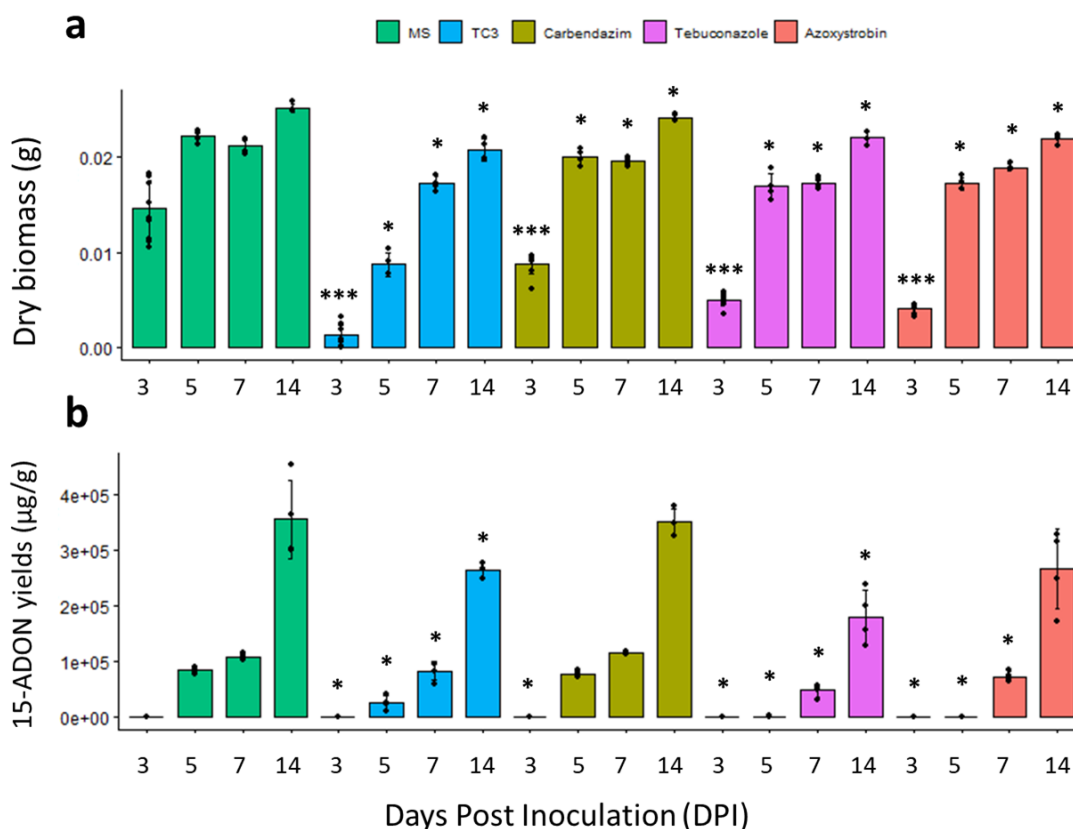


Figure 13. Antifungal and anti-mycotoxin activity of TC3 and synthetic fungicides on *F. graminearum*. Effect of TC3, Carbendazim, Tebuconazole and Azoxystrobin at the respective concentrations of 50µM, 5.25µM, 1.625µM and 5µM on the fungal biomass weight of *F. graminearum* at 3 DPI, 5 DPI, 7 DPI and 14 DPI (a) and on the production of 15-ADON (b) in 3, 5, 7 and 14-day-old broths. Significant differences are labeled (\* $p < 0.05$ , \*\* $p < 0.01$  and \*\*\* $p < 0.005$ ).

LC-MS/MS analysis applied to the fungal mycelium extracts (endometabolome) and culture supernatants (exometabolome) obtained in the exponential (3- and 5-day-old cultures) and stationary (7- and 14-day-old cultures) phases of fungal growth allowed us to detect 3182 m/z signals in mycelium extracts and 5415 m/z signals in supernatant extracts. Among these signals, 1831 m/z signals in mycelium extracts and 3069 m/z signals in supernatant extracts were recovered after filtrating the compounds detected in the blank control without supplementation nor inoculation and after normalization.

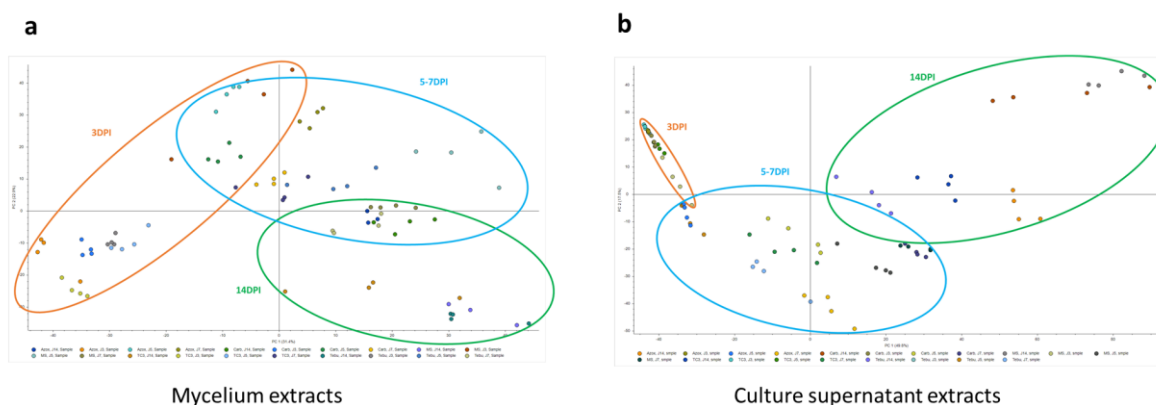


Figure 14. Scores from PCA decomposition of mycelium extracts (a) and culture supernatants extracts (b) at 3 DPI, 5 DPI, 7 DPI and 14 DPI of *F. graminearum* treated or not with TC3, Carbendazim, Tebuconazole and Azoxystrobin at the respective concentrations of 50 $\mu$ M, 5.25 $\mu$ M, 1.625 $\mu$ M and 5 $\mu$ M.

PCA profiles gathering all the conditions (control, TC3, Carbendazim, Tebuconazole and Azoxystrobin- treated cultures at three incubation times) are reported in Figure 14. Differentiation between mycelium extracts was clearly less marked than that of supernatants. Besides, metabolome differentiation was shown to be more driven by the time of culture than by the treatment.

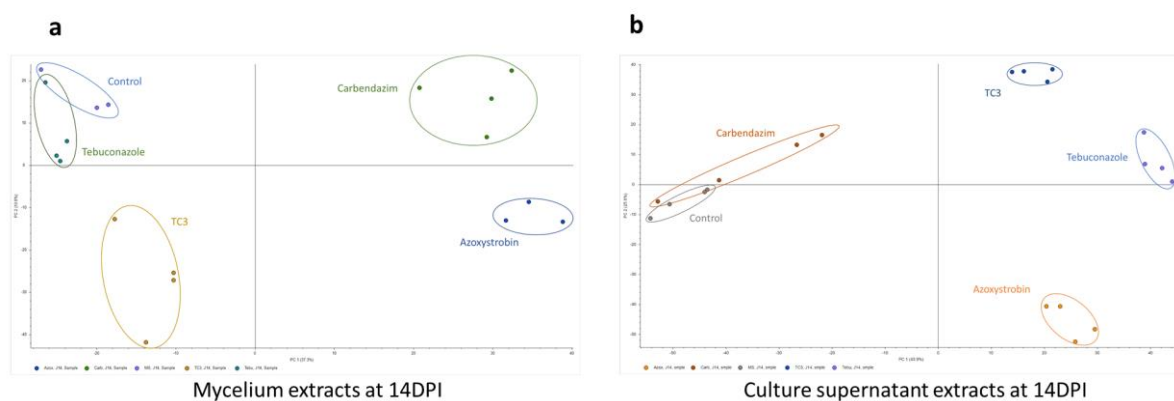


Figure 15. Scores from PCA decomposition of mycelium extracts (a) and culture supernatants extracts (b) at 14 DPI of *F. graminearum* treated or not with TC3, Carbendazim, Tebuconazole and Azoxystrobin at the respective concentrations of 50 $\mu$ M, 5.25 $\mu$ M, 1.625 $\mu$ M and 5 $\mu$ M.

PCA analyses of the endo and exometabolomes at 14 DPI are reported on Figure 15. Globally, the points representing the different biological replicates were shown to be clustered according to the treatment and well separated among treatments. It could however be observed that Tebuconazole and Carbendazim related data were mixed with that of the

control condition for endometabolome and exometabolome, respectively. TC3-treated samples were clearly separated from the other ones, suggesting that the metabolomic perturbations induced by TC3 could be quite different from those induced by the synthetic fungicides. However, Figure 15 also indicated that the tebuconazole samples were the closest to those associated with TC3 treatment for both mycelium and supernatant extracts. The likeness of these two conditions was confirmed by hierarchical clustering (supplementary Fig. 1). Although it needs to be confirmed, this first observation could suggest that, as Tebuconazole, TC3 induced dysfunctions in the ergosterol metabolism. As a reminder, an effect of TC3 on *F. graminearum* envelope has also been highlighted in the transcriptomic analysis described above.

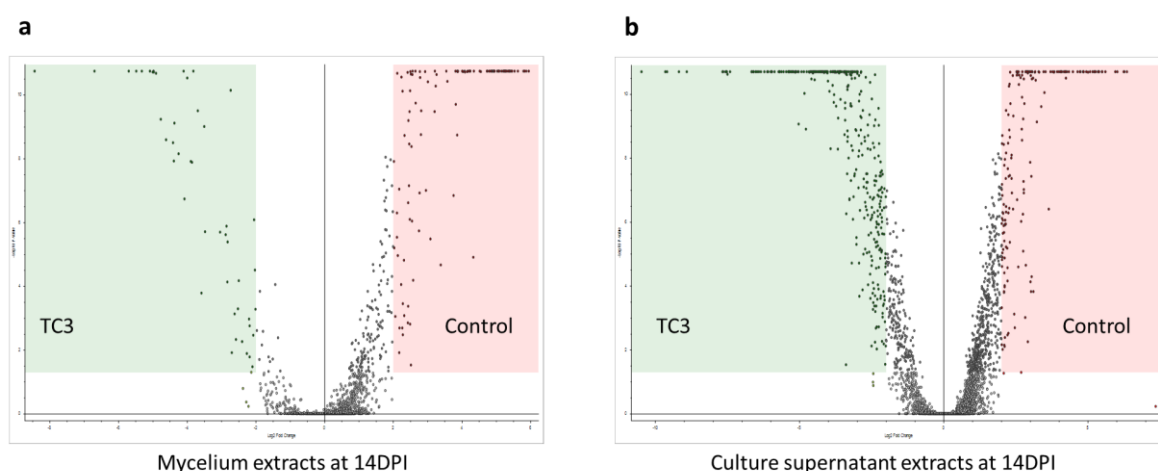
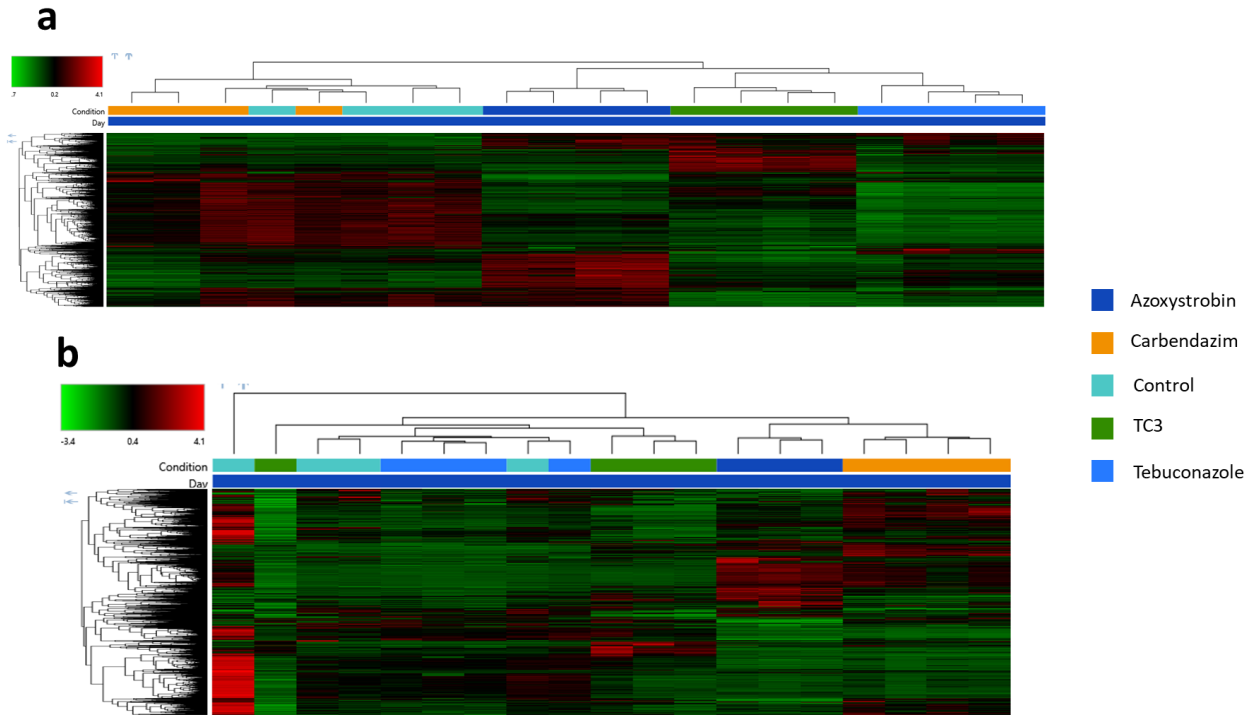


Figure 16. Volcano plot representing the differential concentration of detected molecules in mycelium extracts (a) and culture supernatant extracts (b) between TC3 and the control at 14DPI. Log 2fold change is set a 2 and p-value<0,05.

Concerning the differentially concentrated molecules between the control and TC3 treatment, 143 m/z signals and 576 m/z signals with adjusted p-value Benjamini-Hochberg < 0.05 were observed in mycelium and culture supernatants extracts, respectively. The biomolecules are currently being putatively identified based on m/z signal, accurate mass measurement, literature data and comparisons with databases such as Metabolika, ChemSpider, Mass list and mzCloud. A similar procedure is underway for the fungicide-treated conditions. When achieved, these identifications and their comparison between the different treatments will permit to deepen our knowledge on the effect of TC3 on *F. graminearum* metabolome and provide more clues to precise the mechanisms of action implicated in its antifungal and anti-mycotoxin activities.

Supplementary documents



Supplementary Figure 1. Hierarchical clustering of normalized concentration of detected molecules from culture supernatant extracts (a) and in mycelium extracts (b) between TC3 and the control at 14DPI.



## **Discussion / Conclusion**



## Discussion / Conclusion

Fusarium Head Blight (FHB) is a devastating fungal disease affecting wheat that leads to significant losses in yield and quality and poses a food safety risk due to the production of mycotoxins. Among toxigenic fungal species involved in FHB, *Fusarium graminearum* that produces deoxynivalenol (DON) is acknowledged as the main causal agent. The strategies in place to limit the disease combine agronomic practices, selection of tolerant genotypes and the use of phytochemicals. They are however frequently insufficiently efficient. Actually, when the climatic conditions are favorable for FHB infection, none of these strategies can guarantee acceptable levels of disease symptoms and mycotoxins (below the EU thresholds, n° 1126/2007)<sup>369</sup>. Besides, the over spraying of chemical fungicides has raised numerous concerns about their residual effects and toxicity towards the environment and human health. This over use has also led to the emergence of resistant fungal isolates. In the European Union, a restricted use of chemical pesticides has been approved by regulators through the MRL (maximum residue limit) review program (Regulation 396/2005)<sup>370</sup>. In response to this regulation but also to an increased demand of consumers for natural and environmentally friendly products, research to identify eco-friendly alternatives to synthetic fungicides has significantly stepped up its efforts during the past decade. Numerous biological solutions have been studied for their capacity to reduce FHB and mycotoxins in wheat and among them, natural molecules-based fungicides have gained recent interest. Through a literature review (Leannec-Rialland et al., 2022)<sup>371</sup>, included in the introduction part of this thesis manuscript, we have highlighted the promising potential held by defensin-based plant solutions. Notably, a defensin from the tick *Ixodes ricinus*, DefMT3, was reported as particularly active against *F. graminearum* (Tonk et al., 2015)<sup>358</sup>. This first result has prompted the development of a research program aiming at investigating the capacity of a DefMT3-based solution to be used as an alternative to chemical fungicide to control FHB.

The purpose of this thesis was therefore to demonstrate the efficacy of the DefMT3 and its  $\gamma$ -core TickCore3 (also designed as TC3) against FHB causal agents (with a strong focus on *F. graminearum*) and its capacity to reduce TCTB accumulation as well as to decipher the mechanisms underlying its bioactivity. The main highlights obtained throughout this study are gathered in Figure 1.

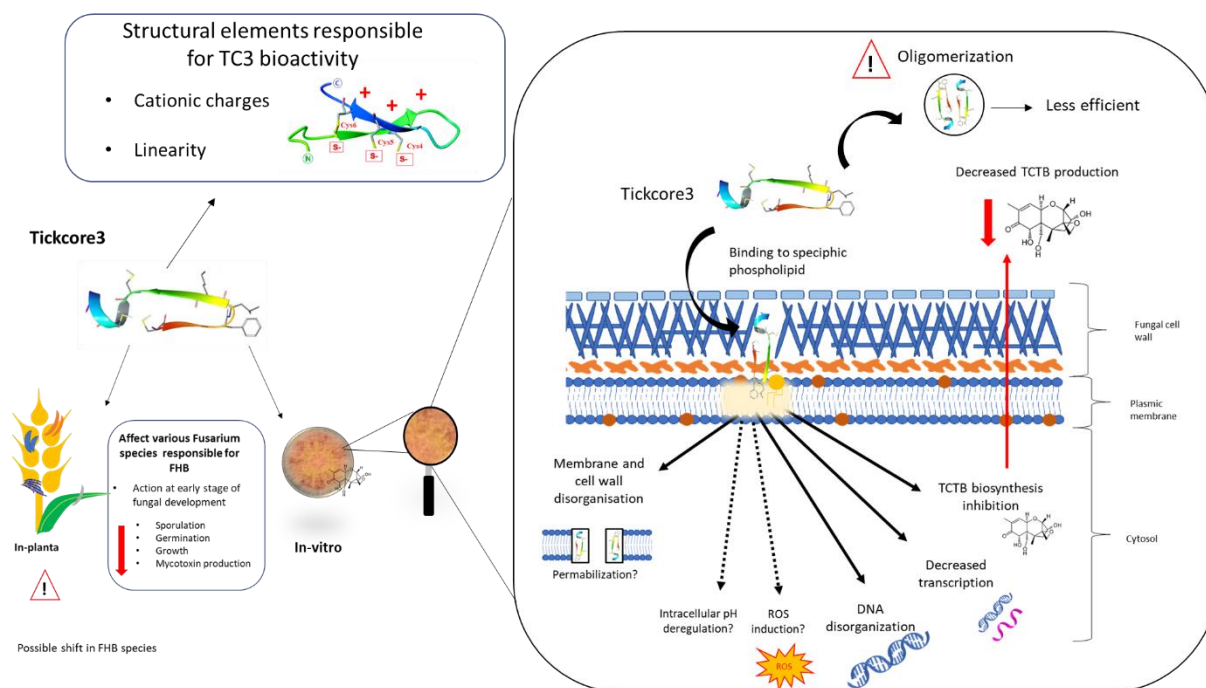


Figure 1. The antifungal and anti-mycotoxin activity of TC3 is related to a multi-faceted mechanism.

### A) The peptide TC3 demonstrated an efficient antifungal and anti-mycotoxin effect towards the main *Fusarium* species responsible for FHB.

While first confirming the bioactivity of the defensin DefMt3, our results have also shown that this activity was essentially related to the  $\gamma$ -core of the defensin, TC3. At low doses (between 12 and 50  $\mu\text{M}$ ), TC3 significantly reduces the fungal development and the production of DON by *F. graminearum*. To consider the diversity of *Fusarium* species involved in FHB and go beyond the reductionist approach “one pathogen-one disease”, TC3 was tested against the main toxigenic *Fusarium* species infecting wheat. In addition to *F. graminearum*, *F. culmorum*, *F. poae* and *F. langsethiae* were also shown as susceptible to TC3 when the peptide was applied at the spore stage. Our data have however revealed different sensitivities of mycotoxin-producing species according to the species and even of the strain. Importantly, the enniatins-producing species *F. avenaceum* appeared as less susceptible to TC3 than the other tested species. This species-dependent efficiency of the peptide raises the concern of potential shift in *Fusarium* population such as in mycotoxin profile contaminating grains mediated by its application in wheat fields. We cannot exclude that a wheat treatment with TC3 could induce a disequilibrium within the FHB complex, with *F. avenaceum* becoming predominant which could lead to an increased accumulation of enniatins in grains. Such an unexpected effect has been observed for azole fungicides by Audenaert *et al.* (2011)<sup>372</sup> who reported an increased occurrence of *F. poae* induced by the treatment. At the opposite, the removal of competitive species more sensitive to the fungicide than *F. graminearum* has been shown to result in adverse effects (no effect or an increase in DON content). This has been evidenced in some situations where the use of strobilurins has eliminated *Microdochium nivale*, a non-toxigenic fungal species that also contributes to FHB, and has favored *F. graminearum* (Pirgozliev *et al.*, 2002)<sup>265</sup>. Therefore, our studies require to be completed by the investigation of TC3 effect on mixtures of *Fusarium* species using *in vitro* and preferentially *in planta* trials.

First *in planta* assays have been implemented during this PhD work. The use of detached wheat leaf assays has allowed corroborating the promising activity of TC3 against *F. graminearum*. The results were less conclusive when the peptide was sprayed on wheat, grown in greenhouses, at flowering before *F. graminearum* inoculation. In this last experiment, only a slight reduction of the fungal spread within the wheat ear was observed. However, in this experiment, neither the concentration of fungal spores, the concentration of TC3 nor the formulation of the TC3 solution were optimized.

Lastly, our data have also revealed that, in certain assays, the efficacy of TC3 was lower than expected. Microscopy observations have shown that the peptide could generate aggregates and we supposed that this oligomerization led to a decreased efficiency. Actually, peptide oligomerization has already been reported as modulating the activity of defensins (Leannec-Rialland et al., 2022)<sup>371</sup>. In some cases, such as for the plant defensin NaD1, oligomerization was associated with a higher activity (Lay et al., 2012)<sup>373</sup>. In a next future, it will be important to elucidate the link between TC3 oligomerization and activity and therefore to provide key clues to improve the stability of the peptide.

#### **B) TC3 is mainly efficient at the fungal spore stage and its efficacy is driven by structural and chemical characteristics**

To start investigating the mode of action of the TC3 peptide, we tried identifying which step of the fungus life cycle was the most susceptible to the treatment. Our results demonstrated that TC3 significantly affected the sporulation and germination but had no effect on the mycelial growth. Besides, some key structural elements involved in TC3 bioactivity were deciphered. The  $\gamma$ -core was shown as more efficient when its linear structure was conserved. Indeed Cys-cyclization was shown to significantly reduce its inhibitory capacity. This result is in contrast with previous reports on human defensins in which cyclization enhanced the antimicrobial activity of  $\gamma$ -cores (Falanga et al., 2017)<sup>374</sup>. This linear form of the peptide was predicted to switch to another structural conformation marked by coil and helix. We also demonstrated that the cationic amino acids are partly responsible for the antifungal and anti-mycotoxin activities of TC3 and that the Lys6 residue seemed to play a determinant role. These data corroborate previous reports that have highlighted the importance of cationic charges for the antimicrobial efficacy of peptides, these cationic charges being involved in electrostatic interactions with the fungal membranes (López Cascales et al., 2018)<sup>375</sup>. Besides, the contribution of the Lys6 residue was suggested to be due to its close location to Phe4 and Leu5, two residues that were predicted to interact with the lipid membrane. These data are close to those observed for the plant defensin NaD1 which binding site was shown to be formed by a Lys residue and a KILRR motif located between the  $\beta$ -strands of its  $\gamma$ -core motif or for the Psd1 defensin in which the Phe15 and the Thr16 residues present in Loop 1 are involved in the interaction with glucosylceramide (Poon et al., 2014; de Medeiros et al., 2010)<sup>376,377</sup>. To demonstrate the importance of Lys6, independently of its cationic charge, it could be relevant to assess the activity of a variant of TC3 with the Lys6 residue replaced by an arginine, another positively charged amino acid.

Using microscopy experiments and a FITC-labeled peptide, we suggested that the peptide was recruited by the spore's envelope of *F. graminearum* and *F. avenaceum*. Accordingly, certain defensins have been shown to bind to specific sphingolipids and phospholipids of the plasma membrane, this binding being a prerequisite for their antifungal activity (Thevissen et al., 2005)<sup>378</sup>. *In silico* simulation predicted the recruitment of TC3 by the *F. graminearum* membrane's upper leaflet more specifically by the phospholipids POPS, POPA and POPG. However, data on the membrane composition used in the simulation were from an old publication (but the only one available, to our knowledge) released by Wiebe et al. in 1989. Further investigations are therefore needed with updated information. Microscopy observations showing the peptide surrounding the fungal envelope could suggest a permeabilization of the membrane according to a carpet like model, one of the three models describing the possible membrane-permeabilizing activity of defensins (Brogden, 2005)<sup>379</sup>. Unfortunately, our microscopy experiment did not allow to visualize a membrane permeabilization neither an internalization of TC3. Such an internalization of TC3 was also suggested by our transcriptomics analysis that has pointed out the downregulation of the expression of genes related to the membrane composition but also of genes associated with the cell-wall. Actually, internalization following interactions with the fungal envelope is a common feature of the mode of action of defensins, as already described for NaD1 toward *Fusarium oxysporum* (Van der Weerden et al., 2008)<sup>380</sup> or *Candida albicans* (Hayes et al., 2013)<sup>381</sup>.

To go further in studying the interactions of TC3 with the *F. graminearum* and *F. avenaceum* spore's envelope, it would be relevant to include a treatment with the SYTOX green dye. SYTOX Green is a high-affinity nucleic acid stain that does not cross the membranes of live cells but easily penetrates cells with compromised plasma membranes. Observation of *F. graminearum* challenged with TC3 and SYTOX Green stain would allow evidencing a possible membrane permeabilization and calculate lysis rates. Furthermore, to discriminate the cell wall and the membrane and visualize more precisely the binding site of TC3, use of TC3 labelled with a fluorophore with less bleaching (FM 1-43 and FM 4-64) and a cell wall specific stain (Calcofluor White M2R, Solophenyl Flavine 7GFE 500, Pontamine Fast Scarlet 48 and Congo Red) with a higher resolution could be relevant (Lichius and Zeilinger, 2019)<sup>382</sup>. Lastly, since exposition time and concentration were shown to regulate the internalization of defensins (Hayes et al., 2018; Tetorya et al., 2022)<sup>383,384</sup>, microscopy observations have to be repeated with different incubation times and TC3 concentrations.

The strongly suspected interaction of TC3 with the fungal membranes and more precisely with the phospholipids POPS, POPA and POPG of *F. graminearum* membranes paves the avenue for additional experiments to understand the different TC3 sensitivities of *Fusarium* species. We can suppose that these different sensitivities are associated with differences in membrane composition. As presented by Jimah et al. (2017)<sup>385</sup>, identifying the lipid targets of proteins and biomolecules is feasible; it was done to demonstrate that phosphatidic acid was the target of a malaria vaccine candidate. We recently started a collaboration with the CNRS laboratory of membrane biogenesis UMR 5200 to decipher the intra- and inter-species

diversity of the *Fusarium* membrane's components. The fatty acids and sterols present in the membrane were extracted and identified/quantified by GCMS. The results are currently being analyzed. Further studies will include the lipid separation and the testing of TC3 on the isolated lipids to determine whether the peptide binds to specific membrane components as it was predicted. After identification of the targeted lipid, it could be highly interesting to generate a *F. graminearum* mutant deleted for the gene related to the synthesis of the identified lipid and test the peptide on it. Such a strategy was previously implemented to demonstrate the importance of glucosylceramide for the AMP EDT151 (Aumer, 2020)<sup>386</sup>.

### **C) The antifungal and anti-mycotoxin activity of TC3 is related to a multi-faceted mechanism**

To reach a comprehensive view of the mechanisms following the binding of TC3 to the fungal envelope, a strategy combining transcriptomics and metabolomics was implemented. The transcriptomic analysis has allowed evidencing the broad perturbations induced in *F. graminearum* exposed to TC3. These dysfunctions are summarized in Figure 1. Among the multiple biological processes, cellular components and metabolic pathways affected by the peptide TC3, it is important to mention the cell wall and membrane organization, DNA organization, DNA transcription, mRNA translation as well as some primary and secondary metabolic pathways. Similar effect of defensins on fungal intracellular targets including DNA synthesis, transcription and/or mRNA translation have already been described (Hale and Hancock, 2007; do Nascimento et al., 2015)<sup>387,388</sup>. Since the process of spore germination has been reported to be accompanied by intense metabolic activities including respiration, RNA and protein synthesis, our results are in accordance with the observations that the germination stage is the most susceptible to the TC3 treatment (Zhou et al., 2018)<sup>389</sup>. Moreover, the first data provided by the metabolic analysis indicated that the mode of action of TC3 could be close to that of tebuconazole, a synthetic fungicide that targets the ergosterol biosynthesis. This first result together with the observed modulation of the expression of genes related to the membrane strongly support that the primary toxic action of TC3 is the fungal membrane disorganization. To go further, the metabolomic analysis will be completed. A putative identification of the m/z signals (and associated metabolic pathways) that discriminate the treated conditions compared to the control will be implemented. Lastly, an HNMR approach which could provide more accurate information on the fungal primary metabolism would be an interesting complementary study.

### **D) Next steps before the development of a biocontrol solution exploiting the bioactivity of TC3 or DefMT3**

Given its antifungal and anti-mycotoxin efficiency, TickCore3 appears as an attractive candidate to replace synthetic fungicides. However, the development of a defensin-based plant care product still faces some important obstacles and additional experiments are required.

### *D.1) One primary issue to solve is the production of TC3 and DefMT3 in high amounts*

All the experiments carried out throughout this study have been done with a batch of chemically synthesized peptide. For short peptides and high-value applications, chemical synthesis is sometimes reported as an economically viable solution (Anderson et al., 2000)<sup>390</sup>. However, the cost and production yield of chemical synthesis is not compatible at all with the development of biofungicide solutions applied to wheat. The extraction and purification of defensins from natural sources is a non-viable method for mass production, being time-consuming and expensive. Thus, optimized process for the production of defensins on a large scale requires still to be defined. The bioproduction of AMPs has been reported as a highly promising method, based on the use of heterologous expression systems such as *E. coli*, yeasts and insects. Due to the antimicrobial activity of TC3 and DefMT3 towards fungi and bacteria (Tonk et al., 2015)<sup>358</sup> and the importance of key structural motifs for their activities, the insect cell-based expression systems might permit to overcome limitations that could hamper their heterologous production in bacteria and yeasts and to allow the properly synthesis of functional peptide structures (Druzinec et al., 2013)<sup>391</sup>. Furthermore, other technics involving the use of fusion proteins or association with a carrier protein could minimize the lethal effects of TC3 and DefMT3 in the host cell, protect it from proteolytic degradation and improve its solubility and folding (Leannec-Rialland et al., 2022)<sup>371</sup>.

### *D.2) Identification of the best formulation to guarantee the efficacy and stability of the peptide is needed*

In our greenhouse tests, the TC3 peptide was dissolved in water solution before being sprayed on wheat spikelets. This has allowed providing promising but limited results. To improve the efficiency of a fungicidal molecule such as TC3, the formulation has to be considered seriously. Indeed, chosen properly, the formulation can improve the biomolecule solubility and stability and consequently its bioavailability. The use of engineered nano-carriers such as nanoencapsulation systems including micro/nano -suspensions, -emulsions, -particles, -capsules and -hybrids are promising formula and could be tested with the TC3 or defensin DefMT3 (Tleuova et al., 2020)<sup>392</sup>. Moreover, spraying of a fungicide is also known to lead to a significant runoff of the product (bouncing, sputtering...). It has been reported that, in most cases, only 40-60 % of the applied product reached the targeted plant organ and that only 0.1 % of the active ingredient reached the targeted pest (Arand et al., 2018)<sup>393</sup>.

### *D.3) High available amount and an optimized formulation would allow assessing the efficacy of the peptide biofungicide (and its potential side-effects) in natural conditions*

Assessing the efficacy of the defensin-based treatment in greenhouse experiments requires to be repeated with different modalities (higher concentrations, higher number of treated plants, different concentrations of inoculated spores and different pathogen pressure, different formulations). But this will not replace the need of field trials with natural inoculation and wheat grown under different agroclimatic environments and with different cultural practices. Moreover, since control measures of FHB and contamination of grains with

mycotoxins (agronomic practices, choice of the cultivar, of the planting and harvest dates...) are known to not acting independently but in a network of multiple interactions (Leslie et al., 2021)<sup>394</sup>, it will be essential to consider the defensin-based treatment as part of an integrated control strategy. And indeed, biofungicide application has been proven to be more efficient when it was included in an integrated pest management system (Palazzini et al., 2007; Xue et al., 2009)<sup>314,322</sup>. Lastly, the association of the defensin with synthetic fungicide could improve the disease management by having complementary effect and reducing the quantity of applied chemicals (Ons et al., 2020)<sup>256</sup>; this will have to be tested.

The implementation of field trials will also allow assessing the potential occurrence of side effects of the biosolution treatment. The risk of a shift in toxigenic fungal community infecting wheat induced by TC3 was previously mentioned: field trials will permit to investigate this risk. In addition, the effect of TC3 or DefMT3 on microbial communities (fungi, bacteria and virus from the wheat phyllosphere and rhizosphere) is another key topic to address to ensure that the treatment would not induce the removal of beneficial microbial agents.

#### *D.4) One of the most challenging step remains however the compliance with the regulation requirements*

As an antifungal peptide with a native chemical structure, the defensin DefMT3 but not the TC3 could be considered as a biofungicide. Indeed, biofungicides refer to formulations exploiting the bioactivity of naturally occurring substances. This implies that some key insights obtained in our study with TC3 would have to be checked with DefMT3. In addition, the lack of poisoning and potential occurrence of hazardous effects on non-targeted species induced by DefMT3 will have to be proven. The registration process of biopesticides is highly challenging with different regulation policies across countries: there is a high possibility that a defensin-based plant care product will never reach the market (Kiewnick, 2007; Lahlali et al., 2022)<sup>341,342</sup>. The biopesticide registration procedure is also cumbersome and expensive and can jeopardize the commercialization of a biopesticide. Complexity and difficulties of registration process that could hamper the development of a DefMT3-product have been intensively discussed in the review paper reported in the introduction part of this manuscript (Leannec-Rialland et al., 2022)<sup>371</sup>.

However, despite the various barriers that could impeditment the development of a DefMT3-based plant care product to minimize FHB and mycotoxins in wheat, the promising efficacy of tick defensins revealed in our study and their associated multifaceted mode of action are strong arguments to motivate the continuation of their investigation. The increased awareness and interest of consumers to eco-friendly products, the observed changes of farmers behavior with the adoption of new agricultural practices, the financial support that can accompany the transition towards sustainable production systems, are additional arguments to not give up! And, in the next decade, the possibility to find a commercialized defensin-based biofungicide to combat FHB and mycotoxins must not be excluded.



## References (the citations refer to the parts apart from the articles)

1. FAO. *World Food and Agriculture - Statistical Pocketbook 2018*. (2018).
2. FAOSTAT. <https://www.fao.org/faostat/en/#home>.
3. FAO. *World Food and Agriculture - Statistical Yearbook 2020*. (FAO, 2020). doi:10.4060/cb1329en.
4. USDA-FAS. *Wheat : Overview for 2018/2019*. (2018).
5. Yadav, P. Nutritional Contents and Medicinal Properties of Wheat: A Review. *Life Sciences and Medicine Research LMSR-22*, (2011).
6. Friesen, T. L., Faris, J. D., Solomon, P. S. & Oliver, R. P. Host-specific toxins: effectors of necrotrophic pathogenicity. *Cell Microbiol* **10**, 1421–1428 (2008).
7. Gurung, S., Sharma, R. C., Duveiller, E. & Shrestha, S. M. Comparative analyses of spot blotch and tan spot epidemics on wheat under optimum and late sowing period in South Asia. *Eur J Plant Pathol* **134**, 257–266 (2012).
8. Xia, L. *et al.* Biomonitoring of Aflatoxin B1 and Deoxynivalenol in a Rural Pakistan Population Using Ultra-Sensitive LC-MS/MS Method. *Toxins (Basel)* **12**, E591 (2020).
9. Parry, D. W., Jenkinson, P. & McLEOD, L. Fusarium ear blight (scab) in small grain cereals—a review. *Plant Pathology* **44**, 207–238 (1995).
10. Sutton, J. C. Epidemiology of wheat head blight and maize ear rot caused by *Fusarium graminearum*. *Canadian Journal of Plant Pathology* **4**, 195–209 (1982).
11. Atanasov, D. *Fusarium-blight (scab) of Wheat and Other Cereals*. (U.S. Government Printing Office, 1920).
12. *Fusarium head blight of wheat and barley*. (APS Press, 2003).
13. Walter, S., Nicholson, P. & Doohan, F. M. Action and reaction of host and pathogen during Fusarium head blight disease. *New Phytologist* **185**, 54–66 (2010).
14. Lenc, L. Fusarium head blight (FHB) and Fusarium populations in grain of winter wheat grown in different cultivation systems. *Journal of Plant Protection Research* **55**, (2015).
15. Bechtel, D. B., Kaleikau, L. A., Gaines, R. L. & Seitz, L. M. The effects of *Fusarium graminearum* infection on wheat kernels. *Cereal chemistry (USA)* (1985).
16. Pirgozliev, S. R., Edwards, S. G., Hare, M. C. & Jenkinson, P. Strategies for the Control of Fusarium Head Blight in Cereals. *European Journal of Plant Pathology* **109**, 731–742 (2003).
17. Kang, Z. & Buchenauer, H. Immunocytochemical localization of fusarium toxins in infected wheat spikes by *Fusarium culmorum*. *Physiological and Molecular Plant Pathology* **55**, 275–288 (1999).
18. Powell, A. J. & Vujanovic, V. Evolution of Fusarium Head Blight Management in Wheat: Scientific Perspectives on Biological Control Agents and Crop Genotypes Protocooperation. *Applied Sciences* **11**, 8960 (2021).
19. Reis, E. M. & Carmona, M. A. Integrated Disease Management of Fusarium Head Blight. in *Fusarium Head Blight in Latin America* (eds. Alconada Magliano, T. M. & Chulze, S. N.) 159–173 (Springer Netherlands, 2013). doi:10.1007/978-94-007-7091-1\_10.
20. Zhu, Z. *et al.* Genome-Wide Association Analysis of Fusarium Head Blight Resistance in Chinese Elite Wheat Lines. *Frontiers in Plant Science* **11**, (2020).
21. Windels, C. E. Economic and social impacts of fusarium head blight: changing farms and rural communities in the northern great plains. *Phytopathology* **90**, 17–21 (2000).
22. McMullen, M. *et al.* A Unified Effort to Fight an Enemy of Wheat and Barley: Fusarium Head Blight. *Plant Dis* **96**, 1712–1728 (2012).
23. McCartney, C. A. *et al.* Fusarium Head Blight Resistance QTL in the Spring Wheat Cross Kenyon/86ISMN 2137. *Frontiers in Microbiology* **7**, (2016).

24. Dill-Macky, R. & Jones, R. K. The Effect of Previous Crop Residues and Tillage on Fusarium Head Blight of Wheat. *Plant Dis* **84**, 71–76 (2000).
25. McMullen, M., Jones, R. & Gallenberg, D. Scab of Wheat and Barley: A Re-emerging Disease of Devastating Impact. *Plant Disease* **81**, 1340–1348 (1997).
26. Choo, T. M. *et al.* Leader barley. *Can. J. Plant Sci.* **89**, 921–924 (2009).
27. Zhang, H., Chen, W. Q., Xu, J., Xu, J. S. & Feng, J. First Report of Fusarium cerealis Causing Fusarium Head Blight on Barley in China. *Plant Dis* **95**, 774 (2011).
28. Tusa, C. *et al.* Aspects of the Fusarium attacks on wheat in Romania. *Probleme de Protectia Plantelor* **9**, 15–31 (1981).
29. Schmaile III. Mycotoxins in Crops: A Threat to Human and Domestic Animal Health. *PHI* (2009) doi:10.1094/PHI-I-2009-0715-01.
30. Arseniuk, E., Foremska, E., G, T., Óral, . & Chełkowski, J. Fusarium Head Blight Reactions and Accumulation of Deoxynivalenol (DON) and Some of its Derivatives in Kernels of Wheat, Triticale and Rye. *Journal of Phytopathology* **147**, 577–590 (1999).
31. Liddell, C. M. Systematics of Fusarium species and allies associated with Fusarium head blight. *Fusarium head blight of wheat and barley* 35–43 (2003).
32. Nelson, P. E., Toussoun, T. A. & Marasas, W. F. O. *Fusarium Species: An Illustrated Manual for Identification*. (Pennsylvania State University Press, 1983).
33. O'Donnell, K. *et al.* DNA sequence-based identification of Fusarium: Current status and future directions. *Phytoparasitica* **43**, 583–595 (2015).
34. Geiser, D. M. *et al.* Phylogenomic Analysis of a 55.1-kb 19-Gene Dataset Resolves a Monophyletic Fusarium that Includes the Fusarium solani Species Complex. *Phytopathology*® **111**, 1064–1079 (2021).
35. O'Donnell, K., Ward, T. J., Geiser, D. M., Corby Kistler, H. & Aoki, T. Genealogical concordance between the mating type locus and seven other nuclear genes supports formal recognition of nine phylogenetically distinct species within the Fusarium graminearum clade. *Fungal Genet Biol* **41**, 600–623 (2004).
36. *The Fusarium Laboratory Manual*. (Wiley, 2006). doi:10.1002/9780470278376.
37. van der Lee, T., Zhang, H., van Diepeningen, A. & Waalwijk, C. Biogeography of Fusarium graminearum species complex and chemotypes: a review. *Food Addit Contam Part A Chem Anal Control Expo Risk Assess* **32**, 453–460 (2015).
38. Pasquali, M. *et al.* A Fusarium graminearum strain-comparative proteomic approach identifies regulatory changes triggered by agmatine. *J Proteomics* **137**, 107–116 (2016).
39. Dweba, C. C. *et al.* Fusarium head blight of wheat: Pathogenesis and control strategies. *Crop Protection* **91**, 114–122 (2017).
40. Bottalico, A. & Perrone, G. Toxigenic Fusarium species and Mycotoxins Associated with Head Blight in Small-Grain Cereals in Europe. *European Journal of Plant Pathology* **108**, 611–624 (2002).
41. Thrane, U. Fusarium. in *Encyclopedia of food microbiology* 901–906 (2000).
42. Xu, X. & Nicholson, P. Community ecology of fungal pathogens causing wheat head blight. *Annu Rev Phytopathol* **47**, 83–103 (2009).
43. Xu, X.-M. *et al.* Predominance and association of pathogenic fungi causing Fusarium ear blight in wheat in four European countries. *Eur J Plant Pathol* **112**, 143–154 (2005).
44. Audenaert, K. *et al.* Fusarium head blight (FHB) in Flanders: population diversity, inter-species associations and DON contamination in commercial winter wheat varieties. *Eur J Plant Pathol* **125**, 445–458 (2009).
45. Oerke, E.-C. *et al.* Spatial variability of fusarium head blight pathogens and associated mycotoxins in wheat crops. *Plant Pathology* **59**, 671–682 (2010).

46. Backhouse, D. & Burgess, L. W. Climatic analysis of the distribution of *Fusarium graminearum*, *F. pseudograminearum* and *F. culmorum* on cereals in Australia. *Australasian Plant Pathology* **31**, 321–327 (2002).
47. Brennan, J. M., Fagan, B., van Maanen, A., Cooke, B. M. & Doohan, F. M. Studies on in vitro Growth and Pathogenicity of European *Fusarium* Fungi. *European Journal of Plant Pathology* **109**, 577–587 (2003).
48. Nielsen, L. K., Jensen, J. D., Rodríguez, A., Jørgensen, L. N. & Justesen, A. F. TRI12 based quantitative real-time PCR assays reveal the distribution of trichothecene genotypes of *F. graminearum* and *F. culmorum* isolates in Danish small grain cereals. *Int J Food Microbiol* **157**, 384–392 (2012).
49. Valverde-Bogantes, E. *et al.* Recent population changes of *Fusarium* head blight pathogens: drivers and implications. *Canadian Journal of Plant Pathology* **42**, 315–329 (2020).
50. Xu, X.-M., Monger, W., Ritieni, A. & Nicholson, P. Effect of temperature and duration of wetness during initial infection periods on disease development, fungal biomass and mycotoxin concentrations on wheat inoculated with single, or combinations of, *Fusarium* species. *Plant Pathology* **56**, 943–956 (2007).
51. Yli-Mattila, T. Ecology and evolution of toxigenic *Fusarium* species in cereals in northern Europe and Asia. *Journal of Plant Pathology* **92**, 7–18 (2010).
52. Kulik, T. *et al.* Whole-genome single nucleotide polymorphism analysis for typing the pandemic pathogen *Fusarium graminearum* sensu stricto. *Front Microbiol* **13**, 885978 (2022).
53. King, R., Urban, M., Hammond-Kosack, M. C. U., Hassani-Pak, K. & Hammond-Kosack, K. E. The completed genome sequence of the pathogenic ascomycete fungus *Fusarium graminearum*. *BMC Genomics* **16**, 544–544 (2015).
54. Stajich, J. E. Fungal Genomes and Insights into the Evolution of the Kingdom. *Microbiology Spectrum* **5**, 5.4.15 (2017).
55. Alouane, T. *et al.* Comparative genomics of eight *Fusarium graminearum* strains with contrasting aggressiveness reveals an expanded open pangenome and extended effector content signatures. *International Journal of Molecular Sciences* **22**, (2021).
56. Goswami, R. S. & Kistler, H. C. Heading for disaster: *Fusarium graminearum* on cereal crops. *Mol Plant Pathol* **5**, 515–525 (2004).
57. Ma, L.-J. *et al.* *Fusarium* pathogenomics. *Annu Rev Microbiol* **67**, 399–416 (2013).
58. Gunupuru, L. R., Perochon, A. & Doohan, F. M. Deoxynivalenol resistance as a component of FHB resistance. *Trop. plant pathol.* **42**, 175–183 (2017).
59. Trail, F. For Blighted Waves of Grain: *Fusarium graminearum* in the Postgenomics Era. *Plant physiology* **149**, 103–110 (2009).
60. Deacon, J. *Fungal Biology*. (Wiley, 2005). doi:10.1002/9781118685068.
61. Khan, Mohd. K. *et al.* *Fusarium* head blight in wheat: contemporary status and molecular approaches. *3 Biotech* **10**, 172 (2020).
62. Brauer, E. K., Subramaniam, R. & Harris, L. J. Regulation and Dynamics of Gene Expression During the Life Cycle of *Fusarium graminearum*. *Phytopathology*® **110**, 1368–1374 (2020).
63. Hallen, H. E., Huebner, M., Shiu, S.-H., Güldener, U. & Trail, F. Gene expression shifts during perithecial development in *Gibberella zeae* (anamorph *Fusarium graminearum*), with particular emphasis on ion transport proteins. *Fungal Genet Biol* **44**, 1146–1156 (2007).
64. Sikhakolli, U. R. *et al.* Transcriptome analyses during fruiting body formation in *Fusarium graminearum* and *Fusarium verticillioides* reflect species life history and ecology. *Fungal Genet Biol* **49**, 663–673 (2012).
65. Lee, J. *et al.* FgVelB globally regulates sexual reproduction, mycotoxin production and pathogenicity in the cereal pathogen *Fusarium graminearum*. *Microbiology* **158**, 1723–1733.

66. Zheng, D. *et al.* The FgHOG1 Pathway Regulates Hyphal Growth, Stress Responses, and Plant Infection in *Fusarium graminearum*. *PLOS ONE* **7**, e49495 (2012).
67. Son, H. *et al.* AbaA Regulates Conidiogenesis in the Ascomycete Fungus *Fusarium graminearum*. *PLOS ONE* **8**, e72915 (2013).
68. Son, H. *et al.* WetA Is Required for Conidiogenesis and Conidium Maturation in the Ascomycete Fungus *Fusarium graminearum*. *Eukaryotic Cell* **13**, 87–98 (2014).
69. Jonkers, W., Dong, Y., Broz, K. & Kistler, H. C. The Wor1-like Protein Fgp1 Regulates Pathogenicity, Toxin Synthesis and Reproduction in the Phytopathogenic Fungus *Fusarium graminearum*. *PLOS Pathogens* **8**, e1002724 (2012).
70. Min, K. *et al.* Transcription Factor RFX1 Is Crucial for Maintenance of Genome Integrity in *Fusarium graminearum*. *Eukaryot Cell* **13**, 427–436 (2014).
71. Shaner, G. Epidemiology of *Fusarium* head blight of small grain cereals in North America. *Fusarium head blight of wheat and barley* 84–119 (2003).
72. Inoue, I., Namiki, F. & Tsuge, T. Plant Colonization by the Vascular Wilt Fungus *Fusarium oxysporum* Requires FOW1, a Gene Encoding a Mitochondrial Protein. *Plant Cell* **14**, 1869–1883 (2002).
73. Rodríguez-Molina, M. C., Medina, I., Torres-Vila, L. M. & Cuartero, J. Vascular colonization patterns in susceptible and resistant tomato cultivars inoculated with *Fusarium oxysporum* f.sp. *lycopersici* races 0 and 1. *Plant Pathology* **52**, 199–203 (2003).
74. Hardham, A. R. Cell Biology of Fungal Infection of Plants. in *Biology of the Fungal Cell* (eds. Howard, R. J. & Gow, N. A. R.) 91–123 (Springer, 2001). doi:10.1007/978-3-662-06101-5\_5.
75. Mary Wanjiru, W., Zhensheng, K. & Buchenauer, H. Importance of Cell Wall Degrading Enzymes Produced by *Fusarium graminearum* during Infection of Wheat Heads. *European Journal of Plant Pathology* **108**, 803–810 (2002).
76. Mandeel, Q. A. Modeling competition for infection sites on roots by nonpathogenic strains of *Fusarium oxysporum*. *Mycopathologia* **163**, 9–20 (2007).
77. Miller, J. D. & Ewen, M. A. Toxic effects of deoxynivalenol on ribosomes and tissues of the spring wheat cultivars Frontana and Casavant. *Natural Toxins* **5**, 234–237 (1997).
78. Brown, N. A., Antoniow, J. & Hammond-Kosack, K. E. The Predicted Secretome of the Plant Pathogenic Fungus *Fusarium graminearum*: A Refined Comparative Analysis. *PLoS One* **7**, e33731 (2012).
79. Rauwane, M. E. *et al.* Pathogenicity and Virulence Factors of *Fusarium graminearum* Including Factors Discovered Using Next Generation Sequencing Technologies and Proteomics. *Microorganisms* **8**, 305 (2020).
80. Jenczmionka, N. J. & Schäfer, W. The Gpmk1 MAP kinase of *Fusarium graminearum* regulates the induction of specific secreted enzymes. *Curr Genet* **47**, 29–36 (2005).
81. Lee, J. *et al.* Genetic Diversity and Fitness of *Fusarium graminearum* Populations from Rice in Korea. *Applied and Environmental Microbiology* **75**, 3289–3295 (2009).
82. Voigt, C. A., Schäfer, W. & Salomon, S. A secreted lipase of *Fusarium graminearum* is a virulence factor required for infection of cereals. *The Plant Journal* **42**, 364–375 (2005).
83. Jansen, C. *et al.* Infection patterns in barley and wheat spikes inoculated with wild-type and trichodiene synthase gene disrupted *Fusarium graminearum*. *Proc Natl Acad Sci U S A* **102**, 16892 (2005).
84. Ilgen, P., Maier, F. & Schäfer, W. Trichothecenes and lipases are host-induced and secreted virulence factors of *Fusarium graminearum*. *Cereal Research Communications* **36**, 421–428 (2008).
85. Schwarz, P. B., Jones, B. L. & Steffenson, B. J. Enzymes Associated with *Fusarium* Infection of Barley. *Journal of the American Society of Brewing Chemists* **60**, 130–134 (2002).

86. Maier, F. J. *et al.* Involvement of trichothecenes in fusarioses of wheat, barley and maize evaluated by gene disruption of the trichodiene synthase (Tri5) gene in three field isolates of different chemotype and virulence. *Molecular Plant Pathology* **7**, 449–461 (2006).
87. Proctor, R. H., Hohn, T. M., McCormick, S. P. & Desjardins, A. E. Tri6 encodes an unusual zinc finger protein involved in regulation of trichothecene biosynthesis in *Fusarium sporotrichioides*. *Applied and Environmental Microbiology* **61**, 1923–1930 (1995).
88. Boddu, J., Cho, S. & Muehlbauer, G. J. Transcriptome Analysis of Trichothecene-Induced Gene Expression in Barley. *MPMI* **20**, 1364–1375 (2007).
89. Wegulo, S. N. Factors influencing deoxynivalenol accumulation in small grain cereals. *Toxins (Basel)* **4**, 1157–1180 (2012).
90. Uzma, F. *et al.* Endophytic fungi—alternative sources of cytotoxic compounds: a review. *Frontiers in pharmacology* **9**, 309 (2018).
91. Alshannaq, A. & Yu, J.-H. Occurrence, Toxicity, and Analysis of Major Mycotoxins in Food. *Int J Environ Res Public Health* **14**, E632 (2017).
92. Commission Regulation (EC) No. 1881/2006 setting maximum levels for certain contaminants in foodstuffs. (2006).
93. McCormick, S. P., Stanley, A. M., Stover, N. A. & Alexander, N. J. Trichothecenes: from simple to complex mycotoxins. *Toxins* **3**, 802–814 (2011).
94. Bennett, J. W. & Klich, M. Mycotoxins. *Clin Microbiol Rev* **16**, 497–516 (2003).
95. Kimura, M., Tokai, T., Takahashi-Ando, N., Ohsato, S. & Fujimura, M. *Molecular and Genetic Studies of Fusarium Trichothecene Biosynthesis: Pathways, Genes, and Evolution*. vol. 71 (2007).
96. Eudes, F., Comeau, A., Rioux, S. & Collin, J. Phytotoxicité de huit mycotoxines associées à la fusariose de l'épi chez le blé. *Canadian Journal of Plant Pathology* **22**, 286–292 (2000).
97. Steinmetz, W. E., Rodarte, C. B. & Lin, A. 3D QSAR study of the toxicity of trichothecene mycotoxins. *European Journal of Medicinal Chemistry* **44**, 4485–4489 (2009).
98. Trusal, L. R. & O'Brien, J. C. Ultrastructural effects of T-2 mycotoxin on rat hepatocytes in vitro. *Toxicol* **24**, 481–488 (1986).
99. Minervini, F., Fornelli, F. & Flynn, K. M. Toxicity and apoptosis induced by the mycotoxins nivalenol, deoxynivalenol and fumonisin B1 in a human erythroleukemia cell line. *Toxicology in Vitro* **18**, 21–28 (2004).
100. Carrasco, L., Barbacid, M. & Vazquez, D. The trichodermin group of antibiotics, inhibitors of peptide bond formation by eukaryotic ribosomes. *Biochimica et Biophysica Acta (BBA) - Nucleic Acids and Protein Synthesis* **312**, 368–376 (1973).
101. Cundliffe, E., Cannon, M. & Davies, J. Mechanism of Inhibition of Eukaryotic Protein Synthesis by Trichothecene Fungal Toxins. *Proceedings of the National Academy of Sciences* **71**, 30–34 (1974).
102. Ueno, Y. & Matsumoto, H. Inactivation of some thiol-enzymes by trichothecene mycotoxins from *Fusarium* species. *Chem. Pharm. Bull.* **23**, 2439–2442 (1975).
103. Cundliffe, E. & Davies, J. E. Inhibition of initiation, elongation, and termination of eukaryotic protein synthesis by trichothecene fungal toxins. *Antimicrob Agents Chemother* **11**, 491–499 (1977).
104. Pace, C. N., Grimsley, G. R., Thomson, J. A. & Barnett, B. J. Conformational stability and activity of ribonuclease T1 with zero, one, and two intact disulfide bonds. *Journal of Biological Chemistry* **263**, 11820–11825 (1988).
105. Gareis, M. Collection of occurrence data of *Fusarium* toxins in food and assessment of dietary intake by the population of EU member states. *Report of Experts Participating in SCOOP Task 3.2.10-Part A: Trichothecene* 13–235 (2003).

106. Edwards, S. G. Fusarium mycotoxin content of UK organic and conventional oats. *Food Additives & Contaminants: Part A* **26**, 1063–1069 (2009).
107. Joint FAO/WHO Expert Committee on Food Additives (JECFA). *Ninety-third meeting - Joint FAO/WHO Expert Committee of Food Additives (JECFA)*. 7 (2022).
108. Hoerr, F. J., Carlton, W. W. & Yagen, B. Mycotoxicosis Caused by a Single Dose of T-2 Toxin or Diacetoxyscirpenol in Broiler Chickens. *Vet Pathol* **18**, 652–664 (1981).
109. Tijerino, A. *et al.* Overexpression of the trichodiene synthase gene *tri5* increases trichodermin production and antimicrobial activity in *Trichoderma brevicompactum*. *Fungal Genet Biol* **48**, 285–296 (2011).
110. Shentu, X., Zhan, X., Ma, Z., Yu, X. & Zhang, C. Antifungal activity of metabolites of the endophytic fungus *Trichoderma brevicompactum* from garlic. *Braz. J. Microbiol.* **45**, 248–254 (2014).
111. Liang, J. M. *et al.* Temporal dynamics and population genetic structure of *Fusarium graminearum* in the upper Midwestern United States. *Fungal Genetics and Biology* **73**, 83–92 (2014).
112. Varga, E. *et al.* New tricks of an old enemy: isolates of *Fusarium graminearum* produce a type A trichothecene mycotoxin. *Environ Microbiol* **17**, 2588–2600 (2015).
113. Kelly, A. *et al.* The geographic distribution and complex evolutionary history of the NX-2 trichothecene chemotype from *Fusarium graminearum*. *Fungal Genetics and Biology* **95**, 39–48 (2016).
114. Wipfler, R. *et al.* Synergistic Phytotoxic Effects of Culmorin and Trichothecene Mycotoxins. *Toxins* **11**, 555 (2019).
115. Woelflingseder, L., Gruber, N., Adam, G. & Marko, D. Pro-Inflammatory Effects of NX-3 Toxin Are Comparable to Deoxynivalenol and not Modulated by the Co-Occurring Pro-Oxidant Aurofusarin. *Microorganisms* **8**, 603 (2020).
116. Varga, E. *et al.* Less-toxic rearrangement products of NX-toxins are formed during storage and food processing. *Toxicology Letters* **284**, 205–212 (2018).
117. Pierron, A. *et al.* Intestinal toxicity of the new type A trichothecenes, NX and 3ANX. *Chemosphere* **288**, 132415 (2022).
118. Jennings, P., Coates, M. E., Turner, J. A., Chandler, E. A. & Nicholson, P. Determination of deoxynivalenol and nivalenol chemotypes of *Fusarium culmorum* isolates from England and Wales by PCR assay. *Plant Pathology* **53**, 182–190 (2004).
119. Prodi, A. *et al.* Difference in Chemotype Composition of *Fusarium graminearum* Populations Isolated from Durum Wheat in Adjacent Areas Separated by the Apennines in Northern-Central Italy. *The Plant Pathology Journal* (2011).
120. Somma, S. *et al.* Phylogenetic analyses of *Fusarium graminearum* strains from cereals in Italy, and characterisation of their molecular and chemical chemotypes. *Crop Pasture Sci.* **65**, 52–60 (2014).
121. Boutigny, A.-L., Ward, T. J., Ballois, N., Iancu, G. & Ioos, R. Diversity of the *Fusarium graminearum* species complex on French cereals. *Eur J Plant Pathol* **138**, 133–148 (2014).
122. Waalwijk, C. *et al.* Major Changes in *Fusarium* spp. in Wheat in the Netherlands. *European Journal of Plant Pathology* **109**, 743–754 (2003).
123. Yli-Mattila, T. *et al.* A novel Asian clade within the *Fusarium graminearum* species complex includes a newly discovered cereal head blight pathogen from the Russian Far East. *Mycologia* **101**, 841–852 (2009).
124. Boutigny, A.-L. *et al.* Quantitative detection of *Fusarium* pathogens and their mycotoxins in South African maize. *Plant Pathology* **61**, 522–531 (2012).

125. Gale, L. R. *et al.* Nivalenol-Type Populations of *Fusarium graminearum* and *F. asiaticum* Are Prevalent on Wheat in Southern Louisiana. *Phytopathology*® **101**, 124–134 (2011).
126. Guo, X. W., Fernando, W. G. D. & Seow-Brock, H. Y. Population Structure, Chemotype Diversity, and Potential Chemotype Shifting of *Fusarium graminearum* in Wheat Fields of Manitoba. *Plant Disease* **92**, 756–762 (2008).
127. Puri, K. D. & Zhong, S. The 3ADON population of *Fusarium graminearum* found in North Dakota is more aggressive and produces a higher level of DON than the prevalent 15ADON population in spring wheat. *Phytopathology* **100**, 1007–1014 (2010).
128. Ward, T. J. *et al.* An adaptive evolutionary shift in *Fusarium* head blight pathogen populations is driving the rapid spread of more toxigenic *Fusarium graminearum* in North America. *Fungal Genet Biol* **45**, 473–484 (2008).
129. Suga, H. *et al.* Molecular characterization of the *Fusarium graminearum* species complex in Japan. *Phytopathology* **98**, 159–166 (2008).
130. Zhang, H. *et al.* Population Analysis of the *Fusarium graminearum* Species Complex from Wheat in China Show a Shift to More Aggressive Isolates. *PLOS ONE* **7**, e31722 (2012).
131. Yoshizawa, T. & Jin, Y. Z. Natural occurrence of acetylated derivatives of deoxynivalenol and nivalenol in wheat and barley in Japan. *Food Addit Contam* **12**, 689–694 (1995).
132. Yang, L., van der Lee, T., Yang, X., Yu, D. & Waalwijk, C. *Fusarium* populations on Chinese barley show a dramatic gradient in mycotoxin profiles. *Phytopathology* **98**, 719–727 (2008).
133. Reynoso, M. M., Ramirez, M. L., Torres, A. M. & Chulze, S. N. Trichothecene genotypes and chemotypes in *Fusarium graminearum* strains isolated from wheat in Argentina. *International Journal of Food Microbiology* **145**, 444–448 (2011).
134. Castañares, E. *et al.* Trichothecene genotypes and production profiles of *Fusarium graminearum* isolates obtained from barley cultivated in Argentina. *International Journal of Food Microbiology* **179**, 57–63 (2014).
135. Malbrán, I., Mourellos, C. A., Girotti, J. R., Balatti, P. A. & Lori, G. A. Toxigenic capacity and trichothecene production by *Fusarium graminearum* isolates from Argentina and their relationship with aggressiveness and fungal expansion in the wheat spike. *Phytopathology* **104**, 357–364 (2014).
136. Scoz, L. B. *et al.* Trichothecene mycotoxin genotypes of *Fusarium graminearum* sensu stricto and *Fusarium meridionale* in wheat from southern Brazil. *Plant Pathology* **58**, 344–351 (2009).
137. Astolfi, P. *et al.* Molecular survey of trichothecene genotypes of *Fusarium graminearum* species complex from barley in Southern Brazil. *International Journal of Food Microbiology* **148**, 197–201 (2011).
138. Sampietro, D. A. *et al.* A molecular based strategy for rapid diagnosis of toxigenic *Fusarium* species associated to cereal grains from Argentina. *Fungal Biology* **114**, 74–81 (2010).
139. Umpiérrez-Failache, M. *et al.* Regional differences in species composition and toxigenic potential among *Fusarium* head blight isolates from Uruguay indicate a risk of nivalenol contamination in new wheat production areas. *International Journal of Food Microbiology* **166**, 135–140 (2013).
140. Quarta, A. *et al.* Multiplex PCR assay for the identification of nivalenol, 3- and 15-acetyl-deoxynivalenol chemotypes in *Fusarium*. *FEMS Microbiology Letters* **259**, 7–13 (2006).
141. Kammoun, L. G., Gargouri, S., Barreau, C., Richard-Forget, F. & Hajlaoui, M. R. Trichothecene chemotypes of *Fusarium culmorum* infecting wheat in Tunisia. *International Journal of Food Microbiology* **140**, 84–89 (2010).
142. Tok, F. M. & Arslan, M. Distribution and genetic chemotyping of *Fusarium graminearum* and *Fusarium culmorum* populations in wheat fields in the eastern Mediterranean region of Turkey. *Biotechnology & Biotechnological Equipment* **30**, 254–260 (2016).

143. Chen, Y., Kistler, H. C. & Ma, Z. Fusarium graminearum Trichothecene Mycotoxins: Biosynthesis, Regulation, and Management. *Annu Rev Phytopathol* **57**, 15–39 (2019).
144. European Food Safety Authority (EFSA). Annual Report of the EFSA Journal 2013. *EFSA* **11**, (2014).
145. Pestka, J. J. Deoxynivalenol: mechanisms of action, human exposure, and toxicological relevance. *Arch Toxicol* **84**, 663–679 (2010).
146. Reddy, K. *et al.* An overview of mycotoxin contamination in foods and its implications for human health. *Toxin Reviews* **29**, 3–26 (2010).
147. Allassane-Kpembi, I. *et al.* New insights into mycotoxin mixtures: the toxicity of low doses of Type B trichothecenes on intestinal epithelial cells is synergistic. *Toxicol Appl Pharmacol* **272**, 191–198 (2013).
148. Feizollahi, E. & Roopesh, M. S. Mechanisms of deoxynivalenol (DON) degradation during different treatments: a review. *Critical Reviews in Food Science and Nutrition* **62**, 5903–5924 (2022).
149. Wu, Q., Kuča, K., Humpf, H.-U., Klímová, B. & Cramer, B. Fate of deoxynivalenol and deoxynivalenol-3-glucoside during cereal-based thermal food processing: a review study. *Mycotoxin Res* **33**, 79–91 (2017).
150. Joint FAO/WHO Expert Committee on Food Additives. Meeting (72nd : 2010 : Rome, I., Organization, W. H. & Nations, F. and A. O. of the U. *Safety evaluation of certain contaminants in food: prepared by the Seventy-second meeting of the Joint FAO/WHO Expert Committee on Food Additives (JECFA)*. <https://apps.who.int/iris/handle/10665/44520> (2011).
151. Ueno, Y., Hosoya, M., Morita, Y., Ueno, I. & Tatsuno, T. Inhibition of the Protein Synthesis in Rabbit Reticulocyte by Nivalenol, a Toxic Principle Isolated from *Fusarium nivale*-Growing Rice. *The Journal of Biochemistry* **64**, 479–485 (1968).
152. Eriksen, G. S. & Pettersson, H. Toxicological evaluation of trichothecenes in animal feed. *Animal Feed Science and Technology* **114**, 205–239 (2004).
153. Alexander, N. J., Proctor, R. H. & McCormick, S. P. Genes, gene clusters, and biosynthesis of trichothecenes and fumonisins in *Fusarium*. *Toxin Reviews* **28**, 198–215 (2009).
154. Chen, Z. Régulation épigénétique de la production de mycotoxines chez *Fusarium graminearum*. (Bordeaux, 2019).
155. Alexander, N. J., McCormick, S. P., Waalwijk, C., van der Lee, T. & Proctor, R. H. The genetic basis for 3-ADON and 15-ADON trichothecene chemotypes in *Fusarium*. *Fungal Genetics and Biology* **48**, 485–495 (2011).
156. Lee, T., Han, Y.-K., Kim, K.-H., Yun, S.-H. & Lee, Y.-W. Tri13 and Tri7 Determine Deoxynivalenol- and Nivalenol-Producing Chemotypes of *Gibberella zeae*. *Applied and Environmental Microbiology* **68**, 2148–2154 (2002).
157. Villafana, R. T., Ramdass, A. C. & Rampersad, S. N. Selection of *Fusarium* Trichothecene Toxin Genes for Molecular Detection Depends on TRI Gene Cluster Organization and Gene Function. *Toxins* **11**, 36 (2019).
158. Ramírez Albuquerque, D., Patriarca, A. & Fernández Pinto, V. Can discrepancies between *Fusarium graminearum* trichothecene genotype and chemotype be explained by the influence of temperature in the relative production of 3-ADON and 15-ADON? *Fungal Biology* **125**, 153–159 (2021).
159. Ramírez Albuquerque, D., Patriarca, A. & Fernández Pinto, V. Water activity influence on the simultaneous production of DON, 3-ADON and 15-ADON by a strain of *Fusarium graminearum* ss of 15-ADON genotype. *International Journal of Food Microbiology* **373**, 109721 (2022).

160. Jiao, F., Kawakami, A. & Nakajima, T. Effects of different carbon sources on trichothecene production and Tri gene expression by *Fusarium graminearum* in liquid culture. *FEMS Microbiology Letters* **285**, 212–219 (2008).
161. Chen, F. *et al.* Combined Metabonomic and Quantitative Real-Time PCR Analyses Reveal Systems Metabolic Changes of *Fusarium graminearum* Induced by Tri5 Gene Deletion. *J. Proteome Res.* **10**, 2273–2285 (2011).
162. Giese, H., Sondergaard, T. E. & Sørensen, J. L. The AreA transcription factor in *Fusarium graminearum* regulates the use of some nonpreferred nitrogen sources and secondary metabolite production. *Fungal Biology* **117**, 814–821 (2013).
163. Gardiner, D. M. *et al.* Early activation of wheat polyamine biosynthesis during *Fusarium* head blight implicates putrescine as an inducer of trichothecene mycotoxin production. *BMC Plant Biol* **10**, 289 (2010).
164. Gardiner, D. M., Osborne, S., Kazan, K. & Manners, J. M. Low pH regulates the production of deoxynivalenol by *Fusarium graminearum*. *Microbiology* **155**, 3149–3156 (2009).
165. Merhej, J., Boutigny, A. L., Pinson-Gadais, L., Richard-Forget, F. & Barreau, C. Acidic pH as a determinant of TRI gene expression and trichothecene B biosynthesis in *Fusarium graminearum*. *Food Additives & Contaminants: Part A* **27**, 710–717 (2010).
166. Merhej, J., Richard-Forget, F. & Barreau, C. The pH regulatory factor Pac1 regulates Tri gene expression and trichothecene production in *Fusarium graminearum*. *Fungal Genetics and Biology* **48**, 275–284 (2011).
167. Merhej, J. *et al.* The velvet gene, FgVe1, affects fungal development and positively regulates trichothecene biosynthesis and pathogenicity in *Fusarium graminearum*. *Molecular Plant Pathology* **13**, 363–374 (2012).
168. Ponts, N., Pinson-Gadais, L., Barreau, C., Richard-Forget, F. & Ouellet, T. Exogenous H<sub>2</sub>O<sub>2</sub> and catalase treatments interfere with Tri genes expression in liquid cultures of *Fusarium graminearum*. *FEBS Letters* **581**, 443–447 (2007).
169. Montibus, M. *et al.* The bZIP Transcription Factor Fgap1 Mediates Oxidative Stress Response and Trichothecene Biosynthesis But Not Virulence in *Fusarium graminearum*. *PLOS ONE* **8**, e83377 (2013).
170. Audenaert, K., Callewaert, E., Höfte, M., De Saeger, S. & Haesaert, G. Hydrogen peroxide induced by the fungicide prothioconazole triggers deoxynivalenol (DON) production by *Fusarium graminearum*. *BMC Microbiol* **10**, 112 (2010).
171. Richard-Forget, F., Atanasova, V. & Chéreau, S. Using metabolomics to guide strategies to tackle the issue of the contamination of food and feed with mycotoxins: A review of the literature with specific focus on *Fusarium* mycotoxins. *Food Control* **121**, 107610 (2021).
172. Lowe, R. G. T. *et al.* A Combined 1H Nuclear Magnetic Resonance and Electrospray Ionization–Mass Spectrometry Analysis to Understand the Basal Metabolism of Plant-Pathogenic *Fusarium* spp. *MPMI* **23**, 1605–1618 (2010).
173. Panagiotou, G., Christakopoulos, P. & Olsson, L. Simultaneous saccharification and fermentation of cellulose by *Fusarium oxysporum* F3—growth characteristics and metabolite profiling. *Enzyme and Microbial Technology* **36**, 693–699 (2005).
174. Smith, J. E., Lay, J. O. & Bluhm, B. H. Metabolic fingerprinting reveals a new genetic linkage between ambient pH and metabolites associated with desiccation tolerance in *Fusarium verticillioides*. *Metabolomics* **8**, 376–385 (2012).
175. Atanasova-Penichon, V. *et al.* Mycotoxin Biosynthesis and Central Metabolism Are Two Interlinked Pathways in *Fusarium graminearum*, as Demonstrated by the Extensive Metabolic Changes Induced by Caffeic Acid Exposure. *Appl Environ Microbiol* **84**, (2018).

176. Liu, C. *et al.* Metabolic Changes of *Fusarium graminearum* Induced by TPS Gene Deletion. *J. Proteome Res.* **18**, 3317–3327 (2019).
177. Tag, A. G. *et al.* A Novel Regulatory Gene, Tri10, Controls Trichothecene Toxin Production and Gene Expression. *Applied and Environmental Microbiology* **67**, 5294–5302 (2001).
178. Seong, K.-Y. *et al.* Global gene regulation by *Fusarium* transcription factors Tri6 and Tri10 reveals adaptations for toxin biosynthesis. *Molecular Microbiology* **72**, 354–367 (2009).
179. Nasmith, C. G. *et al.* Tri6 Is a Global Transcription Regulator in the Phytopathogen *Fusarium graminearum*. *PLOS Pathogens* **7**, e1002266 (2011).
180. Gu, Q. *et al.* Protein kinase FgSch9 serves as a mediator of the target of rapamycin and high osmolarity glycerol pathways and regulates multiple stress responses and secondary metabolism in *Fusarium graminearum*. *Environmental Microbiology* **17**, 2661–2676 (2015).
181. Yu, F.-W., Zhang, X.-P., Yu, M.-H., Yin, Y.-N. & Ma, Z.-H. The potential protein kinase A (Pka) phosphorylation site is required for the function of FgSge1 in *Fusarium graminearum*. *World J Microbiol Biotechnol* **31**, 1419–1430 (2015).
182. Boenisch, M. J. *et al.* Structural reorganization of the fungal endoplasmic reticulum upon induction of mycotoxin biosynthesis. *Sci Rep* **7**, 44296 (2017).
183. Hou, Z. *et al.* A Mitogen-Activated Protein Kinase Gene (MGV1) in *Fusarium graminearum* Is Required for Female Fertility, Heterokaryon Formation, and Plant Infection. *MPMI* **15**, 1119–1127 (2002).
184. Yun, Y. *et al.* Functional analysis of the *Fusarium graminearum* phosphatome. *New Phytologist* **207**, 119–134 (2015).
185. Guo, L. *et al.* Compartmentalized gene regulatory network of the pathogenic fungus *Fusarium graminearum*. *New Phytol* **211**, 527–541 (2016).
186. Jiang, C. *et al.* TRI6 and TRI10 play different roles in the regulation of deoxynivalenol (DON) production by cAMP signalling in *Fusarium graminearum*. *Environmental Microbiology* **18**, 3689–3701 (2016).
187. Yin, T. *et al.* The cyclase-associated protein FgCap1 has both protein kinase A-dependent and -independent functions during deoxynivalenol production and plant infection in *Fusarium graminearum*. *Molecular Plant Pathology* **19**, 552–563 (2018).
188. Merhej, J., Richard-Forget, F. & Barreau, C. Regulation of trichothecene biosynthesis in *Fusarium*: recent advances and new insights. *Applied Microbiology and Biotechnology* **91**, 519–528 (2011).
189. Woloshuk, C. P. & Shim, W.-B. Aflatoxins, fumonisins, and trichothecenes: a convergence of knowledge. *FEMS Microbiol Rev* **37**, 94–109 (2013).
190. Niehaus, E.-M. *et al.* Genetic Manipulation of the *Fusarium fujikuroi* Fusarin Gene Cluster Yields Insight into the Complex Regulation and Fusarin Biosynthetic Pathway. *Chemistry & Biology* **20**, 1055–1066 (2013).
191. Kim, H.-K. *et al.* Functional Roles of FgLaeA in Controlling Secondary Metabolism, Sexual Development, and Virulence in *Fusarium graminearum*. *PLOS ONE* **8**, e68441 (2013).
192. Bok, J. W. & Keller, N. P. LaeA, a Regulator of Secondary Metabolism in *Aspergillus* spp. *Eukaryotic Cell* **3**, 527–535 (2004).
193. Ronne, H. Glucose repression in fungi. *Trends Genet* **11**, 12–17 (1995).
194. Rui, H. & ChenFang, W. The function of the carbon metabolism regulator FgCreA in *Fusarium graminearum*. *Scientia Agricultura Sinica* **51**, 257–267 (2018).
195. Tudzynski, B. Nitrogen regulation of fungal secondary metabolism in fungi. *Front Microbiol* **5**, 656 (2014).
196. Hou, R., Jiang, C., Zheng, Q., Wang, C. & Xu, J.-R. The AreA transcription factor mediates the regulation of deoxynivalenol (DON) synthesis by ammonium and cyclic adenosine

- monophosphate (cAMP) signalling in *Fusarium graminearum*. *Molecular Plant Pathology* **16**, 987–999 (2015).
197. Boutigny, A.-L., Richard-Forget, F. & Barreau, C. Natural mechanisms for cereal resistance to the accumulation of *Fusarium trichothecenes*. *European Journal of Plant Pathology* **121**, 411–423 (2008).
  198. Etier, A., Dumetz, F., Chéreau, S. & Ponts, N. Post-Translational Modifications of Histones Are Versatile Regulators of Fungal Development and Secondary Metabolism. *Toxins* **14**, 317 (2022).
  199. Atanasoff-Kardjalieff, A. K. & Studt, L. Secondary Metabolite Gene Regulation in Mycotoxigenic *Fusarium* Species: A Focus on Chromatin. *Toxins* **14**, 96 (2022).
  200. Mapook, A. *et al.* Ten decadal advances in fungal biology leading towards human well-being. *Fungal Diversity* **116**, 547–614 (2022).
  201. Collemare, J. & Seidl, M. F. Chromatin-dependent regulation of secondary metabolite biosynthesis in fungi: is the picture complete? *FEMS Microbiol Rev* **43**, 591–607 (2019).
  202. Connolly, L. R., Smith, K. M. & Freitag, M. The *Fusarium graminearum* Histone H3 K27 Methyltransferase KMT6 Regulates Development and Expression of Secondary Metabolite Gene Clusters. *PLOS Genetics* **9**, e1003916 (2013).
  203. Studt, L. *et al.* Knock-down of the methyltransferase Kmt6 relieves H3K27me3 and results in induction of cryptic and otherwise silent secondary metabolite gene clusters in *Fusarium fujikuroi*. *Environmental Microbiology* **18**, 4037–4054 (2016).
  204. Studt, L. *et al.* Lack of the COMPASS Component Ccl1 Reduces H3K4 Trimethylation Levels and Affects Transcription of Secondary Metabolite Genes in Two Plant–Pathogenic *Fusarium* Species. *Frontiers in Microbiology* **7**, (2017).
  205. Liu, Y. *et al.* Histone H3K4 methylation regulates hyphal growth, secondary metabolism and multiple stress responses in *Fusarium graminearum*. *Environmental Microbiology* **17**, 4615–4630 (2015).
  206. Janevska, S., Güldener, U., Sulyok, M., Tudzynski, B. & Studt, L. Set1 and Kdm5 are antagonists for H3K4 methylation and regulators of the major conidiation-specific transcription factor gene ABA1 in *Fusarium fujikuroi*. *Environmental Microbiology* **20**, 3343–3362 (2018).
  207. Janevska, S. *et al.* Elucidation of the Two H3K36me3 Histone Methyltransferases Set2 and Ash1 in *Fusarium fujikuroi* Unravels Their Different Chromosomal Targets and a Major Impact of Ash1 on Genome Stability. *Genetics* **208**, 153–171 (2018).
  208. Reyes-Dominguez, Y. *et al.* Heterochromatin influences the secondary metabolite profile in the plant pathogen *Fusarium graminearum*. *Fungal Genetics and Biology* **49**, 39–47 (2012).
  209. Kourmouli, N. *et al.* Heterochromatin and tri-methylated lysine 20 of histone H4 in animals. *Journal of Cell Science* **117**, 2491–2501 (2004).
  210. Schotta, G. *et al.* A silencing pathway to induce H3-K9 and H4-K20 trimethylation at constitutive heterochromatin. *Genes Dev.* **18**, 1251–1262 (2004).
  211. Bachleitner, S., Sulyok, M., Sørensen, J. L., Strauss, J. & Studt, L. The H4K20 methyltransferase Kmt5 is involved in secondary metabolism and stress response in phytopathogenic *Fusarium* species. *Fungal Genetics and Biology* **155**, 103602 (2021).
  212. Rösler, S. M., Kramer, K., Finkemeier, I., Humpf, H.-U. & Tudzynski, B. The SAGA complex in the rice pathogen *Fusarium fujikuroi*: structure and functional characterization. *Molecular Microbiology* **102**, 951–974 (2016).
  213. Almeida, M. I. *et al.* Co-occurrence of aflatoxins B1, B2, G1 and G2, ochratoxin A, zearalenone, deoxynivalenol, and citreoviridin in rice in Brazil. *Food Additives & Contaminants: Part A* **29**, 694–703 (2012).

214. Pleadin, J. *et al.* Contamination of maize with deoxynivalenol and zearalenone in Croatia. *Food Control* **28**, 94–98 (2012).
215. Queiroz, V. A. V. *et al.* Occurrence of fumonisins and zearalenone in maize stored in family farm in Minas Gerais, Brazil. *Food Control* **28**, 83–86 (2012).
216. Rai, A. *et al.* Presence of Zearalenone in Cereal Grains and Its Exposure Risk Assessment in Indian Population. *Journal of Food Science* **83**, 3126–3133 (2018).
217. Mousavi Khaneghah, A., Fakhri, Y. & Sant’Ana, A. S. Impact of unit operations during processing of cereal-based products on the levels of deoxynivalenol, total aflatoxin, ochratoxin A, and zearalenone: A systematic review and meta-analysis. *Food Chemistry* **268**, 611–624 (2018).
218. Kim, J.-E., Son, H. & Lee, Y.-W. Biosynthetic mechanism and regulation of zearalenone in *Fusarium graminearum*. *JSM Mycotoxins* **68**, 1–6 (2018).
219. Gautier, C., Pinson-Gadais, L. & Richard-Forget, F. *Fusarium* Mycotoxins Enniatins: An Updated Review of Their Occurrence, the Producing *Fusarium* Species, and the Abiotic Determinants of Their Accumulation in Crop Harvests. *J. Agric. Food Chem.* **68**, 4788–4798 (2020).
220. Mallebrera, B., Prosperini, A., Font, G. & Ruiz, M. J. In vitro mechanisms of Beauvericin toxicity: A review. *Food Chem Toxicol* **111**, 537–545 (2018).
221. EFSA Panel on Contaminants in the Food Chain (CONTAM). Scientific Opinion on the risks to human and animal health related to the presence of beauvericin and enniatins in food and feed. *EFSA* **12**, (2014).
222. Rodríguez-Carrasco, Y. *et al.* Urinary levels of enniatin B and its phase I metabolites: First human pilot biomonitoring study. *Food and Chemical Toxicology* **118**, 454–459 (2018).
223. Rodríguez-Carrasco, Y. *et al.* Biomonitoring of Enniatin B1 and Its Phase I Metabolites in Human Urine: First Large-Scale Study. *Toxins* **12**, 415 (2020).
224. BIOMIN Mycotoxin Survey Q3 2021 Results. *Biomin* <https://www.biomin.net/science-hub/biomin-mycotoxin-survey-q3-2021-results/>.
225. Smith, M.-C., Madec, S., Coton, E. & Hymery, N. Natural Co-Occurrence of Mycotoxins in Foods and Feeds and Their in vitro Combined Toxicological Effects. *Toxins (Basel)* **8**, 94 (2016).
226. Karlovsky, P. *et al.* Impact of food processing and detoxification treatments on mycotoxin contamination. *Mycotoxin Res* **32**, 179–205 (2016).
227. Peivasteh-Roudsari, L. *et al.* Mycotoxins: Impact on Health and Strategies for Prevention and Detoxification in the Food Chain. *Food Reviews International* **0**, 1–32 (2021).
228. Kabak, B., Dobson, A. D. W. & Var, I. Strategies to Prevent Mycotoxin Contamination of Food and Animal Feed: A Review. *Critical Reviews in Food Science and Nutrition* **46**, 593–619 (2006).
229. Wegulo, S. N., Baenziger, P. S., Hernandez Nopsa, J., Bockus, W. W. & Hallen-Adams, H. Management of *Fusarium* head blight of wheat and barley. *Crop Protection* **73**, 100–107 (2015).
230. Marburger, D. A. *et al.* Crop Rotation and Management Effect on *Fusarium* spp. Populations. *Crop Science* **55**, 365–376 (2015).
231. Tillmann, M., von Tiedemann, A. & Winter, M. Crop rotation effects on incidence and diversity of *Fusarium* species colonizing stem bases and grains of winter wheat. *J Plant Dis Prot* **124**, 121–130 (2017).
232. Obst, A., Lepschy-Von Gleissenthall, J. & Beck, R. On The Etiology of *Fusarium* Head Blight of Wheat in South Germany - Preceding Crops, Weather Conditions for Inoculum Production and Head Infection, Proneness of The Crop to Infection and Mycotoxin Production. *CEREAL RESEARCH COMMUNICATIONS* **25**, 699–703 (1997).

233. Fernandez, M. R., Selles, F., Gehl, D., DePauw, R. M. & Zentner, R. P. Crop Production Factors Associated with Fusarium Head Blight in Spring Wheat in Eastern Saskatchewan. *Crop Science* **45**, 1908–1916 (2005).
234. Pioli, R. N., Mozzoni, L. & Morandi, E. N. First Report of Pathogenic Association Between Fusarium graminearum and Soybean. *Plant Dis* **88**, 220 (2004).
235. Broders, K. D., Lipps, P. E., Paul, P. A. & Dorrance, A. E. Evaluation of Fusarium graminearum Associated with Corn and Soybean Seed and Seedling Disease in Ohio. *Plant Disease* **91**, 1155–1160 (2007).
236. Blandino, M. *et al.* Integrated strategies for the control of Fusarium head blight and deoxynivalenol contamination in winter wheat. *Field Crops Research* **133**, 139–149 (2012).
237. Teich, A. H. Chapter 16 - EPIDEMIOLOGY OF WHEAT (TRITICUM AESTIVUM L.) SCAB CAUSED BY FUSARIUM spp. in *Fusarium* (ed. Chelkowski, J.) vol. 2 269–282 (Elsevier, 1989).
238. Martin, R. A., MacLeod, J. A. & Caldwell, C. Influences of production inputs on incidence of infection by Fusarium species on cereal seed. *Plant disease (USA)* (1991).
239. Yi, C., Kaul, H.-P., Kübler, E., Schwadorf, K. & Aufhammer, W. Head blight (Fusarium graminearum) and deoxynivalenol concentration in winter wheat as affected by pre-crop, soil tillage and nitrogen fertilization / Ähren-Fusarium (Fusarium graminearum) und Deoxynivalenol-Gehalt von Winterweizen in Abhängigkeit von Vorfrucht, Bodenbearbeitung und N-Düngung. *Zeitschrift für Pflanzenkrankheiten und Pflanzenschutz / Journal of Plant Diseases and Protection* **108**, 217–230 (2001).
240. Schaafsma, A. W. & Hooker, D. C. Climatic models to predict occurrence of Fusarium toxins in wheat and maize. *International Journal of Food Microbiology* **119**, 116–125 (2007).
241. De Wolf, E. D., Madden, L. V. & Lipps, P. E. Risk Assessment Models for Wheat Fusarium Head Blight Epidemics Based on Within-Season Weather Data. *Phytopathology*® **93**, 428–435 (2003).
242. Shah, D. A., De Wolf, E. D., Paul, P. A. & Madden, L. V. Predicting Fusarium Head Blight Epidemics with Boosted Regression Trees. *Phytopathology*® **104**, 702–714 (2014).
243. Prandini, A., Sigolo, S., Filippi, L., Battilani, P. & Piva, G. Review of predictive models for Fusarium head blight and related mycotoxin contamination in wheat. *Food and Chemical Toxicology* **47**, 927–931 (2009).
244. Schroeder, H. W. & Christensen, J. J. Factors affecting resistance of Wheat to scab caused by Gibberella zeae. *Phytopathology* **53**, 831–838 (1963).
245. Dhokane, D., Karre, S., Kushalappa, A. C. & McCartney, C. Integrated Metabolo-Transcriptomics Reveals Fusarium Head Blight Candidate Resistance Genes in Wheat QTL-Fhb2. *PLOS ONE* **11**, e0155851 (2016).
246. Buerstmayr, H. *et al.* Molecular mapping of QTLs for Fusarium head blight resistance in spring wheat. I. Resistance to fungal spread (Type II resistance). *Theor Appl Genet* **104**, 84–91 (2002).
247. Cuthbert, P. A., Somers, D. J. & Brulé-Babel, A. Mapping of Fhb2 on chromosome 6BS: a gene controlling Fusarium head blight field resistance in bread wheat (Triticum aestivum L.). *Theor Appl Genet* **114**, 429–437 (2007).
248. McCartney, C. A. *et al.* The evaluation of FHB resistance QTLs introgressed into elite Canadian spring wheat germplasm. *Mol Breeding* **20**, 209–221 (2007).
249. Dokāne, K., Jonkus, D. & Sjakste, T. Evaluation of the RYR1 gene genetic diversity in the Latvian White pig breed. *Biopolym. Cell* **32**, 184–189 (2016).
250. Talas, F., Longin, F. & Miedaner, T. Sources of resistance to Fusarium head blight within Syrian durum wheat landraces. *Plant Breeding* **130**, 398–400 (2011).

251. Zhu, Z. *et al.* Breeding wheat for resistance to Fusarium head blight in the Global North: China, USA, and Canada. *The Crop Journal* **7**, 730–738 (2019).
252. Li, T., Bai, G., Wu, S. & Gu, S. Quantitative trait loci for resistance to fusarium head blight in a Chinese wheat landrace Haiyanzhong. *Theor Appl Genet* **122**, 1497–1502 (2011).
253. Li, T. *et al.* Effective marker alleles associated with type 2 resistance to Fusarium head blight infection in fields. *Breeding Science* **66**, 350–357 (2016).
254. Jia, H. *et al.* A journey to understand wheat Fusarium head blight resistance in the Chinese wheat landrace Wangshuibai. *The Crop Journal* **6**, 48–59 (2018).
255. Buerstmayr, H., Ban, T. & Anderson, J. A. QTL mapping and marker-assisted selection for Fusarium head blight resistance in wheat: a review. *Plant Breeding* **128**, 1–26 (2009).
256. Ons, L., Bylemans, D., Thevissen, K. & Cammue, B. P. A. Combining Biocontrol Agents with Chemical Fungicides for Integrated Plant Fungal Disease Control. *Microorganisms* **8**, 1930 (2020).
257. Bagga, P. Fusarium Head Blight (FHB) of wheat: Role of host resistance, wheat aphids, insecticide and strobilurin fungicide in disease control in Punjab, India. *Cereal Research Communications* **36**, 667–670 (2008).
258. Olotuah, O. F. Comparative control of Fusarium verticillioides infesting maize using Hyptis suaveolens and synthetic insecticide. *Imperial journal of interdisciplinary research* **2**, (2016).
259. Drakulic, J., Ajigboye, O., Swarup, R., Bruce, T. & Ray, R. V. Aphid Infestation Increases Fusarium langsethiae and T-2 and HT-2 Mycotoxins in Wheat. *Applied and Environmental Microbiology* **82**, 6548–6556 (2016).
260. Johal, G. S. & Huber, D. M. Glyphosate effects on diseases of plants. *European Journal of Agronomy* **31**, 144–152 (2009).
261. Fernandez, M. R. *et al.* Glyphosate associations with cereal diseases caused by Fusarium spp. in the Canadian Prairies. *European Journal of Agronomy* **31**, 133–143 (2009).
262. Drakopoulos, D. *et al.* Prevention of Fusarium head blight infection and mycotoxins in wheat with cut-and-carry biofumigation and botanicals. *Field Crops Research* **246**, 107681 (2020).
263. Becher, R., Weihmann, F., Deising, H. B. & Wirsal, S. G. Development of a novel multiplex DNA microarray for Fusarium graminearum and analysis of azole fungicide responses. *BMC Genomics* **12**, 52 (2011).
264. Paul, P. A. *et al.* Efficacy of Triazole-Based Fungicides for Fusarium Head Blight and Deoxynivalenol Control in Wheat: A Multivariate Meta-Analysis. *Phytopathology*® **98**, 999–1011 (2008).
265. Pirgozliev, S. R., Edwards, S. G., Hare, M. C. & Jenkinson, P. Effect of Dose Rate of Azoxystrobin and Metconazole on the Development of Fusarium Head Blight and the Accumulation of Deoxynivalenol (DON) in Wheat Grain. *European Journal of Plant Pathology* **108**, 469–478 (2002).
266. Chen, K. *et al.* New benzimidazole acridine derivative induces human colon cancer cell apoptosis in vitro via the ROS-JNK signaling pathway. *Acta Pharmacol Sin* **36**, 1074–1084 (2015).
267. Mesterházy, Á. Control of Fusarium head blight of wheat fungicides. *Fusarium head blight of wheat and barley* 363–380 (2003).
268. Milus, E. A. & Weight, C. T. Efficacy of Quadris and Benlate applications on wheat scab in Arkansas. in *Proceedings, the* 51–52 (1998).
269. Haidukowski, M. *et al.* Effect of fungicides on the development of Fusarium head blight, yield and deoxynivalenol accumulation in wheat inoculated under field conditions with Fusarium graminearum and Fusarium culmorum. *Journal of the Science of Food and Agriculture* **85**, 191–198 (2005).

270. Hollingsworth, C. R., Motteberg, C. D., Assistant, R. & Thompson, W. G. Assessing Fungicide Efficacies for the Management of Fusarium Head Blight on Spring Wheat and Barley. *Plant Health Progress* **7**, 14 (2006).
271. Spolti, P., Guerra, D. S., Badiale-Furlong, E. & Del Ponte, E. M. Single and sequential applications of metconazole alone or in mixture with pyraclostrobin to improve Fusarium head blight control and wheat yield in Brazil. *Trop. plant pathol.* **38**, 85–96 (2013).
272. Yuan, S. & Zhou, M. A major gene for resistance to carbendazim, in field isolates of *Gibberella zeae*. *Canadian Journal of Plant Pathology* **27**, 58–63 (2005).
273. Gilbert, J. & Haber, S. Overview of some recent research developments in fusarium head blight of wheat. *Canadian Journal of Plant Pathology* **35**, 149–174 (2013).
274. McMullen, M. *et al.* Integrated strategies for Fusarium head blight management in the United States. *Cereal Research Communications* **36**, 563–568 (2008).
275. Ramirez, M. L., Chulze, S. & Magan, N. Impact of environmental factors and fungicides on growth and deoxynivalenol production by *Fusarium graminearum* isolates from Argentinian wheat. *Crop Protection* **23**, 117–125 (2004).
276. Mesterházy, Á. *et al.* Role of Fungicides, Application of Nozzle Types, and the Resistance Level of Wheat Varieties in the Control of Fusarium Head Blight and Deoxynivalenol. *Toxins* **3**, 1453–1483 (2011).
277. Willyerd, K. T. *et al.* Efficacy and Stability of Integrating Fungicide and Cultivar Resistance to Manage Fusarium Head Blight and Deoxynivalenol in Wheat. *Plant Disease* **96**, 957–967 (2012).
278. Paul, P. A. *et al.* Integrated Effects of Genetic Resistance and Prothioconazole + Tebuconazole Application Timing on Fusarium Head Blight in Wheat. *Plant Disease* **103**, 223–237 (2019).
279. Ács, K. *et al.* Reduction of deoxynivalenol (DON) contamination by improved fungicide use in wheat. Part 3. Reduction of Fusarium head blight and influence on quality traits in cultivars with different resistance levels. *Eur J Plant Pathol* **151**, 21–38 (2018).
280. Beyer, M., Klix, M. B., Klink, H. & Verreet, J.-A. Quantifying the effects of previous crop, tillage, cultivar and triazole fungicides on the deoxynivalenol content of wheat grain — a review. *J Plant Dis Prot* **113**, 241–246 (2006).
281. Edwards, S. G. Influence of agricultural practices on fusarium infection of cereals and subsequent contamination of grain by trichothecene mycotoxins. *Toxicology Letters* **153**, 29–35 (2004).
282. Blandino, M. & Reyneri, A. Effect of fungicide and foliar fertilizer application to winter wheat at anthesis on flag leaf senescence, grain yield, flour bread-making quality and DON contamination. *European Journal of Agronomy* **30**, 275–282 (2009).
283. Barber, A. E. *et al.* Effects of Agricultural Fungicide Use on *Aspergillus fumigatus* Abundance, Antifungal Susceptibility, and Population Structure. *mBio* **11**, e02213-20 (2020).
284. Simpson, D. R., Weston, G. E., Turner, J. A., Jennings, P. & Nicholson, P. Differential Control of Head Blight Pathogens of Wheat by Fungicides and Consequences for Mycotoxin Contamination of Grain. *European Journal of Plant Pathology* **107**, 421–431 (2001).
285. Jennings, P., Turner, J. A. & Nicholson, P. Overview of fusarium ear blight in the UK - effect of fungicide treatment on disease control and mycotoxin production. *The BCPC Conference: Pests and diseases, Volume 2. Proceedings of an international conference held at the Brighton Hilton Metropole Hotel, Brighton, UK, 13-16 November 2000* 707–712 (2000).
286. Blandino, M., Minelli, L. & Reyneri, A. Strategies for the chemical control of Fusarium head blight: Effect on yield, alveographic parameters and deoxynivalenol contamination in winter wheat grain. *European Journal of Agronomy* **25**, 193–201 (2006).

287. Bailey, S. W. Climate change and decreasing herbicide persistence. *Pest Management Science* **60**, 158–162 (2004).
288. D'Angelo, D. L. *et al.* Efficacy of Fungicide Applications During and After Anthesis Against Fusarium Head Blight and Deoxynivalenol in Soft Red Winter Wheat. *Plant Disease* **98**, 1387–1397 (2014).
289. Chen, Y. & Zhou, M.-G. Characterization of Fusarium graminearum Isolates Resistant to Both Carbendazim and a New Fungicide JS399-19. *Phytopathology*® **99**, 441–446 (2009).
290. Liu, S. *et al.* Carbendazim Resistance of Fusarium graminearum From Henan Wheat. *Plant Disease* **103**, 2536–2540 (2019).
291. Zhou, Y. *et al.*  $\beta$ 1 Tubulin Rather Than  $\beta$ 2 Tubulin Is the Preferred Binding Target for Carbendazim in Fusarium graminearum. *Phytopathology*® **106**, 978–985 (2016).
292. Duan, Y. *et al.* Development and application of loop-mediated isothermal amplification for detection of the F167Y mutation of carbendazim-resistant isolates in Fusarium graminearum. *Sci Rep* **4**, 7094 (2014).
293. Liu, X. *et al.* Paralogous cyp51 genes in Fusarium graminearum mediate differential sensitivity to sterol demethylation inhibitors. *Fungal Genetics and Biology* **48**, 113–123 (2011).
294. Duan, Y. *et al.* Molecular and biological characteristics of laboratory metconazole-resistant mutants in Fusarium graminearum. *Pesticide Biochemistry and Physiology* **152**, 55–61 (2018).
295. Mamane, A., Baldi, I., Tessier, J.-F., Raheison, C. & Bouvier, G. Occupational exposure to pesticides and respiratory health. *European Respiratory Review* **24**, 306–319 (2015).
296. Piel, C. *et al.* Agricultural exposures to carbamate herbicides and fungicides and central nervous system tumour incidence in the cohort AGRICAN. *Environment International* **130**, 104876 (2019).
297. Hoppin, J. A. *et al.* Pesticides are Associated with Allergic and Non-Allergic Wheeze among Male Farmers. *Environmental Health Perspectives* **125**, 535–543 (2017).
298. Juntarawijit, C. & Juntarawijit, Y. Association between diabetes and pesticides: a case-control study among Thai farmers. *Environmental Health and Preventive Medicine* **23**, 3 (2018).
299. Torres, A. m. *et al.* Fusarium head blight and mycotoxins in wheat: prevention and control strategies across the food chain. *World Mycotoxin Journal* **12**, 333–355 (2019).
300. Mesterházy, Á. *et al.* Reduction of deoxynivalenol (DON) contamination by improved fungicide use in wheat. Part 1. Dependence on epidemic severity and resistance level in small plot tests with artificial inoculation. *Eur J Plant Pathol* **151**, 39–55 (2018).
301. Lee, Y.-H. *et al.* Fungicide Resistance of Fusarium fujikuroi Isolates Isolated In Korea. *The Korean Journal of Pesticide Science* **14**, 427–432 (2010).
302. Ahmed, O. S. *et al.* Naturally occurring phenolic compounds as promising antimycotoxin agents: Where are we now? *Comprehensive Reviews in Food Science and Food Safety* **21**, 1161–1197 (2022).
303. Pal, K. K. & McSpadden Gardener, B. Biological Control of Plant Pathogens. *PHI* (2006) doi:10.1094/PHI-A-2006-1117-02.
304. Vujanovic, V. & Goh, Y. K. Sphaerodes mycoparasitica biotrophic mycoparasite of 3-acetyldeoxynivalenol- and 15-acetyldeoxynivalenol-producing toxigenic Fusarium graminearum chemotypes. *FEMS Microbiology Letters* **316**, 136–143 (2011).
305. Kim, S. H. & Vujanovic, V. Relationship between mycoparasites lifestyles and biocontrol behaviors against Fusarium spp. and mycotoxins production. *Appl Microbiol Biotechnol* **100**, 5257–5272 (2016).
306. Legrand, F., Picot, A., Cobo-Díaz, J. F., Chen, W. & Le Floch, G. Challenges facing the biological control strategies for the management of Fusarium Head Blight of cereals caused by F. graminearum. *Biological Control* **113**, 26–38 (2017).

307. Byrne, M. J. *et al.* Three new biological control programmes for South Africa: Brazilian pepper, Tamarix and Tradescantia. *African Entomology* **29**, 965–982 (2021).
308. Khan, J., Ooka, J. J., Miller, S. A., Madden, L. V. & Hoitink, H. a. J. Systemic Resistance Induced by *Trichoderma hamatum* 382 in Cucumber Against *Phytophthora* Crown Rot and Leaf Blight. *Plant Disease* **88**, 280–286 (2004).
309. Jochum, C. C., Osborne, L. E. & Yuen, G. Y. *Fusarium* head blight biological control with *Lysobacter enzymogenes* strain C3. *Biological Control* **39**, 336–344 (2006).
310. Blaszczyk, L., Siwulski, M., Sobieralski, K., Lisiecka, J. & Jedryczka, M. *Trichoderma* spp. – application and prospects for use in organic farming and industry. *Journal of Plant Protection Research* **54**, (2014).
311. Woo, S. *et al.* *Trichoderma*-based Products and their Widespread Use in Agriculture. *The Open Mycology Journal* **8**, (2014).
312. Fernandez, M. R. The effect of *Trichoderma harzianum* on fungal pathogens infesting soybean residues. *Soil Biology and Biochemistry* **24**, 1027–1029 (1992).
313. Bujold, I., Paulitz, T. C. & Carisse, O. Effect of *Microsphaeropsis* sp. on the Production of Perithecia and Ascospores of *Gibberella zeae*. *Plant Disease* **85**, 977–984 (2001).
314. Xue, A., Voldeng, H., Savard, M. & Fedak, G. Biological management of *Fusarium* head blight and mycotoxin contamination in wheat. *World Mycotoxin Journal* **2**, 193–201 (2009).
315. Palazzini, J. M., Groenenboom-de Haas, B. H., Torres, A. M., Köhl, J. & Chulze, S. N. Biocontrol and population dynamics of *Fusarium* spp. on wheat stubble in Argentina. *Plant Pathology* **62**, 859–866 (2013).
316. Palazzini, J. M., Yerkovich, N., Alberione, E., Chiotta, M. & Chulze, S. N. Reprint of “An integrated dual strategy to control *Fusarium graminearum* sensu stricto by the biocontrol agent *Streptomyces* sp. RC 87B under field conditions”. *Plant Gene* **11**, 2–7 (2017).
317. Nygren, K. *et al.* The mycoparasitic fungus *Clonostachys rosea* responds with both common and specific gene expression during interspecific interactions with fungal prey. *Evolutionary Applications* **11**, 931–949 (2018).
318. He, J., Boland, G. j. & Zhou, T. Concurrent selection for microbial suppression of *Fusarium graminearum*, *Fusarium* head blight and deoxynivalenol in wheat. *Journal of Applied Microbiology* **106**, 1805–1817 (2009).
319. Ghisalberti, E. L. & Sivasithamparam, K. Antifungal antibiotics produced by *Trichoderma* spp. *Soil Biology and Biochemistry* **23**, 1011–1020 (1991).
320. Lavermicocca, P. *et al.* Purification and Characterization of Novel Antifungal Compounds from the Sourdough *Lactobacillus plantarum* Strain 21B. *Applied and Environmental Microbiology* **66**, 4084–4090 (2000).
321. Nourozian, J., Etebarian, H. R. & Khodakaramian, G. Biological control of *Fusarium graminearum* on wheat by antagonistic bacteria. 10.
322. Palazzini, J. M., Ramirez, M. L., Torres, A. M. & Chulze, S. N. Potential biocontrol agents for *Fusarium* head blight and deoxynivalenol production in wheat. *Crop Protection* **26**, 1702–1710 (2007).
323. Crane, J. M. & Bergstrom, G. C. Spatial distribution and antifungal interactions of a *Bacillus* biological control agent on wheat surfaces. *Biological Control* **78**, 23–32 (2014).
324. Gong, W. *et al.* Comparative Secretome Analysis of *Aspergillus niger*, *Trichoderma reesei*, and *Penicillium oxalicum* During Solid-State Fermentation. *Appl Biochem Biotechnol* **177**, 1252–1271 (2015).
325. Grosu, A. I., Siciua, O.-A., Dobre, A., Voaideş, C. & Cornea, C. P. Evaluation of Some *Bacillus* spp. Strains for the Biocontrol of *Fusarium graminearum* and *F. culmorum* in Wheat. *Agriculture and Agricultural Science Procedia* **6**, 559–566 (2015).

326. Wang, G. *et al.* Exopolysaccharide from *Trichoderma pseudokoningii* induces macrophage activation. *Carbohydrate Polymers* **149**, 112–120 (2016).
327. Dunlap, C. A., Bowman, M. J. & Schisler, D. A. Genomic analysis and secondary metabolite production in *Bacillus amyloliquefaciens* AS 43.3: A biocontrol antagonist of *Fusarium* head blight. *Biological Control* **64**, 166–175 (2013).
328. Wang, J., Liu, J., Chen, H. & Yao, J. Characterization of *Fusarium graminearum* inhibitory lipopeptide from *Bacillus subtilis* IB. *Appl Microbiol Biotechnol* **76**, 889–894 (2007).
329. Zhao, P., Quan, C., Wang, Y., Wang, J. & Fan, S. *Bacillus amyloliquefaciens* Q-426 as a potential biocontrol agent against *Fusarium oxysporum* f. sp. *spinaciae*. *Journal of Basic Microbiology* **54**, 448–456 (2014).
330. Chatterton, S. & Punja, Z. K. Chitinase and  $\beta$ -1,3-glucanase enzyme production by the mycoparasite *Clonostachys rosea* f. *catenulata* against fungal plant pathogens. *Can. J. Microbiol.* **55**, 356–367 (2009).
331. Rodríguez, M. a., Cabrera, G., Gozzo, F. c., Eberlin, M. n. & Godeas, A. *Clonostachys rosea* BAFC3874 as a *Sclerotinia sclerotiorum* antagonist: mechanisms involved and potential as a biocontrol agent. *Journal of Applied Microbiology* **110**, 1177–1186 (2011).
332. Larran, S., Simón, M. R., Moreno, M. V., Siurana, M. P. S. & Perelló, A. Endophytes from wheat as biocontrol agents against tan spot disease. *Biological Control* **92**, 17–23 (2016).
333. Toumatia, O. *et al.* Biocontrol and plant growth promoting properties of *Streptomyces mutabilis* strain IA1 isolated from a Saharan soil on wheat seedlings and visualization of its niches of colonization. *South African Journal of Botany* **105**, 234–239 (2016).
334. Roberti, R. *et al.* Induction of PR proteins and resistance by the biocontrol agent *Clonostachys rosea* in wheat plants infected with *Fusarium culmorum*. *Plant Science* **175**, 339–347 (2008).
335. Henkes, G. J. *et al.* *Pseudomonas fluorescens* CHA0 maintains carbon delivery to *Fusarium graminearum*-infected roots and prevents reduction in biomass of barley shoots through systemic interactions. *Journal of Experimental Botany* **62**, 4337–4344 (2011).
336. Ferrigo, D., Raiola, A., Rasera, R. & Causin, R. *Trichoderma harzianum* seed treatment controls *Fusarium verticillioides* colonization and fumonisin contamination in maize under field conditions. *Crop Protection* **65**, 51–56 (2014).
337. Nürnberger, T., Brunner, F., Kemmerling, B. & Piater, L. Innate immunity in plants and animals: striking similarities and obvious differences. *Immunological Reviews* **198**, 249–266 (2004).
338. Chalfoun, N. R. *et al.* Elicitor-Based Biostimulant PSP1 Protects Soybean Against Late Season Diseases in Field Trials. *Frontiers in Plant Science* **9**, (2018).
339. Twamley, T., Gaffney, M. & Feechan, A. A Microbial Fermentation Mixture Reduces *Fusarium* Head Blight and Promotes Grain Weight but does not impact *Septoria tritici* blotch. *Eur J Plant Pathol* **162**, 203–219 (2022).
340. Markets and Markets. *Biopesticides Market by Type (Bioinsecticides, Biofungicides, Bionematicides, and Bioherbicides), Source (Microbials, Biochemicals, and Beneficial Insects), Mode of Application, Formulation (Dry, Liquid), Crop type and Region - Global Forecast to 2027.* (2022).
341. Kiewnick, S. Practicalities of developing and registering microbial biological control agents. *CABI Reviews* **2007**, 11 pp. (2007).
342. Lahlali, R. *et al.* Biological Control of Plant Pathogens: A Global Perspective. *Microorganisms* **10**, 596 (2022).
343. Boulanger, N., Boyer, P., Talagrand-Reboul, E. & Hansmann, Y. Ticks and tick-borne diseases. *Médecine et Maladies Infectieuses* **49**, 87–97 (2019).

344. Nakajima, Y., van Naters-Yasui, A. van der G., Taylor, D. & Yamakawa, M. Two isoforms of a member of the arthropod defensin family from the soft tick, *Ornithodoros moubata* (Acari: Argasidae). *Insect Biochemistry and Molecular Biology* **31**, 747–751 (2001).
345. Fogaça, A. C. *et al.* Cysteine-rich antimicrobial peptides of the cattle tick *Boophilus microplus*: isolation, structural characterization and tissue expression profile. *Developmental & Comparative Immunology* **28**, 191–200 (2004).
346. Hynes, W. L., Ceraul, S. M., Todd, S. M., Seguin, K. C. & Sonenshine, D. E. A defensin-like gene expressed in the black-legged tick, *Ixodes scapularis*. *Medical and Veterinary Entomology* **19**, 339–344 (2005).
347. Johns, R., Sonenshine, D. E. & Hynes, W. L. Identification of a defensin from the hemolymph of the American dog tick, *Dermacentor variabilis*. *Insect Biochemistry and Molecular Biology* **31**, 857–865 (2001).
348. Lai, R., Lomas, L. O., Jonczy, J., Turner, P. C. & Rees, H. H. Two novel non-cationic defensin-like antimicrobial peptides from haemolymph of the female tick, *Amblyomma hebraeum*. *Biochemical Journal* **379**, 681–685 (2004).
349. Nakajima, Y., Van Der Goes van Naters-Yasui, A., Taylor, D. & Yamakawa, M. Antibacterial peptide defensin is involved in midgut immunity of the soft tick, *Ornithodoros moubata*. *Insect Molecular Biology* **11**, 611–618 (2002).
350. Saito, Y. *et al.* Identification and characterization of antimicrobial peptide, defensin, in the taiga tick, *Ixodes persulcatus*. *Insect Molecular Biology* **18**, 531–539 (2009).
351. Todd, S. M., Sonenshine, D. E. & Hynes, W. L. Tissue and life-stage distribution of a defensin gene in the Lone Star tick, *Amblyomma americanum*. *Medical and Veterinary Entomology* **21**, 141–147 (2007).
352. Tsuji, N. *et al.* Babesial Vector Tick Defensin against *Babesia* sp. Parasites. *Infection and Immunity* **75**, 3633–3640 (2007).
353. Wang, Y. & Zhu, S. The defensin gene family expansion in the tick *Ixodes scapularis*. *Developmental & Comparative Immunology* **35**, 1128–1134 (2011).
354. Cabezas-Cruz, A. *et al.* Antibacterial and antifungal activity of defensins from the Australian paralysis tick, *Ixodes holocyclus*. *Ticks and Tick-borne Diseases* **10**, 101269 (2019).
355. Rudenko, N., Golovchenko, M., Edwards, M. J. & Grubhoffer, L. Differential Expression of *Ixodes ricinus* Tick Genes Induced by Blood Feeding or *Borrelia burgdorferi* Infection. *Journal of Medical Entomology* **42**, 36–41 (2005).
356. Rudenko, N., Golovchenko, M. & Grubhoffer, L. Gene organization of a novel defensin of *Ixodes ricinus*: first annotation of an intron/exon structure in a hard tick defensin gene and first evidence of the occurrence of two isoforms of one member of the arthropod defensin family. *Insect Molecular Biology* **16**, 501–507 (2007).
357. Tonk, M. *et al.* Identification and partial characterisation of new members of the *Ixodes ricinus* defensin family. *Gene* **540**, 146–152 (2014).
358. Tonk, M. *et al.* *Ixodes ricinus* defensins attack distantly-related pathogens. *Developmental & Comparative Immunology* **53**, 358–365 (2015).
359. Tonk, M. *et al.* Defensins from the tick *Ixodes scapularis* are effective against phytopathogenic fungi and the human bacterial pathogen *Listeria grayi*. *Parasites Vectors* **7**, 554 (2014).
360. Bulet, P., Stocklin, R. & Menin, L. Anti-microbial peptides: from invertebrates to vertebrates. *Immunol Rev* **198**, 169–184 (2004).
361. Zhang, Z.-T. & Zhu, S.-Y. Drosomycin, an essential component of antifungal defence in *Drosophila*. *Insect Molecular Biology* **18**, 549–556 (2009).

362. Leannec-Rialland, V. *et al.* Tick defensin  $\gamma$ -core reduces *Fusarium graminearum* growth and abrogates mycotoxins production with high efficiency. *Sci Rep* **11**, 7962 (2021).
363. Vela-Corcía, D., Romero, D., de Vicente, A. & Pérez-García, A. Analysis of  $\beta$ -tubulin-carbendazim interaction reveals that binding site for MBC fungicides does not include residues involved in fungicide resistance. *Sci Rep* **8**, 7161 (2018).
364. Roberts, T. R. *et al.* *Metabolic Pathways of Agrochemicals: Part 1: Herbicides and Plant Growth Regulators*. (Royal Society of Chemistry, 2007).
365. Nicaise, V. *et al.* Interaction between the Accumulation of Cadmium and Deoxynivalenol Mycotoxin Produced by *Fusarium graminearum* in Durum Wheat Grains. *J. Agric. Food Chem.* **70**, 8085–8096 (2022).
366. Aamot, H. U. *et al.* Genetic and phenotypic diversity within the *Fusarium graminearum* species complex in Norway. *Eur J Plant Pathol* **142**, 501–519 (2015).
367. Laurent, B. *et al.* Landscape of genomic diversity and host adaptation in *Fusarium graminearum*. *BMC Genomics* **18**, 203 (2017).
368. Ponts, N. Mycotoxins are a component of *Fusarium graminearum* stress-response system. *Front Microbiol* **6**, 1234–1234 (2015).
369. Règlement (CE) n° 1126/2007 de la Commission du 28 septembre 2007 modifiant le règlement (CE) n° 1881/2006 portant fixation de teneurs maximales pour certains contaminants dans les denrées alimentaires en ce qui concerne les toxines du *Fusarium* dans le maïs et les produits à base de maïs (Texte présentant de l'intérêt pour l'EEE). *OJ L* vol. 255 (2007).
370. Règlement (CE) N° 396/2005 du Parlement européen et du Conseil du 23 février 2005 concernant les limites maximales applicables aux résidus de pesticides présents dans ou sur les denrées alimentaires et les aliments pour animaux d'origine végétale et animale et modifiant la directive 91/414/CEE du Conseil Texte présentant de l'intérêt pour l'EEE. *OJ L* vol. 070 (2005).
371. Leannec-Rialland, V. *et al.* Use of Defensins to Develop Eco-Friendly Alternatives to Synthetic Fungicides to Control Phytopathogenic Fungi and Their Mycotoxins. *J Fungi (Basel)* **8**, 229 (2022).
372. Audenaert, K. *et al.* *Impact of Fungicide Timing on the Composition of the Fusarium Head Blight Disease Complex and the Presence of Deoxynivalenol (DON) in Wheat. Fungicides - Beneficial and Harmful Aspects* (IntechOpen, 2011). doi:10.5772/26322.
373. Lay, F. T. *et al.* Dimerization of Plant Defensin NaD1 Enhances Its Antifungal Activity. *J. Biol. Chem.* **287**, 19961–19972 (2012).
374. Falanga, A. *et al.* Cyclic Peptides as Novel Therapeutic Microbicides: Engineering of Human Defensin Mimetics. *Molecules* **22**, 1217 (2017).
375. López Cascales, J. J. *et al.* Small Cationic Peptides: Influence of Charge on Their Antimicrobial Activity. *ACS Omega* **3**, 5390–5398 (2018).
376. Poon, I. K. *et al.* Phosphoinositide-mediated oligomerization of a defensin induces cell lysis. *eLife* **3**, e01808 (2014).
377. de Medeiros, L. N. *et al.* Backbone dynamics of the antifungal Psd1 pea defensin and its correlation with membrane interaction by NMR spectroscopy. *Biochimica et Biophysica Acta (BBA) - Biomembranes* **1798**, 105–113 (2010).
378. Thevissen, K., Francois, I. E., Aerts, A. & Cammue, B. Fungal Sphingolipids as Targets for the Development of Selective Antifungal Therapeutics. *CDT* **6**, 923–928 (2005).
379. Brogden, K. A. Antimicrobial peptides: pore formers or metabolic inhibitors in bacteria? *Nat Rev Microbiol* **3**, 238–250 (2005).
380. van der Weerden, N. L., Lay, F. T. & Anderson, M. A. The Plant Defensin, NaD1, Enters the Cytoplasm of *Fusarium Oxysporum* Hyphae. *J. Biol. Chem.* **283**, 14445–14452 (2008).

381. Hayes, B. M. E. *et al.* Identification and Mechanism of Action of the Plant Defensin NaD1 as a New Member of the Antifungal Drug Arsenal against *Candida albicans*. *Antimicrob. Agents Chemother.* **57**, 3667–3675 (2013).
382. Lichius, A. & Zeilinger, S. Application of Membrane and Cell Wall Selective Fluorescent Dyes for Live-Cell Imaging of Filamentous Fungi. *J Vis Exp* (2019) doi:10.3791/60613.
383. Hayes, B. M. E., Bleackley, M. R., Anderson, M. A. & van der Weerden, N. L. The Plant Defensin NaD1 Enters the Cytoplasm of *Candida albicans* via Endocytosis. *JoF* **4**, 20 (2018).
384. Tetorya, M. *et al.* Plant defensin MtDef4-derived antifungal peptide with multiple modes of action and potential as a bioinspired fungicide. <http://biorxiv.org/lookup/doi/10.1101/2022.10.02.510465> (2022) doi:10.1101/2022.10.02.510465.
385. Jimah, J. R., Schlesinger, P. H. & Tolia, N. H. Liposome Disruption Assay to Examine Lytic Properties of Biomolecules. *Bio-protocol* **7**, e2433–e2433 (2017).
386. Aumer, T., Voisin, S. N., Knobloch, T., Landon, C. & Bulet, P. Impact of an Antifungal Insect Defensin on the Proteome of the Phytopathogenic Fungus *Botrytis cinerea*. *J. Proteome Res.* **19**, 1131–1146 (2020).
387. Hale, J. D. & Hancock, R. E. Alternative mechanisms of action of cationic antimicrobial peptides on bacteria. *Expert Review of Anti-infective Therapy* **5**, 951–959 (2007).
388. do Nascimento, V. V. *et al.* PvD1 defensin, a plant antimicrobial peptide with inhibitory activity against *Leishmania amazonensis*. *Bioscience Reports* **35**, e00248 (2015).
389. Zhou, T. *et al.* Identification of differentially expressed genes involved in spore germination of *Penicillium expansum* by comparative transcriptome and proteome approaches. *MicrobiologyOpen* **7**, e00562 (2018).
390. Andersson, L. *et al.* Large-scale synthesis of peptides. *Biopolymers* **55**, 227–250 (2000).
391. Druzinec, D. *et al.* Optimization of Insect Cell Based Protein Production Processes - Online Monitoring, Expression Systems, Scale Up. in *Yellow Biotechnology II* (ed. Vilcinskas, A.) vol. 136 65–100 (Springer Berlin Heidelberg, 2013).
392. Tleuova, A. B. *et al.* Recent advances and remaining barriers to producing novel formulations of fungicides for safe and sustainable agriculture. *J Control Release* **326**, 468–481 (2020).
393. Arand, K., Asmus, E., Popp, C., Schneider, D. & Riederer, M. The Mode of Action of Adjuvants—Relevance of Physicochemical Properties for Effects on the Foliar Application, Cuticular Permeability, and Greenhouse Performance of Pinoxaden. *J. Agric. Food Chem.* **66**, 5770–5777 (2018).
394. Leslie, J. F. *et al.* Key Global Actions for Mycotoxin Management in Wheat and Other Small Grains. *Toxins* **13**, 725 (2021).



# **Titre : Efficacité et mécanismes d'action des défensines de tiques contre le champignon phytopathogène et toxigène *Fusarium graminearum***

## **Résumé :**

La fusariose de l'épi (FHB), principalement causée par le champignon *Fusarium graminearum*, est une maladie dévastatrice qui affecte les cultures céréalières et entraîne des pertes de rendement importantes et une diminution de la qualité des grains. En effet, *F. graminearum* produit des mycotoxines appelées trichothécènes de type B (TCTB) qui nuisent à la santé humaine et animale. Le peptide appelé TickCore3 (TC3),  $\gamma$ -core de la défensine de tique DefMT3, s'est avéré être un puissant antifongique contre *F. graminearum* et un inhibiteur efficace de la production de TCTB. Les déterminants structuraux et physico-chimiques nécessaires à l'efficacité du peptide ont été clarifiés. Des observations microscopiques ont permis de montrer que le peptide se fixait spécifiquement à l'enveloppe des spores fongiques. En outre, une stratégie associant transcriptomique (RNA-seq) et métabolomique (LC-MS/MS) a été mise en œuvre pour décrypter le mécanisme d'action de TC3. Des changements importants dans le transcriptome de *F. graminearum*, comme dans son métabolome, ont été induits par une exposition au TC3 mettant en évidence un mécanisme à multiples facettes. Les résultats obtenus au cours de cette thèse ont démontré que TC3 était un candidat prometteur pour de nouvelles solutions de protection des végétaux, alternatives aux fongicides de synthèse.

**Mots clés :** défensine, antifongique, champignon phytopathogène, mycotoxine, peptide, tique

---

## **Unité de recherche**

[Mycologie et Sécurité des Aliments, UR1264, 71 Av. Edouard Bourlaux, 33140 Villenave-d'Ornon]

## **Title : Efficacy and mechanisms of action of tick defensins against the phytopathogenic and toxinogenic fungus *Fusarium graminearum***

### **Abstract :**

Fusarium Head Blight (FHB) mainly caused by the fungus *Fusarium graminearum* is a devastating disease affecting cereal crops that leads to significant yield losses and a reduced grain quality. Indeed, *F. graminearum* produces type B trichothecene mycotoxins (TCTB) which are detrimental to the health of humans and livestock. In the present study, a peptide referred to as TickCore3 (TC3), the  $\gamma$ -core of the tick defensin DefMT3, was demonstrated to be a potent fungicidal agent against *F. graminearum* and an efficient inhibitor of the production of TCTB. The structural and physico-chemical determinants required for the peptide efficacy were clarified. Through microscopic observation, the peptide was shown to bind specifically to the fungal spore's envelope. Furthermore, a strategy combining transcriptomic (RNA-seq) and metabolomic (LC-MS) has been implemented to unravel the mechanism of action of TC3. Significant changes in *F. graminearum* transcriptome such as in its metabolome were induced by TC3 exposure evidencing a multi-faceted mechanism. The results obtained during this thesis demonstrated that TC3 could be a promising candidate for the development of new eco-friendly plant protection solutions.

**Keywords :** defensive, antifungal, phytopathogenic fungus, mycotoxin, peptide, tick

---

### **Unité de recherche**

[Mycologie et Sécurité des Aliments, UR1264, 71 Av. Edouard Bourlaux, 33140 Villenave-d'Ornon]